EMERGENCY POINT-OF-CARE ULTRASOUND

SECOND EDITION

Edited by
James A. Connolly
Anthony J. Dean
Beatrice Hoffmann
Robert D. Jarman

WILEY Blackwell

Emergency Point-of-Care Ultrasound

IHEM
iranian house of emergency medicine
خانه متخصصین طب اورژانس ایران

Emergency Point-of-Care Ultrasound

Second Edition

Edited by

James A. Connolly
Anthony J. Dean
Beatrice Hoffmann
Robert D. Jarman

WILEY Blackwell

This edition first published 2017 © 2014, 2017 by John Wiley and Sons Ltd
First edition published 2004 by Blackwell Publishing, Ltd

Registered office:
John Wiley & Sons Ltd, The Atrium, Southern Gate, Chichester, West Sussex, PO19 8SQ, UK

Editorial offices:
9600 Garsington Road, Oxford, OX4 2DQ, UK
The Atrium, Southern Gate, Chichester, West Sussex, PO19 8SQ, UK
111 River Street, Hoboken, NJ 07030-5774, USA

For details of our global editorial offices, for customer services and for information about how to apply for permission to reuse the copyright material in this book please see our website at www.wiley.com/wiley-blackwell

Library of Congress Cataloging-in-Publication data applied for

ISBN: 9780470657577 (Paperback)

A catalogue record for this book is available from the British Library.

Wiley also publishes its books in a variety of electronic formats. Some content that appears in print may not be available in electronic books.

Cover Design: Wiley
Cover Image: Courtesy of Beatrice Hoffmann

Set in 10/12pt Warnock by SPi Global, Pondicherry, India

1 2017

Contents

List of Contributors

Srikar Adhikari MD
Associate Professor of Emergency Medicine
University of Arizona Department of Emergency Medicine;
Section Chief, Emergency Medicine Ultrasound
Tucson, AZ, USA

Pablo Aguillera MD
Assistant Professor of Emergency Medicine
Chair, Department of Emergency Medicine
Pontificia Universidad Católica de Chile (PUC)
Santiago, Chile

Kenton Anderson MD, FACEP
Clinical Assistant Professor
Director of Emergency Ultrasound Research
Department of Emergency Medicine
Stanford University School of Medicine
Stanford, CA, USA

Robert Arntfield MD, RDMS, FRCPC
Associate Professor
Division of Critical Care & Division of Emergency Medicine Department of Medicine
The University of Western Ontario
London, ON
Canada

Paul Atkinson MBBA, FRCEM, FRCPC
Professor and Research Director
Emergency Medicine
St Johns Regional Hospital
Dalhousie University
Saint John, NB, Canada

Sean Bennett MBBCh, FRCA
Consultant in Cardiac Anaesthesia and Intensive Care
University of Hull
Hull Royal Infirmary;
Consultant in Cardiac and Intensive Care Anaesthesia
Castle Hill Hospital, Cottingham, East Yorkshire
UK

Michael Blaivas MD, FACEP, FAIUM
Professor of Medicine
University of South Carolina School of Medicine
Columbia, SC;
Department of Emergency Medicine
St Francis Hospital
Columbus, GA, USA

Jens Børglum MD
Consultant Anaesthetist
Department of Anaesthesiology & Intensive Care
Bispebjerg University Hospital, Copenhagen
Denmark

Mark W. Bowyer MD, FACS, DMCC
Professor of Surgery
Chief, Division of Combat and Trauma Surgery
Director for Surgical Simulation
The Norman M. Rich Department of Surgery
F. Edward Hébert School of Medicine
Uniformed Services University of the Health Sciences
Bethesda, MD, USA

Raoul Breitkreutz, MD
Associate Professor
FINeST, Simulation Centre
Goethe University Hospital of Frankfurt am Main
Frankfurt am Main, Hessen, Germany

Barton Brown MD
Department of Emergency Medicine
Hancock Regional Hospital
Indianapolis, IN
USA

Adam Bystrzycki MBBS, FACEM, PgDip(Echo)
Consultant
Alfred Emergency and Trauma centre
Senior Lecturer Monash University
Australia

Liberty V. Caroon RDMS
Sonographer
Department of Emergency Medicine
Hennepin County Medical Center
Minneapolis, MI
USA

Luigi Cattarossi MD
Department of Pediatrics
San Antonio Abate Hospital
Tolmezzo, Italy

James A. Connolly MBBS, FRCS(Ed), FRCS (Glas), FRCEM
Consultant and Head of Department
Great North Trauma and Emergency Care Centre
Newcastle upon Tyne
UK

Roberto Copetti MD
Department of Emergency
MedicineCattinara HospitalTrieste
Italy

Elena Costantini MD
Department of Anesthesia and Intensive Care
Luigi Sacco Hospital
University of Milan
Italy

Colleen Cuca MD
Hospital zum Heiligen Geist
Teaching Hospital of Goethe-University
Frankfurt am Main
Germany

Sara Damewood MD
Assistant Professor
Section Chief, Emergency Ultrasound
Department of Emergency Medicine
University of Wisconsin School of Medicine and Public Health
Madison, WI
USA

Lisa Munro Davies
Consultant
Department of Emergency Medicine
University Hospitals Bristol NHS Foundation Trust
Bristol Royal Infirmary
Bristol
UK

Anthony J. Dean MD
Professor of Emergency Medicine and of Emergency Medicine in Radiology
Director, Division of Emergency Ultrasonography
Department of Emergency Medicine
University of Pennsylvania
Philadelphia, PA, USA

Mahmoud A. Elbarbary MD, MSc, EDIC, PhD (Deceased)
Consultant and Assistant Professor, Critical Care Medicine
King Saud Bin Abdulaziz University for Health Sciences
Riyadh
Saudi Arabia

J. Matthew Fields MD
Associate Professor of Emergency Medicine
Emergency Ultrasound Fellowship Director
Thomas Jefferson University Hospital
Philadelphia, PA
USA

Jonathan Fischer MD
Attending Physician
Department of Emergency Medicine
Lankenau Medical Center
Wynnewood, PA, USA

Christian Alcaraz Frederiksen MD
Research Associate
Department of Anesthesiology and Intensive Care
Aarhus University Hospital
Aarhus
Denmark

Rajat Gangahar FRCEM
Consultant
Department of Emergency Medicine
Royal Oldham Hospital
Oldham, Lancashire, UK

Lara Goldstein MBBCh, FCEM(SA)
Specialist Emergency Physician
Registrar Programme Director
Division of Emergency Medicine
University of the Witwatersrand;
Gauteng Emergency Medical Services;
Head, Department of Emergency Medicine,
Helen Joseph Hospital
Johannesburg, South Africa

John Gullett MD
Associate Professor
Co-Director Emergency Ultrasound
Department of Emergency Medicine
University of Alabama Birmingham
Birmingham, AL, USA

Tim Harris FACEM, FCEM, DipImmCare, Dip O&G, BM, BS, BMedSci
Consultant and Professor
Department of Emergency Medicine
Pre-Hospital Care and Intensive Care Medicine
Royal London Hospital and London HEMS
Newham University Hospital
Barts Health NHS Trust and QMUL
London, UK

Frank Heringer MD
Frankfurt Institute of Emergency Medicine and Simulation Training
Goethe-University
Frankfurt am Main
Germany

Beatrice Hoffmann MD
Associate Professor of Emergency Medicine
Harvard Medical School
Division Chief, Emergency Medicine Ultrasound
Beth Israel Deaconess Medical Center
Boston, MA
USA

Erskine J. Holmes MBBCh Bio, MRCS, FCEM
Consultant, Emergency Medicine
Wexham Park Hospital
Slough, UK

Richard A. Hoppmann MD
Professor of Medicine
Director, Ultrasound Institute
University of South Carolina School of Medicine
Columbia, SC
USA

Robert D. Jarman MBBS, MSc(Medical Ultrasound), FRCS(Ed), FRCEM(UK), FRCP(Ed), CFEU
Consultant in Emergency Medicine
Royal Victoria Infirmary
Newcastle upon Tyne;
Visiting Professor and MSc Point-of-Care Ultrasound Lead
University of Teesside
Middlesbrough
UK

Dietrich von Kuenssberg Jehle MD, RDMS
Professor of Emergency Medicine
SUNY at Buffalo
Director of Emergency Ultrasonography and Associate Medical Director
Department of Emergency Medicine
Erie County Medical Center
Buffalo, NY
USA

Kenneth Jensen MD
Associate Professor
Department of Anaesthesia and Intensive Care,
Copenhagen University Hospital, Bispebjerg,
Denmark

Phil Johnstone MBBS, FCEM
Consultant, Accident and Emergency
Newcastle upon Tyne Hospitals
NHS Foundation Trust
Newcastle upon Tyne, UK

Peter Juhl-Olsen MD
Research associate
Department of Anesthesiology and Intensive Care
Aarhus University Hospital
Aarhus, Denmark

John L. Kendall MD
Associate Professor
Director of Emergency Ultrasound
Denver Health Medical Center;
Department of Emergency Medicine
University of Colorado School of Medicine
Denver, CO, USA

Andrew M. Kestler MD, MBA, DTMH, FACEP, FRCPC
Clinical Associate Professor
St. Paul's Hospital & University of British Columbia
Vancouver, BC, Canada

Andrew W. Kirkpatrick MD, MHSc
Regional Trauma Services, Departments of
Surgery and Critical Care Medicine,
Foothills Medical Centre,
Calgary, Alberta
Canada

Michael Lambert MD, RDMS, FAAEM
Department of Emergency Medicine
Advocate Christ Medical Center
Oak Lawn, IL,
USA

Hein Lamprecht MBChB, FCEM(SA), FRCEM, DA(UK), CFEU(UK)
Programme Director, Clinical Ultrasound
Stellenbosch University
Cape Town
South Africa

David Lewis MB, BS, FRCS, FCEM, CFEU, PGDipSEM
Associate Professor
Department of Emergency Medicine
Saint John Regional Hospital
Dalhousie University
Saint John, NB
Canada

Resa Lewiss MD
Associate Professor of Emergency
Medicine
University of Colorado;
Director of Point-of-Care Ultrasound
University of Colorado Hospital
Aurora, CO
USA

Veronica M. Madigan MD
School of Biomedical Science
Charles Stuart University
Bathurst, New South Wales
Australia

Jennifer R. Marin MD
Director of Emergency Ultrasound
Division of Emergency Medicine
Children's Hospital of Pittsburgh of UPMC;
Assistant Professor of Pediatrics
University of Pittsburgh School of Medicine
Pittsburgh, PA, USA

Gebhard Mathis MD
Professor of Internal Medicine
Innsbruck University
Austria

Stefan M. Mazur BPhEd, MBChB, PGCertAME, DipIMC, DRTM (RCSEd), CCPU
PreHospital and Retrieval Physician
SAAS MedSTAR;
Consultant in Emergency Medicine
Royal Adelaide Hospital, North Terrace,
Adelaide;
Associate Professor
Public Health Tropical Medicine
James Cook University
Townsville, Australia

Lawrence A. Melniker MD, MS
Vice Chair, Continuous Quality Management
Department of Emergency Medicine
New York Methodist Hospital, Brooklyn;
Assistant Clinical Professor
Department of Medicine
Weill Medical College
Cornell University
Ithaca, NY, USA

Christopher L. Moore MD, RDMS, RDCS, FACEP
Associate Professor
Division Director Emergency Ultrasound
Department of Emergency Medicine
Yale University School of Medicine
New Haven, CT
USA

Craig Morris
ITU Consultant
Derby
UK

Vicki E. Noble MD RDMS
Professor and Vice Chair
Department of Emergency Medicine
University Hospital
Case Western Reserve University School of Medicine
Cleveland, OH, USA

Nova L. Panebianco MD, MPH
Assistant Professor of Emergency Medicine;
Associate Director of Emergency Ultrasound
Department of Emergency Medicine
Hospital of the University of Pennsylvania
Philadelphia, PA, USA

David C. Pigott MD
Professor and Vice Chair for Academic Development
Co-Director, Division of Emergency Ultrasound
Department of Emergency Medicine
University of Alabama at Birmingham
Birmingham, AL, USA

Robert F. Reardon MD
Associate Professor of Emergency Medicine
University of Minnesota Medical School;
Ultrasound Director
Department of Emergency Medicine
Hennepin County Medical Center
Minneapolis, MN
USA

Joshua S. Rempell MD, MPH
Assistant Professor
Cooper Medical School of Rowan University
Cooper University Hospital
Camden, NJ
USA

Simon Richards MHSc, PgC(L&THE), DCR(R)
Senior Lecturer and Programme Lead Medical Ultrasound
Teesside University
Middlesbrough, UK

David B. Richards MD, FACEP
Assistant Professor
Department of Emergency Medicine
Denver Health Medical Center
University of Colorado School of Medicine
Aurora, CO
USA

Peter Ross MD, CCFP(EM), FCFP
Assistant Professor
Memorial University of Newfoundland School of Medicine;
Post Graduate Site Director for Emergency Medicine
Department of Emergency Medicine
Dalhousie University
Saint John, NB
Canada

Conn Russell MD
Consultant in Anaesthesia and Intensive Care Medicine
Department of Anaesthetics and Intensive Care Medicine
Ulster Hospital
Belfast, UK

Fernando Silva MD, MSc
Department of Emergency Medicine
Kaiser Permanente
North California
Napa/Solano Region, USA

Gabriel Simon MD
Department of Emergency Medicine
Nashoba Valley Medical Center
Ayer, MA
USA

Anumeha Singh MD
Faculty
Department of Emergency Medicine
Hartford Hospital
Hartford, CT, USA

Elena Skomorovsky MD
Clinical Instructor
Harvard Medical School
Department of Emergency Medicine
Beth Israel Deaconess Medical Center
Boston, MA, USA

John Sloan
Department of Emergency Medicine
Countess of Chester Hospital
Chester, UK

Erik Sloth MD, PhD, DMSc
Professor
Department of Anesthesiology and Intensive Care
Aarhus University Hospital
Aarhus
Denmark

Brendan E. Smith MBChB, FFA, RCS
Associate Professor
School of Biomedical Science
Charles Stuart University
Bathurst, New South Wales
Australia

Sarah A. Stahmer MD
Clinical Associate Professor of Emergency Medicine
University of North Carolina School of Medicine
Chapel Hill, NC, USA

Seth R. Strote MD
United Hospitalist Service of AMC
Sait Paul, MN, USA

R. Andrew Taylor MD
Clinical Instructor
Department of Emergency Medicine
Yale University School of Medicine
New Haven, CT
USA

Heather Venables
Senior Lecturer
Professional Lead Medical Ultrasound
University of Derby
Derby, UK

Martha Villalba MD
Department of Emergency Medicine
Jesse Brown
Veterans Affairs Medical Center
Chicago, IL, USA

Felix Walcher MD
Dept. of Trauma and Orthopedic Surgery
Frankfurt Institute of Emergency Medicine and Simulation Training
Goethe-University, Frankfurt am Main
Germany

Christopher T. Wall MD
Department of Emergency Medicine
Hennepin County Medical Center
Minneapolis, MN, USA

Mike Wells MBBCh, MSc Med (Emergency Medicine), FCEM(SA), DipPEC(SA)
Specialist Emergency Physician
Consultant, Lecturer and Director of Emergency Ultrasound Training
Division of Emergency Medicine
University of the Witwatersrand;
Netcare Union Hospital Emergency Department
Johannesburg, South Africa

David C. Wherry MD, FACS, FRCS, DMCC
DCW Professor of Surgery
Director, Emerging Technologies
The Norman M. Rich Department of Surgery
F. Edward Hébert School of Medicine
Uniformed Services University of the Health Sciences
Bethesda, MD
USA

Joseph Wood MD, RDMS
Vice Chair and Associate Professor
Department of Emergency Medicine
Mayo Clinic Medical School
Phoenix, AZ, USA

Peter M. Zechner
Internist
Graz
Austria

About the Companion Website

This book is accompanied by a companion website:

www.wiley.com/go/connolly/ultrasound

The website includes:

- Videos
- Chapters 44–50
- Appendix

The videos are clearly signposted throughout the book. Look out for  .

We note with sadness the untimely death of Dr. Mahmoud Elbarbary during the final stages of publication of this volume. Dr. Elbarbary will be missed as a friend and colleague by many of its contributors, and his activities as a scientist, teacher, leader, and international collaborator reflect the spirit of this book.

Introduction

What is Point-of-Care Ultrasound?

James A. Connolly, Anthony J. Dean, Beatrice Hoffmann and Robert D. Jarman

Barely 60 years have passed since the pioneering days of diagnostic ultrasound in the 1950s. The equipment of that time was complicated and bulky, and dedicated technologists with special training were needed to obtain images, and specially trained physicians to interpret them. As this arrangement was well established in radiography, ultrasonography was naturally and rapidly adopted by radiologists. During the late 1960s ultrasound's ability to generate real-time moving images that provided hemodynamic, physiological and pathological data in addition to structural information without the use of contrast agents led to its adoption by cardiologists. The absence of ionising radiation also gave impetus to its use in obstetrics and gynecology. This traditional workflow was continued throughout many Anglo-American medical systems, but interestingly, many European and Asian countries adopted a physician-performed sonography service as part of their unique medical specialty care.

It is not surprising then, that during the 1980s, German ambulance-based traumatologists started to use ultrasonography in the field to detect free peritoneal fluid in victims of blunt trauma. This approach was possible as a result of the development of portable machines of similar size and weight to then-available defibrillator-monitoring equipment. Image quality was inferior to that of cart-based systems, but was still far superior to that of state-of-the-art equipment of the previous generation, and was sufficient for the simple clinical question of the traumatologists: does this patient have free intra-abdominal fluid suggesting the need for immediate operative intervention? This application was adopted by trauma surgeons in North America in the early 1990s, and soon thereafter by emergency physicians. With the adoption of ultrasound by *practitioners* who sought to answer *clinical questions* with a *focused and limited examination*, the field of *sonology* was born.

During the 1990s clinicians from countries with the traditional sonographer-performed ultrasound approach started to implement physician-performed sonography in their practice. For instance, urologists and vascular surgeons in Anglo-American countries discovered speciality applications of ultrasound, while generalists in emergency medicine found cardiac, abdominal and pelvic applications and used them to guide invasive procedures. In the past ten years, the scope of clinician-performed ultrasonography has continued to expand both across and within specialities. Its bedside and point-of care applications have also expanded to the European and Asian countries, where ultrasound traditionally was a physician-performed imaging modality. Most recently, practitioners of critical care medicine, family medicine, anaesthesiology and pediatrics have adopted it, and it is increasingly used by non-physician

Emergency Point-of-Care Ultrasound, Second Edition. Edited by James A. Connolly, Anthony J. Dean, Beatrice Hoffmann and Robert D. Jarman.

Companion website: www.wiley.com/go/connolly/ultrasound

healthcare providers such as nurses (for venous access), paramedics (field triage, pneumothorax assessment, vascular access), and midwives (ante-natal testing). The current edition of this book includes several chapters describing new and evolving applications of bedside ultrasound.

The rapid proliferation of ultrasonography in medical practice has been driven by separate, but mutually reinforcing, historical trends. Technological advances have combined with improvements in the design and ergonomics to make ultrasound equipment more user-friendly, mobile, rapidly deployable and accurate. Ultrasound equipment has become increasingly robust and portable, with many machines capable of running for hours using battery power. At the same time, the decreasing costs have made it more widely available. Finally, the financial burden of hospital admissions has created powerful economic pressures to decrease admission times and maximise the outpatient management of many diseases. This has resulted in increasing numbers of critically ill patients both inside and outside the hospital needing emergency care for acute decompensation of their chronic conditions during night-time and weekend hours, when the manpower and technological resources of the hospital are minimal. At such times, an imaging modality that directly evaluates most of the common causes of critical illness and can be deployed by caregivers at the patient's bedside is of great value. Clinician-performed ultrasonography is that imaging modality, and much of this book is devoted to the use of ultrasound in critical and time-sensitive illnesses.

One of the cardinal features of sonology is 'syndromic' use in clinical settings that are no less serious or complex for being common. The first example of syndromic ultrasound was the FAST, with its concurrent evaluation of the heart (traditionally the purview of cardiologists) and abdomen (traditionally the territory of radiologists or internist- or surgeon-performed sonography in many European and Asian countries). Since that time, ultrasound algorithms have been developed and promulgated for the assessment of abdominal pain, unexplained hypotension, shortness of breath and cardiac arrest, to name a few. This book attempts to help clinicians familiarise themselves with this approach, with a number of chapters devoted to syndromic uses of ultrasound.

As a rule, technology-based medical advances in wealthy societies are of limited utility in resource-poor environments. Clinician-performed ultrasonography is a powerful exception to this rule, for the very reason that its use has been driven by the need to provide expedited care in resource-poor settings that exist even in the richest societies. The back of an ambulance at the scene of a motor vehicle crash in Bavaria, hospital wards at night in Paris, and emergency departments on week-ends and holidays in New York City, all have severely limited manpower and equipment resources. The pressures and stresses of practice in these settings are not unlike those in the developing world, as well as those in wilderness settings, space flight and military environments. This book seeks to be a source of information to any clinician anywhere who is attempting to improve patient care by the use of ultrasonography in a resource-limited setting.

Ultrasound has modified the clinical practice of many specialities. To the extent that it does so by means of the clinician's hands, eyes and brain in real time, it is an extension of the clinical evaluation. (This is not to say that ultrasound is an extension of the *physical examiantion*, any more than a plain film, computed tonography scan or blood test are extensions of the physical examination.) In contrast to the stethoscope – with which it is sometimes compared – ultrasound provides extraordinarily detailed anatomical, physiological and pathological information. Perhaps the greatest similarity between the stethoscope and the ultrasound machine is that the information obtained from both tools is *a function of the expertise residing between the operator's ears*. This should strike a particularly cautionary note to practitioners, since the diagnostic power of ultrasound comes with a commensurate potential for diagnostic error.

The skills of a sonologist can be roughly broken into three distinct types of knowledge. First, there are *cognitive* skills relating to the

patient's disease and the known (or unknown) limitations of ultrasound as a diagnostic test. Second, there are *visual pattern recognition* skills developed through repetitive exposure to ultrasound images of healthy and diseased conditions. Third, there is the *psychomotor* skillset needed to operate the machine, manipulate the transducer, and optimise images. These three distinct – but mutually reinforcing – skills constitute the abilities of the *sonologist*: a healthcare provider who has mastered the '*logos' of ultrasound*.

With this small book we hope to help not only those clinicians who have set themselves the goal of incorporating ultrasound into their clinical practice, but also those who have already embarked on that process and who wish to extend their knowledge. Using copious images and clear succinct text, this book strives to provide the basic cognitive and visual pattern recognition skills needed for basic sonology. The format is designed to fit into a lab-coat pocket, and it is hoped that it will find use as a reference in the clinical environment. Due to its widening utilisation in almost every field of medicine, ultrasonography is increasingly recognised as having a place in undergraduate medical training. We hope that this book will also be a useful introduction to clinical ultrasound for medical students. Clearly, the psychomotor skills of sonology cannot be obtained from a book. In the time-honored traditions of many hands-on fields of medicine, these can only be mastered by *practice*, *practice*, *practice*!

We are deeply indebted to the enormous efforts of the authors of the chapters in this volume, all of whom are acknowledged world leaders in this field. Editing their work has been a source of enlightenment and inspiration. We would also like to thank the pioneer sonologists who beat the path that we now follow when the destination was less clear, and the way less certain. Finally, thanks to our long-suffering families and friends whom we hope have understood our passion and motivation.

Part 1

Physics

1

How Does Ultrasound Work?

Heather Venables

Introduction

The aim of this chapter is to outline the basics of how ultrasound works. The construction of an image and some of the physical principles that govern the behaviour of sound in tissue will be introduced.

What is Ultrasound?

Sound is simply the transfer of mechanical energy from a vibrating source through a medium. *Ultra*sound is defined as sound of a frequency above the human audible range, that is, above 20 kHz.

Piezoelectric crystals within the face of the transducer have the property of contracting or expanding when a voltage is applied across them. A thin layer of a synthetic piezoelectric material can be constructed to vibrate at a resonant frequency within the required range. This acts as a source of ultrasound. A very short (approximately 1 μs) pulse is generated by the transducer and transmitted into the soft tissues. After generation of the 'pulse', the transducer receives no further electricity for a period of time (typically about 100–300 μs) and acts as a 'listening device' to detect returning echoes generated within the medium of the soft tissues.

As the ultrasound wave of a returning 'echo' hits the transducer surface, the piezoelectric crystals vibrate, causing them to generate an alternating electric current. This is transmitted back to the ultrasound machine through the wires attached to the transducer. The magnitude of the voltage of this current is related directly to the amount of energy carried by the returning echo, and will determine the brightness level displayed for this location on the monitor. The machine measures the time that elapses between the *pulse* and the *echo*, and by using the known velocity of sound in soft tissues (1540 m s^{-1}) the distance to the echoing object can be calculated. Many animals (e.g., bats and marine mammals) use the same principle for echo-location of objects in their environment. (It is worth noting that the construction of the transducer with its sensitive crystal elements does not respond favourably if it is dropped or if the wheels of the machine run over its wires.) Diagnostic ultrasound utilises the pulse-echo principle to construct a two-dimensional sectional image of anatomical structures (Figure 1.1).

Constructing the Image

Each pulse of sound transmitted into the patient generates a stream of echoes from multiple reflectors at various depths. As noted, the energy carried by each echo is converted into electrical energy by the piezoelectric crystals. In simple terms, these values are then stored

Emergency Point-of-Care Ultrasound, Second Edition. Edited by James A. Connolly, Anthony J. Dean, Beatrice Hoffmann and Robert D. Jarman.

Companion website: www.wiley.com/go/connolly/ultrasound

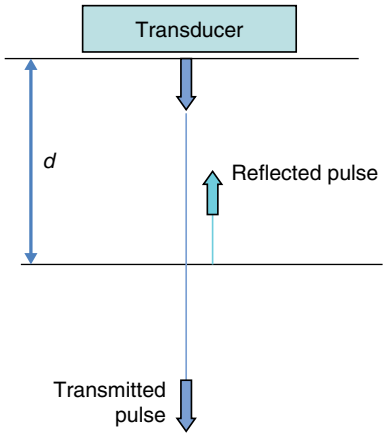

Figure 1.1 The time taken (*t*) for the echo to return to the transducer, and the speed of sound in soft tissue (*v*), can be used to calculate the depth (*d*) of the reflecting interface, where $d = vt/2$.

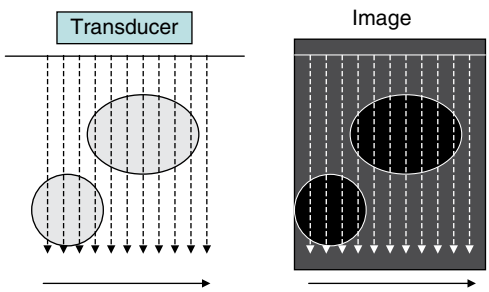

Figure 1.2 Pulses of sound are fired in sequence from multiple adjacent crystals across the face of the transducer. These are used to produce contiguous scan lines from which a single *brightness mode* (B-mode) 'frame' of information can be produced that represents a two-dimensional anatomical cross-section.

within a computer memory as a single 'scan line' of information, and used to determine the brightness levels allocated to points in a vertical line on the image to represent corresponding depths in the patient. By firing pulses of sound in sequence from multiple adjacent crystals across the face of the transducer, numerous contiguous scan lines can be generated and a single 'frame' of information is produced to represent a two-dimensional anatomical cross-section (Figure 1.2). This type of ultrasound imaging is referred to as 'brightness mode' ('B-mode' or 'gray-scale') because the strength of the echoes are represented by the brightness of the ultrasound image at that location.

If performed fast enough, the rapid update of frames can create a 'real-time' dynamic image of the scanning plane. Frame rate is limited by several factors. The ultrasound machine 'waits' for the echoes to return from the maximum depth of interest along each scan line before the next pulse is sent out. Thus, the frame rate depends on the *depth* of interest and the total number of scan lines of the image (*field of view*). Adjusting the depth and field of view allows the operator of the ultrasound machine to optimise the frame rate and the resolution of the image. In general, the image should be adjusted to the minimum depth that will include the entire object of interest.

Making Sense of Ultrasound Images

During an ultrasound examination, most of the diagnostic conclusions about normal and abnormal appearances are based on pattern recognition. This includes a number of key observations:

- the spatial definition of tissue boundaries;
- relative tissue reflectivity;
- echo-texture; and
- the effect of tissue on the transmission of sound.

These appearances are determined by the physical properties of the ultrasound waves and their interactions with tissues. Some of these key interactions are outlined below.

What Happens to a Pulse of Sound as it Travels Through a Patient?

Reflection, scattering and refraction are common to both sound and light waves. An appreciation of this helps us make sense of why structures appear as they do in an ultrasound image.

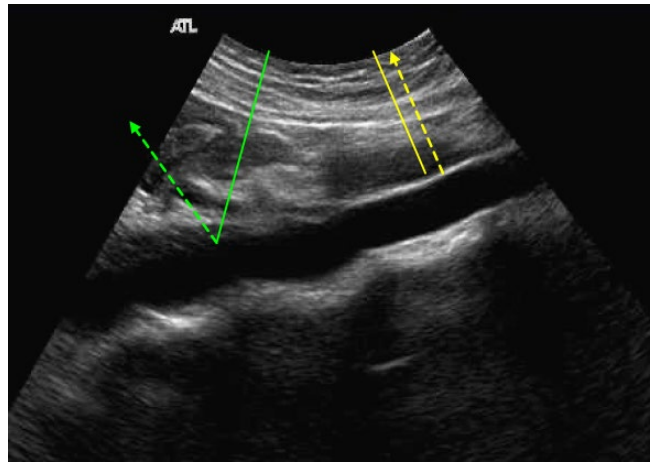

Figure 1.3 The divergent ultrasound beams generated by this curved-array probe demonstrate the effect of angle of insonation on the visualisation of vessel walls. A pulse of sound hitting the wall at 90° (solid yellow arrow) will be reflected back to the transducer (dashed yellow arrow). A pulse hitting the wall at any angle other than 90° will be reflected at an equal and opposite angle (green pathway), with the result that the echo may not be detected by the transducer. This is why in the image, the aortic wall appears well defined in the region of the yellow arrows and cannot be clearly discerned in the region of the green pathway.

Reflection

Reflection of the ultrasound pulse occurs at interfaces between two media that have differences in acoustic *impedance,* which is a medium's physical properties as a transmitter of sound. Impedance is determined primarily by the medium's density and elasticity). At such boundaries, a proportion of the sound energy will be reflected, while the remaining sound energy is transmitted beyond the boundary. If the impedance difference at a boundary is high enough, for example at a soft tissue/air interface or at a soft tissue/solid interface, total reflection occurs and no sound energy is transmitted to deeper structures. Gas-filled structures and bone are therefore a significant challenge in ultrasound imaging.

Specular Reflection

If a reflective boundary is smooth and large, specular reflection occurs. This is similar to when light is reflected from a smooth surface. Typical specular reflectors include the diaphragm, renal capsule and vessel walls.

Where the sound pulse hits a boundary (especially if it is specular) at an angle other than 90°, then by the basic 'law of reflection' it will not be reflected back towards the transducer, which means that the structure will not be detected by the ultrasound machine. Conversely, boundaries will be detected most clearly if they are at 90° to the direction of travel of the ultrasound wave. This phenomenon is demonstrated in Figure 1.3.

Diffuse Reflection

Diffuse reflection occurs where irregularities in the tissue boundary exist that are small compared to the wavelength of the sound. (At 5 MHz this is approximately 0.3 mm or less.) These irregularities cause the sound energy to be reflected in multiple directions – an optical analogy would be to consider the difference between gloss and matt paint. In practice, most soft-tissue boundaries are irregular and produce diffuse reflection to some degree.

Scattering and Echo Texture

Acoustic impedance changes occur at large-scale boundaries, but are also present throughout soft-tissue structures. Small-scale localised changes in acoustic properties act as tiny reflecting targets that *scatter* the sound in many directions. This is what produces the characteristic *echo texture* (graininess) that is associated with solid structures on ultrasound, and the relative *echogenicity* (brightness) of adjacent organs (Figure 1.4).

Attenuation

As sound travels through tissues, it loses energy. A number of interactions contribute to this

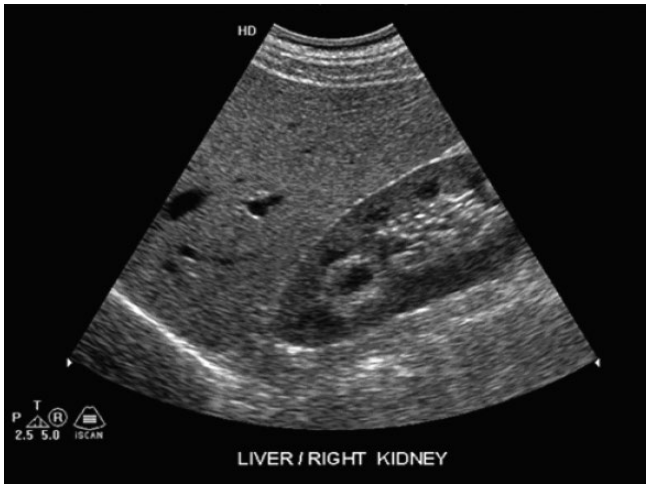

Figure 1.4 Small-scale localised changes in the acoustic properties of many tissues act as tiny reflecting targets that *scatter* the sound in many directions. This produces the characteristic *echo texture* (graininess) associated with solid organs and their relative *echogenicity* (brightness) compared to adjacent organs, as seen in this view of the right lobe of the liver and right kidney.

process of *attenuation*, including reflection, scattering and absorption. This results in the pulse becoming progressively lower in intensity (and therefore producing weaker echoes) the deeper it travels into the patient.

In practice, Time Gain Compensation (TGC: increasing amplification or 'gain' of the electric signals generated by returning echoes from increasingly deep structures) is used to compensate for this reduction in signal strength with depth. Scattering contributes to beam attenuation and increases significantly with increasing frequency of the ultrasound wave. This results in increased attenuation, and thus a reduced *penetration* of the sound beam to deeper structures, when higher transmit frequencies are used.

Absorption

Absorption is the process by which the mechanical energy carried by the pulse is converted into heat within the tissues. Absorption is the most significant form of attenuation in soft tissue. As sound travels though the patient, there is the potential for tissue damage, either through heating or mechanical effects (such as shearing or cavitation). In practice, ultrasound machines are designed to continually minimise the power of the ultrasound waves according to the principle of ALARA ('as low as reasonably attainable'). While deleterious bio-effects caused by diagnostic B-mode ultrasound have never been conclusively demonstrated, in case such bio-effects actually exist (albeit at levels below current powers of detection), ultrasound should be used clinically in situations where the information it provides is of potential net benefit, especially when used in the evaluation of pregnancy.

Why is Frequency Important?

Both, absorption and scattering result in reduced penetration to deeper tissues with higher frequencies. Unfortunately, higher frequencies result in a higher image resolution, and therefore there must be a trade-off between image quality and penetration. In practice, the highest frequency should be used that allows adequate penetration to the depth of interest.

Summary

The power of ultrasound in a clinician's hands will be significantly affected by his or her ability to operate the machine in such a way that it can obtain the highest-quality images. This, in turn, entails an understanding of the physics of ultrasound. This brief overview should serve as an introduction, but further study is called for if the reader wishes to use ultrasound in anything more than a rudimentary fashion, and especially

for the effective use of any of the Doppler applications described in this book. The references listed below provide useful sources of more detailed information.

Further Reading

Gibbs, V., Cole, D., Sassano, A. (2009) *Ultrasound Physics and Technology – How, Why and When?* Churchill Livingstone.

Guidelines for the Safe Use of Diagnostic Ultrasound Equipment (2009) British Medical Ultrasound Society. Available at: http://www.bmus.org/policies-guides/pg-safetystatements.asp

Hoskins, P.R., Thrush, A., Martin, K., Whittingham, T.A. (2010) *Diagnostic Ultrasound Physics and Equipment.* Cambridge Medicine.

Part 2

Ultrasound by Region

Thorax

2

Evaluation of the Chest Wall, Pleura and Lung

Gebhard Mathis and Anthony J. Dean

Introduction

Ultrasound waves are reflected by the bony thorax and scattered by the ventilated lung. For this reason, the utility of sonography in the evaluation of the lung and pleura was until recently overlooked. The ways in which sonography of extra-mediastinal structures can be utilised in the management of the critically ill are outlined in this chapter. Procedural uses of ultrasound in the thorax are discussed elsewhere in this book.

Technique

Equipment

The chest wall and pleura are best imaged with a high-frequency (5–10 MHz) linear array transducer. For evaluation of B-lines and the lung, a curved-array 3.5–5 MHz transducer is preferred. This combination of probes has the advantage of being useful for many other applications, such as abdominal, vascular and small-parts imaging. Skilful manipulation of the transducer, combined with an understanding of respiratory dynamics, will provide views of most parts of the pleura and underlying lung. If only a single transducer is available, a 2–5 MHz microconvex transducer is adequate for the vast majority of situations.

Examination Technique

The examination technique will be determined by a variety of factors, including the diagnostic questions at issue and the patient's clinical condition and habitus. The supine position is used to scan the anterior and lateral chest, while posterior areas are ideally scanned with the patient sitting. If this is not possible, patients are rolled into a decubitus position. Full abduction of the shoulders with the arms crossed behind the head may widen the intercostal spaces, affording better views. The region underlying the shoulder blade can be imaged if the patient puts his/her hand on the contralateral shoulder. If the patient can identify a specific area of pain, this region should be examined first. The scanning depth is usually set at about 4–8 cm for examination of the chest wall and pleura. For the analysis of B-lines and deeper lung structures, the depth is usually set at ≥15 cm.

Scanning of the lung should be systematic and methodical. Each intercostal space should be interrogated from dorsal to ventral with the transducer in both longitudinal and transverse planes with respect to the axis of the body. By using anterior and posterior axillary-lines and a horizontal line superior to the level of the nipple, each hemithorax can be divided into six regions. The presence of pleural sliding should be confirmed in all lung fields. Lung adjacent to the right and left diaphragms can be examined using liver and spleen windows, respectively.

Emergency Point-of-Care Ultrasound, Second Edition. Edited by James A. Connolly, Anthony J. Dean, Beatrice Hoffmann and Robert D. Jarman.

Companion website: www.wiley.com/go/connolly/ultrasound

The axillae should be examined with the patient in the supine position, with the arms fully abducted. The supraclavicular fossa gives views of the brachial plexus, the subclavian vessels and the lung apex. Suprasternal or parasternal windows may afford views of the anterior upper mediastinum.

Normal Sonographic Findings

The superficial surface of the adult ribs gives rise to an intense echo with dense underlying acoustic shadow. Costochondral regions have a hypoechoic oval morphology with adequate through-transmission of ultrasound to underlying structures (Figure 2.1). The normal pleura is 0.2–0.4 mm thick, and hence is at the resolution limits of ultrasound, although the parietal and visceral layers are sometimes distinguishable. The visceral pleura may appear thicker due to complete reflection of the incident beam by the underlying air spaces. Between the two pleural layers, physiological amounts of pleural fluid may appear as an echo-free line. In some patients a hypoechoic layer of extrapleural fat may also be seen (Figure 2.2).

Many horizontal lines appear in the ultrasound image of the lung. The first and most important to be identified is the pleural line, which is seen immediately beneath the ribs. With respiration, the visceral pleura moves with respect to the parietal pleura (*pleural sliding*). In patients with decreased respiratory effort (e.g., due to pain after trauma), subtle motion of the pleura can often be more clearly seen by decreasing the gain, and ensuring that the angle of insonation is perpendicular to the pleura. In the healthy state, occasional B-lines (laser-like vertical reverberation artefacts that reach the bottom of the screen set to a depth of 15 cm; see Video 2.5) and z-lines (laser-like vertical reverberation artefacts that only reach a few centimetres of depth; see Figure 2.7a and Video 2.1) may be seen arising from the visceral pleural line. Widely spaced reverberation artefacts caused by the skin surface and the pleural line ('A'-lines) appear as widely spaced lines

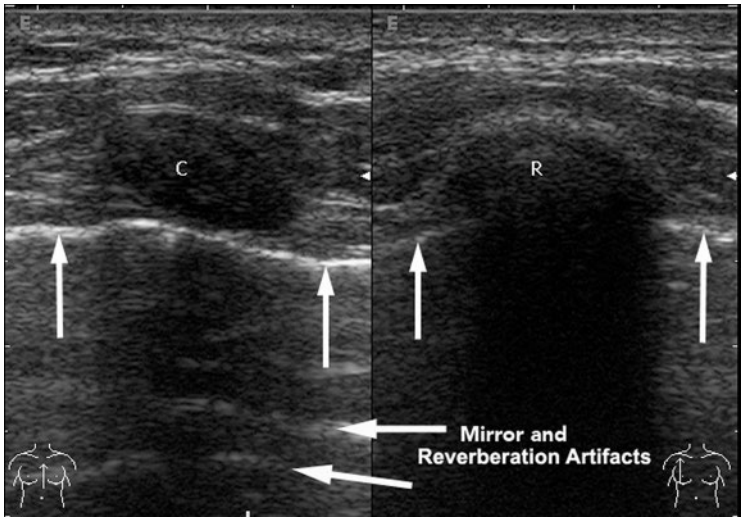

Figure 2.1 Chest wall. Left: The costochondral cartilage (C) allows through-transmission of ultrasound waves so that the underlying pleural line (vertical arrows, both images) can be seen. Right: Ossified rib causes almost complete reflection of sound waves with an underlying sonographic shadow. In cases where it is difficult to identify the pleural line with certainty, its location should be identified immediately underlying the rib and/or cartilage. Horizontal mirror and reverberation artefacts caused by the skin surface and underlying tissue planes are also seen.

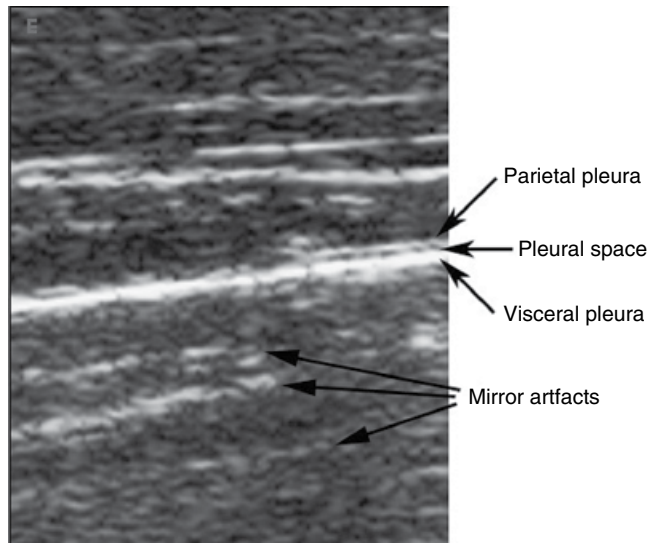

Figure 2.2 Both layers of pleura are echogenic. Usually, the two layers cannot be differentiated by ultrasound unless (as in this case) there is a small layer of fluid between them. This amount of fluid may be physiological (see also Figure 2.19). Horizontal mirror artefacts caused by the fascial layers of the intercostal muscles are seen.

projected into the lung (Figures 2.7b and 2.8; see Videos 2.3 and 2.4). Pleural sliding and 'lung pulse' (cardiac motion transmitted to the lung) can also be demonstrated and recorded with (Video 2.2) or without (Video 2.4) colour Doppler, as well as by M-mode (Figure 2.7c and d). Both of these findings exclude the presence of pneumothorax (at the location of the ultrasound probe; see below).

Chest Wall Lesions

Soft-Tissue Lesions

Suspicious or unclear findings during a physical examination of the chest wall should be examined using ultrasound. In trauma patients, haematomas may be identified as variably hypoechoic structures with blurred internal echoes. The echogenicity of haematomata depends on the erythrocyte content and the stage of organisation. Lymph nodes (usually seen as well-corticated hypoechoic structures with a hyperechoic medulla) and lipomata (usually seen as capsulated structures with fine linear echodensities running parallel with the skin surface) are also visualised using ultrasound.

Rib and Sternum Fractures

Sonographic signs of rib fractures include osseous discontinuity, step-off, adjacent haematomata, pulmonary contusions (discussed below) and pleural effusions (Figure 2.3). Small dislocations and fractures may be identified by a reverberation artefact.

Pleural Diseases

Pleural Effusion

Whilst physiological amounts of pleural fluid (3–5 ml) are detectable with ultrasound, at least 150 ml of effusion is needed for detection by upright chest radiography. Pleural effusions without cellular or proteinaceous aggregates are echo-free. Non-loculated pleural effusions are best detected in both supine and sitting patients in the posterior axillary line above the diaphragm. The morphology of the effusion shows respiratory variation, allowing differentiation from pleural scarring or thickening. Colour Doppler (scale set to detect very low velocity flow) may also be used to distinguish these by demonstrating motion of the liquid. Sonography

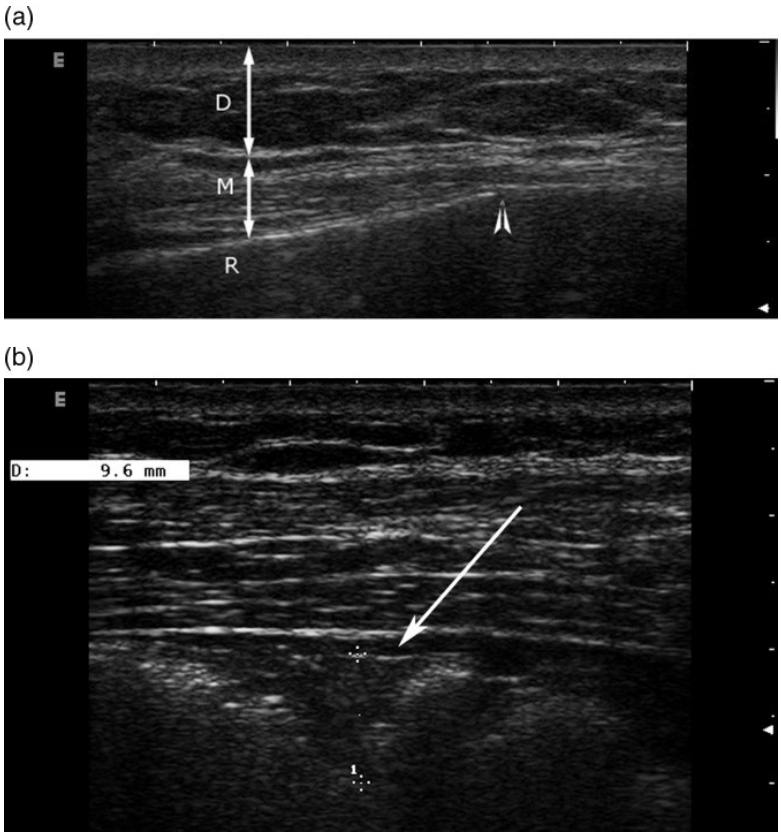

Figure 2.3 (a) A longitudinal image (with respect to the rib) of a subtle rib fracture is seen. Note the angulation as well as the cortical disruption (D = dermal layer, mostly comprised of subcutaneous adipose; M = skeletal muscle (note the striations); R = rib). Due to rib shadowing, the underlying pleural line cannot be seen. (b) An image obtained in the adjacent rib space, parallel to the image in panel (a), providing information about the underlying lung and pleural. A small triangular lung contusion is seen (between the callipers), and a very small associated pleural effusion between the two pleural layers (arrow).

cannot exclude effusions loculated in the interlobar fissures if they are surrounded by well-aerated lung. Lung ultrasound is more accurate than chest radiography in distinguishing between effusion and consolidation, allowing for its use in elucidating opacities of uncertain aetiology identified by chest radiography.

The shape of pleural effusions is highly variable, and an exact measurement of volume is therefore not possible. However, an estimation of volume may be useful when following patients with chronic effusions, and in determining the risk-benefit ratio in performing a thoracentesis in high-risk patients.

In the supine position, the pleural fluid volume is estimated by the formula:

$$Volume(\text{ml}) = 20 \times (\text{maximal thickness in mm in the posterior axillary line.})$$

In sitting patients:

$$Volume(\text{ml}) = \left[\begin{array}{l} (\text{basal lung} - \text{diaphragm} \\ \text{distance incm}) + \\ (\text{cephalocaudal extent of} \\ \text{the effusion in cm}) \end{array} \right] \times 70.$$

The latter formula is shown in Figure 2.4 (it should be noted that small effusions may be overestimated with this formula).

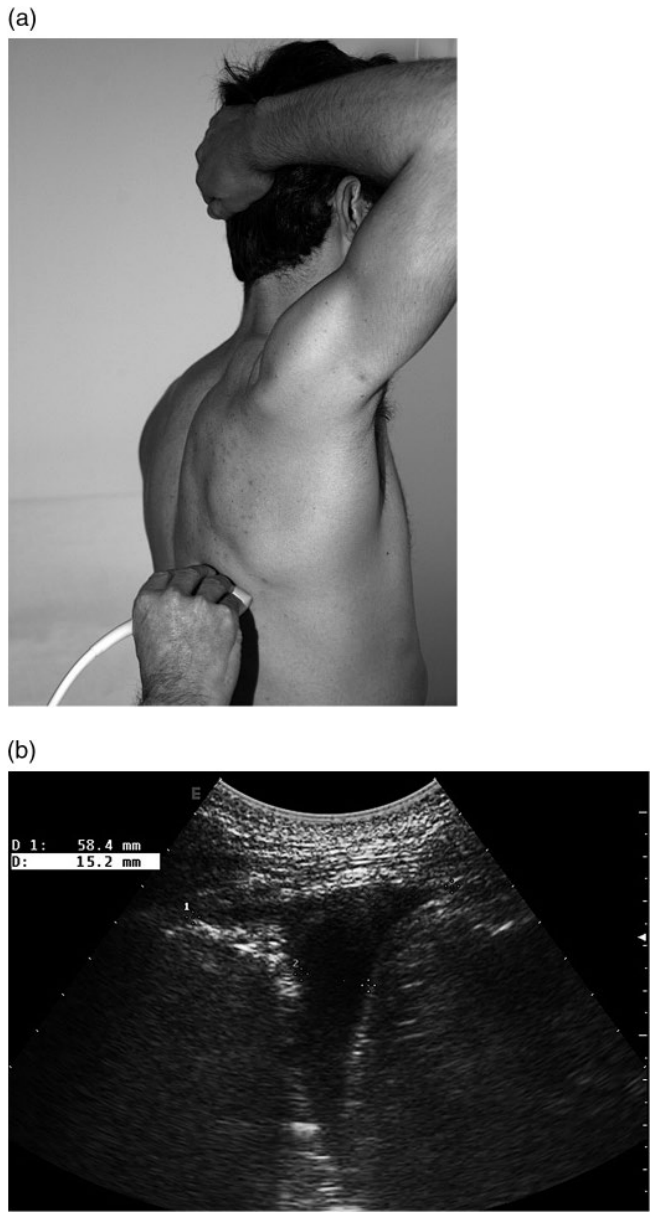

Figure 2.4 (a) Volume estimation of an effusion may be obtained with the patient in the sitting or standing position, by scanning between the scapular and the posterior axillary line. The transducer is usually held in a longitudinal plane (here, the transducer is parallel to the ribs). (b) The volume of the effusion would be estimated as (6 cm + 1.5 cm) × 70 = approximately 500 ml (see text for details).

Ultrasound may also suggest the aetiology of a pleural effusion with important diagnostic and therapeutic implications. Whilst all transudates are echo-free, most exudates are either homogeneously or heterogeneously echogenic, with or without septations, although some may be anechoic (Figure 2.5a and b). Pleural effusion associated with a smoothly thickened pleura may suggest empyema (especially if associated with underlying lung consolidation) (Figure 2.6). Nodules on the diaphragm suggest malignancy.

Ultrasound is an ideal guide for thoracentesis, increasing first-time success rates and reducing complications. (Details of the procedure are provided elsewhere in this book.)

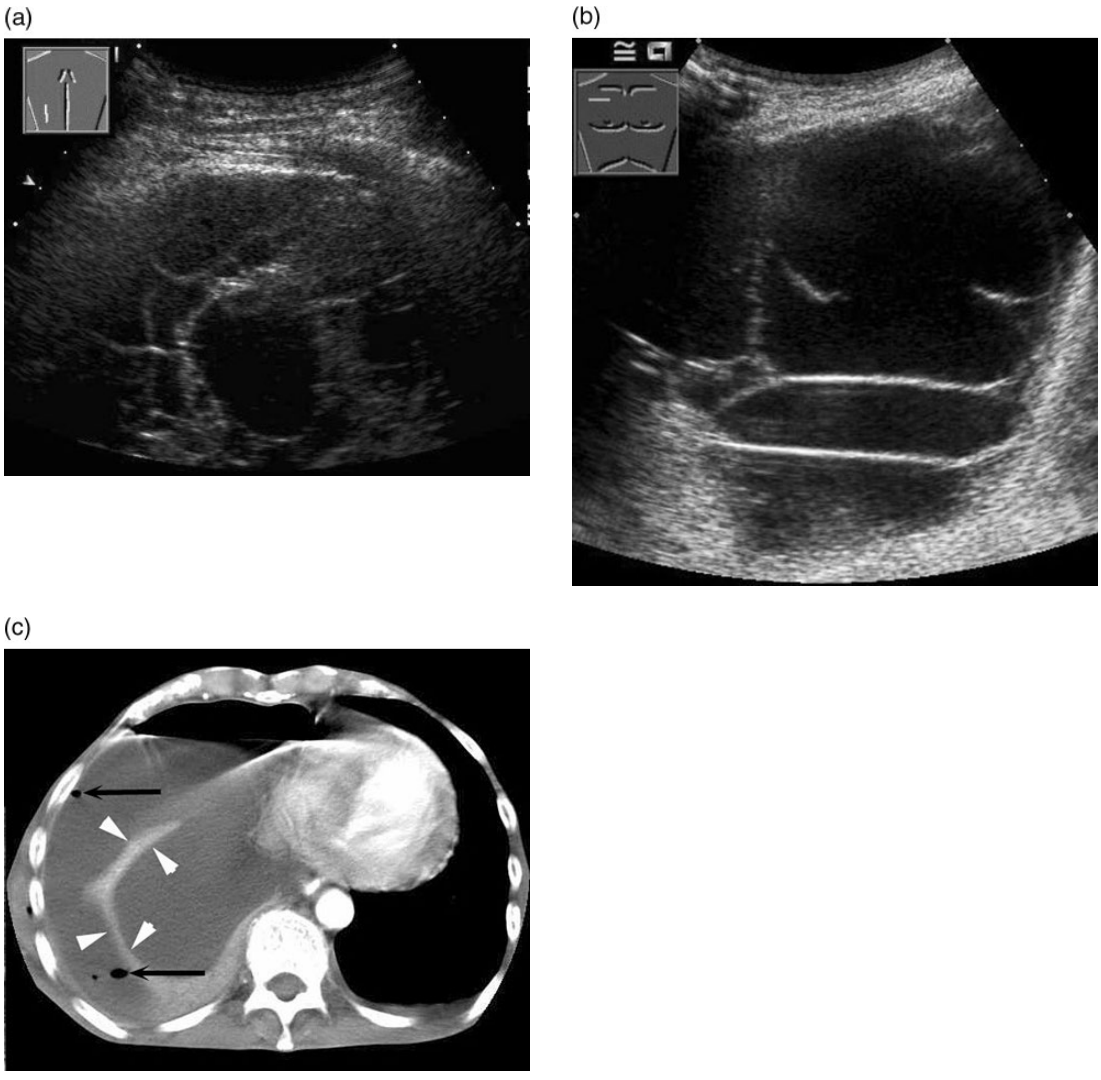

Figure 2.5 (a,b) Two complex septated effusions. The CT from panel (b) is shown in panel (c) with atelectatic lung (white arrowheads) and pockets of gas (black arrows) that suggest the presence of septations because they are not floating. As can be seen, ultrasound identifies septations with greater clarity than CT, and real-time ultrasound allows for drainage with directed access to multiple cavities.

Pneumothorax

With pneumothorax, air between the parietal pleura and lung prevents the ultrasound waves from reaching the visceral pleura, with a resultant loss of pleural sliding (as discussed above). There are several sonographic signs of pneumothorax, most of which require real-time analysis of the ultrasound, although there are subtle findings on still images that suggest pneumothorax (see Figure 2.7). The real-time findings include:

1) Absence of lung sliding (Video 2.3). It should be noted that B-lines and z-lines *by definition* arise from the visceral pleura, so that their presence excludes pneumothorax in that location.

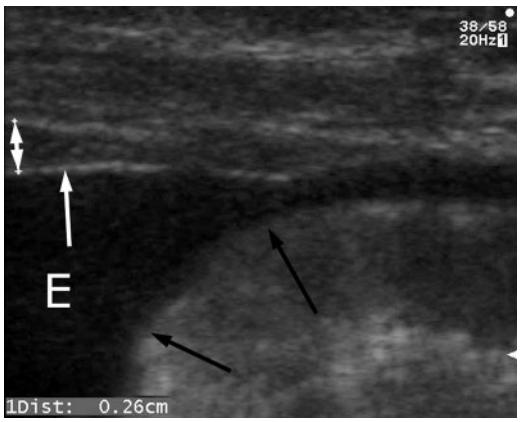

Figure 2.6 Empyema (E), overlying the diaphragm (black arrows). When associated with an effusion, the thickened parietal pleura (white double-headed arrow) suggests empyema. The inner serosal surface of the parietal pleura is indicated by the single white arrow.

2) Absence of lung pulse (Video 2.3, compare with normal in Video 2.1). An absence of lung sliding *and* lung pulse occurs whenever there is pneumothorax beneath the transducer. Occasionally, with normal lung sliding the lung pulse cannot be seen, so the latter in isolation should not be used to rule in pneumothorax.
3) In incomplete pneumothoraces, the transition point between collapsed lung (no lung sliding seen) and expanded lung (lung sliding can be seen) can be identified moving back and forth under the transducer with respiration (Figure 2.8; Video 2.4). This is referred to as the *lung point*, the location of which allows an estimation of the size of the pneumothorax.

In supine patients, the least gravitationally dependent areas are evaluated first (i.e., the anterior chest). The transducer is usually placed inferior to the clavicles in a longitudinal plane, and each rib space is systematically interrogated to the diaphragm in the midclavicular line. On the left side of the chest, if the heart is encountered before the diaphragm, the transducer should be moved laterally to complete the evaluation. If a pneumothorax is found, the lung point may be sought more laterally. If no pneumothorax is identified anteriorly and a pneumothorax is still strongly suspected, lateral scanning may identify a loculated pneumothorax. Pneumothorax can be documented by recording a video clip demonstrating the absence of lung sliding, or by an M-mode image (as described in Figure 2.7).

Any process that causes a loss of pleural sliding and/or pleural adhesions can lead to ultrasound findings of pneumothorax. Examples include inflammatory lung conditions such as pneumonia or pulmonary contusion, and pleural scarring from prior pleural injury or inflammation. Thus, if an absence of lung sliding is identified it is important to confirm that this is due to pneumothorax by ensuring that there are also no B-lines, no lung pulse, and no hepatisation of the underlying lung parenchyma. Bullous emphysema may also give a false appearance of pneumothorax due to effacement of the visceral pleura and underlying lung, often combined with pleural adhesions. Particular caution should be taken in patients with chronic obstructive pulmonary disease (COPD), since they are at high risk of spontaneous pneumothorax but also have a low tolerance of iatrogenic pneumothorax from an unnecessary tube thoracostomy. Despite these potential pitfalls, ultrasound is superior to supine chest radiography in the diagnosis of pneumothorax.

Pleuritis

The sharp localised respirophasic chest pain of pleuritis may be caused by any inflammatory process adjacent to the pleura, including lung infarct, contusion, pulmonary embolus and pneumonia. (The sonographic findings of these are discussed later in this chapter.) Non-specific pleuritis, which is often caused by viral infections, is difficult to diagnose by either clinical examination or radiography. However, in most patients (up to 90%), ultrasound of the visceral pleura displays disruption of the usually smooth pleural line and small subpleural lung consolidations, with or without subtle effusions. Absent or diminished pleural sliding and a focal interstitial syndrome with localised B-lines are further evidence of pleuritis (Figure 2.9).

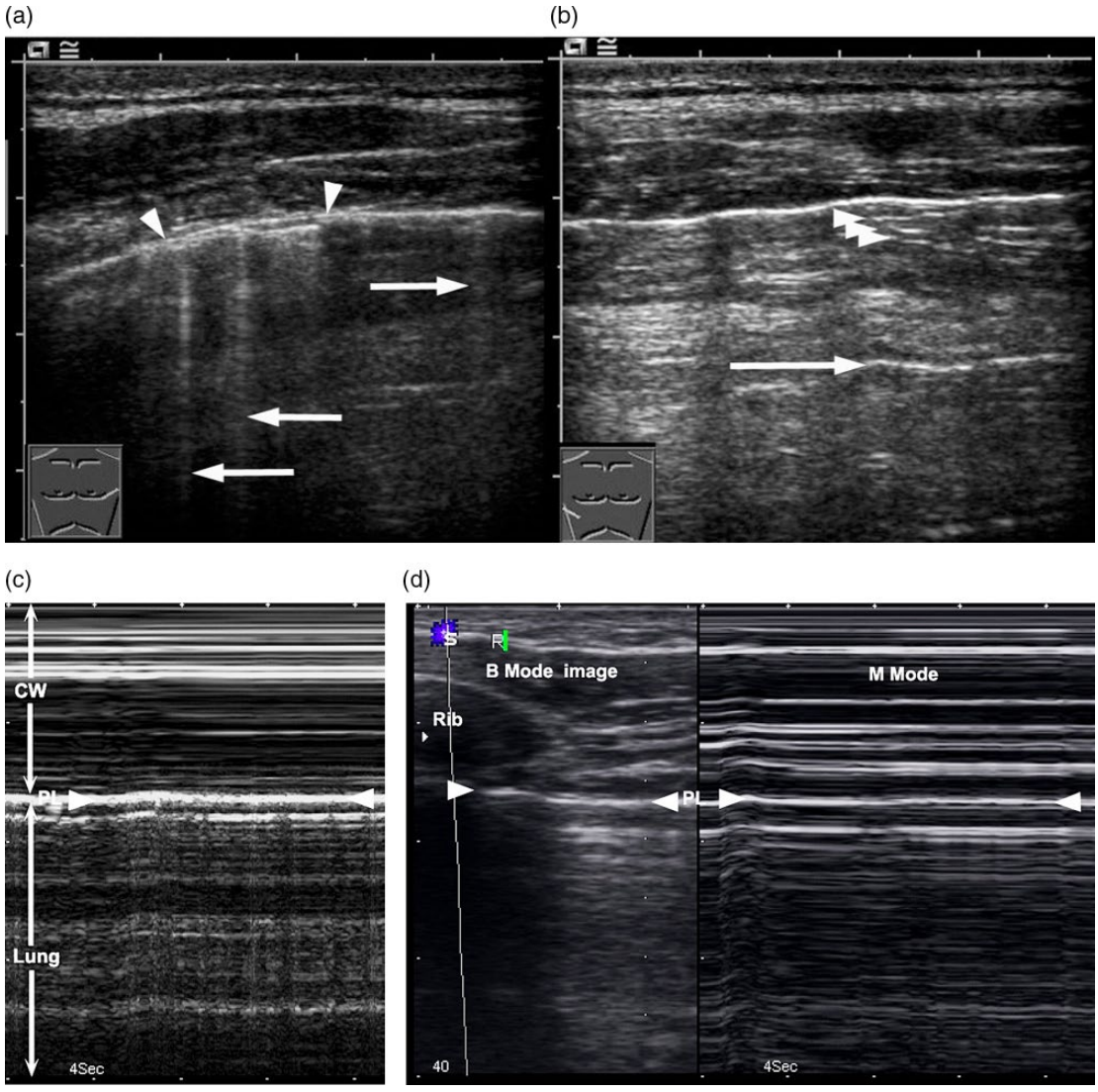

Figure 2.7 (a,b) The images demonstrate the difficulty in distinguishing pneumothorax and expanded lung on still images without using M-mode. (a) Normally expanded lung shows small, subtle pleural-based reverberation artefacts (also called 'z-lines', white arrows) and an area with a loculated pleural effusion that separates the parietal and visceral pleurae (between the arrow-heads). (b) Pneumothorax is suggested by the presence of stronger horizontal reverberation artefact (also known as an 'A-line', white arrow, see also Video 2.4), and by mirror artefacts (arrowheads) as well as absence of the 'Z-lines' seen in panel (a); however, all these findings may occur in normally expanded lung. (c) The M-mode findings of normal expanded lung are shown by a granular appearance of the pleural line itself (PL between arrowheads), and the underlying lung field compared to the straight lines of the chest wall (CW). This appearance is sometimes described as 'waves (straight lines of CW) on the shore (granular appearance of lung)'. (d) Pneumothorax is indicated by the linear horizontal echoes (not granular) below the pleural line, indicating the absence of lung motion. This finding is sometimes called the 'barcode' or 'stratosphere' sign.

Interstitial Syndrome

Increased extravascular (i.e., interstitial) lung water can be caused by a variety of diseases including heart failure, acute respiratory distress syndrome (ARDS), pulmonary fibrosis, inhalation injury and interstitial lung infections, all of which generate a similar sonographic pattern easily identifiable by bedside ultrasonography. In most cases, ultrasound cannot determine the specific aetiology, although it is often suggested by the clinical context. In other situations, ultrasonography can rapidly distinguish among conditions with similar presentations but with mutually exclusive treatment; for example, shortness of breath due to pulmonary oedema versus exacerbation of COPD.

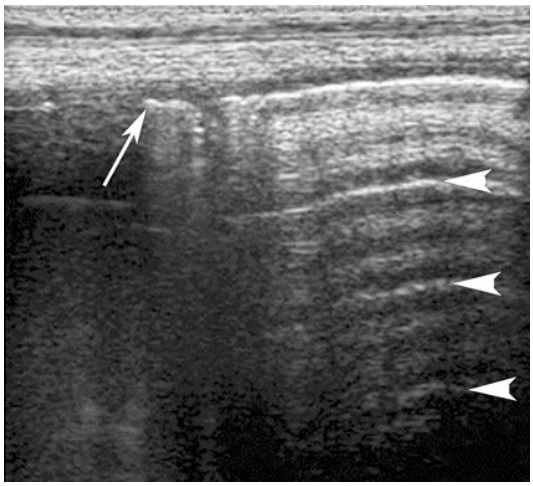

Figure 2.8 Pneumothorax. The lung point (arrow) is the transition point between expanded (to left of arrow) and collapsed (to right of arrow) lung. It is best appreciated in real time. To the left of the arrow lung sliding would be seen, to the right there would be absence of sliding. The lung point moves back and forth across the image with respiration (see Video 2.4). In this case, A-lines are best seen in the area of collapsed lung, although they are also usually seen in normal expanded lung.

B-lines are discrete reverberation artefacts arising from the pleural line that spread to the bottom of the screen without fading, and move synchronously with lung sliding (Figure 2.10; see Videos 2.5 and 2.6). They are the hallmark sonographic sign of the interstitial syndrome. Ideally, eight zones of the thorax are interrogated (Figure 2.11), but a quick anterior scan of one region on each side of the chest may often be sufficient. A positive region is defined by the presence of a rib space with three or more B-lines. With increasing severity, the extravascular lung water gives rise to confluent B-lines. Under such circumstances, some authorities recommend estimating the percentage of the rib space filled by the confluent B-lines and multiplying that by 10 to estimate the 'number' of B-lines at that location. Lung ultrasound is superior to chest radiography in the identification and exclusion of significant interstitial syndrome. Focal regions of

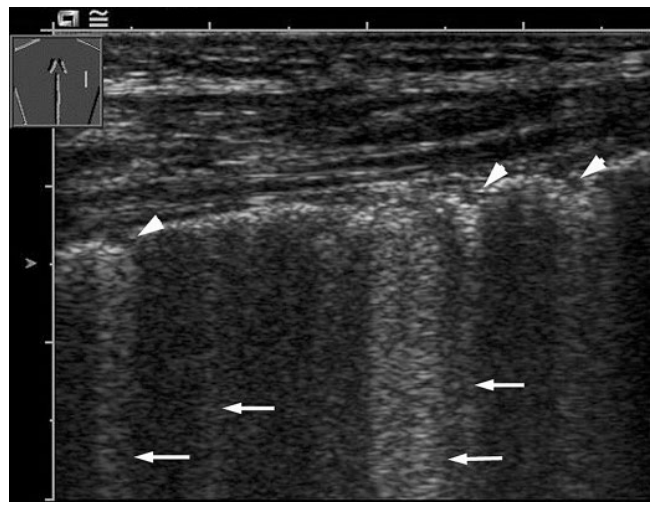

Figure 2.9 Pleuritis may be due to any inflammatory process adjacent to the pleura (see text). In the case of non-specific pleurisy, the normally smooth visceral pleura is irregular with small subpleural consolidations (arrowheads) or nodules and a focal B-line pattern (arrows). Ultrasound examination should be done at the location of the patient's symptoms.

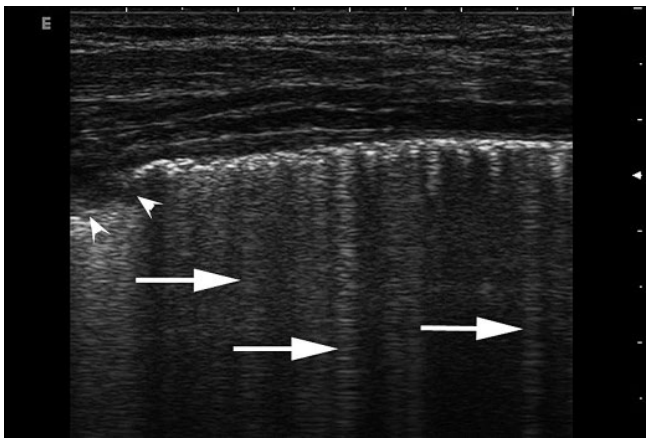

Figure 2.10 Multiple B-lines in diffuse interstitial syndrome demonstrated by a linear array transducer (some indicated by arrows). B-lines are vertical reverberation artefacts that arise from the pleural line and extend to the bottom of the screen without fading, moving synchronously with lung sliding. Many authorities prefer to use a curved-array probe set to a depth of about 15 cm to be certain that the reverberation artefacts extend to an adequate depth. On the left there is a small subpleural consolidation (arrowheads).

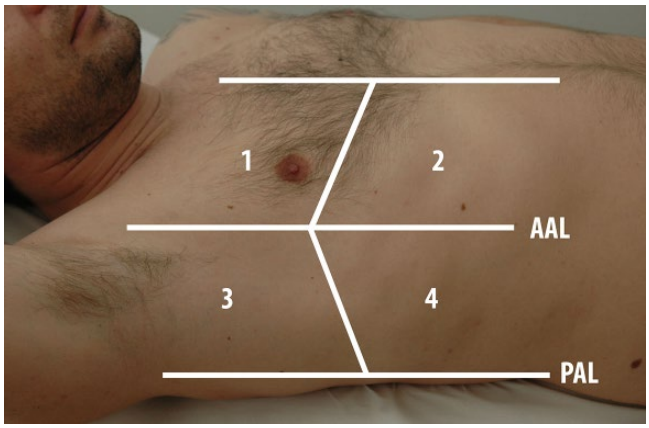

Figure 2.11 One widely used system for evaluating the chest for interstitial syndrome in which a rib space is sampled from each of eight regions on the anterior and lateral thorax. This image shows the four regions on the right side.

interstitial syndrome may be seen in the presence of pleuritis, pneumonia, pulmonary infarction and lung contusion.

In addition to the differentiation of cardiac and pulmonary causes of acute respiratory failure, B-lines have been shown to be useful in the risk stratification of patients with chest pain and dyspnoea once pulmonary fibrosis has been excluded, and to monitor response to treatment of volume overload in both cardiac and renal failure.

Lung Consolidations

In healthy persons, ultrasound imaging of the lung parenchyma is not possible because the ultrasound waves are completely reflected, scattered, and absorbed by the air-filled lung underlying the visceral pleura. Pulmonary processes that cause consolidation allow the transmission of ultrasound waves, but they can only be visualised sonographically when they abut the pleura, have an overlying sonographic window, and have no overlying subcutaneous emphysema or pneumothorax. Consolidations that are completely surrounded by normal air-filled lung are therefore sonographically occult.

Pneumonia

In the early stages of pneumonia, the consolidated lung has a sonographic appearance similar to that of liver (*hepatisation*) except that it contains arborising air bronchograms and numerous echogenic foci that measure a few

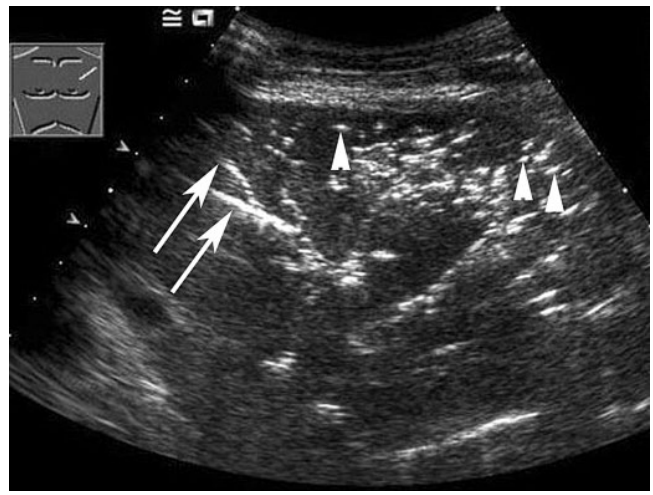

Figure 2.12 A large pneumonia seen as consolidated lung with liver-like echotexture and multiple highly echoic air bronchograms (arrows) and pockets of trapped air (vertical arrowheads) is seen. Unless seen in longitudinal section, air bronchograms (tubular structures) and air pockets (discrete) can only be distinguished with real-time scanning (see Video 2.7).

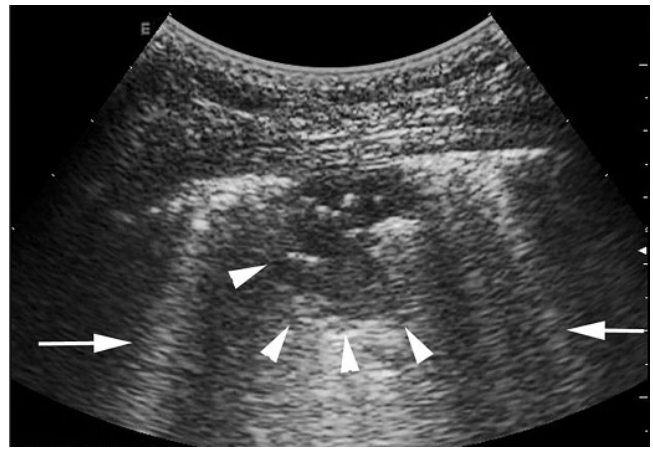

Figure 2.13 In this small pneumonia caused by the H_1-N_1 virus, the consolidation has a typically irregular 'shredded' contour (arrowheads). The adjacent pleura shows focal areas of B-lines (arrows). Other viral pneumonias may show less aeration.

millimetres in diameter and result from pockets of trapped air within the consolidation. Viral or fungal pneumonias are often more poorly ventilated and therefore contain fewer air bronchograms. In contrast to those seen in obstructive atelectasis, the air bronchograms associated with pneumonia are dynamic (Figure 2.12; Video 2.7). The transition zone between pneumonic consolidations and unaffected lung has an irregular 'shredded' appearance unless the consolidation abuts a major fissure. (Figure 2.13). Fluid bronchograms may also be present, seen as anechoic/hypoechoic branched tubular structures (Video 2.7). A persistent fluid bronchogram prompts suspicion of an obstructive cause for the pneumonia and may call for bronchoscopy. The characteristic colour-flow Doppler findings of pneumonia include a profuse vascular flow with normally arborising vessels (Figure 2.14 and video 2.8).

With progression, bacterial pneumonias may coalesce and form abscesses that appear as round or oval hypoechoic foci without inner vascular flow on colour Doppler. The smooth echo-dense margin of a capsule may be seen. If a patient does not respond to antibiotics, a microbiologic specimen may be obtained by ultrasound-guided needle aspiration.

As the pneumonia resolves, improving aeration of lung is sonographically evidenced by diminishing hepatisation, which is replaced by areas of reflection and reverberation artefacts

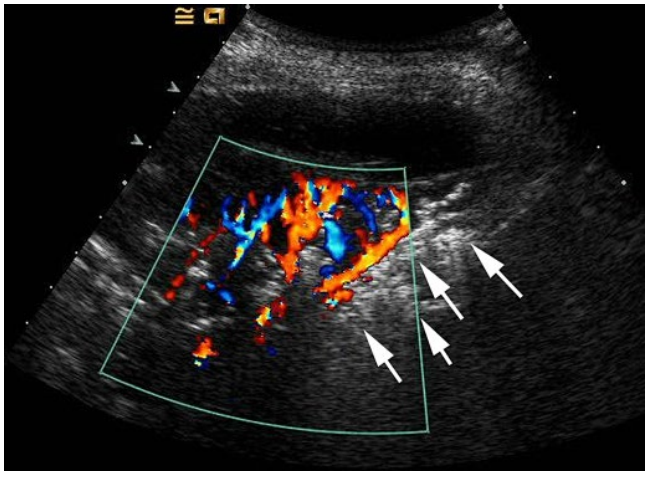

Figure 2.14 The pneumonia seen in Figure 2.12 shows a profuse pattern of vascularisation on colour Doppler sonography. On gray-scale the 'shredded' transition zone between consolidated and aerated lung (arrows) is seen.

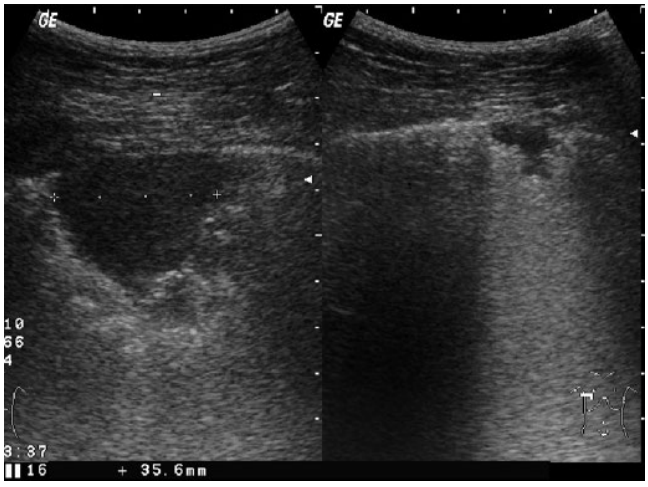

Figure 2.15 Two typical lung consolidations due to pulmonary embolism. They are pleural-based, mostly triangular, sometimes polygonal or round, with relatively well-demarcated margins.

('shred' zones) that are ultimately replaced by normal (non-transmissive) lung. The sonographic resolution of pneumonia is a more accurate reflection of the patient's clinical course than that of chest radiography.

Pulmonary Embolism

Following the occlusion of a pulmonary artery, surfactant loss within its vascular distribution leads to alveolar collapse. Interstitial fluid and erythrocytes flow into the alveolar space causing haemorrhagic infarcts that tend to abut the visceral pleura, creating good conditions for chest sonography. The frequency of reperfusion of these pulmonary infarcts has been shown to be much higher than previously reported as demonstrated by computed tomography (CT) and ultrasound. The sonographic signs of pulmonary embolism are multiple (usually) small (typically 1–3 cm, sometimes larger or smaller) pleural-based, echo-poor consolidations with sharp margins and with minimal or absent central colour-flow by colour-Doppler (Figure 2.15; Video 2.9).

With suspected pulmonary embolism, the examination should start at the site of localised pain, if the patient has one. If the patient has

dyspnoea without pain, the examination is started at the dorsobasal lung regions, where two-thirds of emboli are localised. Patients unable to sit up may be examined in an oblique or decubitus position.

There are some impediments to the use of lung sonography for the diagnosis of pulmonary embolism. For a complete examination, every rib space from spine to sternum should be systematically evaluated, but this requires a relatively mobile and cooperative patient. The patient is asked to 'hug' his or her chest, placing both hands on the contralateral shoulder. The examination should be performed slowly so as to allow the lung in each rib space to be evaluated throughout the respiratory cycle and to minimise the likelihood that a small infarct escapes detection beneath a rib. Time constraints may therefore limit the ability of sonologists caring for critically ill patients to perform a complete and thorough examination. Even with adequate time, a proportion of pulmonary emboli will lodge in arteries that supply lung abutting the mediastinum or major fissures, rendering them sonographically inaccessible.

The overall sensitivity and specificity of chest sonography in pulmonary embolism are 80% and 94%, respectively. Depending on the clinical context, the lung evaluation should be performed in conjunction with echocardiography (which is sensitive and specific in the detection of haemodynamically significant emboli; see Chapters 5 and 6) and leg vein sonography if pulmonary embolism is not identified. With this approach, bedside sonography can potentially 'kill three birds with one stone' by evaluating the source, transit point and destination of thromboemboli, in some reports raising the sensitivity of sonography to 92%. Thoracic ultrasound in combination with laboratory tests is a particularly attractive alternative to CT in cases of renal failure, pregnancy, contrast allergy, or when CT is unavailable. Given its widespread availability, relative cheapness and the avoidance of ionising radiation, sonography may also be preferable in settings where the approximately 8% false-negative rate is deemed acceptable in the evaluation of this disease.

Pulmonary Carcinomas and Metastases

Malignant invasion of the chest wall frequently causes local pain. Targeted ultrasound-based investigation of the region may allow for the immediate identification of this condition. Lung carcinomas and metastases are sonographically visualised as hypoechoic or heterogeneously echogenic structures that are usually rounded or polygonal, sometimes with echo-poor necrotic areas. The margins are often sharp, but the lesions may be speculated with finger-like extensions into the ventilated lung. In colour-flow evaluation, the tumour-vessels appear irregular and corkscrew-like (Figure 2.16). Dynamic ultrasound examination may identify malignant invasion of the chest wall or subclavian vessels more clearly than CT (sensitivity 89–100% for ultrasound versus 42–68% for CT).

Atelectasis

The partial or complete absence of ventilation of lung has several causes, and leads to atelectasis.

Compression atelectasis is usually due to massive pleural effusion. Sonographically, it appears as an area of hepatised lung containing minimal air (in contrast to pneumonias; see above). The consolidations may appear wedge-shaped or resemble a pointed hat. Similar to pneumonia, the transition to ventilated lung may be irregular and shaggy (Figure 2.17). The compressed lung may be seen to float in the effusion, like a waving hand (Video 2.10). Partial re-expansion may occur during inspiration and after drainage of the effusion. On colour-flow Doppler the vessels within the atelectatic lung will show a normal branching pattern.

Obstructive atelectasis appears sonographically as mostly hypoechoic regions of hepatisation, with little or no effusion. In the acute phase of obstruction, air bronchograms may be seen. With the passage of time, secretory congestion within the bronchi may lead to fluid bronchograms which appear like vessels on B-mode but lack a colour-flow Doppler signal. The appearance is similar to that of pneumonia, but with significantly less air bronchograms (Figure 2.18).

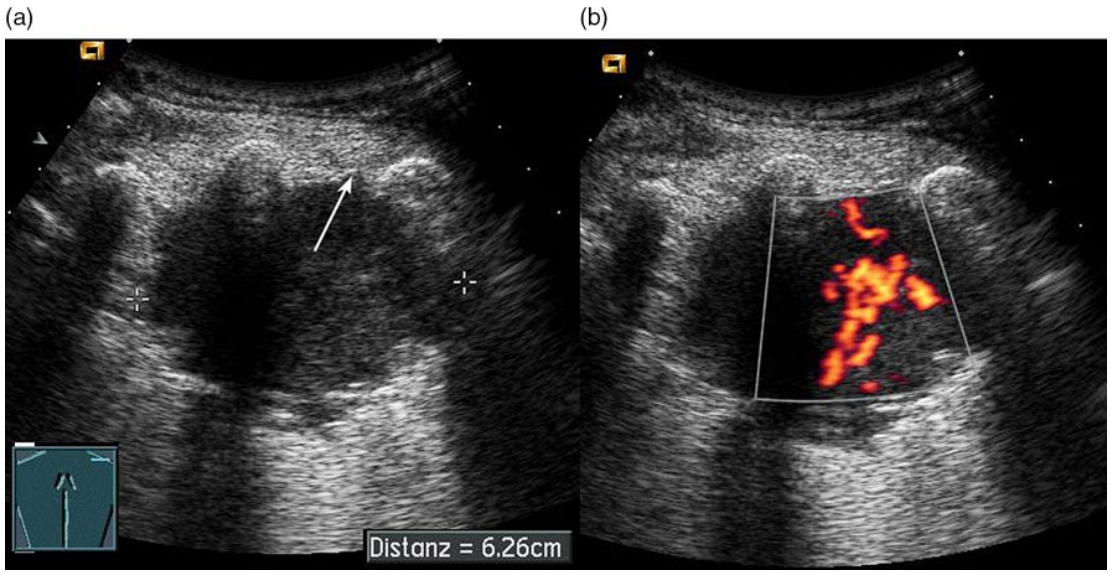

Figure 2.16 Lung cancer appears as a rounded consolidation at the site of the patient's pain. (a) The disrupted pleural line (arrow) indicates that the tumour has infiltrated the chest wall, resulting in a loss of pleural sliding. (b) The characteristically exaggerated blood flow on colour Doppler due to neovascularisation is often described as a 'vascular inferno'. An ultrasound-guided biopsy confirmed the diagnosis.

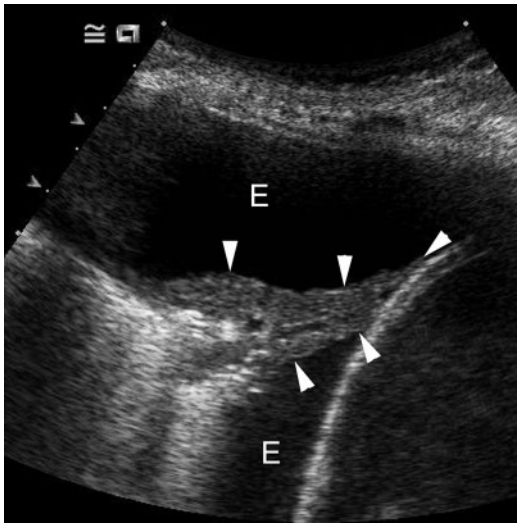

Figure 2.17 Compression atelectasis. A triangular-shaped lung consolidation (arrowheads) is seen floating in a simple effusion (E) with a shred sign at the transition between collapsed and normally expanded lung.

Obstructive atelectasis may have a variable shape, with clear margins if it abuts a fissure. Sometimes an underlying central tumour can be identified.

Plate-like atelectasis, frequently seen on plain film, is due to regional areas of hypoventilation and collapse. It is usually surrounded by normally expanded lung, making it difficult to identify sonographically.

Lung Contusion

In cases of blunt chest trauma – especially multiple rib fractures – pulmonary contusions are seen better on sonography than by plain-film radiography. Alveolar oedema and haemorrhage are visualised as shallow hypoechoic sub-pleural consolidations with irregular borders with respect to adjacent ventilated lung. These are more pronounced in the presence of concomitant pleural effusion (Figure 2.19). A focal

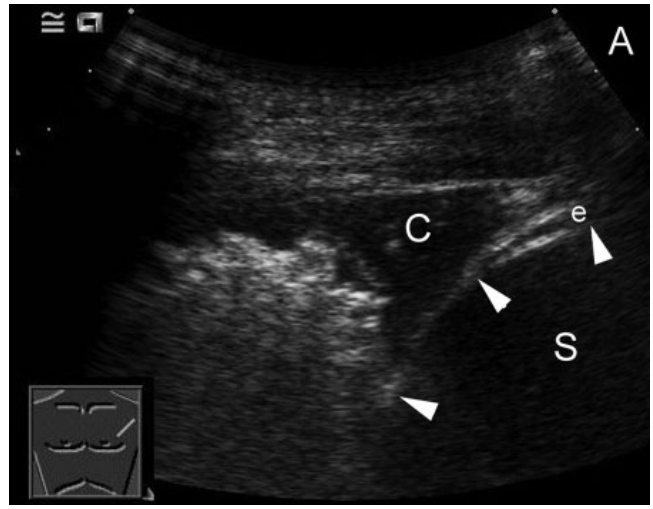

Figure 2.18 Obstructive atelectasis can be seen in the costophrenic sulcus with B-hepatisation similar to that of pneumonia, but with fewer air bronchograms (C). There is a small associated effusion (e) adjacent to the diaphragm (arrowheads), and underlying spleen (S).

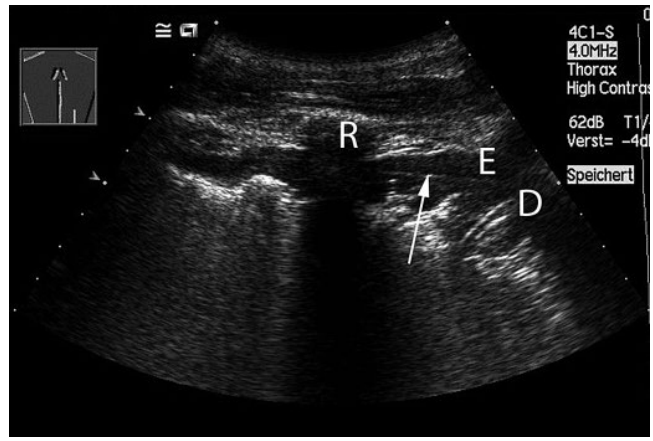

Figure 2.19 A lung contusion in a patient with two rib fractures appears as an extensive shallow consolidation beneath the visceral pleura (arrow). There is a small pleural effusion or self-limited haemothorax (E). R = rib, with shadow; D = diaphragm.

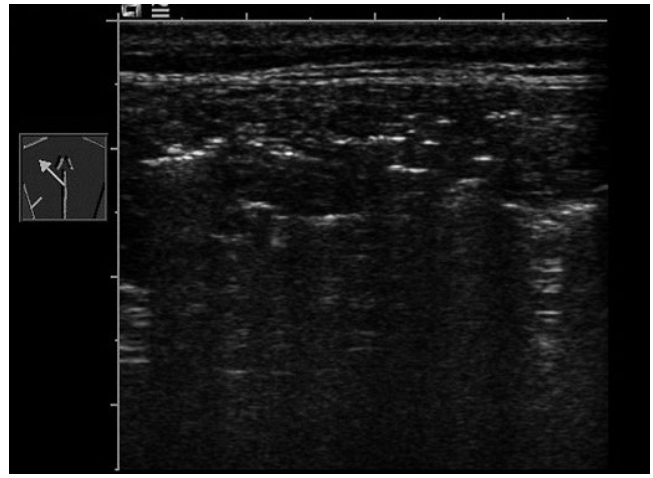

Figure 2.20 In subcutaneous emphysema, numerous air pockets cause irregular echoes, and prevent transmission of the ultrasound waves, with the result that neither ribs nor pleural line are clearly identifiable.

Table 2.1 Sonographic differentiation among various causes of lung consolidation.

Condition	Echogenicity	Bronchograms	Margins	Shape	Vascularisation	Other
Pneumonia	Moderately hypoechoic with intensely echogenic areas	Air early Air and fluid late	Irregular, 'shaggy', poorly defined, 'shred sign'. Underlying 'comet tail' artefacts (like B-lines, but not arising from the pleura)	Any	Profuse	Abscesses later
Pulmonary embolus	Hypoechoic	Absent	Sharp	Pleural-based, often triangular	Absent	Two or more
Lung cancer and metastases	Heterogeneous Hypoechoic regions may indicate infarcted areas	Less	Often smooth, may be spiculated	Often rounded, may be spiculated	Irregular at margins. Sometimes 'vascular inferno'	May be seen to involve pleura, chest wall, or vessels
Compression atelectasis	Hypoechoic	Absent; may see partial expansion with inspiration and after thoracentesis	Transition to lung irregular, but less so than pneumonia.	Often starts in costophrenic angles, extends between pleural surfaces. Usually 'pointy hat' triangular shape. Smooth borders floating in effusion	Normal	
Obstructive atelectasis	Hypoechoic	Fluid (except early when air bronchograms may be seen)	Shaggy and 'shredded' (like pneumonia)		Normal	
Lung contusion	Hypoechoic	Absent	Irregular, but less so than pneumonia Underlying 'comet tail' artefacts may be seen	Shallow consolidation underlying the visceral pleura	Normal	

interstitial syndrome is described in 95% of multiple rib fractures. Overlying subcutaneous emphysema (Figure 2.20) may impede the evaluation, but in patients able to tolerate a full anterior and posterior lung evaluation, ultrasound is as accurate as CT in detecting traumatic pulmonary contusions.

Pearls and Pitfalls

Pearls:

- Particular attention should be directed to the site of the patient's pain.
- The examining hand and the transducer should be immobile with respect to the chest wall.
- Lung ultrasound complements echocardiography: many findings are further elucidated by examination of the heart, and vice-versa.

Pitfalls:

- Lung ultrasound is unable to detect diseases that are surrounded by normal aerated lung, and do not abut the chest wall or diaphragm.
- A relatively limited number of sonographic findings are seen in a wide variety of lung diseases. With practice, many diseases can be identified by specific permutations of sonographic findings and by the clinical context (see Table 2.1).
- Reverberation artefacts and pleural irregularities may give the false impression of lung pathologies.
- Evaluation of pneumothorax is particularly difficult in patients with COPD.

Summary

Chest sonography can rapidly identify, or narrow the differential diagnosis for many thoracic complaints. Many causes of dyspnoea can be identified by ultrasound, including extravascular lung water in heart failure and ARDS, other interstitial lung diseases, and lung consolidations. In the evaluation of chest pain, chest ultrasound may allow for the rapid and accurate diagnosis of pleural conditions, pneumonia and pulmonary embolism. Chest sonography has a special role in the evaluation of trauma because it is the fastest means of diagnosing several common life-threatening conditions, including pneumothorax, haemothorax and pericardial tamponade.

Further Reading

Görg, C., Bert, T. (2004) Transcutaneous colour Doppler sonography of lung consolidation: review and pictorial essay. Part 2: CDS patterns of pulmonary consolidations. *Ultraschall. Med.*, **25**, 285–291.

Kirkpatrick, A.W., Simis, M., Lampland, K.B., *et al*. (2004) Hand-held thoracic sonography for detecting post-traumatic pneumothoraces: the extended focused assessment with sonography for trauma. *J. Trauma*, **57**, 288–295.

Lichtenstein, D.A., Menu, Y. (1995) A bedside ultrasound sign ruling out pneumothorax in the critically ill: lung sliding. *Chest*, **108**, 345–348.

Mathis, G. (1997) Thorax sonography – Part I: Chest wall and pleura. *Ultrasound Med. Biol.*, **23**, 1141–1153.

Mathis, G., Blank, W., Reißig, A., *et al*. (2005) Thoracic ultrasound for diagnosing pulmonary embolism. A prospective multicenter study of 352 patients. *Chest*, **128**, 1531–1538.

Niemann, E., Egelhof, T., Bongratz, G. (2009) Transthoracic sonography for detecting pulmonary embolism – a meta analysis. *Ultraschall. Med.*, **30**, 150–156.

Reißig, A., Kroegel, C. (2007) Sonographic diagnosis and follow-up of pneumonia: a prospective study. *Respiration*, **74**, 537–547

Reuss, J. (2011) The Pleura, in *Chest Sonography* (ed. G. Mathis), Springer-Verlag, Berlin, Heidelberg, New York, pp. 27–54

Soldati, G., Testa, A., Silva, F.R., *et al*. (2006) Chest ultrasonography in lung contusion. *Chest*, **130**, 533–538.

Volpicelli, G., Blaivas, M,, Mahmoud, E., Lichtenstein, D., Mathis, G., Kirkpatrick, A., *et al*. (2012) International evidence-based recommendations for point of care ultrasound. *Intensive Care Med.*, **38**,(4), 577–591.

3

Point-of-Care Ultrasonography of the Thoracic Aorta

R. Andrew Taylor and Christopher L. Moore

Introduction

Aneurysmal disease of the aorta is the 18th most common cause of death among all ages in the United States, and the 15th most common cause in patients aged over 65 years, accounting for more than 13 000 deaths annually, and with the incidence likely to increase as the population ages. Thoracic aortic aneurysm precedes thoracic aortic dissection in 95% of cases, with aortic dissection having a mortality rate of more than 1% per hour after its onset, and a 36–72% cumulative mortality within 48 hours of diagnosis. Clinical characteristics, electrocardiograms and chest x-radiographs are of marginal utility during the decision-making process, with one study finding that only 43% of aortic dissections are diagnosed on presentation in the emergency department.

While computed tomography (CT) angiography of the chest remains the 'gold standard' for the diagnosis of thoracic aortic pathology, echocardiography is a well-accepted method of assessing the thoracic aorta and has the advantage of not involving radiation or intravenous contrast. Transoesophageal echocardiography (TOE) provides superior visualisation of much of the thoracic aorta, but requires sedation, airway management, and is typically not available as a point-of-care test. While somewhat more limited for aortic visualisation, transthoracic echocardiography (TTE) is quick, non-invasive and increasingly available as a point-of-care test. TTE will form the focus of this chapter.

Normal Anatomy and Scanning Technique

Anatomy

Ultrasound imaging of the aorta is facilitated by a thorough understanding of the anatomy. The ascending aorta extends from the valve to the innominate artery. Its first part, from the annulus to the sinotubular junction, including the sinuses of Valsalva, is termed the 'aortic root'. The aortic arch begins at the innominate artery and terminates at the left subclavian artery, where the descending aorta starts. The thoracic aorta is a complex three-dimensional structure, and measurements should be made in a plane that is transverse to the main axis of the vessel at that point. On TTE, the aorta can be measured at several locations, including the annulus, the sinotubular junction, the ascending aorta and the descending aorta. Thoracic aortic diameters are correlated with age (mean diameters increasing about 1 mm per decade), gender (males typically about 2 mm larger than females) and body surface area. Typical reported upper-limit-of-normal diameters (more than

Emergency Point-of-Care Ultrasound, Second Edition. Edited by James A. Connolly, Anthony J. Dean, Beatrice Hoffmann and Robert D. Jarman.

Companion website: www.wiley.com/go/connolly/ultrasound

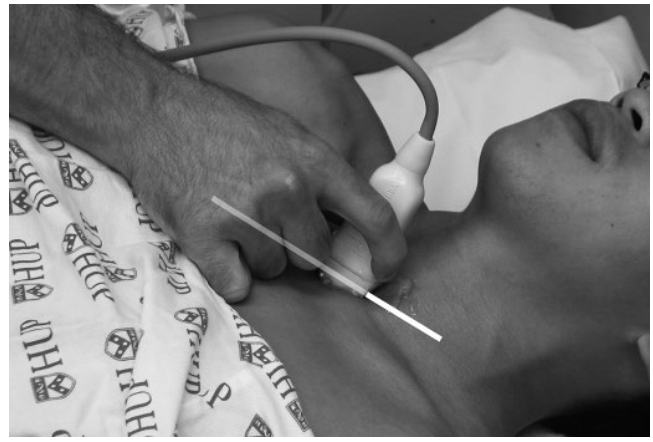

Figure 3.1 The suprasternal window. The approximate plane of the probe along the axis of the aortic arch is indicated, although this will vary from patient to patient. Figure © A. J. Dean.

two standard deviations above the mean) for the ascending aorta and arch is 4 cm, and for the descending aorta 3 cm. Since these dimensions are obtained from patients of both sexes, and of all ages and sizes, then younger, smaller and/or female patients would have a lower cut-off for aneurysm, with the opposite being true for larger, older and/or male patients. It is important to understand that the limit of resolution of measurement is several millimetres, and also that there are discrepancies between different imaging modalities and planes of interrogation.

Sonographic Technique

In TTE evaluation of the thoracic aorta, the primary views are the parasternal long-axis (PLAX) and suprasternal (Figure 3.1), although apical four- and two-chamber, subxiphoid and parasternal short-axis views may provide additional information. The PLAX plane allows visualisation of the aortic root, the proximal ascending aorta, and a transverse view of the descending aorta behind the left atrium (Figure 3.2). In the PLAX, the most reliably visualised and measured portion is the aortic root, in particular the sinus of Valsalva. In a standard parasternal view, only 1–2 cm of the ascending thoracic aorta will likely be seen. Improved imaging, up to the proximal 4–5 cm, can be obtained by moving up an intercostal space or two, placing the patient in a left decubitus position, and/or by rocking the probe in a more cephalad direction. Measurements should be made in imaging planes that demonstrate the maximal diameter of the interrogated region by the leading-edge to leading-edge method (i.e., from the outside part of the anterior wall of the aorta to the inside part of the posterior wall, similar to biparietal diameter measurements), as demonstrated in the upper two measurements in Figure 3.3. Care should be taken to allow enough depth for viewing the descending aorta. It is measured in the same manner as the abdominal aorta, from outside wall to outside wall.

In the suprasternal view, the aortic arch with its three major branch vessels (the right innominate, the left carotid and the left subclavian arteries) can be seen (Figure 3.4; Video 3.1) along with, at times, the right pulmonary artery and left atrium. While it is sometimes difficult to achieve adequate images, suprasternal views are traditionally acquired by placing the phased-array probe in the suprasternal notch, but they may also be obtained in the supraclavicular fossae. The imaging plane is then aligned with the aortic arch, often corresponding with the indicator pointing to the patient's left shoulder. Optimisation is achieved by extending and rotating the patient's head, if they can tolerate such action. The carotid arteries should be followed down into the arch and the arch interrogated as fully as possible. It is important to have a thorough understanding of normal anatomy of this view, so as to avoid the pitfall of mistaking a

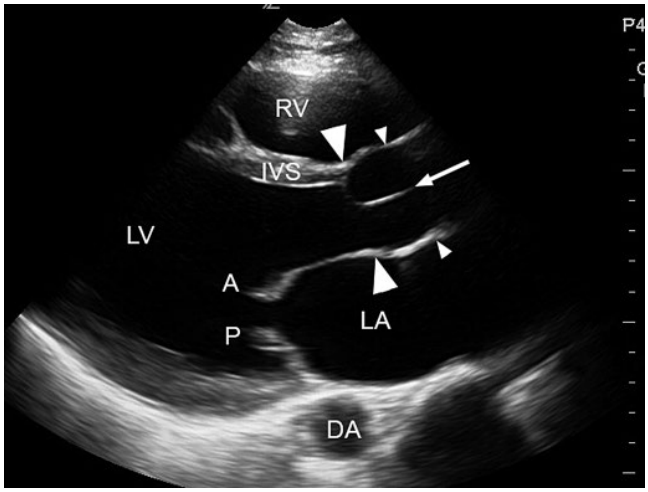

Figure 3.2 Demonstration of the parasternal long-axis view. The aortic annulus can be seen between the large arrowheads, as well as the apposed valve leaflets in diastole (arrow). Between the annulus and the sinotubular junction (small arrowheads) can be seen the sinuses of Valsalva. The left ventricle (LV), anterior and posterior mitral valve leaflets (A and P, respectively), left atrium (LA), right ventricle (RV), and descending aorta (DA) can be seen. Here, a right-sided pleural effusion can be seen adjacent to the DA. Figure © A. J. Dean.

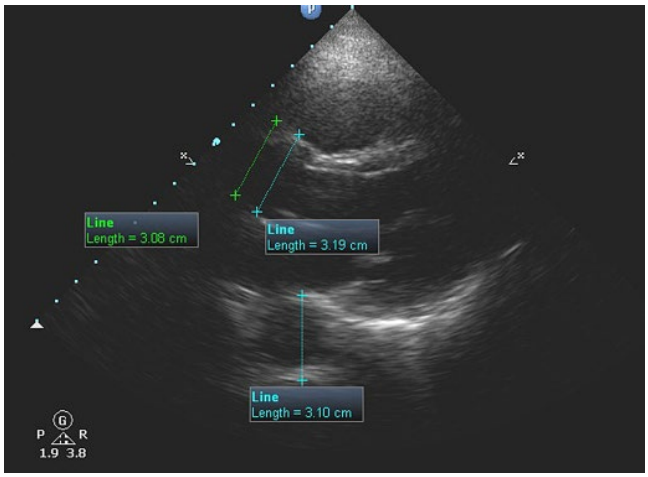

Figure 3.3 Parasternal long-axis view with measurements at the sinus of Valsalva (3.19 cm), sinotubular junction (3.08 cm) and descending aorta (3.10 cm). Note that, in contrast to the ascending aorta, the descending aorta is measured from one outside-wall to the other outside-wall. The latter method is also used for the abdominal aorta.

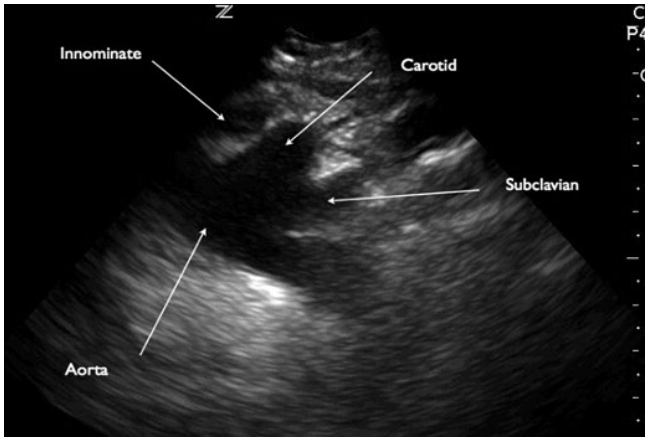

Figure 3.4 Suprasternal view. The right pulmonary artery and left atrium are not seen (see Video 3.1).

venous structure next to the aorta as a dissection. Because of the location of the probe in the suprasternal notch and overlying the trachea, this position can be uncomfortable for the patient and care should be taken to avoid excessive pressure.

Several other views may help in visualising the thoracic aorta. A right parasternal approach in the right lateral decubitus may provide a window to the descending aorta, especially if it is dilated to the right of the sternum. A cross-sectional view of the aortic root is provided by the parasternal short-axis (PSAX). A parasternal longitudinal view of the retrocardiac aorta is often obtained by a plane somewhere between the PLAX and PSAX. Apical two- and four-chamber views, as well as lung consolidation or large pleural effusions, may provide windows to the descending aorta. These views, along with their associated aortic areas of visualisation, are summarised in Table 3.1.

Table 3.1 TTE windows and views afforded of the thoracic aorta.

TTE views	Associated views of the aorta
Left parasternal long-axis	Proximal ascending, transverse descending
Suprasternal	Aortic Arch and branches
Parasternal short-axis	Cross-section of aortic root and longitudinal descending
Subxiphoid	May reveal distal descending
Apical two- and four-chamber	Distal descending
Right parasternal	May reveal mid descending

TTE, transthoracic echocardiography.

Pathologic Findings

Aortic Dilation and Aneurysm

As TTE is more frequently utilised at the point-of-care, it has the potential to play a vital role in screening patients at risk for aortic dilation and aneurysm, and in identifying patients who may benefit from operative intervention (Figure 3.5) As noted previously, normal aortic root diameters are related to gender, habitus and age. Some authorities define 'dilation' as a diameter greater than 3.7 cm at the sinus of Valsalva or 3.5 cm at the sinotubular junction and ascending aorta, with dilation greater than 4.5 cm being defined as aneurysmal. Dilation or aneurysm may present along any portion of the thoracic aorta, and its presence should prompt evaluation of the entire aorta as 25% of patients with thoracic aneurysms have concomitant abdominal aneurysms. Of note, atherosclerotic disease tends to affect the aorta distal to the ligamentum

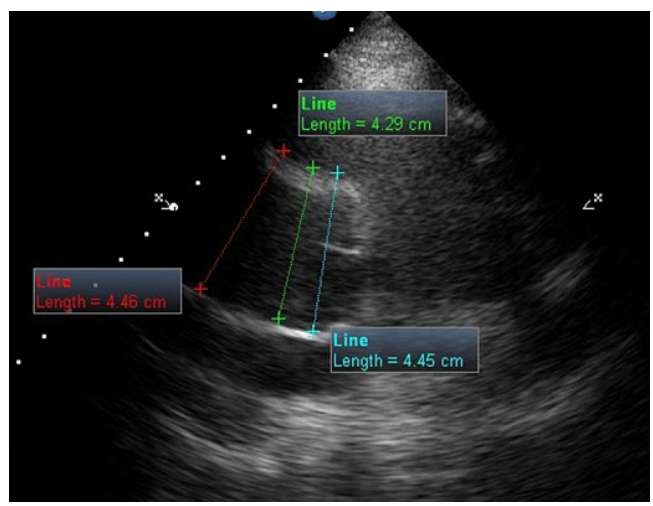

Figure 3.5 Parasternal long-axis view demonstrating aortic root dilation.

Table 3.2 Indications for elective surgical treatment of the ascending aorta.

Aortic diameter >5.5 cm
Aortic diameter >5.0 cm with any of the following:
• Marfan syndrome or other genetic disorders
• Bicuspid aortic valve
• Tricuspid aortic valve with moderate to severe regurgitation
• Expansion 5 mm per year
Aortic diameter >4.5 cm in Marfan syndrome or bicuspid valve with any of the following:
• First-degree relative with ascending aortic dissection or rupture
• Ratio of aortic diameter to body surface area >2.75 cm m^{-2}
• Expansion 5 mm per year
• Concomitant indication for aortic valve replacement
• Pregnancy is desired

arteriosum, so that diseases originating proximal to this point tend to have a systemic, congenital or infectious aetiology (such as arteritis, syphilis, Marfan's disease). Like abdominal aneurysms, an increasing size in thoracic aneurysms is strongly associated with an increasing risk of rupture, dissection or death. A large retrospective study conducted by Davies *et al.* demonstrated this finding with a significantly increased risk for aortas of >6 cm in diameter. However, this relationship does not mean that a small aneurysm size excludes the possibility of rupture or dissection. Because smaller aneurysms are much more common, 25% of ruptures occur in patients with only mild degrees of enlargement. Thus, the first priority of the clinician who identifies a thoracic aneurysm in a patient being evaluated for chest symptoms is whether it is an incidental finding, or whether it might be the cause of the patient's complaints. In the former situation, additional imaging (typically CT angiography) consultation and intervention can proceed electively. The elective operative guidelines for aortic dilations of various sizes are listed in Table 3.2. If there is any suspicion that the patient's symptoms are caused by the aneurysm, an aortic emergency must be ruled out urgently.

Aortic Dissection

Any TTE evaluation of the thoracic aorta for aortic dissection is focused on identifying aortic dilation and an intimal flap. Enia *et al.* showed that aortic root dilation is 91% sensitive for the detection of ascending aortic dissection. The latter findings further supported data provided by Roudaut *et al.*, who found that aortic dilation is 95% sensitive for aortic dissection of any type. A specificity of 100% for dissection was achieved when the three echocardiographic findings were identified: enlargement of the aortic root, thickening of the aortic wall, and the presence of an intimal flap. However, with ranges of 59–85% sensitivity and 63–96% specificity reported for TTE, this test is less accurate than TOE, CT or magnetic resonance imaging (MRI) when directly seeking aortic dissection. This stems from the difficulty of obtaining complete images of the aortic arch and descending aorta with TTE.

Intimal flaps may be visualised along any portion of the thoracic aorta, and may extend into the abdominal aorta (Figure 3.6). Important in the evaluation for intimal flaps is their differentiation from artefact. Clues to artefact versus intimal flap include the following:

1) True intimal flaps have a random motion with respect to the aortic wall as compared to a more fixed location for artefacts (this may be better appreciated using M-mode).
2) Side-lobe artefacts seen in the sinotubular junction may look like an intimal flap, but these attenuate in intensity within the aortic lumen whereas true flaps do not.
3) Colour flow imaging may help in differentiating venous from arterial flow, as adjacent veins (such as the brachiocephalic) may confused with the aorta. Wall thickness, compressibility, and real-time scanning should also clarify uncertain cases (Figure 3.7).

Direct visualisation of aortic pathology can also be combined with indirect signs of ascending dissection, particularly the presence of pericardial effusion in combination with a dilated aortic root or visualised flap (Figure 3.6).

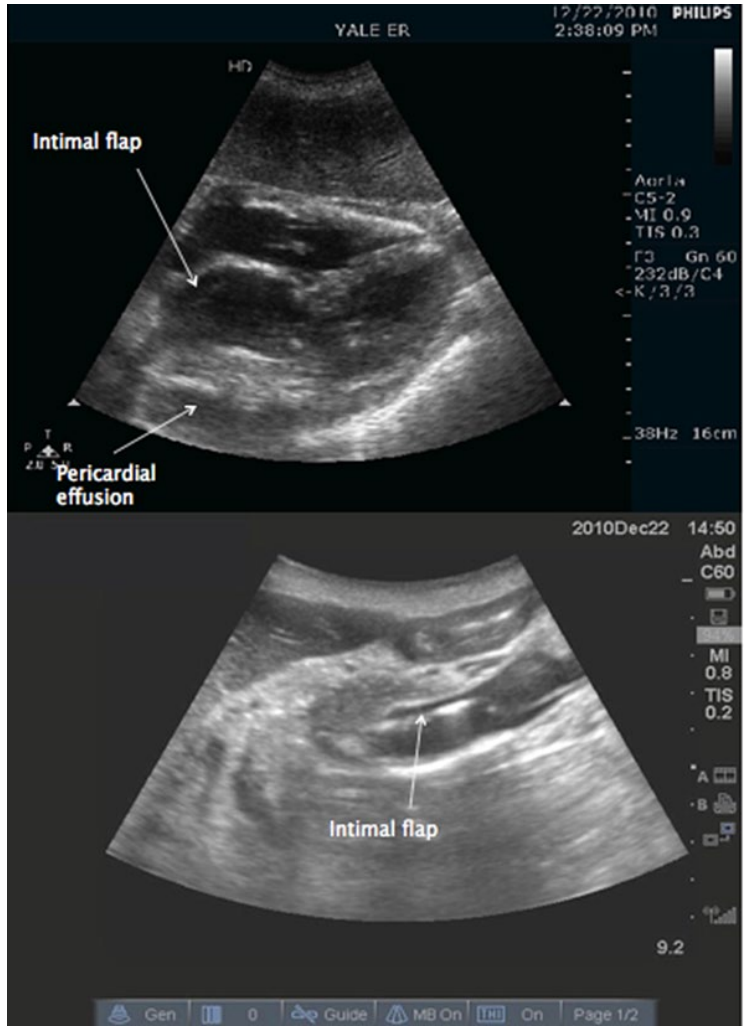

Figure 3.6 Aortic dissection extending from the aortic root (upper image, subxiphoid view) into the abdomen (lower image). Note the presence of the pericardial effusion in the subxiphoid view (see Video 3.2).

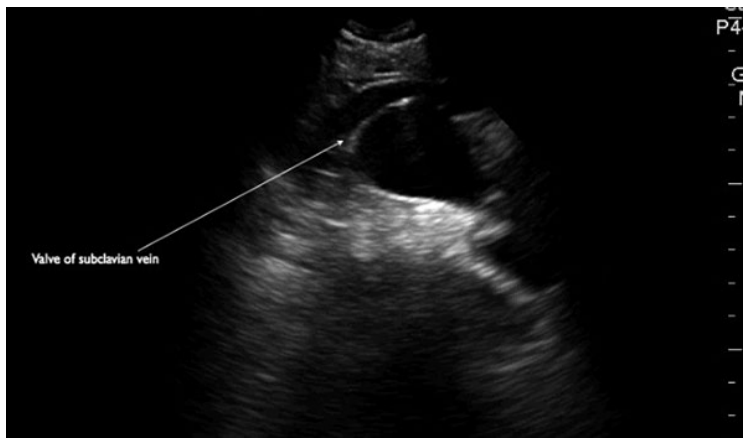

Figure 3.7 Intimal flap pitfall. The subclavian vein valve can be interpreted as an aortic intimal flap.

Pearls and Pitfalls

- While TTE is reasonably sensitive for ascending aneurysm and specific for dissection, a negative TTE does not rule out aortic pathology, and may be particularly limited for descending thoracic aortic pathology.
- Assess the aorta in as many windows and imaging planes as are available.
- Position the patient in the right and left lateral decubitus positions as needed.
- Allow for enough depth to visualise the descending aorta in parasternal views.
- Be aware of artefacts or normal anatomy that may be mistaken for aortic intimal flaps.
- Remember that, depending on the plane of interrogation, TTE measurements may differ from those on other imaging modalities (TOE, CT, MRI).

Summary

A focused ultrasound revealing aneurysm or dissection will expedite care, while a normal examination in patients at low risk will provide reassurance and prompt investigations for alternative causes.

Further Reading

Barbry, T., Bouhemad, B., Leleu, K., de Castro, V., Remerand, F., Rouby, J.J. (2006) Transthoracic ultrasound approach of thoracic aorta in critically ill patients with lung consolidation. *J. Crit. Care*, **21** (2), 203–208.

Davies, R.R., Gallo, A., Coady, M.A., Tellides, G., Botta, D.M., Burke, B., *et al*. (2006) Novel measurement of relative aortic size predicts rupture of thoracic aortic aneurysms. *Ann. Thorac. Surg.*, **81** (1), 169–177.

Di Credico, G. (2000) The International Registry of Acute Aortic Dissection (IRAD): New insights on aortic dissection. *Ital. Heart J. Suppl.*, **1** (7), 943–944.

Elefteriades, J.A., Farkas, E.A. (2010) Thoracic aortic aneurysm clinically pertinent controversies and uncertainties. *J. Am. Coll. Cardiol.*, **55** (9), 841–857.

Enia, F., Ledda, G., Lomauro, R., Matassa, C., Raspanti, G., Stabile, A. (1989) Utility of echocardiography in the diagnosis of aortic dissection involving the ascending aorta. *Chest*, **95** (1), 124–129.

Fojtik, J.P., Costantino, T.G., Dean, A.J. (2007) The diagnosis of aortic dissection by emergency medicine ultrasound. *J. Emerg. Med.*, **32** (2), 191–196.

Labovitz, A.J., Noble, V.E., Bierig, M., Goldstein, S.A., Jones, R., Kort, S., *et al*. (2010) Focused Cardiac Ultrasound in the Emergent Setting: A Consensus Statement of the American Society of Echocardiography and American College of Emergency Physicians. *J. Am. Soc. Echocardiogr.*, **23** (12), 1225–1230.

Mao, S.S., Ahmadi, N., Shah, B., Beckmann, D., Chen, A., Ngo, L., Flores, F.R., Gao, Y.L., Budoff, M.J. (2008) Normal thoracic aorta diameter on cardiac computed tomography in healthy asymptomatic adult; impact of age and gender. *Acad. Radiol.*, **15** (7), 827–834.

Nienaber, C.A., Vonkodolitsch, Y., Nicolas, V., Siglow, V., Piepho, A., Brockhoff, C., *et al*. (1993) The diagnosis of thoracic aortic dissection by noninvasive imaging procedures. *N. Engl. J. Med.*, **328** (1), 1–9.

Roudaut, R.P., Billes, M.A., Gosse, P., Deville, C., Baudet, E., Fontan, F., *et al*. (1988) Accuracy of M-mode and two-dimensional echocardiography in the diagnosis of aortic dissection – an experience with 128 cases. *Clin. Cardiol.*, **11** (8), 553–562.

Solomon, S.D., Bulwer, B. (2007) *Essential Echocardiography. A Practical Handbook with DVD*. 1st edition, Humana Press.

Sullivan, P.R., Wolfson, A.B., Leckey, R.D., Burke, J.L. (2000) Diagnosis of acute thoracic aortic dissection in the emergency department. *Am. J. Emerg. Med.*, **18** (1), 46–50.

4

Anatomy/Ultrasonography of the Heart

Conn Russell

Introduction

The heart is surrounded by the aerated lungs and bony thoracic cage, all of which create a challenging environment for the acquisition of ultrasound images. For this reason, a small-footprint, phased-array ultrasound transducer is optimal. Windows are found in three main regions where lung coverage is minimal, namely the left parasternal, apical and subcostal areas. The suprasternal window is traditionally used for additional views of the aortic arch (see Chapter 3). The phased-array transducer and cardiac presets differ from the general radiology curvilinear probe and non-cardiac presets by providing a higher frame rate, and better black/white resolution of the rapidly moving cardiac structures. The long axis of the heart lies in a plane between the right shoulder and left hip, and all relations are to this plane rather than to the cranial-to-caudal long axis of the body.

Probe Orientation

There are important differences in the orientation of the ultrasound probe used for transthoracic echocardiography and traditional ultrasonography. Indeed, this can be a source of confusion for those with a background of non-cardiology ultrasound, or vice versa. Cardiology and radiology each developed imaging conventions independently. The differences are important to emergency and critical care clinicians who simultaneously perform point-of-care ultrasound examinations of structures above and below the diaphragm.

By the convention of radiologists, the transducer marker ('pointer') corresponds to the left side of the screen. Conversely, for echocardiologists the marker corresponds with the right side of the screen. These screen conventions are embedded in the presets for abdominal and cardiac scanning, respectively, and therefore the same transducer position leads to scans that are mirror images of each other, depending on the preset (Figure 4.1). These differences in convention can be confusing for those scanning with different transducers and/or presets, when evaluating a combination of cardiac and other organs in a single patient. For this reason, many sonologists over-ride the 'factory presets' on their machines so that all probes create images in the same orientation for a given marker direction. This avoids the need to 'flip the probe' depending on which transducer is being used.

Improving Image Quality

A full echocardiology examination will usually take place with a stable patient, in a dark room, and take up to 30 minutes to complete.

Emergency Point-of-Care Ultrasound, Second Edition. Edited by James A. Connolly, Anthony J. Dean, Beatrice Hoffmann and Robert D. Jarman.

Companion website: www.wiley.com/go/connolly/ultrasound

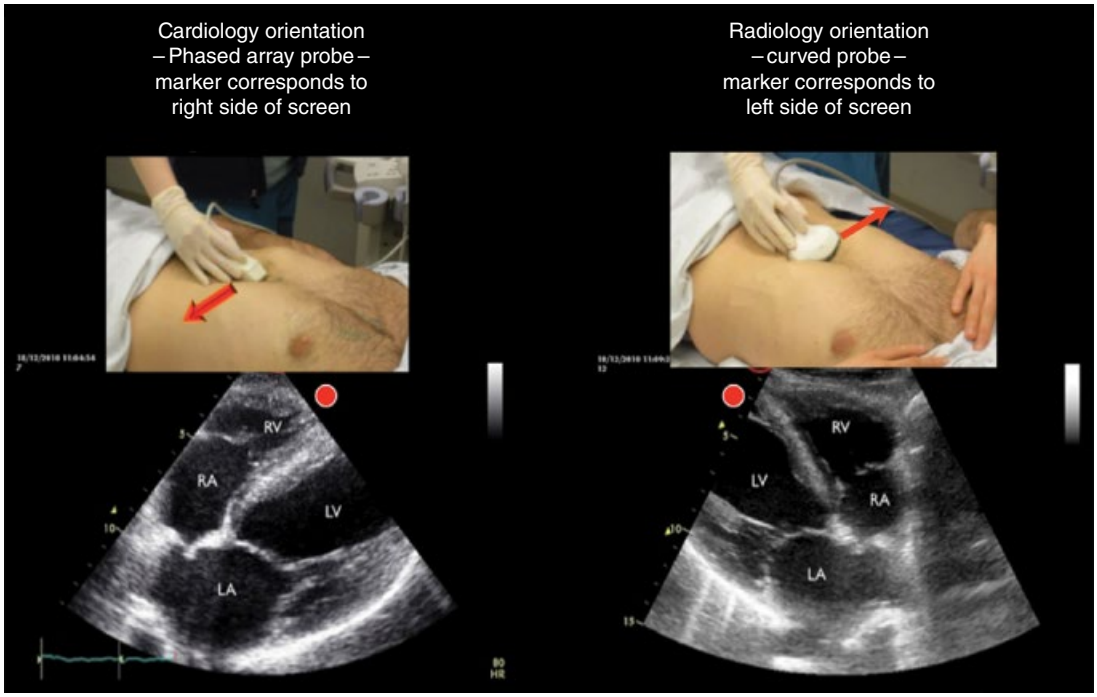

Figure 4.1 Differences in transducer orientation and image generation in transthoracic echocardiography and general radiology in obtaining a subcostal view. In both cases, the marker points to the left side of the patient's body (arrows). However, the corresponding orientation on the screen is different for the cardiac (left) and general abdominal (right) transducers, resulting in mirror images.

A detailed qualitative and quantitative interrogation of the chambers and valves is carried out in B-mode, M-mode, and Doppler. Such standards are neither achievable nor necessary in the majority of acutely ill patients, in whom the answers to a few basic clinical questions may be invaluable to management and diagnosis. It is, however, important to recognise the inherent limitations of a focused examination, and at the same time to obtain optimal images so that as much information as possible can be obtained from it. Sub-optimal images are common and may be due to many factors, including poor position, background lighting, electrical interference and mechanical ventilation, dressings, and the patient's inability to cooperate. It has been shown, however, that images sufficient to answer specific focused questions are possible in the majority of cases.

A few general principles will aid in optimising image acquisition:

- Ultrasound gel is needed to allow the passage of the ultrasound beams from the transducer into the patient; however, excessive amounts may lead to a slippery probe and/or slipping of the probe on the chest wall.
- The transducer is best held towards the tip, resting the heel of the hand and/or the fingertips on the patient to stabilise it.
- Subjects who have poor windows in the upper chest (parasternal windows) often have better lower windows (apical four-chamber, subcostal) and vice versa due to reciprocal variations in position of the heart with respect to the sternum and the diaphragm.
- The parasternal and apical views are almost always improved in the left lateral decubitus position, with the left arm placed under

patient's head. This position may not be possible for critically ill patients.
- The subcostal view may be improved by placing the patient supine, with knees drawn up. Abdominal pain, obesity or presence of bowel gas will interfere with the ability to obtain optimal images.
- Assessment of the inferior vena cava is a component of the cardiac examination (this is addressed in detail in Chapter 10).
- Patient information should be entered, and, time permitting, electrocardiogram leads connected. Clips and images should be stored.

The *Focussed Echocardiographic Examination* is a modified and simplified version of the traditional British Society of Echocardiography adult transthoracic echocardiography dataset, available for download from their website (see references).

Cardiac Windows, Planes and Views

There are three primary windows used to interrogate the heart: parasternal, apical and subxiphoid (also referred to as 'subcostal'). In each window the probe can be rotated allowing for assessment in at least two orthogonal planes. Often, the planes in each window are named according to the primary axes/planes of the heart, which are: (i) the long axis; (ii) the short axis; and (iii) the four-chamber plane. The names of the cardiac views combine a 'window' plus a cardiac plane/axis, for example 'parasternal long axis', 'apical four-chamber', or 'subxiphoid short axis'. The following is a description of the cardiac views most used in clinician-performed ultrasound.

The Parasternal Window

Parasternal Long-Axis (PLAX) Plane

The parasternal window lies in the left sternal edge, 2nd–4th intercostal space. In the PLAX, the transducer marker points towards the patient's right shoulder if using the cardiology screen convention (Figure 4.2). Obtaining this view may be difficult with chronic hyperinflation of the lungs or positive-pressure ventilation, where the lung becomes interposed between the heart and anterior chest wall. If possible, the patient should be placed on their left side with the left arm supporting their head (Figure 4.3) and the breath held in expiration. These manoeuvres are often not feasible with acutely ill patients.

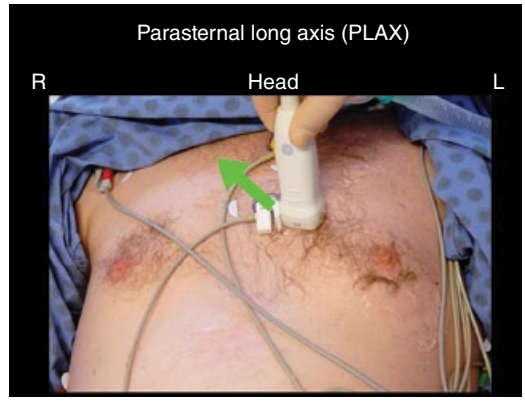

Figure 4.2 Transducer orientation for the PLAX window. The probe marker is directed towards the right shoulder (arrow) for the cardiology screen orientation. The probe is being held in this way for demonstration only.

The PLAX shows the following structures in a single plane: left atrium (LA), mitral valve, left ventricle (LV), left ventricular outflow tract, aortic valve and aortic root. A partial longitudinal view of the right ventricle is seen anterior to the septum. Patients' hearts have highly variable cardiac axes that requires small adjustments in position to be made to obtain a full long-axis view. In general, patients with abdominal obesity have hearts that lie more transversely with respect to the body, while those with hyperinflated lungs have a 'vertical' cardiac lie, with the heart in an almost sagittal orientation with respect to the axis of the body. It may be helpful to imagine the thorax sliced along the long axis between the right shoulder and left hip; the PLAX will then be seen by looking from the patient's left side (Figure 4.4). This view provides information about many structures in the heart, as well as pressure relationships between

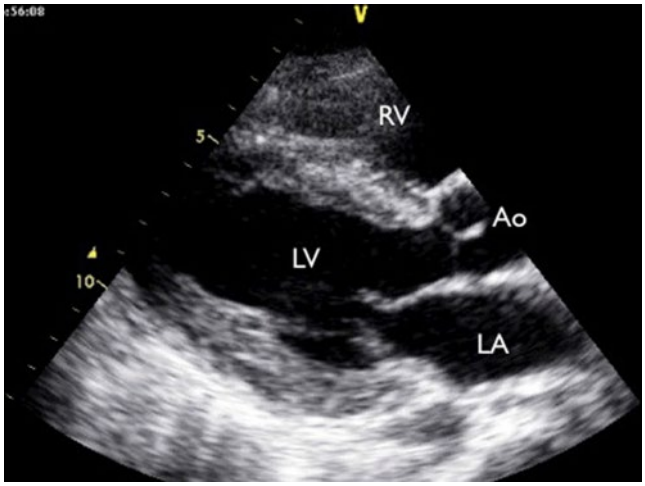

Figure 4.3 PLAX view showing key the structures discussed in text. Ao, aorta; LA, left atrium; LV, left ventricle; RV, right ventricle.

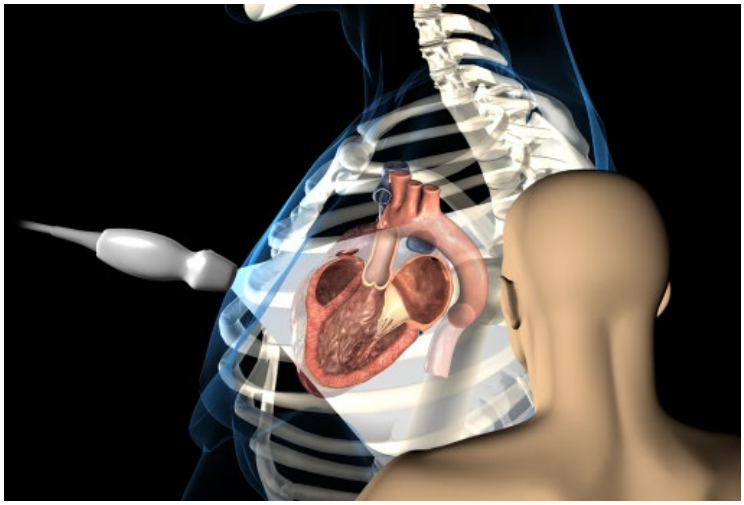

Figure 4.4 Depiction of the PLAX by viewing the chest from the patient's left side. © CAE Healthcare Inc., 2010; All Rights Reserved. Reproduced with permission from the CAE Healthcare-ICCU e-learning Curriculum on the Use of Bedside Ultrasound. Available at: www.iccuelearning.com.

the two ventricles based on their relative sizes and septal motion. In health, the right-to-left ventricular ratio should be about 0.6:1. It should always less than 1:1.

Parasternal Short-Axis (PSAX) Plane

To obtain the PSAX, the transducer remains in the same window used to obtain the PLAX, but is rotated 90° clockwise so that the marker now points to the patient's left shoulder (Figure 4.5a). This view will demonstrate both ventricles in cross-section (Figure 4.6 and Video 4.1 Reference source not found.). With fanning of the transducer this view allows the visualisation of structures from the base of the heart to the apex. On the left, these include (in approximate order) the aortic root and left atrium, the aortic valve, the aortic outflow tract, the mitral valve in transverse view, the chordae tendineae, the papillary muscles, and the apex. With respect to the right heart, fanning from the base first reveals the pulmonary trunk, pulmonic valve, and right ventricular outflow tract in a single plane, followed by the tricuspid valve, and the entire RV to its apex (Video 4.1 Reference source not found.). Putting a cursor through the

centre of the PLAX image before rotating to PSAX helps to highlight the area that will be seen in cross-section when the probe is rotated. The PSAX allows a full appreciation of the ventricular ratios, and is the most intuitive view for the assessment of left ventricular function.

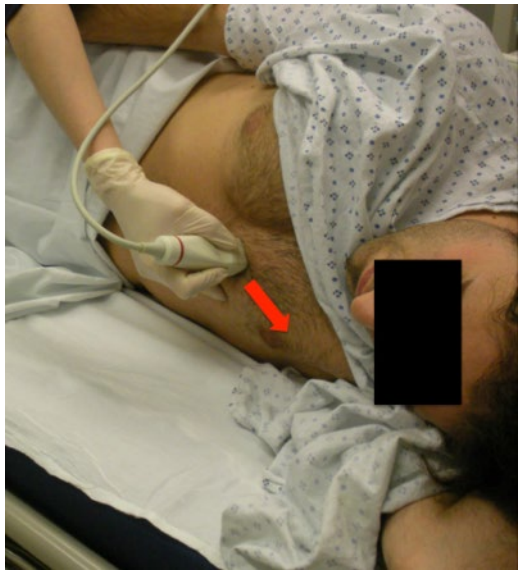

Figure 4.5 Transducer orientation for the PSAX window. The patient is in a left decubitus position with the left arm supporting the head. The probe marker is directed towards the left shoulder (arrow) for the cardiology screen orientation. Note the position of the sonologist's fingers stabilising the transducer on the chest wall. Figure © A. J. Dean.

Figure 4.6 PSAX image showing the paired papillary muscles. Note the relative sizes of the left ventricle (LV) and right ventricle (RV).

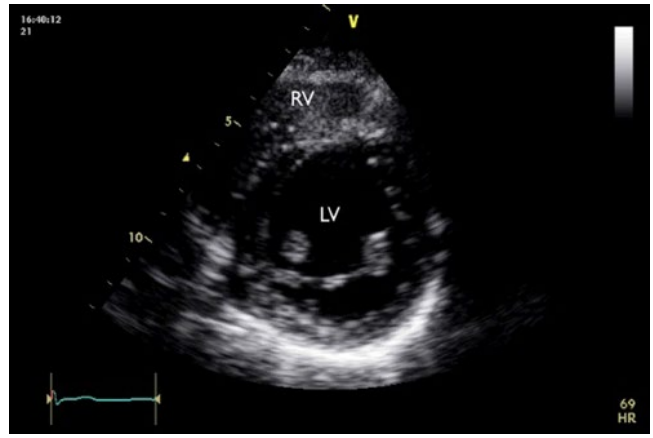

Apical Window

The plane most commonly assessed using the apical window is the four-chamber. With more advanced scanning skills, the two-chamber and five-chamber planes are also used [see Chapter 5 (especially Table 5.2) and Chapter 6].

Apical Four-Chamber (A4C) View

The transducer is positioned at the apex of the heart, pointing up towards the patient's right shoulder and with the marker directed at the patient's left/3 o'clock position using the cardiology convention (Figure 4.7). More depth is usually required for this view. Ideally, the atrial and ventricular septa should make a direct line towards the probe (Figure 4.8). If the septa are directly towards the transducer, small movements medially or laterally on the chest wall may be required. If the atria are poorly visualised, fanning the transducer (usually to point more cephalad) may bring these chambers into view. Further cephalad tilting will show the aortic outflow tract leading to the aortic valve and aorta to be seen in the 'five-chamber view'. The A4C view allows the imaging of all chambers for function and size, and of both the mitral and tricuspid valves. If Doppler evaluation is planned, this is ideal for measuring tricuspid, mitral and aortic transvalvular blood flows as they are directly towards or away from the transducer in this view.

Subxiphoid/Subcostal (SC) Window

This window is most commonly used to obtain images in the four-chamber plane, but also provides excellent short axis views, especially in patients with hyperinflated lungs or enlarge livers. For the four-chamber plane the transducer is held almost flat against the abdomen, immediately caudal to the xiphisternum, pointing up towards the left scapula with the marker at the 3 o'clock position (Figure 4.9). The left lobe of liver serves as an acoustic window. The patient should be supine or slightly head-up, and can draw their knees up to relax the abdominal musculature. Firm pressure is often required,

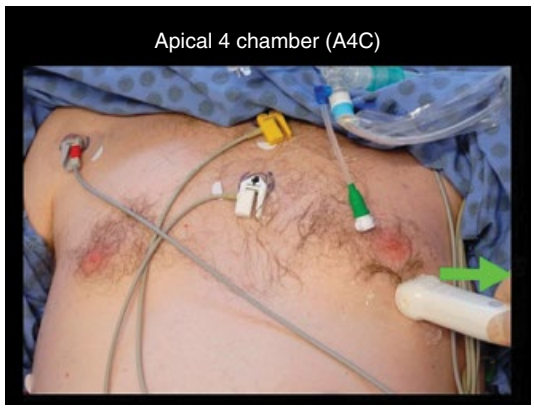

Figure 4.7 Typical transducer location and orientation for the apical four-chamber (A4C) window. Using the cardiology screen orientation, the marker is directed towards the patient's left ('3 o'clock'). In dehydrated patients the apex tends to be more towards the midline, whereas for patients with cardiomegaly it tends to be more lateral.

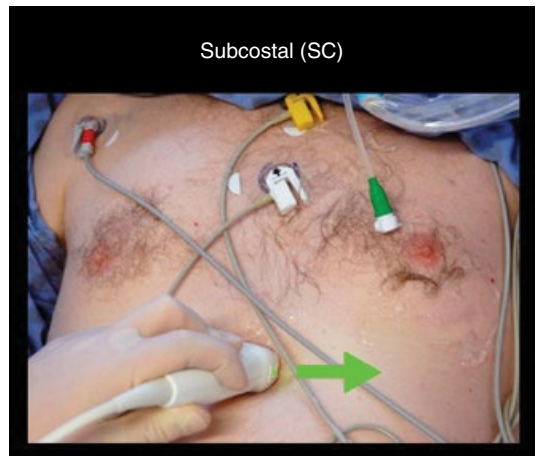

Figure 4.9 Transducer orientation for the subcostal window. Using the cardiology screen orientation, the marker is directed towards the patient's left ('3 o'clock').

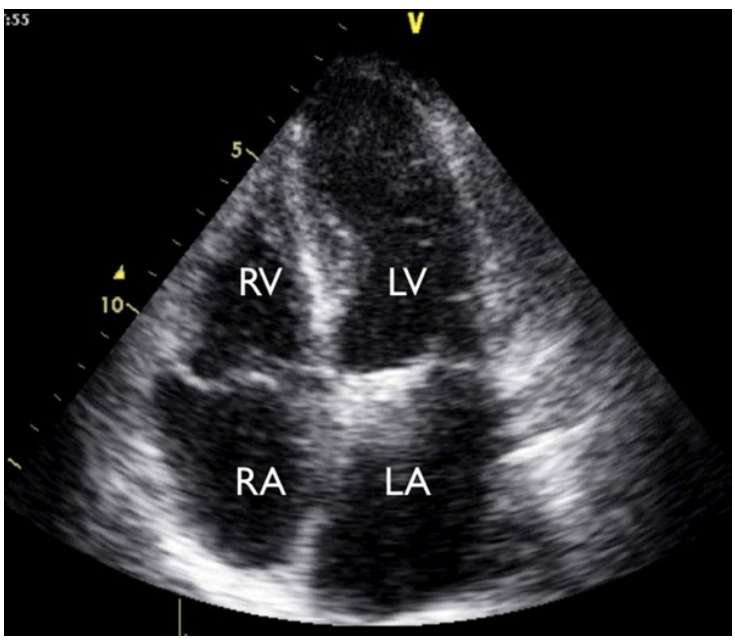

Figure 4.8 Apical four-chamber view. The septum is slightly displaced to the left of the image to allow complete visualisation of the left ventricular free wall. LA, left atrium; LV, left ventricle; RA, right atrium; RV, right ventricle.

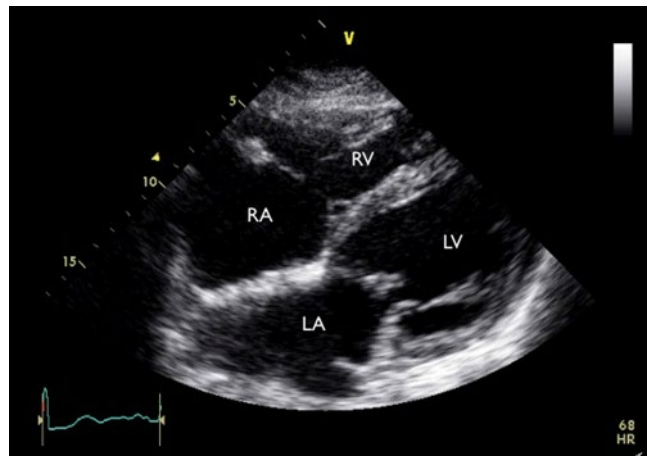

Figure 4.10 A subcostal image showing all four chambers. LA, left atrium; LV, left ventricle; RA, right atrium; RV, right ventricle.

which can cause some discomfort with abdominal pathology. This window is most useful in asthenic patients, or those with increased lung volumes. It is most challenging with high body-mass index patients and those with protruberant abdomens.

The imaging plane in the heart is the same as that for the apical four-chamber view from an orthogonal direction, so that all the structures seen in that view can be seen here (Figure 4.10). The SC view is often the easiest to obtain, especially in trauma and cardiac arrest, as it does not impede cardiac massage, and these patients generally cannot be placed in left lateral decubitus position to help with other windows. The SC window provides information about the key concerns in cardiac arrest, including the pericardium (for possible tamponade), cardiac activity, and evidence of massive pulmonary embolus. It allows for immediate assessment of the inferior vena cava and right pleural spaces by fanning down and to the right, and fanning more anterior and cephalad provides views of the aortic root.

Pearls and Pitfalls

- As with all ultrasound applications, an ergonomic set-up with both the patient and the operator in comfortable positions will increase the likelihood of success.
- Parasternal and apical windows are markedly improved by scanning the patient in a left lateral decubitus position.
- Good technique with probe manipulation and the adjustment of 'knobs' will increase the likelihood of obtaining images adequate for rendering essential information.
- The PLAX plane is typically from the right shoulder to the left hip.
- Whatever the PLAX plane for a given patient, the PSAX plane is perpendicular to that plane.
- The most common error in obtaining the apical four-chamber plane is failure to angle the probe sufficiently towards the patient's right shoulder.
- Regardless of the transducer being used, the cardiac preset should be selected if available.
- Small movements are often all that are needed to improve the image by navigating between the ribs.
- Less-experienced sonologists should take the opportunity to evaluate as many hearts as possible to become familiar with differences in habitus and cardiac windows. This also helps to develop 'visual pattern recognition' in assessments of the heart and cardiac function.
- With increasing experience, sonologists develop the knowledge of 'when to admit defeat'. It is not possible to obtain ideal images in every patient.
- An increasing skill also allows more experienced sonologists to obtain key information through one of several alternative windows.

Further Reading

Chambers, J., Masani, N., Hancock, J., *et al.* A Minimum Dataset for a Standard Adult Transthoracic Echocardiogram. Available at: www.bsecho.org.

Jensen, M.B., Sloth, E., Larsen, M., *et al.* (2004) Transthoracic echocardiography for cardiopulmonary monitoring in intensive care. *Eur. J. Anaesthesiol.*, **21**, 700–707.

5

Basic Point-of-Care Echocardiography

Interpretation and Haemodynamic Assessment

Craig Morris

Introduction

Even fairly basic echocardiography provides information that significantly modifies diagnosis and management of critically ill patients. This chapter will review how ultrasound can be incorporated into the assessment of undifferentiated shock and hypotension. Common haemodynamic patterns encountered in critically ill patients will be reviewed. For the purposes of this chapter, basic echocardiography is taken to include qualitative visual inspection ('eyeballing'), two-dimensional (2D) and M-mode linear measurements, and their derivatives. Throughout the chapter the term 'critically ill' is intended to refer to severely unwell patients in any location, and does not imply 'within an intensive care unit'.

The Ultrasound Examination

Key technical components of the clinician-performed cardiac examination are listed in Table 5.1. Ideally, the patient should be positioned in a semi-recumbent posture, rotated to the left with the left arm elevated (to open the rib spaces), and be able to cooperate with requests to hold their breath. The room should be darkened to allow a minimal use of gain. Such ideal conditions are rarely realised during an 'emergency' scan; posture may be limited by pain, dyspnoea, or an inability to cooperate, time is limited, and it may be impossible to lower the ambient lighting conditions. Despite these limitations a flexible approach to scanning usually results in at least one useable window providing diagnostic or actionable information.

The relevant sonoanatomy and views are discussed in detail elsewhere (see Chapter 4). It is the present author's practice to perform a rapid diagnostic single view, the left ventricle short-axis (LV SAX) 'dancing doughnut' view via either the parasternal or subcostal windows, followed by a more detailed examination as emergency therapy is ongoing. This approach is analogous to the FAST examination, where the examination may be abandoned at any stage if adequate diagnostic information is obtained or the images prove inadequate. This SAX view of the mid-papillary level of the left ventricle allows a visual estimation of left ventricular function, as well as measurement of the fractional shortening (FS) or fractional area of contraction (FAC) (Figure 5.1). As noted, a flexible approach to both the choice and sequence of views is called for. FS is a simple and reproducible measurement but it is preload-dependent, and because it only takes a one-dimensional measurement of the three-dimensional left ventricular cavity it can only ever be considered an approximate measurement. The key features of the primary cardiac views are detailed in Table 5.2.

Emergency Point-of-Care Ultrasound, Second Edition. Edited by James A. Connolly, Anthony J. Dean, Beatrice Hoffmann and Robert D. Jarman.

Companion website: www.wiley.com/go/connolly/ultrasound

Table 5.1 Equipment and settings.

Equipment or setting	Appropriate for point-of-care echocardiography
Probe	Phased-array, with cardiac preset and smaller footprint allows view between ribs. Curvilinear probes may access the subcostal window but often have no cardiac presets, which produces 'jerky' low frame rates and with the marker to the right.
Depth	Typically 15–16 cm. Certain views (e.g., apical or subcostal) may be >25 cm in obese patients.
Gain	Personal preferences vary. Gain generally yields optimal images at lower settings, but for evaluation of function gain must be increased until the endocardium is well defined. Gain does not improve resolution and amplifies artefact as well as detail. 'Auto-gain' is available on some machines, but does not work for all patients. Time gain compensation (TGC) adjusts gain for different depths.
Dynamic range (also known as Log Compression)	On cardiac examination presets, the dynamic range is compressed (i.e., low), allowing for stark contrast between blood and endocardium, at the expense of resolution of the myocardial detail.
Imaging modes used	Predominantly 2D and M-mode (see below). Focused application of colour Doppler may assist valve interrogation, while spectral Doppler may assist valve gradient or stroke volume determinations.
Comments	In all echocardiography the quality of the 2D image determines the quality of 'additional' modes. Machines with a 'cardiac' preset optimise the above, including producing an image with a high frame rate (>20 per second) to provide a 'smooth' image and resolution of rapidly moving structures (e.g., valves). Additional modes (e.g., tissue harmonic imaging) may help to reduce unwanted artefacts.

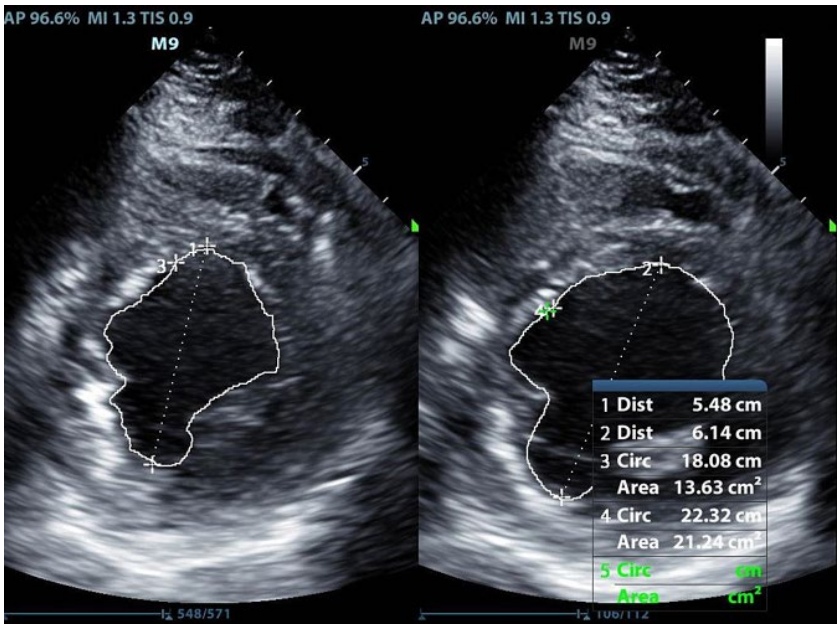

Figure 5.1 A parasternal short-axis (PSAX) mid-papillary view in systole (left) and diastole (right) showing the methods of estimating both fractional shortening (FS) and fractional area of contraction (FAC). The FS is (6.14 – 5.48)/6.14 = 0.26/6.14 = 4%. The FAC is (22.3 – 13.6)/22.3 = 8.7/22.3 = 39%. PSAX and PLAX views from the apex to the aortic valve can be seen in Videos 5.1 and 5.2. These clips reveal hypokinesis of the inferior wall, which leads to the artefactually low FS obtained by these measurements. Systematic visual evaluation of the entire ventricle in at least two orthogonal planes will decrease the potential for error caused by static measurements. Many studies have confirmed the accuracy of visual estimation in the assessment of LVEF. Figure © A. J. Dean.

Table 5.2 Key features of the primary cardiac views.

View	Probe position and orientation	Structures identified	Comments
Subcostal four-chamber (SC 4C)	Subxiphoid region, flat on abdomen, with marker to patient's left	Both ventricles and atria, relative sizes. Good views of dependent pericardial sac for pericardial fluid	Relative ventricle size may be misleading on this view. Good view for patients with COPD or on PPV due to depression of diaphragm
Subcostal short-axis (SC SAX)	Subxiphoid region with probe rotated counterclockwise from SC 4C	Papillary muscles (anterolateral and posteromedial) join body of the LV	Can replace the PSAX in the presence of chest disease or if the patient is on PPV
Inferior vena cava (IVC)	Subxiphoid or right intercostal region with marker to the head (long) or the patient's left (TRV), identifying the hepatic vein	Size and variation of IVC through respiratory cycle	Of limited value with PPV
Parasternal long-axis (PLAX)	2nd–4th intercostal space, marker to right shoulder	LV septum and posteroinferior wall in basal and mid regions, MV, AV and LVOT, LA, RVOT	LV apex typically not seen
Parasternal short-axis (PSAX)	2nd–4th intercostal space probe to left shoulder	Three primary planes: most cephalad AV SAX, then MV commissure, then chordae tendineae to papillary muscles joining LV inferolateral wall	Analogous to the SC SAX plane with the probe moved through 90° over the chest. Non-invasive CO with Doppler VTI of PA.
Apical four- chamber (A4C)	At the true LV apex	LA, RA, LV and RV with associated MV and TV. Allows visual estimation of relative chamber sizes and LV function	Typically further lateral and inferior to the palpable apex beat. Doppler evaluation of valvular disease.
Apical five-chamber (A5C)	Tilting the probe anteriorly demonstrates the LVOT '5th chamber'	Limited value in point-of-care scanning, but allows 2D inspection of AV mobility and opening	Non-invasive CO assessment with Doppler VTI of LVOT.
Apical two-chamber (A2C)	Rotate from A4C through 90° clockwise so that marker is towards the ceiling	Demonstrates LV and LA and MV with interrogation of the anterior (marker side) and inferior LV walls	Combining the A4C and A2C allows the LV to be seen in two perpendicular planes and assessment of global LV function
Apical three-chamber/ long axis (A3C/LAX)	Rotate approx 30° further from A2C		Essentially same plane as PLAX rotated through 90°
Interatrial septum	Visualised from PSAX AV level, A4C, SC4C	Allows determination of relative sizes and movement of the interatrial septum	This assessment is compromised by MR and TR
Suprasternal	Placed in the suprasternal notch looking caudad with marker oblique aiming posteriorly approx. 45°	Aortic arch descending aorta	Search for dissection flap; non-invasive CO with Doppler VTI

Probe orientation is based on traditional echocardiographic screen orientation: probe marker transmits to the right side of the screen. MV, mitral valve; AV, aortic valve; TV, tricuspid valve; OT, outflow tract; PA, pulmonary artery; MR, mitral regurgitation; TR, tricuspid regurgitation; COPD, chronic obstructive pulmonary disease; CO, cardiac output; VTI, velocity–time integral. For other abbreviations, see text.

Normal Findings at Echocardiography: 2D and M-Mode

With experience, an great deal of diagnostic information can gained by qualitative visual assessment, sometimes referred to as 'eyeballing'. There is good evidence that, *in experienced hands*, this is an accurate and reproducible approach but it requires good technique, experience and practice in visual pattern recognition. Where possible, focused quantitative measurements during point-of-care assessment will complement visual assessment by:

- Confirmation of visual impressions, for example of an apparently 'dilated' left ventricle.
- Objective documentation of changes in the patient's clinical condition and response to therapy over time.
- Communication of metrics that can be reassessed and/or shared by other clinicians caring for the patient.
- enhanced credibility in dealing with providers from other specialties.

Conversely, the danger of entering erroneous information into a cardiac calculations package should not be underestimated. Ideally, qualitative and quantitative assessment are integrated, allowing for an evaluation that combines the clinical, metric, and visual pattern recognition skills of the sonologist (Table 5.3; see Figure 5.1 and Videos 5.1 and 5.2).

Haemodynamic Patterns in the Critically Ill

Haemodynamic assessment refers to the simultaneous measurement of cardiovascular pressure *and* flow parameters, allowing the inference of resistance. Point-of-care echocardiography is typically *part* of a haemodynamic assessment and should be integrated with clinical, laboratory, and other imaging data. Point-of-care haemodynamic management includes:

1) A clinical diagnostic phase, that is, 'What is wrong with this patient and what is the cause of shock?'
2) A haemodynamic diagnostic phase; that is, 'How can I classify the haemodynamic disturbance?.
3) A therapeutic phase: treatment of the abnormalities identified in points 1 and 2.
4) A review phase: evaluation of response to therapy with further corrections and adaptations.

While many 'normotensive' patients may demonstrate evidence of shock (i.e., inadequate tissue perfusion), hypotension alone is an important finding with an adverse prognostic significance. Patients presenting to emergency departments with hypotension have a relatively high mortality. In septic patients, progressing from severe sepsis to septic shock increases mortality from 30% to 50%.

Many methods have been advocated to classify shock and hypotension. One fairly simple approach (modified from the *Pocket Guide to Preoperative and Critical Care Echocardiography*; without assessment of filling pressures) considers just two parameters: (i) preload based on ventricular size, and (ii) left ventricular function. The most useful plane is the short axis [either parasternal (PSAX) or subcostal (SC SAX) at the mid-papillary level] (see Table 5.4).

1) Preload or 'filling' conditions. Echocardiography allows a 2D assessment of volaemic status based on simple linear (left ventricular end-diastolic diameter; LVEDD) or left ventricular end-diastolic area (LVEDA) assessment of morphology (Figure 5.1). An inferior vena cava (IVC) assessment may also be used in the assessment of preload. Conversely, traditional monitors (e.g., central venous pressure or right heart catheterisation) have been used to measure pressure and derived volumes through assuming compliance relationships.
2) Systolic function may be assessed by a variety of techniques of increasing complexity, from 'eyeballing' to linear changes (FS) to area changes (FAC) (see Figure 5.1 and Videos 5.1 and 5.2).

Table 5.3 Tips and caveats in qualitative and quantitative cardiac assessment.

Structure	Tips and caveats
LV dimensions	These are traditionally recorded from the PLAX using M-mode, where the best definition of the endocardium/blood is seen. LVEDD <3.5 cm suggests hypovolaemia, LVEDD >5.5 cm suggests dilatation, and IVS >1.2 cm suggests abnormal LV wall thickening. Identifying LVH is a good surrogate for diastolic dysfunction, especially in the presence of a dilated LA.
LV function	The LV contracts principally by radial shortening with lesser longitudinal contraction in contrast to the RV. When eyeballing the LV in the SAX view, place a finger in the centre and ask 'Are all walls moving *and thickening*?' On PLAX, use M-mode to identify the LVEDD and LVESD and calculate the FS%. As a rule of thumb, FS% × 2 approximates the LVEF. Many machines will generate an extrapolation of the FS% as the Teicholz EF%, but this tends to underestimate the true EF%.
LA	This should be approximately the size of the aortic root and <4 cm at its largest (ventricular systole) on PLAX. A small LA suggests ongoing hypovolaemia in patients in shock.
LVOT and aortic root	The LVOT diameter is measured at the junction of the AV cusps and annulus and used in cardiac output calculation. The PLAX provides views of the aortic root. Normal AV leaflets should open to the walls of the sinus of Valsalva. Aortic diameter increases with age, but should be <4 cm. While significant stenosis is relatively easily excluded on 2D, AV regurgitation cannot be excluded without using the Doppler modality.
MV	Has a long anterior and shorter posterior leaflet. It should be thin and mobile and open with two distinct phases during ventricular diastole. Similar considerations as for AV regarding stenosis and regurgitation.
RV dimensions	The RV should not exceed two-thirds of a normal-sized LV in any comparable plane. Mild RV dilatation may be taken up to RV = LV. It is considered severe where RV > LV.
RV function	The RV is a complex geometrical structure but may be easily described for point-of-care purposes by assessing the longitudinal contraction. This is most reliably assessed by the tricuspid annular plane systolic excursion (TAPSE) from the A4C, where M-mode measures the free TV annulus movement. Normal >1.6 cm
Pericardium	Significant quantities of pericardial fat are not unusual, and fresh fluid should appear as a true black anechoic space; fat has a more striated appearance. Identification of pericardial fluid does *not* always equal tamponade (e.g., chronic effusion) and this requires further evaluation. Typically fluid >1 cm acutely will cause problems and should prompt more specialist assessment; fluid >3 cm represents a very significant collection. Effusions may be loculated, leading to effects on isolated cardiac chambers (e.g., post cardiac surgery).

Abbreviations: EDD, end-diastolic diameter; ESD, end-systolic diameter; IVS, interventricular septum; EF, ejection fraction. For other abbreviations, see text.

Table 5.4 Categories of haemodynamic derangement based on echocardiographic findings.

Clinical syndrome	LV size (preload)	LV systolic function	Comments
Hypovolaemia or vasodilatation	↓	↑	Unless LV impairment prevents compensation. Hypovolaemia may be either absolute (e.g., haemorrhage) or relative (e.g., septic vasodilatation).
Hyperdynamic	↔ or ↓	↑	May occur with (as per line above) or without hypovolaemia (normal end-diastolic volume and adequately filled IVC). The syndromes overlap extensively.
LV systolic failure	↔ or ↑	↓	Normal LV systolic function does not exclude heart failure; isolated diastolic heart failure occurs in 50% of patients.
RV failure or obstruction	↓	↔ or ↑	The RV is typically dilated. In RV failure associated with pulmonary hypertension, interventricular septum findings include flattening and paradoxical motion. May lead to decreased LV size.

For abbreviations, see text.

The normal LVEDD on the mid-papillary LVSAX ranges from 3.5 to 5.5 cm, the normal FS is 25–40%, and the LVEDA is 8–15 cm^2 (with papillary muscles excluded from the measured area). The normal FAC is >55%, similar to the left ventricular ejection fraction (LVEF). A LVEDD <3.5 cm and LVEDA <8 cm^2 strongly suggest low preload conditions. Further confirmation on the preload state may be gained from assessing the IVC and observing the atria and interatrial septal movements (see Figures 5.2 and 5.3, and Videos 5.3 and 5.4). As noted in

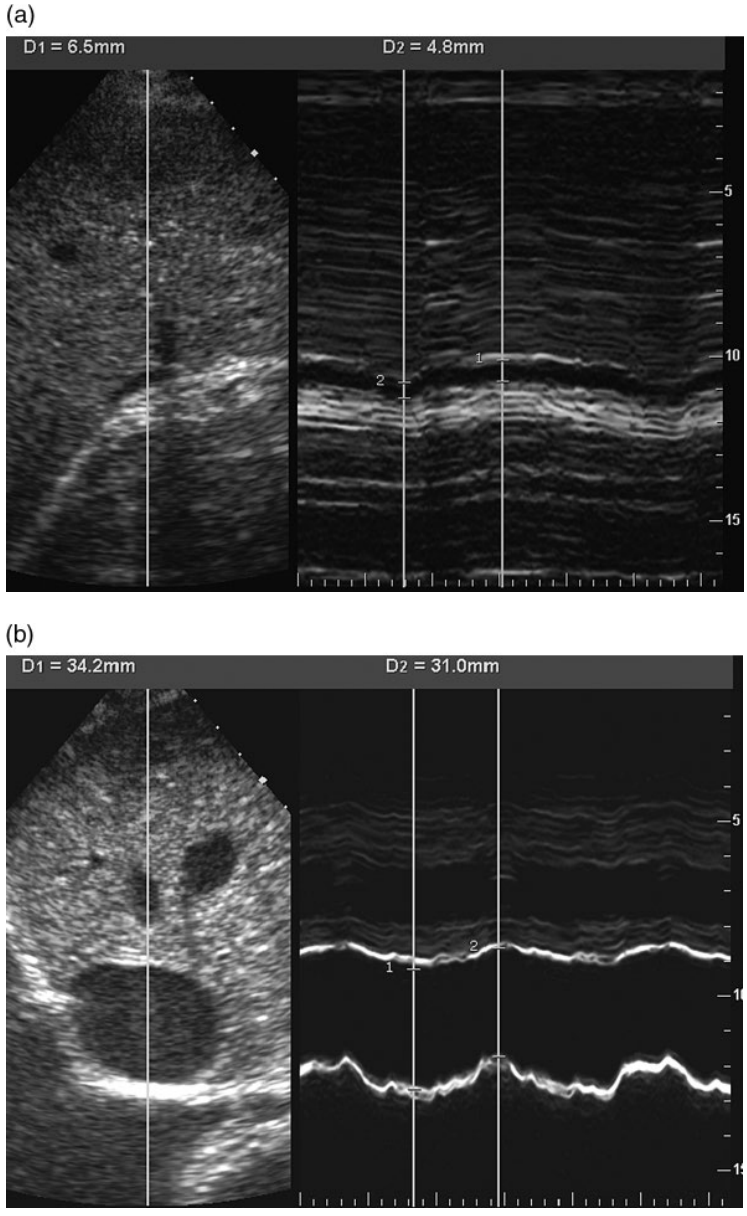

Figure 5.2 Transverse transhepatic (intercostal) views of (a) a dehydrated patient with a slit-like IVC, and (b) a patient with volume overload and congestive heart failure. In each panel the B-mode image of the IVC is seen on the left, with a corresponding M-mode record on the right. Figures © A. J. Dean.

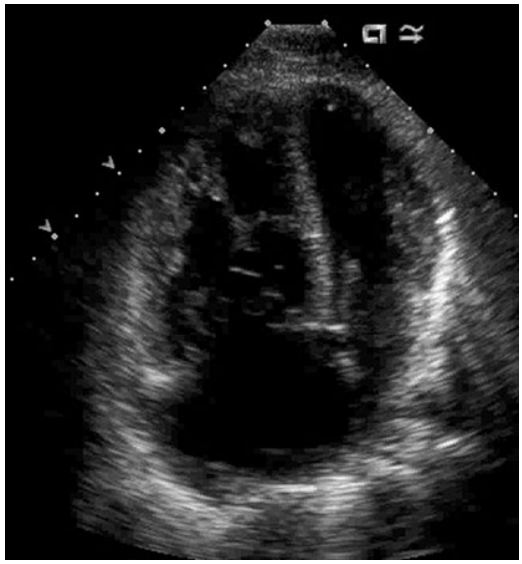

Figure 5.3 An apical four-chamber view of a patient with chronic pulmonary hypertension. The right ventricular cavity is larger than the left, with abnormally thickened walls (normal ≤7 mm), and septal bowing towards the underfilled left ventricle (left ventricular end-diastolic diameter <3.5 cm). The atrial septum can also be seen to be bowing toward the left side. Figure © A. J. Dean.

Table 5.3, a left ventricular wall thickness >12 mm in diastole suggests hypertrophy, and is strongly suggestive of diastolic dysfunction. More refined techniques for the assessment of left ventricular diastolic function are considered in Chapter 6.

Under most circumstances, the clinician is focused on resuscitating the left ventricle and restoring the systemic circulation. Here, the left atrial pressure (LAP) is a far more useful target than the right atrial pressure or central venous pressure (CVP). The interatrial septum should be mildly convex towards the right in an adequately hydrated patient (absent valvular disease). While the left atrial collapse demonstrated in Video 5.3 may be difficult to identify in a rapidly beating, underfilled heart, its presence should usually prompt fluid loading. The left atrium can also be assessed in the PLAX view in comparison to the aorta. Under normal circumstances the left atrium, the aorta and the right ventricle should be approximately the same size in this view (see Figure 5.4 and Videos 5.5 and 5.6). It is the present author's overwhelming experience that patients thought to be 'fully fluid-resuscitated' on the basis of CVP, compounded by concerns about inducing pulmonary oedema, often actually have a low LAP. Indeed, they often remain fluid-responsive and fluid therapy may be curtailed once the left atrium reaches normal dimensions and the interatrial septum a more central position.

Advanced Echocardiography and 'Departmental Scans'

There is on-going debate about the value of 'focused' or 'problem based' (e.g., does this patient have left ventricular impairment?) versus 'comprehensive' echocardiographic examination. Each has its merits, determined primarily by the patient's condition, the clinical setting, and available resources. A point-of-care echocardiogram may generate a haemodynamic diagnosis (e.g., cardiogenic shock due to left ventricular systolic impairment). Conversely, comprehensive studies – which in most settings and times cannot be arranged on an emergency basis – may be of less value in managing the critically ill, but may generate information that is useful for the longer-term management of the patient (e.g., left ventricular impairment with ejection fraction <35%). A variety of organisations have made recommendations regarding both focused and comprehensive or 'departmental' echocardiography examinations (see References).

This debate also raises the issue of the limits of a clinician-performed echocardiography, beyond which all examinations should be performed by imaging specialists. In reality, differences in skill, experience and training mandate that each sonologist understands his or her limitations, and use this as a basis for decisions about requesting 'departmental' speciality-performed. Some general principles are as follows:

- Most echocardiographic abnormalities serious enough to cause critical illness are not

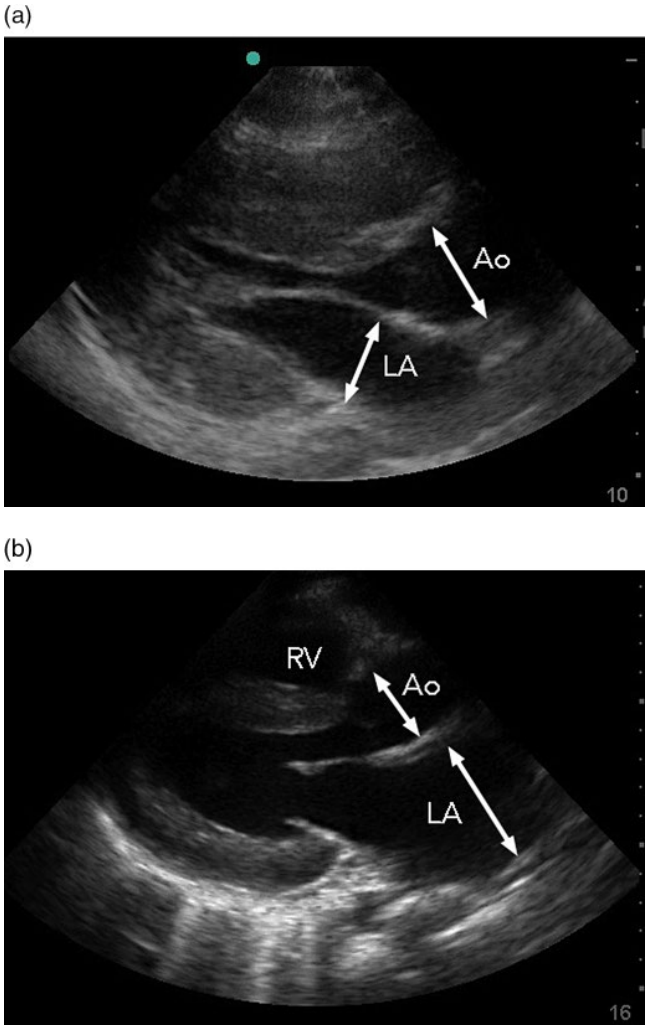

Figure 5.4 The PLAX view seen in (a) is the same as that of Video 5.5. The patient complained of acute chest pain and shortness of breath with a known history of hypertrophic cardiomyopathy and a baseline high LVEF. The patient is currently hypovolaemic (as revealed by a collapsing IVC, not seen here). The LVEF is approximately 80%. The diameter of the left atrium (LA) is mildly reduced compared to the aortic root (Ao). (b) The same cardiac plane from a patient with restrictive cardiomyopathy and severely depressed LVEF. The LA is very much enlarged compared to the aorta. The right ventricle (RV) appears unremarkable. Figure © A. J. Dean.

'subtle', making minor derangements requiring speciality training for their identification less important in this patient population.

- Many echocardiographic abnormalities serious enough to cause critical illness are singular not multiple, often making their recognition easier.
- Direct knowledge of the clinical context (augmented for intensivists by extended periods of care) can provide the clinician sonologist with important advantages over imaging specialists. For example, the management of acute dyspnoea in a patient with a grossly dilated right ventricle is likely to be influenced by a history of either recent immobilisation, ongoing cancer, or longstanding chronic obstructive pulmonary disease (Figure 5.3).
- Certain pathologies group together, such as hypertension, left ventricular hypertrophy

(LVH), aortic valve degeneration and aortic stenosis.

- Ultrasound evaluations of the critically ill are not limited to the heart! In ambiguous cases it should be augmented by evaluation of the lungs, IVC and serosal spaces of the trunk. For example, to diagnose hypovolaemia with an IVC in excess of 3 cm diameter is probably erroneous.
- Focus on what you can fix. It is less important to identify pathologies that cannot be (acutely) treated, such as severe aortic stenosis.
- Know the inherent limitations of point-of-care echocardiography; for example, its ability to exclude infective endocarditis or aortic dissection, or to assess the severity of a regurgitant valve lesions.
- An impaired left ventricle does not equate with a low cardiac output, especially if the right ventricular function is vigorous. Both ventricles must have an identical stroke volume, so barring catastrophic valve failure or septal defects, even with impairment, the left ventricular output must be the same as the right ventricular output.
- Point-of-care echocardiography should be integrated with the entire clinical picture, and be scrutinised with judgement and common sense. Isolated echocardiographic findings may be misleading. For example, a patient may live functionally for many years with an ejection fraction of 10%. A sudden deterioration of condition should not necessarily be ascribed to worsening heart failure *per se*, and alternative aetiologies should be sought.

Further Reading

Recommendations Regarding Various Types of Echocardiographic Protocol:
http://www.bsecho.org/home/
http://asecho.org/guidelines/guidelines-standards/

Other Reference Material

McGowan, J.H., Cleland, J.G. (2003) Reliability of reporting left ventricular systolic function by echocardiography: a systematic review of 3 methods. *Am. Heart J.*, **146** (3), 388–397.

Rose, C., Donnan, G., Royse, A. (2006) *Pocket Guide to Preoperative and Critical Care Echocardiography*. McGraw-Hill.

Via, G., Hussain, A., Wells, M., Reardon, R., El Barbary, M., *et al.* (2014) International evidence-based recommendations for focused cardiac ultrasound. International Liaison Committee on Focused Cardiac UltraSound (ILC-FoCUS); International Conference on Focused Cardiac UltraSound (IC-FoCUS). *J. Am. Soc. Echocardiogr.*, **27** (7), 683;e1–e683; e33.

6

Beyond Basic Point-of-Care Echocardiography

Sean Bennett

Introduction

The aim of this chapter is to examine more advanced echocardiography within the setting of emergency care. Thus, it remains relevant to the practitioner in the emergency department, the recovery room and in the intensive care unit (ICU). Whilst the chapter does not include advanced diagnostics or time-consuming protocols, it does include the use of transoesophageal echocardiography (TOE) in addition to transthoracic echocardiography (TTE). Technical points will be discussed and reinforced using case histories.

When is Basic Not Enough?

Generally, more advanced echocardiography is called for when inadequate information has been obtained due to poor echo windows or when, after a basic echocardiogram, the patient's condition is still unclear and it is likely that more echocardiographic information will provide important information. Generally, in critical care an echocardiogram will begin with TTE and then move on to TOE if required.

Practical Issues

Echocardiography laboratory conditions are rare in a critical care setting. As with basic ultrasound, time spent in patient preparation and ergonomic set-up is likely to be more than repaid in faster scanning and better images. If time permits, attachment of ECG leads is ideal, to link ultrasound findings precisely with the cardiac cycle. In many cases, not all the TTE views will be obtainable, and the scan remains focused on information needed to answer an immediate clinical question. For example, the subcostal view, although rarely used in the laboratory, often provides the best view of the heart and surrounding structures in ventilated patients undergoing resuscitation.

All attempts to obtain needed information by TTE before resorting to TOE. If TOE is required, all local as well as systemic conditions and contraindications should be considered. Check for either iatrogenic or pathologic coagulopathy. Most anaesthetists are familiar with passing probes, but this must be done with great care in the ICU. Cervical spine injury is a relative, and oesophageal pathology usually an absolute contraindication to TOE. Exceptions exist: for

Emergency Point-of-Care Ultrasound, Second Edition. Edited by James A. Connolly, Anthony J. Dean, Beatrice Hoffmann and Robert D. Jarman.

Companion website: www.wiley.com/go/connolly/ultrasound

example in a case of a young girl with a cervical spine fracture and suspected aortic dissection a negative TOE obviated the need for thoracic surgery in a setting where angiography was not available.

Prior to TOE, the airway should be secured, and the patient lightly anaesthetised and paralysed. This reduces procedure time and risk of complications. Gastric views should be sought only if mid-oesophageal views fail to provide the necessary information. If gastric views are needed, the stomach should only be entered once. A nasogastric tube does not prevent gastric images but the tube should first be aspirated. When removing the TOE probe the nasogastric tube position should be checked before restarting the feed. Damage to the teeth, mouth and upper airway is common. Oesophageal damage occurs in less than 0.5% of patients, but is more serious.

The American Heart Association (AHA) guidelines suggest that aortic dissection and haemodynamic instability are the Class 1 indications for an echocardiogram. For clinicians managing critically ill patients, the threshold to perform a point-of-care echo is lower. Based on the present author's experience, a practical list of the conditions that should prompt echocardiography is provided in Table 6.1.

Table 6.1 Indications for TTE/TOE in the critical care setting.

- Haemodynamic instability, especially with:
  - Suspected LV or RV dysfunction or pulmonary embolism
  - Suspected hypovolaemia
  - Suspected tamponade
  - Suspected acute valvular pathology (prompted by any murmur)
  - History of cardiac or metastatic neoplasm
  - Recent cardiac catheterization
- Suspected endocarditis
- Hypoxaemia
- Possible aortic pathology
- Ventilated patients with a history of chest trauma

Ventricular Assessment

Visual assessment of the left ventricle may be misleading, especially in mitral valve disease, sepsis, myocardial infarction and with image 'drop-out'. As discussed in Chapter 5, measurements may add significant information. Cardiac output is rarely calculated by echocardiologists, but many advanced sonologists assess this in managing the critically ill.

Videos 6.1–6.3 are taken from the same patient. In Video 6.1, despite some image drop-out a mixed pathology of the mitral and aortic valves can be seen. In these cases, the valves should be assessed first. Here, the aortic stenosis (AS) will cause left ventricular hypertrophy (LVH) and a small left ventricular end-diastolic diameter (LVEDD). However, the aortic regurgitation (AR) will cause an increase in LVEDD. The AS is more severe, as shown in the short axis (Video 6.2). The mitral regurgitation (MR) is not severe but may well cause the appearance of better forward flow than is actually the case (Video 6.3). This ejection fraction was measured at 50%, but in fact performance was at least 10% lower and the patient required inotropes.

Video 6.4 and Figures 6.1–6.3 show a patient with mitral disease in whom it was wondered '… is there was a pericardial effusion causing low blood pressure and high central venous pressure (CVP)?' The patient was awake. TTE showed a fractional area change (FAC) of just under 50%, but the areas were abnormal [maximum normal end-diastolic area (EDA) of 22 cm^2 with an end- diastolic diameter (EDD) of 6.1 cm (maximum normal EDD 5.3 cm)]. The patient had no effusion and was hypervolaemic with dilated heart failure. Initial treatment with diuretics was indicated with addition of inotropes if necessary.

Figure 6.4 is the TOE scan of a young septic patient showing an EDD of 5.3 cm. An early echocardiogram can avoid fluid overload and prompt the timely use of inotropes. Follow-up echocardiography typically shows a good recovery of left ventricular function. Similarly, left ventricular obstruction can occur pathologically,

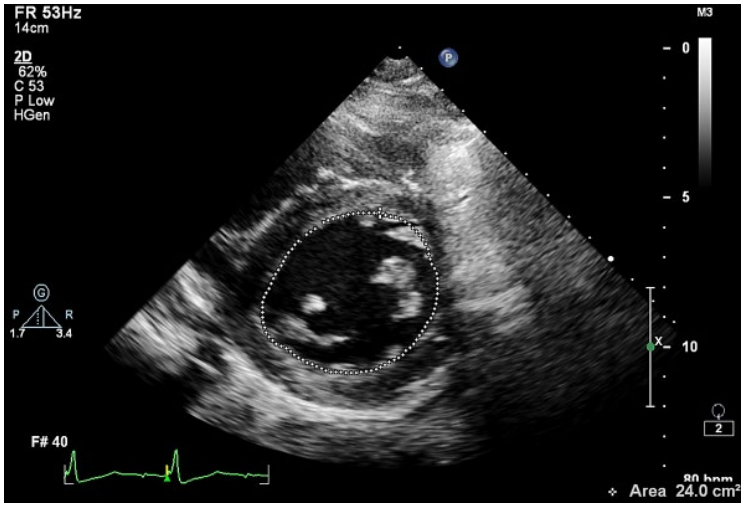

Figure 6.1 TTE short-axis: End-diastolic area.

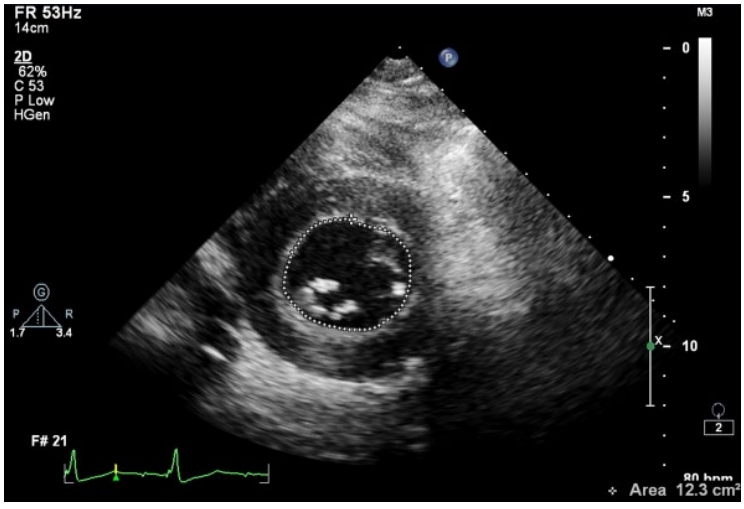

Figure 6.2 TTE short-axis: End-systolic area.

following mitral valve surgery, or in the hypovolaemic patient receiving inotropes. Echocardiography will show this clearly and define treatment.

Reliable detection of subtle regional wall motion abnormalities (WMAs) is beyond the skill of most sonologist, but gross WMAs may be correlated with the ECG and help to direct therapy. The right ventricle can also be affected. It is shown in Video 6.5 that whilst right ventricular movement is maintained at the base and lateral wall, the inferior wall is severely hypokinetic (Videos 6.5a and b). A common approach to assessing right ventricular function is to simply note its relative size to the left ventricle (it should be <60% of the left ventricle). In biventricular failure, both are dilated.

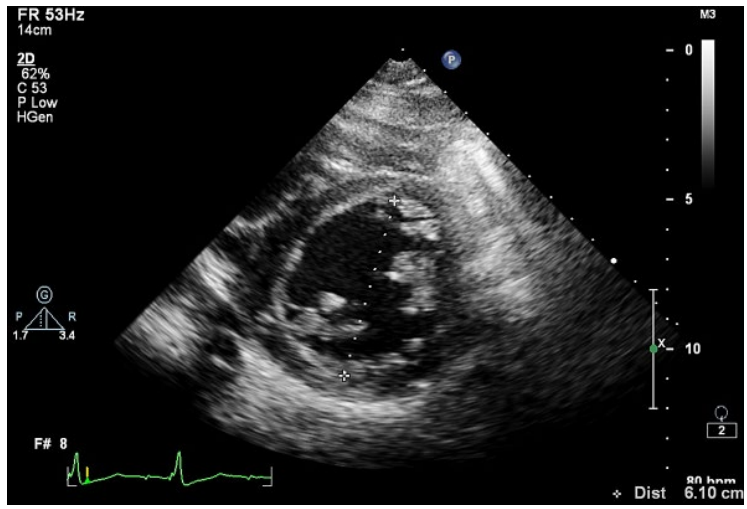

Figure 6.3 TTE short-axis: End-diastolic diameter.

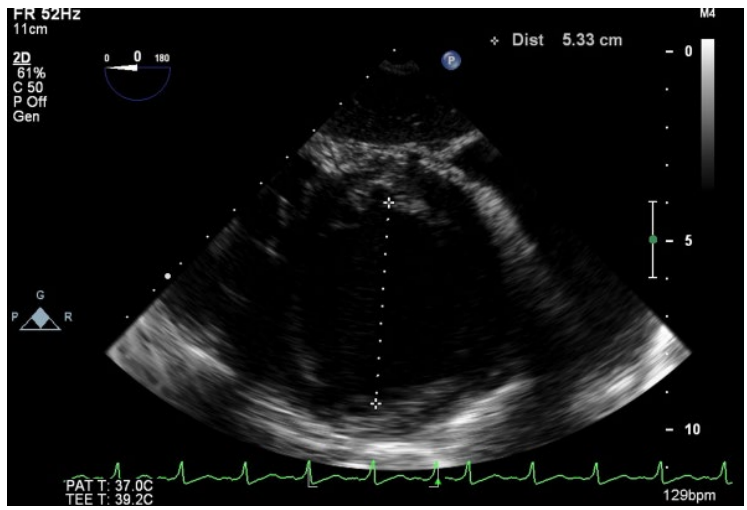

Figure 6.4 TOE transgastric short-axis: End-diastolic diameter.

Volume Status

Examination of trends in EDA and EDD are very useful, especially in conjunction with fluid challenge to assess the need for volume resuscitation. Video 6.6 shows a classic transgastric view with reduced EDA suggesting hypovolaemia. However, AS and hypertension both cause concentric hypertrophy, which creates a smaller EDA.

Young septic patients become severely hypovolaemic while maintaining blood pressure. Video 6.7 shows a swine-flu patient with inferior vena cava (IVC) collapse. Video 6.8 shows right ventricular collapse (not from the small pericardial effusion) and a dynamic left ventricle. Initial empiric management of low blood pressure will be fluid in the majority of cases.

Further information can come from looking at the mitral valve inflow E wave, which should be greater than 60 cm s^{-1} in a normal ventricle (Figure 6.5). Pulmonary vein inflow shows the S (systolic) and D (diastolic) wave. In this patient the S wave is less than D (Figure 6.6), but in

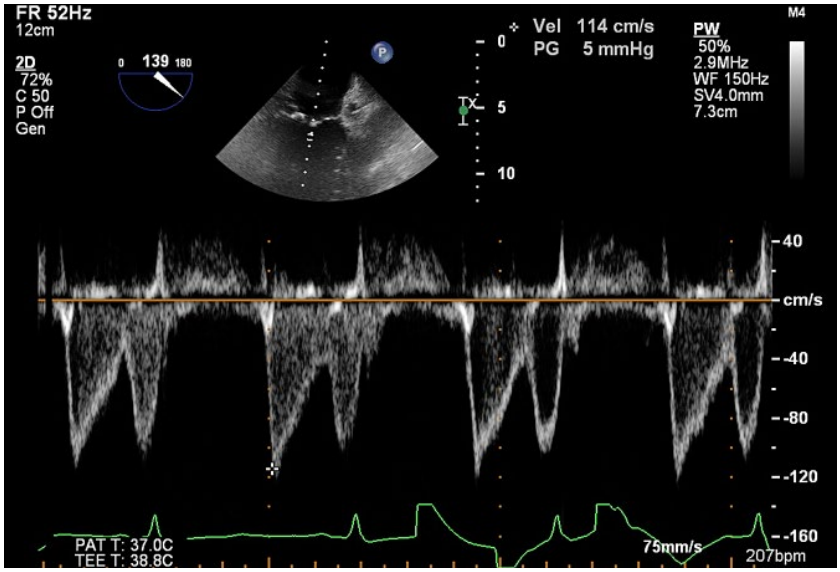

Figure 6.5 TOE Doppler tracing showing mitral inflow E and A waves.

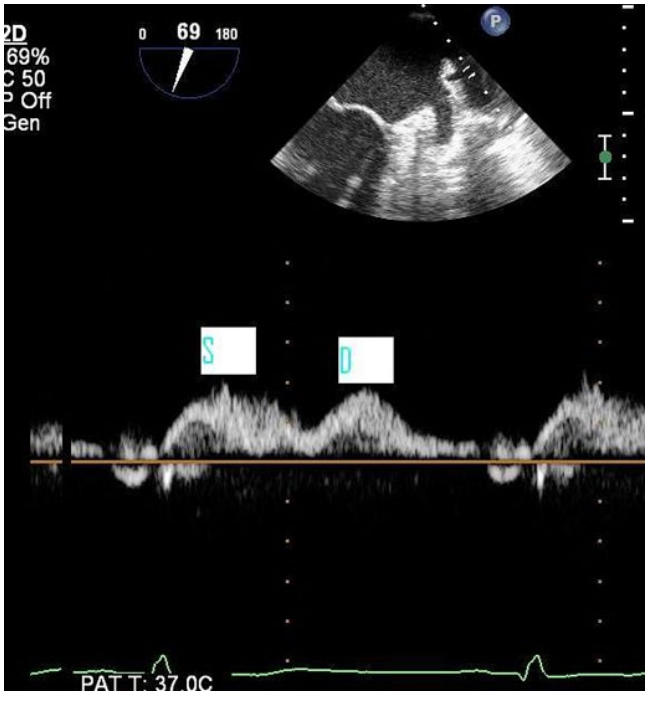

Figure 6.6 TOE pulsed-wave Doppler tracing of the left upper pulmonary vein showing systolic (S) and diastolic (D) flow. The velocity scale is not shown, but would ideally be lowered to give greater velocity resolution.

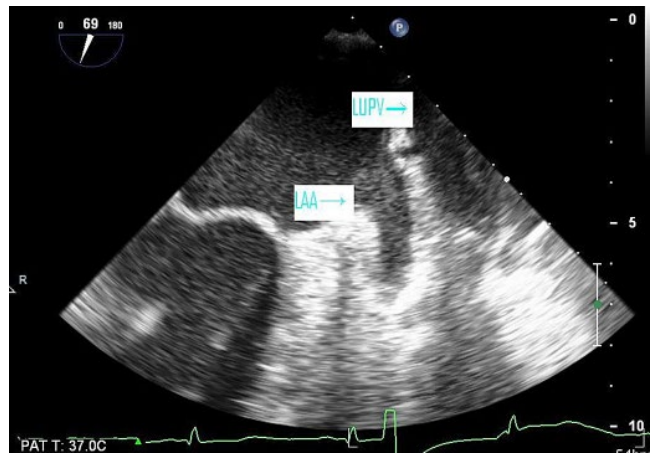

Figure 6.7 TOE anatomy of the left upper pulmonary vein (LUPV) and left atrial appendage (LAA).

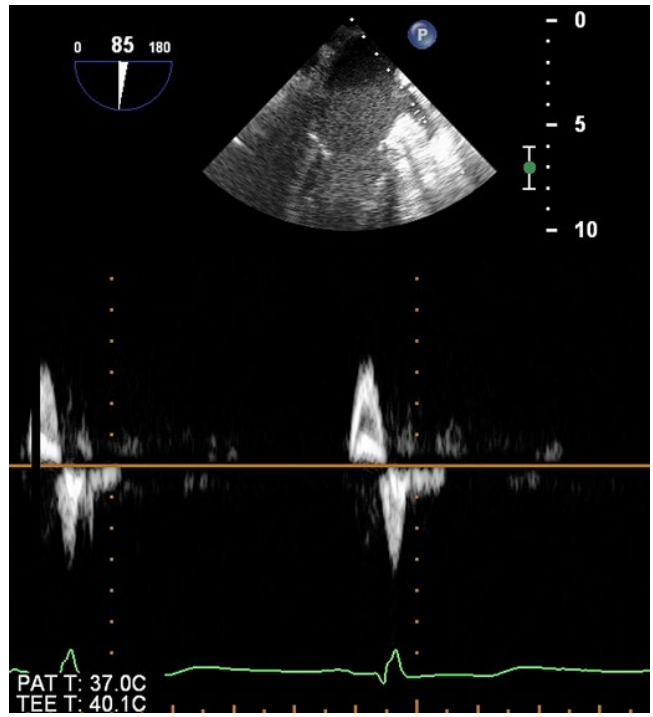

Figure 6.8 TOE view shown in Figure 6.7 with pulsed-wave Doppler trace of temporally limited (to systole) bidirectional flow in the left atrial appendage.

normal patients S > D. E <60 cm s^{-1} and S < D it suggest hypovolaemia. Pulmonary vein flow is best measured using TOE, and care is required to ensure that the measurement is within 1 cm of the vein opening, and that the Doppler gate is not placed in the left atrial appendage (LAA), which is found inferiorly (Figure 6.7) and also gives an entirely different Doppler pattern (Figure 6.8).

Pericardial Effusion

A large pericardial effusion >3 cm is easily identified on TTE and with clinical signs of tamponade has clear management. Small localised effusions can be confined to the right heart (Figure 6.9), even to the right atrium. Symptoms are variable but may present with palpitations caused by atrial arrhythmias. Caution is called

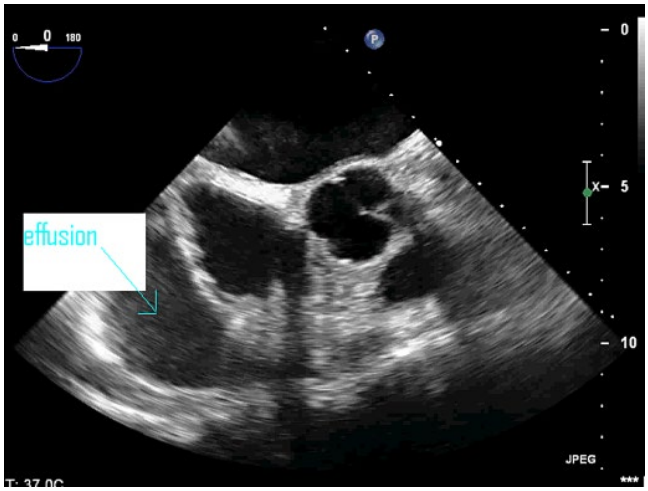

Figure 6.9 TOE view of right-sided pericardial effusion.

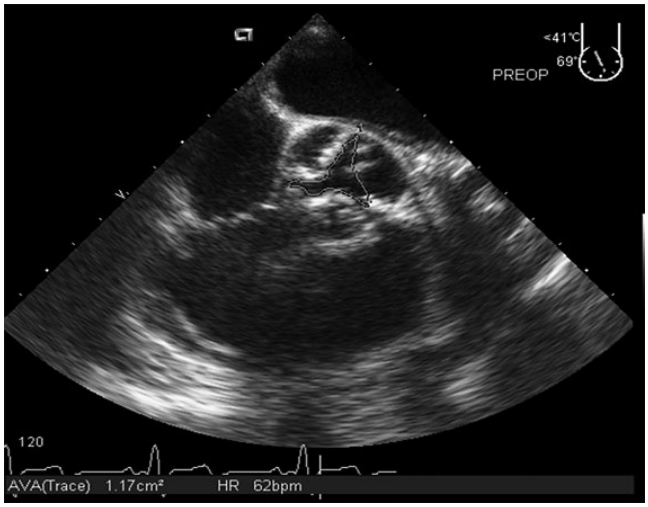

Figure 6.10 TOE view of a bicuspid aortic valve in short axis.

for since even 'small' loculated effusions have been known to cause cardiac arrest.

Valvular Pathology

Aortic stenosis is common. An area <1.0 cm^2 is severe, but lesser degrees can be important when the patient is stressed. The visualisation of leaflet mobility and planimetery in the short axis are useful (Figures 6.10 and 6.11). A bicuspid aortic valve is abnormal (Video 6.9). Velocity and gradients should be measured with an awareness of left ventricular function. With TOE, a transgastric view is required to obtain a continuous-wave Doppler signal if the window is not accessible on TTE. In general, a gradient of >50 mmHg or a velocity of >3 m s^{-1} is highly important. Aortic regurgitation is significant if the defect can be visualised in the short axis (Figure 6.12).

Mitral regurgitation is common, and post-myocardial infarction can present as a surgical emergency, diagnosed with echocardiography. Figure 6.13 shows a classic posterior leaflet prolapsed in a patient who had been undiagnosed and ventilated for three weeks. Subsequent surgical repair enabled the patient to leave hospital within two weeks. The evaluation

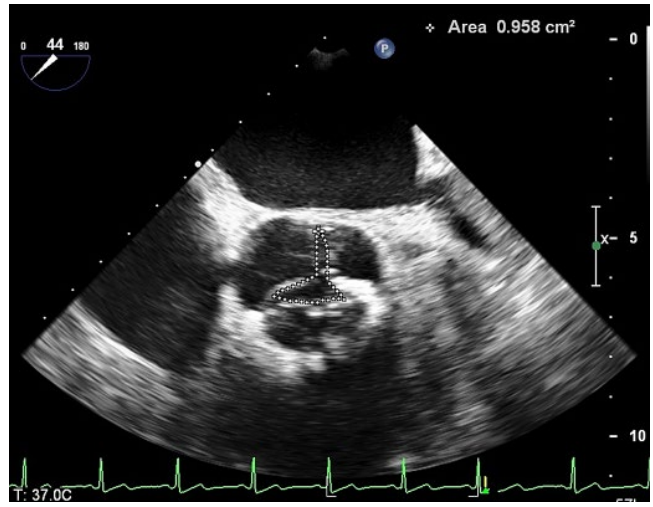

Figure 6.11 TOE view of the AV short axis: Aortic valve area (AVA) planimetry.

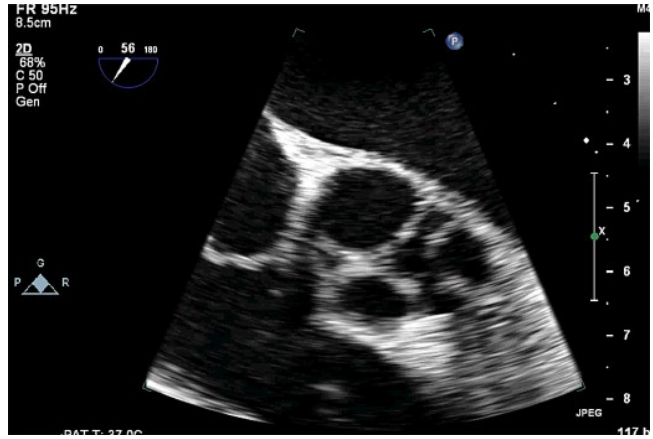

Figure 6.12 TOE transgastric AV long-axis view with continuous-wave Doppler gradient.

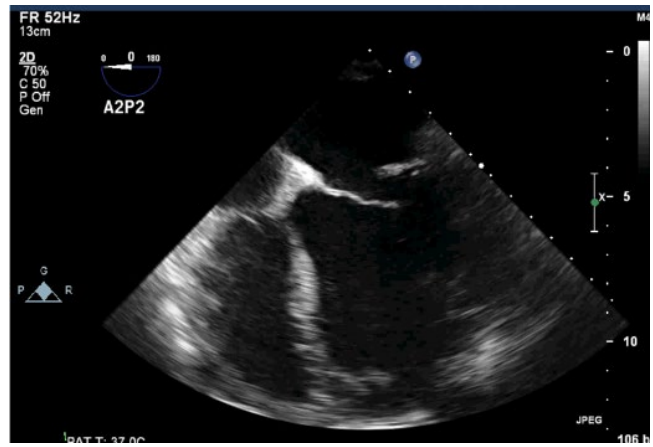

Figure 6.13 TOE four-chamber view: the prolapsing posterior mitral leaflet is on the right of the image. The anteior leaflet can be seen below (anterior in TOE) and to the left on the image. The structures below the valve (from right to left on the image) are the left ventricle, the septum, and the right ventricle.

of mitral regurgitation requires advanced echocardiography. Mitral stenosis is less common but is easily diagnosed by visualising the valve and measuring a Doppler-derived gradient. A mean gradient of >10 mmHg is significant.

Cardiac Tumours and Abnormal Soft-Tissue Masses

The most common cardiac soft-tissue mass is thrombus (Figure 6.14), which can occur in any chamber. It is a sign of a poor heart with a low blood flow. Atrial myxoma is uncommon, but rewarding if found; the patient may be asymptomatic intermittently symptomatic with light-headedness or syncope, or collapsed due to atrioventricular obstruction (Figure 6.15).

Endocarditis

Endocarditis may have become more common because of increased awareness of the disease. Increased prevalence of intravascular devices, intravascular procedures and injection drug use may also be responsible. It may occur in outpatients with fever of unknown origin, or in chronically hospitalized patients. Figure 6.16 shows the mid-oesophageal atrioventricular long-axis view. This requires TOE for confirmation, though further evaluation may be required, and always a follow-up. Long-term sequelae may be avoided if there is no valvular destruction.

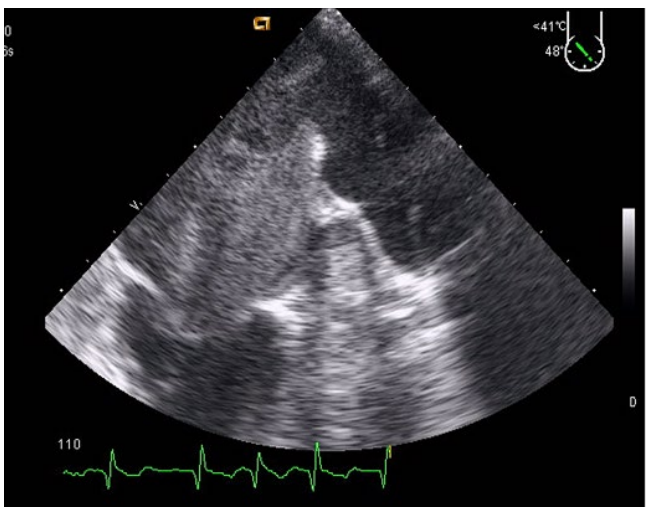

Figure 6.14 TOE rotated four-chamber mid-oesophageal view of left atrial-mitral stenosis and thrombus in the left atrial appendage (LAA).

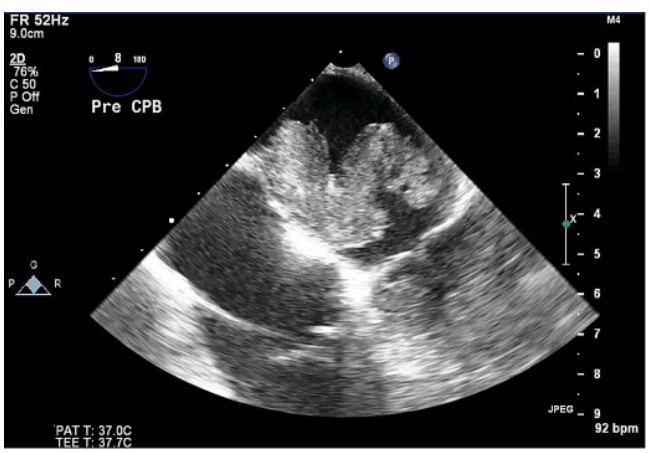

Figure 6.15 TOE four-chamber view: atrial myxoma.

Hypoxaemia

Echocardiography can help in the diagnosis of many causes of hypoxaemia, including commonly finding pleural effusions. As is true for many point-of-care ultrasound applications, the larger something is, the easier it is to see, such as in large effusions (Figure 6.17; TOE at atrioventricular level with the probe rotated). However, it is less easy when the effusion is smaller (Figure 6.18; TTE). The rule is always to look at the pleura when performing a scan. Drainage is indicated if hypoxia or pulmonary atelectasis is present (Figure 6.19), or if the diagnosis may be helped by taking a pleural fluid sample.

Atrial septal defects (ASDs) can be missed on TTE. If the index of suspicion is high, TOE evaluation can be done using the high mid-oesophageal four-chamber and the bicaval view (Figure 6.20).

Aortic Pathology

An important diagnosis not to miss is aortic dissection. It is not difficult to diagnose using echocardiography (Video 6.10) in the mid-oesophageal aortic long-axis view. This case shows both dissection and aneurysm. In many

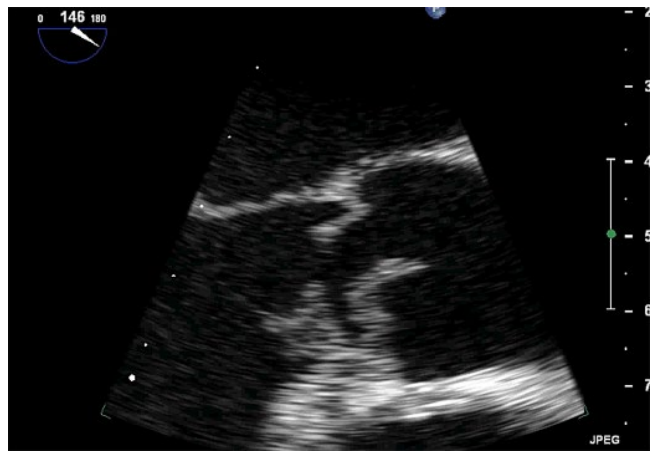

Figure 6.16 TOE long axis of the aortic valve showing loss of apposition of the valve leaflets with a vegetation under the anterior (lower in this view) leaflet due to endocarditis.

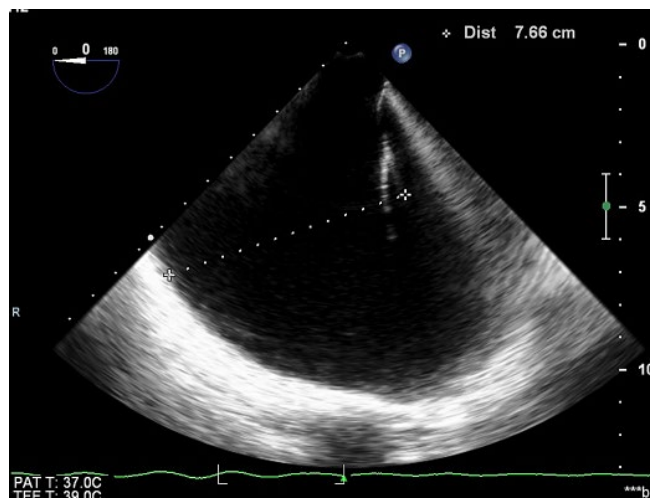

Figure 6.17 TOE: large pleural effusion.

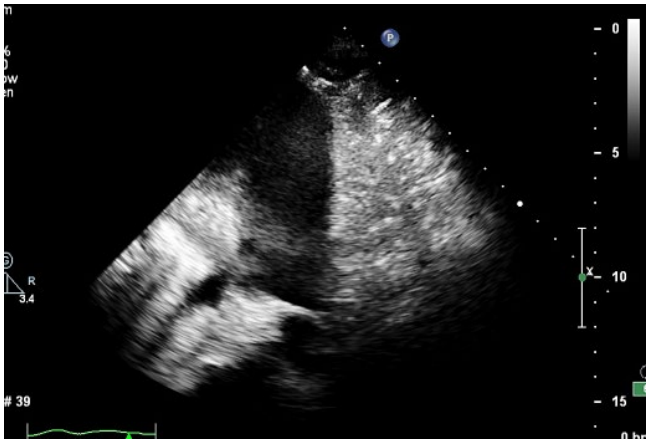

Figure 6.18 TTE: moderate pleural effusion.

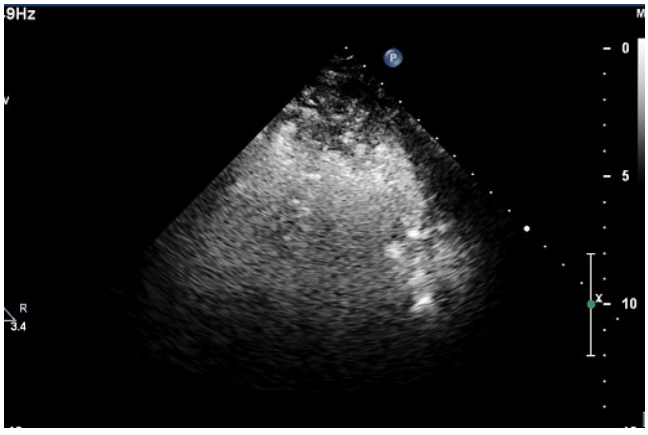

Figure 6.19 TTE: pulmonary atelectasis.

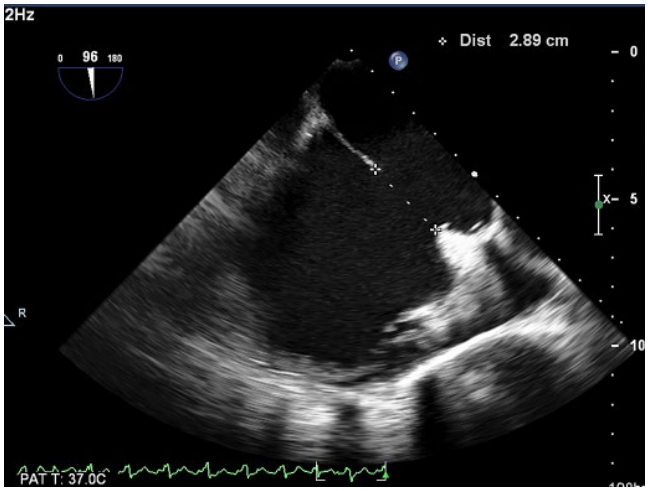

Figure 6.20 Rotated bicaval view of large atrial septal defect.

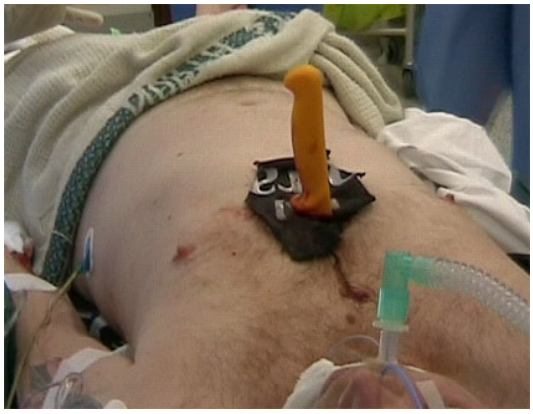

Figure 6.21 Knife stabbing in the chest.

cases there is aortic regurgitation, a chaotic flap, and a pericardial effusion. Considering the diagnosis may the most important part of identifying this disease.

Chest Trauma

Major vessel damage is often revealed by pleural and pericardial effusions. TOE can be very useful in avoiding unnecessary thoracotomy. For example, when a subject was stabbed in the chest with a knife (Figure 6.21), TOE showed that there was no internal bleeding and that key vascular structures were not involved. The knife was safely removed under continuous TOE surveillance. Chest trauma requiring ventilation is an indication for echocardiography.

Conclusions

Echocardiography has been shown to make a difference in critical care. For expediency, as well as avoidance of unnecessary transport, this should be performed at the bedside. TOE can enhance the level and detail of information available by TTE but is an invasive procedure with attendant risks. Much diagnostic and monitoring information is available from cardiac ultrasound. With increasing training and experience, both TTE and TOE are incrementally valuable to the clinician caring for critically ill patients.

Further Reading

Beaulieu, Y., Marik, P. (2005) Bedside ultrasonography in the ICU, Part 1. *Chest*, **128**, 881–895.

Bonow, R., Carabello, B.A., Chatterjee, K., *et al.* (2006) ACC/AHA 2006 Guidelines for the Management of Patients with Valvular Heart Disease. *J. Am. Coll. Cardiol.*, **48** (3), e1–e148.

Cheitlin, M.D., Armstrong, W.F., Aurigemma, G.P., *et al.* (2003) ACC/AHA/ASE Committee to Update the 1997 Guidelines for the Clinical Cardiology/American Heart Association Task Force on Practice Guidelines Echocardiography: Summary Article: A Report of the American College of ACC/AHA/ASE 2003 Guideline Update for the Clinical Application of Echocardiography. *Circulation*, **108**, 1146–1162.

Griffee, M.J., Merkel, M.J., Wei, K.S. (2010) Echocardiography in haemodynamic assessment of septic shock. *Crit. Care Clin.*, **26** (2), 365–382.

Habib, G., Badano, L., Tribouilloy, C., *et al.* (2010) Recommendations for the practice of echocardiography in infective endocarditis. *Eur. J. Echocardiogr.*, **11** (2), 202–219.

Kil, U.H., Jung, H.O., Koh, Y.S., *et al.* (2008) Prognosis of large, symptomatic pericardial effusion treated by echo-guided percutaneous pericardiocentesis *Clin. Cardiol.*, **31** (11), 531–537.

Kircher, B.J., Himelman, R.B., Schiller, N.B. (1990) Noninvasive measure of right atrial pressure from the inferior vena cava. *Am. J. Cardiol.*, **66**, 493–496.

Kjaergaard, J., Akkan, D., Iversen, K., *et al.* (2007) Right ventricular dysfunction as an independent predictor of short- and long-term mortality in patients with heart failure. *Eur. J. Heart Failure*, **9**, 610–616.

Labovitz, A.J., Noble, V.E., Bierig, M., *et al.* (2010) Focused cardiac ultrasound in the

emergent setting: A Consensus Statement of the American Society of Echocardiography and American College of Emergency Physicians. *J. Am. Soc. Echocardiogr.*, **23**, 1225–1230.

Price, S., Via, G., Sloth, E., *et al*. (2008) Echocardiography practice, training and accreditation in the intensive care: document for the World Interactive Network Focused on Critical Ultrasound (WINFOCUS). *Cardiovasc. Ultrasound*, **6**, 49.

Via, G., Breitkreutz, R., Price, S. (2009) Detailed echocardiography protocols for the critical patient. *J. Trauma*, **66** (2), 589–590.

Abdomen

7

Ultrasound Assessment of the Abdominal Aorta in the Acute Setting

Simon Richards

Introduction

The lifetime incidence of abdominal aortic aneurysm (AAA) is 8.9% in males and 2.2% in females, with the peak incidence occurring in males during their ninth decade of life. The main concern with AAA is rupture. For asymptomatic aneurysms, the risk of rupture is very low, at less than 2.0% per annum if the diameter of the aneurysm is less than 4.5 cm. For aneurysms of 4.5–5.5 cm, the risk is 2–4% per year. Once an aneurysm reaches 5.5 cm in diameter the annual risk of rupture equals or exceeds the risk of surgical intervention, and treatment will be considered – either open or endovascular repair. The mortality rate for an elective open repair is approximately 5%. These statistics apply only to asymptomatic aneurysms. Any aneurysm that is causing acute symptoms ('leaking', 'expanding') has a high rupture rate requiring immediate intervention, regardless of its size. If an AAA ruptures, the mortality rate is 60–80%, despite treatment, and therefore the key challenge for the physician evaluating a patient with abdominal pain in whom an aneurysm has been identified is to decide whether the symptoms are due to the aneurysm or something else.

Many patients with ruptured AAA present to the emergency department without the classic triad of pain, hypotension and pulsatile abdominal mass. Patients more often present with several alternative diagnoses – with the potential for delayed diagnosis and thus a catastrophic outcome. Clinical examination is unreliable, and whilst computed tomography (CT) is the reference standard for detecting a rupture (Figure 7.1), the patient must be haemodynamically stable before it can be considered. Moreover, CT may result in delays due to logistical and transport issues, as well as the risks arising from removal of the patient from the resuscitation area. Ultrasound (US) provides an opportunity to perform a highly accurate, quick and simple examination at the point-of-care (POC), to identify the presence or absence of an aneurysm. Once an AAA has been identified, appropriate management can be expeditiously planned without interruption of ongoing resuscitation.

The Abdominal Aorta

The abdominal aorta (aorta) originates at the diaphragm and is a continuation of the descending thoracic aorta. It lies anterior to the lumbar vertebrae within the retroperitoneum, and descends to the left of the midline to the level of the fourth lumbar vertebra (L4), where it bifurcates into the left and right common iliac arteries. It runs parallel and in close proximity to the left of the inferior vena cava (IVC). In adults, the normal calibre of the aorta is between 1.4 and

Emergency Point-of-Care Ultrasound, Second Edition. Edited by James A. Connolly, Anthony J. Dean, Beatrice Hoffmann and Robert D. Jarman.

Companion website: www.wiley.com/go/connolly/ultrasound

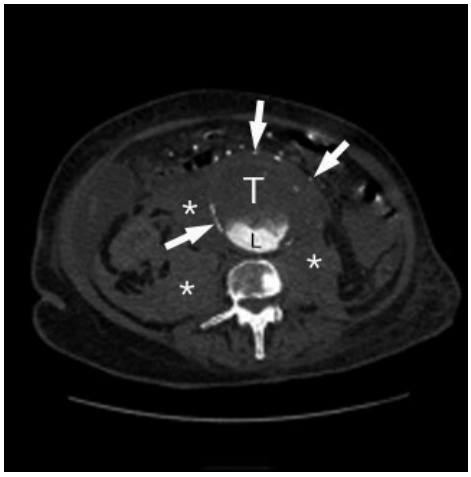

Figure 7.1 A ruptured abdominal aortic aneurysm on CT. The arrows indicate calcifications in the wall of the vessel, with adjacent retroperitoneal haematoma (*). Between the lumen filled with contrast (L) and the vessel wall is organized thrombus (T). Image courtesy of Maja Jafari.

2.5 cm. The widest diameter of the aorta is at the diaphragm, but it tapers as it descends to the bifurcation. The coeliac axis, superior mesenteric artery (SMA) and the renal arteries can readily be visualised and used to determine if an aneurysm is supra or infra-renal. The anatomy and the sonographic appearance of these structures can be seen in Figures 7.2–7.5.

The common iliac arteries bifurcate into the internal and external iliac arteries. The external iliac arteries pass inferiorly through the false pelvis medial to the psoas muscle to become the common femoral arteries as they traverse the inguinal canal. The internal iliac arteries descend into the true pelvis and supply blood to the pelvic organs and musculature. In adults, the calibre of the common iliac arteries is between 1.1 and 1.4 cm.

What is an Aneurysm?

An aneurysm is defined as a permanent, localised dilation of >50%, and involving all three layers of the vessel wall. As stated previously, the normal calibre of the aorta is between 1.4 and 2.5 cm, but once an aorta's maximum diameter

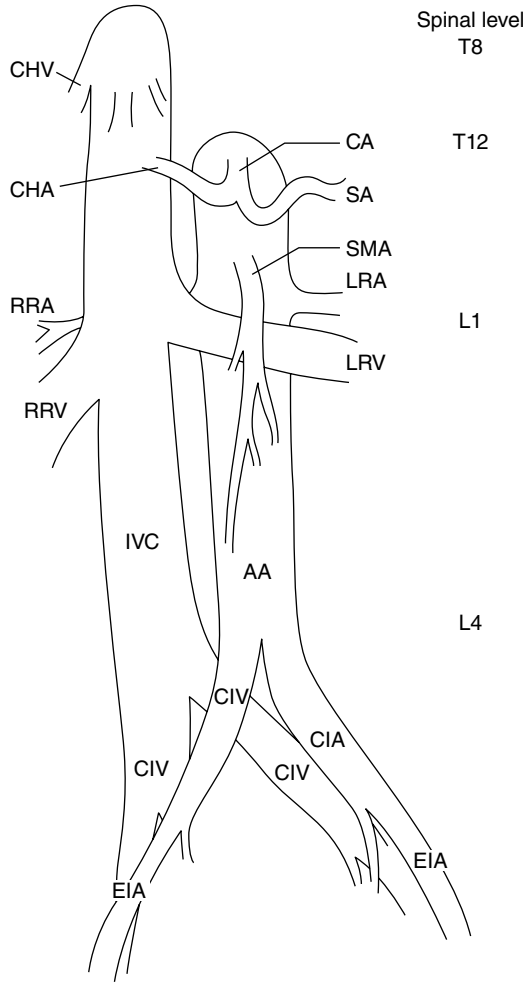

Figure 7.2 Line drawing showing major relationships with the great vessels of the abdomen.

reaches 3 cm it is classed as aneurysmal. An aortic diameter between 2.5 and 3 cm is described as ectatic, unless the section of aorta under examination is focally dilated by >50%, in which case it would be classified as a small aneurysm. The iliac arteries are defined as aneurysmal if their diameter is greater than 1.4 cm. Again, sizes can vary so it is worth comparing the diameter of the contralateral artery to gauge the true nature of the vessel.

Aneurysms vary in size, shape and location:

- An aneurysm with a dilation of the entire circumference of the vessel is termed '*fusiform*'.

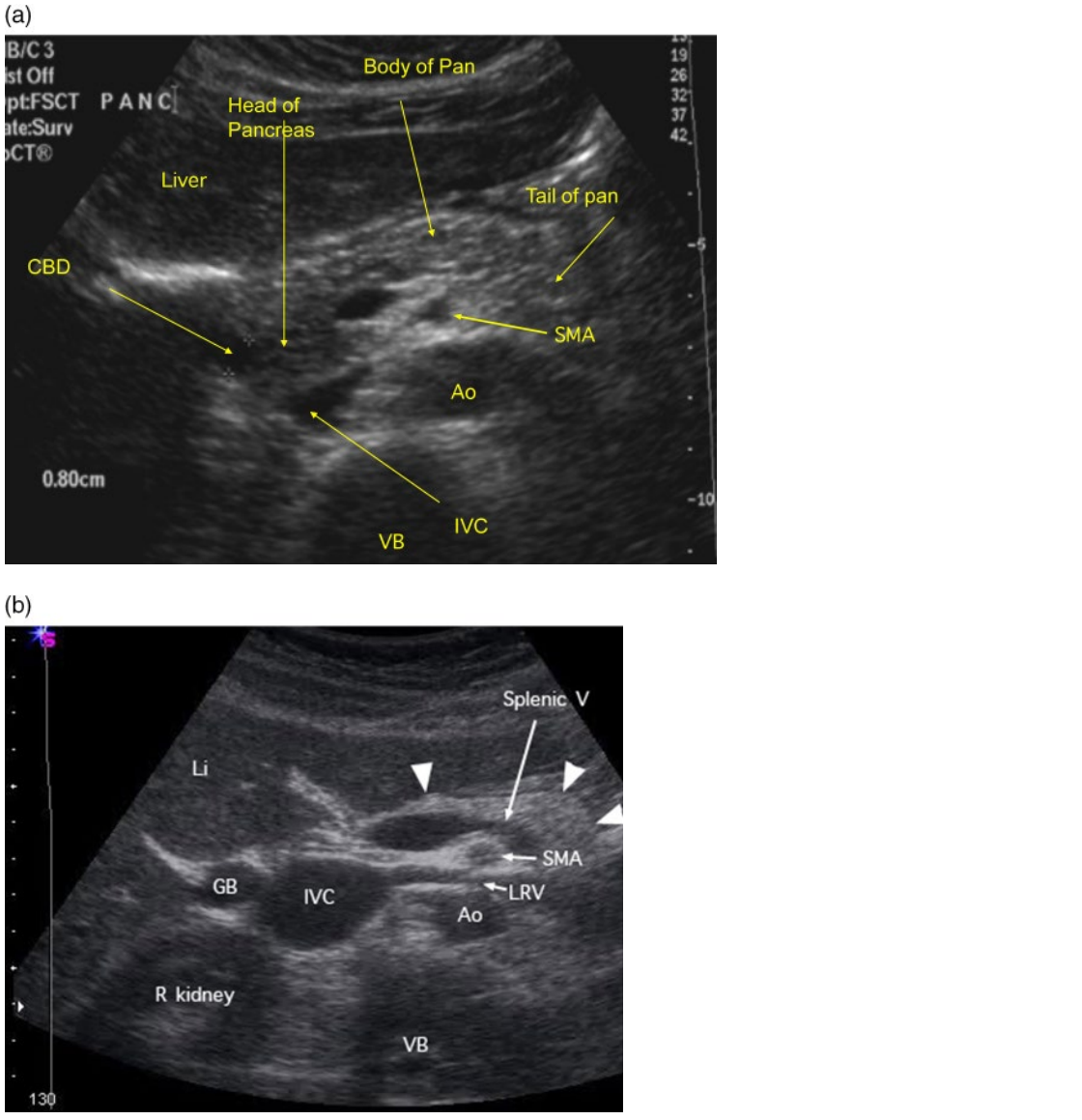

Figure 7.3 The anatomic structures seen in a transverse plane at the level of the pancreas in the upper abdomen. The vertebral body VB should be identified first, then, immediately anterior, the inferior vena cava (IVC) and aorta (Ao). The superior mesenteric artery (SMA) is usually directly anterior to the aorta. Anterior to that the splenic vein which runs posterior to the body and tail of the pancreas (arrowheads in b). The most anterior structure, forming a sonographic window is the liver (Li). CBD, common bile duct; GB, gallbladder; LRV, left renal vein.
Figure 7.3b © A.J. Dean.

- An aneurysm demonstrating a focal dilation of one part of the circumference is termed '*saccular*'.
- A '*dissection*' occurs when the intima, media or adventitia separate from one another, allowing for thrombus formation and/or a pseudolumen within the arterial wall. Dissections can occur in normal-calibre vessels or be associated with aneurysms. Dissections can frequently be identified but

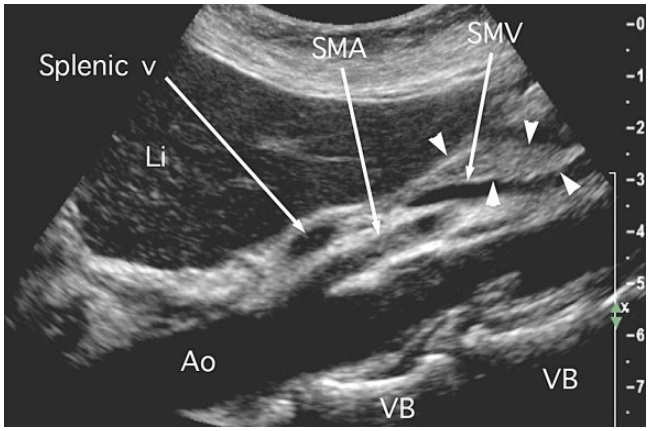

Figure 7.4 Aorta shown in the longitudinal plane. The aorta (Ao) lies immediately anterior to the vertebral bodies (VB). Arrowheads indicate the body of the pancreas overlying the superior mesenteric vein (SM). In many patients, the liver (Li) does not provide such a good sonographic window. SMA, superior mesenteric artery, SMV superior mesenteric vein.

(a)

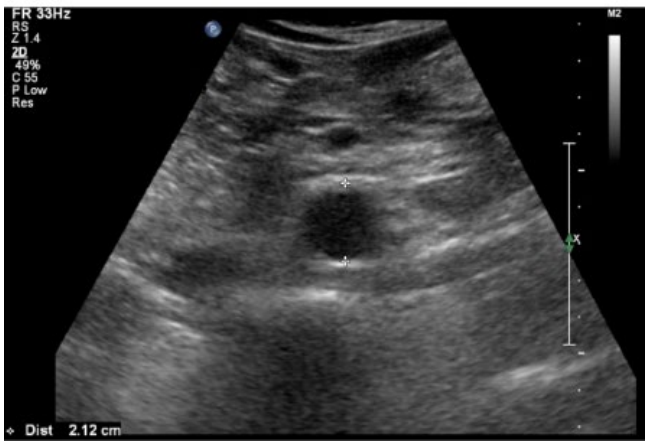

(b)

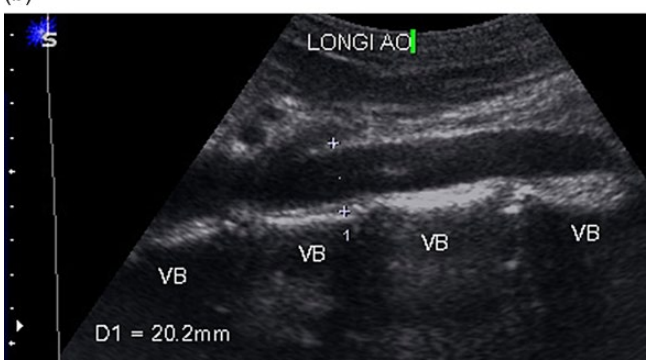

Figure 7.5 Transverse (a) and longitudinal (b) views of the aorta. In panel (a) the posterior calliper is mistakenly placed on the inside rather than the outside wall. Figure 7.5b © A.J. Dean.

cannot be reliably excluded using POC ultrasound (Video 7.5).
- The location of the aneurysm should be determined. They can be '*supra-renal*', '*infra-renal*', or both.

How to Scan the Abdominal Aorta and Iliac Arteries

The following describes an effective examination which can be performed at the POC, to identify the presence or absence of an AAA. An ultrasound examination performed by imaging specialists typically take up to 20 minutes, and include a level of detail which is not required in the acute setting or emergency department.

An AAA can only be excluded if the aorta is seen along its entire length in both the longitudinal and transverse planes.

Equipment and Presets

- A curvilinear, low-frequency transducer around 3 MHz is ideal.
- An abdominal preset should be used, with a medium to low dynamic range.
- Standard general ultrasound orientation should be used.
- The depth should be set below the surface of the vertebral body and the focus at the level of the great vessels, and adjusted throughout the examination to optimise image quality.
- Harmonic imaging may help in the presence of bowel gas.
- B-mode imaging and anatomic landmarks should be used to differentiate between the aorta and IVC, *not Doppler imaging*.

Normal Appearances of the Abdominal Aorta and Inferior Vena Cava

Although it might seem obvious, the aorta and IVC can be mistaken for one another by less-experienced sonologists. The key features of each are listed in Table 7.1. It should be noted that both the aorta and IVC are *pulsatile vessels*.

Table 7.1 How to differentiate between the aorta and the IVC.

IVC	Aorta
To the right of the midline	To the left of the midline
Enters the abdomen high (T8), immediately below the right atrium. Runs through the liver with anterior entry of hepatic veins	Enters the abdomen relatively low (inferior to the liver, around T12)
Has no anterior branches below hepatic veins	Has prominent anterior branches in abdomen (coeliac and SMA)
Thin-walled	Thick-walled (two distinct components are visible with a high-quality ultrasound machine)
No calcification	Calcification may be present
Pulsatility: both vessels are pulsatile	
Shape varies from round to slit-like	Round shape
Larger unless compressed or slit-like	Smaller unless aneurysmal
Can be compressed in slim patients, and demonstrates respiratory variation unless plethoric or completely collapsed.	Non-compressible, no respiratory variation.
Can be seen entering right atrium	Sometimes seen posterior to heart (usually obscured by lung below level of heart in sub-xiphoid window)

The Technique

1) Place the probe in transverse section (TRV) on the patient's midline immediately below the xiphisternum. For less experienced sonologists, the vertebral body is the first structure to identify because it defines the location of the great vessels (they are found immediately anterior) and the appropriate depth. The left lobe of the liver, the aorta, and the IVC should be identified (Table 7.1 and Figures 7.2a and 7.5a). The sector width may be narrowed to optimise image quality. The probe is slid and fanned – depending on available sonographic windows between loops of the bowel – inferiorly to the bifurcation to examine the entire length of the vessel. Scanning should be systematic and methodical to avoid skipping any areas of the vessel (Video 7.1a).
2) To obtain longitudinal images, the probe is again placed on the patient's midline immediately below the xiphoid process. When a longitudinal image is found (Figures 7.4 and 7.5b; Video 7.1b) the transducer is slid or rocked caudally to the bifurcation.
3) The aorta should be measured at its widest point in the antero-posterior (AP) plane (Figures 7.5–7.7). The vessel should be measured 'outside wall to outside wall' (the

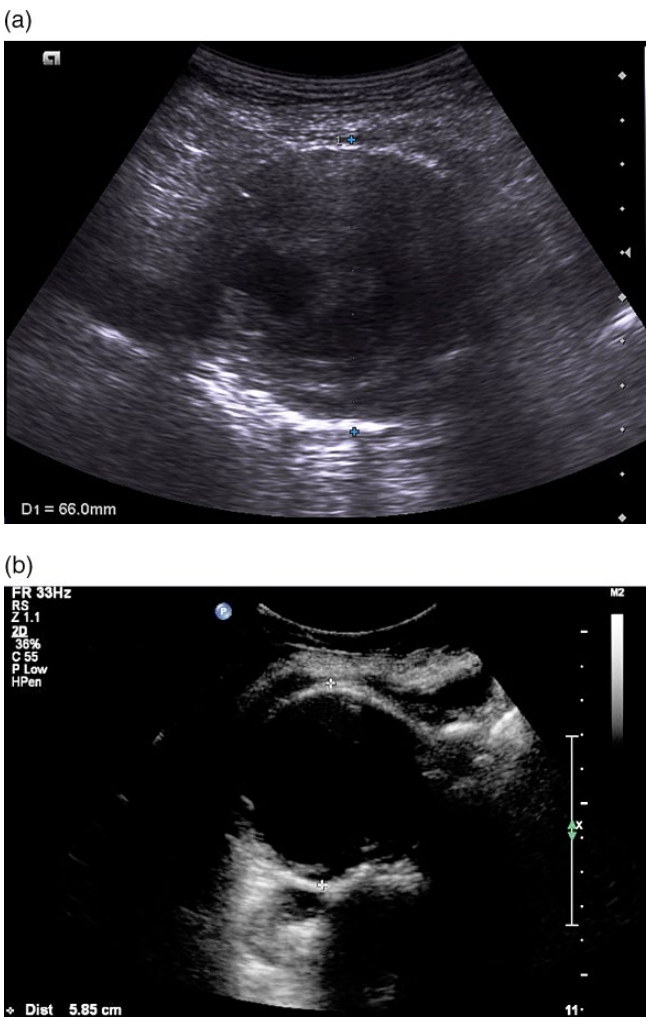

Figure 7.6 Transverse images of two large aortic aneurysms. (a) The extensive intraluminal thrombus can be appreciated in (a). In (b) The dynamic range has been set lower, making it more difficult to appreciate thrombus, but with the advantage that it is easier to identify the aortic wall. In panel (b) the posterior calliper is mistakenly placed on the inside wall. Figure 7.6a © A.J. Dean.

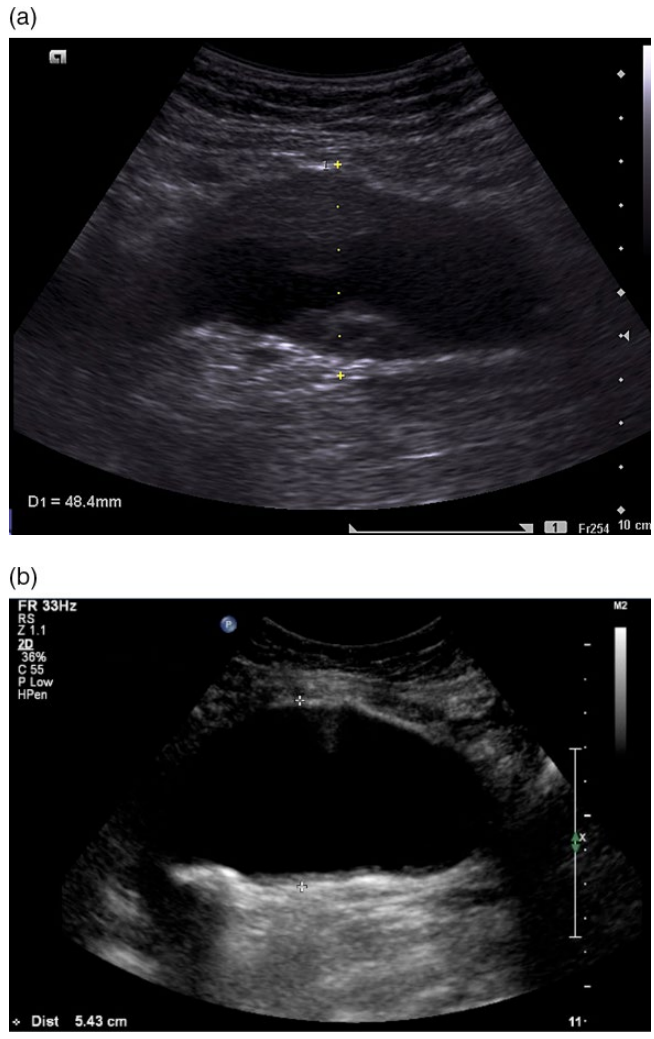

Figure 7.7 The aneurysms seen in Figure 7.6 are shown here in longitudinal section. Both figures again show the effects of high (a) and low (b) dynamic range settings. Figure 7.7a © A.J. Dean.

anterior of the anterior wall to the posterior of the posterior wall).

4) If an AAA is present, its origin and extent should be determined – if clinical circumstances allow. It is relatively simple to see if the aneurysm extends to the bifurcation; however, it is considerably more difficult to identify the renal arteries. If the latter cannot be identified, the SMA and celiac arteries arise 1 and 2 cm, respectively, above the renal arteries, allowing for estimation of their location. Alternatively, if the superior extent of the aneurysm is inferior to the pancreas it is infra-renal.
5) The iliac arteries can also be examined using ultrasound, although an isolated aneurysm without AAA is rare and the assessment is often more technically challenging. They can be demonstrated in both longitudinal and transverse section. The iliac arteries should be measured at the widest point in the AP plane (Figures 7.8 and 7.9).
6) Coronal. If the aorta is obscured by bowel gas it may be possible to image it by scanning in the mid-axillary line using the coronal plane. The spleen or liver serve as acoustic windows on the left or right, respectively (Figure 7.10). This examination is technically

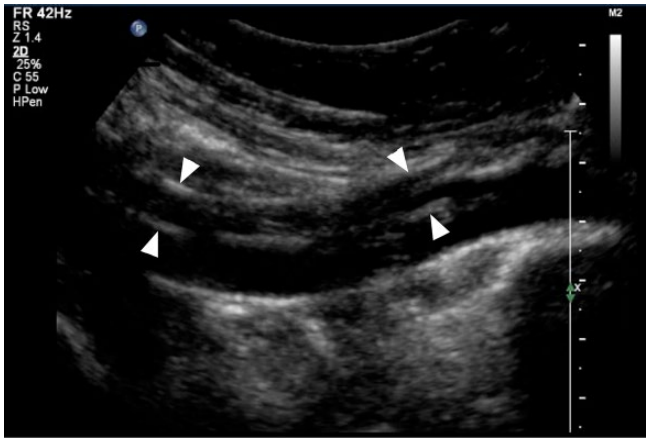

Figure 7.8 The external iliac artery (between arrowheads) is typically more superficial than the vein, as in this image. In most patients, especially those with higher body mass index, bowel gas prevents a complete assessment of the iliac vessels.

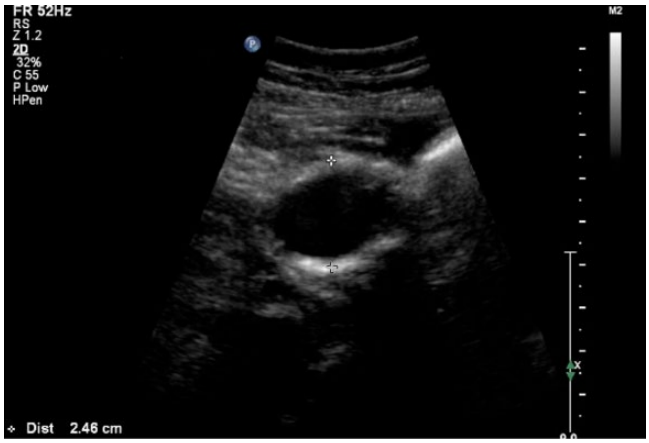

Figure 7.9 An iliac artery aneurysm, identified between the callipers.

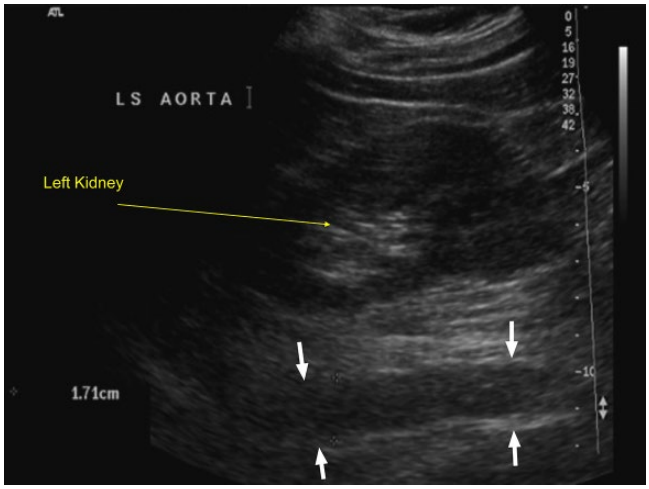

Figure 7.10 This coronal view of the aorta (between arrows) through the left flank may be useful in cases where the vessel is obscured by bowel gas. It may also be identified from the right, using the liver as a window, in which case it will be seen deep to the inferior vena cava.

challenging and rarely allows for uninterrupted imaging of the entire length of the vessel.

Ultrasound Appearances of an Aneurysm

On ultrasound, an aneurysm appears as an abnormal dilatation of the artery (see Figures 7.6 and 7.7; Videos 7.2–7.4). Thrombus is commonly seen within the lumen, and calcification may occur within the arterial wall or within chronic thrombus, casting an acoustic shadow. When measuring an AAA it is very important to *measure from the outside of the arterial walls*, not the lumen of the artery or the flow channel within the thrombus.

How to Measure an AAA

When measuring the aorta, the widest point should be chosen and the callipers should be carefully placed on the *outside of the walls* to measure the vessel in the AP and transverse planes. When measuring any tubular structure it is important to achieve a 'true' section (see Figures 7.11 and 7.12). Ideally, the ultrasound beam should be perpendicular to the vessel for all measurements. Many factors can undermine the accuracy of measurement, but since the primary goal in the acute setting is to avoid missing the diagnosis (false-negative findings), it is important to understand which errors may lead to an *underestimation* of the diameter of the vessel. If the ultrasound beam is not perpendicular in the transverse view, the obtained section will be oblique (see Figure 7.11). This error is sometimes referred to as 'salami slicing' and will give rise to an overestimation of the diameter.

Conversely, if the longitudinal plane is off the central axis of the vessel (see Figure 7.12), the true diameter of the vessel will be underestimated. Other factors that should be borne in mind include:

Figure 7.11 Demonstration of how, in transverse imaging, the diameter of the vessel can be overestimated when the imaging plane is not exactly perpendicular to the vessel.

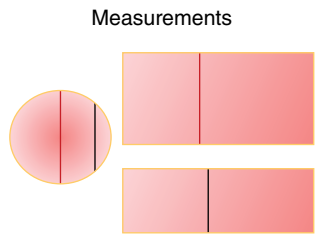

Figure 7.12 Demonstration of how the true diameter of a vessel can be underestimated in the longitudinal plane if the scanning plane is not at the widest part of the vessel.

- Ultrasound has very good axial resolution, and measuring in the AP plane utilises this benefit.
- Measurements in the transverse plane may be less accurate for two reasons: (i) the lateral borders of the vessel may be obscured by edge artefact; and (ii) ultrasound has relatively poor lateral resolution.

Both planes should be scanned in order to perform the most reliable sonographic evaluation. The transverse plane demonstrates the entire circumference of the vessel at any given level, allowing for detection of a saccular aneurysm in the lateral walls of the vessel. These can easily be overlooked in the longitudinal plane, which tends to focus on the anterior and posterior walls. However a complete scan depends on exhaustive real-time visualization of the entire vessel from the diaphragm to the bifurcation without any skipped regions. This can be challenging due to bowel gas, especially in the transverse colon,

which can often extend for up to 5 cm across the epigastrium. The transverse plane is also advantageous in patients with ectactic aortas, since the irregular morphology of these vessels makes it impossible to obtain a true longitudinal section. Furthermore, as noted above, the transverse plane has the advantage that it cannot result in an *under*estimation of aortic diameter. Conversely, the longitudinal plane may result in underestimation of the vessel but it allows for assessment of the location and extent of an aneurysm. The relative advantages and disadvantages of the two scanning planes are reviewed in Videos 7.2–7.4. As noted previously, aneurysms should be measured from outside wall to outside wall.

Ultrasound Appearances of Open Repair and Endovascular Aortic Repair (EVAR) Stent Grafts

It is important to remember that a previous repair does not exclude a patient from having a ruptured AAA, usually caused by leakage at the site where the endovascular graft was sutured to the native aorta ('endoleak'). This may result in leakage of blood into the native vessel surrounding the graft and result in pressures within the aneurysm that can lead to rupture. Less commonly, new aneurysms can form *de novo* in the native vessel above or below the graft. When examining a patient who has had a repair of an AAA a residual aneurysm sac will be seen, as neither method – EVAR or open repair – removes the dilated section of artery. Within the sac the prosthetic vessel appears as an echogenic tubular structures; thrombus may also be seen surrounding it (see Figure 7.13).

Pearls and Pitfalls

- Saccular aneurysms are localised and *may occur on any surface of an otherwise normal-appearing aorta*. For this reason, the aorta should be systematically examined along its length without any skip areas, especially in the transverse plane.
- Bowel gas, obesity and calcification will limit the diagnostic quality of the examination. A 'jiggling' motion of the transducer combined with pressure may succeed in displacing bowel gas. Sometimes windows can be obtained off the median plane.
- The extent of the aneurysm and/or rupture are most accurately demonstrated using CT.
- Edge artefact may make the lateral wall of the aorta difficult to evaluate.
- *Do not measure the flow channel inside the thrombus of the aneurysm. Measure the outer limit of the vessel walls!* This pitfall most commonly occurs due to excessive gain. Set gain so that the column of blood within the vessel appears *black*, and clearly identify the outer limit of the vessel wall.
- Longstanding aneurysms frequently contain thrombus that is heavily calcified, making the error described in the previous pitfall even more likely to occur. Again, this pitfall can best be avoided by optimal gain adjustment, and fairly low dynamic range settings.
- The *presence of an AAA does not mean that it is necessarily responsible for the patient's abdominal pain*. Ultrasound findings should be interpreted according to the clinical context.
- A *small AAA (4–5 cm) can still become symptomatic*, with the potential for acute rupture.
- The *absence of free abdominal fluid does not exclude acute AAA*. Most patients with acute AAAs that survive long enough to be evaluated in a healthcare facility have ruptured into the retroperitoneal space, causing temporary stabilisation. By definition, such haemorrhage will not result in intraperitoneal free fluid.
- Ultrasound does not reliably identify even very large retroperitoneal haematoma.
- If an examination is limited due to bowel gas or for other technical reasons, record this in the documentation, and incorporate it in the clinical decision-making based on the ultrasound.
- If an AAA is detected in a patient in shock, it should be presumed to be ruptured or leaking until proven otherwise.

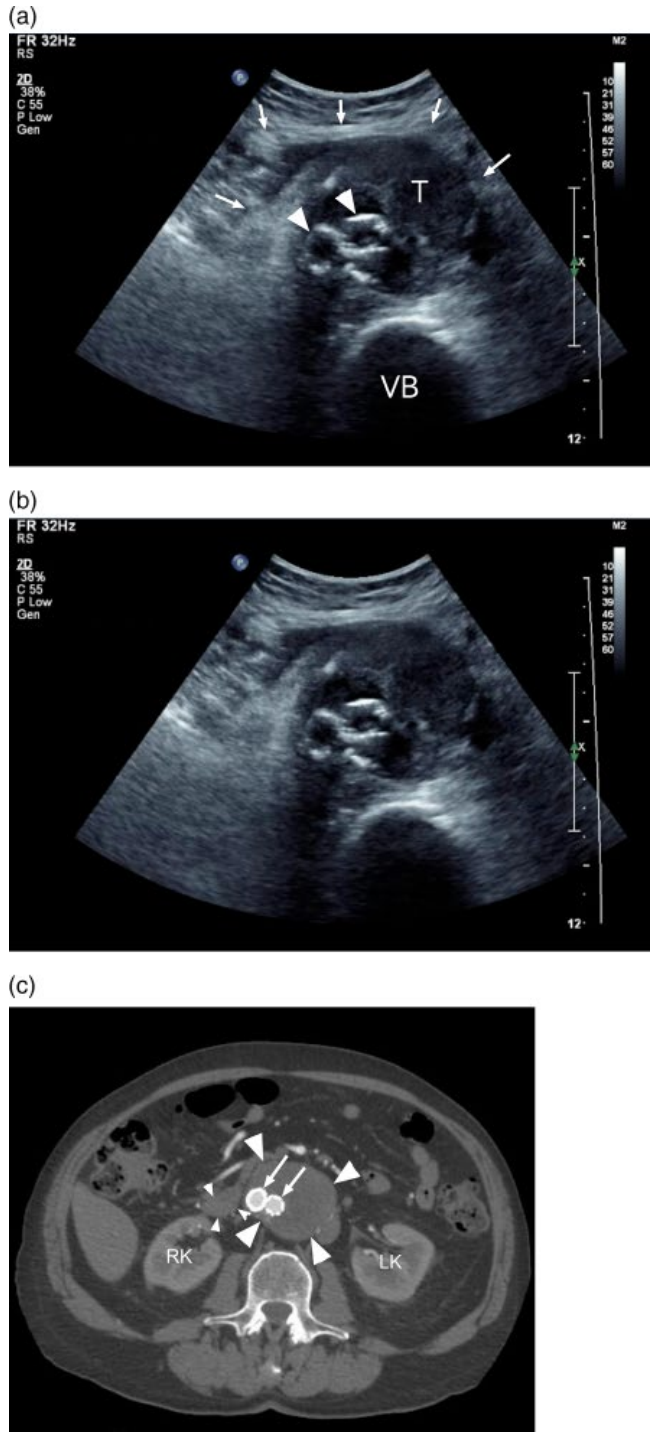

Figure 7.13 (a) A transverse ultrasound image of an AAA (arrows) containing an endovascular stent (arriwheads) supplying the iliac arteries. There is echogenic thrombus (T) within the vessel, as well as some anechoic uncoagulated fluid. To determine whether this fluid is chronically or acutely leaking blood, colour-flow Doppler analysis needs to be made. Anterior to the vessel there is a small anechoic area which could be due to chronic inflammation but could also be suspicious for leakage. (b) The same image as in panel (a) but without markers. (c) A CT image from the same patient. Note that the endovascular stents (arrows) appear to contain highly radiopaque contrast material, without any evidence of leakage into the aneurysmal native aorta (large arrowheads). The compressed inferior vena cava can also be seen (small arrowheads). [RK: right kidney; LK: left kidney). (CT image courtesy of Maja Jafari.)

- An AAA can only be excluded if the aorta is examined along its length in both the longitudinal and transverse planes.
- The accuracy of ultrasound evaluation of the aorta is *correlated with experience*. In this application of clinician-performed ultrasound (as in all others), practice makes more perfect, and less-experienced sonologists should exercise particular caution in their clinical decision-making based on the ultrasound.

Further Reading

Basnyat, P.S., Biffin, A.H.B., Moseley, L.G., Hedges, A.R., Lewis, M.H. (1999) Mortality from ruptured abdominal aortic aneurysm in Wales. *Br. J. Surg.*, **87** (7), 966–967.

Brady, A.R., Fowkes, F.G.R., Greenhalgh, R.M., Powell, J.T., Ruckley, C.V., Thompson, S.G. (2000) Risk factors for postoperative death following elective surgical repair of abdominal aortic aneurysm: results from the UK Small Aneurysm Trial. *Br. J. Surg.*, **87** (6), 742–749.

Concannon, E., McHugh, S., Healy, D.A., Kavanagh, E., Burke, P., Moloney, C.M., Walsh, S.R. (2014) Diagnostic accuracy of non-radiologist performed ultrasound for abdominal aortic aneurysm: systematic review and meta-analysis. *Int. J. Clin. Pract.*, **68** (9), 1122–1129.

Costantino, T., Bruno, E., Handly, N., Dean, A.J. (2005) Accuracy of emergency medicine ultrasound in the evaluation of abdominal aortic aneurysm. *J. Emerg. Med.*, **29**, 455–460.

Hoffmann, B., Bessman, E., Um, P., Ding, R., McCarthy, M.L. (2011) Successful sonographic visualisation of the abdominal aorta differs significantly among a diverse group of credentialed emergency department providers. *Emerg. Med. J.*, **28** (6), 472–476.

Kunh, M., Bonnin, R.L.L., Davey, M.J., Rowland, J.L., Langlois, S.L.P. (2000) Emergency department ultrasound scanning for abdominal aortic aneurysm: accessible, accurate, and advantageous. *Ann. Emerg. Med.*, **36** (2), 219–223.

Rubano, E., Mehta, N., Caputo, W., Paladino, L., Sinert, R. (2013) Systematic review: emergency department bedside ultrasonography for diagnosing suspected abdominal aortic aneurysm. *Acad. Emerg. Med.*, **20** (2), 128–138.

Singh, K., Bonna, K.H., Jacobsen, B.K., Bjork, L., Solberg, S. (2001) Prevalence of and risk factors for abdominal aortic aneurysm in a population-based study. The Tromso Study. *Am. J. Epidemiol.*, **154** (3), 236–244.

Studer, M., Hempel, D., Rouhani, S., Dubsky, H., Pivetta, E., Kimberly, H. (2014) Addition of a lateral view improves adequate visualisation of the abdominal aorta during clinician performed ultrasound. *Am. J. Emerg. Med.*, **32** (3), 256–259.

Vardulaki, K.A., Prevost, T.C., Walker, N.M., Day, N.E., Wilmink, A.B.M., Quick, C.R.G., Ashton, H.A., Scott, R.A.P. (1998) Growth rates and risk of rupture of abdominal aortic aneurysms. *Br. J. Surg.*, **85**, 1674–1680.

8

Focussed Assessment with Sonography in Trauma – The FAST Exam

Rajat Gangahar

Introduction

The prompt recognition and treatment of occult sources of haemorrhage is the cornerstone of initial management of patients with major trauma. Four common sites in the body – the chest, abdomen, long bones and pelvis/retroperitoneum – and one outside it should be evaluated ('blood on the floor and four more'). Among these sites, the pleural and peritoneal cavities are a major diagnostic challenge due to their ability to conceal large volumes of blood without specific symptoms and signs until haemorrhage is far advanced. Ultrasound has been described as an aid in the evaluation of truncal trauma since the 1970s, and over the past two decades it has become established as an important screening tool in this setting.

Ultrasound was initially directed to the diagnosis of haemopericardium, but its role was soon extended to the detection of abnormal free fluid in the pleural and peritoneal spaces. This integrated, limited, focussed examination became known as the Focussed Assessment with Sonography in Trauma (FAST). Although, in the context of trauma, abnormal free fluid is presumed to be blood, the clinician must be mindful that chronic medical conditions may be the basis of these findings. The FAST exam is *not directed to the identification of solid organ or hollow viscous injuries*, since the technique required for these requires advanced skills and a more time-consuming examination.

Computed tomography (CT) scanning provides detailed solid organ evaluation, and is the 'gold standard' for assessing abdominal injury in patients who are physiologically stable. Unfortunately, CT requires the transport of patients out of the resuscitation suite, which limits its utility for patients who are unstable. Diagnostic peritoneal lavage (DPL) is now rarely used, but it has a higher sensitivity than FAST for detecting intra-abdominal blood. However, such high sensitivity results in a lower specificity, with non-therapeutic laparotomies reported at rates of between 6% and 26%. DPL is also an invasive procedure that is susceptible to complications.

To date, published data have shown that FAST performed by emergency physicians has a specificity of 95–100% and a sensitivity between 69% and 98%. FAST can probably detect as little as 250 ml of free fluid in Morrison's pouch, the test being rapid, repeatable and without contraindications. The exam is an adjunct to clinical assessment and not a substitute for it. A negative FAST does not exclude the presence of intra-abdominal blood, especially when pre-test suspicion is high. The scan may be repeated if initially negative, and this has been shown to increase sensitivity. Due to a higher specificity than sensitivity, the FAST exam – like many point-of-care ultrasound applications – is better at ruling-in pathology than at excluding it.

Emergency Point-of-Care Ultrasound, Second Edition. Edited by James A. Connolly, Anthony J. Dean, Beatrice Hoffmann and Robert D. Jarman.

Companion website: www.wiley.com/go/connolly/ultrasound

The FAST Technique

A low-frequency (2.5–5 MHz) transducer is used for this application. A curved-array general abdominal probe is commonly used, although a phased-array or small-footprint curvilinear transducer may also be used.

Free fluid appears black on ultrasound, and it is sought in potential spaces that are interrogated via four standard 'windows' or 'views' (see Figure 8.1):

- Right upper quadrant (RUQ; includes right pleural space).
- Left upper quadrant (LUQ; includes left pleural space).
- Pelvic view.
- Sub-xiphoid view.

Acute haemorrhage may have a grey echotexture if it has formed clots, and the latter may be difficult to distinguish from fat (especially omentum). If clotted blood is suspected the sonologist should look for tell-tale areas of black unclotted free fluid. The order of the FAST views can be modified based on the patient's mechanism and pattern of injury.

The Right Upper Quadrant (RUQ) View

This view is commonly done first. More than 60% of positive FAST examinations will show evidence of free fluid in this location. The view should enable visualisation of both the hepatorenal and subphrenic potential spaces and the right costophrenic recess of the pleural cavity.

The transducer is initially placed in the anterior axillary line, but with a generous application of coupling gel, allowing the sonologist to range freely to find the best intercostal space. Optimal windows are usually obtained using a plane that is parallel with the ribs. The marker is directed posteriorly and cephalad in this plane. The initial depth setting should be set to around 15 cm. The goal is to obtain a *complete dynamic examination of each of the potential spaces* of concern rather than a series of still images (see Figure 8.2 and Video 8.1a and b). Morrison's pouch is generally at the level of the 7th–9th intercostal spaces, but counting ribs is not usually helpful or practicable so the sonologist should become familiar with the sonographic anatomy. The transducer is fanned at every level to interrogate the entire region.

In a normal subject, scanning of the RUQ will show the liver and the right kidney contiguous, unless there is a layer of perinephric fat interposed. The area above the diaphragm in a patient with no pleural fluid demonstrates a *mirror image artefact*, that is, the appearance of normal liver echo-texture is seen above the diaphragm.

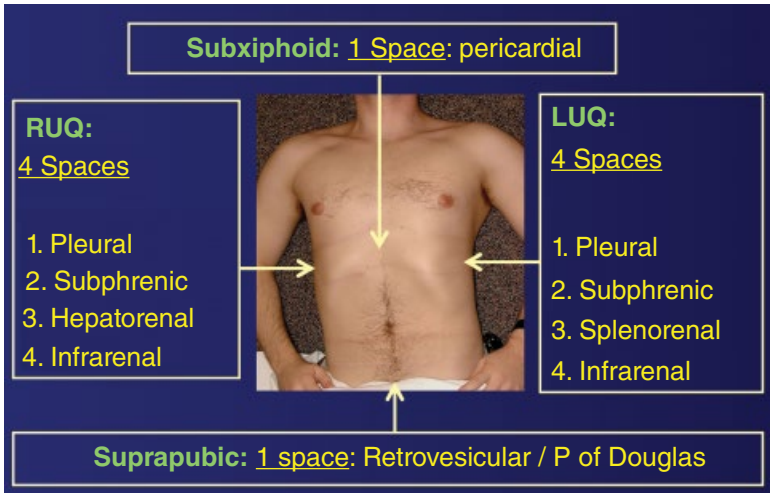

Figure 8.1 The four general areas to be evaluated in the FAST exam, and the potential spaces that need to be interrogated in each.

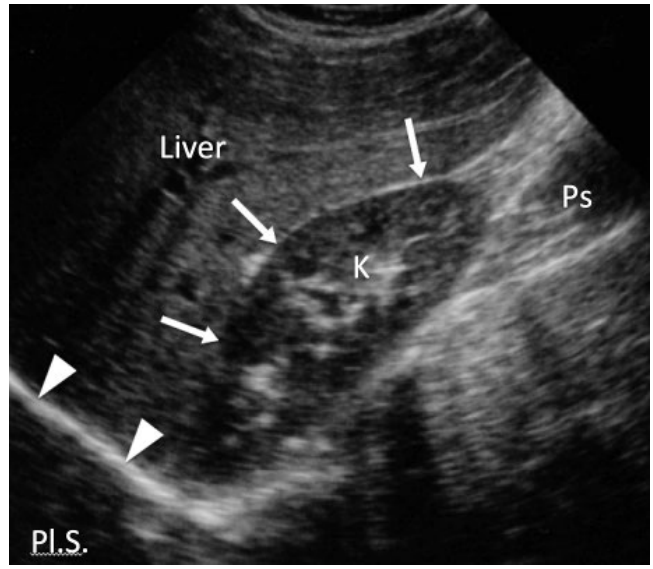

Figure 8.2 Ultrasound of a normal right upper quadrant, showing each of the four potential spaces. The diaphragm is indicated by the white arrowheads, and the hepatorenal space (Morison's pouch) by white arrows. Above the diaphragm, mirror-image artefact can be seen. Note that in most patients all four potential spaces are not visible in a single view. Pl.S, plural space; Ps, psoas muscle; K, kidney. Figure © A. J. Dean.

Free fluid appears black on ultrasound, and can be identified in any of the previously mentioned potential spaces. These are (in top-to-bottom order):

- Above the diaphragm (pleural space).
- Between the liver and diaphragm (sub-diaphragmatic, or subphrenic space).
- Between the liver and kidney (Morison's pouch).
- At the inferior pole of the kidney (space continuous with the colic gutter).

Free fluid has no walls and usually has a 'pointy' shape with angles and corners as it tracks tissue planes (Figure 8.3). These features help to distinguish RUQ free fluid from both the gallbladder and the inferior vena cava (IVC). The latter is tubular and may be tracked to the right atrium; colour-flow Doppler may be helpful if there is uncertainty. Fluid in the pleural space appears black and replaces the mirror image artefact (see Figure 8.3 and Videos 8.2–8.5). A mixed echogenicity picture may be seen with an older, more organised haemothorax, or an exudate/empyema collection. A 'tongue' of atelectatic lower lung may be seen moving with the respiratory cycle.

It is worth noting that, should a patient have a positive Morison's scan, there is usually no value in performing any other abdominal views unless there is a question about the accuracy or significance of a trace positive finding. The pericardial and pleural spaces should still be evaluated.

The Left Upper Quadrant (LUQ) View

The LUQ view is technically the most challenging as it lacks the large hepatic window that is exploited on the right. The transducer is placed between the mid and posterior axillary lines, with the operator's knuckles almost on the trolley. The preferred plane is again parallel to the ribs, with the probe marker cephalad. The initial depth setting can often be less than 15 cm. As with the RUQ, the probe is moved both cranially and caudally and fanned anteriorly and posteriorly to fully interrogate all potential spaces in the LUQ, which are analogous to those in the RUQ. These are (in top-to-bottom order) (see Video 8.6):

- Above the diaphragm (pleural space).
- Between the spleen and diaphragm (sub-diaphragmatic, or subphrenic space).
- Between the spleen and kidney.
- At the inferior pole of the kidney (continuous with the colic gutter).

(a)

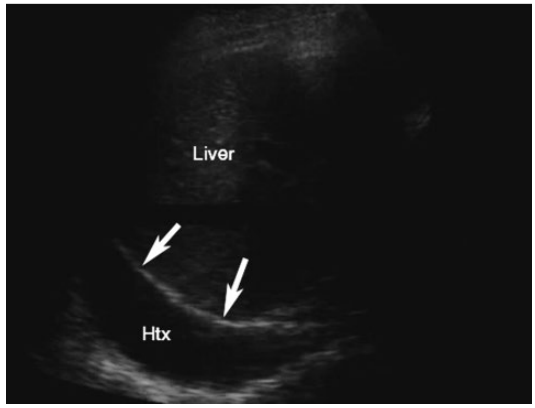

(b)

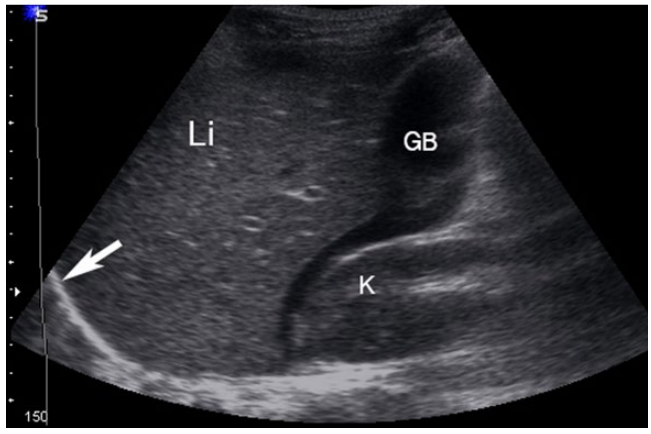

(c)

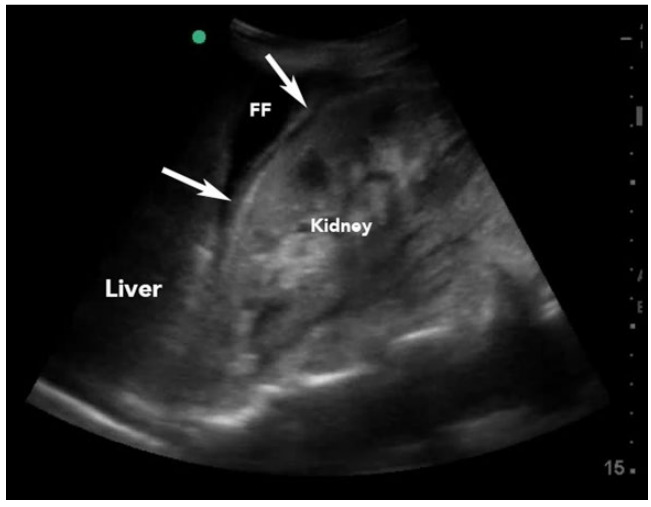

Figure 8.3 Abnormal free fluid as seen in the right upper quadrant (RUQ) windows of the FAST exam. (a) A haemothorax (Htx) is seen above the diaphragm (white arrows). (b) Free fluid is seen in Morison's pouch between the liver (Li) and the kidney (K). In real time this could be seen to be distinct from the gallbladder (GB). (c) Another case of fluid in Morison's pouch, in which the overlying liver is barely seen. Free fluid (FF) can be seen on both sides of the renal capsule (white arrows), suggesting both haemoperitoneum and parenchymal renal injury. (d) Free fluid (FF) at the inferior pole the kidney and surrounding the liver (L) edge. (e) A case of subtle free fluid between the inferior pole of the kidney (K) and a loop of gas-filled bowel (B). A rib shadow (RS) is also seen. All figures © A. J. Dean.

(d)

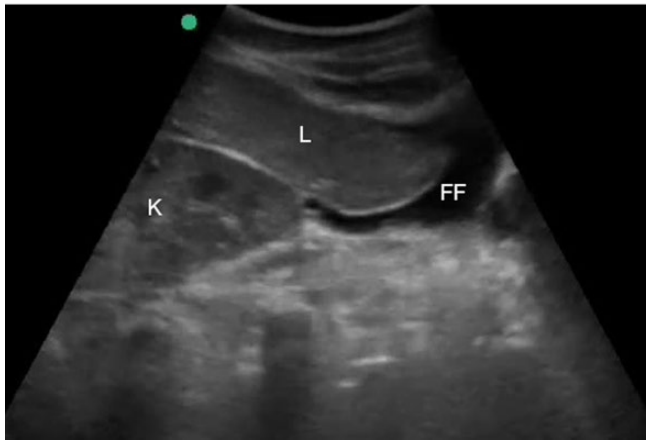

(e)

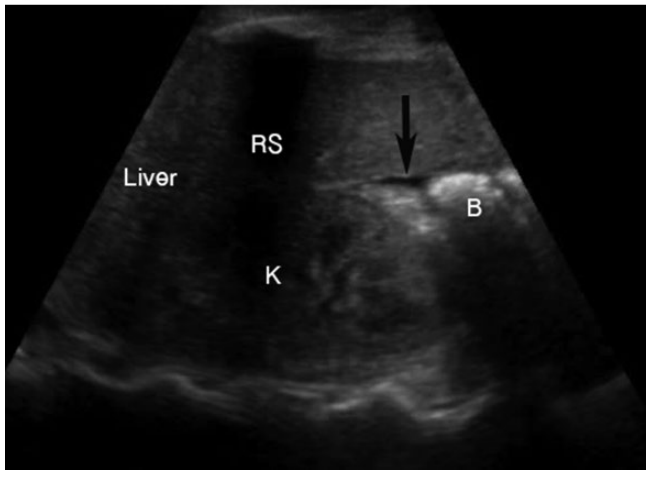

Figure 8.3 (Continued)

In most normal subjects the diaphragm is seen overlying the spleen, which in turn is closely apposed to the upper pole of the kidney (again, unless the patient has interposed perinephric fat). As in the RUQ, in the absence of haemothorax a mirror-image reflection of the spleen is seen above the diaphragm (Figure 8.4 and Video 8.6). It is worth noting that in the LUQ, free fluid often collects around the inferior pole of the spleen and in left sub-diaphragmatic space, so that these must be carefully interrogated (see Figure 8.5 and Video 8.7a–c).

Colour flow Doppler may be used to differentiate free fluid from splenic hilar blood vessels, with which it may occasionally confused (Figure 8.5c and d). A left pleural collection will abolish the mirror-image artefact and the supra-diaphragmatic space will appear black. A fluid-filled stomach (this is not uncommon in patients involved in car crashes) can be recognised by its location, the gastric rugae, the presence of reverberation artefacts from gas bubbles, and its 'non-pointy' shape (see Figure 8.5c).

The Pelvic or Suprapubic View

This view is the first to be done on patients entrapped in an upright position. The transducer

(a)

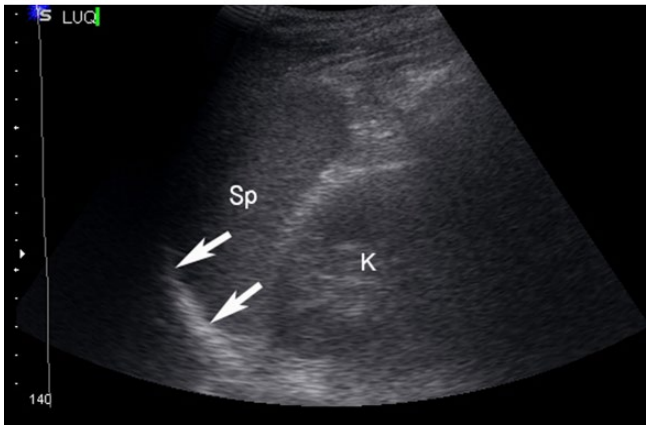

(b)

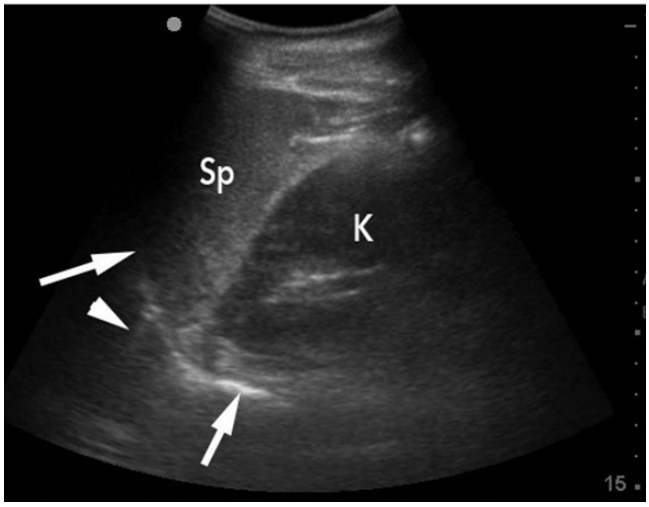

(c)

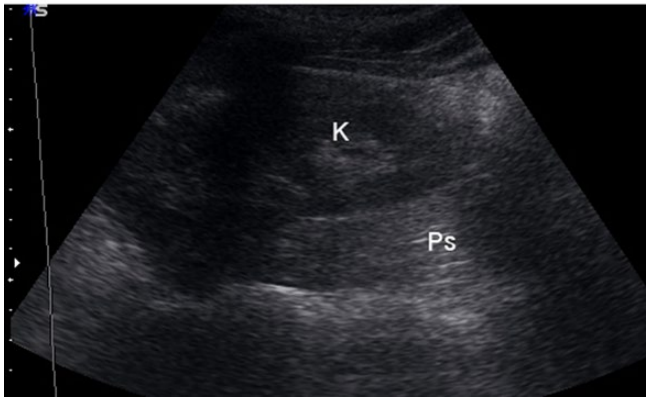

Figure 8.4 Images of a normal left upper quadrant (LUQ) exam. (a, b) The spleen (Sp) can be seen adjacent to the kidney (K). Superior to the diaphragm (arrows) the mirror artefact can be seen, excluding the possibility of haemothorax. (b) The presence of a reverberation artefact (also known as a z-line) above the diaphragm (arrowhead) is another indication of the presence of lung tissue, therefore excluding haemothorax. In the LUQ, all four potential spaces are really seen in any single view. (c) The inferior pole of the kidney is seen overlying the psoas muscle (PS). All figures © A. J. Dean.

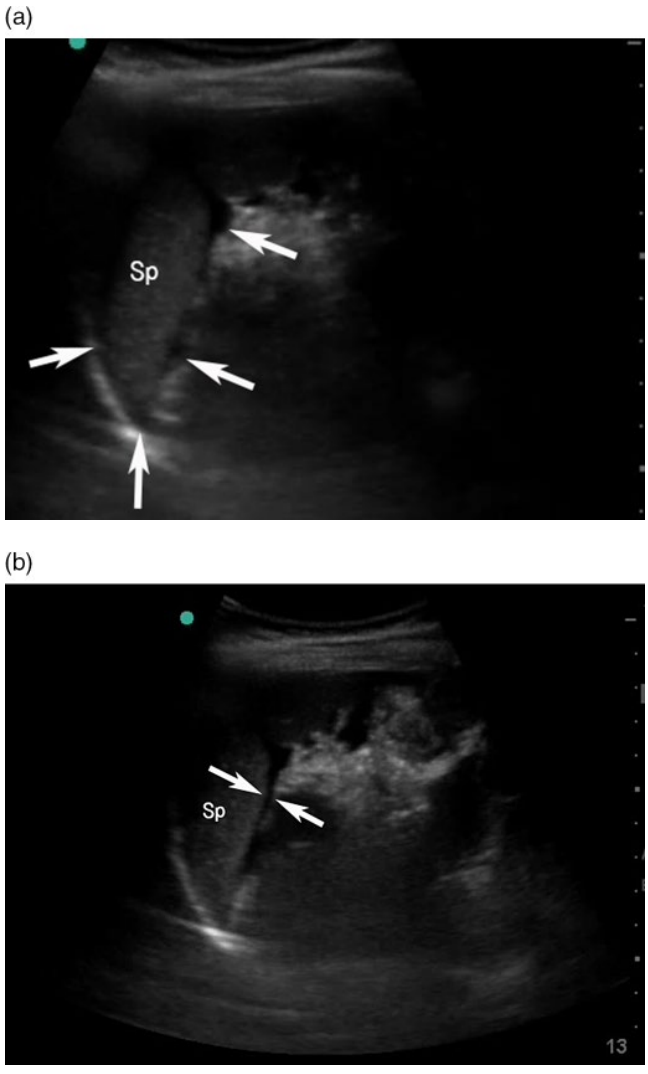

Figure 8.5 Abnormal collections of free fluid in the left upper quadrant (LUQ) (arrows). (a, b) Free fluid can be seen surrounding the spleen. (c, d) Free fluid can be seen surrounding the superior pole of the spleen and in the subphrenic space. It is more commonly found in this location in the splenorenal space. The arrowheads indicate the splenic vessels. The presence of reverberation artefact above the diaphragm (between the white triangles) indicates the presence of lung, thus ruling out haemothorax. (d) In many patients the stomach (St), rather than the kidney, is inferior to the spleen. (e) Free fluid surrounding loops of bowel overlying the inferior pole of the kidney (K) and psoas muscle (Ps) can be seen. All figures © A. J. Dean.

is placed transversely (with the probe marker pointing to the patient's right) just superior to the symphysis pubis and angled somewhat caudally. The initial depth setting should be around 15 cm. The potential spaces of interest are the recto-vesical space in the male, and the recto-uterine space (pouch of Douglas) in the female. With larger volumes of haemorrhage the vesico-uterine space may also fill with free fluid. After transverse interrogation, the probe is rotated in a clockwise direction 90° to obtain a longitudinal view, which may be more sensitive for free fluid.

(c)

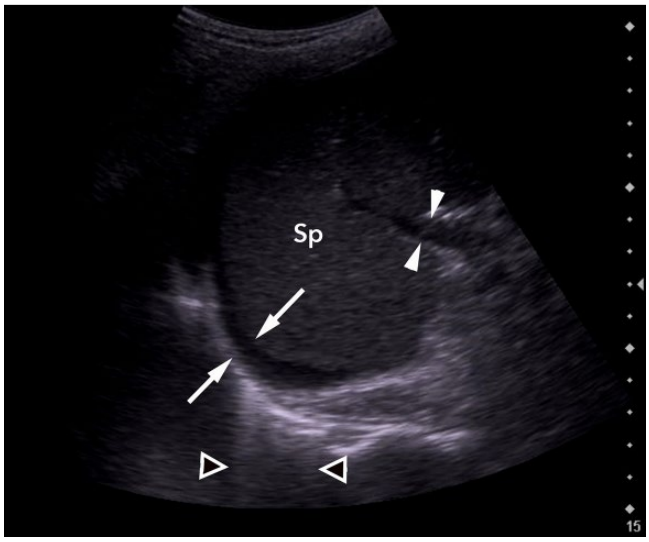

(d)

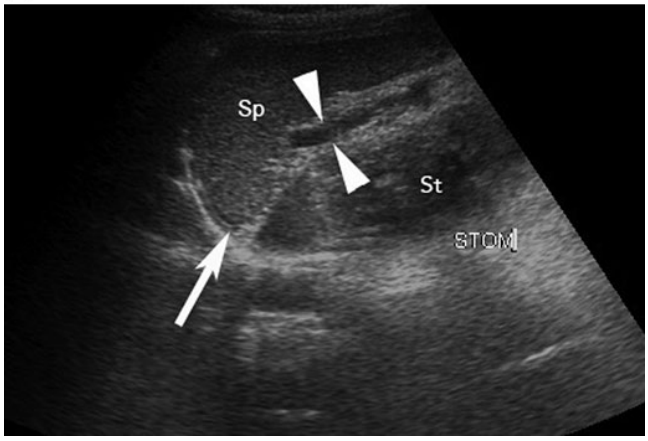

(e)

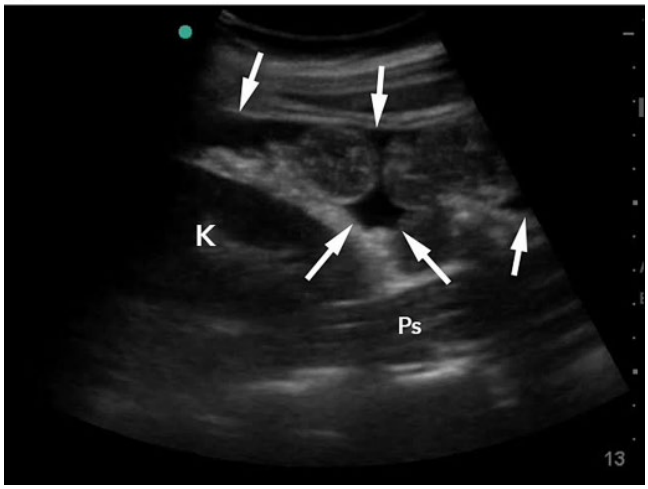

Figure 8.5 (continued)

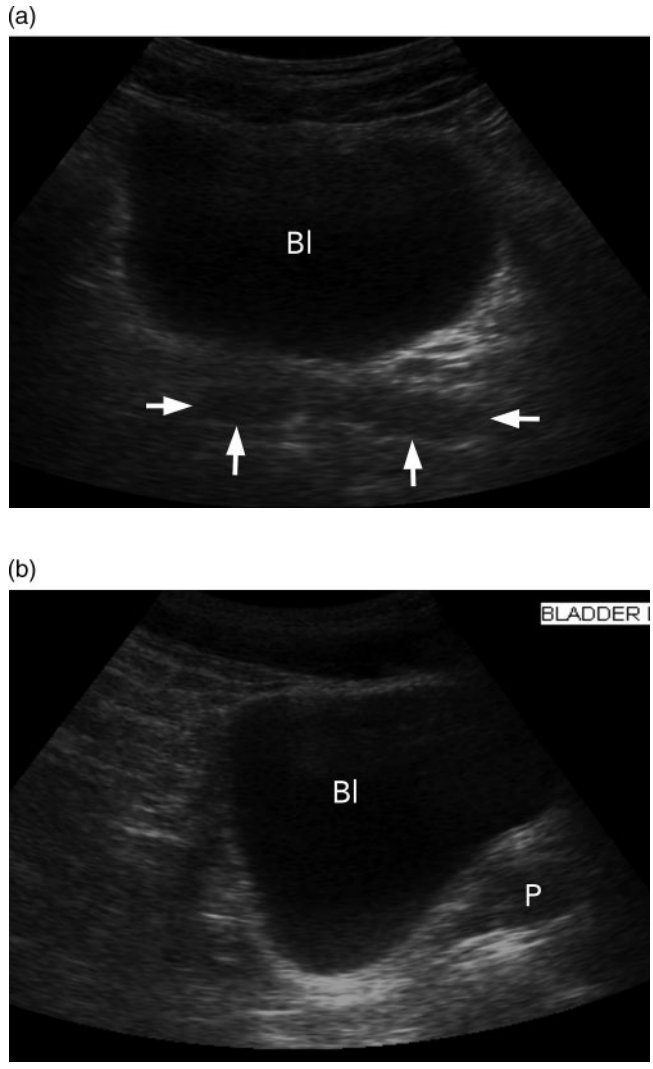

Figure 8.6 Normal suprapubic views of the pelvis. (a) In a transverse view of the male, paired seminal vesicles (arrows) can be seen in behind the bladder. As noted in the text, this plane is below the peritoneal reflection. (b) In the midline sagittal plane of the male, the prostate (P) can also be seen. The seminal vesicles are not seen in this plane. (c) In the transverse view of the female pelvis, the uterus (Ut) can be seen behind the bladder, and behind that, the air-filled rectum (between arrowheads). (d) In the longitudinal view of the female pelvis, the vagina (between arrowheads) can be seen in the characteristic location behind the bladder with an anteroflexed uterus. The arrow indicates the location of the pouch of Douglas, where free fluid commonly first accumulates. All figures © A. J. Dean.

Free fluid may be identified in the following areas on these views (see Figures 8.6 and 8.7 and Videos 8.8 and 8.9):

- Superior, lateral and posterior to the bladder.
- In the recto-vesical or the recto-uterine spaces.
- Surrounding loops of bowel.

The 'pointy' appearance of free fluid is differentiated from fluid within the bowel, which exhibits peristalsis, contains gas, can be tracked in real time as a tubular structure, and may demonstrate a 'corrugated' appearance (from the plicae circulars; see Video 8.9d). In females, small amounts of fluid in the pouch of Douglas (up to 15 ml) may be normal.

It is important to be aware of the location of the most caudal/inferior reflection of the peritoneum. In the male it is *cephalad* to the seminal vesicles, which are paired hypoechoic structures apposed to the posterior bladder wall immediately superior to the prostate (Figure 8.6a and Videos 8.8c and 8.9c). In the female it is at the inferior extent of the cervix

(c)

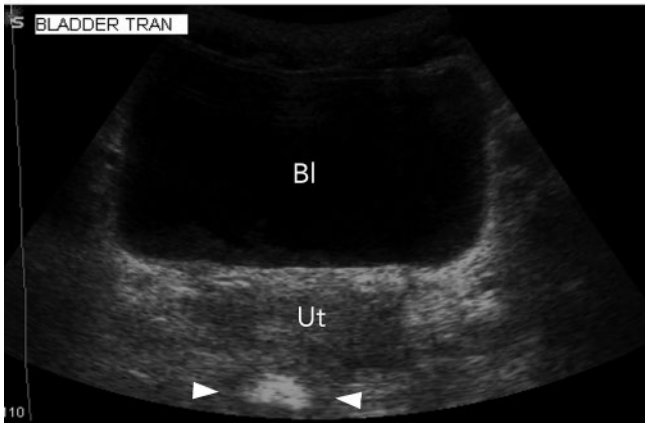

(d)

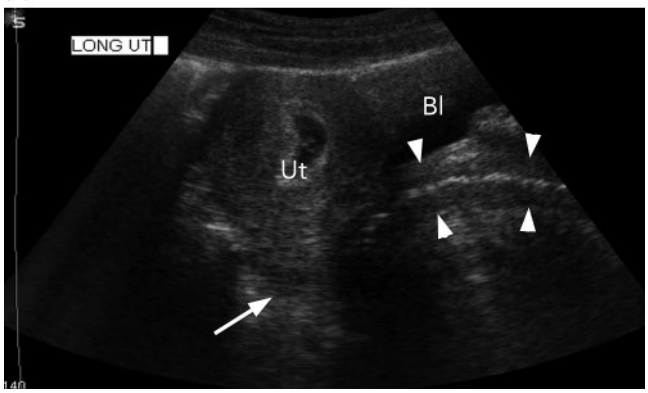

Figure 8.6 (Continued)

(Figure 8.6d and Video 8.8b). *Sonographic evaluation at or below these landmarks is fruitless and potentially misleading* because the FAST is not accurate in detecting extraperitoneal fluid collections. As in every region evaluated in the FAST, it is essential for the operator to fan systematically through the entire region in both the transverse and longitudinal planes.

Visualisation of the pelvis can be difficult with a small or empty bladder. In the female an anteverted uterus will lie quite inferior and anterior, and may provide an adequate window of the pouch of Douglas (Figure 8.6d). If the bladder is empty and there is a high index of suspicion despite a negative FAST, and there are no contraindications, a Foley catheter may be inserted and 250–500 ml of saline introduced to create an acoustic window. The most common reason for non-visualisation of the bladder is failure to place the transducer immediately superior to the symphysis pubis, and/or failure angle the transducer sufficiently inferiorly.

In the normal suprapubic examination, the gain settings usually need to be decreased to make the urine in the bladder appear black (not grey). Despite this, tissues behind the bladder may still appear excessively white due to the artefact of *posterior acoustic enhancement* (Figure 8.7a). This artefact can result in free fluid being overlooked, but can be resolved by

Figure 8.7 Various cases of pelvic haemoperitoneum. (a) Free fluid (arrows) can be seen between the bladder (Bl) and uterus (Ut) (same patient as Video 8.9a). Posterior acoustic enhancement is demonstrated behind the bladder. (b) A sagittal scan reveals extensive free fluid (arrows) and clot superior to the bladder adjacent to loops of bowel (Bo). (c) A longitudinal view of the pelvis in a case of bladder rupture. The bladder (outlined by arrowheads) is collapsed and contains clot. Superior to the bladder there is a large volume of free fluid (FF) and clot. All figures © A. J. Dean.

(a)

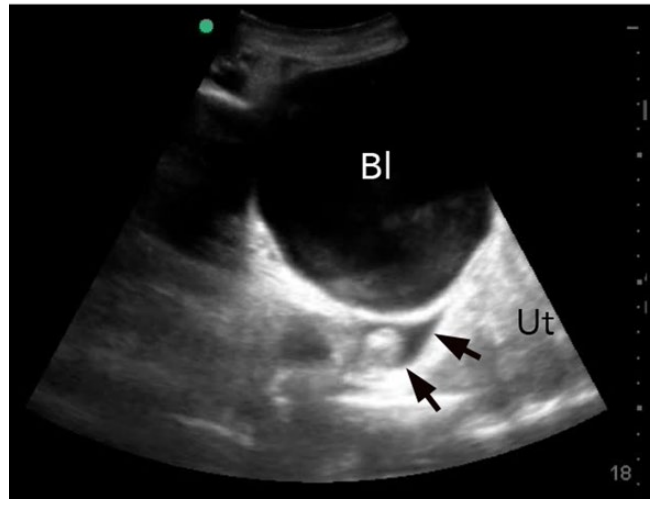

(b)

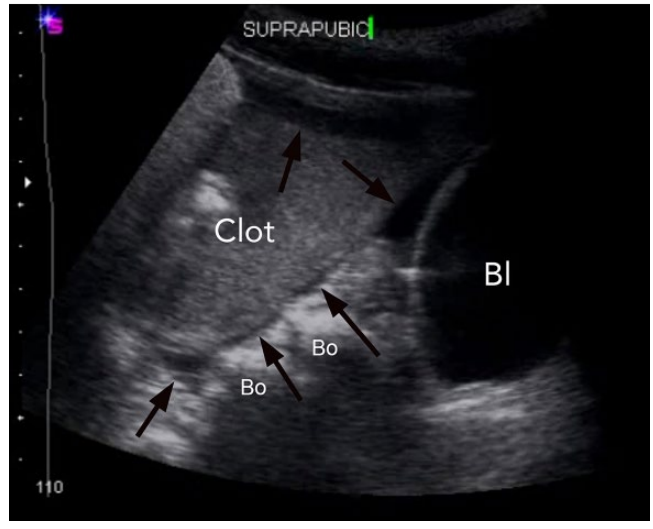

(c)

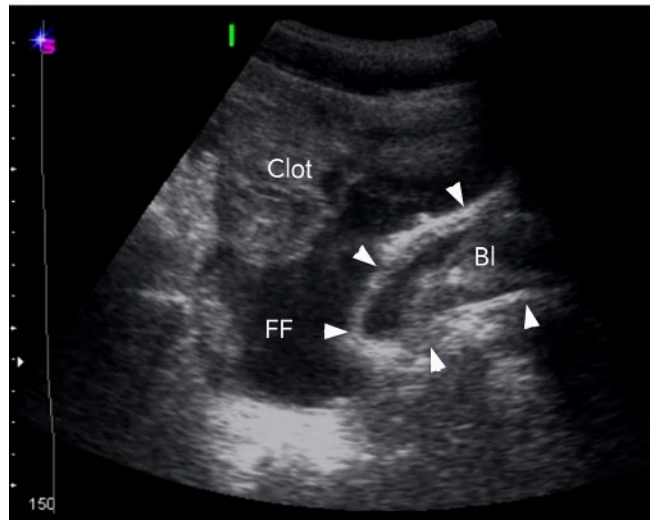

an adjustment of the 'far gain' so that structures that *should be black* (e.g., pelvic blood vessels) are *actually black*.

Less-experienced sonologists may mistake iliac vessels for free fluid. The vessels have a characteristic continuous tubular and branching structure, are 'roundy' (not 'pointy'), and demonstrate flow with Doppler. The seminal vesicles can also be mistaken for free fluid, but they too are 'roundy', symmetrical, with a characteristic location (Figure 8.6a and Video 8.9c). Larger collections of free fluid may be mistaken for the bladder (Video 8.9d), and to avoid this the dome of the bladder should be carefully identified in the longitudinal plane, and there should be no fluid superior/cephalad to this structure (Figure 8.7b and Video 8.9b). Rarely, the placement of a urethral catheter may be needed to clarify the issue.

The Sub-Xiphoid View

This view evaluates the pericardial sac for the presence of fluid that might represent haemopericardium. The transducer is placed in a transverse, almost coronal, plane as close as possible to the xiphoid process, using the liver as an acoustic window. The probe is directed towards the patient's left shoulder, with the marker to the patient's right. The position of the heart immediately behind the sternum dictates that the probe lies *almost flat on the patient's abdomen*, with an initial depth setting of around 20 cm. A four-chamber view of the heart is seen, with the right atrium and ventricle lying anteriorly and inferiorly (i.e., closer to the top of the ultrasound screen) (Figure 8.8).

Common reasons for non-visualisation of the heart via the subxiphoid window include:

- The depth of the ultrasound screen is set too shallow.
- The angle of the probe is too steep and pointing towards the upper abdomen rather than into the chest cavity.
- Air in the gastrointestinal tract is interposed between the transducer and liver. A protuberant abdomen can have this effect by displacing the liver and diaphragm superiorly. Ask a cooperative patient to "…take a deep breath and hold", or try to move the probe to the patient's right to obtain improved liver windows.

If a subxiphoid view cannot be obtained, then the parasternal views of the heart should be used (see Chapters 4 and 5).

The primary objective of the cardiac evaluation in the FAST exam is an evaluation of the pericardium which, under normal circumstances, is seen as a single echogenic line around the heart (Figures 8.8 and 8.9; Video 8.10). The pericardium cannot be distinguished from the diaphragm adjacent to the liver. Pericardial fluid appears as a black stripe between the parietal and visceral pericardium. It is important to evaluate posterior to the heart, since free fluid may initially collect in this location. An anterior anechoic area without any posterior component might be an epicardial fat pad; these tend to occur adjacent to the coronary vessels, to move with the myocardium, to have a somewhat globular shape, and to have the characteristic echotexture of fat (fine internal striations). They can be quite prominent in overweight patients.

The parietal pericardium can modify its volume chronically, but not acutely, and for this reason the rate of change in volume of pericardial fluid is much more important than its absolute volume. In acute trauma a volume of less than 100 ml accumulating quickly may cause tamponade. In contrast, chronic effusions of >1000 ml due to medical diseases are not uncommon. If a circumferential pericardial fluid collection is seen, the right ventricle should be evaluated for diastolic collapse. Any collapse of the right atrium is also suggestive of significantly increased intrapericardial pressures. The sonographic diagnosis of tamponade is covered in Chapter 33. Since the clinical signs of tamponade are late and unreliable, ultrasound can significantly accelerate the recognition of this condition, allowing for more timely intervention.

(a)

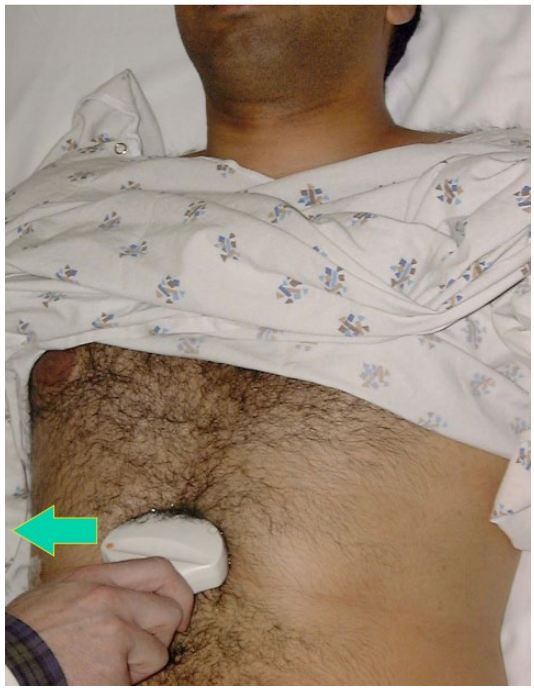

(b)

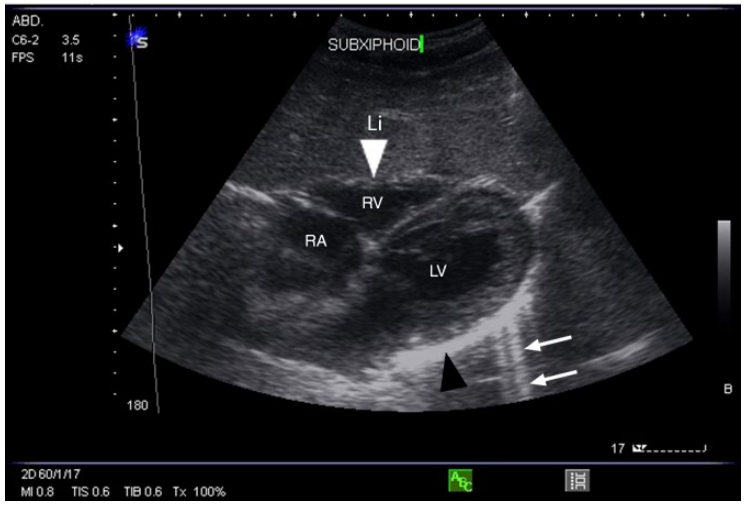

Figure 8.8 (a) Probe placement for the subxiphoid view. The arrow indicates the direction of the probe marker. (b) A typical normal subxiphoid four-chamber view of the heart (RA, right atrium; RV, right ventricle; LV, left ventricle) using the liver (Li) as a window. Both the anterior and posterior pericardium (white and black arrowheads, respectively) should be checked for the presence of fluid. Reverberation artefacts (arrows) are frequently seen posterior to the heart, and indicate the location of the visceral pleura and thereby the presence of the underlying lung parenchyma. Note the depth setting of 18 cm to evaluate the posterior pericardium. Figures © A. J. Dean.

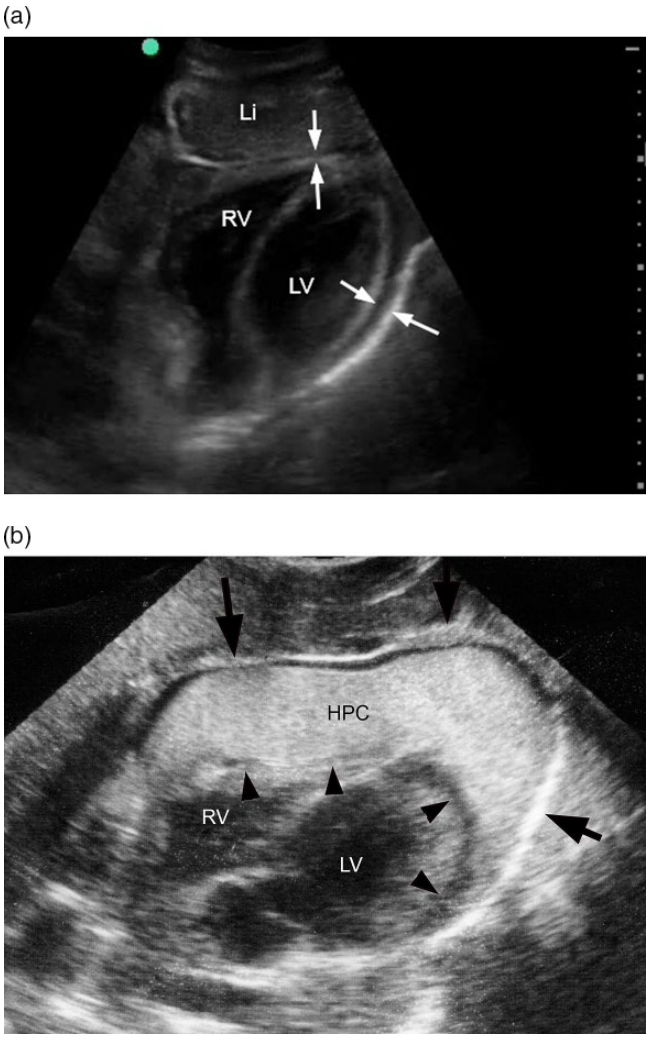

Figure 8.9 (a) A small circumferential haemopericardium (between arrows). (b) Subxiphoid view of a patient who sustained a cardiac arrest minutes after being struck by a car. The potential space between the visceral (arrowheads) and parietal pericardium (arrows) is filled with organised clot (HPC). There is a thin peripheral layer of unclotted blood. As a result of these ultrasound findings, and because the arrest was witnessed, an open thoracotomy was performed and the haemopericardium was evacuated with return of vital signs and subsequent cardiac repair. The patient survived and was discharged with full neurologic function. Abbreviations as Figure 8.8. Figures © A. J. Dean.

Extended FAST Examination

The extended FAST (e-FAST) examination is an evolution of the traditional FAST. In addition to searching for free fluid, the e-FAST seeks to identify pneumothorax. This condition is discussed in detail in Chapter 2.

Algorithm for FAST

FAST is not a substitute for CT, which is indicated for the further evaluation of patients with a significant risk of internal injury and a negative FAST, as well as for providing anatomic information in stable patients

with a positive FAST, to determine operative approaches or options for more conservative management.

The management of stable patients with a negative FAST exam depends on a variety of considerations relating to the patient, including an estimated pre-test probability of disease, comorbid conditions, age, mechanism of injury and psychosocial issues. Geographical and site-specific considerations are also important, including the availability of CT and of surgeons and operative suites, transportation issues, and local trauma centre protocols. In many settings, patients with stable vital signs and a negative FAST exam are observed for a period of 4–6 hours, at which time they undergo a repeat FAST scan. If the second examination is negative and the patient remains well, he or she is discharged home with carefully explained return-precautions. An International Consensus Conference developed the following algorithm for the use of the FAST examination:

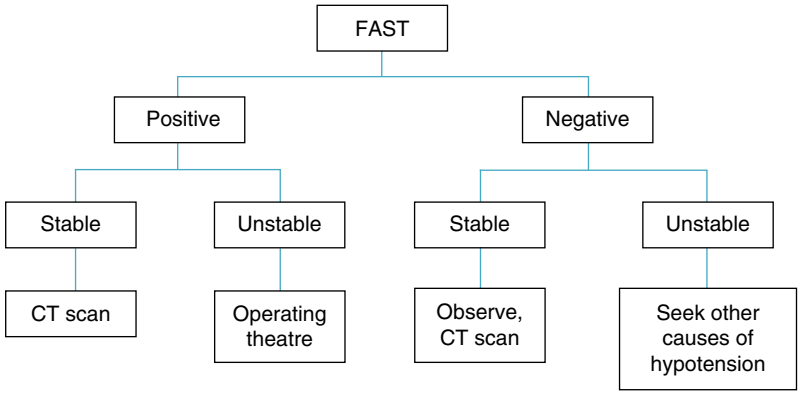

Limitations and Discussion

There are several limitations to the FAST. First, like any ultrasound evaluation, it is dependent on the skill of the sonologist. Probably the single greatest pitfall is failure to perform a systematic, thorough real-time scan of each of the potential spaces described above. While normal anatomy is predictable, injuries are unique, resulting in idiosyncratic rates, locations and patterns of haemorrhage. Patient-related factors that may impede optimal imaging include habitus, obesity, bowel gas, subcutaneous emphysema, and thoracic or abdominal wall injuries. Patients may present with chronic abnormal fluid collections, which need to be differentiated from acute haemorrhage. These can often be identified by clinical history. Sonologists skilled in the optimisation of gain settings can differentiate the absolutely anechoic quality of ascites (or pleural transudates) from the subtle echogenicity of blood.

When confronted by a hypotensive patient, the sonologist should bear in mind that "…you need blood to bleed". A patient who has sustained significant external haemorrhage may have a negative FAST despite internal organ injuries. An absolutely collapsed inferior vena cava would support this possibility. FAST has a lower sensitivity in penetrating abdominal trauma. It does not identify retroperitoneal or pelvic wall haemorrhage, and is not accurate

in identifying solid organ injury *per se*. With high specificity and lower sensitivity (probably 80–90% in experienced hands), FAST should be used more to 'rule-in' disease rather than rule it out, unless the pre-test probability of a disease is low. As with all diagnostic testing, FAST should be integrated with all other information obtained from the clinical evaluation.

The results of the first Sonographic Outcomes Assessment Program Trial (SOAP) trial showed that patients who had a FAST exam compared to those receiving routine trauma care without FAST had 64% lesser time to operative care, underwent fewer CT scans, spent 27% fewer days in hospital, had fewer complications (Odds Ratio 0.16), and their healthcare charges were 35% less when compared to controls. Despite these findings, the Cochrane Review concluded in 2013 that there was insufficient evidence to determine whether FAST is beneficial in trauma management.

While the widespread availability of multiplanar CT has decreased the role of FAST in many settings, most trauma patients in the world are still treated in locations without this technology. Even where CT is available, FAST is important for triage in multiple casualty situations. It is also likely that recent studies demonstrating identifiable life-time cancer risks associated with CT will promote an increasingly targeted use of CT. Such approaches will be particularly important for younger patients – the population at greatest risk for trauma – and are likely to be integrated with information obtained using ultrasound.

Pearls and Pitfalls

- When starting the evaluation of each window, it is better to err on the side of too-much depth than too little. This allows for the identification of anatomic landmarks, and an overview of the entire area. Perform a slow systematic real-time sweep through the entire extent of all potential spaces. A shallower depth adjustment can be made to interrogate specific structures in more detail.
- If a potential space or region cannot be adequately evaluated, record this limitation in the report.
- In some patients, adhesions or other anatomic anomalies may prevent free fluid from accumulating in the usual potential spaces. The operator should maintain 'peripheral vision' during the examination for collections of abnormal free fluid in other locations.
- Pathological free fluid tends to be 'pointy', while physiological collections of fluid tend to have 'rounded' shapes.
- In the LUQ, the region of the posterior tip of the spleen and adjacent subphrenic area should be carefully evaluated.
- Perinephric fat has the following characteristics (Figure 8.10 and Video 8.11a and b):
  - It is bilateral.
  - With appropriate gain adjustments it has the characteristic stranded echotexture of adipose tissue.
  - It will not alter shape or size in decubitus position.
  - It should cohere with the patient's body habitus.
- Traces of free fluid in the RUQ or LUQ might be confirmed by placing the patient in the Trendelenberg position or decubitus positioning and rescanning.
- 'Blood is needed to bleed'. With a patient in shock and a negative FAST, check the IVC. If it is completely collapsed, consider other sites of haemorrhage.
- A patient with a positive abdominal FAST still needs evaluation of the pleural and pericardial spaces.
- Repeating the FAST scan increases its sensitivity.
- Clotted blood does not appear black. Search for tell-tale areas of black unclotted free fluid to confirm the diagnosis.

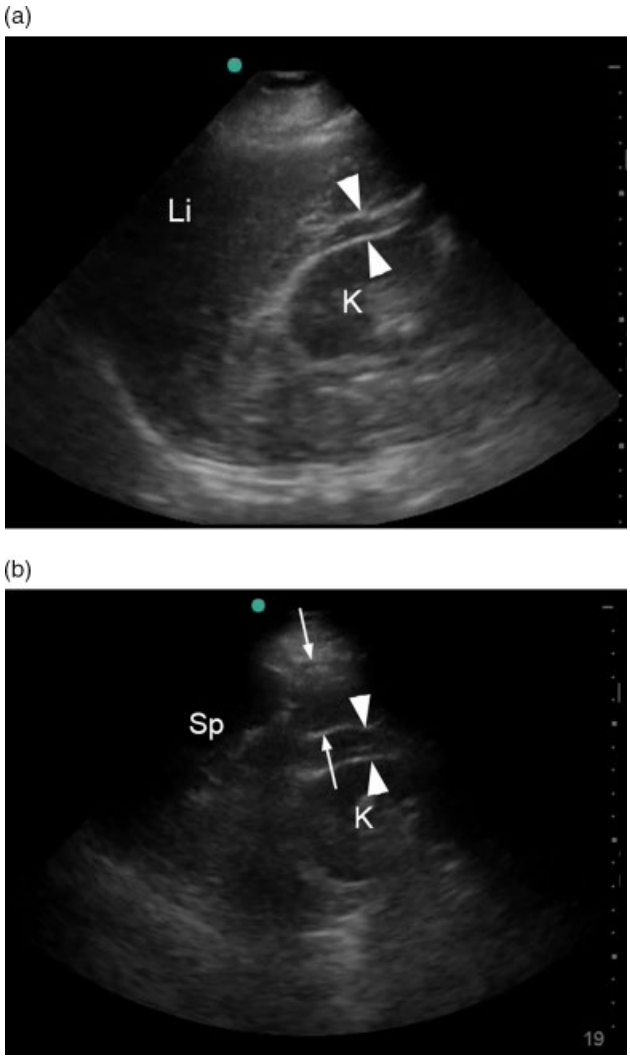

Figure 8.10 (a) A still image of the right upper quadrant view shown in Video 8.11a. Perinephric fat with characteristic internal echoes (between arrowheads) is seen between the liver (Li) and kidney (K). (b) An image from an obese patient shows a layer of perinephric fat (between arrowheads) underneath another layer of fat (between arrows), most likely pro-peritoneal or omentum (same patient as in Video 8.11b). Figures © A. J. Dean.

Further Reading

American College of Surgeons (ACS) (1997) Advanced Trauma Life Support for Physicians. ACS, Chicago, IL.

Jansen, J.O., Yule, S.R., Loudon, M.A. (2008) Investigation of blunt abdominal trauma. *Br. Med. J.*, **336**, 938.

Jehle, D., Guraiono, J., Karamanoukian, H. (1993) Emergency department ultrasound in the evaluation of blunt abdominal trauma. *Am. J. Emerg. Med.*, **11**, 342–346.

Yoshi, H., Sato, M., Yamamoto, S. (1998) Usefulness and limitations of ultrasonography in the initial evaluation of blunt abdominal trauma. *J. Trauma Injury*, **45**, 45–51.

Ma, O.J., *et al.* (1993) Prospective analysis of a rapid trauma ultrasound examination by emergency physicians. *J. Trauma Injury Infect. Crit. Care*, **38**, 879–885.

McKenney, M.G., Martin, L., Lentz, K. (1996) One thousand consecutive ultrasounds for blunt abdominal trauma. *J. Trauma Injury Infect. Crit. Care*, **40**, 607–612.

Melniker, L.A., Leibner, E., McKenney, M.G., Lopez, P., Briggs, W.M., Mancuso, C.A. (2006) Randomized controlled clinical trial of point-of-care, limited ultrasonography for trauma in the emergency department: the first sonography outcomes assessment program trial. *Ann. Emerg. Med.*, **48** (3), 227–235.

Rozycki, G.S., *et al.* (1993) Prospective evaluation of surgeons' use of ultrasound in the evaluation of the trauma patient. *J. Trauma*, **34**, 516–527.

Scalea, T.M., Rodriguez, A., Chiu, W.C., Brenneman, F.D., Fallon, W.F., Jr, Kato, K., McKenney, M.G., Nerlich, M.L., Ochsner, M.G., Yoshii, H. (1999) Focused Assessment with Sonography for Trauma (FAST): results from an international consensus conference. *J. Trauma*, **46** (3), 466–472.

Stengel, D., Bauwens, K., Rademacher, G., Ekkernkamp, A., Güthoff, C. (2013) Emergency ultrasound-based algorithms for diagnosing blunt abdominal trauma. *Cochrane Database of Systematic Reviews*, Issue 7, Article no. CD004446.

9

Advanced Gastrointestinal Ultrasound

Identifying Appendicitis, Pneumoperitoneum, Intussusception and Diverticulitis

Beatrice Hoffmann and Sara Damewood

With the increasing role of point-of-care ultrasound in emergency medicine, a growing number of gastrointestinal sonography applications are now taught and practised in emergency departments. Some of those advanced ultrasound indications are the detection of acute appendicitis, visualising free air in patients presenting with symptoms of acute abdomen, or diverticulitis for adult and intussusception for paediatric patients. The practice of the above applications will be introduced in this chapter.

ACUTE APPENDICITIS

Introduction and History

Acute appendicitis remains the most common surgical emergency of the abdomen. It carries a high rate of false clinical diagnosis, as several other conditions causing abdominal pain can present with very similar physical examination and laboratory findings. For these reasons, clinicians are utilising several imaging modalities to improve their diagnostic accuracy.

The first case report of ultrasound being used to diagnose acute appendicitis dates back to 1981, when Preusser described sonographic findings of suppurative appendicitis in an 87-year-old patient, that was subsequently confirmed at surgery. Five years later, a sonographic examination technique of the appendix using a high-frequency probe, termed 'graded compression', was described by Pyualert *et al.* The technique builds largely on the concept that the inflammatory response in intestinal tissues such as the appendix will lead to wall oedema and surrounding mesenteric inflammation, and decreases compressibility of the bowel. The technique also creates a better visual field to assess deeper structures by simply pushing overlying and air-containing bowel loops obscuring the view out of the way and gradually pushing the transducer towards deeper structures.

The results of the first two clinical trials testing this new technique were reported in 1987 and 1988. In a 1987 trial of 111 consecutive patients with suspected appendicitis, Pyualert and coworkers found a sensitivity of 75% for non-perforated appendicitis, 80% for perforated appendix, and 89% for appendiceal mass, with 100% specificity. Notably, sonography changed the diagnosis and management in over one-quarter of patients. One year later, in 1988, Schwerk *et al.* reported even better results, with 95.5% accuracy of ultrasound in 404 consecutive patients, reducing the negative appendectomy rate by 50%. These initial results were very impressive, as they are similar to today's accepted diagnostic standards for acute appendicitis ultrasound. Moreover, these studies were conducted with ultrasound equipment and technology available in the mid-1980s.

Emergency Point-of-Care Ultrasound, Second Edition. Edited by James A. Connolly, Anthony J. Dean, Beatrice Hoffmann and Robert D. Jarman.

Companion website: www.wiley.com/go/connolly/ultrasound

This supports the notion that the most important denominator for accurate appendicitis sonography might be operator experience and skill.

Over the next 30 years, several large trials and meta-analyses reported ultrasound sensitivity for acute appendicitis at 78–88%, and its specificity between 83% and 94%. Occasionally, studies performed by a single operator with an obviously high skill level showed sensitivities and specificities as high as 96% and 99%, respectively. Results with this accuracy are compatible or even superior to those achieved with computed tomography (CT) or even magnetic resonance imaging (MRI).

Comparison with CT and MRI

Overall, both CT and MRI are more *sensitive* diagnostic tools for the diagnosis of acute appendicitis. Specificities, however – especially when CT and sonography are compared – are largely compatible. The advantages of CT and MRI include a greater independence from patient body habitus and less operator dependence, as there is no variable component of a true 'manual examination' requiring spatial aptitude from the operator as there is for ultrasound. Operators are only reading and interpreting sets of standardised images. The disadvantages include the exposure to ionising radiation associated with CT, and the inconsistent availability of MRI. Both imaging modalities are significantly more expensive to conduct than ultrasound. Sonography, when performed by appropriately trained operators, should offer an initial safe, rapid and reproducible diagnostic means to identify appendicitis, as well as a range of differential diagnoses in the patient with abdominal pain.

Normal Sonographic Findings

The anatomic location of the appendix is usually found in the right iliac fossa at the junction of the terminal ileum and proximal caecum. The base of the appendix typically originates about 2 cm proximal from the ileocaecal valve. There are many potential anatomical variations to the location of the caecum and appendix, which makes the sonographic examination of the appendix one of the most challenging. However, finding the normal appendix might be just as important as finding an abnormal appendix for high sonographic accuracy, and the detection of common alternative diagnoses to acute appendicitis with sonography has long been established (Table 9.1).

The normal appendix is easily compressible with the graded compression technique, and does not display peristaltic activity. A normal appendix usually measures ≤6 mm, measured from outer-to-outer wall in the anterior-posterior (AP) diameter. In this axial view it will appear as an oval structure when compressed, and normal values can range from 2 to 11 mm. It is important to remember that the overall axial diameter of the appendix is an important – but by far not the most specific – sonographic sign of acute appendicitis. The normal appendiceal wall measures ≤2 mm, also measured in AP view. Here, the appendix appears as a target sign; the outer, dark-appearing layer corresponds to the muscularis propria of the intestinal wall, the medium and more echodense layer corresponds to the submucosa, while the inner, sonolucent layer, represents the mucosa. In long axis, the appendix appears as a blind-ending tubular structure. The normal length of the appendix can range from 2 to 20 cm. It is usually largest in children and young adults, and decreases in size with advancing age. It is essential to visualise the entire appendix from the fundus to the tip, to detect any segmental inflammation (Figures 9.1–9.3). It is important to remember that the base of the appendix is usually fairly predictably located proximal to the ileocaecal valve, at the point of convergence of the three taeniae coli of the caecum, right at the posteriomedial wall. However, the location of the tip of the appendix (where inflammation can originate) and the actual location of the caecum can vary greatly.

Table 9.1 Selected differential diagnoses detectable with sonography in patients with abdominal pain.

Differential diagnosis	Common sonographic findings
Crohn's disease	Thickened and a-peristaltic terminal ileum (TI), localised pain with graded compression over TI, potential abscess or fistula formation with stranding.
Mesenteric lymphadenitis	Enlarged and tender mesenteric lymph nodes.
Enteritis	Fluid-filled bowel loops with normal wall thickness and prominent peristalsis.
Intussusception	Target sign with invaginated bowel wall and containing bowel content.
Colitis	Enlarged, oedematous colon wall with mesenteric and omental stranding.
Diverticulitis	Stranding and oedema with local wall thickening of the colon; the diverticulum may contain a fecolith or air and is surrounded by hyperechoic, non-compressible tissue, representing the inflamed mesentery and omentum.
Incarcerated hernia	Peritoneal wall defect with herniated bowel content with or without strangulation and ileus.
Ileus	Dilated bowel loops, fluid-filled, increased or decreased peristalsis, sedimentation of bowel content, ascites and bowel wall thickening (late findings).
Renal colic/cystitis	Dilated renal collecting system with or without dilated ureter with potential visualised renal stone.
Tubo-ovarian abscess, salpingitis, ovarian torsion, ectopic pregnancy	Tumour- or mass-like structure adjacent to the uterus with potential findings of tubal ring with foetus (ectopic) or dilated tubular structure with internal mucosal folds (salpingitis).
Psoas abscess or haematoma	Retroperitoneal tumour.

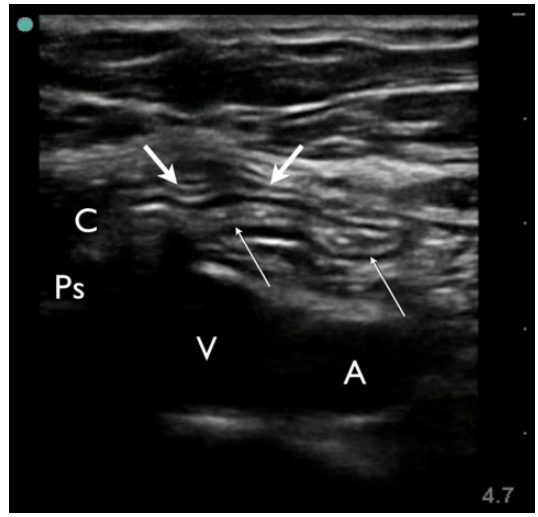

Figure 9.1 Normal appendix (thin arrows) visualized below the terminal ileum (thick arrows). This appendix is located ventral to the iliac artery (A) and vein (V) and medial to the psoas muscle (Ps) and caecum (C).

Scanning Technique

The approach to sonography of the appendix mirrors that of other bowel ultrasound examinations. The first part of scanning is performed with a curvilinear, 3–5 MHz frequency probe that allows for an overview of the anatomy and potential pathophysiology. The next step is scanning with a high-frequency linear probe using graded compression. The goal of this second step is to evaluate the patient's anatomy with high resolution and in detail.

It is prudent to perform a systematic approach, given the complexity of the right lower abdominal anatomy and the variability of the location of the caecum/appendix.

Scanning Locations

The initial step is usually a 'self-localisation technique', in which the patient is asked to point to the area of maximum pain. The second step is a systematic scanning of the anatomy of the right lower quadrant. For this part of the examination the pericaecal area is found by placing the transducer

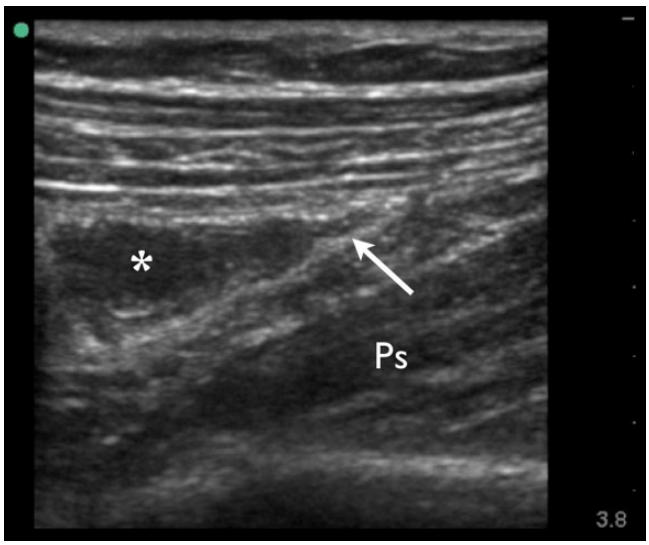

Figure 9.2 Normal proximal appendix (arrow) on psoas muscle (Ps) and caecum (*).

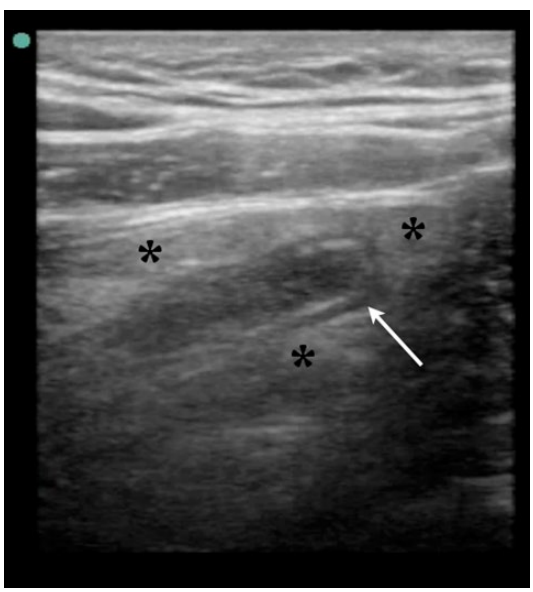

Figure 9.3 Acute appendicitis. Enlarged appendix with preserved wall layers (arrow) and stranding (*).

in the right lower abdomen, moving it to the lateral area, and searching for typical large-bowel lumen. The caecum is frequently the most lateral and inferior large-bowel structure in the right lower abdomen, and is larger in size than the small bowel, often contains more air than the small bowel, and will rest on the psoas. Other ways to identify the caecum are to find the right hepatic flexure next to the liver and to trace it inferiorly. Alternatively, the probe can be used to scan from the iliac vessels into the iliac fossa laterally, often following the terminal ileum and crossing the psoas. Once the caecum is visualised, the appendix should be sought at the tip, or just posterior, medial or even lateral to the caecum. If an appendix is not easily identified using this technique, then the transducer should be oriented in parallel to the iliac vessels. The middle portion of the appendix can be found anterior to the iliac vessels, while the distal portion dips into the pelvis. An additional area of interest is the region posterior to the terminal ileum – the inferior ileocaecal recess – which can be found by identifying the area lateral to the iliac vessels and anterior to the psoas muscle when tracing the terminal ileum. Once the appendix is found, gentle and gradually increasing pressure should be applied with the probe to dispel gas and faecal material from any overlying bowel loops that may obstruct the area of interest and to demonstrate compressibility (or otherwise) of the appendix.

Acute Appendicitis Findings

Helpful sonographic findings for the diagnosis of acute appendicitis, with details of their sensitivity and specificity, are listed in Table 9.2.

Table 9.2 Sonographic findings suggesting appendicitis.

Finding	Sensitivity (%)	Specificity (%)
Appendix diameter >6 mm	100	68
Blind ending identified	100	37
Round diameter	100	37
Non-compressible	97	20
Hyperechoic mesenteric fat surrounding appendix	86	97
Localised pain over appendix	86	68
Lack of intralumenal gas	85	79
Increased perfusion of appendix	79	31
Free intraperitoneal fluid	60	58
Appendicolith	28	96
Enlarged mesenteric lymph nodes	20	70

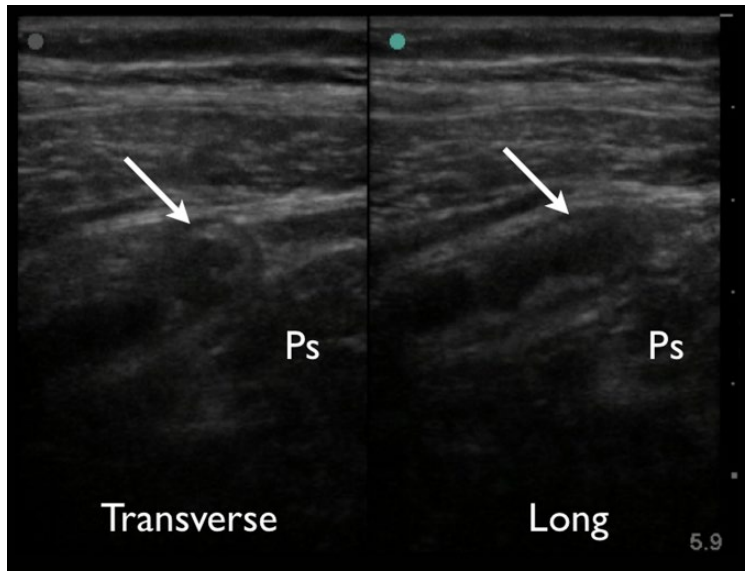

Figure 9.4 Appendicitis (arrow) with transverse and longitudinal images on psoas muscle (Ps).

Some of the most high-yield sonographic criteria are: (i) visualising a non-compressible full-length appendix with round (not oval) diameter when compressed, greater or equal to 6 mm in axial diameter; (ii) visualising an appendicolith; (iii) peri-appendiceal stranding with hyperechoic and oedematous mesenteric fat surrounding the appendix at the meso-appendix; and (iv) localised pain during 'sonopalpation', when the probe is directly placed over the appendix and pressure is applied (Figures 9.4–9.6).

Pearls and Pitfalls

There are several stages of appendiceal inflammation that can be visualised with sonography. These can be divided into non-necrotic and necrotic stages, as listed in Table 9.3.

In women, the appendix can sit adjacent to the right ovary, and appendicitis might be identified on pelvic ultrasound. To identify a retrocaecal appendix it may be necessary to have the patient positioned on their left side and approach the

caecum through a lateral flank view. The retrocaecal appendix will lie posterior to the caecum in this view. Finally, a full bladder may displace structures of the right lower abdominal quadrant into the lateral pelvis or mid abdomen.

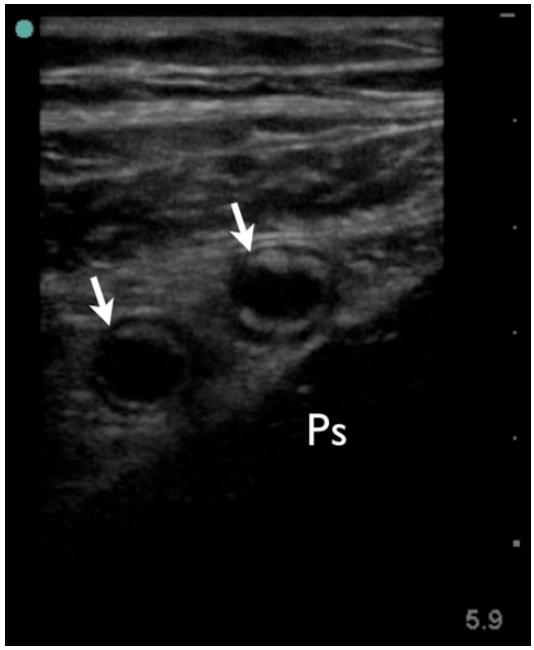

Figure 9.5 A curved inflamed appendix (arrows) resting on the psoas muscle (Ps) with stranding.

Occasionally, the proximal part of the appendix can contain an obstructing appendicolith that leads to segmental appendicitis and subsequent appendicitis. The proximal end of the appendix may appear normal, while the distal tip will be inflamed. It is imperative to visualise the entire length of the appendix not to miss a segmental appendicitis.

In the setting of a ruptured appendix, the appendix may appear normal-sized, collapsed, or difficult to identify at all due to a loss of the typically target-sign and echogenic ring structure. Fluid and oedema and a right lower quadrant mass might surround the area.

Loops of small bowel in the right lower quadrant can be mistaken for the appendix. Remember to look for peristalsis to delineate between the small bowel and the appendix, as well as to search for other signs of appendicitis around the structure in question, such as hyperaemia and fat stranding.

Other inflammatory processes can be mistaken for appendicitis (as noted in Table 9.1). When performing an endovaginal ultrasound, a dilated fallopian tube in short-axis view may have a similar appearance to appendicitis, but has mucosal folds present that are not seen with the appendix. Tubo-ovarian abscesses and diverticulitis can also cause fat stranding in the right lower quadrant.

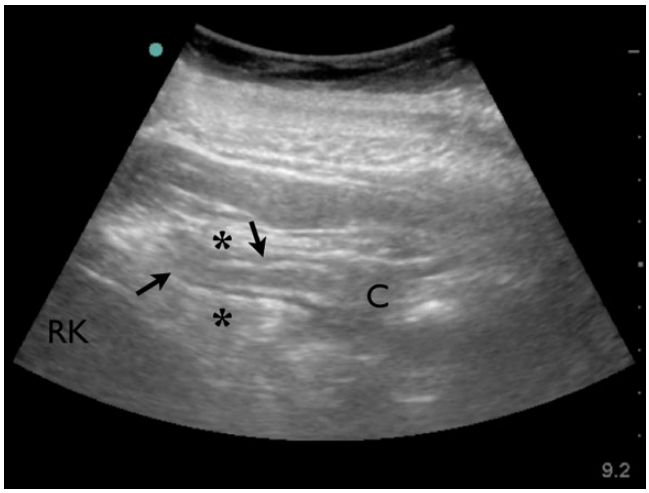

Figure 9.6 Acute appendicitis with mesenteric stranding (*) and caecum (C). The appendix is located close to the right kidney (RK) and right liver lobe.

Table 9.3 Stages of appendicitis and sonographic findings.

Stages of appendicitis	Sonography findings
Non-necrotic stages	
Appendicitis catarrhalis	An enlarged and non-compressible appendix is visualised, all wall layers are distinguishable and show increased vascular flow.
Phlegmone	Enlarged and thickened wall that is either intact or layers are now indistinguishable, increased vascularity on Doppler and usually oedema and inflammation in the peri-appendiceal and often peri-caecal area.
Necrotic stages	
Gangrenous appendicitis	Shows loss of visualisation of all wall layers and loss of perfusion on Duplex, frequently appendix presents with large diameter in axial view.
Perforated appendicitis	Can present with variable sonographic findings; often shows loss of wall layers, with inconsistent-appearing wall thickness or areas of loss of detectable wall altogether, localisation of potential free fluid or air inclusions, and formation of perityphlic abscess. Appendix structure can become unrecognisable if severe inflammation and abscess formation occurs.

PNEUMOPERITONEUM

Introduction and History

Although air has been lamented as a hindrance to ultrasound image acquisition and interpretation, an appreciation of the sonographic characteristics of air and physiological presentation is helpful in interpreting normal and abnormal abdominal ultrasounds. Air interfacing with sound waves creates reverberation artefacts that are easy to locate and, depending on the location, can be allocated to physiological or pathological air. Air artefacts are normally visualised within the lumen of the air-containing gastrointestinal tract, and also during respirations of the air-filled lungs. Extraluminal, intraluminal or intramural air is considered pathological and can sometimes be the only pathological finding suggesting an acute emergency process.

A German study by Seitz and Reisling in 1982 was the first to describe the sonographic findings of free intra-abdominal air in a group of patients who had air injected after paracentesis. Sonography was found to be 100% sensitive for detecting pneumoperitoneum, even for volumes as low as 1 ml. This study was the first to report many of the known findings and characteristics of extralumenal free abdominal air on sonography. The investigators went on to evaluate ultrasound's accuracy in about 4000 consecutive patients presenting with non-traumatic abdominal pain to an emergency department reaching 90% sensitivity and 100% specificity. Over 25 years later, Moriwaki *et al.* evaluated sonography's performance in trauma patients with abdominal pain, and found it to have 85% sensitivity and 100% specificity for acute pneumoperitoneum in 483 consecutive patients. Over the past 30 years, several smaller trials have confirmed and validated these original findings by Seitz and Reisling.

Scanning Technique and Location

The patient is initially examined in the supine position with the bed tilted to 30° elevation at the head. A linear array probe is oriented cephalad and placed in the right upper abdomen, to visualise any free air now migrating and residing in the peritoneal recess anterior to the liver. Such air will show the classic peritoneal enhancement (Figures 9.7 and 9.8). The patient is then placed in a 45° left lateral decubitus position, with the probe placed in the mid-axillary line, over the ventral interface of the liver with the peritoneum, and air will appear as a hyperechoic artefact within the interface of liver and peritoneum, and will not move with respirations. When compared

with the physiological air artefact from lung expanding into the costophrenic angle with inspiration and overshadowing the upper abdomen, a pleural-peritoneal gap can be visualised (Figure 9.8). Gentle pressure on the caudal end of the probe can expel the air from the anterior peritoneal recess to other areas in the peritoneum, and with releasing pressure the reverberation artefact will re-appear. Originally described by Seitz and Reisling, the term 'scissors manoeuvre' was later postulated by Karahan *et al.* for this phenomenon. Free intraperitoneal air can be visualised in all areas, usually collecting or migrating towards the most elevated point of the peritoneum. Free retroperitoneal air shows similar characteristics, but usually does not migrate with patient re-positioning. In a report by Nürnberg *et al.*, retroperitoneal free air was most commonly seen ventral to the right kidney, but it can be identified at the left kidney, aorta and inferior vena cava (IVC), as well as around the duodenum and pancreas or within the pancreatic ducts.

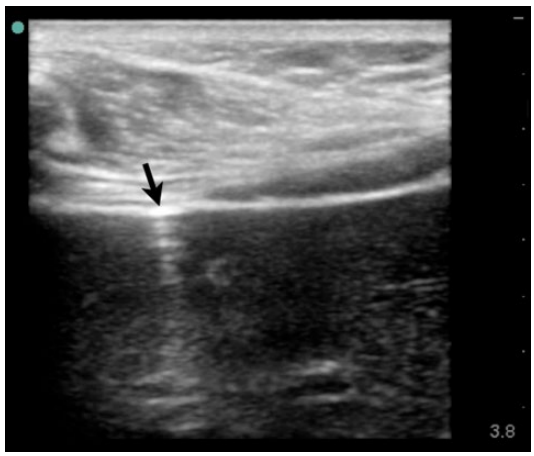

Figure 9.7 A small hyperechoic-appearing amount of free air (arrow) is detected at the peritoneum ventral to liver tissue with reverberation artefacts.

Pearls and Pitfalls

Apply only gentle pressure to the abdomen when initially scanning through the epigastric region, as pneumoperitoneum can be easily displaced from view, leading to a false-negative study. Air in locations other the peritoneal cavity gives similar reverberation artefacts. Subcutaneous and intramuscular emphysema can be mistaken for pneumoperitoneum. However, in these cases, the

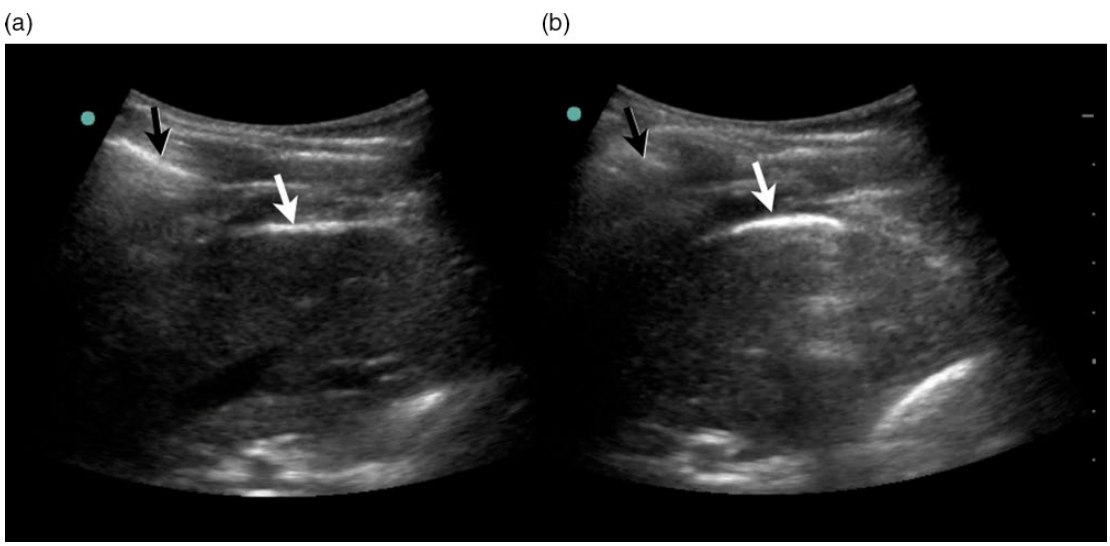

Figure 9.8 Free intraperitoneal air (white arrow) at right upper quadrant with lung (black arrow) in inspiration creating the pleuro-peritoneal step-off (left side of image). This phenomenon is less visible in expiration (right image).

reverberation artefact originates will not dissipate with applied pressure from the probe. Peritoneal free air can be differentiated from air in the lung by monitoring the artefact's behaviour with breathing and identifying the diaphragm from the peritoneum. True pneumoperitoneum will not change with respiration. Air in the duodenum and other portions of the gastrointestinal tract will move with peristalsis and does not cross the ventral surface of the liver, unlike intraperitoneal free air.

In general, pneumoperitoneum appears as echogenic foci with ring down or reverberation artefact between the anterior left liver lobe and anterior abdominal wall when the patient is supine, and between the right liver lobe and inner thoracic wall when the patient is lying to the left. Retroperitoneal free air instead frequently collects at the right kidney, with the same reverberation artefact as pneumoperitoneum. However, the artefact will not change with re-positioning the patient.

INTUSSUSCEPTION

Introduction

Intussusception is rare in adults and common in children. It occurs when a portion of the intestine invaginates into an adjacent bowel segment. Associated mesentery, nerves and vessels are telescoped along with the bowel, causing a compression of blood flow and leading to segmental swelling and obstruction. Intussusception occurs frequently in children aged less than 2 years, with a recent review article citing an incidence of 0.75–1.0 per 1000 children in European emergency departments. Intussusception can also occur in adults, especially in the setting of neoplasm, and here most cases occur in the small bowel.

Scanning Technique and Location

The most common site of intussusception is ileocaecal. Therefore, investigation of the colon for intussusception begins in the right lower quadrant or the area of the patient's pain. If the patient is unable to relate a reliable history – as is often the case with paediatric patients – the entire colon needs to be investigated in stepwise fashion. Initially, a high-frequency linear array probe should be used with applied graded compression to dispel unnecessary bowel gas. A curvilinear probe may be used if deep penetration is necessary. A high-frequency linear probe can visualise detail into any pathology of the bowel wall and can usually distinguish the three bowel wall layers.

Sonographic Findings

The most recognisable sonographic sign of intussusception is the target sign. This is typically appreciated in a transverse view of the colon, and it will appear as a complex round mass with a hypoechoic outer rim composed of concentric echogenic rings. The inner part of the target is the lumen of the invaginating portion of bowel and associated mesenteric fat, while the outer part of the target sign is the receiving outer portion of bowel (Figures 9.9 and 9.10).

Once the intussusception is identified in transverse, Doppler can be used on the tissue to show what blood flow is present to the segments of bowel. The affected segment is visualised in a sagittal plane by slowly rotating the probe 90° caudally. Frequently, the invagination will be visualised with the hyperechoic telescoping portion of bowel appearing inside the sometimes oedematous and relatively hypoechoic bowel segment.

Pearls and Pitfalls

Small bowel can be differentiated from large bowel by size, location and the absence of haustrae. Like testicular torsion, intussusception may be intermittent, so that a patient with real disease may have a normal exam. Other potential causes of the patient's abdominal pain should be considered.

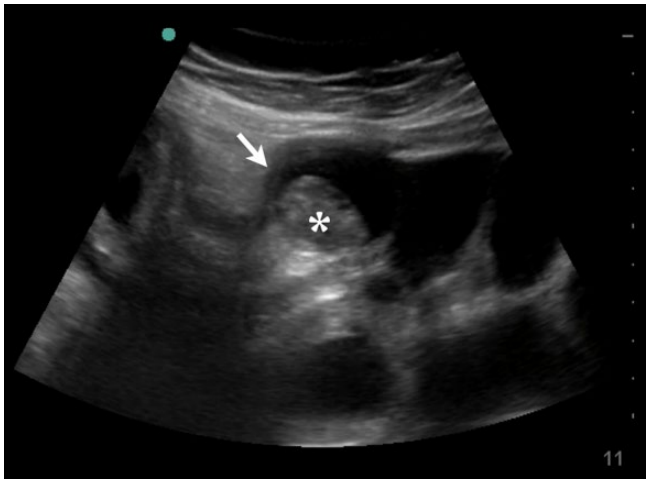

Figure 9.9 Image of ileo-colic intussusception. Arrow shows intussuscipiens, and * the intussusceptum bowel segment.

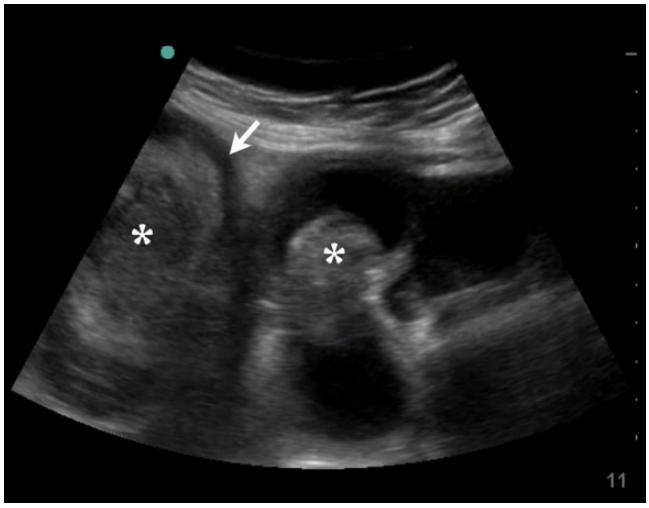

Figure 9.10 Large bowel intussusception. Left * shows target sign and intussusception in transverse view; the right * shows the intussusception in longitudinal. Arrow: outer wall of intussuscipient bowel.

DIVERTICULITIS

Introduction

Acute colonic diverticulitis is a common cause of abdominal pain in middle-aged to elderly patients. A diverticulum is an outpouching of weak intestinal wall areas in the large bowel. These pouches can become inflamed and obstructed, leading to diverticulitis, sometimes with abscess formation and microperforation. Abdominal CT nears 100% specificity for detecting acute colonic diverticulitis, but sonography is a useful tool in the hands of an experienced sonographer that can be rapidly obtained and easily repeated (without radiation) to investigate bowel pathology, and might be an alternative imaging tool in uncomplicated diverticulitis.

Scanning Technique and Location

The sigmoid colon is the most frequent location for diverticular disease, although diverticula can occur in any section of the colon. Right-sided diverticulitis is less common in adults of the Western hemisphere, but has been

identified in young and Asian patients, and is congenital in origin. Although the entire length of the large bowel should be investigated, starting in the left lower quadrant or at the patient's stated location of pain will likely yield pathological findings. A large curvilinear probe is used to scan the abdomen to obtain an overview and identify potential areas of interest, and also review. Following this step, the high-frequency linear array probe should be used to investigate the bowel in a stepwise fashion, with care given to apply gentle compression to each segment to dispel bowel gas and small bowel loops out of view.

Pathology

Diverticulitis appears as a small pouch with a hypoechoic wall extending from a thickened colon wall with colitis findings (Figures 9.11 and 9.12) with echogenic material, likely faeces or air, within the pouch (Figure 9.13). This pattern of hyperechoic area inside an hypoechoic

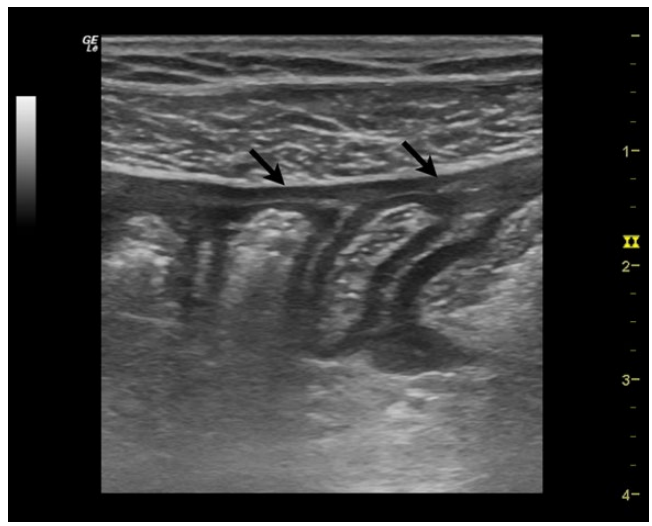

Figure 9.11 Colitis with oedematous bowel wall showing swollen layers of bowel wall (arrows).

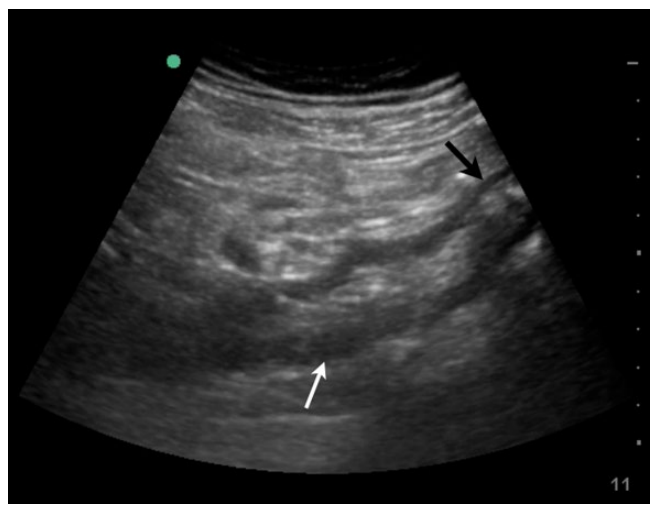

Figure 9.12 Colitis with area of enlarged and swollen bowel wall (white arrow) tapering off into segment of less inflammation with decreased bowel wall thickness (black arrow).

structure can appear similar to the kidney, and has been termed the 'pseudokidney' sign, as first defined by Parulekar.

The affected length of bowel wall will appear thickened and oedematous, typically greater than 4 mm thick (Figure 9.12). The offending diverticula will frequently have surrounding echogenic fat stranding (Figure 9.13). Microperforation frequently occurs with diverticulitis, but larger perforations can occur, leading to abscesses and even pneumoperitoneum. An abscess will appear as a hypoechoic fluid collection adjacent to the diverticula with air shadows and reverberation artefact. Fistulas or abscess can form and may link to adjacent loops of bowel. Fistulas can be visualised as hypoechoic linear canals connecting the diverticula, colon and abscess (Figure 9.14).

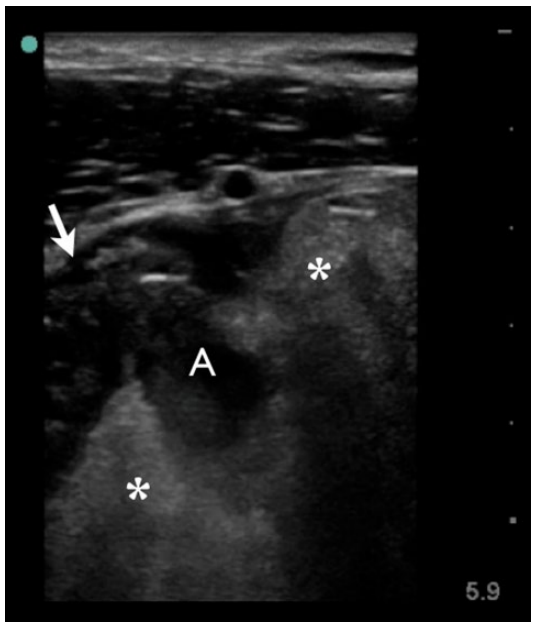

Figure 9.13 Acute diverticulitis with oedematous large bowel (arrow) and inflamed diverticulum with abscess formation (A) with stranding (*).

Pearls and Pitfalls

Care should be given to apply gentle graded compression on the affected segment of bowel, so as to allow the patient to tolerate the sonogram, as well as for the investigator to adequately visualise pathological findings. Parenteral analgesia is often helpful. Appendicitis and right-sided diverticulitis have similar clinical presentations, but the management of these two conditions is different. Right-sided diverticulitis can often be conservatively managed, while appendicitis remains a surgical emergency. Therefore, a strong effort should be made to achieve a clear sonographic visualisation of the appendix in all patients with right lower quadrant pain.

Other common sonographic findings such as acute pancreatitis or pancreatitis with pseudocyst

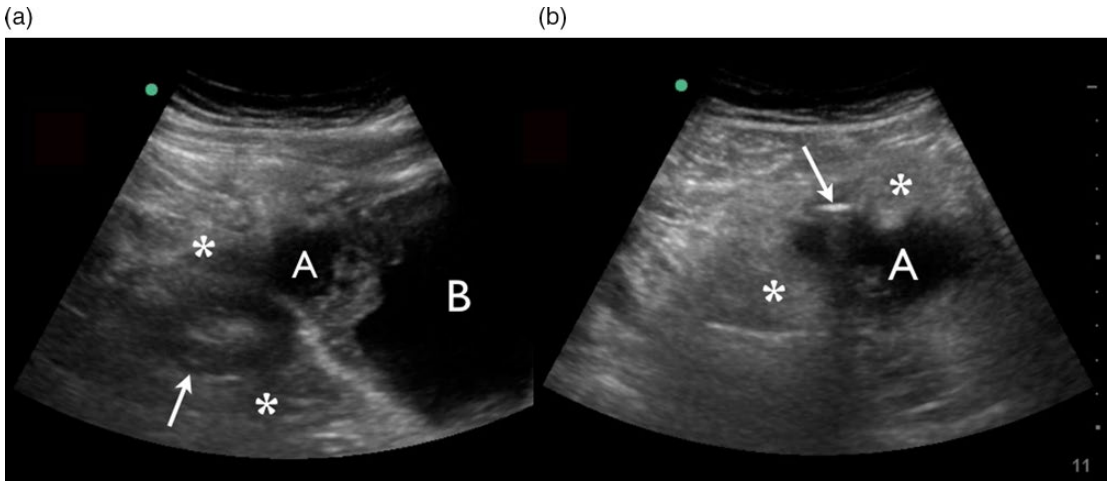

Figure 9.14 (a) Image of diverticulitis with abscess formation (arrow) and tissue inflammation (*). B, bladder; A, fluid pocket. (b) Stranding (*) with flee fluid (A) and micro-perforation with air-fluid level in the pelvis (arrow).

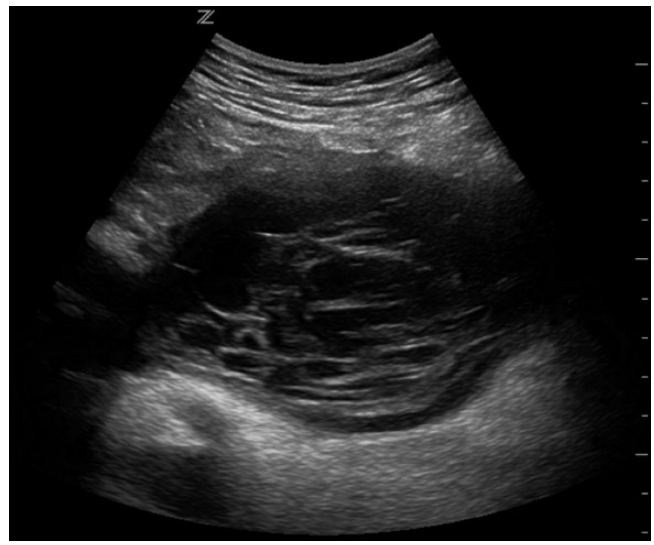

Figure 9.15 Large complex pancreatic cyst.

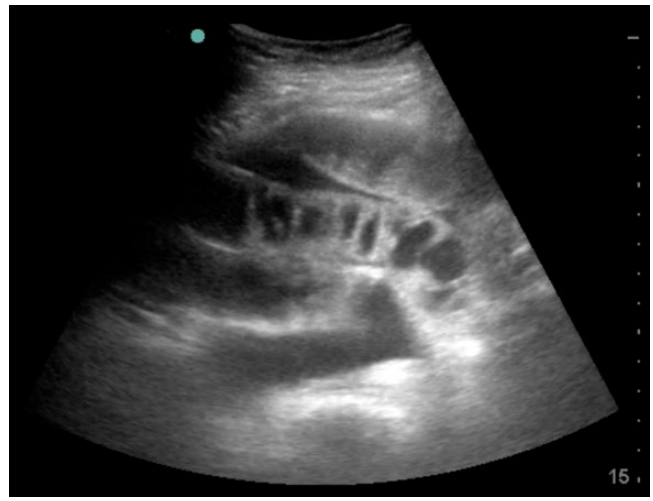

Figure 9.16 Ileus with thickened bowel wall, sedimentation of bowel content and ascites.

development (Figure 9.15) or ileus (Figure 9.16) can be encountered when using bedside ultrasound. Advanced scanning knowledge is usually required to identify these pathologies and to correlate such findings with the clinical presentation.

Further Reading

Binnebösel, M., Otto, J., Stumpf, M., *et al*. (2009) [Akute Appendizitis – Moderne Diagnostik. Der chirurgische Ultraschall] (article in German). *Chirurgia*, **80**, 579–587.

Buckley, O., Geoghegan, T., O'Riordain, D.S., *et al*. (2004) Computed tomography in the imaging of colonic diverticulitis. *Clin. Radiol.*, **59**, 987.

Hoffmann, B., Nürnberg-Westergaard, M. (2012) Focus on abnormal air: diagnostic ultrasonography for the acute abdomen. *Eur. J. Emerg. Med.*, **19** (5), 284–291.

Hollerweger, A. (2006) Acute appendicitis: Sonographic evaluation. *Ultraschall. Med.*, **27**, 412–426.

Huppertz, H., Soriano-Gabarró, M., Grimprel, E., *et al*. (2006) Intussesception among young

children in Europe. *Pediatr. Infect. Dis. J.*, **25**, S22–S29.

Jüngling, A., Holzgreve, A., Kaiser, R. (1998) [Indications for appendectomy from the ultrasound-clinical viewpoint] (article in German). *Zentralbl. Chir.*, **123** (Suppl. 4), 32–37.

Karahan, O., Kurt, A., Yikilmaz, A., Kahriman, G. (2004) New method for the detection of intraperitoneal free air by sonography: scissors maneuver. *J. Clin. Ultrasound*, **32**, 381–385.

King, W.C., Shuaib, W., Vijayasarathi, A., Fajardo, C.G., Cabrera, W.E., Costa, J.L. (2015) Benefits of sonography in diagnosing suspected uncomplicated acute diverticulitis. *J. Ultrasound Med.*, **34** (1), 53–58.

Kori, T., Nemoto, M., Maeda, M., *et al*. (2000) Sonographic features of acute colonic diverticulitis: the 'dome sign'. *J. Clin. Ultrasound*, **28**, 340–346.

Lianos, G., Xeropotamos, N., Bali, C., Baltoggiannis, G., Ignatiadou, E. (2013) Adult bowel intussusception: presentation, location, etiology, diagnosis and treatment. *G. Chir.*, **34** (9-10), 280–283.

Moriwaki, Y., *et al*. (2009) Ultrasonography for the diagnosis of intraperitoneal free air in chest-abdominal-pelvic blunt trauma and critical acute abdominal pain. *Arch. Surg.*, **144**, 137–141.

Nürnberg, D., Mauch, M., Spengler, J., Holle, A., Pannwitz, H., Seitz, K. (2007) Sonographic diagnosis of pneumoretroperitoneum as a result of retroperitoneal perforation. *Ultraschall. Med.*, **28**, 612–621.

Parulekar, S.G. (1985) Sonography of colonic diverticulitis. *J. Ultrasound Med.*, **4**, 659–666.

Preusser, R. (1981) [Ultrasonic diagnosis of acute suppurative appendicitis: a case report (author's translation; article in German). *Wien. Klin. Wochenschr.*, **93** (18), 587–588.

Puyalert, J.B., Rutgers, P.H., Lalisang, R.I., de Vries, B.C., van der Werf, S.D., Dörr, J.P., Blok, R.A. (1987) A prospective study of ultrasonography in the diagnosis of appendicitis. *N. Engl. J. Med.*, **317** (11), 666–669.

Puylaert, J.B. (1986) Acute appendicitis: US evaluation using graded compression. *Radiology*, **158**, 355–360.

Puylaert, J.B. (2012) Ultrasound of colon diverticulitis. *Dig. Dis.*, **30** (1), 56–59.

Raymond-Dufresne, É., Ghanayem, H. (2012) Towards evidence-based emergency medicine: best BETs from the Manchester Royal Infirmary. BET 2: Can emergency physicians safely rule in or rule out paediatric intussusception in the emergency department using bedside ultrasound? *Emerg. Med. J.*, **29** (10), 854–855.

Rettenbacher, T., Hollerweger, A., Macheiner, P., Rettenbacher, L., Tomaselli, F., Schneider, B., Gritzmann, N. (2001) Outer diameter of the vermiform appendix as a sign of acute appendicitis: evaluation at US. *Radiology*, **218** (3), 757–762.

Schwerk, W.B., Wichtrup, B., Maroske, D., Rüschoff, J. (1988) [Ultrasonics in acute appendicitis. A prospective study] (article in German). *Dtsch. Med. Wochenschr.*, **113** (13), 493.

Seitz, K., Reisling, K.D. (1982) Ultrasound detection of free air in the abdominal cavity. *Ultraschall. Med.*, **3**, 4–6.

Valentino, M., Serra, C., Ansaloni, L., Mantovani, G., Pavlica, P., Barozzi, L. (2008) Sonographic features of acute colonic diverticulitis. *J. Clin. Ultrasound*, **37**, 457– 463.

Wang, N., Cui, X.Y., Liu, Y., Long, J., Xu, Y.H., Guo, R.X., Guo, K.J. (2009) Adult intussusception: a retrospective review of 41 cases. *World J. Gastroenterol.*, **15** (26), 3303–3308.

10

Intravascular Volume Assessment by Ultrasound Evaluation of the Inferior Vena Cava

Anthony J. Dean

Background

Ultrasound evaluation of inferior vena cava (IVC) diameter and collapse was initially investigated by nephrologists for use with dialysis. Subsequently, cardiologists investigated it as a surrogate parameter for right atrial pressure, and more recently it has been adopted by intensivists and emergency physicians as a rapid and non-invasive tool to evaluate intravascular volume status. In patients suspected of significant abnormalities of intravascular volume status (depletion or overload), IVC evaluation may rapidly confirm or exclude that derangement.

For example, the test is often used in patients with undifferentiated illnesses, potentially involving multiple organ systems (e.g., shock, dyspnoea, unexplained hypotension), and in such cases the IVC evaluation is usually a component of a more extensive ultrasound examination that may include the heart, lungs, pleural spaces and peritoneal cavity (see Chapter 33). Because of the non-invasive nature and rapidity of the ultrasound examination, it can be repeated as often as necessary and so is valuable in assessing a patient's progress and/or response to therapy. The skills needed for IVC assessment can be learned relatively easily, but like most areas of bedside ultrasonography there are both tricks to make the evaluation quicker and more reliable, and potential pitfalls for the unwary.

The IVC is the major capacitance vessel of the body. As such, its primary role is to serve as a reservoir, providing a ready supply of blood to fill the right side of the heart in diastole. For this reason, and because the pressure differentials between iliac veins and the right atrium are small, the vessel is relatively voluminous (larger diameter than the aorta) with walls which, in non-volume overload states, are pliable and collapsible. The diameter of the IVC varies both with the cardiac and respiratory cycles.

With respect to the cardiac cycle, the IVC is at its most collapsed immediately after opening of the tricuspid valve in early diastole, and most distended at the time of atrial contraction at the end of ventricular diastole. It is frequently possible to appreciate the triple waveform described in physiology textbooks for the internal jugular vein in a moderately underfilled IVC.

When assessing IVC collapsibility, it is very important to distinguish the cardiac and respiratory cycles. The latter are longer, with the IVC maximally distended during expiration and most collapsed during inspiration. The beat-to-beat cardiac waveform is superimposed on this respiratory variation.

An extensive body of literature describes the relationship between sonographically obtained

Emergency Point-of-Care Ultrasound, Second Edition. Edited by James A. Connolly, Anthony J. Dean, Beatrice Hoffmann and Robert D. Jarman.

Companion website: www.wiley.com/go/connolly/ultrasound

IVC parameters and both intravascular volume and cardiac filling pressures. There is strong evidence that, in a given patient (whose IVC is not already fully distended), an increased intravascular volume will result in an increased IVC diameter, a decrease in the respiratory variation of vessel, and a more circular shape in cross-section. A decreasing intravascular volume will have the opposite effects (unless the IVC is already completely empty).

Sonographic Technique

The IVC is best visualised with a 2–4 MHz phased-array or curvilinear probe. There are two windows generally accepted for IVC evaluation: the traditional window has been the subxiphoid, while an alternative is a transhepatic window through the right intercostal spaces. In both cases, the ultrasound waves are transmitted through the liver.

The subxiphoid view has the disadvantage that in many patients the liver window is small or absent, and the transducer pressure needed to obtain adequate views may not be well tolerated, especially by patients with protuberant abdomens and/or shortness of breath. The intercostal window, in contrast, has a large area of underlying liver without interposed bowel, and application of the transducer in this location is less likely to impede respiratory dynamics. The major drawback of the intercostal approach is that the technical skills required for obtaining views of the IVC require a higher degree of manual dexterity and practice.

Regardless of the window chosen, the first task is to identify the IVC, and distinguish it from the many other tubular structures in the upper abdomen, most importantly, the aorta. In order to distinguish these two vessels with certainty, both should be identified in a single transverse image. The two vessels will be seen in cross-section anterior to the shadowing artefact of the vertebral bodies (Figure 10.1). Because the aorta passes through the diaphragm into the posterior thorax around the level of the 12th thoracic vertebral body, and superior to that may be obscured by lung, it is usually necessary to identify the two vessels at this level (Figure 10.2). The IVC can then be followed cephalad, in real time, to be demonstrated entering the right atrium.

The assessment of IVC diameter and collapse is usually made at a level immediately below the hepatic veins (often described as '1–3 cm below the diaphragm'). The sonographic features of the IVC and aorta are compared in Table 10.1. An alternative technique for finding the IVC is

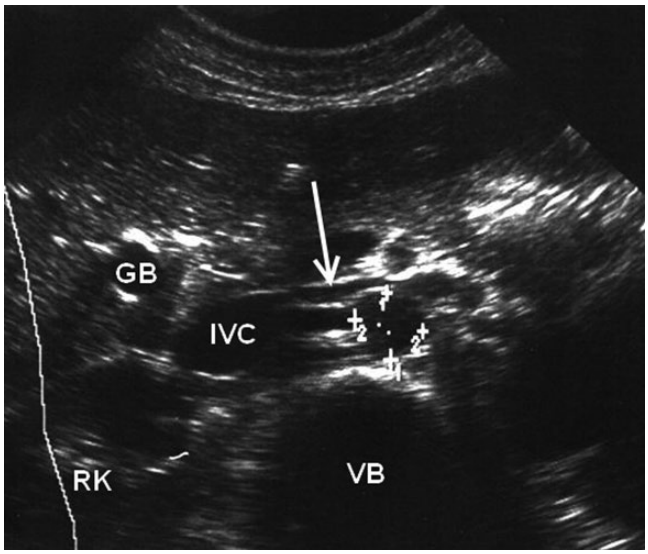

Figure 10.1 Transverse image of the abdomen at the level of the renal vessels. The vertebral body (VB) can be seen with its characteristic shadowing that extends to the bottom of the image. The inferior vena cava (IVC) is seen adjacent to the aorta (callipers). The right kidney (RK) and the gallbladder (GB) can be seen. The left renal vein is indicated by the tip of the arrow. The right renal artery can be seen immediately underneath it.

to obtain a subxiphoid transverse view of the heart and then to fan the transducer inferiorly, demonstrating the right atrium transitioning to the IVC in real time.

The commonest pitfall among inexperienced sonographers is misidentification of some other structure as the IVC, most commonly in severe hypovolaemia when the IVC is completely collapsed. The most frequently substituted structure is the aorta (see Figure 10.9 and Video 10.8), but the hepatic veins, portal veins, gallbladder and pleural effusions may also cause errors (see Figure 10.6). Identification of both the aorta and the IVC in the transverse plane, and visualisation of the IVC entering the right atrium, should ensure accurate IVC identification (Figure 10.3a,b).

Vessel pulsatility *cannot* be used to identify the IVC since, as discussed above, the IVC is a *pulsatile vessel* (see Video 10.3). With experience, caval pulsations in which the most rapid movement is inwards at the beginning of diastole can be distinguished from aortic pulsations, in which the most pronounced movement is outward at the beginning of systole (see Figure 10.9). However this is a distinction that is only reliably recognised with extensive practice in IVC sonography.

Both, longitudinal and transverse planes each have potential flaws that can only be identified by sonographic evaluation in the complementary plane (see Table 10.2). Therefore, *it is necessary always to assess the IVC in both planes*.

Longitudinal Plane

The longitudinal plane has been the traditional choice of cardiologists for measurements of the IVC. It allows the rapid identification of extrinsic structures causing compression to the IVC

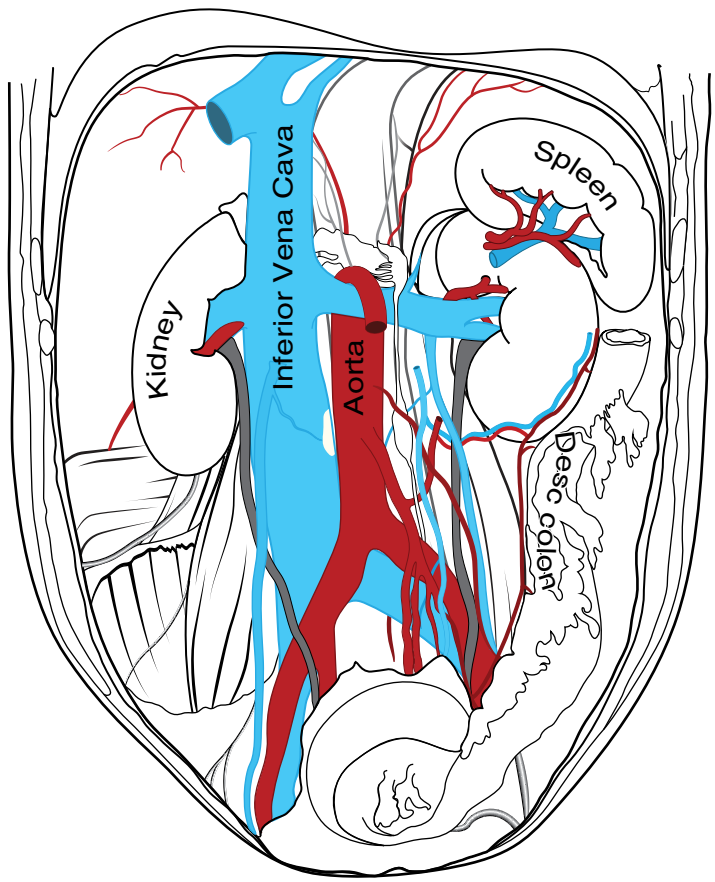

Figure 10.2 Anatomy of the great vessels, demonstrating key anatomical features and relative positions. Note that the aorta enters the abdominal cavity approximately four vertebral levels below the IVC. Above the diaphragmatic hiatus, the aorta can usually not be seen due to interposed lung.

Table 10.1 Sonographic features of the IVC and aorta.

IVC	Aorta
Patient's right	Patient's left
Continuous with the right atrium	If visible above the diaphragm, is seen passing posterior to the heart
Exits abdomen through dome of diaphragm immediately inferior to heart (approximate T8 vertebral body)	Enters abdomen lower (approximate T12 vertebral body) adjacent to vertebral body. Descending thoracic aorta may sometimes be seen behind diaphragm and heart
Compressible, usually ovoid	Non-compressible, round
Thinner walls	Thicker walls
No anterior branches below hepatic veins	Coeliac axis and mesenteric arteries posing anterior to aorta
Size variable, usually larger (unless severe hypovolaemia)	Smaller (unless aneurysmal)
Usually respiratory variation	No respiratory variation
Pulsatile (both respiratory and cardiac beat-to-beat variation)	Pulsatile (beat-to-beat variation only)

(most commonly the diaphragm or liver; see Figure 10.4 and Videos 10.4 and 10.5a and b), and also provides a view of the confluence of the hepatic veins, enabling measurements immediately inferior to this point. Conversely, it is easier for less-experienced sonologists to fail to find a collapsed IVC and/or to misidentify the aorta in this plane. It is also not uncommon for the IVC to slide off a longitudinal plane during the respiratory cycle, resulting in an overestimation of the IVC collapse index (IVC-CI).

Transverse Plane

Assessment in the transverse plane allows for the simultaneous identification of both the IVC and aorta. It also allows for visualisation of the maximum diameter of the vessel throughout the respiratory cycle. However, it requires more skill to identify the appropriate level for measurement inferior to the hepatic vessels. In addition, extrinsic compression of the vessel may not be recognised, resulting in an underestimation of the IVC diameter and/or an overestimation of the IVC-CI. With respect to quantitative assessment, both planes yield similar results.

Acquiring IVC Measurements

A variety of sites have been used to measure the IVC, including the caval-right atrium (RA) junction, inferior to the junction of the hepatic veins, and at the take-off of the left renal vein. Most sonologists make measurements 1–3 cm inferior to the junction of the hepatic veins.

IVC-CI measurements can be made using B-mode images obtained as stills or clips, with calliper measurement during inspiration and expiration (Figure 10.5), or by M-mode tracing with the sampling beam placed through the middle of the vessel throughout the respiratory cycle (Figure 10.6). The M-mode sweep speed should be set at the slowest possible setting, ideally allowing for the assessment of more than one complete respiratory cycle. Whether the transverse or longitudinal plane is being used to make M-mode measurements, the sampling plane is placed in a location such that it remains below the hepatic veins throughout the respiratory cycle. The sonologist should not try to move the probe up and down with the movement of the hepatic veins.

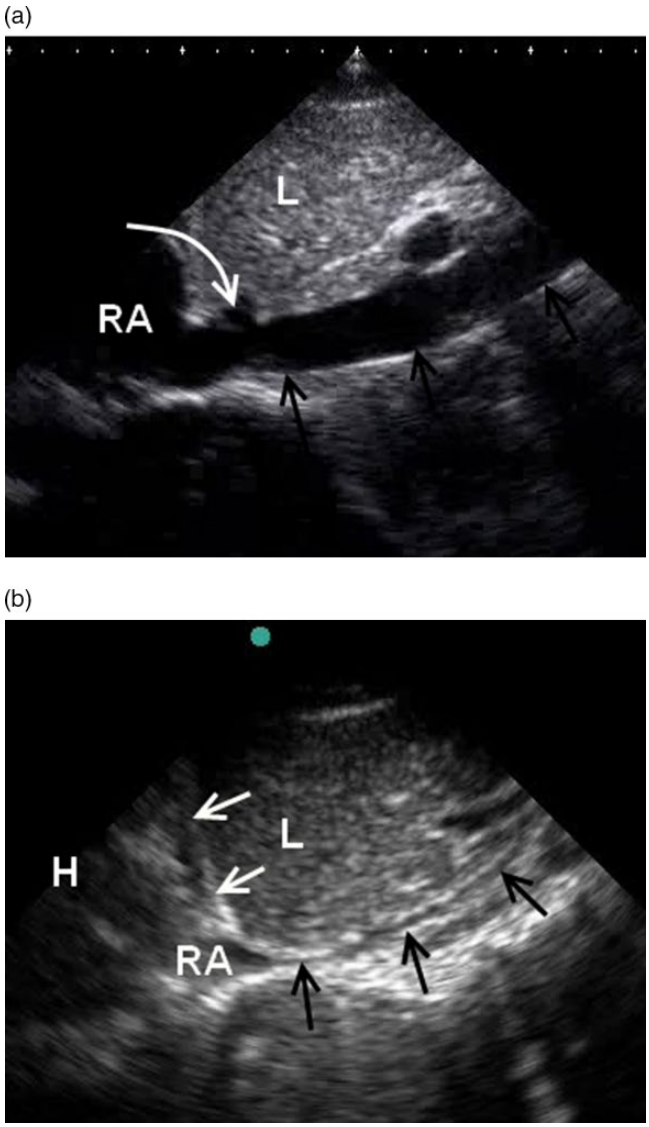

Figure 10.3 Two longitudinal views of IVC (black arrows), which can be seen entering the right atrium (RA) of the heart (H). (a) The IVC is well filled and the structures are easy to identify. The hepatic vein is indicated by the curved white arrow. (b) The IVC is almost slit-like and could easily be overlooked. The liver (L) can be seen inferior to the diaphragm (white arrows). Videos 10.1 and 10.2 show these two IVC examinations in real time.

Although a variety of methods have been advocated in an attempt to standardise the negative intrathoracic pressure of inspiration, it is almost impossible to standardise patient effort or airway factors. Accordingly, most intensivists and emergency physicians perform the test with the patient supine while breathing at rest. The measurement of IVCD-min occurs during inspiration, and the smallest identified diameter is used. The IVCD-max is the maximum identifiable diameter during expiration, and usually occurs at the time of atrial contraction. The electronic callipers are placed at the inner walls across the centre of the IVC.

Table 10.2 Relative advantages and disadvantages of longitudinal and transverse planes for scanning and measuring the IVC (advantageous features are shown in **bold** text).

Longitudinal	Transverse
Allows precise determination of distance below hepatic veins	Requires visual estimate of level by distance to hepatic veins
Allows direct visualisation of strictures of the vessel or of external structures that are compressing the IVC	Strictures and external compression may go unrecognised
Allows direct visualisation of the IVC entering the right atrium in a single image/plane	Visualisation of the IVC entering the atrium requires more skill and experience: following the structures in real time through scanning planes
An unwary sonologist may mistake the aorta for the IVC, especially with collapsed IVC	**Allows sonologist to 'positively identify' both IVC and aorta in single image**
Cylinder-tangent effect: scanning plane may come off middle of IVC through side-to-side respiratory movement of the vessel	**The widest part of vessel can be directly visualised through the respiratory cycle**
Cannot make qualitative estimate of IVC shape	**Allows for qualitative assessment of IVC shape: 'plethoric', 'normal (ovoid)', or 'slit-like'**

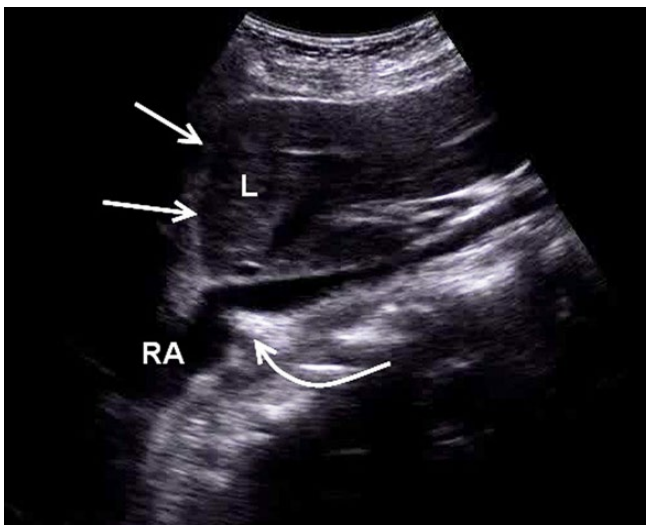

Figure 10.4 A longitudinal view of the IVC with a marked deformity of the posterior wall (curved white arrow), most likely due to the diaphragm. In a transverse view this could be mistaken for collapse. L, liver; the diaphragm is shown by white arrows. Video 10.4 demonstrates this examination in real time.

Interpreting the Ultrasound Examination

Assessment of the IVC is made both qualitatively (shape) and quantitatively (absolute size and collapse index).

Qualitative Assessment

The shape of the IVC can often relay key information. For example, the cross-section of the IVC becomes progressively flatter with intravascular volume depletion, finally becoming slit-like throughout the respiratory and cardiac

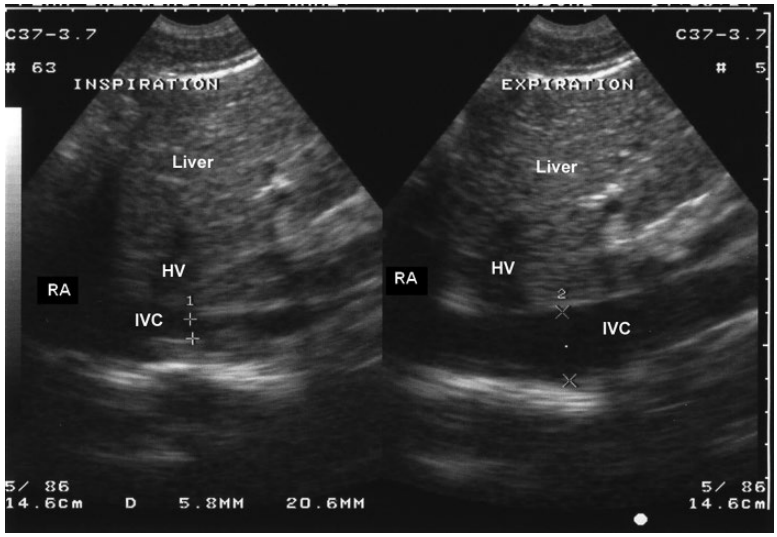

Figure 10.5 In the traditional method of measuring IVC collapse, the vessel (IVC, between callipers) is imaged in a longitudinal plane on inspiration (left image) and expiration (right image) immediately below the hepatic veins (HV). The callipers reveal diameters of 5.8 and 20.6 mm, respectively, for a high normal collapse index of approximately 70%. RA, right atrium.

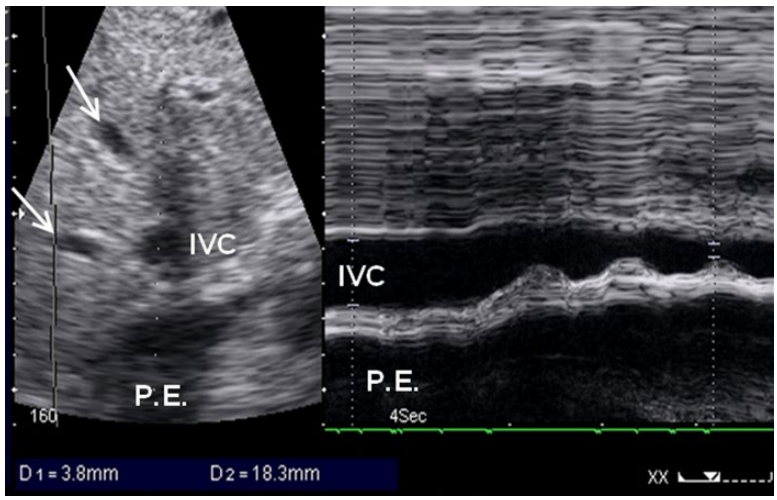

Figure 10.6 Left: A B-mode still image demonstrating a transverse view of the inferior vena cava (IVC), a pleural effusion (P.E.), and the hepatic veins (arrows). Right: Corresponding M-mode image showing approximately 80% collapse. The sonologist must be careful not to mistake pleural effusions for the IVC on M-mode images. This image would be improved by a slower sweep speed, allowing for more than one full respiratory cycle.

cycles with profound hypovolaemia (Figure 10.3 and Videos 10.3 and 10.6). In contrast, the IVC of a hypervolaemic patient tends to be circular and unvarying in diameter (Figure 10.7 and Video 10.7).

With practice, the appearance of the IVC as either round with minimal respiratory and cardiac variation, or completely flat, as well as the various gradations between these two extremes, can be rapidly recognised. Depending on how

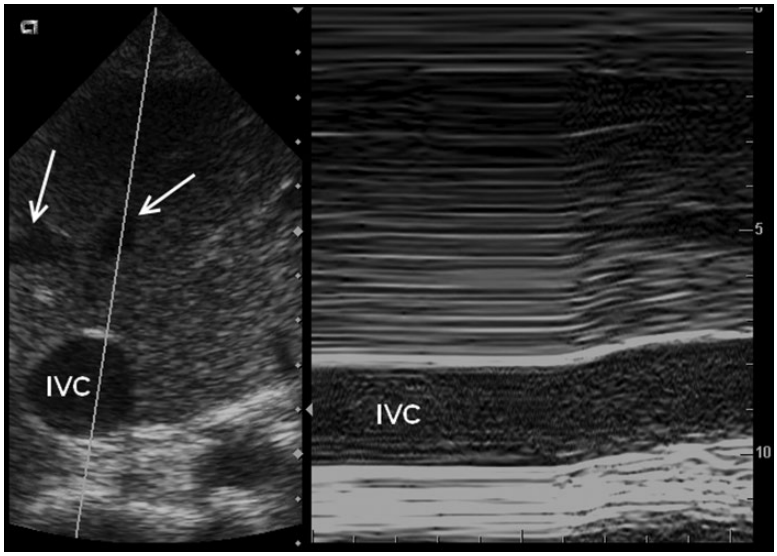

Figure 10.7 M-mode image of a transverse view of a plethoric inferior vena cava (IVC). Arrows indicate hepatic veins. Compare to Video 10.7.

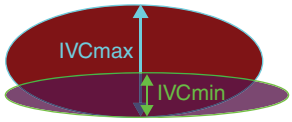

Figure 10.8 Schematic representation of the relationships used to calculate the IVC collapse index.

flat or how plethoric the vessel appears, a clinical judgement can be rapidly made to estimate the likelihood that further volume expansion or diuresis are likely to be helpful to the patient.

Quantitative Assessment

Both absolute size and collapse index can be used as quantitative measures of the IVC. When taking an isolated measurement of the IVC to evaluate intravascular status, the absolute size is usually recorded at its peak diameter during expiration (IVCDe). Recent American Society of Echocardiologist standards have advocated 21 mm as an upper limit of normal for IVC diameter. Conversely, a diameter less than 9 mm is highly suggestive of significant intravascular volume depletion in patients with hypotension or who are in shock. Experienced sonologists will know that 'normal' IVC diameters vary widely, however, and it is possible to have an IVC larger than this without being volume-overloaded, and a diameter less than this without being intravascularly volume-depleted. For example, patients with chronic congestive heart failure may be clinically volume-depleted despite a relatively large IVC. Patient habitus and conditioning also affect IVC diameter, with height and aerobic conditioning being associated with larger IVCs. Despite the lack of consensus regarding a 'normal' IVC diameter in expiration there is strong evidence that, in a given patient, volume expansion causes an increase in IVCDe while volume depletion results in a decrease in IVCDe.

The variation in IVC diameter through the respiratory cycle increases in hypovolaemic states and diminishes in hypervolaemic states. The metric for this variation is the IVC collapse index (IVC-CI), which is calculated using the following equation (Figure 10.8):

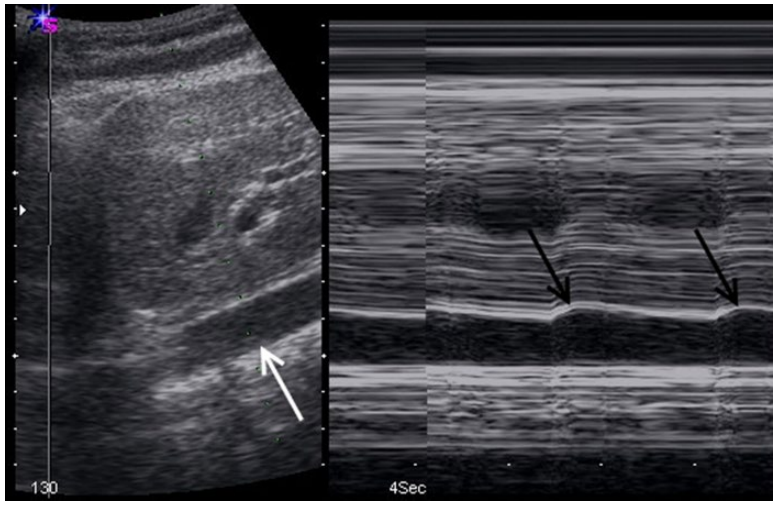

Figure 10.9 B-mode image revealing a longitudinal view of the aorta (white arrow) which has been mistaken for the IVC. The aorta has thicker walls, and in the M-mode image on the right, it can be recognized by its rapid outward movement at the beginning of systole (black arrows). Video 10.8 showing the aorta in longitudinal.

$$\text{IVC-CI} = \left(\text{IVCD-max} - \text{IVCD-min}\right)/\text{IVCD-max}$$

where IVCD-max is the maximal IVCD, measured in expiration, and IVCD-min is the minimal IVCD, measured in inspiration.

Although absolute cut-off values for a normal IVC-CI do not exist, the IVC-CI in normal healthy subjects is typically between 25% and 75%. The clinical utility of an isolated IVC-CI is greatest when the value approaches the extremes. When the IVC-CI is used to assess a dynamic response to therapy, serial values can ensure progression towards a goal (e.g., a 'plump' IVC with less than 25% IVC-CI in a patient with septic shock).

It is important to note that with an increasingly collapsed IVC, the use of the IVC-CI is misleading. For example, a patient with an IVC diameter of 3 mm that collapses to 2 mm is severely hypovolaemic, despite the IVC-CI of only 33%. In this circumstance, more telling parameters are the IVCDe and the slit-like shape.

Special Circumstances

Peadiatric IVC Assesment

IVC assessment in children indexes the IVC diameter against the aortic diameter in order to adjust for size and habitus. In contrast to adults, the measurement is usually made at approximately the level of the renal arteries. A well-hydrated child should have an IVC that is the same diameter as the adjacent aorta or greater. The smaller the IVC in comparison to the aorta, the more confident the clinician can be that the child is hypovolaemic.

Mimics of Volume Overload

There are several causes of IVC dilatation unrelated to intravascular volume. Fortunately, only a small minority of cases of acute shock are due to volume overload. While a large IVCD-max or an IVC-CI approaching 0% are usually the result of hypervolaemia and/or congestive heart failure, other conditions that cause impaired cardiac filling or forward flow have a similar sonographic appearance. Examples include positive-pressure ventilation, cardiac tamponade, tricuspid or pulmonic valvular disease, pulmonary hypertension (due to chronic cardiopulmonary conditions, or acute pathology such as pulmonary embolism), right ventricular infarction, and left-sided heart failure.

Many patients with ventricular hypertrophy and/or chronic heart failure require high filling pressures that will be reflected by a plethoric

IVC. In addition, measurements of the hepatic IVC in patients with liver fibrosis or cirrhosis should be interpreted with caution because the extensive attachments of the IVC to the stiffened hepatic parenchyma can limit the ability of the IVC to collapse.

Whilst many of these conditions can be identified sonographically, the techniques may not be familiar to less-experienced bedside sonologists. For this reason, sonographic findings of hypervolaemia (like most diagnostic tests) should be interpreted in the context of the patient's clinical situation. For sonologists familiar with them, tests for volume-responsiveness should be performed (see Chapters 33 and 36).

Mimics of Hypovolaemia

There are fewer conditions that give rise to the mistaken impression of an empty IVC, and these tend to be more easily recognisable. Intra-abdominal masses (usually hepatic) that compress the IVC may give the false impression of a hypovolaemic state when imaged in the transverse plane. As noted, such a mass should be identifiable in the longitudinal plane.

Increased intra-abdominal pressure, as seen in abdominal compartment syndrome, can cause IVC compression and lead to misidentification of a volume-depleted state. In such cases the presence of high central venous pressures should be confirmed by an ultrasound assessment of the internal jugular veins and superior vena cava.

The Effects of Positive-Pressure Ventilation

Positive-pressure ventilation alters IVC parameters in several ways. By impeding venous return into the thorax it increases IVC diameter, and by reversing the usual pressure changes through the respiratory cycle it undermines the utility of IVC-CI assessment. Studies suggest that the IVC-CI in ventilated patients is significantly lower than that encountered when the patient is removed from the ventilator, so that any IVC-CI >10–20% may be an indicator of fluid-responsive shock.

However, there is no consensus regarding the magnitude of the effect of positive-pressure ventilation. Conversely, a collapsed IVC in the setting of positive-pressure ventilation is almost always indicative of significant hypovolaemia.

Pearls and Pitfalls

- While there are many conditions that can cause an apparently plethoric IVC other than volume overload, it is very rare that a collapsed IVC does not betoken *pathological intravascular volume depletion*, mandating volume resuscitation. This makes IVC assessment a powerful tool in the initial assessment of any patient with undifferentiated shock.
- Always scan the IVC in both transverse and longitudinal planes.
- Both the IVC and aorta should always be positively identified. The IVC should be identified as a tubular structure in the appropriate location with respect to the aorta, and demonstrated in real time to enter the right atrium.
- The measurement of IVC-CI is not useful in patients with a collapsed or slit-like IVC. In almost all circumstances, the qualitative identification of a slit-like appearance or a maximum diameter less than 5 mm is indicative of severe hypovolaemia.
- IVC assessment is of limited use in intubated patients, except if the IVC is found to be underfilled, in which case the patient is almost always significantly volume-depleted.
- Since the IVC has both beat-to-beat and respiratory variation in diameter, it is important to use the respiratory variation in estimating IVC-CI, not the cardiac beat-to-beat variation. To best appreciate this, the M-mode sweep speed should be set to 'low'.

Further Reading

Ando, Y., Yanagiba, S., Asano, Y. (1995) The inferior vena cava diameter as a marker of dry weight in chronic hemodialyzed patients. *Artif. Org.*, **19** (12), 1237–1242.

Bendjelid, K., Romand, J., Walder, B., Suter, P., Fournier, G. (2002) Correlation between measured inferior vena cava diameter and right atrial pressure depends on the echocardiographic method used in patients who are mechanically ventilated. *J. Am. Soc. Echocardiogr.*, **15**, 944–949.

Brennan, J.M., Blair, J.E., Goonewardena, S., *et al.* (2007) A comparison by medicine residents of physical examination versus hand-carried ultrasound for estimation of right atrial pressure. *Am. J. Cardiol.*, **99** (11), 1614–1616.

Carr, B.G., Dean, A.J., Everett, W.W., Ku, B.S., Mark, D.G., Okusanya, O., Horan, A.D., Gracias, V.H. (2007) Intensivist Bedside Ultrasound (INBU) for volume assessment in the intensive care unit: a pilot study. *J. Trauma Injury Infect. Crit. Care*, **63** (3), 495–502.

Chen, L., Hsiao, A., Langhan, M., Riera, A., Santucci, K.A. (2010) Use of bedside ultrasound to assess degree of dehydration in children with gastroenteritis. *Acad. Emerg. Med.*, **17** (10), 1042–1047.

Feissel, M., Michard, F., Faller, J.P., Teboul, J.L. (2004) The respiratory variation in inferior vena cava diameter as a guide to fluid therapy. *Intensive Care Med.*, **30**, 1834–1837.

Levine, A.C., Shah, S.P., Umulisa, I., *et al.* (2010) Ultrasound assessment of severe dehydration in children with diarrhea and vomiting. *Acad. Emerg. Med.*, **17** (10), 1035–1041.

Lyon, M., Blaivas, M., Brannam, L. (2005) Sonographic measurement of the inferior vena cava as a marker of blood loss. *Am. J. Emerg. Med.*, **23**, 45–50.

Mark, D.G., Ku, B.S., Carr, B.G., Everett, W.W., Okusanya, O., Horan, A., Gracias, V.H., Dean, A.J. (2007) Directed bedside transthoracic echocardiography: preferred cardiac window for left ventricular ejection fraction estimation in critically ill patients. *Am. J. Emerg. Med.*, **25** (8), 894–900.

Mitaka, C., Nagura, T., Sakanishi, N., Tsunoda, Y., Amaha, K. (1989) Two-dimensional echocardiographic evaluation of inferior vena cava, right ventricle, and left ventricle during positive-pressure ventilation with varying levels of positive end-expiratory pressure. *Crit. Care Med.*, **17** (3), 205–210.

Pershad, J., Myers, S., Plouman, C., Rosson, C., Elam, K., Wan, J., Chin, T. (2004) Bedside limited echocardiography by the emergency physician is accurate during evaluation of the critically ill patient. *Pediatrics*, **114**, e667–e671.

Rudski, L.G., Lai, W.W., Afilalo, J., Hua, L., Handschumacher, M.D., Chandrasekaran, K., Solomon, S.D., Louie, E.K., Schiller, N.B. (2010) Guidelines for the echocardiographic assessment of the right heart in adults: a report from the American Society of Echocardiography endorsed by the European Association of Echocardiography, a registered branch of the European Society of Cardiology, and the Canadian Society of Echocardiography. *J. Am. Soc. Echocardiogr.*, **23** (7), 685–713.

Stawicki, S.P., Braslow, B.M., Panebianco, N.L., *et al.* (2009) Intensivist use of hand-carried ultrasonography to measure IVC collapsibility in estimating intravascular volume status: correlations with CVP. *J. Am. Coll. Surg.*, **209** (1), 55–61.

Wallace, D.J., Allison, M., Stone, M.B. (2010) Inferior vena cava percentage collapse during respiration is affected by the sampling location: an ultrasound study in healthy volunteers. *Acad. Emerg. Med.*, **17** (1), 96–99.

Yanagawa, Y., Nishi, K., Sakamoto, T., Okada, Y. (2005) Early diagnosis of hypovolemic shock by sonographic measurement of inferior vena cava in trauma patients. *J. Trauma*, **58**, 825–829.

11

Emergency Ultrasound in First-Trimester Pregnancy

Andrew M. Kestler and John L. Kendall

Introduction

This chapter is directed towards all practitioners engaged in the evaluation of acute pelvic symptoms in the first trimester of pregnancy. Clinician-performed ultrasound in this clinical setting has become a standard of practice and training world-wide. It has been described in remote or under-resourced environments including Rwanda and Liberia. In addition to the material presented here, supervised hands-on experience is necessary to attain proficiency in the procedure.

The justifications for including a first-trimester ultrasound examination among the 'core' applications of clinician-performed ultrasound are many. First, presentations of first-trimester pregnancy complications are common. Second, a recent systematic review by McRae and others showed that clinician-performed ultrasound has a very high specificity (approaching 100%) for detecting an intrauterine pregnancy, and thus indirectly excluding an ectopic pregnancy. Third, clinician-performed ultrasound investigations have been shown to decrease the evaluation time for both patients in whom the diagnosis of ectopic is excluded, and those needing operative intervention.

Indications

The primary goal of first-trimester emergency ultrasound is to identify an *intrauterine* pregnancy (IUP) in pregnant patients presenting with abdominal pain and/or vaginal bleeding. The identification of an IUP effectively rules out an ectopic pregnancy (rare exceptions are discussed below). Other applications of clinician-performed pelvic ultrasound (as discussed in this chapter) – including pregnancy dating – are secondary goals that facilitate decision-making in cases of threatened abortion or pregnancy loss.

Technique

Transabdominal and transvaginal views are both useful in the assessment of patients with first-trimester complaints. Transabdominal ultrasound (TAU) may be more acceptable to the patient and should be the initial approach. It may be combined with the evaluation of intra-abdominal free fluid in the hepatorenal space or elsewhere. When TAU yields the necessary information, there is usually no need to perform a transvaginal ultrasound (TVU) examination.

Emergency Point-of-Care Ultrasound, Second Edition. Edited by James A. Connolly, Anthony J. Dean, Beatrice Hoffmann and Robert D. Jarman.

Companion website: www.wiley.com/go/connolly/ultrasound

A transvaginal examination is considered by some to be more invasive, and requires additional skills for those familiar with abdominal sonography. However, it typically produces higher-resolution images and a higher specificity in identifying an intrauterine pregnancy.

TAU views are easier to obtain through the acoustic window of a full bladder, whereas TVU is optimal with an empty bladder. Many institutions have traditionally placed a Foley catheter to fill the urinary bladder for transabdominal views. This is not necessary if the sonologist is proficient in TVU.

Transabdominal Technique

A curvilinear transducer usually performs best, but a phased-array transducer may also be used. The operator places the transducer just cephalad to the pubic symphysis, initially in the transverse position with the marker to the patient's right (Figure 11.1 and Video 11.1). Slow

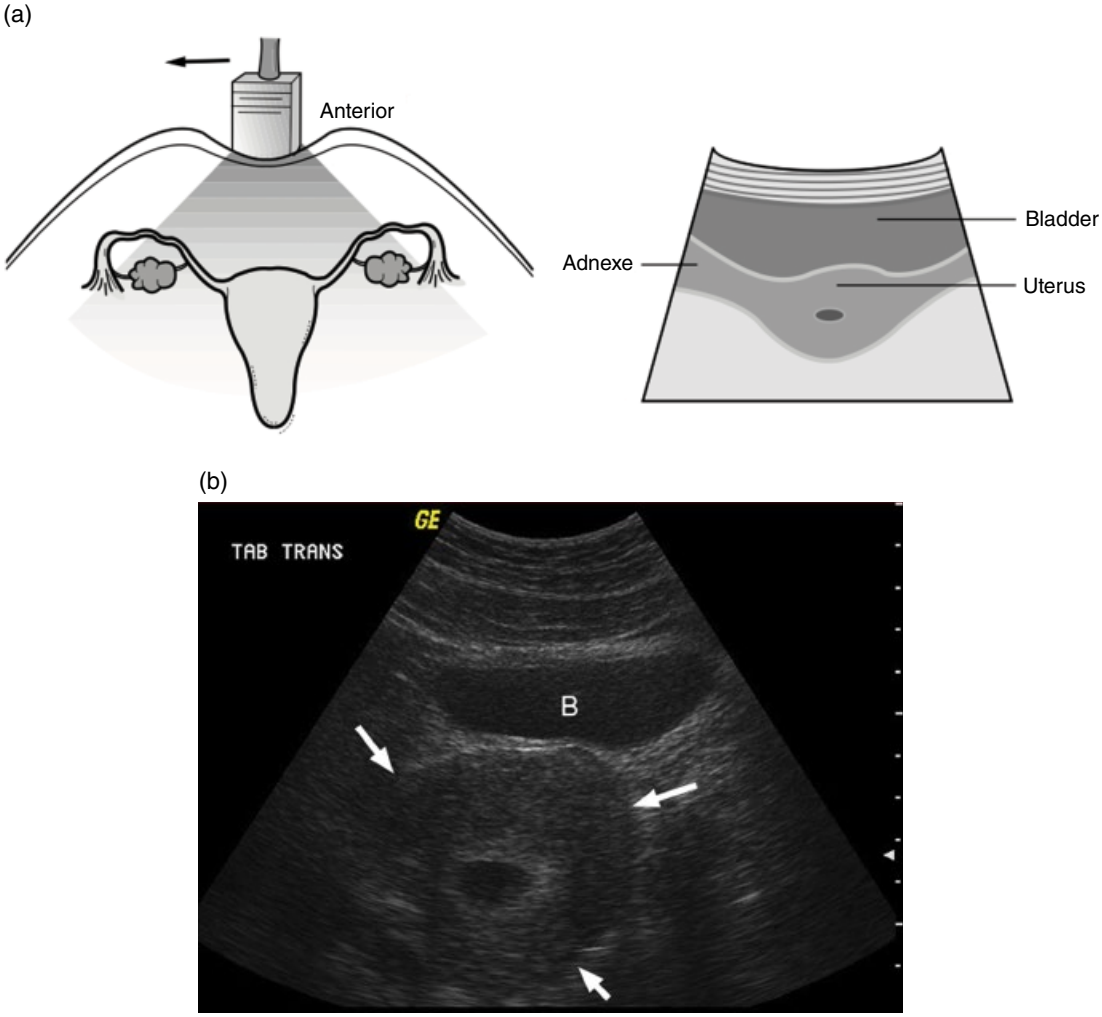

Figure 11.1 (a) Diagram of an ultrasound transducer placed transabdominally in the transverse scanning plane. (b) Ultrasound image taken with the transducer placed transabdominally in the transverse scanning plane. The usual location of the uterus (arrows) immediately behind the bladder (B) is seen. The myometrium (relatively hypoechoic) surrounds a layer of endometrium (relatively hyperechoic) within which an anechoic non-specific intrauterine sac is seen.

fanning from caudad to cephalad will typically demonstrate the urinary bladder inferiorly and the uterus superiorly. Fanning should systematically demonstrate views from cervix to fundus, while directing the probe slightly laterally will usually demonstrate the ovaries as well as any adnexal masses. The transducer should then be rotated 90° clockwise to demonstrate a long-axis view of the uterus. Fanning from side to side will typically permit an examination of the entire lateral extent of the pelvis, including both adnexa and the uterus (Figure 11.2 and Video 11.2). This view allows for demonstration of the *anchoring anatomy* of this examination:

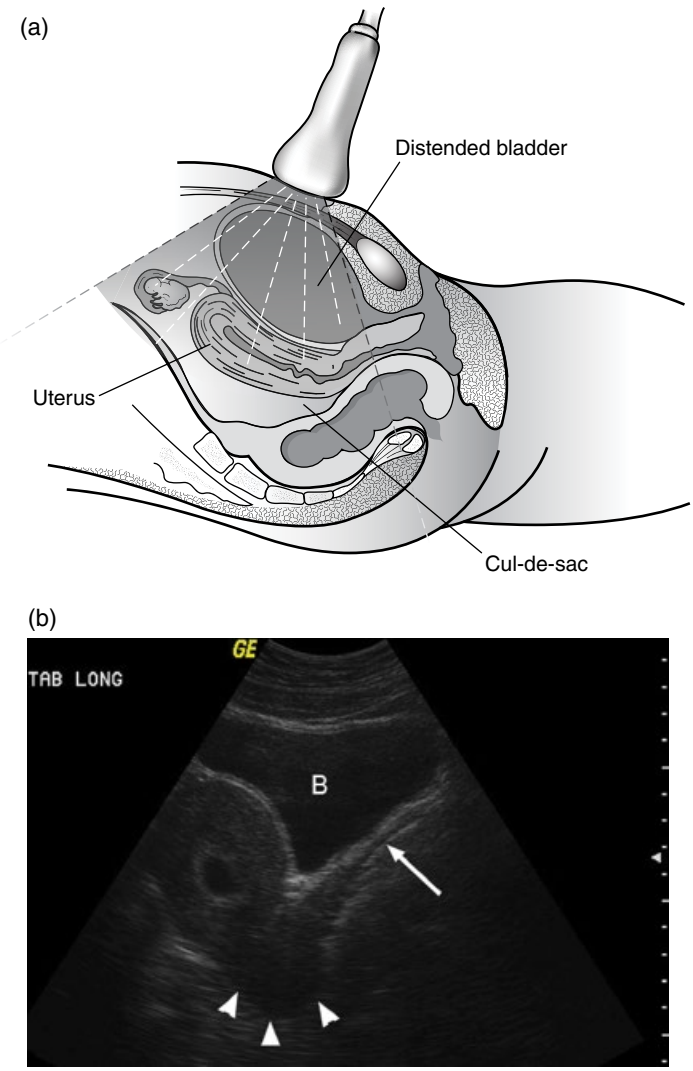

Figure 11.2 (a) Diagram of an ultrasound transducer placed transabdominally in the longitudinal scanning plane. (b) Longitudinal image of the same patient as in Figure 11.1. The vagina and endovaginal stripe (arrow) can be seen immediately behind the bladder (B). The cul de sac is the post-dependent portion of the peritoneal cavity and lies posterior to the cervix (arrowheads). A non-specific intrauterine sac is again seen.

the vagina is located posterior to the bladder, and demonstrated to be connected to the cervix, which is in turn continuous with the uterus (Figure 11.2b and Video 11.2). Demonstration of an IUP in this plane definitively identifies it as being intrauterine, thereby avoiding the most serious error of this exam: identification of a pregnancy and *failure to recognise that it is outside the uterus*.

Transvaginal Technique

If an intrauterine pregnancy has not been identified on TAU, the next step for those with the equipment and the training is to perform an TVU. This exam can identify intrauterine pregnancy about a week earlier than TAU. In the interests of efficiency, a clinician-performed TVU will be performed immediately before or after the pelvic examination since the set-up and need for a chaperone are the same for both. The patient is placed in the lithotomy position, ideally on a stretcher with stirrups. In the absence of a pelvic examination table, the patient may be examined in the frog-leg position with support under the buttocks to elevate the pelvis. Without pelvic support it is not possible to move the transducer handle posteriorly in order to visualise the uterus anteriorly and superiorly. Gel should be placed on the transducer tip before applying a disposable sheath, which is then externally lubricated. The transducer tip is inserted slowly into the vaginal canal in the sagittal plane, with the indicator towards the ceiling. The operator maintains a view on the image screen as the transducer is advanced along the anterior vaginal wall, with the goal of final placement in the anterior fornix for the 90% of patients with an anteroverted uterus (Figure 11.3). For patients with a retroflexed uterus, the tip of the transducer will be in the posterior fornix for the examination (Figure 11.3). Fanning gently from side to side will once again enable real-time views of the entire lateral extent of the pelvis from the internal iliac vessels on one side to the other (Video 11.3). The transducer is then rotated 90° anticlockwise to obtain a short-axis view of the uterus (Figure 11.4 and Video 11.4). Although transvaginal views may initially be disorienting, they become familiar with a little experience. The primary goal of the clinician-performed examination is methodical fanning from the cervix to fundus in order to rule in or exclude IUP, but with experience a systematic examination of the adnexa can also be performed.

Sonographic Findings

Normal Pregnancy

The clinician sonologist should be familiar with how the findings of normal pregnancy correlate to gestational age. The usual sonographic signs are listed in Table 11.1, along with their dates of appearance. Although intradecidual signs and double-decidual signs are listed to familiarise the reader with the terms, they will not be further discussed at this point (Figure 11.5). These findings are subjective, and do not provide definitive signs of IUP in the context of clinician-performed sonology. The definitive findings of an IUP are yolk sac (Figure 11.6), and/or foetal pole (Figure 11.7). While not essential, measurements of crown–rump length (CRL)] and cardiac activity can be made (Figure 11.8). The normal range for a foetal heart rate (FHR) from a gestational age of 8 weeks onward is 120–160 beats per minute. Prior to that, FHRs are usually in the range of 90–100 bpm. Normal pregnancies are surrounded by a minimum of 5 mm of myometrium (see Pitfalls below).

Table 11.1 Findings of IUP by dates.

Sonographic sign	Transvaginal visible at:	Transabdominal visible at:
Intradecidual sign	4–5 weeks	N/A
Double decidual sign	5 weeks	6 weeks
Yolk sac*	5–6 weeks	6–7 weeks
Foetal pole*	5–6 weeks	6–7 weeks
Cardiac activity*	6 weeks	8 weeks

* Definitive for intra-uterine pregnancy, if seen in uterus.

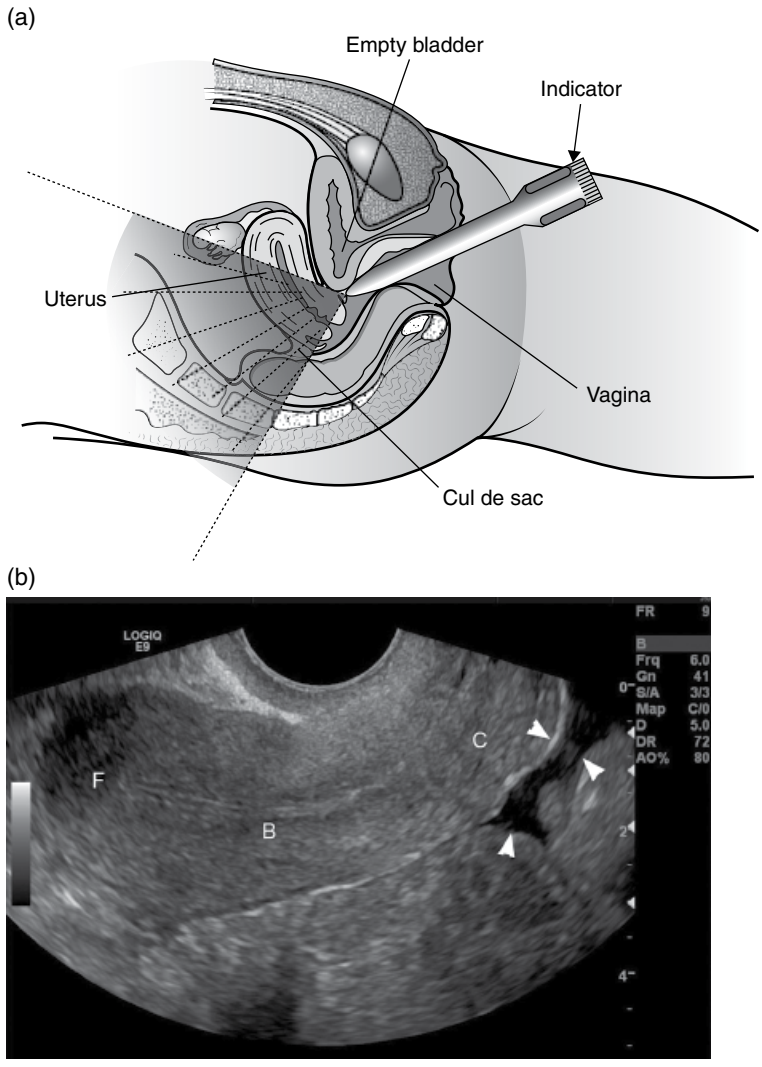

Figure 11.3 (a) Diagram of an ultrasound transducer placed endovaginally in the sagittal scanning plane. (b) An endovaginal scan of a typical non-gravid anteroverted uterus in the sagittal scanning plane. The cervix (C), body (B) and fundus (F) can be seen. The uterus has almost no endometrial lining, suggesting that the patient has just finished menstruating or is post-menopausal. Note the small amount of fluid in the cul-de-sac (arrowheads). If the patient had a positive pregnancy test, this scan would be suspicious for ectopic pregnancy.

Gestational Age Calculations

To assist clinical decision-making, the sonologist should be familiar with techniques to determine gestational age using foetal measurements. Measurement of the gestational sac (Figure 11.9) and the CRL (Figure 11.10) are most useful in the first trimester, although the former parameter is more prone to measurement variability. Many ultrasound machines will calculate a gestational age based on the average of several gestational sac measurements (mean sac diameter; MSD). Later pregnancy measurements include the bi-parietal diameter (BPD) (Figure 11.11) and femur length (FL) (Figure 11.12).

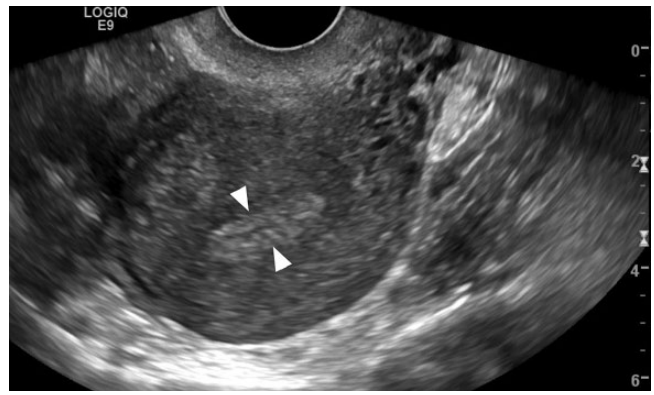

Figure 11.4 Endovaginal transverse view of the uterus with the transducer in the coronal plane. A thin layer of endometrium can be seen (arrowheads).

Abnormal Findings

It is not the primary role of the clinician sonologist to definitively identify an ectopic pregnancy. However, certain secondary findings may be increase suspicion for the diagnosis. Relevant findings include adnexal mass or pelvic/intra-peritoneal free fluid. Optimal gain settings and experience are needed to recognise the extensive clot that may be present with a ruptured ectopic pregnancy. Clot has a heterogeneous soft-tissue echodensity not dissimilar from that of bowel and peritoneal fat. To distinguish an adnexal mass, the sonologist should be familiar with the normal appearance of the ovaries (Figure 11.13). Pelvic free fluid can be categorised by degrees: a "small" volume of free fluid typically up to 15 ml can be physiological, extending up to one-third of the length of the [non-enlarged] uterus (Figure 11.14). 'Moderate free fluid' extends up to two-thirds of the length of the uterus (Figure 11.15), while a 'large' volume of fluid extends more than two-thirds of the uterus length. In the absence of a clear IUP, the larger the volume of fluid the greater the likelihood of an ectopic pregnancy. The findings of fluid reaching the upper abdomen (Morrison's pouch and the splenorenal space should be examined) or the presence of complex free fluid in the pelvis (Figures 11.16–11.18) confer an even greater likelihood of a ruptured ectopic pregnancy. Ultimately, the only way to definitively diagnose an ectopic pregnancy is to identify an extra-uterine gestational sac (Figure 11.19), but this finding is only present in 10–24% of cases.

The clinician sonologist should be familiar with other signs suggestive of an abnormal pregnancy, although such findings usually require consultative ultrasound for their confirmation. When an ectopic pregnancy is not a clinical concern, most consultative studies can be performed on an urgent rather than emergency basis. The absence of foetal heart activity by seven weeks of gestation (in the presence of other findings definitive for IUP) suggests foetal demise. A FHR lower than 120 bpm may be normal up to eight weeks of gestation. Later, foetal bradycardia may suggest an abnormal pregnancy. Heterogeneous material in the uterus suggests an incomplete abortion, but this finding also occurs with the pseudogestational sac of ectopic (Figure 11.20) and molar pregnancy. An empty uterus is interpreted in the context of the quantitative β-human chorionic gonadotrophin (β-hCG) and other clinical and sonographic findings (see below). A gestational sac greater than 20 mm without other diagnostic findings is consistent with a blighted ovum, or anembryonic pregnancy (Figure 11.21). A molar pregnancy can vary in appearance with components of 'grape-like' vesicles and diffuse heterogeneous echodensities described as a 'snowstorm' within the uterus (Figure 11.22), or other non-specific findings.

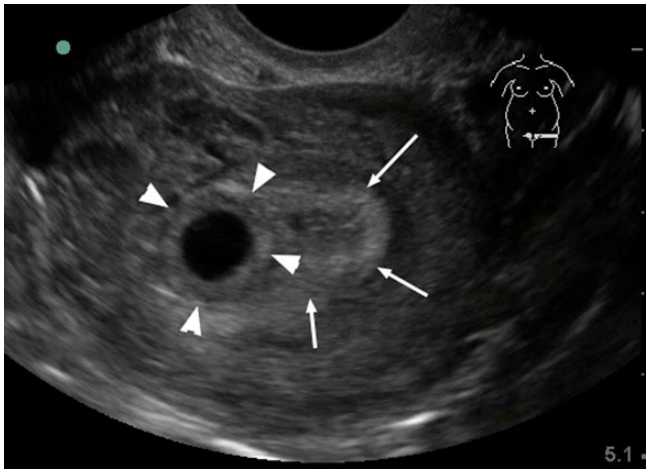

Figure 11.5 Coronal TVU of uterus demonstrating a double-decidual sign with an 'inner' (arrowheads) and 'outer' (arrows) layer of endometrium. In this image there is no definitive finding of IUP.

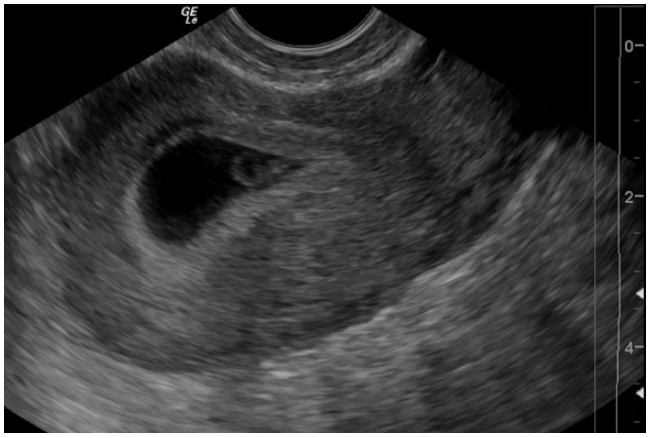

Figure 11.6 A sagittal TVU image showing a yolk sac and foetal pole. The double-decidual sign can still be faintly seen.

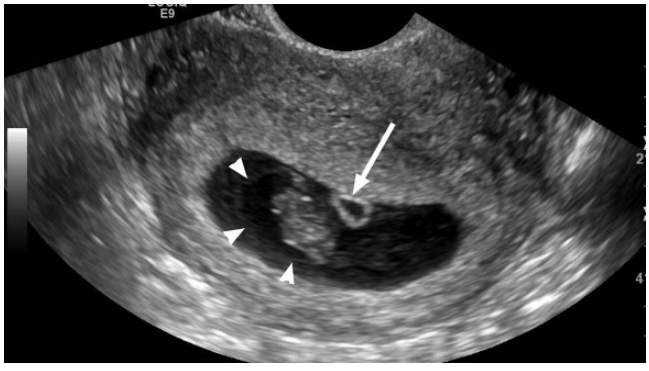

Figure 11.7 A transverse TVU image of the uterus demonstrating a collapsing yolk sac (arrow) and foetal pole. The amniotic membrane (arrowheads), not to be confused with the yolk sac, can also be seen.

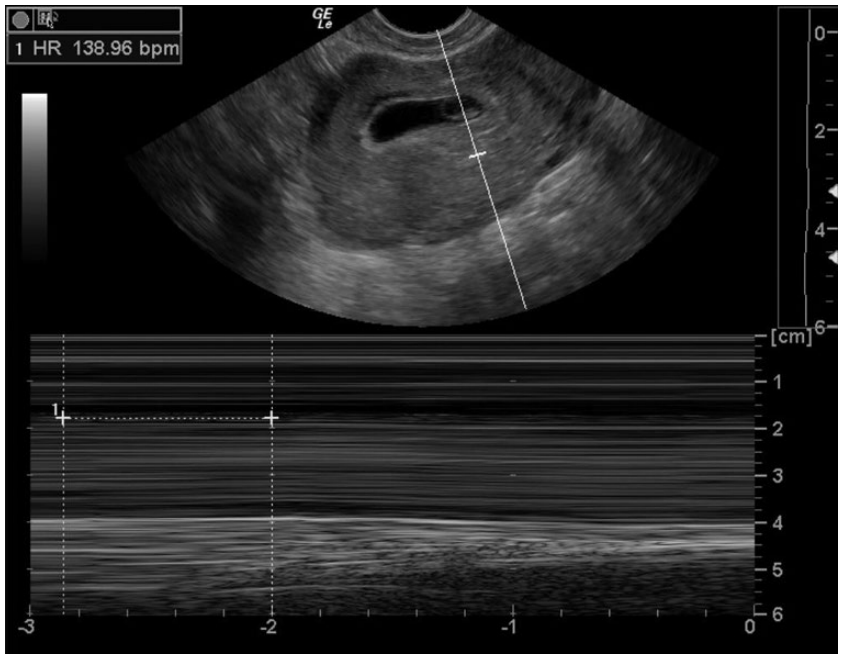

Figure 11.8 M-mode TVU image of an embryo demonstrating foetal cardiac activity at 138 beats per minute.

Figure 11.9 Coronal (a) and sagittal (b) TVU demonstrating calculation of mean sac diameter (MSD). In both images a collapsing amniotic sac (*not* yolk sac; see Figure 11.7) can be seen. The absence of definitive findings of IUP at this stage, in combination with the poorly defined heterogeneous endometrium with shaggy internal margins and areas of apparent liquefaction or haemorrhage (arrows), strongly suggest that this is an abnormal and non-viable IUP.

(a)

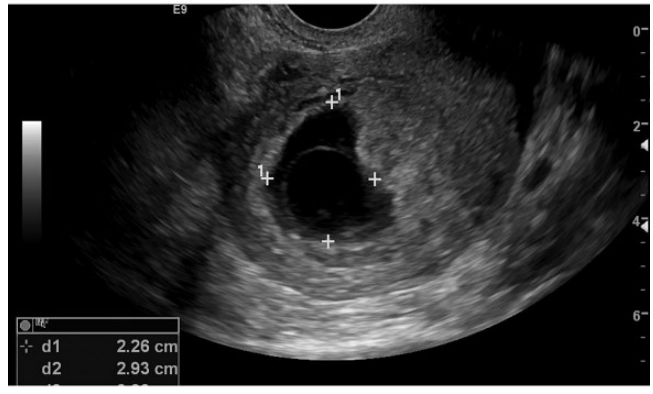

(b)

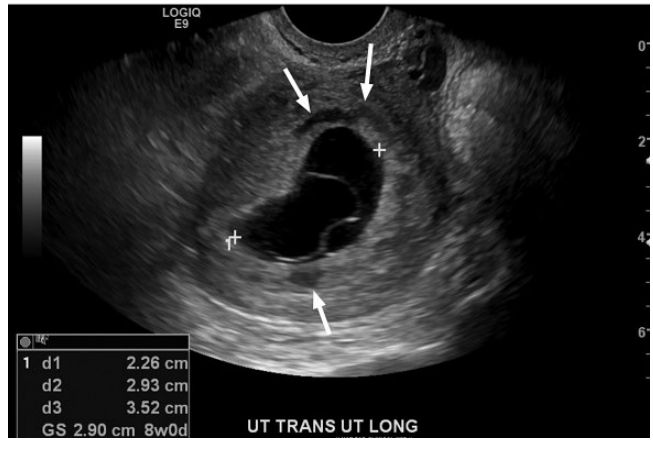

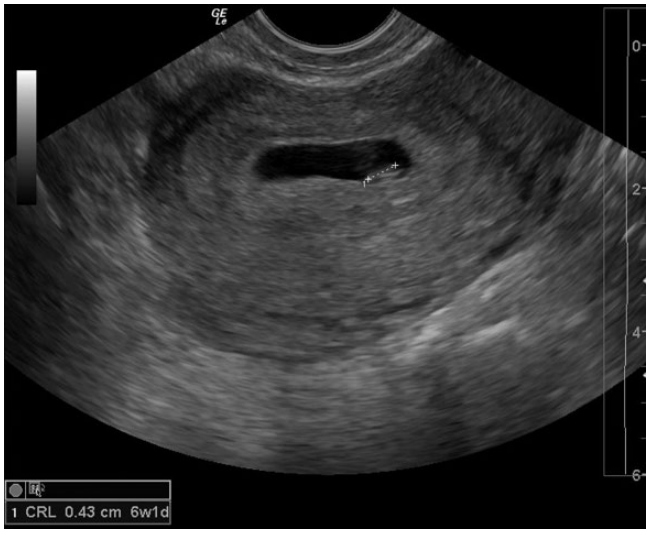

Figure 11.10 Ultrasound image demonstrating the crown–rump length (CRL) measurement of a six-week, one-day gestational age embryo.

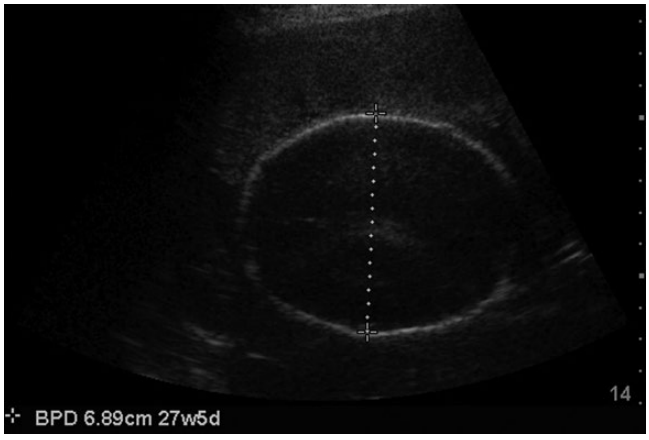

Figure 11.11 TAU image demonstrating the biparietal diameter (BPD) measurement of a 27-week, five-day-old foetus. The gain is set too low. The measurement should be made from the inside table on one side to the outside table of the bone on the other.

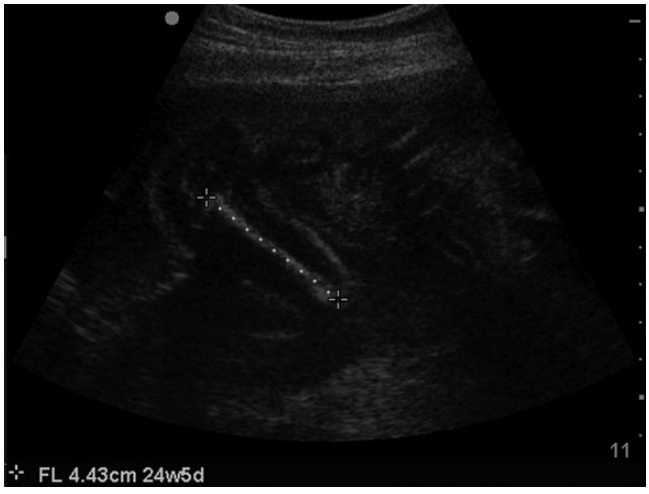

Figure 11.12 Ultrasound image demonstrating the femur length (FL) measurement of a 24-week, five-day-old foetus.

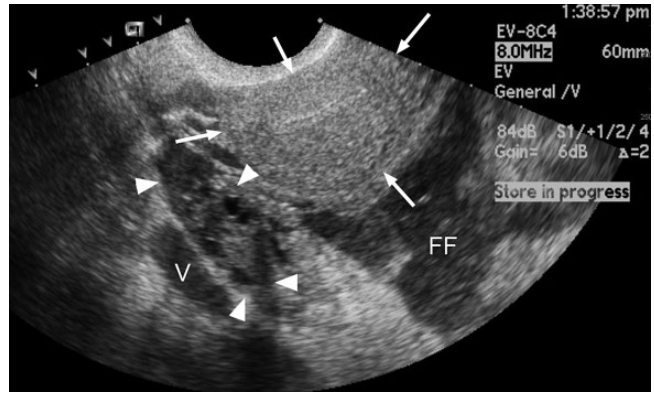

Figure 11.13 TVU image of a normal-appearing right ovary (arrowheads) adjacent to an empty uterus. The location of the ovary adjacent to the internal iliac vein (V) is common. The presence of a large volume of heterogeneous free fluid (FF) is suggestive of the presence of a ruptured ectopic pregnancy.

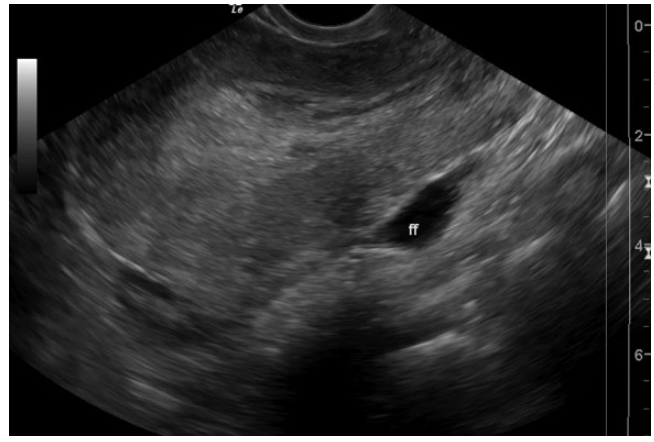

Figure 11.14 Longitudinal TVU image demonstrating small (physiological) volume of free fluid (ff) in the cul-de-sac.

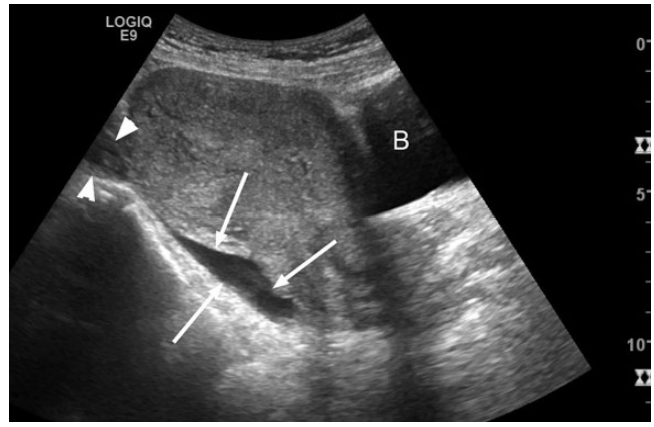

Figure 11.15 TAU image with a moderate amount of free fluid in the cul de sac (arrows) behind a uterus without identifiable decidual reaction (endometrium). Abnormal free fluid tends to have a 'pointy' shape. in contrast to anatomical collections of fluid such as those in the bladder (B) or bowel (arrowheads).

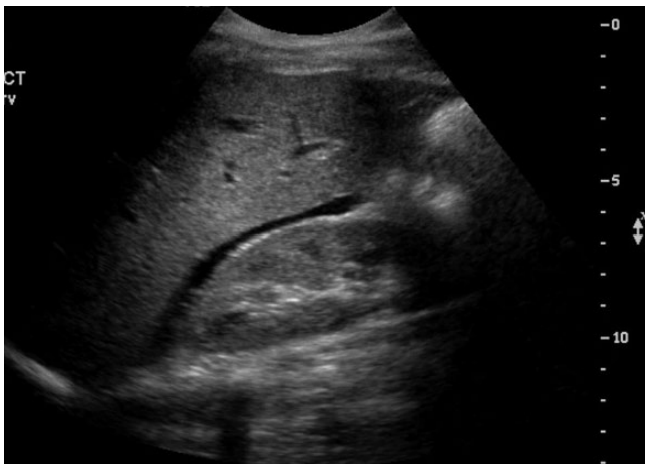

Figure 11.16 Right upper quadrant image of Morrison's pouch demonstrating free intraperitoneal fluid in a patient with ectopic pregnancy.

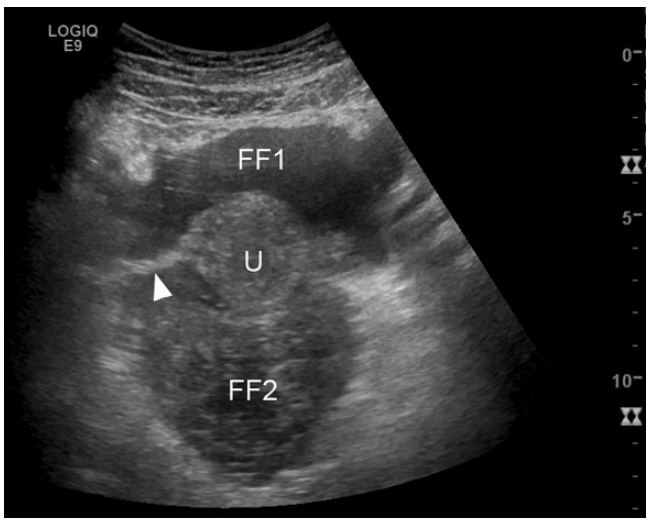

Figure 11.17 TAU showing an empty uterus and uterine ligament (arrowhead) surrounded by a large volume of complex free fluid anteriorly (FF1) and in the recto-uterine space (FF2).

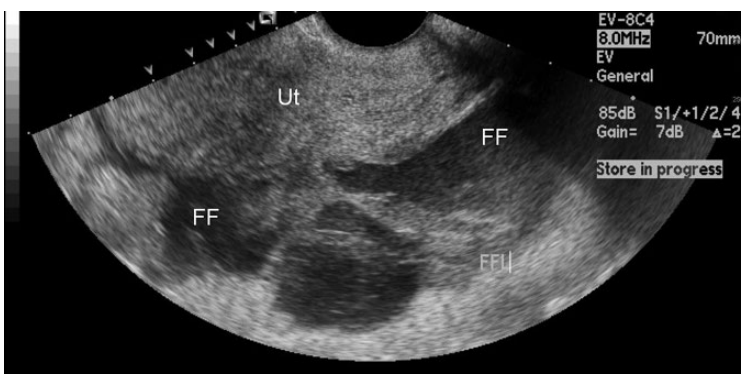

Figure 11.18 TVU demonstrating an empty uterus with no decidual reaction and large volume of complex fluid (FF) in the cul-de-sac.

(a)

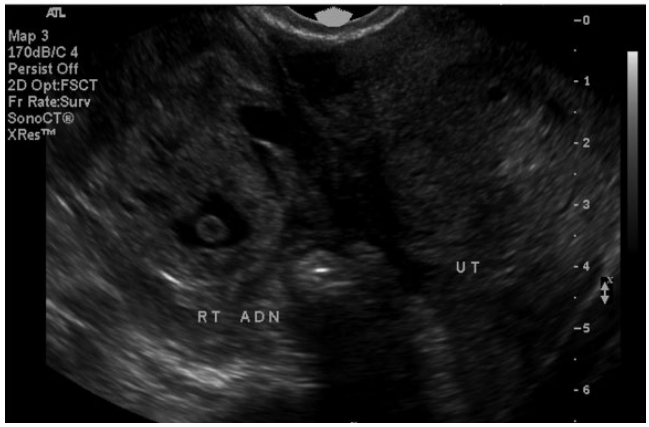

(b)

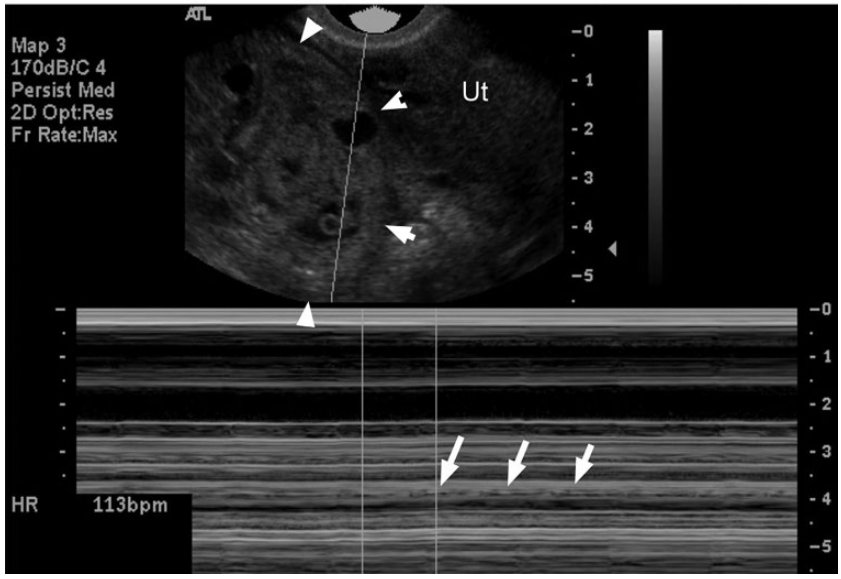

Figure 11.19 (a) Transvaginal ultrasound image demonstrating an extra-uterine yolk sac within a mass adjacent to the empty uterus (UT) in the right adnexa (RT ADN). (b) TVU of the same case showing greater detail of the empty uterus (Ut) with a large complex adnexal mass (arrowheads) containing a yolk sac and foetal pole. M-mode reveals cardiac activity (arrows).

Pitfalls

Sonographic findings should be used in conjunction with clinical judgement. The greatest and most serious pitfall is the mistaken assumption that an apparently normal yolk sac, embryo, foetal heart motion or foetal motion is actually in the uterus. Strict adherence to definitive criteria for IUP and demonstration of the previously described "anchoring anatomy" in the images of the gestational sac can help to avoid this pitfall. The sonologist should be watchful for gestational sacs that appear either too high (interstitial or "corneal" ectopic) or too low in the uterus (cervical ectopic). These are relatively rare locations for ectopic, but are particularly

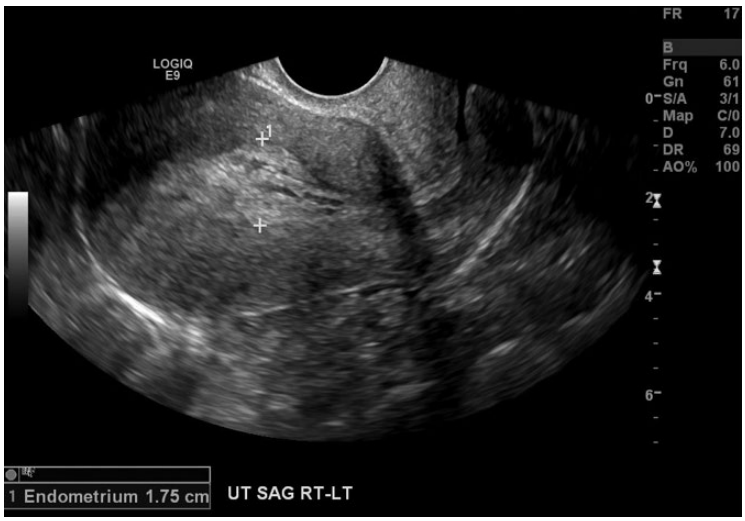

Figure 11.20 Longitudinal TVU image demonstrating complex endometrial material (between callipers) in a patient with an incomplete spontaneous abortion.

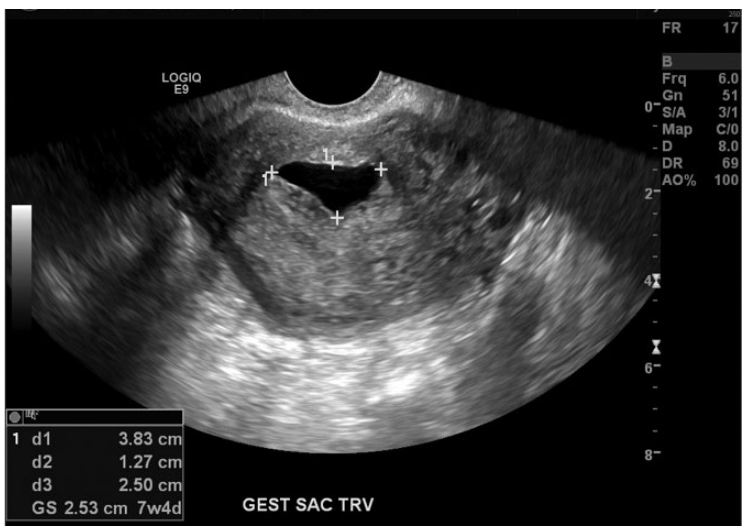

Figure 11.21 Ultrasound image of a non-specific intrauterine sac measured at seven weeks', four days' gestational size. A corresponding embryo was not visualised. The poor decidual reaction and the irregular internal margins of the sac are suggestive of foetal demise or anembryonic pregnancy.

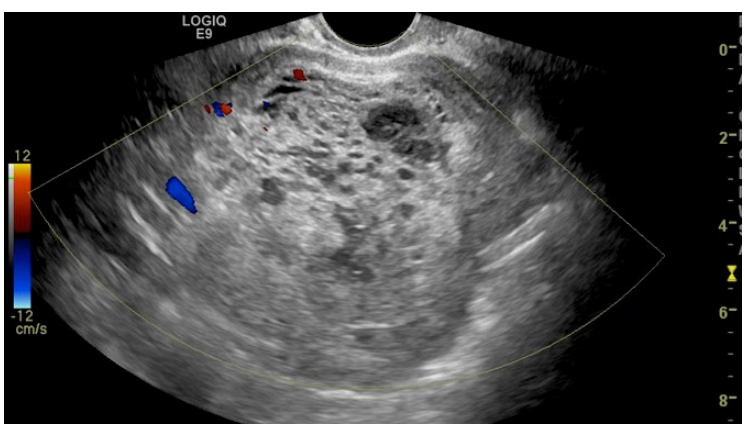

Figure 11.22 Ultrasound image demonstrating findings typical of a molar pregnancy.

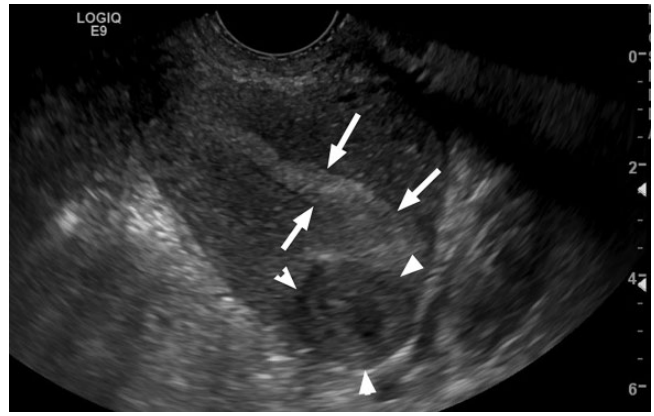

Figure 11.23 TVU image of an interstitial pregnancy (arrowheads) in a patient with a retroverted uterus. Note the absence of myometrium surrounding the sac. The endometrium (arrows) may be seen.

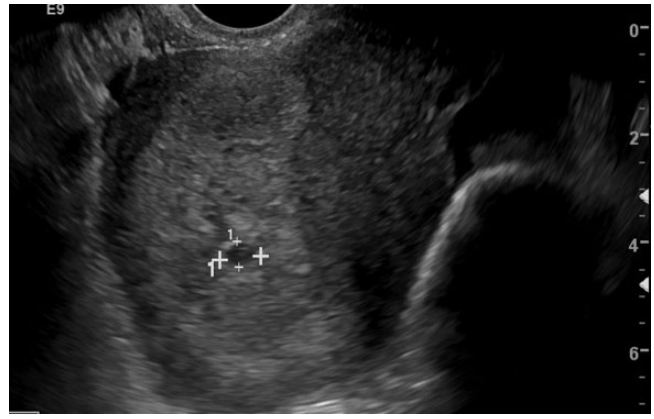

Figure 11.24 TVU image of a pseudo-gestational sac. Note the pronounced decidual reaction stimulated by the ectopic gestational hormones.

dangerous because they often cause severe haemorrhage. To assess for these ectopic locations, myometrial thickness ("mantle") should be measured in all planes around a gestational sac, and should be greater than 5 mm in all directions (Figure 11.23). A misdiagnosis of pseudo-gestational sac (Figure 11.24) for IUP can be avoided if criteria of a yolk sac, foetal pole or cardiac activity are used for a definitive diagnosis of IUP. A sonographic IUP in the presence of clinical or sonographic findings suggestive of an ectopic pregnancy should raise suspicion for a heterotopic pregnancy. Once quoted to occur in approximately 1 in 30 000 pregnancies, the incidence of heterotopic pregnancy may be closer to 1 in 3600, and can be as high as 1 in 100 for women undergoing fertility treatment.

The 'Indeterminate Scan'

Around 20% of first-trimester ultrasound examinations are indeterminate. The images may show an empty uterus or an intra-uterine gestational sac without a clear-cut foetal pole or yolk sac (Figure 11.25). These sonographic findings may reflect either a normal early pregnancy (<5.5 weeks) or an ectopic pregnancy. In this situation, the measurement of serum β-hCG level may provide additional guidance (see below). In many institutions an indeterminate scan mandates a consultative ultrasound prior to discharge. In Tayal's study, in which 300 patients with indeterminate scans in the ED were followed to their final diagnosis, 53% had embryonic demise, 29% had an IUP, 15% had an ectopic pregnancy, and 3% had an unknown outcome.

The Integrated Algorithm

Algorithms to guide management of the 'indeterminate scan' are based on the quantitative measurement of β-hCG and the concept of a 'discriminatory level'. In a normal pregnancy, serum β-hCG levels double every two to three days until they reach a plateau at approximately 8–12 weeks' gestation. The 'discriminatory level' is the level of β-hCG at which a double-decidual sign (DDS) should be detectable by ultrasound. The discriminatory level is affected by the assay, the sonographic approach, ultrasound equipment, and the skill of the sonologist: quoted ranges are 1000–2000 IU/l for TVU and 3000–6500 IU/l for TAU. Algorithms that have been studied and published typically use TVU and a conventional discriminatory level of 1500–2000 IU/l (Figure 11.26). It is important to note that a serum β-hCG level far below the discriminatory level does not decrease the risk for ectopic pregnancy, or the probability of identifying it. In fact, in one study it was found that patients presenting to the emergency department first

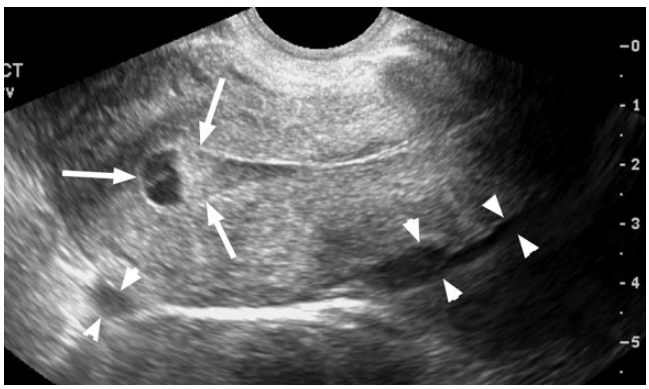

Figure 11.25 EVU image demonstrating heterogeneous intrauterine material that includes a possible sac without definitive findings for IUP (arrows). The scant decidual reaction suggests anembryonic pregnancy, although the free fluid in the cul de sac (arrowheads) would prompt concern for this being the pseudogestational sac of an ectopic pregnancy.

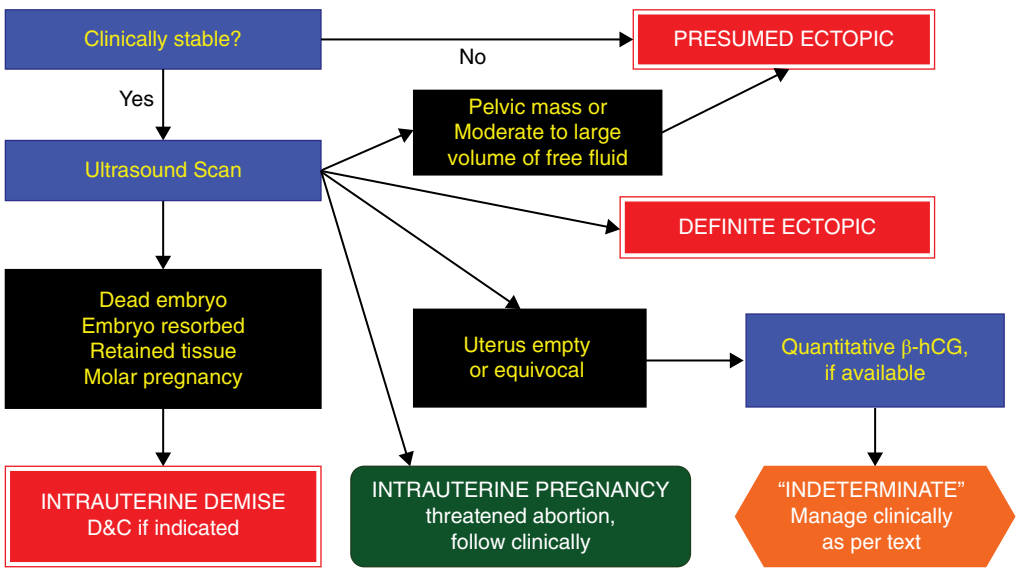

Figure 11.26 Suggested algorithm for the management of early pregnancy pain or bleeding.

trimester pelvic symptoms with a serum β-hCG level below 1000 IU/l were at a fourfold *increased* risk for ectopic implantation compared to those whose β-hCG was > 1000 IU/l. It is also important to note that the DDS is not a *definitive* sign of IUP, so that further clinical judgement is needed if this is the only finding. No useful nomogram has been established relating the quantitative β-hCG with the definitive sonographic signs of IUP (yolk sac, foetal pole, foetal heart motion).

Protocols will vary depending on the clinical setting and available resources. Some sonologists may not have access to the equipment, or the training to perform TVU. TAU detects definitive signs of IUP about a week later than TVU, and this results in a larger proportion of indeterminate examinations. If immediate results of β-hCG levels are not available an indeterminate scan may mandate a more conservative strategy, such as admission for observation.

Disposition

One possible protocol is suggested in Figure 11.26. Overall, the first-trimester ultrasound examination will greatly enhance clinical decision-making, both in terms of accuracy and speed, but the sonologist must recognise that there will always be about 20% of patients who have no definitive diagnosis at the end of their evaluation. Clinician-performed ultrasound typically identifies IUP in about 70% of patients presenting with first-trimester abdominal pain or vaginal bleeding. The vast majority of these patients may be discharged with a diagnosis of threatened abortion or lower-abdomen pain of unknown cause. This assumes that an appropriate follow-up is available, and that alternative diagnoses have been considered. A first-trimester finding of free fluid and an empty uterus in a patient with unstable vital signs is likely to speed the time to the definitive management of ectopic pregnancy. Such patients may be managed without a consultative ultrasound examination. Stable patients with findings suggestive of an ectopic pregnancy will require urgent gynaecological consultation (the need for consultative ultrasound depends on local protocols). Patients with abnormal findings not suggestive of an ectopic pregnancy will require a timely outpatient consultative ultrasound and gynaecology follow-up, with clear return precautions for new or worsening symptoms. Patients with indeterminate scans may be discharged with instructions for serial repeat serum β-hCG levels every two to three days until a definitive diagnosis is made.

Further Reading

American College of Emergency Physicians (2003) Clinical Policy: Critical Issues in the Initial Evaluation and Management of Patients Presenting to the Emergency Department in Early Pregnancy. *Ann. Emerg. Med.*, **41**, 123–133.

American College of Emergency Physicians (2009) Policy Statement: Emergency Ultrasound Guidelines. *Ann. Emerg. Med.*, **53**, 550–570.

Kaplan, B.C., Dart, R.G., Moskos, M., *et al.* (1996) Ectopic pregnancy: prospective study with improved diagnostic accuracy. *Ann. Emerg. Med.*, **28**, 10–17.

Mahony, B.S., Filly, R.A., Nyberg, D.A., *et al.* (1985) Sonographic evaluation of ectopic pregnancy. *J. Ultrasound Med.*, **4**, 221–228.

McRae, A., Edmonds, M., Murray, H. (2009) Diagnostic accuracy and clinical utility of emergency department targeted ultrasonography in the evaluation of first-trimester pelvic pain and bleeding: a systematic review. *Can. J. Emerg. Med.*, **11**, 355–364.

Panebianco, N.L., Shofer, F., Fields, J.M., Anderson, K., Mangili, A., Matsuura, A., Dean, A.J. (2025) The utility of transvaginal ultrasound in the ED evaluation of complications of first trimester pregnancy. *Am. J. Emerg. Med.*, **30** (6), 743–748.

Rempen, A (1988) Vaginal sonography in ectopic pregnancy. A prospective evaluation. *J. Ultrasound Med.*, **7**, 381–387.

Rodgerson, J.D., Heegaard, W.G., Plummer, D., Hicks, J., Clinton, J., Sterner, S. (2001) Emergency department right upper quadrant ultrasound is associated with a reduced time to diagnosis and treatment of ruptured ectopic pregnancies. *Acad. Emerg. Med.*, **8** (4), 331–336.

Tayal, V.S., Cohen, H., Norton, H.J. (2004) Outcome of Patients with an Indeterminate Emergency Department first-trimester pelvic ultrasound to rule out ectopic pregnancy. *Acad. Emerg. Med.*, **11**, 912–917.

12

Second- and Third-Trimester Pregnancy

Elena Skomorovsky, John Gullett and David C. Pigott

Introduction

Ultrasonography is the imaging modality of choice for evaluating pregnancy. While standard practice in the evaluation of patients in their first trimester, the use of clinician-performed ultrasound in the second and third trimesters is less widespread. Nevertheless, there are several techniques that may prove valuable in managing pregnant patients in the acute-care setting. These applications have the potential for even greater impact in resource-poor settings where they can be used to identify those patients with complicated labour.

In this chapter, attention is focused on clinical applications that may influence the management of patients presenting in mid to late pregnancy with symptoms such as bleeding, trauma, abdominal pain or labour. Certain conditions need urgent diagnosis at this stage in pregnancy including placenta previa, foetal viability, pregnancy dating, and foetal lie.

General Technique

Transabdominal Imaging

Transabdominal ultrasound (TAU) is sufficient for the majority of examinations in the second and third trimesters. The gravid uterus is large and filled with fluid, making a standard curvilinear or phased-array probe appropriate, although a curvilinear transducer is designed for this use and is preferable if available.

The normal uterus in the second or third trimester should be immediately recognisable. A full bladder will improve visualisation of the lower uterus and cervix (Figure 12.1).

Transvaginal Imaging

Transvaginal ultrasound (TVU) is rarely useful with the enlarged second- and third-trimester uterus, although it may be advantageous for evaluating the lower uterine segment or cervix when there is concern for previa. This technique is described in detail in Chapter 11. A shallower insertion depth should be used when there is concern for placenta previa. Using this semi 'perineal' approach with the transducer just inside the introitus is not absolutely contraindicated when previa is a concern, but it is generally best reserved for an experienced sonologist.

Second and Third Trimester – Normal Findings

Gestational Dating

When presented with a gravid patient of uncertain gestational age with almost any acute disease process it is important to establish gestational age promptly to determine viability. Premature

Emergency Point-of-Care Ultrasound, Second Edition. Edited by James A. Connolly, Anthony J. Dean, Beatrice Hoffmann and Robert D. Jarman.

Companion website: www.wiley.com/go/connolly/ultrasound

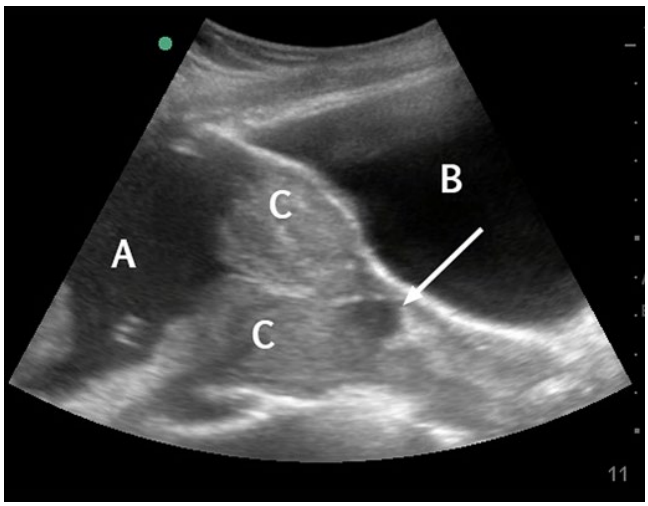

Figure 12.1 Longitudinal view of the lower uterine segment containing amniotic fluid (A), and cervix (C) seen behind the bladder (B), There appears is a small fluid collection in the vagina (arrow).

labour is defined as less than 35 weeks. Viability varies by locality (generally around 20 weeks), but is an important factor in the decision to deliver or to delay labour. Many techniques are available for calculating gestational age in the second and third trimesters. The simplest techniques are femur length, biparietal diameter and head circumference. The accuracy of these methods varies at different stages of pregnancy, and decreases through the third trimester. Measuring with multiple techniques improves accuracy. Nonetheless, in the acute setting any one of these methods should provide a reasonable estimation of gestational age.

Biparietal Diameter

Foetal biparietal diameter (BPD) is a reasonable first-line technique for determining gestational age using a single measurement. It has been found to be accurate to within 7–11 days with a normally developed foetal skull.

An axial view of the foetal skull is obtained with the following landmarks visible:

- The midline falx cerebri.
- Bilateral hyperechoic bean-shaped choroid plexi posteriorly.
- Bilateral hypoechoic thalami central and immediately adjacent to the falx bilaterally.
- The hypoechoic septum pellucida also immediately adjacent to the falx, but more anterior.

Measuring callipers should be placed at the outer skull table of one temporal side and the inner skull table on the other side (Figure 12.2). Most types of ultrasound machine have the ability to calculate the foetal age from this measurement.

Femur Length

The straightforward anatomy makes femur length (FL) a simple choice for dating in the emergency department, and can be used to measure gestational age as early as 10 weeks. This method has been shown to be accurate within ± 2.8 weeks after 10 weeks' gestation. The femur is easily located by identifying the distinctive vertebrae of the spine, following the spine to the pelvis/hip, and identifying the femur. The femur should be measured along the axis of the diaphysis; the epiphyses should be excluded and only the osseous part of the femur is measured (Figure 12.3). Skeletal dysplasias may alter the result. If one measurement seems incorrect, it should be confirmed using another method.

Head Circumference

Head circumference (HC) is a reliable technique, even in the presence of many growth dysplasias. The landmarks and axial plane are the same as described for BPD. Callipers are placed on the outer calvarial mantles at the midline

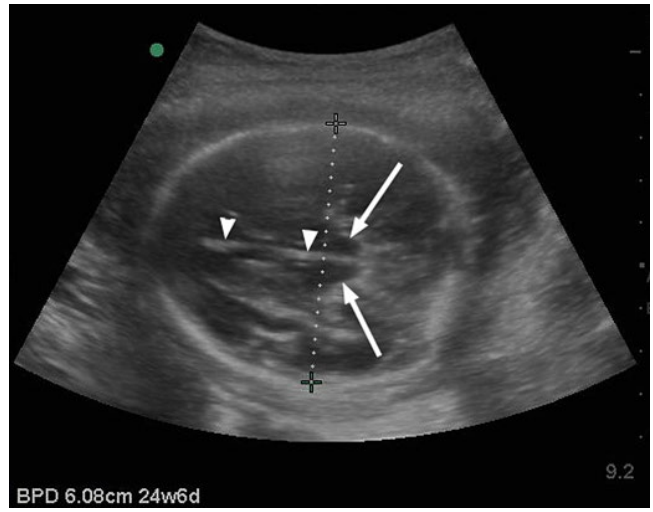

Figure 12.2 Biparietal diameter measured in the correct plane of the thalamus (arrows) from inner table to outer table of the skull. The corpus calosum is also seen (arrowheads).

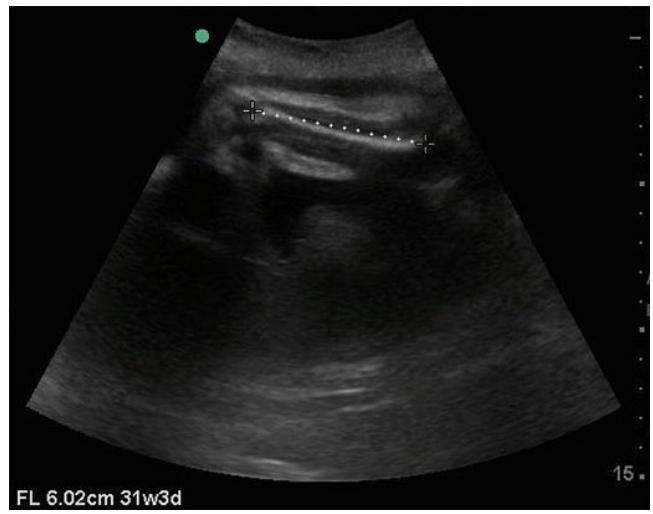

Figure 12.3 Femur length. Note that only the metaphyseal extent of the bone is included. Depth settings could be shallower in this image to avoid so much wasted space.

anterior and posterior skull, while the circular calliper is oriented along the outer circumference of the skull (Figure 12.4).

Foetal Cardiac Activity

Foetal heart rate (FHR) is an important measurement for assessing foetal well-being, though it should be noted that a single ultrasound measurement is not a substitute for foetal tocometry, when indicated. The technique is the same, regardless of trimester. When the heart is identified, M-mode is activated and the cursor line placed across the foetal heart where cardiac motion is greatest. The M-mode tracing will demonstrate a characteristic repetitive pattern of cardiac contractions. To calculate the heart rate, two calliper markers are placed between the two adjacent heartbeats (Figure 12.5).

Foetal Lie

When a patient presents in active labour it is important to determine the foetal position. Early detection of breech position allows for preparation for a complex delivery or initiation of tocolysis pending obstetrical consultation.

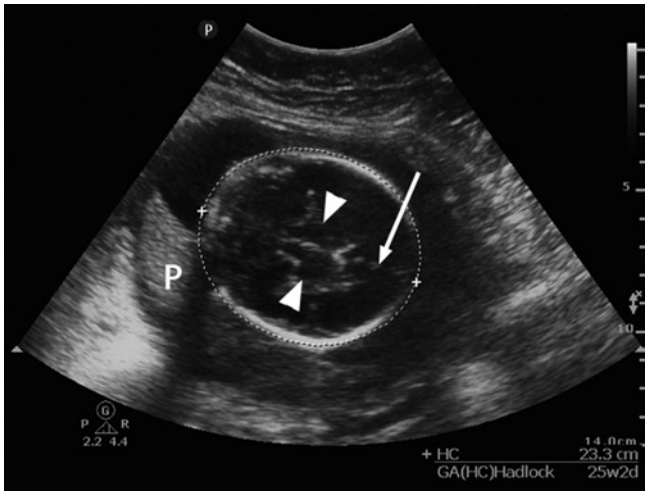

Figure 12.4 Head circumference, again in plane with the thalamus (arrowheads). The placenta (P) and corpus calosum are also seen (arrow). Note how with effacement of the myometrium in the later stages of pregnancy, the interface between the myometrium and placenta is undetectable in many places in this image. For this reason, placental abruption may be impossible to detect on ultrasound.

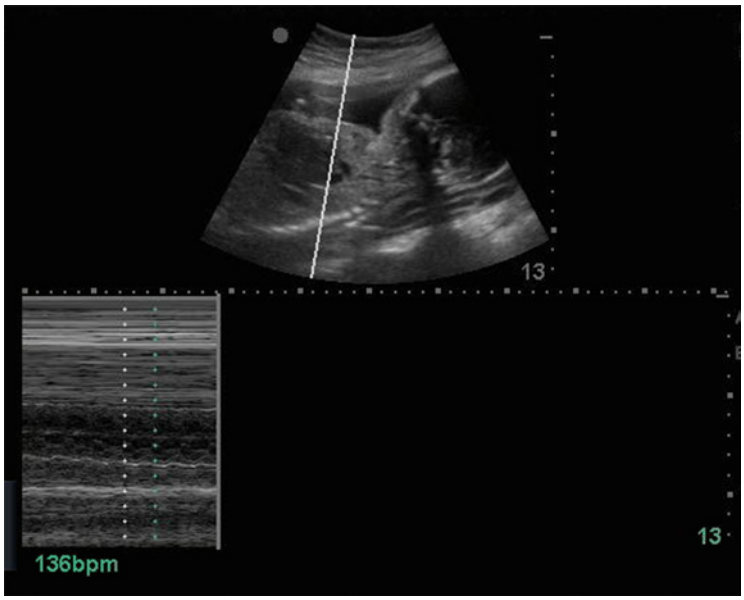

Figure 12.5 M-mode measurement of foetal heart rate. The callipers are placed on corresponding points on two adjacent heartbeats.

The foetal spine has a characteristic appearance on ultrasound, and this indicates the orientation of the foetus. It can be followed to either the foetal head or pelvis to determine foetal lie. If the head is seen in the fundus, the foetus is in a breech position. The most common type of breech presentation is a *frank breech*, where the lower extremities are located adjacent to the foetal head in the fundus. When the feet are seen downward in the pelvis instead of upward near the foetal head in the fundus, this would signify a *complete breech* presentation. *Transverse lie* is identified by the orientation of the spine and might lead later to shoulder presentation. While abnormal positions will usually self-correct during pregnancy, in active labour they are likely to lead to a complicated delivery or need for a caesarean section.

Placental Location

Placental location should be part of the basic initial assessment of any patient presenting to the emergency department in active labour to

exclude placenta previa, especially when an obstetric consultation is not readily obtainable. The placenta appears as hyperechoic material adherent to the inside of the uterine wall. On transabdominal ultrasound the entire placenta can usually be visualised to establish its lie. When the edges of the placenta are carefully examined it enables the clinician to characterise placental lie based on its location as normal (anterior, posterior, fundal) or abnormal (low-lying, marginal, partial or complete previa) (see Figure 12.1).As noted above, when there is suspicion for low-lying placenta, transvaginal ultrasound should be performed by the experienced scanner.

Cervical Assessment

Cervical evaluation is most often employed to predict preterm labour. The cervix is identified posterior to the bladder in a sagittal plane by its location between the vagina and the body of the gravid uterus. The thin hyperechoic line of the endocervical canal may be seen. The cervix can be assessed by its length and its thickness. To determine length, measurement of the cervix is taken from the internal to external os (Figure 12.6). When a cervix is <2.5 cm long before 24 weeks of gestation it is considered short and this carries a higher risk of preterm labour prior to 35 weeks. The cervix can also be assessed for effacement, which appears as a shortening of the endocervical canal until it is obliterated completely. While ultrasound offers significant information for decision-making, this application should be used with caution as it has not been validated in the hands of clinician sonographers at this time.

Amniotic Fluid Assessment

Assessment of amniotic fluid volume (AFV) allows for identification of premature rupture of membranes, oligohydramnios/anhydramnios, or suggest congenital defects. Numerous foetal complications can be associated with a reduced or increased AFV, ranging from congenital defects to poor perinatal outcomes. The simplest technique to evaluate AFV is the single deepest pocket (SDP; also known as the maximum vertical pocket, MVP) technique. This method involves visualising the largest pocket of fluid not containing any foetal extremity or umbilical cord, and measuring the vertical extension of the pocket at a right-angle to the uterine contour (Figure 12.7). The measurement of a pocket depth <1 cm – named the '1-cm rule' – was shown to be a good predictor of oligohydramnios, frequently associated with foetal growth restriction. The normal MVP is 2–8 cm.

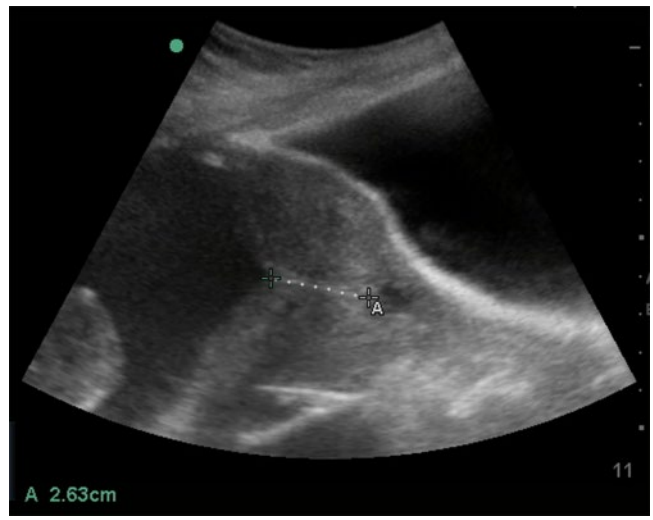

Figure 12.6 Cervical length is measured from the internal to external cervical os.

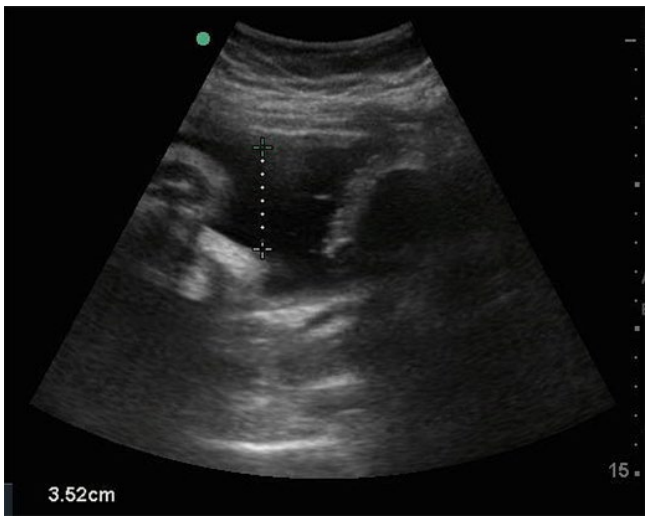

Figure 12.7 Single deepest pocket for estimating amniotic fluid volume. The deepest vertical pocket should be 2–8 cm.

Second and Third Trimester Pregnancy – Pathology

Foetal Demise

There are clear signs that signify foetal demise, such as an absence of cardiac activity in the visualised heart. There are also imaging impressions indicative of impending and inevitable foetal death, such as an absence of amniotic fluid. Such findings would require urgent obstetric consultation if the foetus is viable. Hence, the patient who presents with premature, preterm rupture of membranes (PPROM) should be rapidly evaluated for foetal viability.

Molar Pregnancy

Molar pregnancy is often diagnosed during the first trimester, but patients may also present later in pregnancy if prenatal care is limited. Some of the diagnostic criteria include markedly elevated serum levels (>120,000) of β-human chorionic gonadotrophin (β-hCG) and a variety of ultrasound findings including the 'snowstorm in the uterus' and the "bunch of grapes" caused by numerous by hydropic chorionic villi typically without the presence of an identifiable foetus. This heterogeneous mass fills the uterus. The management of molar pregnancy usually requires surgical intervention with dilation and curettage, followed by serial serum β-hCG measurements and close outpatient follow-up.

Placental Abruption

Placental abruption typically presents with symptoms of uterine pain and decreased foetal movement with or without vaginal bleeding, and physical findings of a hard tender uterus with or without shock on examination. Haemorrhage may be vaginal or internal and occult. The latter type poses serious risks to both mother and foetus due to delayed diagnosis, and can result in severe complications such as disseminated intravascular coagulopathy (DIC). Ultrasound has not been shown to be accurate in detecting abruption, so that diagnosis is clinical. If it is suspected, findings of subplacental fluid or haematoma will confirm the diagnosis and may help to expedite obstetric consultation.

Placenta Previa

The diagnosis of placenta previa should be considered when a low-lying placenta (within 2 cm of the os) is visualised (Figures 12.8 and 12.9). The reported accuracy of TVU for the diagnosis of placenta previa is superior to that of TAU, approaching 96–98%.

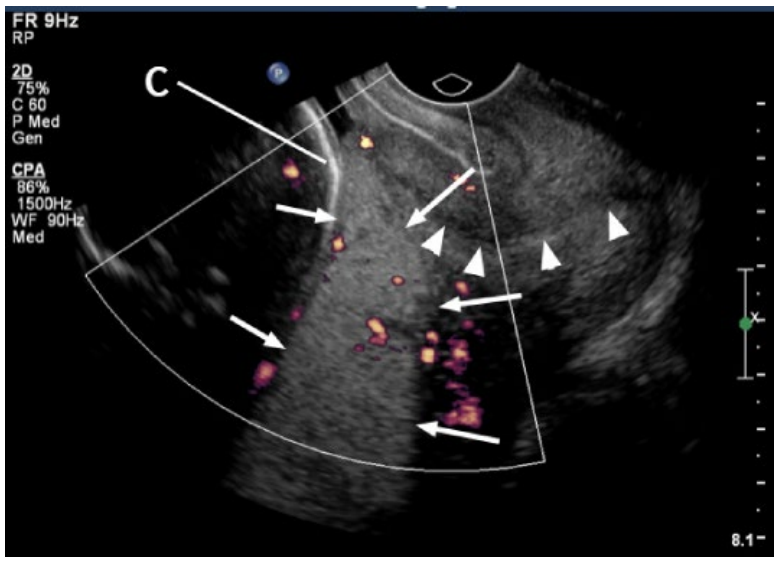

Figure 12.8 Longitudinal transvaginal ultrasound of partial placenta previa. The endocervical canal (arrowheads) is partially covered by the placenta (arrows). The calvarium of the foetus can be seen (C).

Figure 12.9 Transabdominal ultrasound of placenta previa in the longitudinal plane. The placenta (P) completely covers the internal cervical os (between the arrowheads).

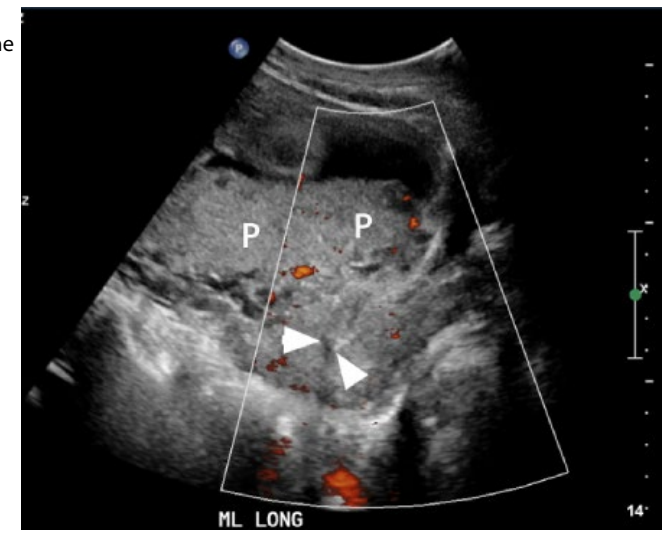

Uterine Perforation

Uterine perforation is a potential complication of any invasive intrauterine procedure, usually occurring during dilation and curettage or voluntary termination of pregnancy. These injuries may not be immediately evident, and delayed presentation is not uncommon. This can lead to life-threatening haemorrhage or peritonitis. Uterine perforation is not directly seen with ultrasound, but rather indirect signs should be noted. For instance, intraperitoneal or pelvic haematomas as well as free fluid are suggestive in the right clinical context.

Retained Products of Conception

Retained products of conception (RPOC) includes placental and/or foetal tissue that remains in the uterus after a spontaneous or

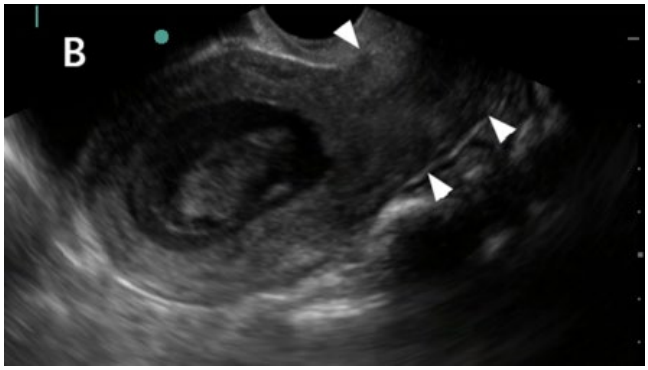

Figure 12.10 Transvaginal longitudinal plane image showing the cervix (between arrrowheads) and the uterus containing retained products. The patient had had a spontaneous abortion one month prior, and presented with persistent pain and bleeding. The bladder (B) is seen. Ideally, this should be emptied prior to endovaginal scanning.

elective abortion, or after delivery. Ultrasound signs of intrauterine haemorrhage or haematoma following a spontaneous abortion may be indistinguishable from retained foetal or placental tissue. However, when hyperechoic material is identified within the endometrial cavity some time after an abortion or delivery, and the patient is having pain and persistent bleeding, then RPOC should be considered. The use of power Doppler to visualise the blood flow within the retained tissue may risk-stratify patients in need of surgical intervention (Figure 12.10).

Summary

As with all applications of clinician-performed ultrasound, evaluation of second- and third-trimester complications of pregnancy requires experience and awareness of one's limitations. This is especially true for diagnoses that are not time-critical, and therefore allow for evaluation by imaging specialists. The use of clinician-performed ultrasound in this context should be goal-directed. When imaging specialists and/or gynaecological or obstetric resources are limited, ultrasound in the hands of the treating care-providers may provide critical information to better guide the management of a pregnant patient.

Further Reading

American College of Emergency Physicians (2001) ACEP emergency ultrasound guidelines - 2001. *Ann. Emerg. Med.*, **38** (4), 470–481.

Ananth, C.V., Wilcox, A.J. (2001) Placental abruption and perinatal mortality in the United States. *Am. J. Epidemiol.*, **153** (4), 332–337.

Crane, J.M., Hutchens, D. (2008) Transvaginal sonographic measurement of cervical length to predict preterm birth in asymptomatic women at increased risk: a systematic review. *Ultrasound Obstet. Gynecol.*, **31** (5), 579–587.

Elsayes, K.M., Trout, A.T., Friedkin, A.M., Liu, P.S., Bude, R.O., Platt, J.F., Menias, C.O. (2009) Imaging of the placenta: a multimodality pictorial review. *Radiographics*, **29** (5), 1371–1391.

Filly, R.A., Hadlock, F.P. (2000) Sonographic Determination of Menstrual Age, in Ultrasonography in Obstetrics and Gynecology, 4th edition (ed. P.W. Callen), WB Saunders, Philadelphia.

Hadlock, F.P., Deter, R.L., Harrist, R.B., Park, S.K. (1984) Estimating fetal age: computer-assisted analysis of multiple fetal growth parameters. *Radiology*, **152**, 497.

Hadlock, F.P., Harrist, R.B., Martinez-Poyer, J. (1991) How accurate is second trimester fetal dating? *J. Ultrasound. Med.*, **10**, 557.

Hadlock, F.P., Harrist, R.B., Shah, Y.P., *et al.* (1987) Estimating fetal age using multiple parameters:

a prospective evaluation in a racially mixed population. *Am. J. Obstet. Gynecol.*, **156**, 955.

Hill, L.M., Guzick, D., Hixson, J., *et al.* (1992) Composite assessment of gestational age: a comparison of institutionally derived and published regression equations. *Am. J. Obstet. Gynecol.*, **166**, 551.

Hohler, C.W. (1984) Ultrasound estimation of gestational age. *Clin. Obstet. Gynecol.*, **27** (2), 314–326.

Lazarus, E., Hulka, C., Siewert, B., *et al.* (1999) Sonographic appearance of early complete molar pregnancies. *J. Ultrasound Med.*, **18** (9), 589–594.

Lazebnik, N., Lazebnik, R.S. (2004) The role of ultrasound in pregnancy-related emergencies. *Radiol. Clin. North Am.*, **42** (2), 315–327.

Manning, F.A., Hill, L.M., Platt, L.D. (1981) Qualitative amniotic fluid volume determination by ultrasound: Antepartum detection of intrauterine growth retardation. *Am. J. Obstet. Gynecol.*, **139**, 254.

Manning, F.A., Platt, L.D. (1980) Antepartum fetal evaluation development of a fetal biophysical profile score. *Am. J. Obstet. Gynecol.*, **136**, 787.

Ott, W.J. (2005) Reevaluation of the relationship between amniotic fluid volume and perinatal outcome. *Am. J. Obstet. Gynecol.*, **192**, 1803.

Oyelese, Y., Smulian, J.C. (2006) Placenta previa, placenta accreta, and vasa previa. *Obstet. Gynecol.*, **107** (4), 927–941.

13

Gynaecological Ultrasound in Emergency Medicine

The Non-Pregnant Female Patient with Abdomino-Pelvic Pain

Martha Villalba and Michael Lambert

Introduction

Ultrasound is currently the best initial imaging modality for the assessment of gynaecological causes of acute pelvic or abdominal pain. It is quick, accurate, cost-effective, available at the patient's bedside, and it avoids exposure to ionising radiation. In this chapter attention will be focused on ovarian cysts, ovarian torsion and tubo-ovarian abscesses. The narrow focus delineates the need for possible surgical intervention in the case of ovarian torsion and tubo-ovarian abscess. Ovarian cyst is included because it is the most common gynaecological cause of acute pelvic pain in non-pregnant patients

Uterus, Ovary, Follicles and Cysts

The uterus is a pear-shaped organ located between the bladder and sigmoid colon. It consists of the fundus, body and cervix. In the postpubertal patient it measures about 8 cm long, 5 cm wide and 3 cm deep, and consists of three layers: the outer serosa; the muscular middle layer; and the endometrium. In more than 90% of patients, the fundus points towards the anterior abdominal wall (anteverted). In the minority it is directed towards the spine (retroverted). When an angle exists between the cervix and fundus and the fundus points anteriorly, the uterus is said to be anteflexed (Figure 13.1c); when it points posteriorly, it is described as retroflexed (Figure 13.1d). The ovaries change in predictable ways to their hormonal milieu. It is therefore important to determine where a patient is in her menstrual cycle. During the follicular phase about five to eight follicles form. A dominant follicle develops by day 10 of the menstrual cycle, and it can reach up to 2.5 cm in diameter. In response to a gonadotrophin surge, the dominant follicle releases an oocyte. After ovulation, the dominant follicle's walls collapse and the corpus luteum develops from its remains. On ultrasound, the corpus luteum measures on average 1.5 cm in diameter and demonstrates irregular, thick walls. If colour Doppler is applied, a 'ring-of-fire' might be seen at the corpus luteum's periphery, with a lack of central flow. The corpus luteum stops secreting hormones, and then involutes if pregnancy does not occur. The cycle is repeated as menstruation begins (Figure 13.2).

Ovarian Cysts

Definition

The overwhelming majority of ovarian cysts are physiological in origin. They appear unilocular and anechoic, with smooth well-defined margins.

Emergency Point-of-Care Ultrasound, Second Edition. Edited by James A. Connolly, Anthony J. Dean, Beatrice Hoffmann and Robert D. Jarman.

Companion website: www.wiley.com/go/connolly/ultrasound

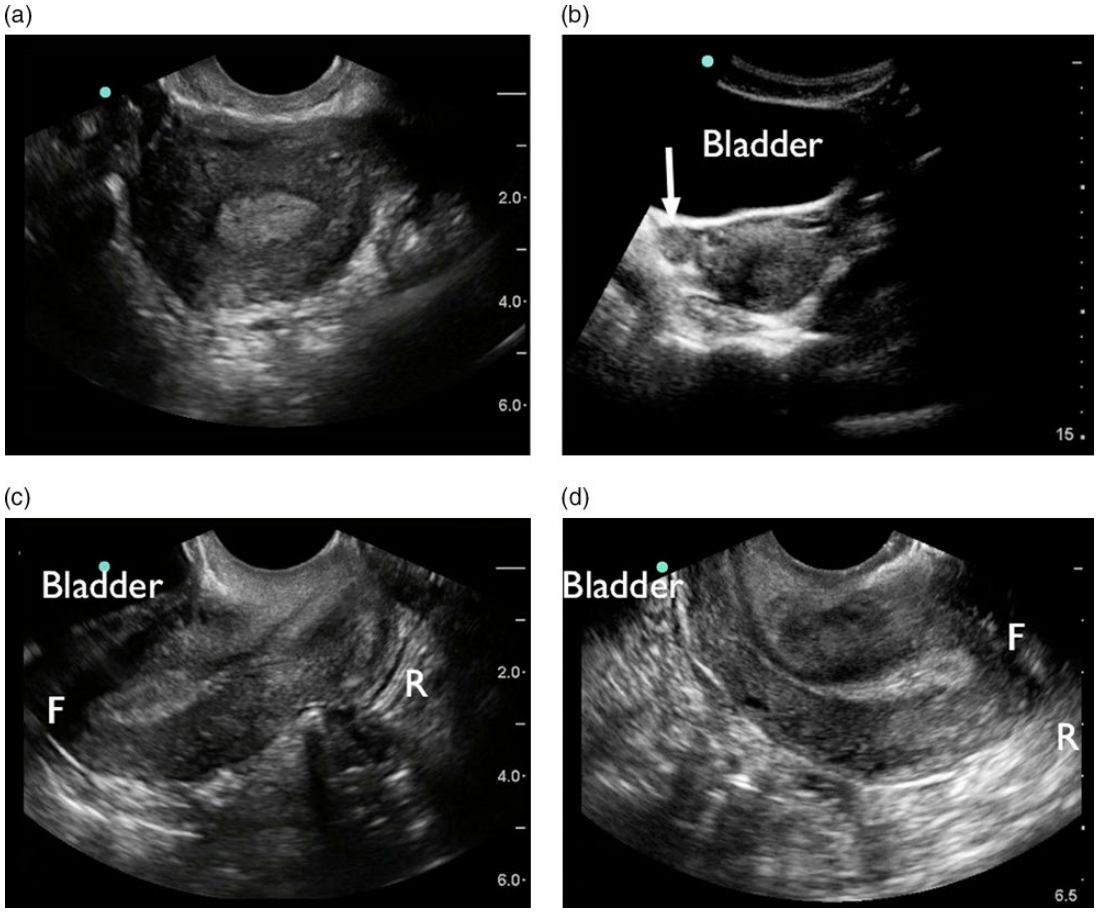

Figure 13.1 Sonographic images of the uterus. (a) Transvaginal imaging, uterus in coronal plane. The relatively hyperechoic endometrium is surrounded by a uniformly thick myometrium. (b) Transabdominal imaging with uterus in transverse plane. The right ovary (arrow) can be seen. (c) Transvaginal sagittal image of a normal anteroverted uterus. The fundus (F) is anterior (towards the left of the image). The distinction between endometrium and myometrium is again clear. (d) Transvaginal sagittal view of the retroverted uterus. Note that the fundus (F) is directed posteriorly (towards the right of the image). In both (c) and (d), the rectum (R) is seen on the right.

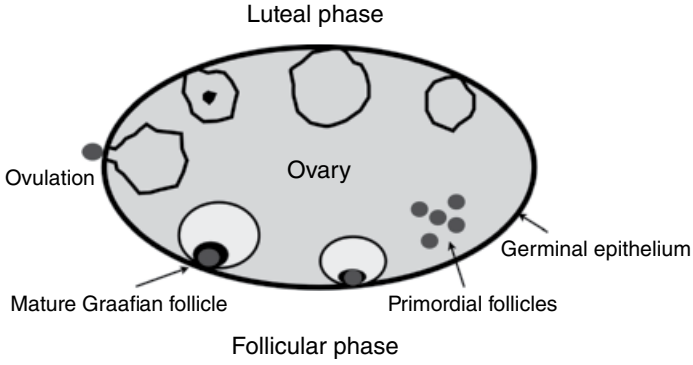

Figure 13.2 Representation of the ovarian cycle starting on the right with the germinal epithelium, and rotating clockwise over a typical 28-day cycle. It should be noted that none of the structures is referred to as a 'cyst'. This term, when properly used, should only be applied to structures whose largest diameter is greater than 2.5 cm. Smaller structures, if they are simple (clear margins and anechoic), are referred to as 'follicles' to avoid potential confusion to physicians or anxiety to patients. Ultrasound characteristics of functional cysts are described in the text.

Table 13.1 Types of cyst commonly found in or adjacent to the ovary.

1. Follicular
2. Functional
3. Paraovarian
4. Dermoid
5. Endometrioma
6. Serous cystadenoma
7. Mucous cystadenoma
8. Hydrosalpinx
9. Cancerous
10. Borderline

There is not a specific size criterion that distinguishes a cyst from a physiological ovarian follicle, but many authorities reserve the term 'cyst' for structures with any dimension greater than 2.5 cm. The most common type of ovarian cyst in women of reproductive age are 'functional cysts', and are thought to represent the failure of a normal follicle to rupture or regress in response to hormonal changes that occur in the menstrual cycle. A variety of other cyst types exist, including dermoid, paraovarian, cystadenomas and hydrosalpinx (Table 13.1). With training and experience, up to 90% of all cysts can be confidently diagnosed with ultrasound alone.

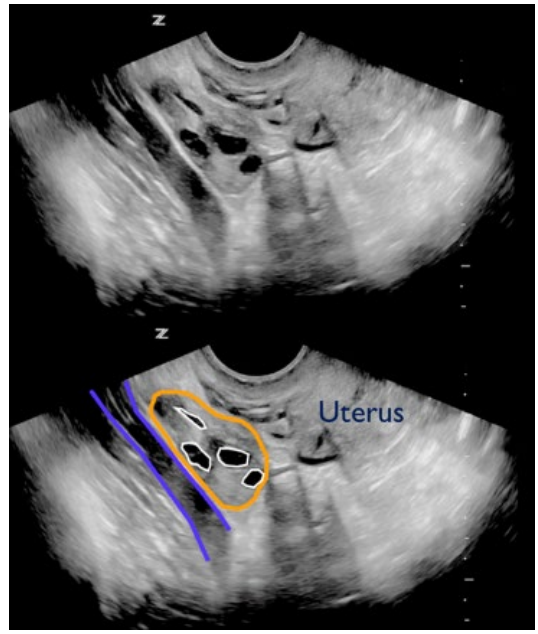

Figure 13.3 Two identical images, the one below is color-coded. Endovaginal view of the normal ovary with follicles. The pelvic probe is in coronal plane orientation and directed towards the patient's right adnexa, with the right iliac vessels visible on the left of the image (blue) and the ovary (yellow) located in between iliac vessel and uterus. Several follicles are seen (white). The gain settings are too high on this image (iliac vessels do not appear black), and less depth would have improved the resolution. The normal ovarian parenchyma has the same or slightly lower echogenicity than the normal myometrium.

Clinical Presentation

Ovarian cysts that become symptomatic can develop at any time in life. The onset of pain can be sudden, as in a ruptured ovarian cyst, or subacute, as in the instance of a slowly enlarging cyst. Rupture may cause peritonitis, symptomatic hypotension and abdominal distention prompting emergency evaluation.

Ultrasound Findings

Ovarian cysts are readily identifiable on ultrasound, either via transabdominal or endovaginal approaches. Transabdominal imaging allows for a better overall view of the structures of the pelvis and the abdomen, as well as the intraperitoneal complications (such as free fluid from rupture or hydronephrosis from obstructed ureter). On the other hand, the high-frequency endovaginal probe can be closely approximated to the ovary itself, allowing for images with superior resolution.

To understand the sonographic morphology of ovarian cysts, it is helpful to compare their features with those of a normal adult ovary, and to review the anatomical relationship of ovaries within the pelvis. Typically, the normal-sized ovary averages 2.5–5 cm in length, 1.5–3 cm in width and is 0.6–1.5 cm thick. It is located in the pelvis, medial to the internal iliac vessels (Figures 13.3–13.5). Several follicles might be visible within the ovarian tissue, if imaging occurs during the follicular phase.

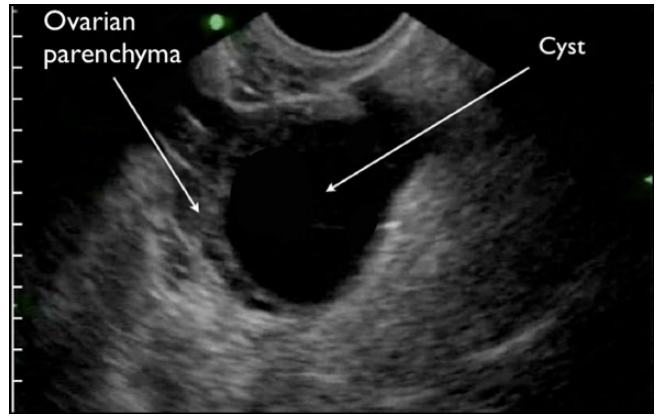

Figure 13.4 Transvaginal ultrasound showing a large anechoic and smoothly marginated ovarian cyst >6 cm in size with adjacent ovarian tissue.

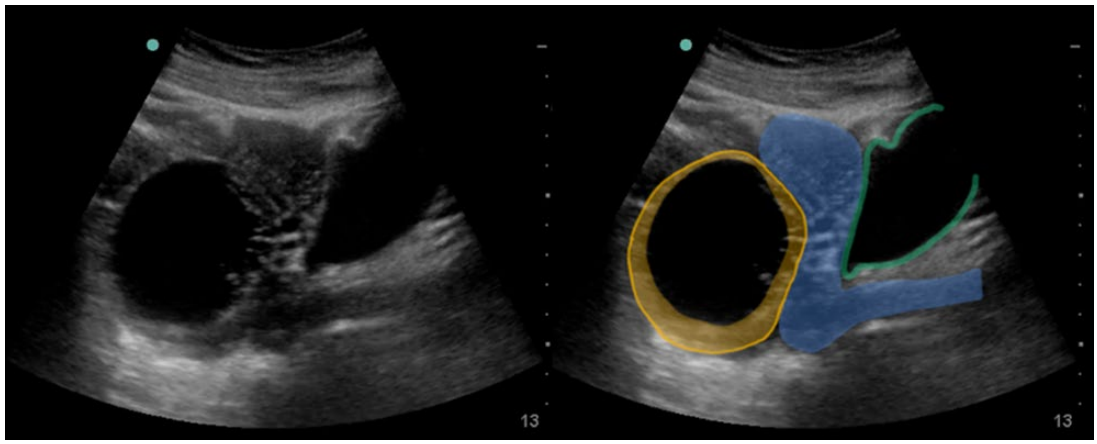

Figure 13.5 Two identical images, the one on the right is color-coded. Large anechoic ovarian cyst with surrounding ovarian tissue (yellow) on sagittal transabdominal ultrasound. The adjacent uterus is shown in blue, the bladder in green. Figure courtesy of Beatrice Hoffmann MD.

Functional ovarian cysts are rounded, anechoic, smoothly marginated and unilocular. They can displace adjacent ovarian tissue to the periphery (Figure 13.4), they can range in size from 2.5 cm to over 15 cm, and are typically hypo- or anechoic, with posterior enhancement. As cysts become larger the surrounding ovarian stromal tissue becomes increasingly effaced, to the point that it can be difficult to visualise on ultrasound.

Haemorrhage into an ovarian cyst or corpus luteum is common. The collapsed corpus luteum can re-expand with blood after oocyte release, leading to a characteristically evolving sonographic appearance. In the acute phase, fresh blood is anechoic, but as the blood coagulates, it forms a thrombus with mixed echogenicity. With thrombolysis, residual fibrin strands give the clot a reticular appearance (Figure 13.6). In contrast to the septa associated with malignancy or abscess, fibrin strands usually do not traverse the lumen of the cyst, and are more delicate in appearance (<3 mm in thickness). Finally, a blood clot, unlike a solid mass, will develop concave outer walls as the clot retracts. The presence of these characteristics supports the diagnosis of a haemorrhagic cyst. In *rupture*, the cyst's walls collapse and free fluid in the pelvis is visualised (Figure 13.6).

With regards to the management of a cyst based on its size, it is recommended that cysts larger than 5 cm be identified in the ultrasound report. These patients should undergo yearly follow-up. Cysts ranging from 2.5 to 5 cm

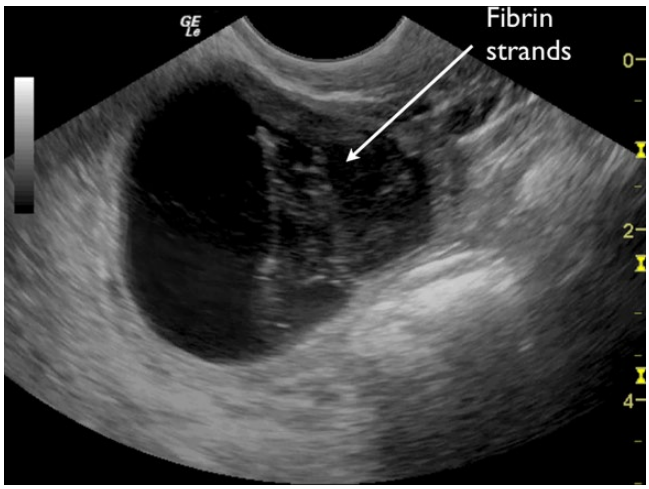

Figure 13.6 Subacute haemorrhagic ovarian cyst with fibrinolysis of the clotted blood leading to fibrin strands. The culmination of this process often results in fine septations within the cyst.

Table 13.2 Differential diagnosis of cystic masses in the pelvis.

1. Ovarian cysts and tumours (see Table 13.1)
2. Ovarian torsion
3. Tubo-ovarian abscess
4. Hydrosalpinx
5. Ectopic pregnancy
6. Diverticulitis with abscess
7. Appendicitis
8. Urolithiasis with ureterocoele or cystocoele
9. Terminal ileitis with abscess
10. Endometriosis
11. Mesenteric and omental cysts

require no follow-up, whereas at sizes greater than 7 cm magnetic resonance imaging should be considered as the cyst's walls can be difficult to thoroughly interrogate. The differential diagnoses of cystic structures in the pelvis is reviewed in Table 13.2.

Ovarian Torsion

Clinical Presentation

Similar to the testicle, twisting or rotation of the ovary can lead to compromised perfusion by obstruction of first the venous outflow (can occur at lower pressures), and then arterial inflow. Ovarian torsion typically occurs during the early reproductive years. It is very rare in a normal-sized ovary (<15 ml, or approximately 2 cm × 2 cm × 3 cm). A corpus luteum is a common cause of ovarian enlargement. Others include other types of ovarian masses and polycystic ovary syndrome, and ovarian hyperstimulation from progestational therapy. Long fallopian tubes in the paediatric population have also been associated with torsion.

Symptoms and signs of ovarian torsion are variable. The classic presentation begins with severe, poorly localised, lower-abdomen pain that worsens over a few hours. However, the presentation can be more insidious. In one review the duration of pain was documented as lasting for several hours to weeks, and many patients presented with non-specific nausea and vomiting. Most patients had minimal findings on abdominal and pelvic examinations, and no peritoneal signs.

Ultrasound Findings

The most common sonographic finding in torsion is ovarian enlargement. As noted, this is the most important predisposing factor for torsion, and with the onset of vascular compromise, a vicious cycle ensues with impaired venous and lymphatic drainage leading to oedema and an increase in ovarian size (Figure 13.7). The enlarged ovary also might demonstrate multiple

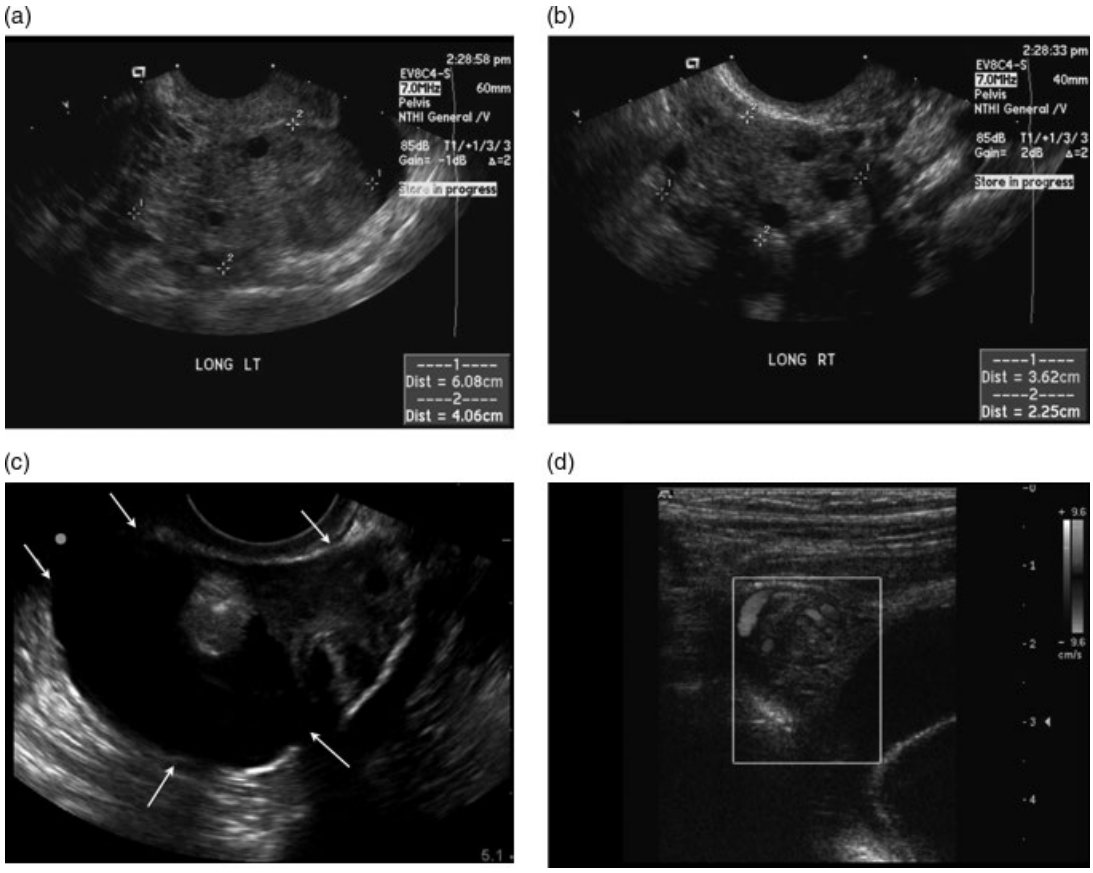

Figure 13.7 Ovarian torsion. (a) Enlarged torsed left ovary measuring 6 × 4 cm (callipers) with tissue oedema and surrounding free fluid seen on the right side of the image. (b) Right ovary of the same patient with normal appearance and size (callipers). (c) Enlarged torsed ovary (white arrows) with large ovarian cyst and free fluid below and to the right of the ovary on the image (image courtesy of Beatrice Hoffmann MD). (d) Whirlpool sign (image courtesy Dr S.B. Vijayraghavan, Coimbatore, India).

large peripheral follicles, or have a cystic or solid appearance, sometimes with heterogeneous debris and septations (Figure 13.7c).

Doppler Sonography

The use of duplex and colour Doppler sonography is important in cases of possible torsion. However, the clinician-sonologist should be cautious in its use for several reasons. Ovaries have a dual blood supply, from both the adnexal artery and the adnexal branch of the uterine artery. This vascular redundancy can mask signs of compromised blood flow. In addition, the presence of abnormal architecture or intraovarian haemorrhage can interfere with thorough Doppler interrogation. Furthermore, as a result of the previously noted evolution of vascular compromise, there are many reports of preserved arterial flow in surgically proven ovarian torsion. Even if perfusion is actually present, it is possible that the patient has had spontaneous detorsion, leaving them at high risk of re-torsion. As a rule of thumb, if there is a high clinical suspicion for torsion the presence of flow on Doppler does not rule it out. The most reassuring finding is of a normal-sized ovary, since torsion is very rare without ovarian enlargement.

An effective Doppler examination requires experience and good technique. Vascular interrogation should always take place across multiple planes because this will increase the chances of detecting flow. Venous parenchymal flow should be carefully sought and recorded. On spectral Doppler it appears as a low-velocity, non-pulsatile flow usually seen above and below the line due to the random motion of blood cells. Colour flow imaging can be used to compare central versus peripheral ovarian flow to help predict ovarian viability. A research team that conducted one small study found an absence of central flow in non-viable ovaries, but in viable ovaries some central venous flow could be depicted.

A final area of interrogation is the vascular pedicle, which includes the fallopian tube, broad ligament and the vessels that supply the ovary. Ultrasound literature describes the identification of a twisted vascular pedicle as being highly suggestive of torsion. In grey-scale imaging along the axis of the pedicle, concentric, hypoechoic rings, which can give a snail shell or 'string of beads' appearance, are visualised. In colour Doppler imaging of this area the vessels give the appearance of what is known as the 'whirlpool sign' (Figure 13.7d). An absence of flow of the twisted pedicle was indicative of ovarian non-viability in one small study.

Tubo-Ovarian Abscess and Pelvic Inflammatory Disease

Definition

Tubo-ovarian abscess (TOA) is a collection of purulent material located in the ovary, fallopian tubes, and often the surrounding structures. It is typically the end result of acute pelvic inflammatory disease (PID). There are an estimated one million women in the United States that develop PID annually, and 15% of these women will develop a tubo-ovarian abscess. TOA has been reported in nearly one-third of women hospitalised annually with PID; the sum equates to almost 100,000 women being hospitalised each year. TOAs can occasionally be the result of an infection spreading from nearby organs, such as appendicitis or diverticulitis. Other rare aetiologies include actinomycosis, tuberculosis or xanthogranulomatous inflammation.

Clinical Presentation

PID occurs when disease-causing organisms migrate from the vagina to the upper genital tract. The classic presentation includes abdomino-pelvic pain, vaginal discharge, fever and leukocytosis, similar to TOA, but without a palpable mass on pelvic examination. Unfortunately, numerous cases exist of patients with documented TOAs, presenting without any of these signs. In one study it was found that 35% of women presenting with TOA were afebrile and 23% had a normal white blood cell count. The clinical spectrum of PID ranges from subclinical endometritis to severe salpingitis, hydrosalpinx, pyosalpinx, tubo-ovarian abscess, pelvic peritonitis and perihepatitis. The management of these entities differs and, as noted, clinical diagnosis is not reliable. Consequently, imaging is needed to identify the presence of TOA in the setting of PID. The two most widely utilised imaging modalities for TOA are ultrasound and computed tomography (CT). There is debate amongst clinicians as to the 'gold standard' for diagnosing TOA in this setting, as CT seems to have an improved sensitivity (78–100%) over ultrasound (75–82%), depending on the study setting. However, the benefits of CT come at a higher financial cost and concerns about radiation exposure. Ultrasound may be the appropriate initial diagnostic imaging study based on its availability, performance at the patient's bedside, cost savings and absence of ionising radiation.

Ultrasound Findings

In PID, the normal echo architecture of the endometrium and myometrium are distorted with blurring of their margins (Figures 13.8 and 13.9). As pus develops within the fallopian

(a)

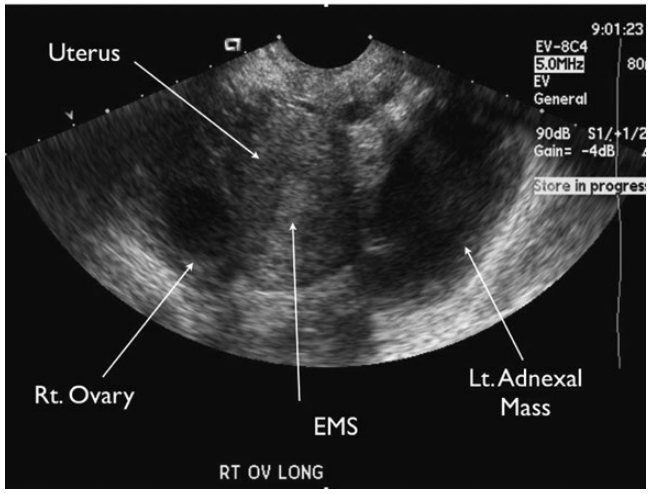

(b)

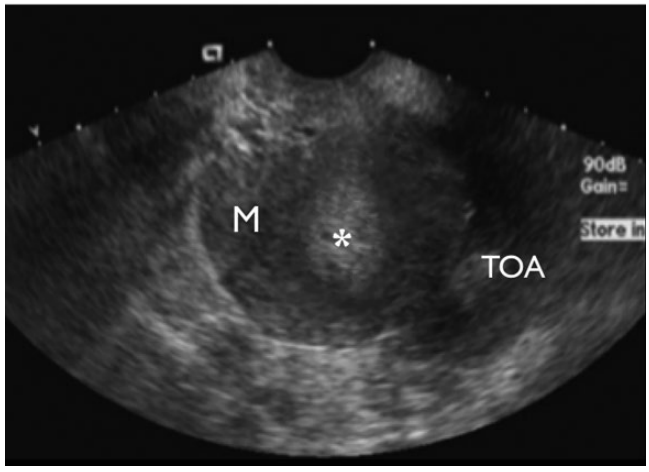

Figure 13.8 Transverse endovaginal images of two cases of tubo-ovarian abscess. In (a), there is blurring of the demarcation between the endometrium (EMS) and the surrounding myometrium. A large hypoechoic inhomogeneous fluid collection, which appears to be contained within smooth margins is consistent with pyosalpinx. In (b), there is again blurring of the margin between myometrium (M) and the endometrium (*). On the right of the image (patient's left adnexa), there is heterogeneoulsy echogenic free fluid (suggested by its "pointy" shape), which is the tubo-ovarian abscess (TOA).

Figure 13.9 Patient with PID and TOA. There is loss of recognisable uterine (U) endometrial and myometrial architecture. Free fluid (FF) is seen behind the uterus. A complex left adnexal mass (TOA) and pyosalpinx (*) are visualised.

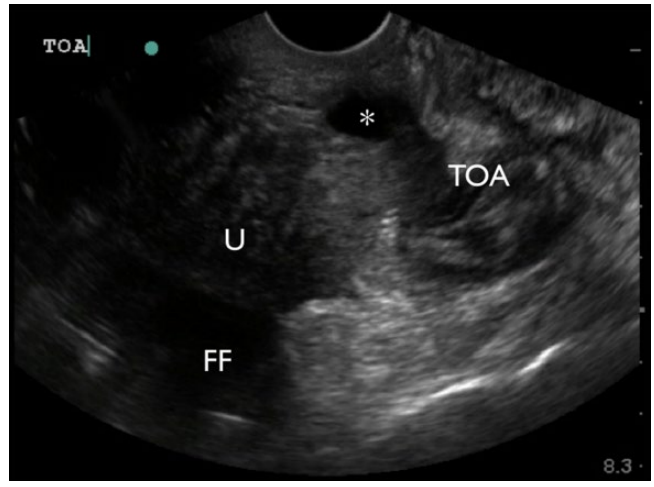

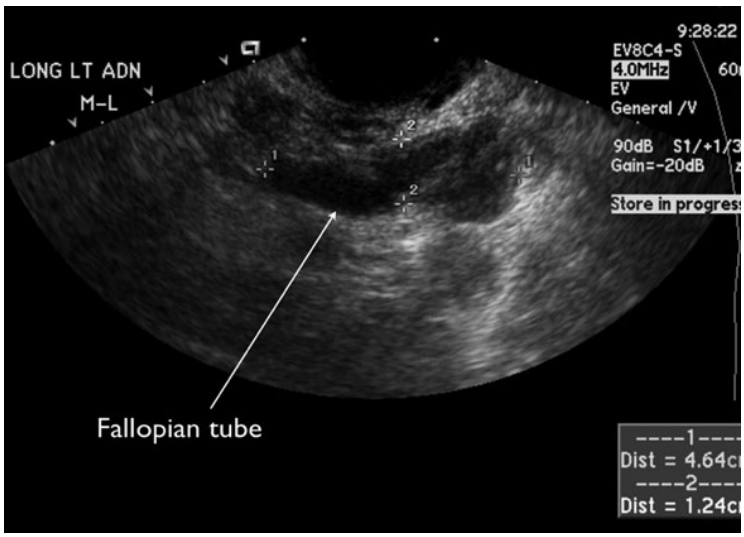

Figure 13.10 Hydrosalpinx. Longitudinal transvaginal sonogram showing the characteristic folded tubular configuration of a distended fallopian tube filled with fluid, and a well-defined echogenic thickened wall.

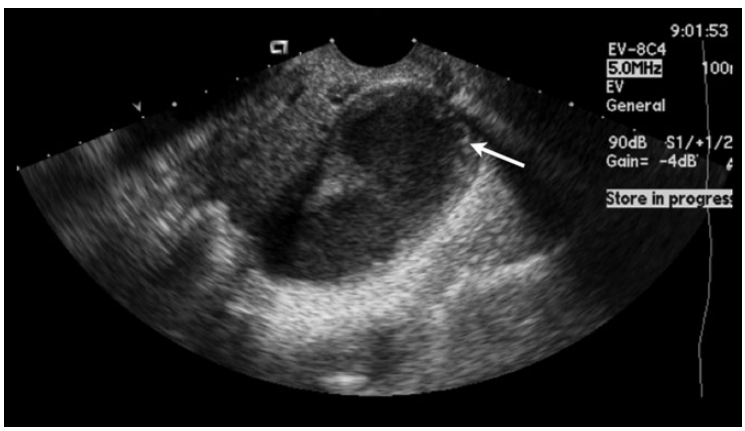

Figure 13.11 Pyosalpinx. Sagittal endovaginal ultrasound shows a distended fallopian tube with thickened wall with cogwheel phenomenon (arrow) and low-amplitude internal echoes, related to purulent material.

tubes, they become distended (Figures 13.8a, 13.10 and 13.11). The distended fallopian tube may demonstrate thickened walls with prominent inner folds, referred to as the 'cogwheel sign' (Figure 13.11). The ovaries may also be enlarged and distorted, appearing as a complex adnexal soft tissue mass (see Figure 13.9). Anechoic areas that are frequently visualised adjacent to these complex masses may be due to free fluid or focal areas of hydro- or pyo-salpinx (Figures 13.8a and 13.9).

TOA and PID in summary

Pelvic inflammatory disease ranges from mild illness to TOA. Women with clinically suspected PID should undergo an ultrasound examination of the pelvis to determine if a TOA is present. Some patients with a high suspicion of TOA undiagnosed by ultrasound may benefit from further imaging by CT or MRI. The majority of TOAs can be managed conservatively with broad-spectrum antibiotics and

close observation; however, about 30% of patients will require surgery or drainage of the abscess. The actual size of the TOA may predict patients who require surgical intervention. Emergency gynaecological consultation should then be initiated.

Pearls and Pitfalls

- Start the ultrasound examination with the transabdominal approach. For many diseases, transvaginal scanning may provide additional or more detailed information.
- Perform transvaginal examinations with a chaperone present.
- The presence of flow does not rule out torsion or torsion–detorsion.
- The transducer can be used to gently 'palpate' areas that are suspicious under direct visualisation. Similarly, asking the patient "where it hurts most" can steer the sonologist to the location of disease.
- Keep the thumb on the probe indicator to assure a correct plane and angle of the probe.
- Comply with local guidelines for transvaginal probe cleaning.

Further Reading

Agency for Healthcare Research and Quality (2006) Management of Adnexal Masses. Evidence Report/Technology Assessment, No. 130. Agency for Healthcare Research and Quality, Rockville, ME.

Albayram, F., Hamper, U.M. (2001) Ovarian and adnexal torsion: spectrum of sonographic findings with pathologic correlation. *J. Ultrasound Med.*, **20** (10), 1083–1089.

Baltarowich, O.H., Kurtz, A.B., Pasto, M.E., Rifkin, M.D., Needleman, L., Goldberg, B.B. (1987) The spectrum of sonographic findings in hemorrhagic ovarian cysts. *Am. J. Roentgenol.*, **148**, 901–905.

Blaustein, A. (1977) Noneoplastic cysts of the ovary, in P*athology of the Female Genital Tract* (ed. A. Blaustein), Springer-Verlag, New York.

Hall, D.A. (1983) Sonographic appearance of normal ovary, of polycystic disease, and of functional ovarian cysts. *Semin. Ultrasound*, **4**, 149.

Hosek, W.T. OB/GYN ultrasound, in *Sonoguide* (ed. B. Hoffmann) Copyright ACEP, 2008. Available at: http://www.sonoguide.com/obgyn.html. Accessed 13th October 2015.

Houry, D., Abbott, J.T. (2001) Ovarian torsion: a fifteen-year review. *Ann. Emerg. Med.*, **38**, 156–159.

Landers, D.V., Sweet, R.L. (1983) Tubo-ovarian abscess: contemporary approach to management. *Rev. Infect. Dis.*, **5**, 876–884.

Morgan, A. (2001) Adnexal mass evaluation in the emergency department. *Emerg. Med. Clin. North Am.*, **19**, 799–816.

Pena, J.E., Ufberg, D., Cooney, N., Dennis, A.L. (2000) Usefulness of Doppler sonography in the diagnosis of ovarian torsion. *Fertil. Steril.*, **73**, 1047–1050.

Vijayaraghavan, S.B. (2004) Sonographic whirlpool sign in ovarian torsion. *J. Ultrasound Med.*, **23** (12), 1643–1649.

Villalba, M.L., Bang, H., So Minna, MacKenzie, J.D., Ledbetter, S., Rybicki, F. (2005) An ovary with a twist: a case of interesting sonographic findings of ovarian torsion. *J. Emerg. Med.*, **29** (4), 443–446.

Wiesenfeld, H.C., Sweet, R.L. (1993) Progress in the management of tuboovarian abscess. *Clin. Obstet. Gynecol.*, **36**, 433–444.

14

Focused Hepatobiliary Ultrasound

Resa Lewiss

Introduction

Patients presenting to the emergency department with right upper quadrant and epigastric pain frequently need evaluation for a hepatobiliary aetiology. Bedside ultrasound in this situation is a rapid and effective means of evaluation.

History of Hepatobiliary Ultrasound in the Emergency Department

During the past thirty years, ultrasound has made the transition from novel concept to a preferred method of evaluation for many forms of hepatobiliary pathology. In 1978, a report in the *Journal of Investigative Radiology* noted that ultrasound was poised to replace oral cholecystography as the basic modality of biliary imaging. By 1980, an article in the *New England Journal of Medicine* recommended ultrasound as "…the diagnostic technique of choice" for suspected calculous gallbladder disease. In 1988, a retrospective study conducted by Jehle demonstrated that bedside ultrasound in the emergency department was highly sensitive and specific for the diagnosis of acute calculous cholecystitis. These findings were further supported by the results of a prospective study published in 1994 by Schlager. Over the course of the last decade, the use of ultrasound for hepatobiliary imaging has gained widespread acceptance, as evidenced by the 2009 Council of Residency Directors consensus document listing biliary ultrasound as a core application for emergency medicine resident education.

Focused Ultrasound in Diagnosing Hepatobiliary Pathology

Clinician-performed ultrasound helps the physician answer focused questions for patient care. In the hepatobiliary context it may be used, for example, to determine the presence or absence of gallstones, or the presence or absence of pericholecystic fluid, or the presence or absence of ductal obstruction, depending on the level of experience and training of the sonologist.

Sonographic evaluation of the liver is both more extensive and less focused, and may be less suited for emergency department evaluation. In viral hepatitis, for example, the liver will have decreased echogenicity, a finding that requires the sonographer to understand subtle variations of liver tissue. While evaluation of the liver may eventually become a standard for bedside examination, it is currently beyond the scope of discussion for this chapter.

Emergency Point-of-Care Ultrasound, Second Edition. Edited by James A. Connolly, Anthony J. Dean, Beatrice Hoffmann and Robert D. Jarman.

Companion website: www.wiley.com/go/connolly/ultrasound

Radiology versus Clinician-Performed Ultrasound

Several studies have compared bedside ultrasound of the gallbladder with sonograms performed in the department of radiology, using the radiology ultrasound as the 'gold standard'. Miller and Kendall each noted that emergency physicians are able to identify gallstones well, with sensitivities of 94% and 96%, respectively. Scruggs conducted a retrospective analysis of the bedside sonographic identification of gallstones in 575 studies, and reported a lower sensitivity (88%) for emergency physicians to detect gallstones, and a 91% positive predictive value.

Ultrasound versus Computed Tomography versus HIDA Scanning

Despite the widespread use of ultrasound, computed tomography (CT) and hepatobiliary iminodiacetic acid (HIDA) scans for the evaluation of biliary pathology, there is a paucity of published literature comparing the various modalities, especially with regards to the diagnosis of acute disease. A review published in 2007 in *Ultrasound Clinics* supports ultrasound as the initial evaluation of choice for imaging the gallbladder and biliary tract, obtaining contrast-enhanced CT or radionuclide or magnetic resonance imaging in cases of technically limited ultrasound studies, or for cases where the cause of biliary obstruction is not apparent despite adequate ultrasound imaging.

The Normal Gallbladder

Basics

Biliary ultrasound should be performed utilising a low-frequency (3–5 MHz) transducer. Using the liver as an acoustic window, the gallbladder will appear as a fluid-filled, cystic structure. Its size van be very variable, and in the post-prandial state can be small (3 cm in length) and completely collapsed (Figures 14.1 and 14.2). The gallbladder should be visualised in longitudinal and transverse planes, and the anterior wall of the gallbladder should be measured preferably in a transverse plane with respect to the gallbladder. A normal wall thickness is less than 3 mm, unless collapsed in the post-prandial state. The common bile duct is located laying anterior to the portal vein in the porta hepatis, which defines the left margin of the quadrate lobe. The porta hepatis is therefore always medial to the gallbladder fossa. The right bile duct is sometimes measured in focused scanning because it is easier to find. It can be located by connecting the neck of the gallbladder and the right portal vein, connected by the median lobar fissure (Figure 14.1). From inner wall to inner wall, it measures less than 6 mm, or the patient's age in years divided by 10, whichever is greater.

Points and Pitfalls

- The gallbladder can be located almost anywhere between the midline and the midaxillary line. It can also have a very varied axis from transverse, with the fundus pointed to the patient's left to almost transverse in the opposite direction, with the axis directed to the patient's right iliac crest. Experience, optimal gain settings and a systematic scanning approach are required to locate the organ efficiently and rapidly.
- The gallbladder is always located immediately under the liver edge, so this structure (the liver edge) should be kept in view throughout the search (Figure 14.1a).
- Begin with the probe marker pointing to the patient's right to accurately identify surrounding landmarks. It may be necessary to rotate the probe in order to achieve ideal views. While searching for a structure it is often helpful to have the depth of field set deeper than the anticipated target in order to widen the area of search in any given plane. Depth can be adjusted more shallow to interrogate the organ when it is located.

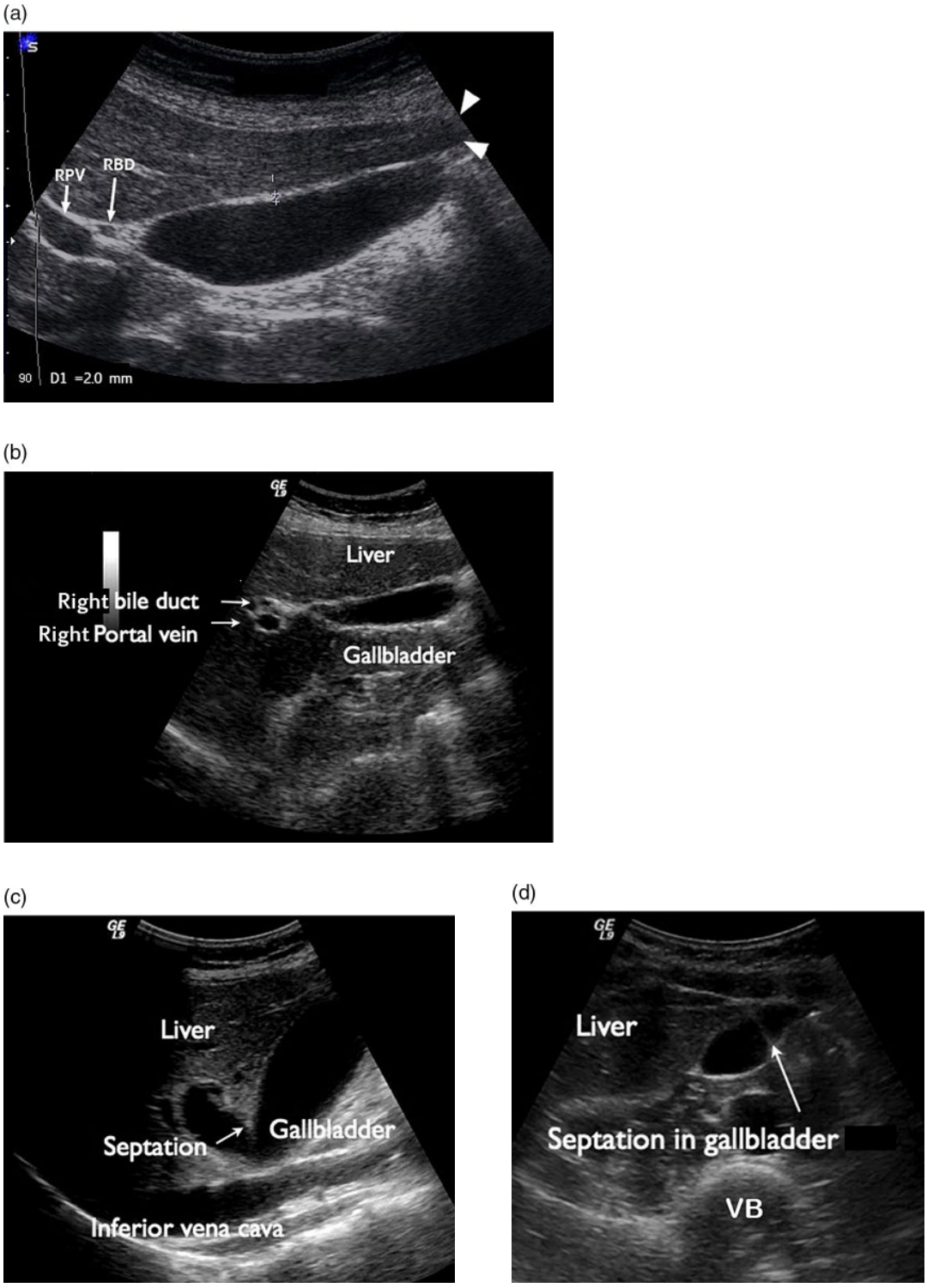

Figure 14.1 (a–d) Views of normal gallbladders demonstrating the varied shape, axis, and location. (a, b) A fibrous band (the median longitudinal fissure) can be seen extending from the neck to the classic 'triad' consisting of the right portal vein (RPV), the right hepatic artery and right bile duct (RBD). The normal anterior gallbladder wall is seen as a thin, crisp, well-defined echogenic line. The liver edge is indicated in (a) by the arrowheads. (c) A longitudinal view shows a folded GB with a septation, and its relationship to the inferior vena cava (IVC). (d) A transverse view shows another appearance of a septated gallbladder. The IVC overlying the vertebral body (VB) can again be seen.

- One technique is to begin at the epigastrium with the patient in the supine position, and to move the transducer laterally along the costal margin until the gallbladder comes into view.
- If the gallbladder is not easily visualised, the patient should be asked to 'take a deep breath and hold', bringing the liver edge below the costal margin temporarily for continued scanning. Moving the patient into the left lateral decubitus position may accomplish the same goal. Other positions to consider include sitting the patient upright or having the patient sit up on knees and hands.
- If these techniques are unsuccessful, the transducer should be placed parallel to the lower ribs anteriorly, and the intercostal spaces should be used for scanning.
- Measure the anterior gallbladder wall to assess thickness. The posterior wall is less accurately measured since it is contiguous with peritoneal fat and bowel, and the exact extent of the wall is not easily defined against these structures (Figures 14.1 and 14.2). Due to lateral cystic shadowing, measurements of the side of the gallbladder (those lying parallel with the direction of the ultrasound beam) are also unreliable (Figure 14.3).
- The common bile duct can be small and difficult to locate. It often takes on the appearance of train-tracks or two parallel, hyperechoic lines anterior to the portal vein. Utilising the left lateral decubitus position and deep inhalation can also assist in visualising a common bile duct that is difficult to locate. As noted, the porta hepatis is anatomically always medial to the gallbladder, so it is often identifiable using high epigastric views with the liver in deep inspiration as a sonographic window.

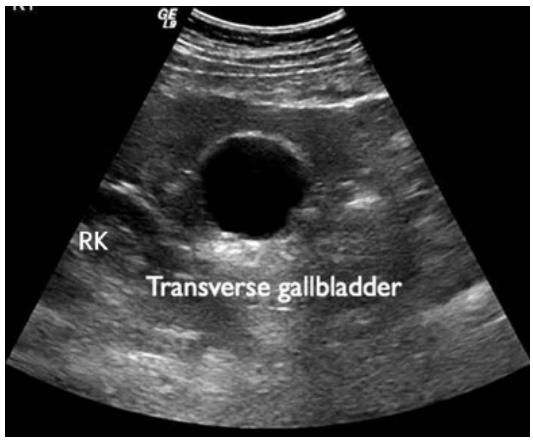

Figure 14.2 A transverse view of a normal gallbladder in a typical location medial and anterior to the right kidney (RK). The anterior wall, which is again seen as a crisp well-defined echogenic line, is the ideal location for GBW measurement. As discussed in the text, the lateral and posterior walls are more difficult to measure accurately.

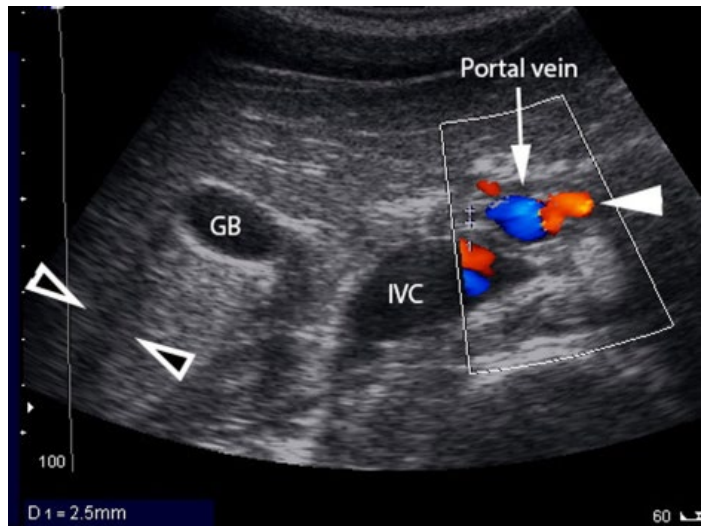

Figure 14.3 A transverse view of the porta hepatitis shows the portal vein, proper hepatic artery (arrowhead) and common bile duct (callipers, 2.5 mm) lying medial (patient's left) to the gallbladder. Between the structures is the quadrate lobe of the liver. Note the proximity of the inferior vena cava (IVC), which also demonstrates colour flow. The artefact of lateral cystic shadowing (white outline arrowheads) can be seen, as well as the consequent difficulty of making accurate measurements of the lateral walls. Image © A.J. Dean.

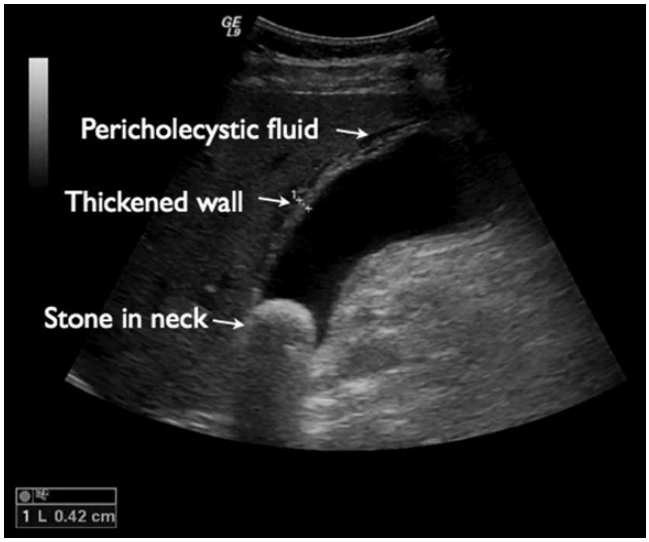

Figure 14.4 In this longitudinal view a large stone is seen impacted in the gallbladder neck. The image shows evidence of an irregular wall, with layers of oedema. There is a continuum between pericholecystic fluid and mural oedema, as in this case; however, the distinction is clinically moot since both reflect an acute inflammatory process consistent with cholecystitis.

Cholelithiasis

Basics

Gallstones will appear as hyperechoic foci in dependent portions of the gallbladder, and often cast an acoustic shadow (Figures 14.4–14.8). They can vary in size and quantity. Most stones, unless impacted in the gallbladder neck or floating (cholesterol stones), collect in dependent locations in the gallbladder. Smaller stones (<2 mm) may not shadow or, if numerous, they may create a 'curtain' of shadow (Figures 14.6–14.8).

Points and Pitfalls

- Small stones may be easily overlooked, but are of equal or greater clinical significance than large ones, since they can more easily become impacted in the neck of the gallbladder or the common bile duct. Optimisation of gain, depth and focus settings on the posterior wall and neck may be necessary in order to detect these stones.
- Obstructing gallstones in the gallbladder neck are the most clinically significant. They are also the easiest to overlook due to the deep location, varied anatomy, frequent associated lateral cystic shadowing, and proximity to gas-filled bowel. Meticulous examination of this part of the gallbladder, if possible from multiple angles, is necessary for a complete examination (see Video 14.1).
- Polyps may resemble gallstones sonographically, but do not shadow and are adherent to the gallbladder wall. They are therefore not mobile (Figure 14.9). Changing the patient's position may help to distinguish a polyp from a stone.
- Biliary sludge appears as a low-amplitude echo without shadowing contained within the gallbladder (Figure 14.10). The sludge/bile interface has a bizarre convoluted shape. Biliary sludge is the first step in the process of precipitation and formation of gallstones, and will be seen in patients with extended fasting and may resolve completely. Its role in biliary colic and acute cholecystitis is unclear.

A 'wall-echo-shadow' (WES) sign is seen when a chronically contracted gallbladder becomes densely packed with gallstones to the exclusion of bile (Figures 14.11 and 14.12). Patients with this condition can develop acute episodes of cholecystitis. This appearance can mimic other, more serious conditions such as porcelain gallbladder (as discussed below).

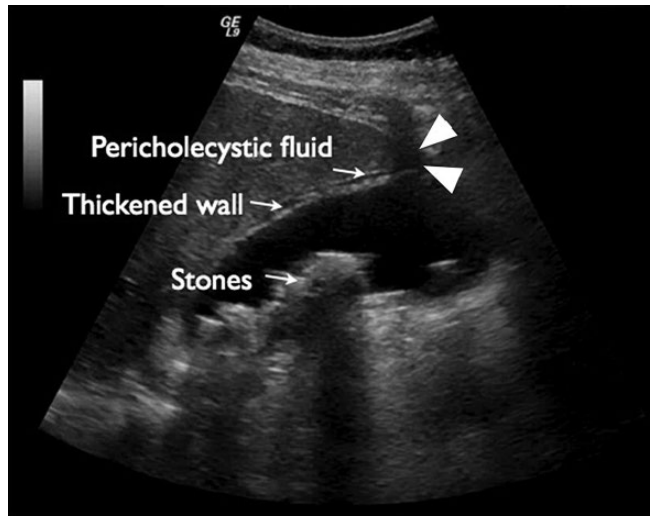

Figure 14.5 A longitudinal view of an enlarged gallbladder seen in its characteristic location under the liver edge (arrowheads). There are several stones with shadowing. While the wall does not appear particularly thick, qualitative assessment reveals irregular areas of thickening and oedema, both of which are suggestive of acute inflammation consistent with cholecystitis.

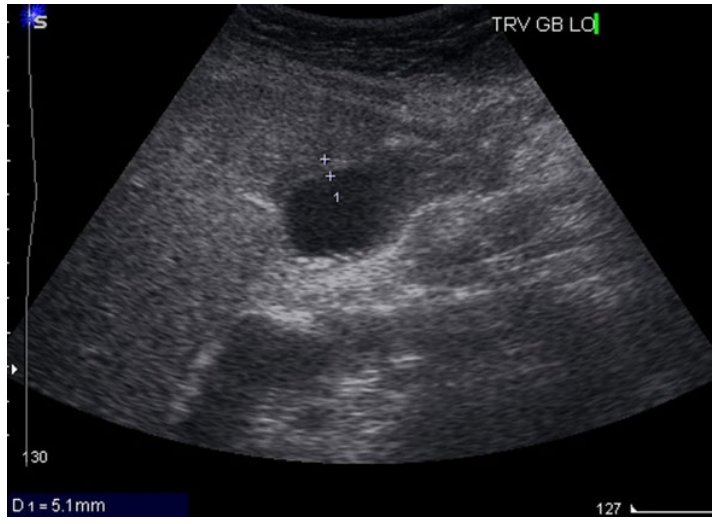

Figure 14.6 A transverse view of the gallbladder with multiple small non-shadowing stones. These can be distinguished from sludge by the discrete echogenic foci. Even though the wall is barely thickened at 5.1 mm, it reveals irregular thickening suggestive of cholecystitis. The gain settings on this image are too high; lower settings might have revealed subtle shadowing behind the gallstones, © A.J. Dean.

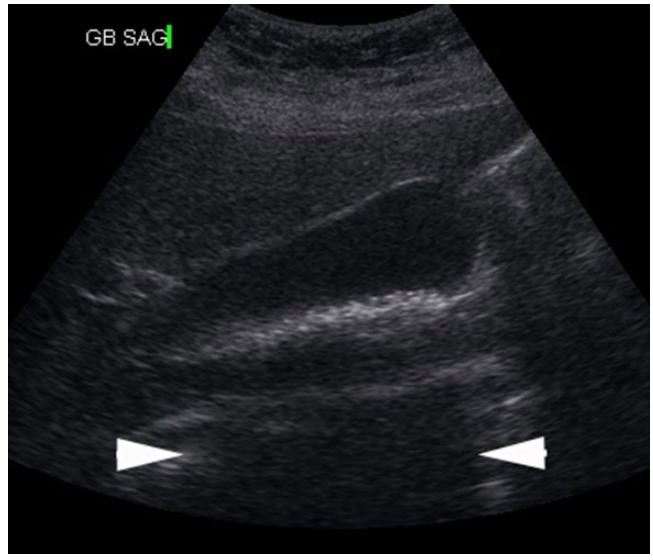

Figure 14.7 A longitudinal view of the gallbladder with multiple small stones. The stones create an aggregate shadow, confirming their presence (between arrowheads), © A.J. Dean.

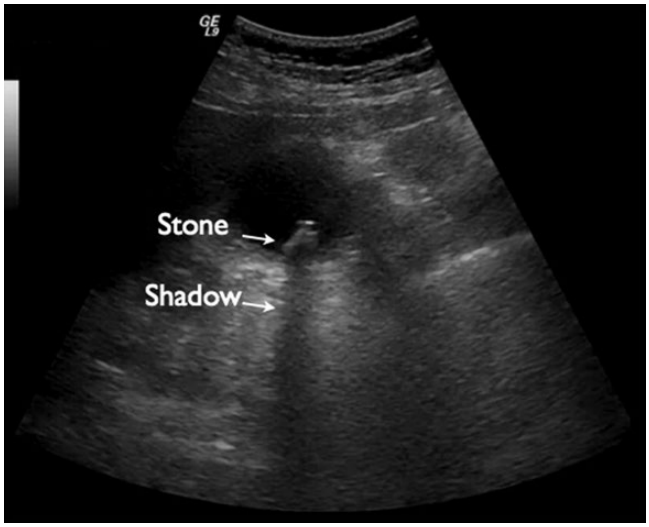

Figure 14.8 A transverse view of the gallbladder showing a single shadowing stone. The walls are poorly defined, and there is a suggestion of thickening, but this cannot be stated with certainty from this view.

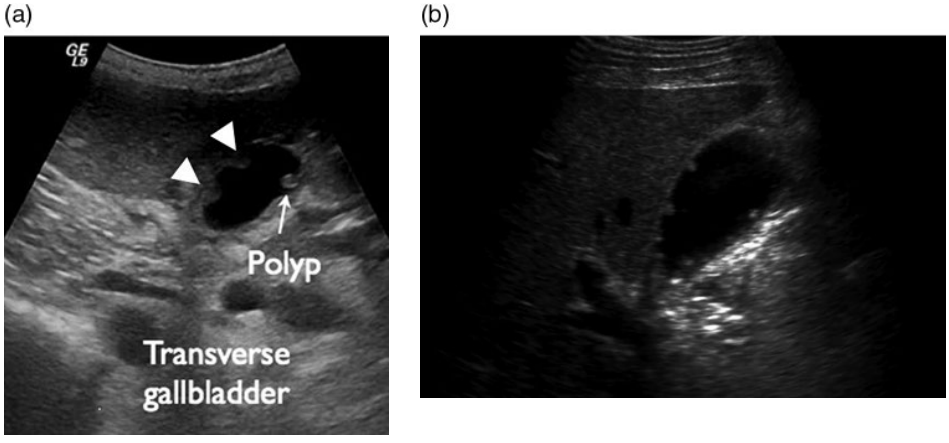

Figure 14.9 (a) A pedunculated polyp which can be distinguished from a gallstone by the absence of shadowing can be seen. On the opposite wall, there are two sessile polyps (arrowheads). (b) A gallbladder with multiple polyps (see also Video 14.2). Image (b), © A.J. Dean.

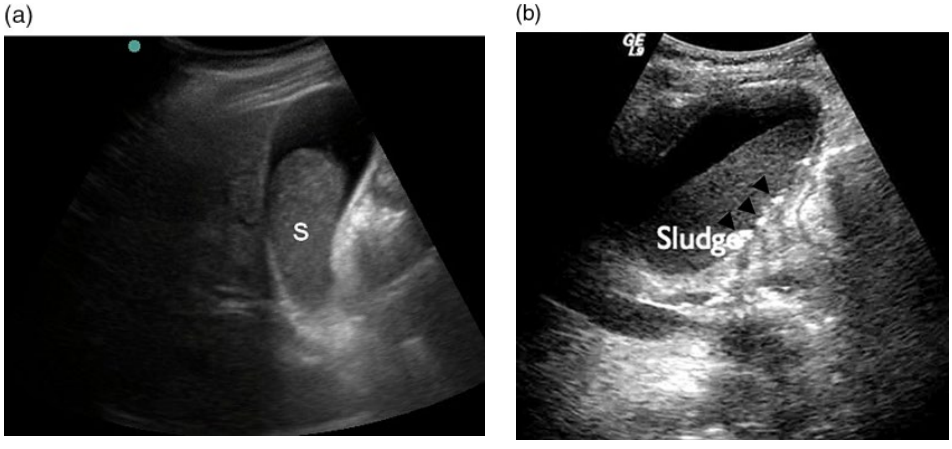

Figure 14.10 Two images showing sludge. (a) The sludge has a characteristic bizarre shape; the gallbladder otherwise appears normal. (b) A longitudinal view also shows multiple dependent small stones (arrowheads). The anterior wall of the gallbladder is irregularly thickened, suggesting the presence of cholecystitis. Image (a), © A.J. Dean.

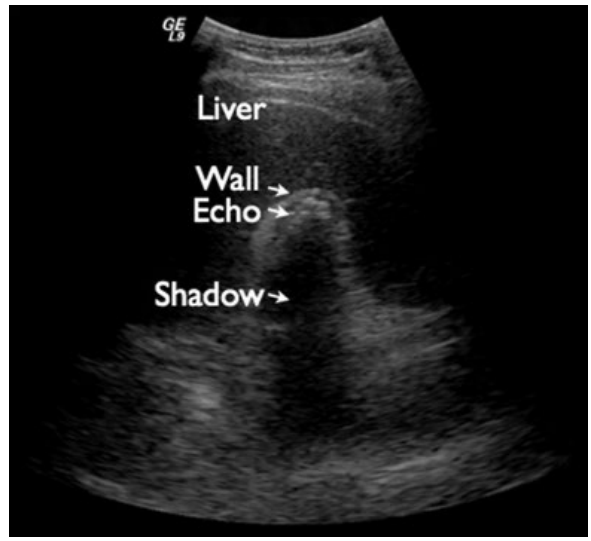

Figure 14.11 A transverse view of a gallbladder showing the wall-echo-shadow sign, indicating chronic cholecystitis that results in a contracted gallbladder full of stones, without any evidence of residual bile.

(a)

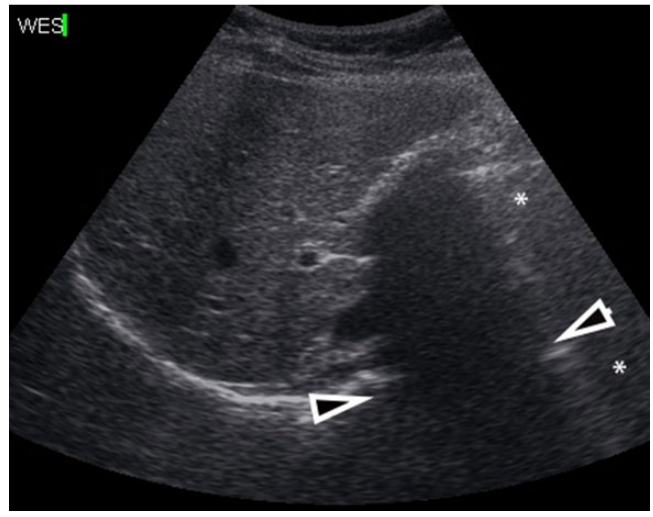

(b)

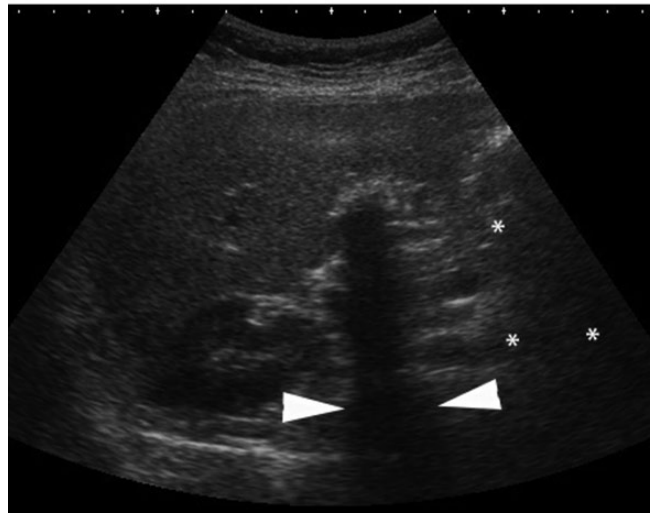

Figure 14.12 Longitudinal (a) and transverse (b) views of another case of wall-echo-shadow sign. In the absence of bile, less-experienced sonologists may have difficulty in finding the gallbladder. With gain settings optimised so that blood vessels in the liver appear completely black, the clean (very dark) shadows caused by the multiple gallstones (arrowheads) can be identified, in marked contrast to the 'dirty' shadows (**) caused by bowel gas. Images © A.J. Dean.

Acute Cholecystitis

Basics

The sonographic diagnosis of acute cholecystitis is based on a constellation of findings: gallstones, gallbladder wall thickening, pericholecystic fluid, dilated common bile duct, and a sonographic Murphy's sign. With progressive gallbladder wall inflammation, there is a continuum between gallbladder wall oedema, pericholecystic fluid, and frank gangrenous necrosis (Figures 14.4–14.6, 14.13 and 14.14). Gallbladder wall oedema due to surgical disease appears as irregular thickening and heterogeneous echodensity of the wall. Sometimes, irregular sloughing mucosa can be identified within the lumen. The thickening of acute cholecystitis is qualitatively different from the thickening due to medical causes because it affects the wall irregularly and discontinuously. Pericholecystic fluid will appear as an hypoechoic to an anechoic stripe directly surrounding the gallbladder wall. The sonographic Murphy sign consists of placement of the probe directly over the gallbladder and provocation of the patient's symptoms. This should be confirmed by demonstrating an *absence of tenderness* with probe pressure in locations more distant from the gallbladder.

Points and Pitfalls

- Gallbladder wall thickening is a normal finding in the contracted post-prandial gallbladder.

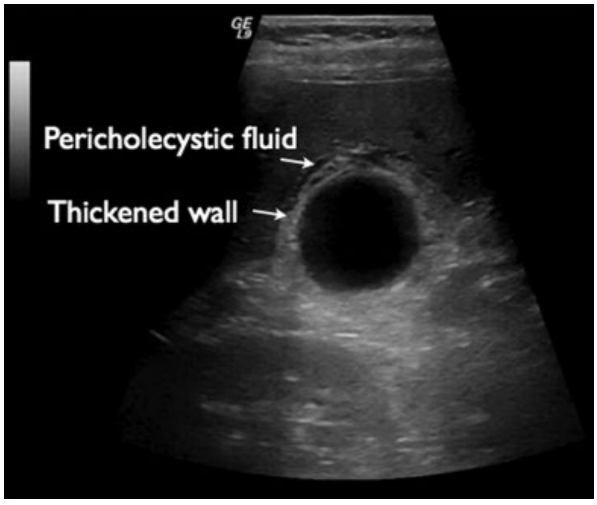

Figure 14.13 Transverse view of a gallbladder with cholecystitis. The wall is heterogeneously echogenic, with areas of focal oedema and surrounding pericholecystic fluid.

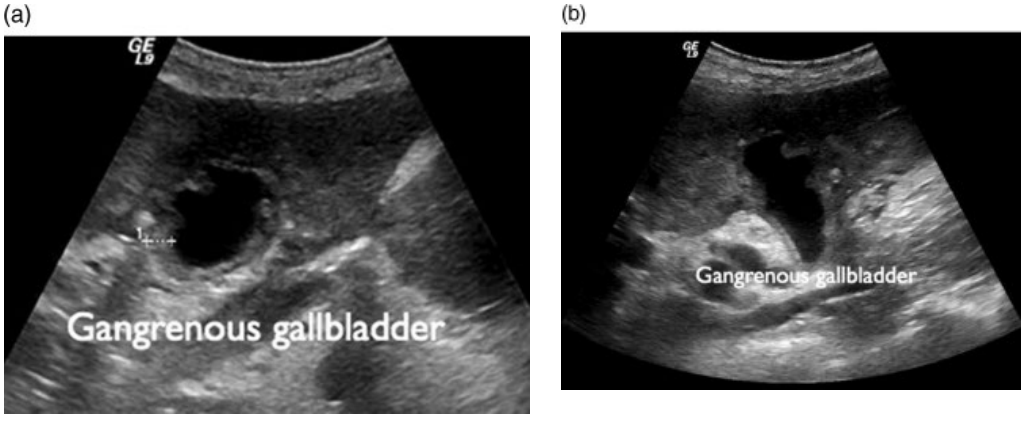

Figure 14.14 Transverse (a) and longitudinal (b) views of a gangrenous gallbladder demonstrating advanced cholecystitis with necrosis and sloughing of mucosa into the lumen.

Many systemic medical conditions can also cause gallbladder wall thickening, including congestive heart failure, renal failure, volume overload, hepatitis, ascites and HIV. Clinical correlation is necessary to determine whether gallbladder wall thickening is a sign of cholecystitis in any given instance.

The Prognostic Value of Signs

While various studies have demonstrated a range in the sensitivity and specificity of different sonographic findings for determining the presence of true acute biliary disease, there appears to be consensus that a sonographic Murphy's sign, in the presence of either stones or a thickened gallbladder wall, is both highly sensitive and highly specific. Similarly, the absence of both a sonographic Murphy's sign and stones has a negative predictive value on the order of 95%.

Special Considerations

Acalculous Cholecystitis

Acalculous cholecystitis is rare in non-hospitalised patients. Ultrasound findings will be similar to those associated with acute cholecystitis, and may include wall thickening, pericholecystic fluid and a sonographic Murphy's sign. Risk factors include diabetes, sepsis, immunocompromise, parenteral nutrition and mechanical ventilation.

Gangrenous Cholecystitis

Emphysematous cholecystitis, caused by gas-forming organisms in the gallbladder wall, may lead to a gangrenous organ. Ultrasound findings such as an asymmetrically thickened gallbladder wall or localised pericholecystic fluid or distortion of the clear wall boundaries are suggestive of this condition. Fine reverberation artefacts may be detected emanating from the wall due to the presence of gas. The gallbladder may be filled with echogenic debris representing abscess. Older age and diabetes are risk factors.

Porcelain Gallbladder

A porcelain gallbladder appears as a diffusely hyperechoic structure due to calcium deposits in the gallbladder wall as a result of chronic cholecystitis. If the gallbladder contains stones this may be confused with a WES sign. Due to an association between porcelain gallbladder and biliary cancer, further investigation is required and CT is usually the next step in the evaluation.

Biliary Duct Obstruction

Basics

A common bile duct measuring >6 mm may be indicative of obstruction, which may be secondary to stones within the duct (choledocholithiasis) (Figures 14.15 and 14.16). The common bile duct can also be obstructed by

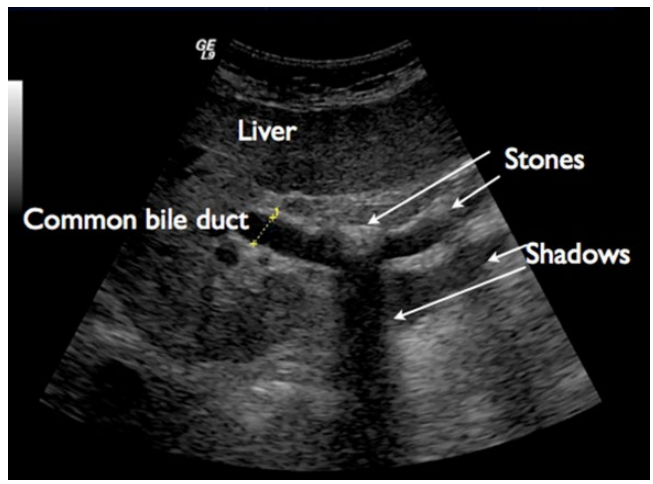

Figure 14.15 Choledocholithiasis: a longitudinal image of a dilated common bile duct with two shadowing intraluminal gallstones.

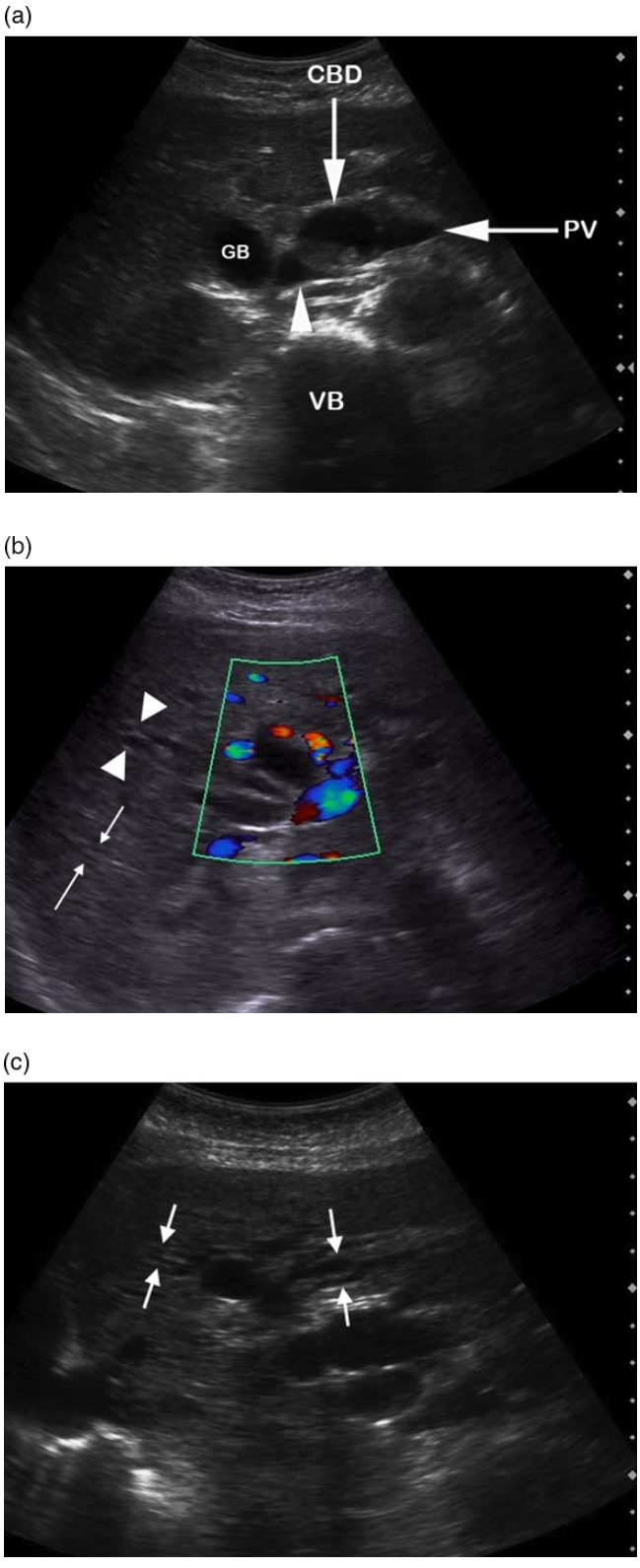

Figure 14.16 (a–c) Images of common bile duct (CBD) obstruction and intrahepatic cholestasis (IHC) due to pancreatic head neoplasm. (a) A transverse view demonstrates the porta hepatis with a CBD containing sludge and with a diameter >2 cm (compare to the 1-cm depth markers). The sludge compresses both the portal vein and inferior vena cava (arrowhead; VB: vertebral body). (see Video 14.3, from which this image was taken). (b) and (c) show images of severe IHC with colour-flow Doppler in (a) confirming that the dilated vessels are not vascular. Centrally, this is sometimes called the 'too many tubes sign'. (c) More peripherally, the 'parallel tracks' and 'shotgun' signs are seen (between the arrowheads and arrows). Images © A.J. Dean.

extrinsic compression from masses, most often arising from the pancreas (e.g., pancreatic adenocarcinoma). Less commonly, the common bile duct can be dilated due to a stricture, the majority of which are iatrogenic, though they may also be caused by pancreatic cancer or by chronic conditions such as pancreatitis or recurrent stones in the duct. The common bile duct is located in close proximity to the portal vein, and the use of colour flow can help to distinguish it from nearby vascular structures. It should be noted that in patients who had had their gallbladders removed, or in the elderly, the diameter of the common bile duct might normally be more than 6 mm. Many clinicians use the rule of 'age in decades' in millimetres as the upper limit of normal bile duct size. For a 75-year-old, this would be 7.5 mm.

Points and Pitfalls

- The common bile duct size increases with age. In an elderly patient, a measurement greater than 6 mm may not signify gallbladder pathology.
- An obstructing stone in the bile duct can cause signs of cholecystitis on ultrasound, as well as gallstone pancreatitis. Laboratory testing and further imaging for these entities may be required.

Current Value of Ultrasound as a Clinical Decision-Making Tool

Numerous studies have documented the reliability of emergency department ultrasound for determining the presence of acute biliary disease. It is probably best viewed in terms of providing a binary (yes or no) answer to a focused question. When findings are highly suggestive of an acute process, steps can be taken to more quickly obtain appropriate consultations, perform laboratory investigations, and begin therapeutic interventions. When the examination does not demonstrate significant sonographic findings, acute biliary disease is unlikely. In cases of high pre-test probability, or when bedside scanning is limited or equivocal, further investigations with CT, MRI or HIDA scanning may be needed.

Summary

Over the past two decades ultrasound has become accepted as the ideal first-line imaging for the evaluation of hepatobiliary pathology. In the hands of clinician sonologists, it is safe, easily available and accurate. It is important to recognise that technically limited or equivocal studies mandate further evaluation and imaging, with CT scan as a common next step.

Further Reading

Berk, R.N., Leopold, G.R. (1978) The present status of imaging of the gallbladder. *Invest. Radiol.*, **13** (6), 477–489.

Billittier, A.J., Abrams, B.J., Brunetto, A. (1996) Radiographic imaging modalities for the patient in the emergency department with abdominal complaints. *Emerg. Med. Clin. North Am.*, **14** (4), 789–850.

Cooperberg, P.L., Burhenne, H.J. (1980) Real-time ultrasonography. Diagnostic technique of choice in calculous gallbladder disease. *N. Engl. J. Med.*, **302** (23), 1277–1279.

Jehle, D., Davis, E., Evans, T., Harchelroad, F., Martin, M., Zaiser, K., Lucid, J. (1989) Emergency department sonography by emergency physicians. *Am. J. Emerg. Med.*, **7** (6), 605–611.

Kendall, J.L., Shimp, R.J. (2001) Performance and interpretation of focused right upper quadrant ultrasound by emergency physicians. *J. Emerg. Med.*, **21** (1), 7–13.

Miller, A.H., Pepe, P.E., Brockman, C.R., Delaney, K.A. (2006) ED ultrasound in hepatobiliary disease. *J. Emerg. Med.*, **30** (1), 69–74.

Rubens, D.J. (2007) Ultrasound imaging of the biliary tract. *Ultrasound Clin. North Am.*, **2** (3), 391–413.

Schlager, D., Lazzareschi, G., Whitten, D., Sanders, A.B. (1994) A prospective study of ultrasonography in the ED by emergency physicians. *Am. J. Emerg. Med.*, **12** (2), 185–189.

Scruggs, W., Fox, J.C., Potts, B., Zlidenny, A., McDonough, J., Anderson, C.L., Larson, J., Barajas, G., Langdorf, M.I. (2008) Accuracy of ED beside ultrasound for identification of gallstones: retrospective analysis of 575 studies. *West. J. Emerg. Med.*, **9** (1), 1–5.

Shah, K., Wolfe, R.E. (2004) Hepatobiliary ultrasound. *Emerg. Med. Clin. North Am.*, **22** (3), 661–673.

Spence, S.C., Teichgraeber, D., Chandrasekhar, C. (2009) Emergent right upper quadrant sonography. *J. Ultrasound Med.*, **28** (4), 479–496.

15

Renal Ultrasound

Lisa Munro Davies

Introduction

Bedside ultrasound is a useful tool in patients presenting with complaints of flank or abdominal pain. Its major application in this setting is the detection of hydronephrosis secondary to obstructing ureteral calculi. It can also be used to exclude the presence of abdominal aortic aneurysm (AAA), an important 'can't miss' diagnosis (see Chapter 7).

A renal ultrasound examination includes evaluation of the kidneys, the ureters (to the extent that they are visible), and the bladder. In addition to detecting hydronephrosis, renal ultrasound can narrow the differential diagnosis in patients presenting with renal failure, anuria and some renal infections. Abdominal/pelvic computed tomography (CT) is more sensitive in detecting these as well as alternative diagnoses pathologies under consideration in these patients. However, ultrasound has the advantage of providing rapid information at the point of care and does not expose the patient to ionising radiation.

Anatomy and Sonoanatomy

The kidneys are paired retroperitoneal organs, located deep to the posterolateral lower rib cage within the paravertebral gutters. The left kidney lies inferior to the spleen, usually spanning the T11 to L2 vertebral levels. The right kidney lies inferior to the liver, approximately one vertebral level lower than the left kidney. The superior poles of the kidneys are tilted slightly posterior and medial with respect to the inferior poles.

The three main layers of the kidney are the *cortex*, the *medulla*, and the *sinus* (Figures 15.1–15.3). Immediately beneath the capsule (Gerota's fascia) is the cortex. The columns of Bertini are projections of the cortex that extend into the medulla. These columns separate the *renal pyramids*, which have a characteristic hypoechoic appearance on ultrasound, especially in younger patients, in whom they can be mistaken for renal cysts (Figure 15.2a and c). The corticomedullary junction may be difficult to discern without optimal gain settings. The apex of each renal pyramid forms a papilla, which excretes urine into a corresponding minor calyx. The minor calyces coalesce to form the major calyces, which merge to form the renal pelvis; the latter tapers through the renal hilum into the proximal ureter. The transition between the renal pelvis and the ureter is the *ureteropelvic junction* (UPJ), which is usually at the level of the hilum, although it can occur more distally in patients with an extrarenal pelvis. The UPJ is a common site of obstruction from ureterolithiasis. Collectively, the minor calyces, major calyces, blood vessels and surrounding fatty tissue

Emergency Point-of-Care Ultrasound, Second Edition. Edited by James A. Connolly, Anthony J. Dean, Beatrice Hoffmann and Robert D. Jarman.

Companion website: www.wiley.com/go/connolly/ultrasound

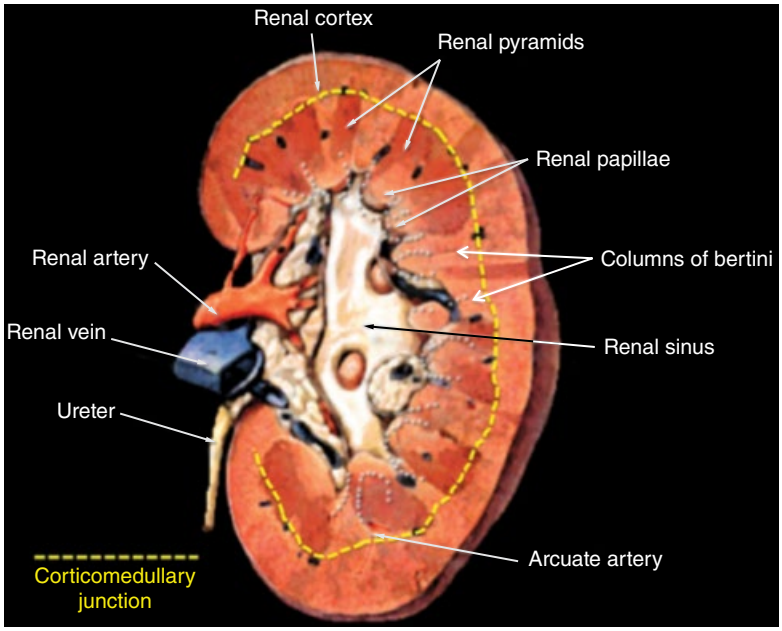

Figure 15.1 Normal kidney anatomy. The dotted line indicates the corticomedullary junction. The renal sinus includes the collecting system, vasculature and renal sinus fat. Figure © Matt Nixon and Sonoguide; reproduced with permission from Beatrice Hoffmann.

constitute the *renal sinus*, which is a highly echogenic central region of the kidney. The collecting system and ureters are normally drained of urine by active peristalsis several times per minute, so that they are not seen on ultrasound unless distended by urine in hydronephrosis.

Multiple structures enter and exit through the hilum, including the blood vessels, lymphatics and ureters. The ureters course inferiorly across the psoas muscles, crossing the common iliacs at the pelvic brim, descending inferiorly, then anteriorly and medially to empty into the bladder via the *ureterovesicle junctions* (UVJs), which form two of the corners of the trigone. The ureter is difficult to follow below the pelvic inlet due to overlying bone, although in lower-body mass index patients experienced sonologists are able to follow them into the pelvis, scanning through the lower abdomen. The bladder can extend to the level of the umbilicus in cases of severe urinary retention.

Scanning Technique

A 3–5 MHz abdominal probe is typically used. The scanning technique is slightly different for the right and left kidneys.

Scanning of the right kidney begins with the patient supine. In many cases an examination of the entire kidney is possible using the liver as a window. The probe marker is pointing superiorly/posteriorly (Figure 15.4), though optimal longitudinal images are usually obtained with the probe parallel with the ribs. When a good view is obtained the sonologist fans the probe to scan the entire organ in real time. The probe is then turned 90° counterclockwise and the kidney is scanned systematically from pole to pole in the transverse plane (Figure 15.2; Videos 15.1 and 15.2).

The left kidney requires more posterior windows (Figures 15.3 and 15.5), and the kidney is scanned directly (without using the spleen as a window). A decubitus (Figure 15.5b) or a sitting position may be helpful. Again, the kidney is

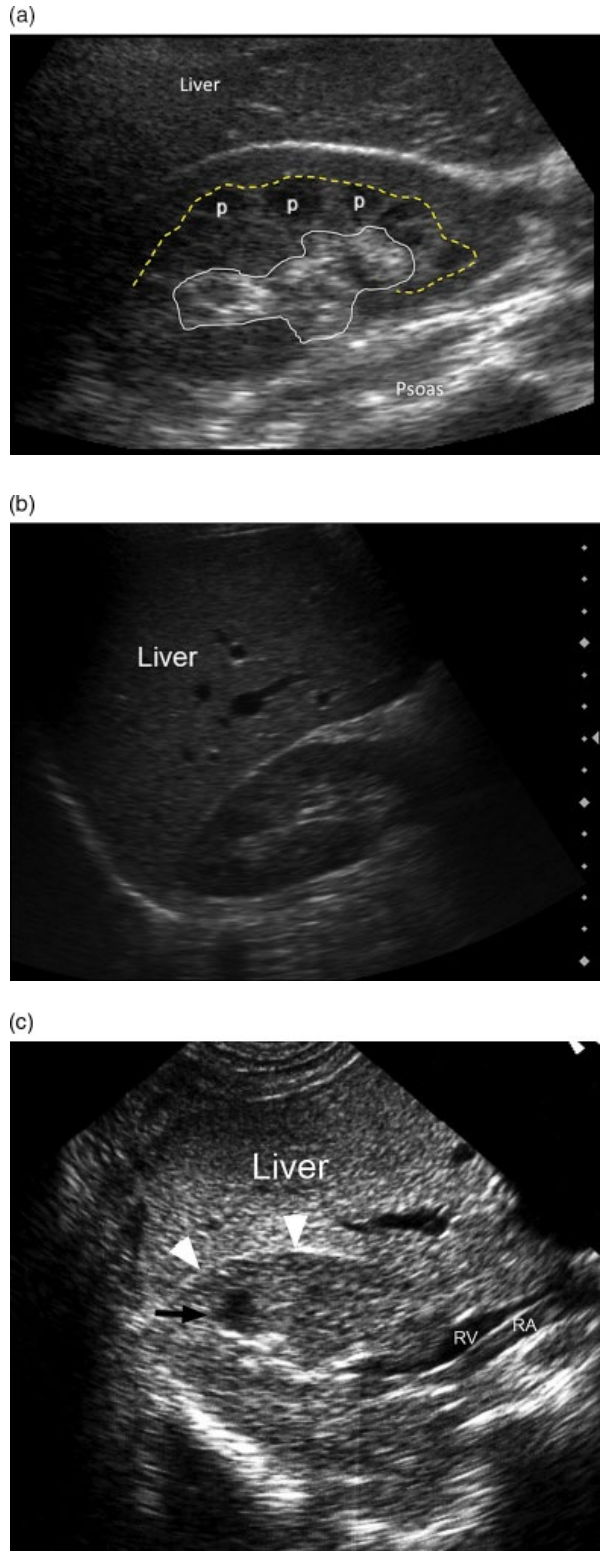

Figure 15.2 The right kidney. (a) The dotted line indicates the boundary between the cortex and medulla. Inside this line, several hypoechoic pyramids (p) are seen. (b) Longitudinal image, where the pyramids and renal sinus are less distinct. The depth to the kidney indicates that this view is obtained from an anterior lateral position, using the liver as a window. (c) Transverse view of the normal right kidney, with a single prominent pyramid (black arrow). The kidney is slightly less echogenic than the liver, separated by Gerota's fascia (white arrowheads). The renal vein (RV) and renal artery (RA) enter at the hilum. All figures © A. J. Dean.

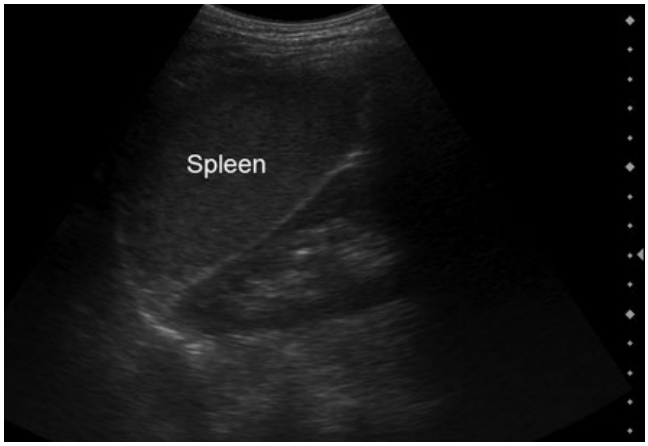

Figure 15.3 Longitudinal view of the upper half of the left kidney. Because the normal spleen affords much more limited views than the liver, the inferior pole is obscured by bowel gas. Images of the left kidney, especially the inferior pole, are usually obtained directly through the flank. Figure © A. J. Dean.

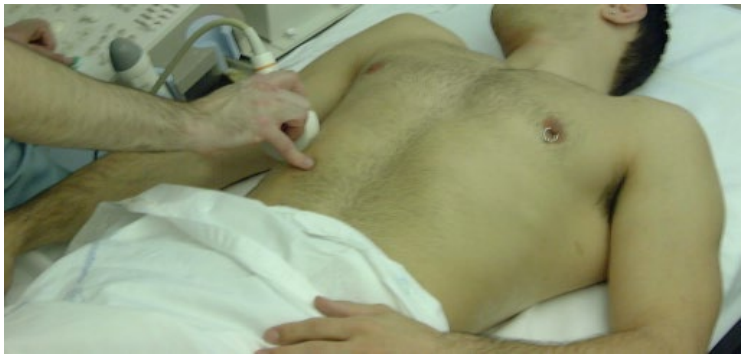

Figure 15.4 Typical probe position for scanning of the right kidney using the liver as a window. Figure © A. J. Dean.

scanned in both longitudinal and transverse planes. Both kidneys should be examined for purposes of comparison and to ensure that the patient indeed has two kidneys, since a unilateral, horseshoe or pelvic kidney alters management.

The bladder can almost always be easily visualised by placing the probe immediately superior to the pubis (see Chapter 8; Figure 8.6 and Videos 8.8a–c for longitudinal and transverse images of the bladder in the male and female). The commonest pitfall in scanning the bladder is excessive gain. This results in an inability to distinguish significant findings posterior to the bladder, particularly hydroureter, ureteral stones, shadowing from bladder stones or free fluid (Figure 15.6).

Pathology

Ureterolithiasis

The commonest goal of emergency renal ultrasound is to identify the presence of obstructive uropathy manifesting as hydronephrosis and/or hydroureter. The causative stone may not be identified on ultrasound, although it is frequently seen behind the bladder at the UVJ. However, in the presence of microscopic hematuria, unilateral hydronephrosis on bedside ultrasound has a sensitivity of 83% and a specificity of 92% for the diagnosis of ureterolithiasis compared to abdominal/pelvic CT as the 'gold standard'.

(a)

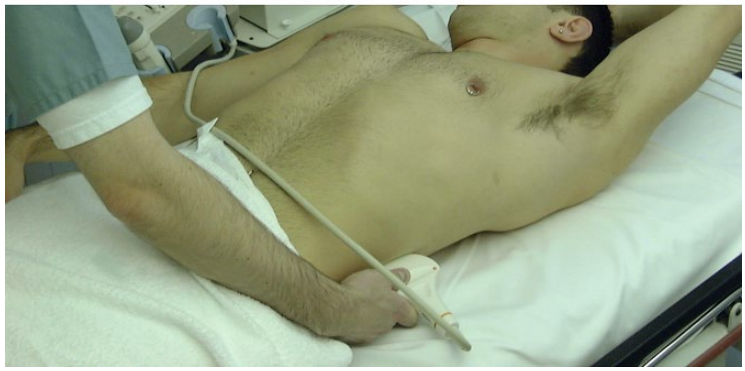

(b)

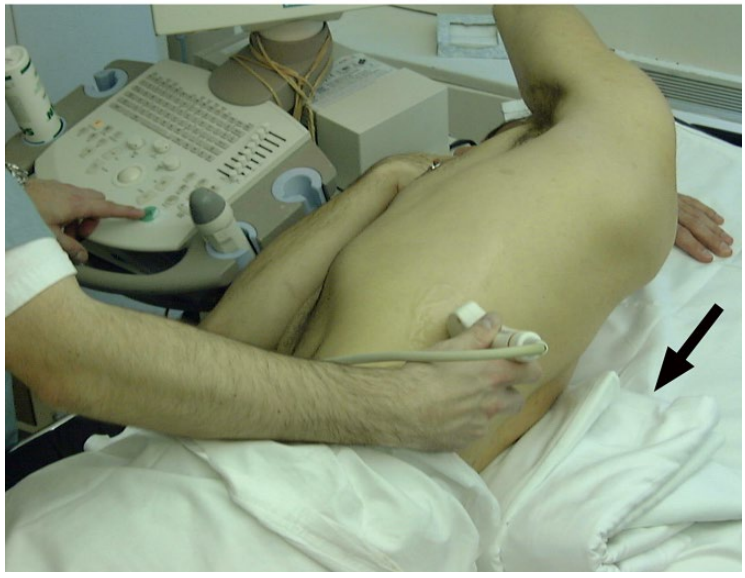

Figure 15.5 Typical probe position for scanning of the left kidney. The transducer is typically more posterior than for the right kidney. (a) Adequate images may be obtained with the patient supine, although it may be necessary to place the patient in a decubitus position with a bolster (black arrow) placed under the contralateral ribs to widen the intercostal spaces on the left (b). Figures © A. J. Dean.

Despite the inferior test characteristics of ultrasound for the diagnosis of ureterolithiasis compared to CT, and the inability to identify the size and location of most stones, ultrasound provides immediate information at the bedside and also spares the patient exposure to ionising radiation. This is particularly important in younger patients with recurrent renal colic. Ultrasound also may provide prognostic information regarding the likelihood of stone passage, as the absence of hydronephrosis appears to predict a smaller stone size.

Hydronephrosis is seen on ultrasound as echo-free areas within the brightly echogenic renal sinus (Figures 15.7 and 15.8; Videos 15.4 and 15.5). Hydronephrosis is graded according

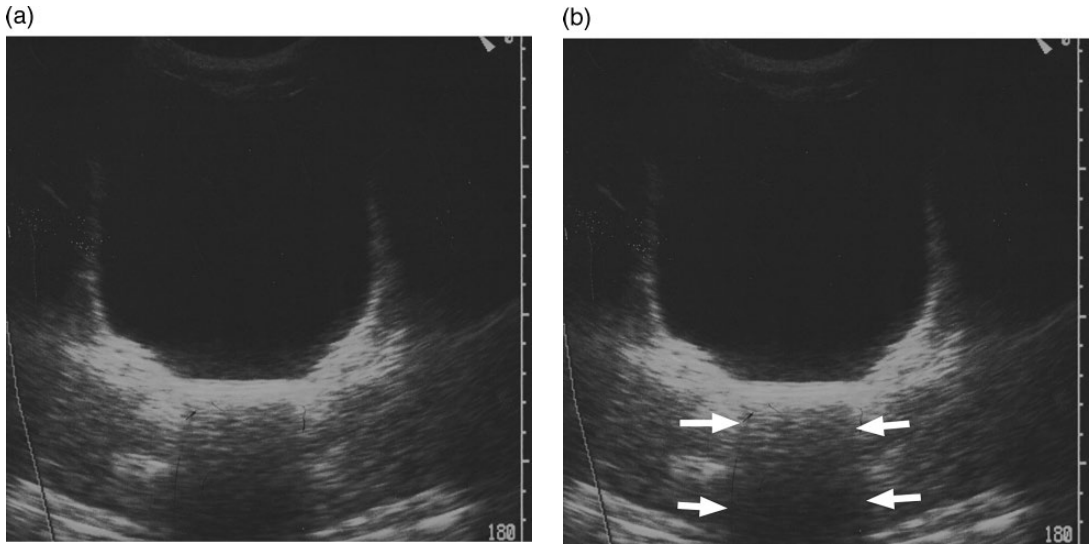

Figure 15.6 The effect of posterior acoustic enhancement behind the bladder. (a) A patient being evaluated for urinary retention had this image interpreted as 'distended bladder, otherwise normal'. (b) As a result of failure to reduce gain to allow for posterior acoustic enhancement, the increased echogenicity of multiple layering stones, and the shadowing behind them (arrows) were overlooked. Figures © A. J. Dean.

to the severity of ultrasound findings which are related to both the degree of obstruction, and the length of time that it has been present. A four-grade system is delineated in Table 15.1. Hydronephrosis is also frequently described using 3 grades: "mild (Grade 1)", "moderate (Grade 2)" and "severe (Grade 3). The latter system combines the first two grades of the system described in Table 15.1. Small, partially obstructing stones may not result in hydronephrosis, whereas grade IV hydronephrosis is typically seen only in those with high-grade, chronic ureteral obstruction. Dehydration from vomiting or other causes may prevent the development of hydronephrosis. Scanning may be repeated after hydration. Conversely, pregnancy or a distended bladder may cause hydronephrosis (usually bilateral) in the absence of an obstructing stone. A fluid-filled extrarenal pelvis is occasionally seen. It is not evidence of obstruction unless hydronephrosis is seen within the renal sinus (Figure 15.8d).

Calculi appear on ultrasound as bright, echogenic foci with posterior shadowing (Figure 15.9; Video 15.6). In the renal sinus the echo is often indistinguishable from the surrounding fat, so that stones are identified by the shadowing alone. Ureteral stones most commonly become lodged at the UVJ, a location where they can readily be identified by ultrasound (Figure 15.10; Videos 15.5b and 15.7). Gain settings should be adjusted so that the bladder appears completely black. Far gain needs to be decreased to compensate for posterior acoustic enhancement. Structures behind the bladder should have a complete range of greys, rather than being all light grey or white (see Figure 15.6). In equivocal cases, the UVJ can be interrogated using power Doppler where a 'twinkle artefact' may be generated by the stone.

Ureteral jets are sought by activating colour Doppler in the plane of the posterior trigone in the transverse plane (Figure 15.11; Video 15.8). The colour window should be as small as possible to include the posterior bladder only, the colour velocity scale should be low, and the colour gain adjusted as high as possible without the generation of gain artefact. Left and right ureteral jets can be simultaneously evaluated. The ureters have a highly variable rate of peristalsis, but in well-hydrated patients this occurs several times per minute. No jet will be seen on

Figure 15.7 (a, b) Two examples of mild hydronephrosis, which can easily be overlooked or mistaken for renal vessels, requiring confirmation in real time or using colour-flow Doppler (see panel (c) and Video 15.3). Figures © A. J. Dean.

(a)

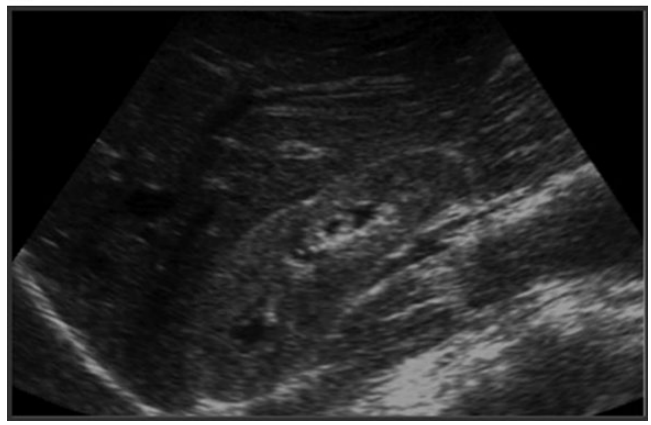

(b)

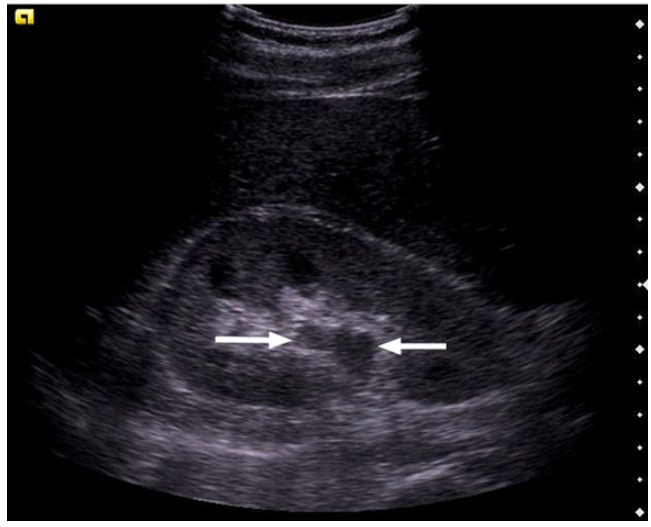

(c)

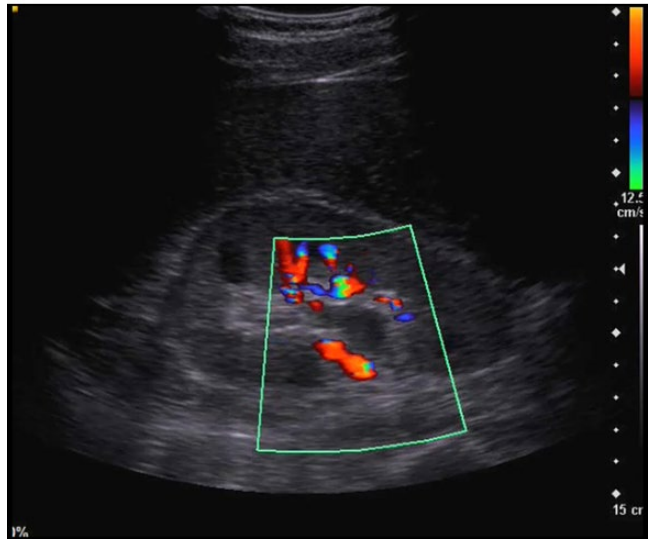

(a)

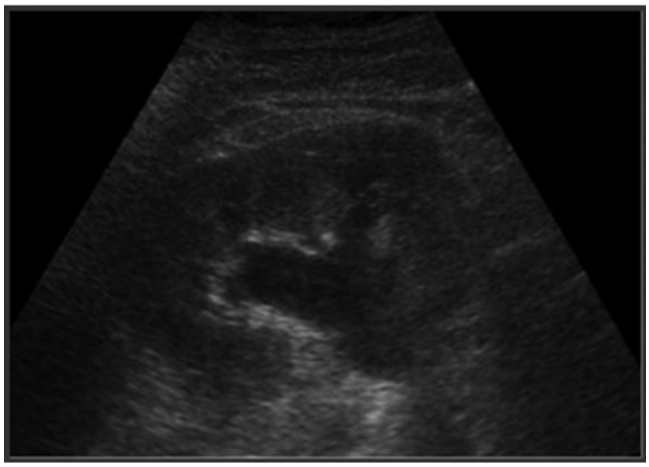

(b)

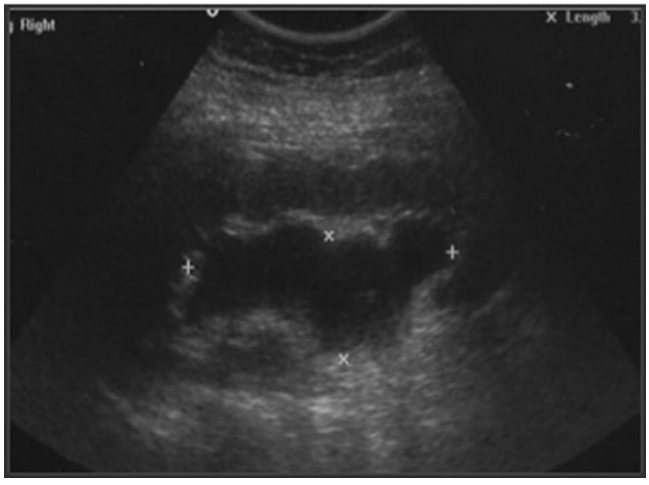

(c)

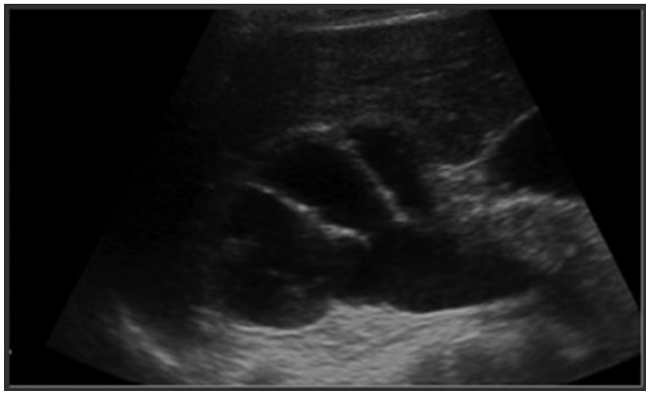

Figure 15.8 Three examples of moderate (a) and severe (b, c) hydronephrosis.

Figure 15.8 (Continued)
(d) An extrarenal pelvis on the left kidney can be seen (arrows). There is no evidence of hydronephrosis. Figures © A. J. Dean.

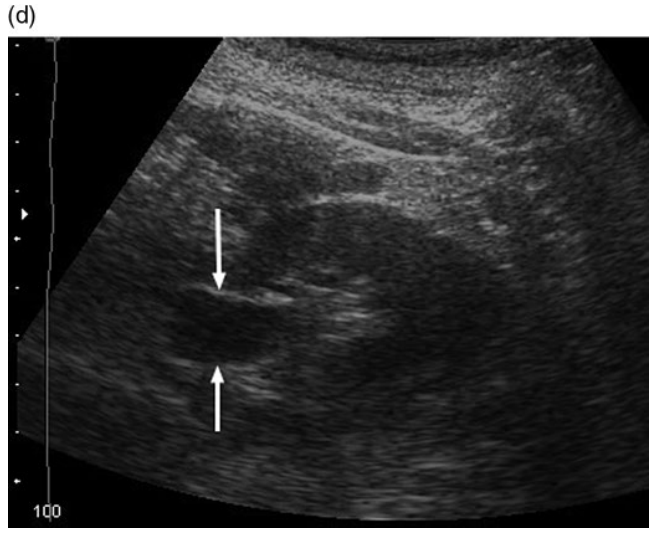

Table 15.1 Grading of hydronephrosis.

Grade 1 (Early or mild)	Minimal separation of the intrarenal collecting system.
Grade 2 (Moderate)	Mild dilation of the renal pelvis, no calyceal dilatation (Figure 15.7b).
Grade 3 (Severe)	Renal pelvic dilation with calyceal dilatation (Figure 15.8a and b).
Grade 4 (Severe, chronic obstruction)	Hydronephrosis with thinning of the renal parenchyma (Figure 15.8c).

the side of the obstruction, whereas the contralateral ureter should discharge normally. With partial obstruction almost any pattern is possible, including increased or diminished flow, sometimes with a continuous dribbling jet.

Renal Infection

Pyelonephritis is not reliably detected by ultrasound, although in some cases it may result in hypoechoic areas of cortex or blurring of the corticomedullary demarcation. A renal abscess appears as a hypoechoic area within the renal parenchyma. Perinephric abscesses may be seen as hypoechoic fluid collections within the perinephric space (Figure 15.12).

Chronic Renal Failure

In chronic renal failure the kidneys often appear small and hyperechoic (Figure 15.13).

Renal Cysts

Renal cysts can be located in any region of the kidney, although usually they occur in the periphery. Benign cysts are thin-walled and anechoic with well-demarcated borders and no further testing is warranted (Figure 15.14; Video 15.9). Cysts that have irregular borders, septations, calcifications or heterogeneous echodensity should be referred for further imaging and urological consultation. Cysts located in the renal sinus should not be mistaken for hydronephrosis. Subcapsular cysts can grow to a large size, and may be mistaken for hepatic cysts, or even the gallbladder. Patients with polycystic kidney disease may have multiple cysts of various sizes with compression and thinning of the adjacent renal parenchyma on ultrasound imaging (Figure 15.15; Video 15.10).

Renal Cancer

Renal cancer has a varied appearance on ultrasound. Any unexplained mass or disruption of renal architecture should be considered

(a)

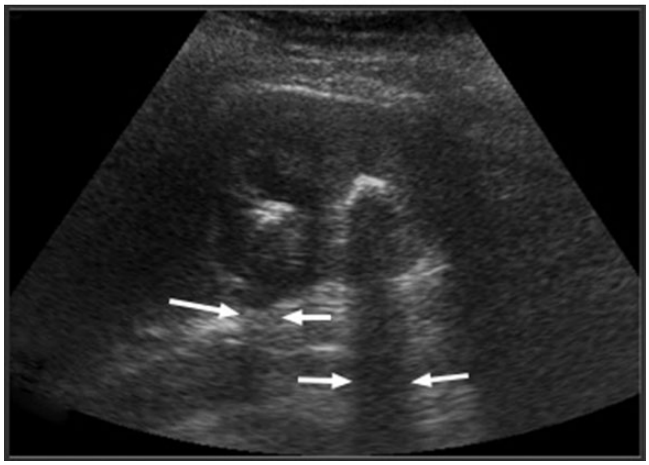

(b)

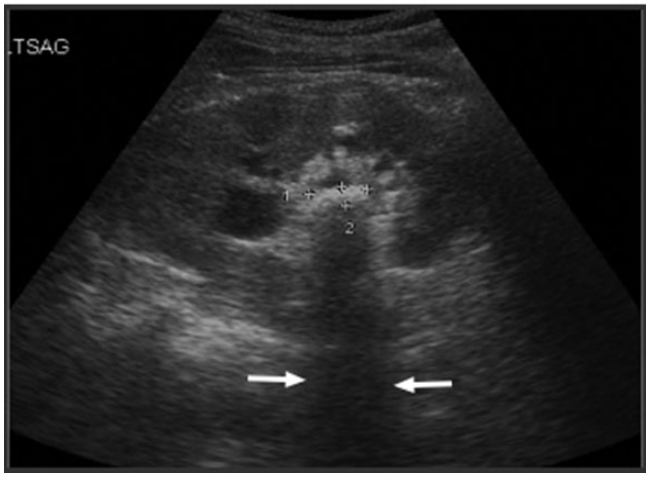

Figure 15.9 Two cases of renal stones, the echogenicity of which is similar to that of renal sinus fat. The stones identified by their shadows (arrows). (b) Mild hydronephrosis, indicating the presence of ureterolithiasis in addition to the renal stone(s). The kidneys require evaluation with both a shallower (for optimal resolution of renal structures) and a deeper field of view (for appreciation of shadowing). Figures © A. J. Dean.

for referral for consultative imaging (Figure 15.16).

Bladder Dysfunction

A number of clinical settings exist where evaluation of the bladder and bladder volumes may be useful:

- In patients with suprapubic pain or voiding difficulty, bladder outlet obstruction can be suspected when large amounts of retained urine are seen on ultrasound.
- Patients presenting with acute kidney injury (acute renal failure) should be screened to exclude an obstructive cause.
- In patients in whom the diagnosis of spinal cord injury or cauda equina syndrome are being considered, post-void urinary retention greater than 100–200 ml mandates further imaging evaluation.

Figure 15.10 Three cases of ureterovesicle junction stones (white arrows). Surrounding oedema is commonly seen, as in the transverse images (panels a and b). (c) (same case as Video 15.7a) The stone is in the plane of the mildly distended ureter (black arrows). Figures © A. J. Dean.

(a)

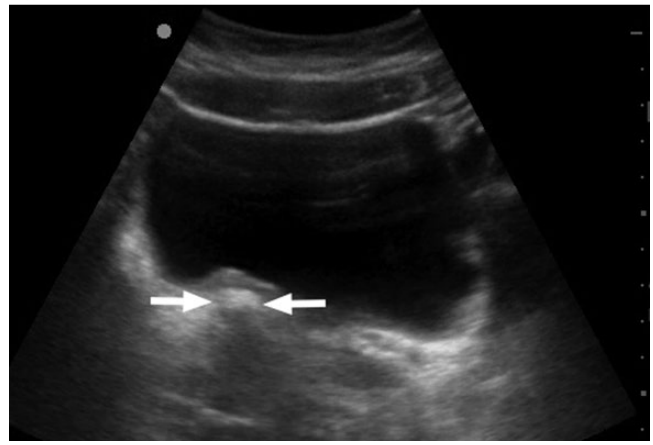

(b)

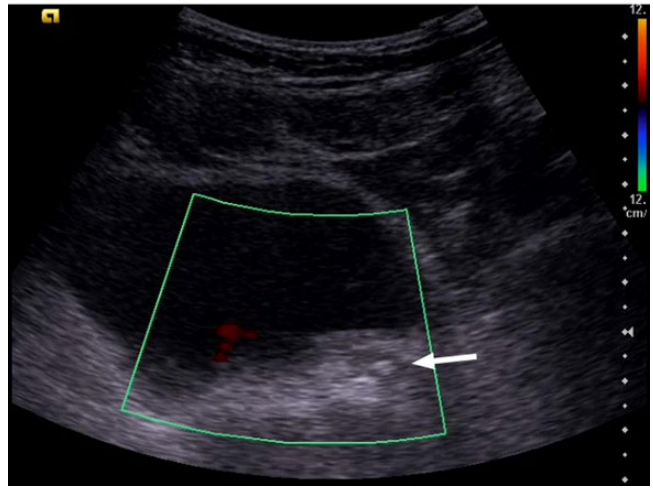

(c)

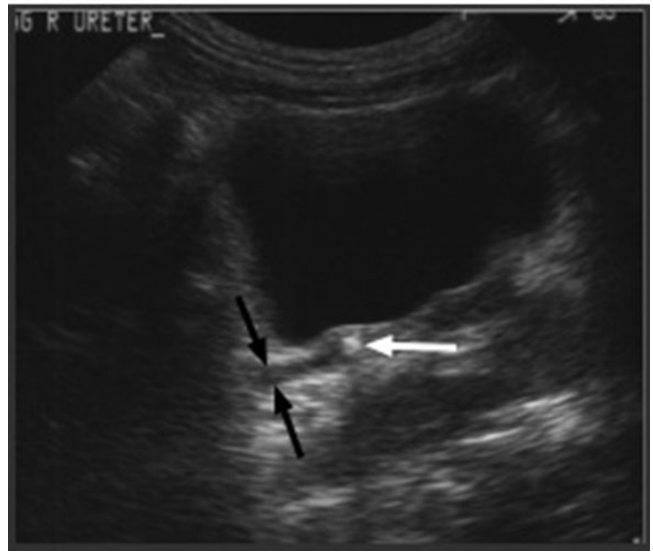

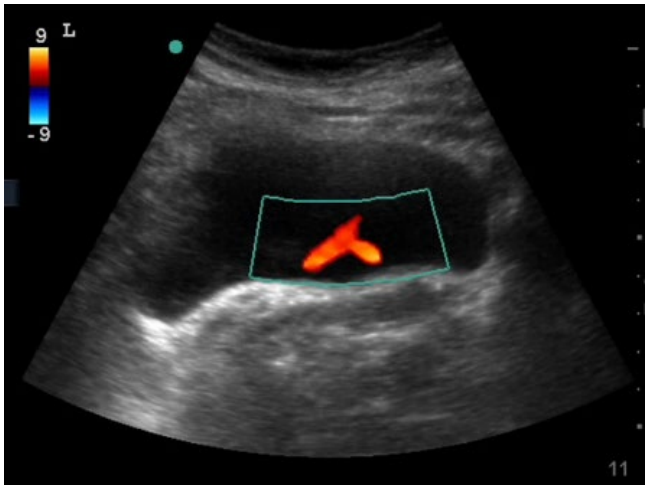

Figure 15.11 Bilateral ureteral jets. Note that the colour Doppler window is appropriately adjusted to be small (to avoid low frame rates), and the velocity scale is also set low (±9 cm s^{-1}) to pick up low-flow signals. The overall depth setting is unnecessarily deep. Figures © A. J. Dean.

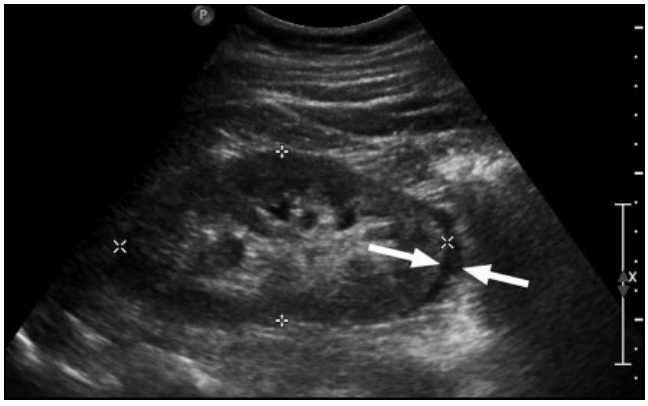

Figure 15.12 Perinephric fluid (between arrows), in this case caused by passage of a ureteral stone leading to a urinoma (there is also mild hydronephrosis). In cases of pyelonephritis, similar sonographic findings of perinephric fluid can be seen in some cases. Figure © A. J. Dean.

In addition to the measurement of volume, ultrasound not infrequently reveals unheralded prostatic hypertrophy or neoplasm (Figure 15.17a,b), diffuse bladder wall thickening from detrusor hypertrophy (Figure 15.19b) and/or trabeculations or diverticula (also suggestive of chronic obstruction) (Figure 15.19c; Video 15.12). Bladder stones and bladder neoplasms can also be identified (Figures 15.18 and 15.19c).

For measurement of bladder volume, the bladder dimensions in three orthogonal directions are multiplied together. Several correction factors have been advocated (including none), although many use a correction factor of 0.7. In health, the bladder empties completely with voiding, although older patients with detrusor dysfunction may have a residual volume of 50–100 ml. A detailed discussion of the various neurogenic diagnoses suggested by the appearance (smooth versus trabeculated ± diverticula) and wall thickness of the bladder with post-void residual urine is beyond the scope of this text.

Bladder Masses and Foreign Bodies

Foley catheters have a characteristic appearance on ultrasound when the balloon is inflated (Figure 15.19). Bladder stones are hyperechoic with posterior shadowing (Figure 15.19c; Video 15.12). Bladder and prostate tumours

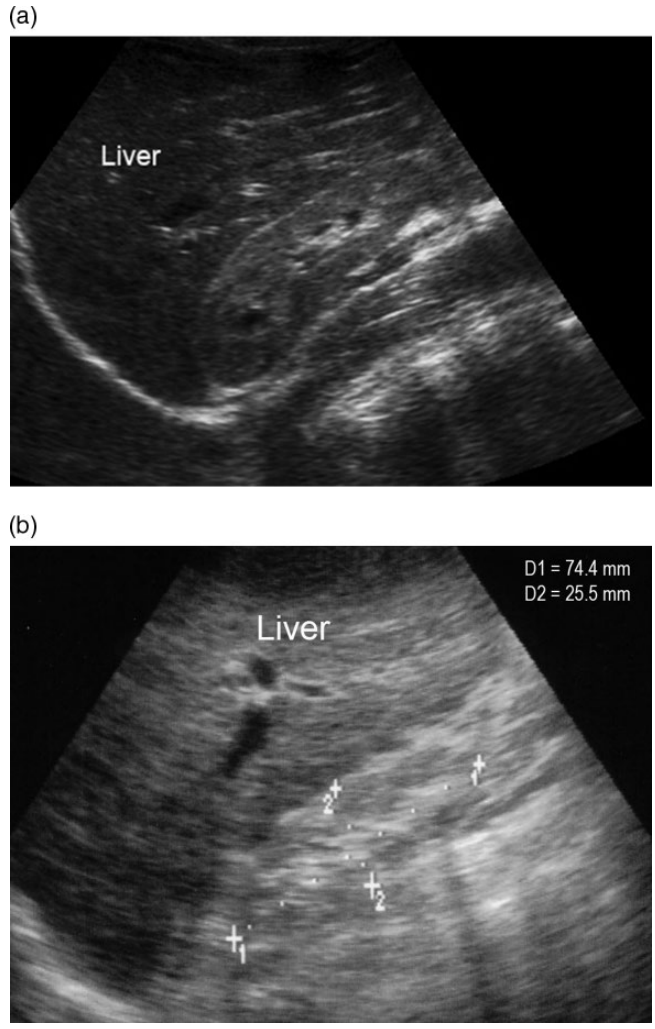

Figure 15.13 (a) A case of mild medical renal disease (MRD) with a normal-sized mildly hyperechoic kidney. (b) The MRD is advanced with a severely atrophic, highly echogenic kidney (indicated by calipers). Figures © A. J. Dean.

may be seen on ultrasound (Figure 15.17). The adjustment of gain and scanning from different angles will usually distinguish tumours from artefacts (most commonly side lobe) occasionally seen in the bladder.

Pearls and Pitfalls

- Scan both kidneys and bladder in all circumstances: unilateral absence or severe disease of a kidney will always affect management. Many bladder findings are readily evident on ultrasound, and frequently affect management.
- For evaluation of hydronephrosis the patient should be adequately hydrated, but not have a distended bladder or be actively diuresing.
- As with grey-scale imaging, successful Doppler evaluation of the kidneys and bladder require understanding and application of relevant 'knobology'.
- Gain settings need to be reduced to interrogate structures behind the bladder.

(a)

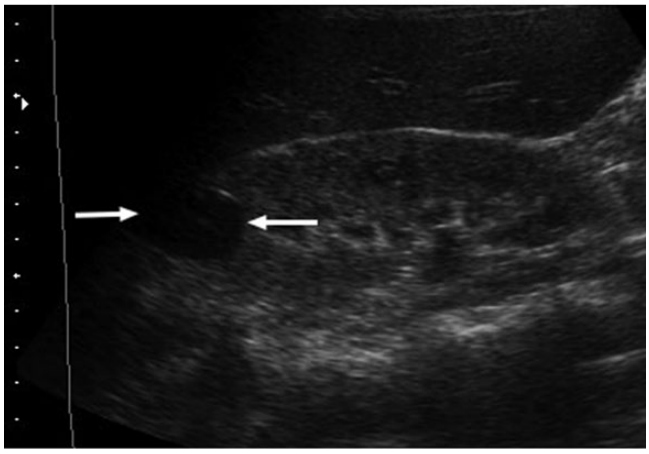

(b)

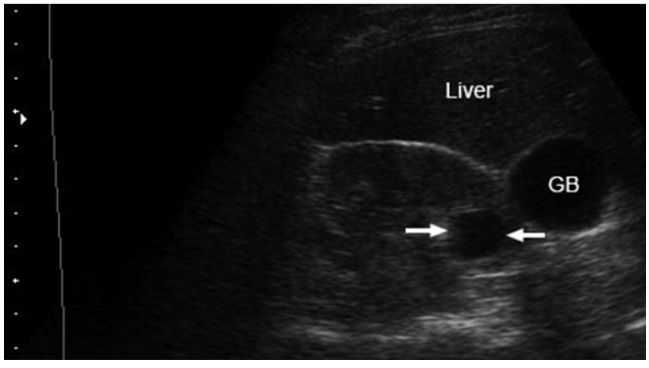

(c)

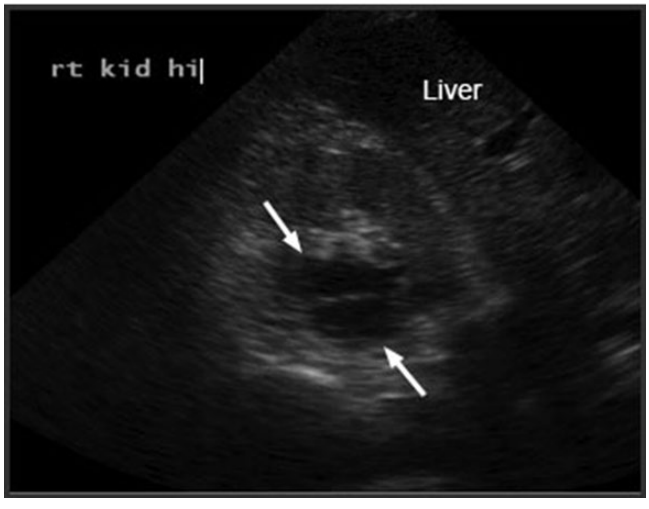

Figure 15.14 (a, b) Two cases of simple renal cysts (arrows; GB = gallbladder). (c) A complex cyst with irregular margins and an internal septation. This requires further work-up. Figures © A. J. Dean.

Figure 15.15 A case of polycystic kidney disease (also seen in Video 15.10). On a still image this may give the impression of severe hydronephrosis, but the cysts are seen outside the renal sinus fat, and in real time the fluid collections are shown to be discrete (non-continuous). Figures © A. J. Dean.

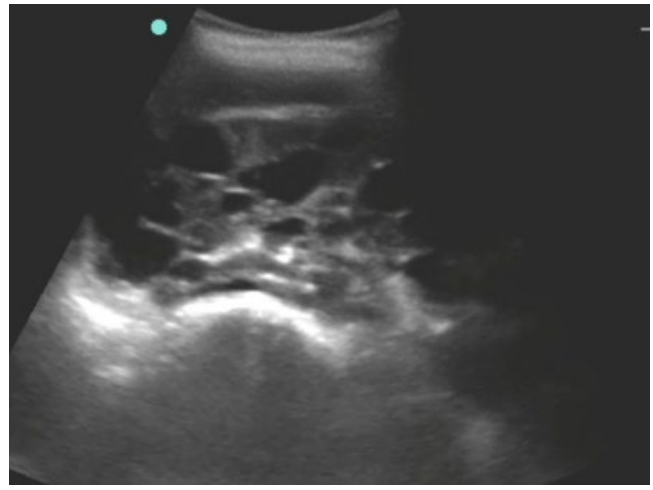

Figure 15.16 A case of renal cell carcinoma. The highly irregular anechoic area should not be confused with a simple cyst or hydronephrosis. Figure © A. J. Dean.

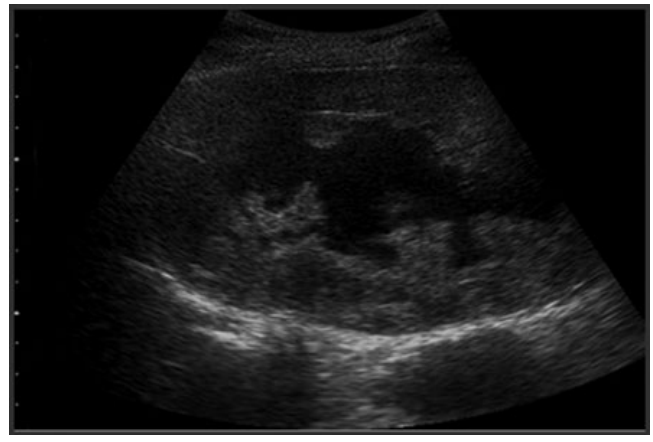

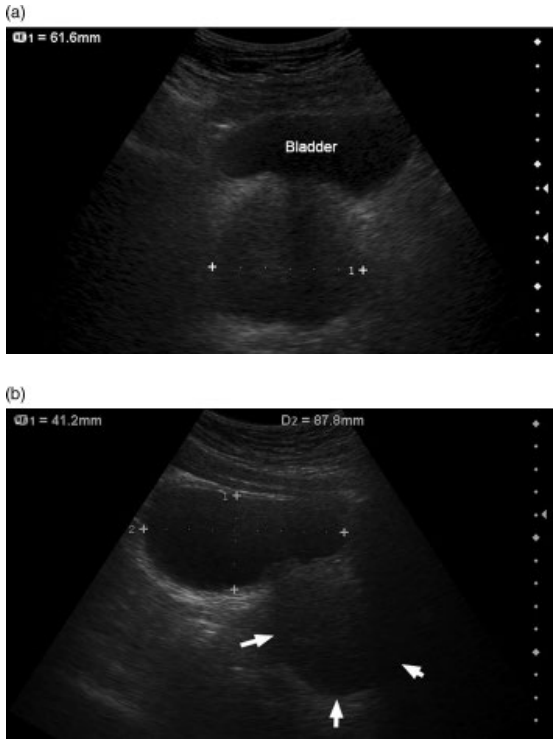

Figure 15.17 Transverse (a) and longitudinal (b) images of prostatic hypertrophy. The margins are smooth. In panel (b) the bladder is being measured for post-void residual, and the prostate is seen to have a slightly exophytic component. In older patients, the caudal margin of the prostate is frequently obscured by the shadow of the calcified symphysis pubis. Using a radius of 3 cm, the volume of this approximately spherical prostate is 160 ml (usual range 15–30 ml). (c) The enlarged prostate has irregular lobulations and margins (arrowheads). (d) The very large prostate protrudes into the bladder lumen (see also Video 15.11 from this case). The abnormalities in panels (c) and (d) are suspicious for neoplasia. Calcifications, as in panel (c), are present in approximately 50% of men aged over 50 years. Figures © A. J. Dean.

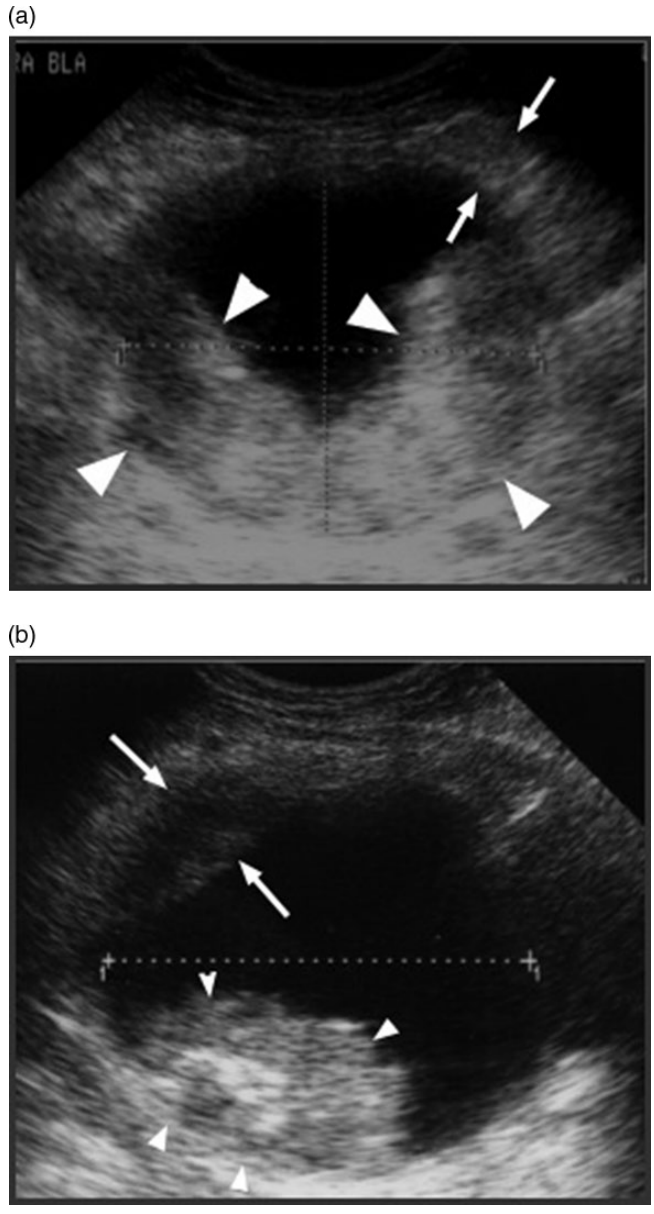

Figure 15.18 Transverse (a) and longitudinal (b) views of bladder cancer (between arrowheads). The non-affected bladder wall (arrows) appears thickened, suggesting chronic outlet obstruction. Figures © A. J. Dean.

- While not as accurate as CT for the evaluation of ureterolithiasis, ultrasound may significantly reduce the utilisation of ionising radiation, without any effect on outcomes. Ultrasound may also help to identify patients at higher risk of complications and to risk-stratify patients with low or high pre-test probability of disease.

(a)

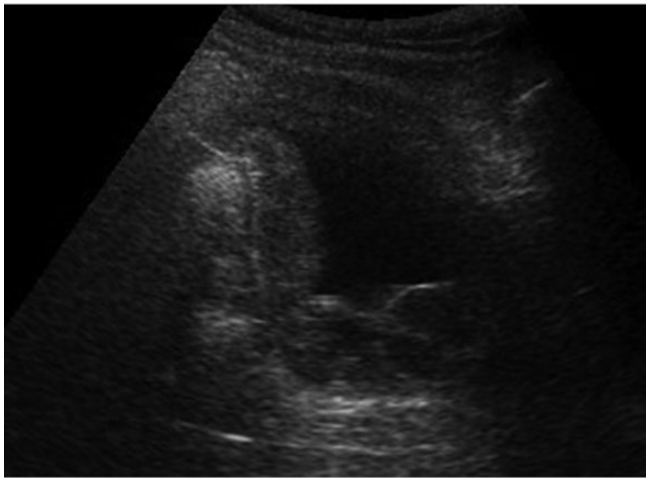

(b)

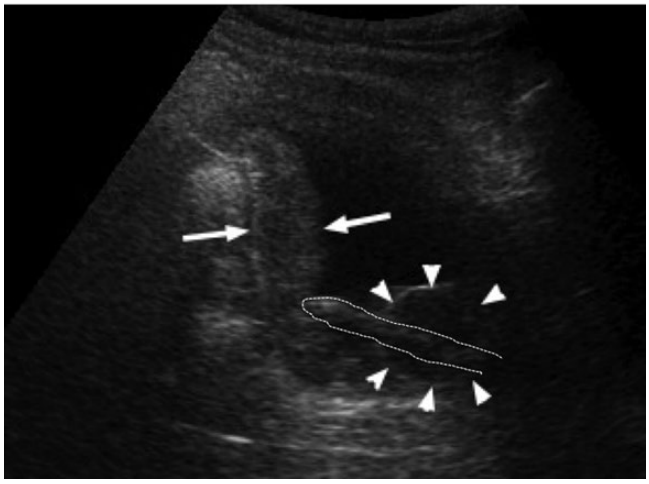

(c)

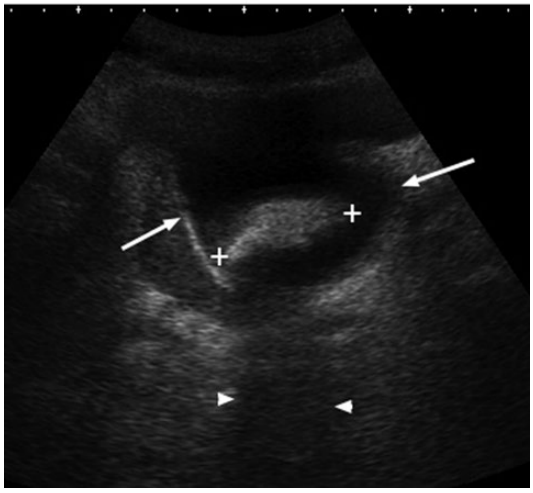

Figure 15.19 (a) Longitudinal image of the bladder of a patient with a Foley catheter placed for acute urinary retention. (b) The same image with arrowheads to indicate the balloon. Note the hypertrophied bladder wall (arrows). (c) (see also Video 15.12 of the same case) A large stone (between callipers) with shadowing (arrowheads) is seen within a bladder diverticulum (arrows). Under the left arrow there is an area of focal wall thickening, suggesting local inflammation or infection. Figures © A. J. Dean.

Further Reading

Gaspari, R.J., Horst, K. (2005) Emergency ultrasound and urinalysis in the evaluation of flank pain. *Acad. Emerg. Med.*, 12 (12), 1180–1184.

Goertz, J.K., Lotterman, S. (2010) Can the degree of hydronephrosis on ultrasound predict kidney stone size? *Am. J. Emerg. Med.*, 28 (7), 813–816.

Kelly, C.E. (2004) Evaluation of voiding dysfunction and measurement of bladder volume. *Rev. Urol.*, 6 (Suppl. 1), S32–S37.

Pei, Y., Obaji, J., Dupuis, A., Paterson, A.D., Magistroni, R., Dicks, E., Parfrey, P., Cramer, B., Coto, E., Torra, R., San Millan, J.L., Gibson, R., Breuning, M., Peters, D., Ravine, D. (2009) Unified criteria for ultrasonographic diagnosis of ADPKD. *J. Am. Soc. Nephrol.*, 20 (1), 205.

Smith-Bindman, R., Aubin, C., Bailitz, J., *et al.* (2014) Ultrasonography versus computed tomography for suspected nephrolithiasis. *N. Engl. J. Med.*, 371, 1100–1110.

16

Ultrasound Evaluation of the Acute Scrotum

J. Matthew Fields

Introduction

Acute scrotal pain and/or swelling are common emergency department complaints. Ultrasound is a key component of the evaluation, as it is able to identify testicular torsion – the highest emergency scrotal condition – as well as many other alternative diagnoses including epididymitis, orchitis, spermatic corditis (also known as funiculitis), torsion of a testicular appendage, scrotal abscess, testicular neoplasms, intestinal herniae and, in the setting of trauma, hematoma or testicular fracture. Point-of-care ultrasound performed by the treating physician is likely to expedite diagnosis and management.

Technique and Anatomy

Testicular ultrasound is performed with the patient in the supine position. A rolled towel placed between the patient's legs helps to elevate the scrotum. A second towel placed across the thighs and beneath the scrotum further isolates the scrotum for ultrasound evaluation (Figure 16.1). A high-frequency (10 MHz) linear transducer should be used with a protective cover (an examination glove can serve) for hygiene. Testicular evaluation begins with B-mode visualisation of the testicle size and parenchyma in the long and short axes, being sure to scan entirely through each testicle.

Under normal conditions the scrotal wall typically measures 2–8 mm and the testicle approximately 4 × 3 × 2.5 cm. The testicle is homogeneously echogenic, with the exception of the hyperechoic mediastinum testis that can usually be seen in long-axis views (Figure 16.2a). The head of the epididymis is attached to the superior pole of the testis adjacent to the spermatic cord. The body and tail are usually less prominent unless inflamed (Figure 16.2b). The appendix testis is rarely seen unless outlined by a hydrocele. Moving the probe cephalad allows visualisation of the spermatic cord as it ascends to the inguinal canal.

After B-mode evaluation, testicular flow can be assessed with pulsed-wave Doppler using colour, power and spectral displays. Power Doppler is more sensitive in detecting low-flow states than colour Doppler, and may be helpful in identifying venous flow (the most sensitive test for torsion). When using colour or power Doppler, the sampling field can be placed simultaneously over both testicles or over each individually, using a split screen for comparison (Figure 16.3). Spectral Doppler can be targeted over any region of flow seen on colour or power Doppler to determine if it is arterial or venous (Figure 16.4). Arterial flow is identified by unidirectional flow with a peak systolic velocity (PSV) and minimum diastolic velocity (MDV) (Figure 16.4b). Arterial flow is characterised by the resistive index (RI) = (PSV – MDV)/PSV). In the healthy state, the RI of normal intra-testicular arteries

Emergency Point-of-Care Ultrasound, Second Edition. Edited by James A. Connolly, Anthony J. Dean, Beatrice Hoffmann and Robert D. Jarman.

Companion website: www.wiley.com/go/connolly/ultrasound

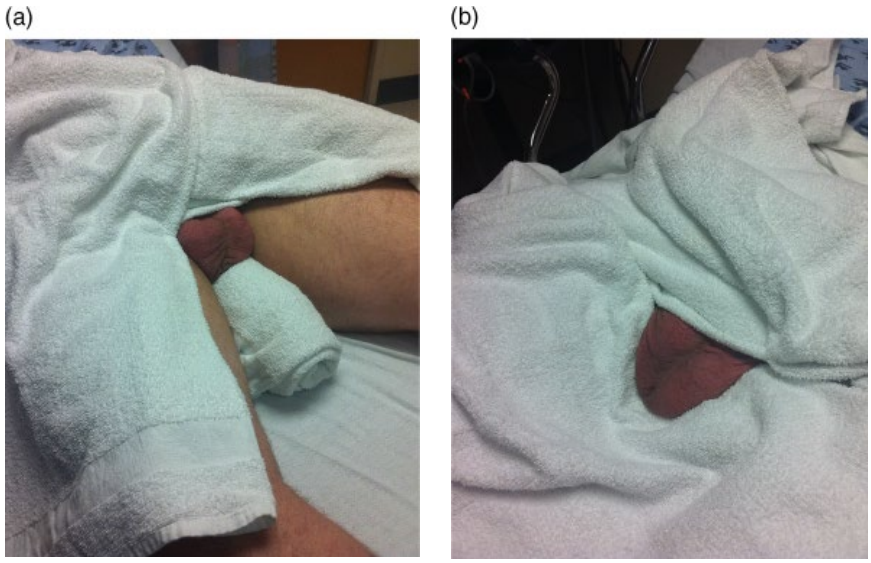

Figure 16.1 (a) A rolled towel placed between the thighs helps to elevate the scrotum. (b) An additional towel placed across the legs and beneath the scrotum further isolates the scrotum for ultrasound evaluation.

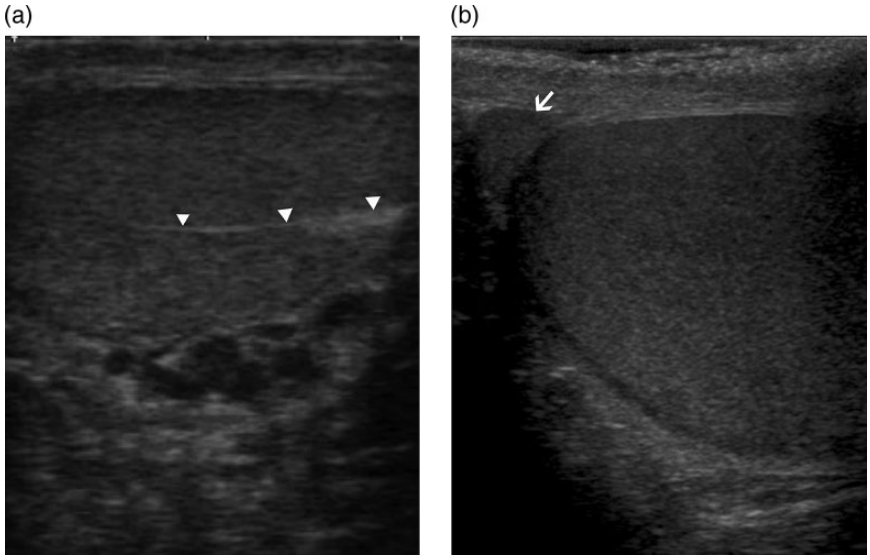

Figure 16.2 Normal testicles with homogeneous echotexture. (a) The mediastinum testis is seen as a hyperechoic stripe (triangles). (b) The epididymal head is seen adjacent to the superior pole of the testicle (arrow).

ranges from 0.48 to 0.75, but it rises with ischaemia. Venous flow is an unvarying low-velocity signal, often bidirectional due to non-laminar motion of the blood cells (Figure 16.4a).

When using Doppler the sonologist should be familiar with how to adjust gain, scale (pulse repetition frequency) and sampling gate size. Wall filters are rarely helpful and should be turned off. In addition, a good scanning technique requires an ergonomic set-up and hand-stabilisation to minimise motion artefact.

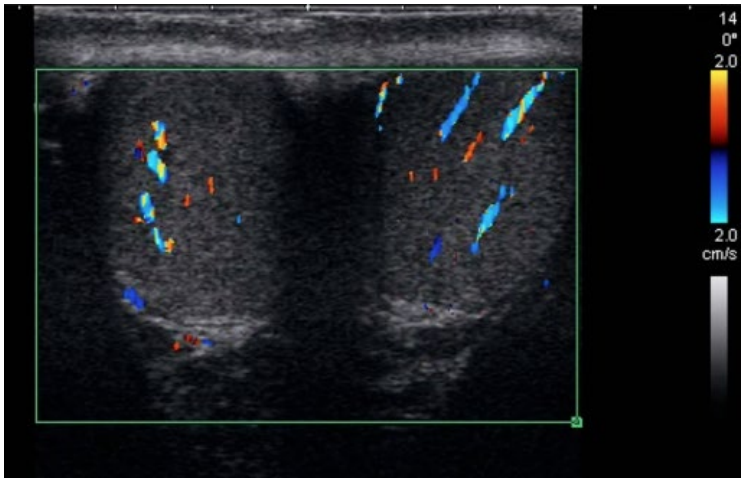

Figure 16.3 Simultaneous testicle visualisation ('buddy view') with colour Doppler allows comparison of echo texture, size and flow. Both testes in this case have a normal homogeneous echotexture and similar flow.

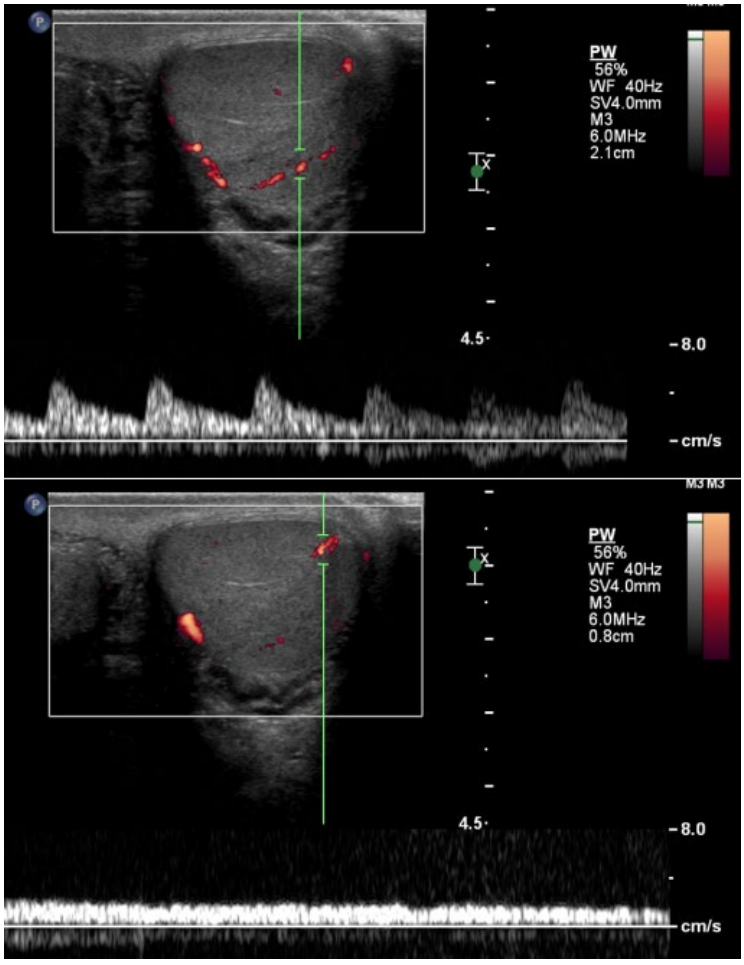

Figure 16.4 Arterial (upper image) and venous (lower image) spectral Doppler tracings. A loss of venous flow is often the first sign of torsion.

Testicular Torsion

The salvage rate of a torsed testicle begins to decrease as early as 3 hours after symptom onset, making rapid diagnosis mandatory. Bedside clinician-performed ultrasound improves the time to diagnosis, especially in settings where imaging specialists are not available at all times.

Ultrasonographic signs of testicular torsion can be divided into B-mode and Doppler findings (Table 16.1). The earliest B-mode finding is enlargement of the testicle due to vascular congestion (Figure 16.5a). As torsion progresses there is a loss of the normal homogeneous echotexture, with areas of oedema, haemorrhage and necrosis. With colour or power Doppler examination the flow will be decreased or absent in the affected testicle (Figure 16.5a). Loss of venous perfusion, which disappears before arterial flow, is the most sensitive sonographic finding, but identifying the flow in the testicular venules can be challenging in a normal testicle, even for experienced sonologists. Arterial evaluation may show an increase in the RI (above 0.75) due to decreased (or even reversed) diastolic flow. As torsion progresses, the arterial flow will become decreased (compared with the contralateral side) or undetectable (Figure 16.5b). With spontaneous or manual detorsion flow will initially become hyperaemic unless infarction has already occurred (Figure 16.6).

While, bedside ultrasound may rule in torsion, a lack of findings does not necessarily rule it out. First, the testicle is perfused by three distinct arteries – the spermatic, [vas] deferential and cremasteric – all of which anastomose in the tail of the epididymis. The cremasteric artery is outside the spermatic cord and is therefore unaffected by torsion. In addition, the other two arteries may not be completely occluded by a given degree of torsion. Second, in cases of detorsion, reactive hyperaemia and persistent ischaemic injury/infarction may 'cancel one another out' on Doppler flow analysis, resulting in apparently 'normal' flow. Finally, some patients detorse and present with a completely normal ultrasound evaluation. Such patients are clearly at high risk for retorsion, which might not result in such a benign outcome. Even in the hands of imaging specialists, ultrasound has only 86–97% sensitivity, so the bedside sonologist should be very cautious in ruling out this diagnosis. Bedside ultrasound may also be used to perform a repeat examination if a patient's pain worsens, or to provide objective evidence of perfusion after manual detorsion at the bedside.

Pitfalls

- Potential pitfalls include detorsion hyperaemia (as previously discussed) and the misidentification of capsular blood flow as testicular. In addition, motion artefact may give the impression of flow where there is none.

Other Causes of Testicular Complaints

Epididymitis is inflammation of the epididymis, and the most common cause of inflammation within the scrotum. Ultrasound reveals

Table 16.1 B-mode and Doppler findings of testicular torsion.

Time of finding	B-mode findings	Doppler findings
Early	Normal or enlarged	Decrease/loss of venous flow on spectral Doppler
Mid	Enlarged size with striated pattern of oedema.	As above, plus decrease in arterial flow causing elevated resistive index on spectral Doppler
Late	Loss of echotexture, haemorrhage, necrosis	As above, plus loss of arterial flow on power and spectral Doppler

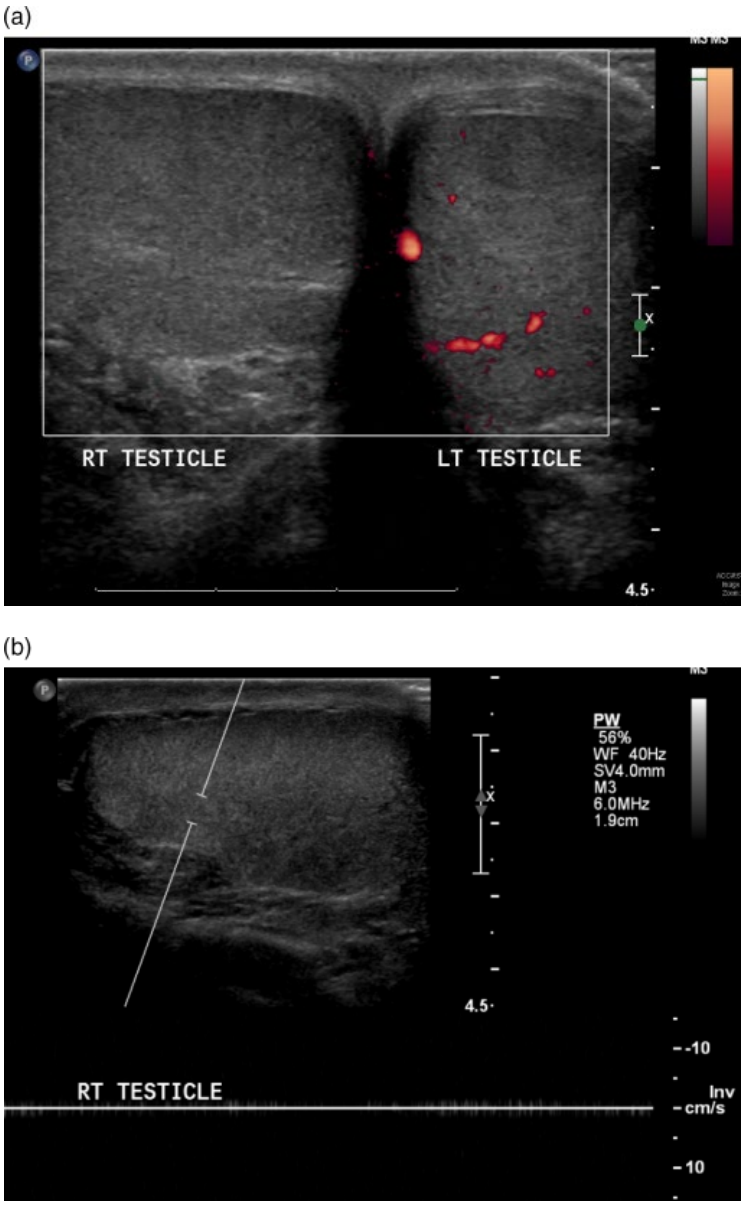

Figure 16.5 (a) Testicular torsion of the right testicle with loss of power Doppler signal and enlarged size. The echotexture appears preserved, suggesting that the torsion is early in presentation. (b) Spectral Doppler with no detectable arterial or venous flow in a case of testicular torsion.

enlargement and hyperaemia of the epididymal head, frequently with a concomitant hydrocoele (Figure 16.7). Contralateral comparison is helpful unless the symptoms are bilateral. The entire epididymis should be evaluated, since in some cases inflammation may be focal. Inflammation results in an increased vascular flow to the testicle, in contrast to the decreased flow seen in torsion. When *orchitis* is present, increased blood flow, swelling and loss of echo texture may be seen in the testicle (Figure 16.7). With prolonged severe orchitis, oedema within the

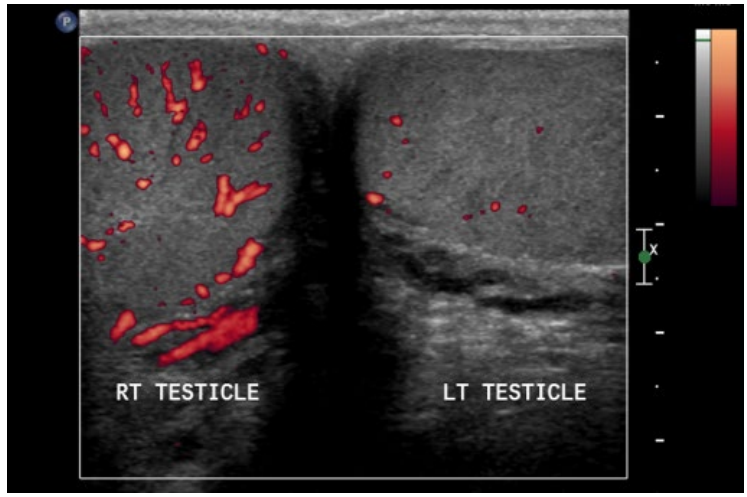

Figure 16.6 The same case as seen in Figure 16.5 with testicular hyperaemia in the previously torsed right testicle after manual detorsion at the bedside.

(a)

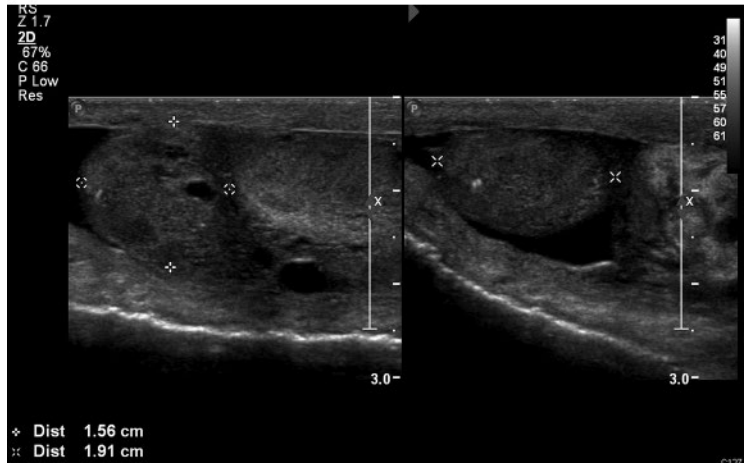

(b)

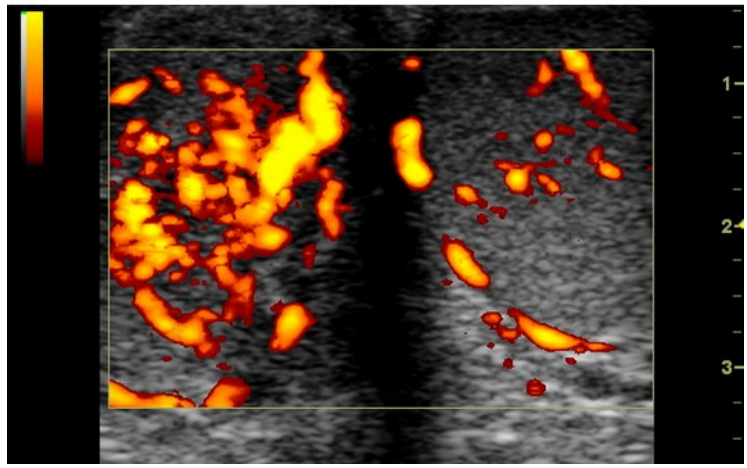

Figure 16.7 (a) Epididymitis with enlargement of the epididymal head (measured by callipers; left and right). (b) Orchitis demonstrating testicular oedema and increased flow to the testicle on power Doppler.

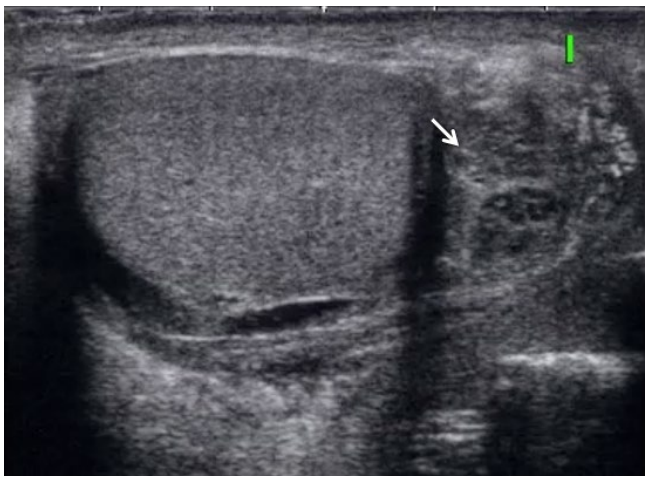

Figure 16.8 Corditis. Isolated swelling and inflammation of the spermatic cord (arrow) are visible.

minimally distensible tunica may lead to ischaemia and infarction. In addition, the spermatic cord can also become inflamed (termed *corditis* or *funiculitis*), either in combination with epididymitis or in isolation, and may be the source of the patient's testicular complaint (Figure 16.8).

The *appendix testis* lies adjacent to the epididymal head and is difficult to visualise in the normal state. With torsion – most commonly in prepubertal boys – it becomes enlarged and therefore is more easily visualised. There is a loss of blood flow in the appendage with hydrocoele and, occasionally, adjacent epididymal inflammation.

Herniation of bowel into the scrotum may be visualised on ultrasound (Figure 16.9). On ultrasound, if the bowel is not strangulated, it will continue to demonstrate peristalsis. Dynamic changes of the herniated bowel may also be seen if the patient is asked to Valsalva.

Traumatic injury to the testicle may result in testicular fracture or intracapsular haematoma (Figure 16.10). The latter condition may result in loss of the testis due to arterial disruption, compounded by a cycle of oedema, ischaemia and infarction similar to that seen in severe orchitis. Both conditions result in a disorganised heterogeneously echogenic appearance. Haemorrhage progresses from initially hyperechoic whorls to anechoic (after fibrinolysis).

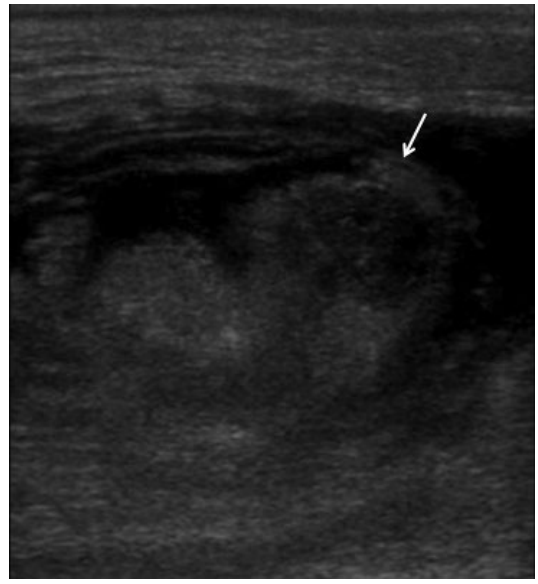

Figure 16.9 Herniation of a loop of bowel (arrow) into the inguinal canal.

Epididymal cysts are a frequent incidental finding and occur in approximately 30% of older males. They rarely require further management unless they are symptomatic. The clinical context usually leads to the distinction among hydrocoele, pyocoele and haematocoele, although only the hydrocoele is completely anechoic. Varicocoele and spermatocoele are beyond the scope of this chapter, but are not difficult to identify.

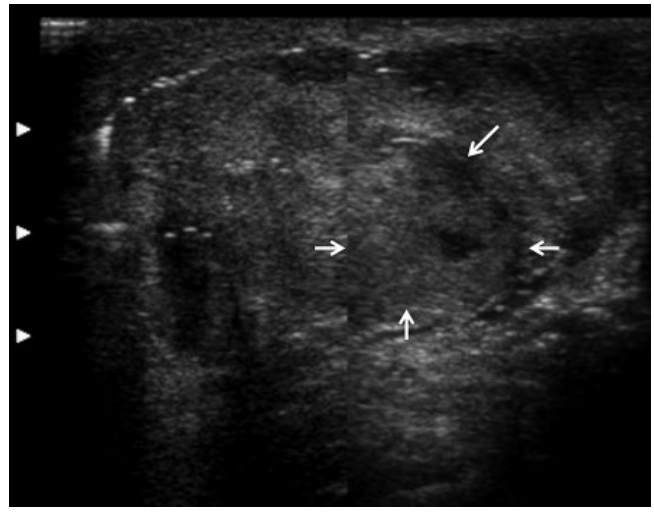

Figure 16.10 Shattered testicle as a result of blunt trauma. There is disruption of the capsule with an area of haemorrhage (arrows).

(a)

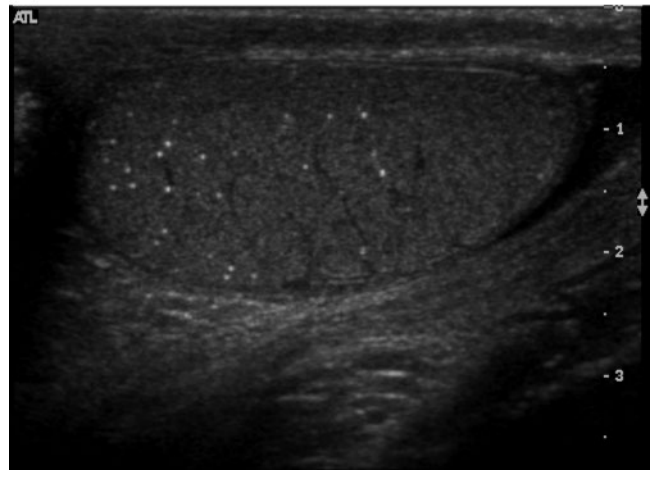

(b)

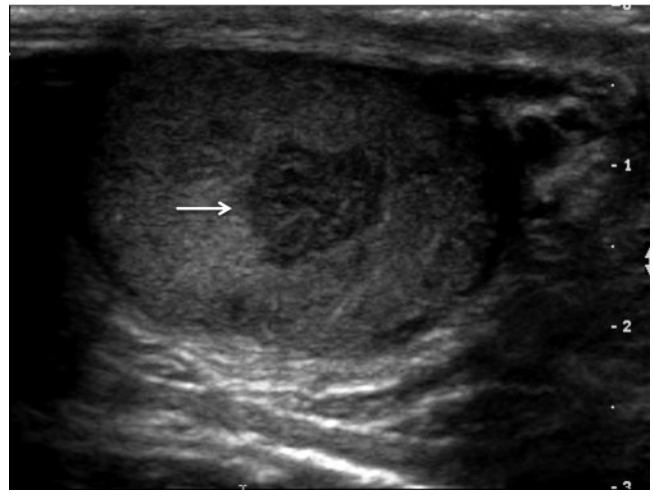

Figure 16.11 (a) A testicle with stromal irregularities and calcifications which may be signs of neoplasm. (b) A testicle with stromal irregularities and a central irregular hypoechoic region indicative of a seminoma (arrow).

Occasionally, an ultrasound examination of a testicle will reveal enlargement, stromal irregularities or *microlithiasis*. These findings suggest neoplasm, so that patients should be referred for further evaluation by a urologist and imaging specialist. Five or more microcalcifications per ultrasound field are considered abnormal, and patients are typically followed with annual ultrasound examinations. Masses may vary in size and appear cystic or solid. The testicular stroma will often appear non-homogeneous with focal areas of swelling and haemorrhage (Figure 16.11).

Summary

Bedside ultrasound is a valuable component in the work-up of testicular complaints. It is easily performed at the bedside and has the ability to diagnose and confirm multiple aetiologies of testicular pain. While ultrasound has the ability to speed diagnosis, the emergency physician should be cautious of ruling out the presence of pathology, especially torsion.

Further Reading

al Mufti, R.A., Ogedegbe, A.K., Lafferty, K. (1995) The use of Doppler ultrasound in the clinical management of acute testicular pain. *Br. J. Urol.*, **76** (5), 625–627.

Barada, J., Weingarten, J., Cromie, W. (1989) Testicular salvage and age-related delay in the presentation of testicular torsion. *J. Urol.*, **142** (3), 746–748.

Blaivas, M., Brannam, L. (2004) Testicular ultrasound. *Emerg. Med. Clin. North Am.*, **22** (3), 723–748, ix.

Bomann, J.S., Moore, C. (2009) Bedside ultrasound of a painful testicle: before and after manual detorsion by an emergency physician. *Acad. Emerg. Med.*, **16** (4), 366.

Middleton, W., Thorne, D., Melson, G. (1989) Color Doppler ultrasound of the normal testis. *Am. J. Roentgenol.*, **152** (2), 293.

Extremities

17

The Lower Limb and the Upper Limb

David Lewis and John Gullett

The Lower Limb

Ultrasound of the lower limb includes the groin, hip joint, thigh, knee, calf, foot and ankle. There are many potential clinical applications in the acute setting, including (but not exclusively) acute sportsman's groin, occult hip fracture, quadriceps or hamstring tears, knee ligament injuries, calf pain, tendon injuries, ankle ligament injuries, joint effusions and swollen leg.

Assessments of lower-limb fractures and the limping child are described in detail in Chapters 28 and 22, respectively.

The majority of lower-limb structures can be visualised with a high-frequency linear transducer. Occasionally, the use of a curvilinear transducer may be required for deeper structures or in obese patients.

The Groin

Emergency physicians will be familiar with the ultrasound appearance of the femoral triangle, bounded by the inguinal ligament superiorly, sartorius laterally and adductor longus medially. However, their focus is usually on the femoral vein rather than the muscles and tendons.

Although not within the scope of this chapter, ultrasound is frequently used to assess chronic sportsman's groin, including occult inguinal hernia and adductor tendinopathy. In the acute setting, however, the focus is more on muscle tears, avulsion fractures and apophyseal injuries in the adolescent.

Technique

Clinical examination directs ultrasound examination to the point of maximal tenderness. Pain on resisted movements is used to identify the likely site of injury. The procedure involves:

- Placing the transducer over the area of tenderness.
- Identifying the muscle groups and seeking overt muscle injury or haematoma.
- Orientating the transducer first transversely and then longitudinally to the muscle and following proximally to its insertion.

Pathology

The adductors are commonly injured during running sports. Ultrasound can be used to identify the site of injury and to grade the injury (as described earlier). In adolescents, particular attention should be paid to the insertion of the rectus femoris at the anterior inferior iliac spine (AIIS), a common site of acute avulsion and apophyseal injury (Figure 17.1). Ultrasound will demonstrate avulsion fragments, epiphyseal separation and haematoma.

Emergency Point-of-Care Ultrasound, Second Edition. Edited by James A. Connolly, Anthony J. Dean, Beatrice Hoffmann and Robert D. Jarman.

Companion website: www.wiley.com/go/connolly/ultrasound

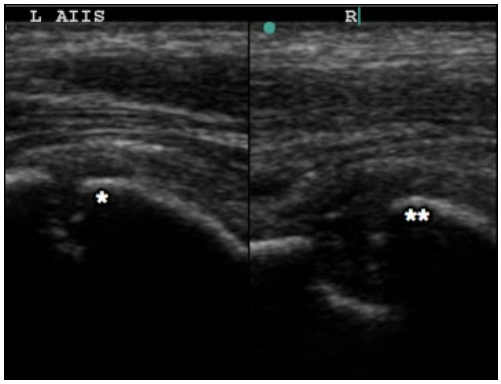

Figure 17.1 Normal rectus femoris insertion (*). Avulsion of the right anterior inferior iliac spine (**).

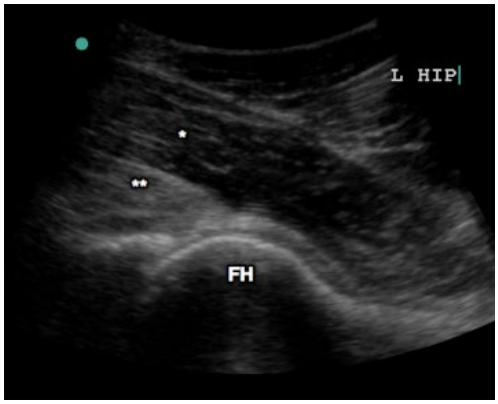

Figure 17.2 Adult hip, showing ilio-psoas muscle (*) and ilio-psoas tendon (**). FH, Femoral head.

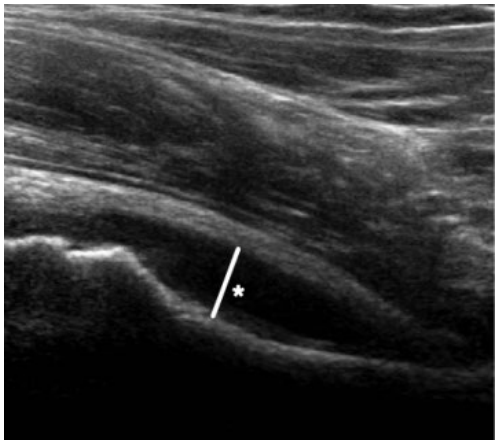

Figure 17.3 Image of hip effusion (*).

The Hip Joint

The main indications for hip ultrasound are occult hip fracture, hip effusion and psoas tendon injury.

Technique

- The patient lies supine on the couch.
- Place the transducer transversely over the proximal femur.
- Move the transducer cranially until the femoral neck comes into view.
- Rotate the transducer along the axis of the femoral neck and move medially to visualise the anterior joint capsule, femoral head and acetabulum.
- Identify the ilio-psoas tendon (Figure 17.2).

Pathology

A hip effusion can be seen displacing the capsule away from the femoral neck. Upward convexity of the femoral neck suggests an effusion. Measure the maximum distance between the femoral neck and the capsule. Compare with the contralateral hip. Asymmetry or an absolute value of >5–10 mm is abnormal and suggests that an effusion is present (Figure 17.3).

Undisplaced impacted fractures of the neck of femur can be difficult to visualise on plain radiographs. Where there is a suspicion of femoral neck fracture, despite a normal/inconclusive radiograph, ultrasound can be useful. In this context the presence of an effusion (haemarthrosis) is highly suggestive of an occult femoral neck fracture.

Pitfalls

- Ultrasound cannot distinguish the cause of the effusion.
- The absence of a hip effusion does not exclude septic arthritis.

The Thigh

The thigh can be divided into the posterior (hamstring), anterior (quadriceps) and medial (adductor) compartments. Muscle injuries in the thigh are either due to overstretching/contracting or direct contusion ('dead-leg').

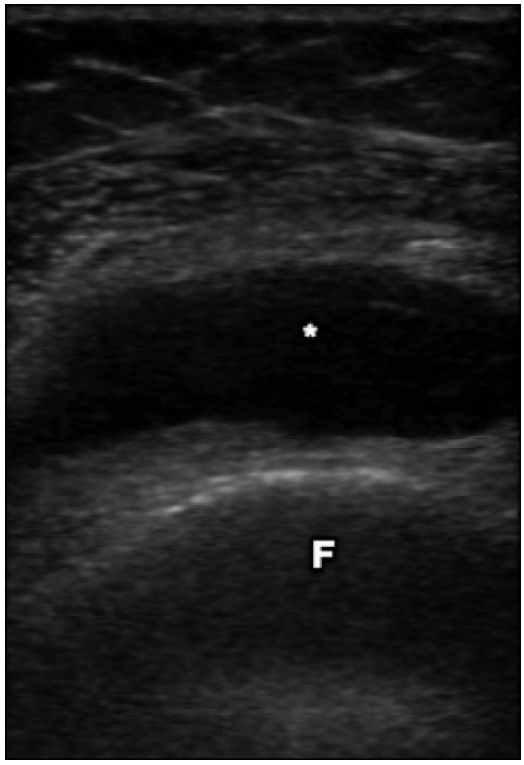

Figure 17.4 Transverse image of thigh showing quadriceps haematoma (*). F, Femur.

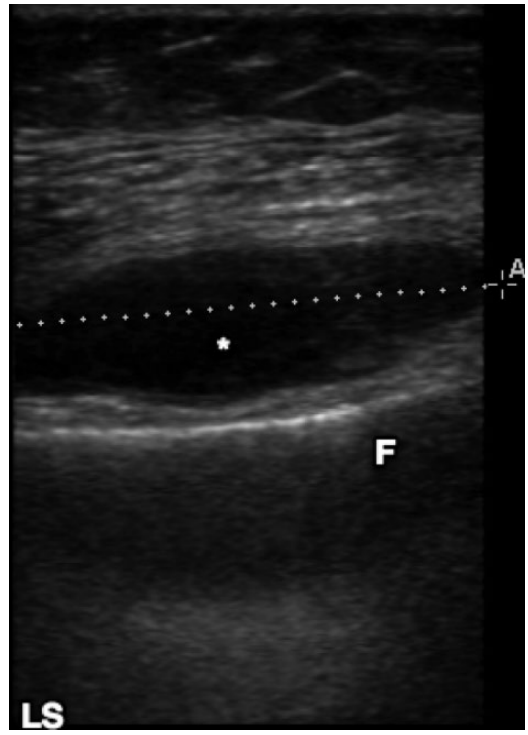

Figure 17.5 Longitudinal image of thigh showing the quadriceps haematoma (*). F, Femur.

Technique

- Ultrasound assessment is guided by clinical examination.
- Muscle groups are identified and assessed in both transverse and longitudinal orientation and followed to both proximal and distal insertions.

Acute Pathology

- Hamstring tears.
- Rectus femoris tears.
- Quadriceps contusion, intramuscular haematoma (Figures 17.4 and 17.5).

Pearls and Pitfalls

- Comparative views of the contralateral muscle compartment can be helpful.
- A 'quick-scan', moving the transducer in transverse proximally and distally through the muscle group, will often allow pathology to be seen more easily.
- Early assessment (<12 h) may fail to demonstrate small tears.
- Too much transducer pressure may obscure small haematomas.

The Knee

In patients who present with non-traumatic knee swelling, ultrasound can be used to differentiate bursitis from joint effusion. It can be used to guide joint aspiration. Ultrasound can also help to differentiate the causes of posterior knee swelling.

Following trauma, ultrasound can be used to examine the collateral ligaments and assess for haemarthrosis. *Patellar tendinosis* is a chronic condition causing anterior knee pain, and can be easily diagnosed with ultrasound.

Technique

- The patient lies supine on the couch with the knee flexed to 30° and supported by a rolled towel.

- The history and clinical examination direct a focussed ultrasound assessment.
- The patellar tendon is assessed in transverse and longitudinal planes (Figure 17.6a,b).
- Look for tendon integrity, thickening (>5 mm) and hypoechogenicity. Assess for prepatellar and infrapatellar bursitis, which do not communicate with the knee joint, and for suprapatellar bursitis, which does communicate with the knee joint in 85% of adults.
- Assess the medial and lateral collateral ligaments longitudinally, both at rest and under varus/valgus strain (Figure 17.7).
- Look for haemarthrosis and/or joint space opening suggestive of ligament rupture.
- The posterior knee (popliteal fossa) is best assessed with the patient prone and the knee extended. Look for the presence of a semimembranosus-gastrocnemius bursitis (Baker's cyst), which can be seen originating between

(a)

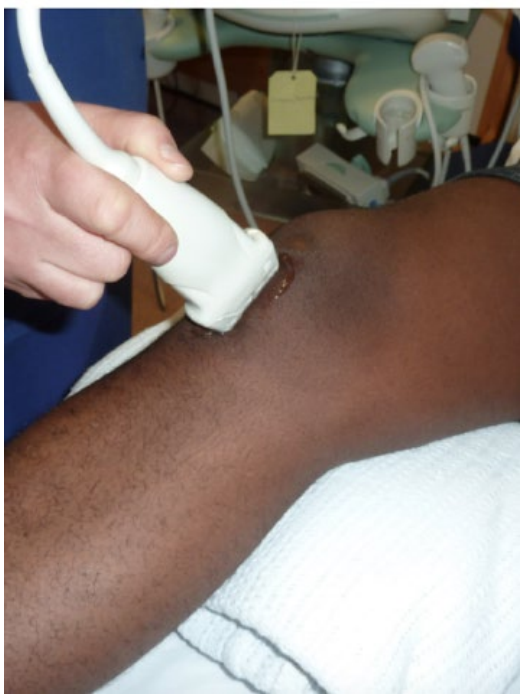

(b)

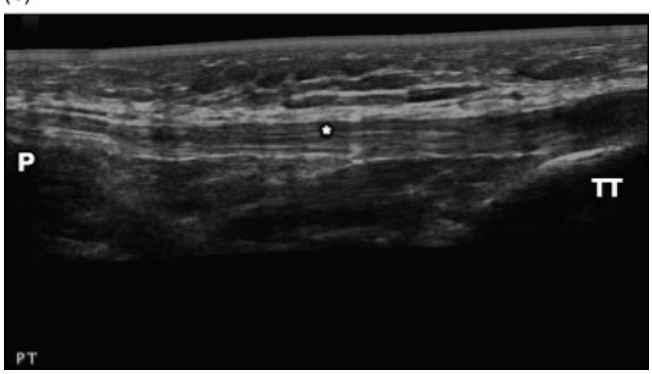

Figure 17.6 (a) Probe placement over patella tendon for longitudinal view. (b) Longitudinal landscape view of the anterior knee showing course of the patellar tendon (*). P, Patella; TT, Tibial tuberosity.

these two muscles behind the medial femoral condyle. A ruptured Baker's cyst is diagnosed by calf swelling, pain, redness and the presence of fluid in the subcutaneous tissues.

Pathology

- Patellar tendinopathy.
- Bursitis.
- Collateral ligament injury.
- Haemarthrosis.
- Baker's cyst (Figure 17.8).

The Achilles Tendon

The Achilles tendon is formed by the fusion of soleus and gastrocnemius. It has a flat anterior margin and a convex posterior margin. A normal tendon will have an anteroposterior diameter of 5–6 mm. A number of bursae are closely related. The retroachilles bursa lies between the skin and the distal insertion of the tendon, while the retrocalcaneal bursa lies deep to the tendon just above its insertion into the calcaneum.

The majority of Achilles tendon ruptures occur 5–6 cm above the insertion, having been weakened by chronic tendinopathy. High-force tears can occur in healthy tendons at the musculotendinous junction. Avulsion tears at the insertion are usually related to steroids, renal disease or quinolone use.

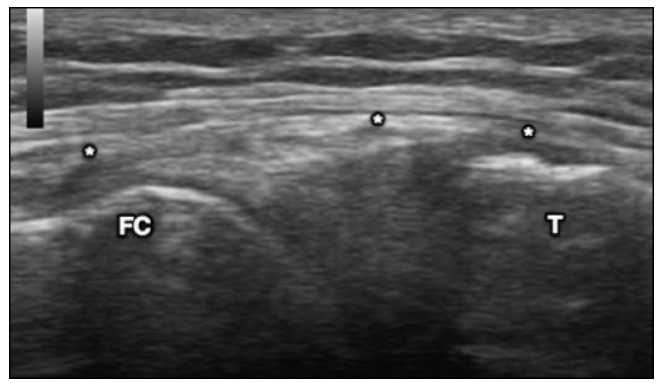

Figure 17.7 Medial knee showing the medial collateral ligament (*). FC, Femoral condyle; T, Tibia.

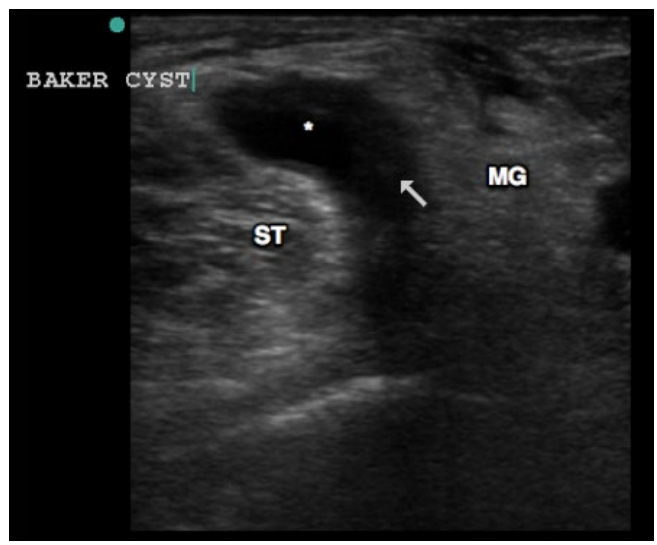

Figure 17.8 View of the posterior knee showing a Baker's cyst (*). ST, Semimembranosus tendon; MG, Medial head of the gastrocnemius.

Technique

- The patient is positioned prone, with their feet hanging over the end of the stretcher (Figure 17.9a).
- Assess the Achilles tendon in transverse and longitudinal planes (Figure 17.9b). The normal tendon will appear ribbon-like with a typical hyperechoic fibrillar pattern.
- Look for tendon integrity, fusiform thickening (>6 mm) and hypoechogenicity.
- Assess the bursae for the presence of fluid.
- Dynamic examination can be used to assess for the separation of tendon ends during passive ankle dorsiflexion.

Pathology

Achilles tendon rupture (Figure 17.10).

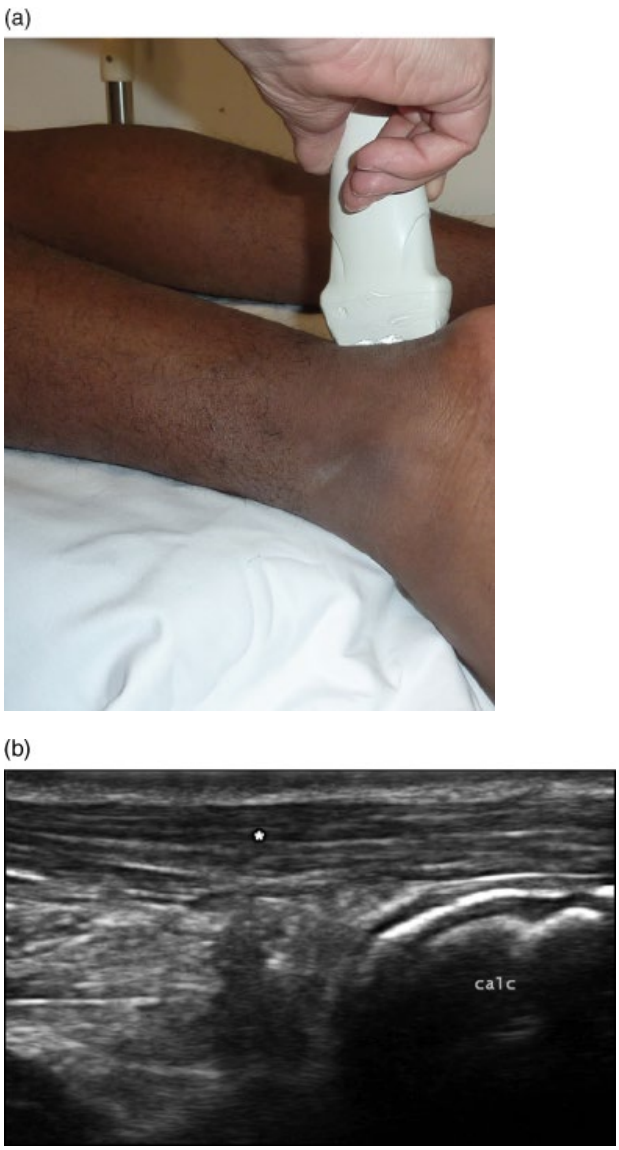

Figure 17.9 (a) Probe placement over the posterior ankle for a longitudinal view of the Achilles tendon. (b) Longitudinal view of the posterior ankle showing the Achilles tendon (*). calc, Calcaneus.

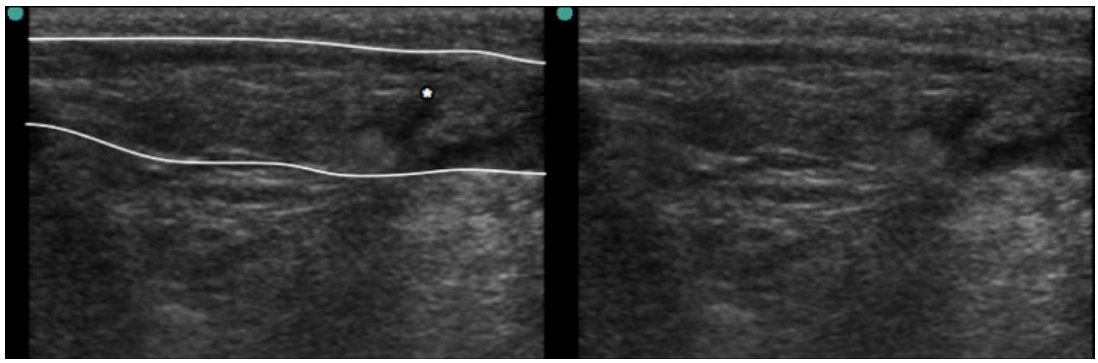

Figure 17.10 Ruptured Achilles tendon in longitudinal view. Left image shows the outline of the tendon (white line) and the site of rupture (*).

The Ankle

The main indications for ankle ultrasound in the acute setting include the assessment of ligaments in severe ankle sprains and diagnosis of joint effusions. Typically, 85% of severe ankle sprains involve the lateral ligaments, namely the anterior talofibular ligament (ATFL), the posterior talofibular ligament (PTFL) and the calcaneofibular ligament (CFL).

Technique

Anterior talofibular ligament (ATFL):

- The patient is placed supine with the knee flexed and the foot flat on the stretcher. The ankle is in slight inversion (Figure 17.11a).
- Place the transducer over the distal fibular and orientate it transversely. The ligament is visualised spanning between the lateral malleolus and the talus (Figure 17.11b). Assess its appearance and look for fluid or blood.
- Apply anterior drawer stress and observe for any separation of the talus from the lateral malleolus.

Calcaneofibular ligament (CFL) and posterior talofibular ligament PTFL:

- The patient is placed supine with the knee flexed and the ankle dorsiflexed.
- Orientate the transducer longitudinally for CFL and transversely for PTFL.

Ankle joint:

- The ankle joint is best visualised anteriorly.
- Place the transducer over the distal tibia in the longitudinal plane. Move the transducer distally and observe the anterior recess between the tibia and talar dome. A small amount of synovial fluid can be seen here in the normal ankle joint. More than 3 mm or any asymmetry with the contralateral ankle is considered to be an effusion (see Figures 17.2 and 17.3 for examples of joint effusions).

Pathology

- ATFL rupture (Figure 17.12).
- Ankle effusion.

The Calf

Patients frequently present with acute calf pain and swelling. Point-of-care ultrasound allows not only proximal deep-vein thrombosis (DVT) to be excluded (see Chapter 18) but also an alternative diagnosis to be made.

The differential diagnosis of painful/swollen calf also includes superficial thrombophlebitis, ruptured Baker's cyst, cellulitis, subcutaneous haematoma, intramuscular haematoma, calf muscle tear, Achilles tendinopathy and ruptured tendo-Achilles.

(a)

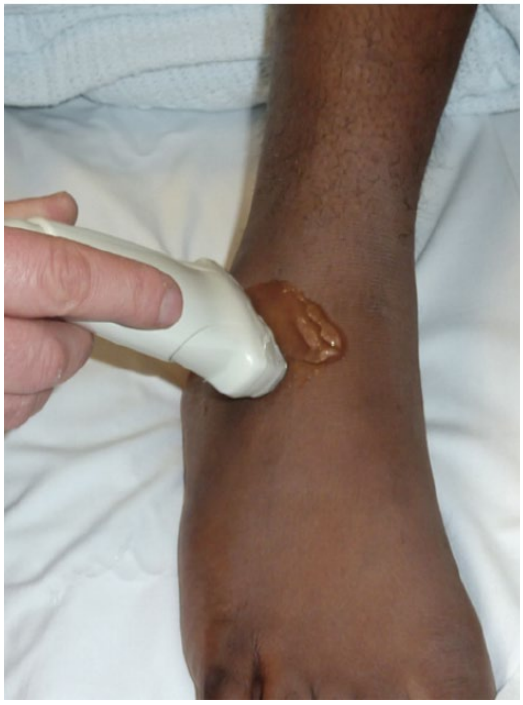

(b)

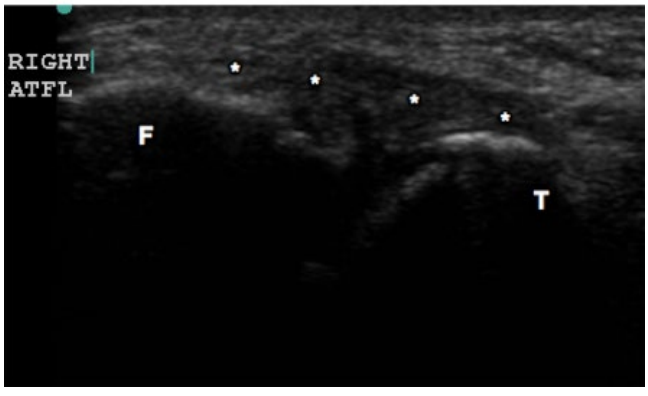

Figure 17.11 (a) Probe placement for visualisation of the anterior talofibular ligament (ATLF). (b) Anterior talofibular ligament (*). F, Fibula; T, Talus.

Technique

Although the history and examination will direct the assessment, a thorough 'swollen leg' protocol is recommended:

- DVT scan (see Chapter 18).
- Knee joint for effusion.
- Posterior knee for Baker's cyst (see Figure 17.8).
- Calf skin and subcutaneous tissues for cellulitis (Figure 17.13), abscess and haematoma.
- Calf muscles for haematoma, tear or oedema.
- Achilles tendon.

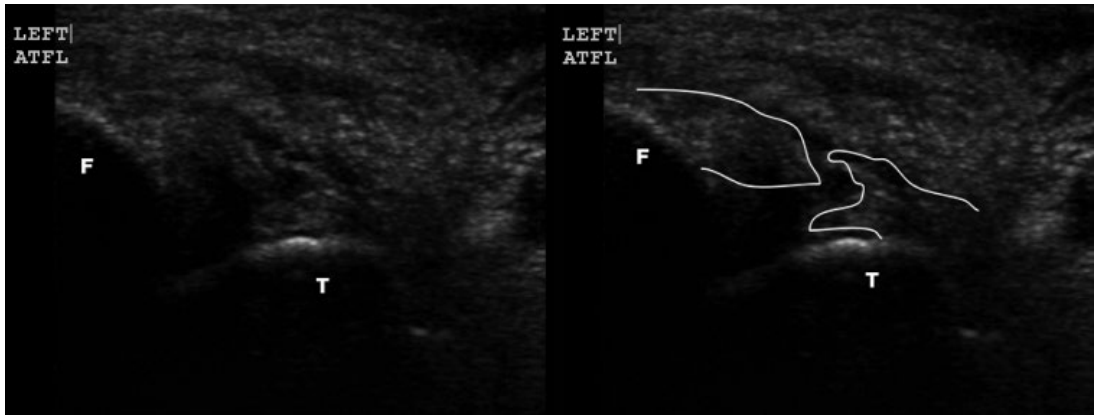

Figure 17.12 Ruptured anterior talofibular ligament (ATFL), Right image with outlined ruptured ATFL. F, Fibula; T, Talus.

Figure 17.13 Typical 'cobblestone' oedema appearance of cellulitis over the lower extremity.

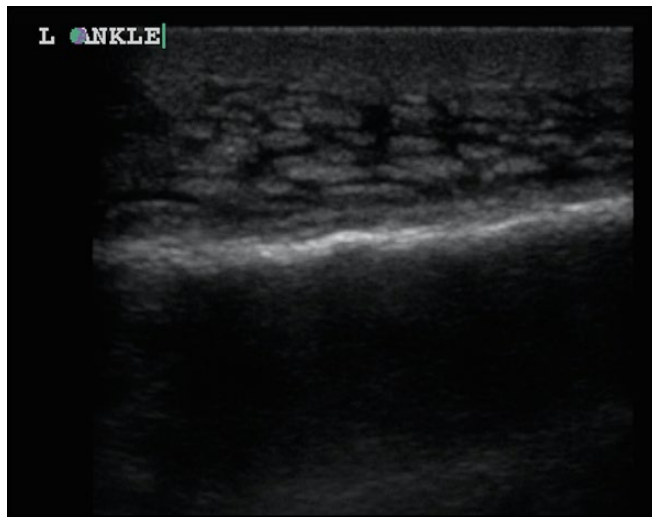

The Upper Limb

Point-of-care ultrasound is commonly used to assist in the clinical assessment of acute upper-limb conditions. These include non-traumatic shoulder pain, shoulder injury, biceps rupture, elbow joint effusion, forearm fracture, metacarpal fracture, tendon injuries, foreign bodies and palmar abscess assessment. Ultrasound use in fracture and foreign body management is described in detail in Chapter 28 and Chapter 30, respectively.

Shoulder

Ultrasound of the shoulder joint can be technically challenging and requires a good deal of experience for its correct interpretation. As with all point-of-care ultrasound investigations, it should be used to answer focussed questions based on the findings of the history and examination. The large number of eponymous examination tests associated with the shoulder joint is a clear indication of their low diagnostic value. Ultrasound can be very useful in distinguishing a rotator cuff tear or subacromial bursitis from tendinopathy.

Technique

- The patient is seated slightly to the side of a chair or stool, providing for maximal shoulder range of motion.
- Place the machine on the same side of the patient as the shoulder to be examined. In this way, both the sonographer and the patient can see the screen. Demonstrating the normal anatomy and any abnormalities can be helpful and will improve the patient experience.
- The sonographer stands behind the patient providing support for the hand on the patient during the examination (Figures 17.14 and 17.15).

For *patient position #1* (Probe position; Figure 17.16): with the shoulder adducted, the upper arm against the side, the elbow flexed and the wrist fully supinated, place the transducer transversely over the bicipital groove. Identify the long head of the biceps tendon within the groove (Figure 17.17).

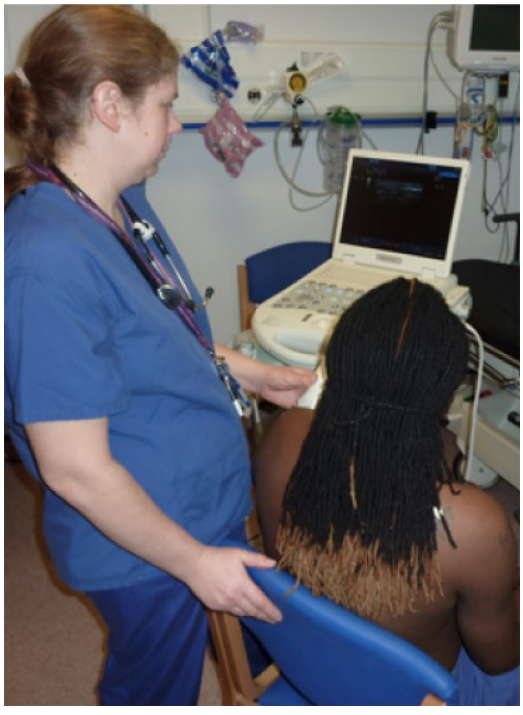

Figure 17.14 Ultrasound of the shoulder. Preparing the patient's position.

- Normal tendon thickness is between 5 mm and 10 mm. Move the transducer down along the biceps tendon to the overlying insertion of the pectoralis major. An absence of the bicipital tendon within the groove suggests tendon rupture.
- Rotate the transducer and examine the biceps tendon in a longitudinal plane. Heel/toe transducer angulation will compensate for anisotropy (Figure 17.18).

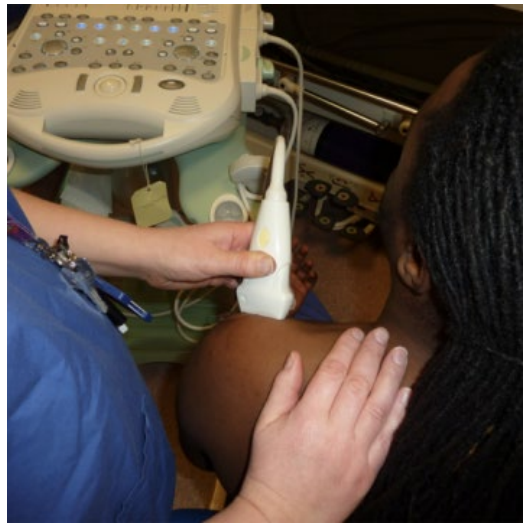

Figure 17.15 Ultrasound of the shoulder. Supporting the patient's shoulder.

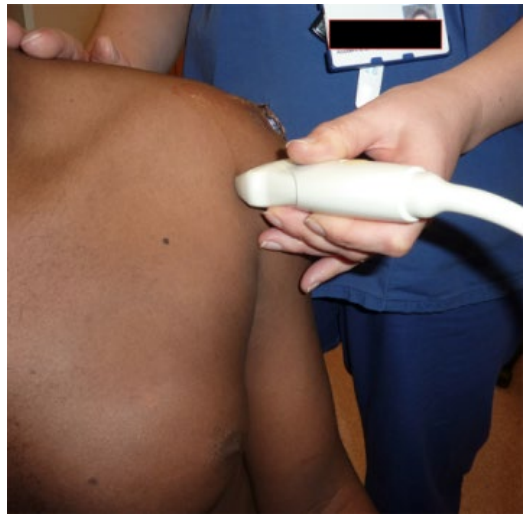

Figure 17.16 Ultrasound of the shoulder. Patient position #1 during the ultrasound examination.

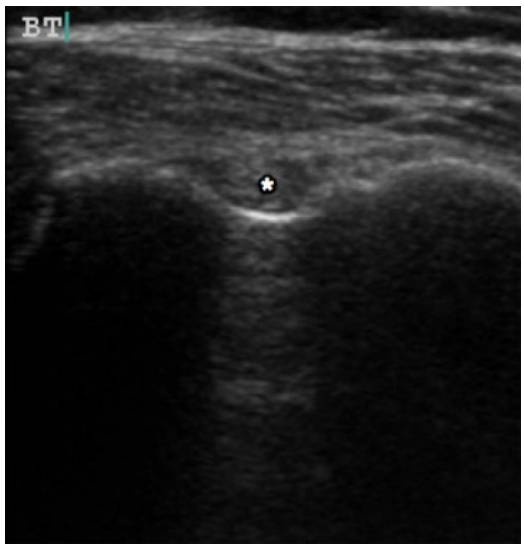

Figure 17.17 Image of the bicipital groove, showing the biceps tendon (*) in transverse view.

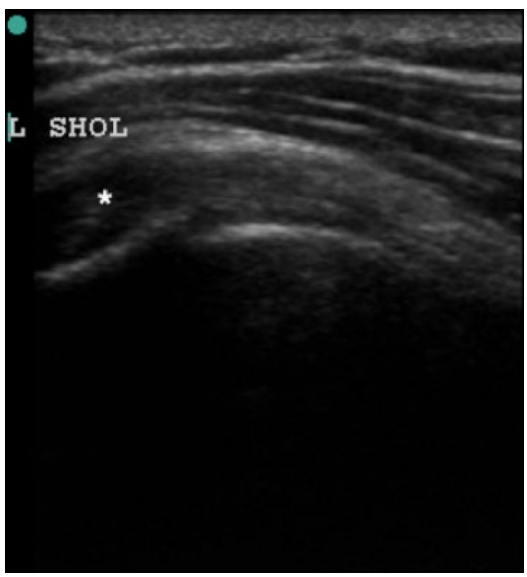

Figure 17.18 Biceps tendon in longitudinal view of the left shoulder showing anisotropy (*).

- Note the presence of any fluid around the tendon. A small quantity of fluid is often seen within the biceps tendon sheath in the lower part of the bicipital groove. Larger quantities can suggest either bicipital tendon pathology or may reflect pathology within the shoulder joint.

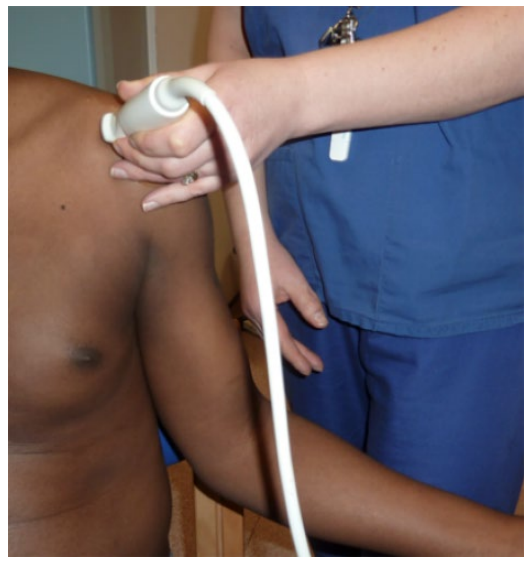

Figure 17.19 Ultrasound of the shoulder. Patient and probe position #2 during the ultrasound examination.

For *patient position #2* (Probe position; Figure 17.19): with the shoulder adducted and externally rotated and the upper arm against side with the elbow flexed and the wrist fully supinated. Place the transducer transversely over the bicipital groove. Observe the subscapularis tendon as it comes into view from underneath the coracoid, moving from medial to lateral on the screen as the shoulder externally rotates (Figure 17.20).

- Rotating the transducer by 90° allows the subscapularis to be examined in cross-section, enabling the multipennate nature of the tendon to be visualised.
- Return the patient to position #1 and move the transducer to just above the bicipital groove to see the rotator cuff interval, the space between the subscapularis and supraspinatus, occupied by the long head of biceps tendon (Figure 17.21).
- The anterior free edge of the supraspinatus lies alongside the intra-articular portion of the biceps tendon and is a common location for visualising tears (Figure 17.22).

For *patient position #3* (Probe position; Figure 17.23): with the shoulder adducted and internally rotated and the hand in the ipsilateral back pocket, palm posteriorly, place the

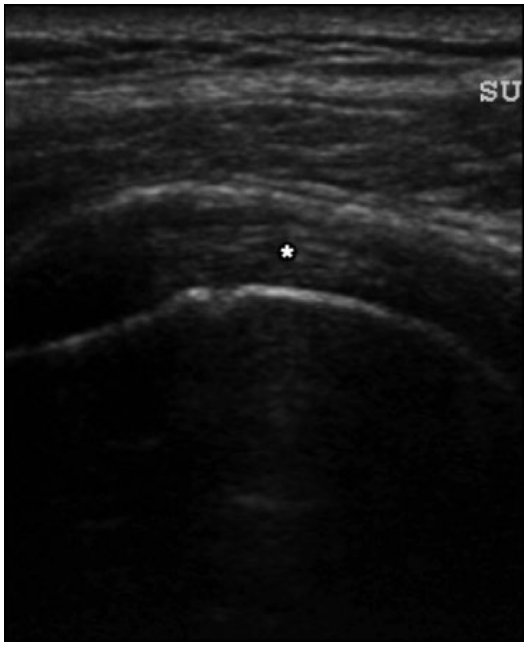

Figure 17.20 View of the subscapularis (*) in longitudinal view.

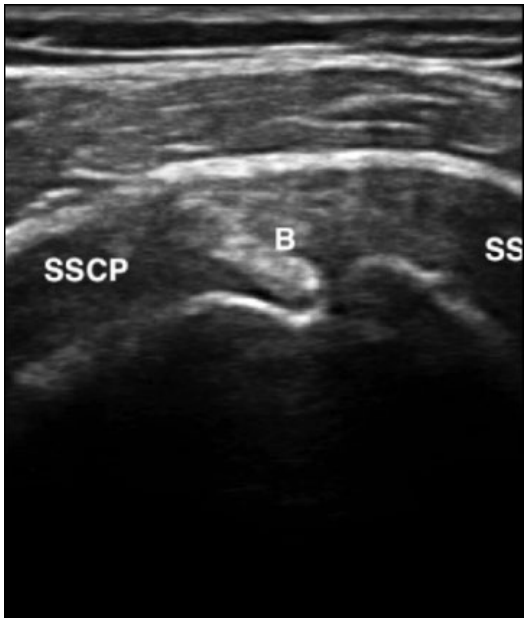

Figure 17.21 Image of the rotator cuff interval, showing the space between the subscapularis (SSCP) and supraspinatus (SS), occupied by the long head of biceps tendon (B).

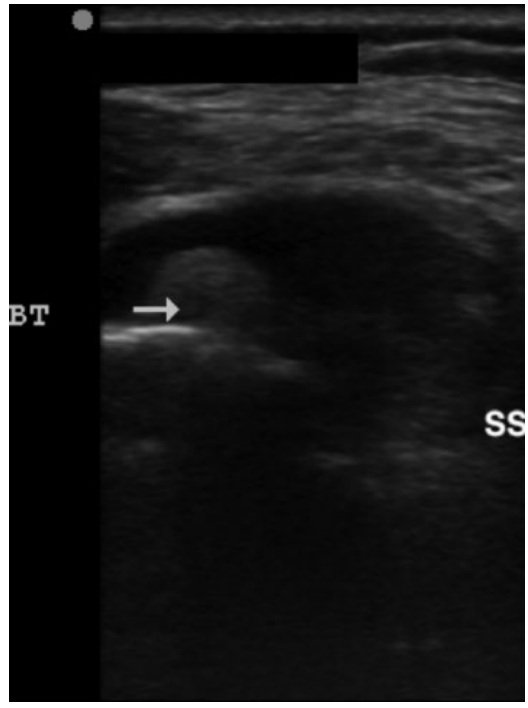

Figure 17.22 Image of the biceps tendon (BT, arrow) and the tear-free edge of suprasinatus (SS).

transducer in a coronal plane over the supraspinatus. Visualise the acromion.

- Follow the supraspinatus down to its insertion at the greater tuberosity, observing the 'bird's beak' appearance (Figure 17.24).
- The subacromial bursa lies between the deltoid and supraspinatus. Examine for the presence of fluid or oedema (Figure 17.25).
- Assess the convexity of the supraspinatus. Loss of convexity suggests a full-thickness supraspinatus tear. Assess the appearance of the supraspinatus tendon. Look for full-thickness tears (Figure 17.26).
- Thickening and hypoechogenicity suggest tendinopathy (Figure 17.27).
- Hyperechoic specks or acoustic shadows suggest calcific tendonitis (Figure 17.28).
- Move the transducer posteriorly to assess the infraspinatus. Rotate the transducer by 90° to assess these tendons in cross-section. Evaluate any areas of pathology carefully in two planes.

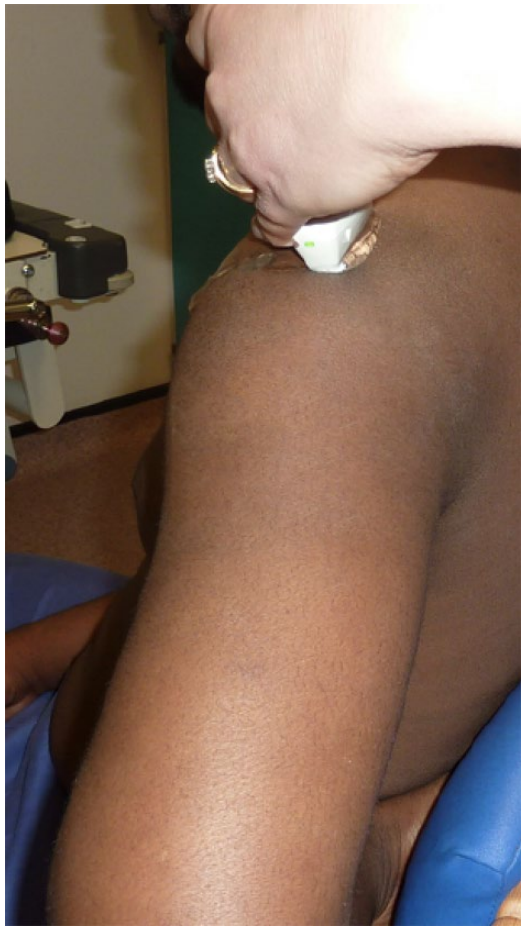

Figure 17.23 Patient position #3 during the ultrasound examination of the shoulder.

For *patient position #4* (Probe position; Figure 17.29): dynamic examination of subacromial impingement.

- Hold the transducer in a coronal plane over the supraspinatus. Visualise the acromion. The sonologist slowly and passively abducts the shoulder by elevating the elbow with the non-scanning hand. Observe the supraspinatus pass beneath the acromion. Correlate the onset of pain with position of the supraspinatus or greater tuberosity in relation to the acromion. Observe for bulging of the subacromial bursa as the shoulder abducts.

For *patient position #5*: with the shoulder adducted and the hand on the knee and the

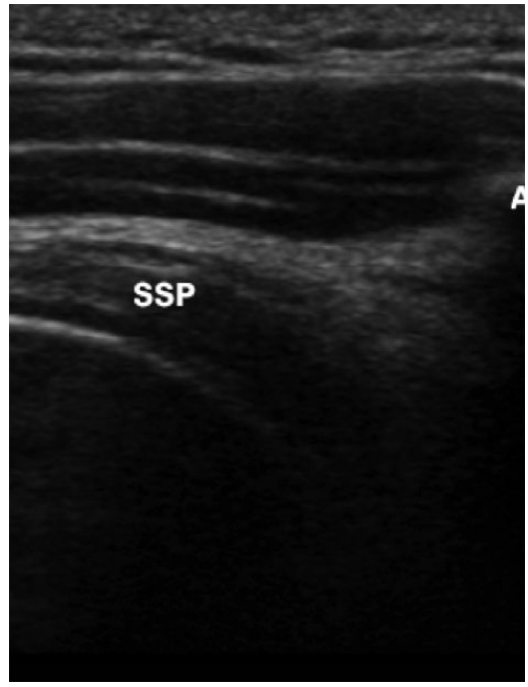

Figure 17.24 Supraspinatus tendon (SSP); (A) Acromion.

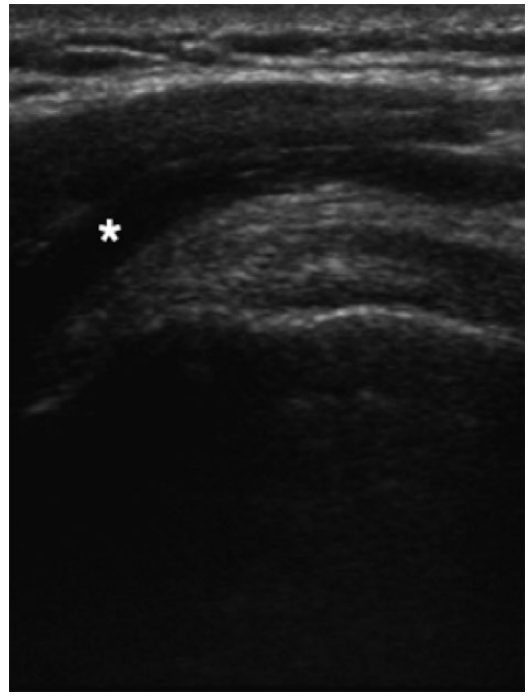

Figure 17.25 Subacromial bursitis with fluid (*).

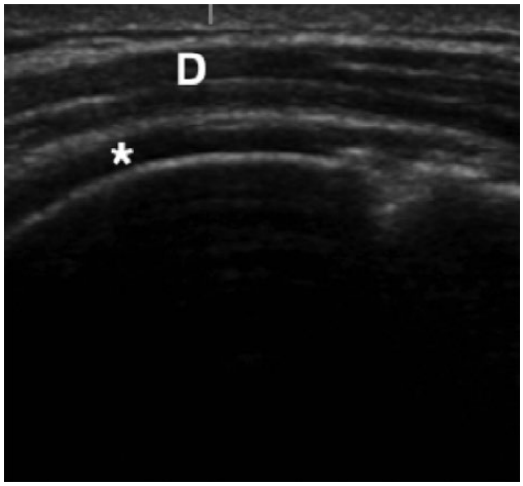

Figure 17.26 Full-thickness tear of the supraspinatus. D, Deltoid; (*) absent suprasinatus.

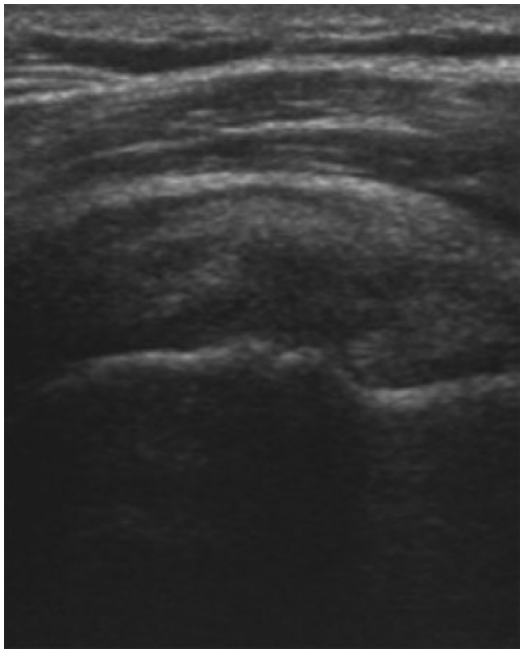

Figure 17.27 Supraspinatus tendinopathy.

wrist pronated, move the transducer posteriorly in a transverse orientation to examine the posterior glenoid and labrum.

- Assess for the presence of joint effusion and glenohumeral alignment. Significant displacement can be seen in both posterior and anterior glenohumeral joint dislocation. Post-reduction joint position can usefully be checked using this ultrasound view prior to moving the patient for formal radiography.
- Finally, place the transducer inline over the acromioclavicular joint (ACJ). Assess for a normal joint space (3–5 mm) and normal capsule bulge (2–3 mm). Degenerative disease results in joint narrowing and joint effusion with increased capsular bulge. Widening of the joint space can be seen in ACJ subluxation/dislocation.

Pearls and Pitfalls

Pearls: Use patient position 4 for ultrasound-guided subacromial bursa steroid injections. Hold the transducer with the non-dominant hand and perform the procedure with your dominant hand. Observe the needle tip enter the subacromial space, using the same technique as ultrasound-guided central line placement. Use a mixture of 1% lidocaine (2 ml) and a long-acting steroid (e.g., triamcinolone, 40 mg). Inject the solution under direct ultrasound guidance, observing distension of the subacromial bursa.

Pitfalls: Anisotropy of biceps tendon can mimic tendon rupture. Use the heel/toe transducer position to compensate for anisotropy. Hypoechoic muscle slips visualised in the medial portion of rotator cuff tendons can mimic tendon tears.

The Elbow

There are a limited number of acute elbow conditions that benefit from ultrasound assessment. Rupture of the distal biceps tendon is usually a straightforward clinical diagnosis.

Epicondylitis tends to develop gradually and is usually managed in primary care.

Elbow effusions can be subtle and are often difficult to diagnose clinically. Following injury, and in the absence of a radiographically visible fracture, the presence of an elbow effusion may indicate an occult fracture (e.g., radial head or supracondylar). Elevation of the anterior and posterior fat pads on a plain lateral radiograph is used as a marker of joint effusion. Ultrasound can detect smaller effusions.

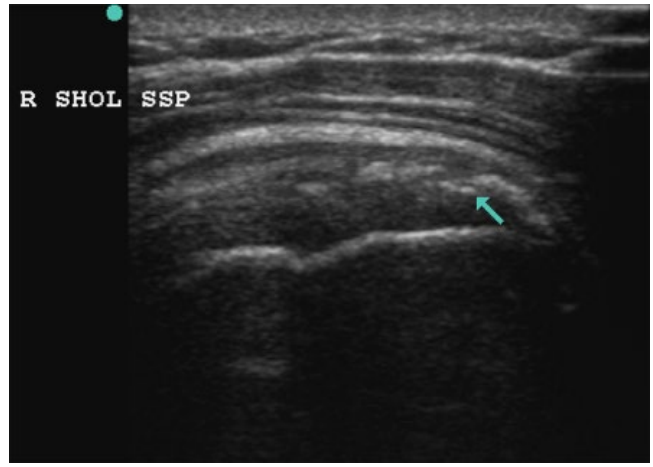

Figure 17.28 Calcific tendonitis (arrow) of the supraspinatus (SSP).

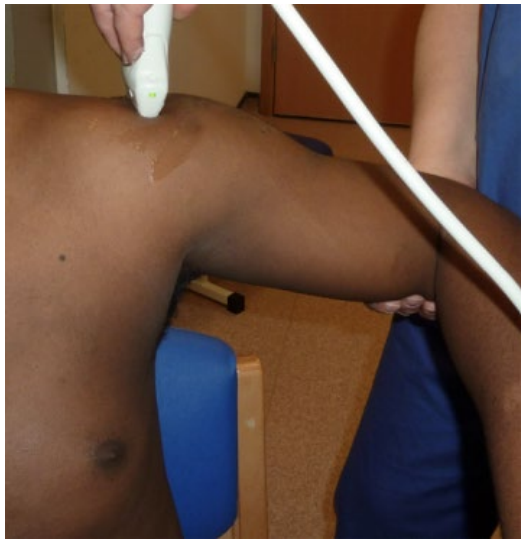

Figure 17.29 Ultrasound of the shoulder. Patient position #4 during the ultrasound examination.

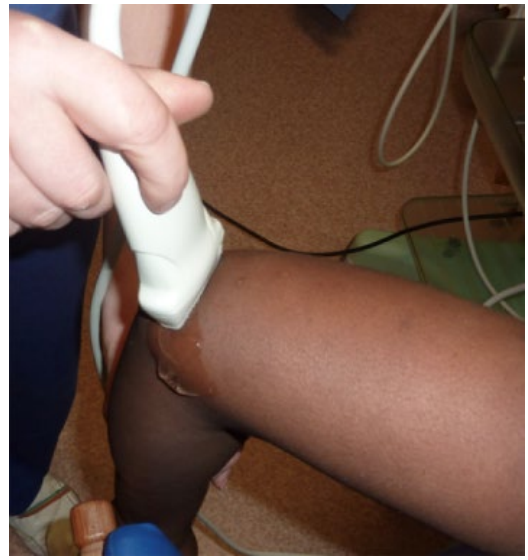

Figure 17.30 Ultrasound of the elbow. Patient and probe position during the ultrasound examination.

Technique

- With the elbow flexed, the transducer is placed in a transverse plane over the posterior elbow and olecranon fossa (Figure 17.30).
- Assess for fluid displacement of fat pad.

Pearls and Pitfalls

Pitfall: While the absence of an effusion on ultrasound would make the diagnosis of septic arthritis unlikely, it does not rule it out.

Pearl: Drainage of an elbow haemarthrosis will result in significant symptom relief for the patient. It is performed with the elbow flexed. A lateral approach is used, passing the needle posterior to the radial head into the effusion. Ultrasound can be used to guide needle placement.

Wrist and Hand

Other than fracture management and foreign body localisation, ultrasound is also used to

assess wrist and hand tendons for injury or inflammation.

Tenosynovitis of the wrist tendons can be easily diagnosed with ultrasound, with synovial proliferation and tendon sheath effusion. In de Quervain's tenosynovitis, ultrasound will demonstrate thickening of the tendon sheath.

Digital tendon rupture is usually a straightforward clinical diagnosis. However, ultrasound can be used to demonstrate the position of the retracted proximal end, which can be helpful for the surgeon.

Further Reading

Al-Shawi, A., Badge, R., Bunker, T. (2008) The detection of full thickness rotator cuff tears using ultrasound. *J. Bone Joint Surg. Br.*, **90B** (7), 889–892.

Bruyn, G.A.W., Schmidt, W.A. (2009) How to perform ultrasound-guided injections. *Best Pract. Res. Clin. Rheumatol.*, **23** (2), 269–279.

Campbell, D.G., Menz, A., Isaacs, J. (1994) Dynamic ankle ultrasonography – a new imaging technique for acute ankle ligament injuries. *Am. J. Sports Med.*, **22** (6), 855–858.

Chew, K., Stevens, K.J., Wang, T.-G., Fredericson, M., Lew, H.L. (2008) Introduction to diagnostic musculoskeletal ultrasound - Part 2: Examination of the lower limb. *Am. J. Phys. Med. Rehab.*, **87** (3), 238–248.

de Jesus, J.O., Parker, L., Frangos, A.J., Nazarian, L.N. (2009) Accuracy of MRI, MR arthrography, and ultrasound in the diagnosis of rotator cuff tears: a meta-analysis. *Am. J. Roentgenol.*, **192** (6), 1701–1707.

Finlay, K., Ferri, M., Friedman, L. (2004) Ultrasound of the elbow. *Skel. Radiol.*, **33** (2), 63–79.

Girish, G., Finlay, K., Landry, D., O'Neill, J., Popowich, T., Jacobson, J., *et al.* (2007) Musculoskeletal disorders of the lower limb-ultrasound and magnetic resonance imaging correlation. *Can. Assoc. Radiol. J.*, **58** (3), 152–166.

Hashimoto, B.E., Kramer, D.J., Wiitala, L. (1999) Applications of musculoskeletal sonography. *J. Clin. Ultrasound*, **27** (6), 293–318.

Jacob, D., Cohen, M., Bianchi, S. (2007) Ultrasound imaging of non-traumatic lesions of wrist and hand tendons. *Eur. Radiol.*, **17** (9), 2237–2247.

Konermann, W., Gruber, G. (1998) Standardized ultrasound examination of the upper extremity – shoulder joint and elbow joint. *Ultraschall. Med.*, **19** (3), 130–138.

Lee, D.H., Robbin, M.L., Galliott, R., Graveman, V.A. (2000) Ultrasound evaluation of flexor tendon lacerations. *J. Hand Surg. Am.*, **25A** (2), 236–241.

Mack, L.A., Matsen, F.A., Kilcoyne, R.F., Davies, P.K., Sickler, M.E. (1985) US evaluation of the rotator cuff. *Radiology*, **157** (1), 205–209.

Naredo, E., Aguado, P., De Miguel, E., Uson, J., Mayordomo, L., Gijon-Banos, J., *et al.* (2002) Painful shoulder: comparison of physical examination and ultrasonographic findings. *Ann. Rheum. Dis.*, **61** (2), 132–136.

Nazarian, L.N. (2008) The top 10 reasons musculoskeletal sonography is an important complementary or alternative technique to MRI. *Am. J. Roentgenol.*, **190** (6), 1621–1626.

O'Reilly, M.A.R., Massouh, H. (1993) The sonographic diagnosis of pathology in the Achilles tendon. *Clin. Radiol.*, **48** (3), 202–206.

Peetrons, P., Creteur, V., Bacq, C. (2004) Sonography of ankle ligaments. *J. Clin. Ultrasound*, **32** (9), 491–499.

Rutten, M., Maresch, B.J., Jager, G.J., Malefijt, M.C.D. (2007) Injection of the subacromial-subdeltoid bursa: blind or ultrasound-guided? *Acta Orthopaed.*, **78** (2), 254–257.

Singh, A.K., Malpass, T.S., Walker, G. (1990) Ultrasonic assessment of injuries to the lateral complex of the ankle. *Arch. Emerg. Med.*, **7** (2), 90–94.

Winter, T.C., Teefey, S.A., Middleton, W.D. (2001) Musculoskeletal ultrasound – an update. *Radiol. Clin. North Am.*, **39** (3), 465.

18

Ultrasonography of Deep Venous Thrombosis

Joshua S. Rempell and Vicki E. Noble

Introduction

Venous thromboembolism (VTE) ranges in spectrum from small deep-vein thromboses (DVT) to life-threatening pulmonary emboli (PE). Diagnosing and treating DVTs and the prevention of PE is crucial in emergency medicine. DVT occurs frequently (estimated annual incidence 0.1% with up to two million cases annually).

DVT of the lower extremity is further subdivided into distal (calf)-vein thrombosis (thrombi below the knee) and proximal-vein thrombosis (thrombi above knee) Proximal-vein thrombosis is of greater clinical concern and is more commonly associated with serious, chronic disease and a higher risk of PE. In one study, over 90% of acute PE were found to be due to emboli originating in the proximal leg veins. The rate of propagation from DVT to PE is estimated at between 10% and 50%. Left untreated, PE carry a significant mortality rate (up to 20–30%) in emergency department patients. Estimates of annual deaths in the United States attributable to PE are 50 000 to 100 000.

Given the high prevalence, associated morbidity and mortality, DVT is a critical diagnosis to consider and to make reliably in the emergency department. Traditional physical examination findings, such as palpable thrombosed vein, oedema, warmth and superficial venous dilation, are unreliable findings for the diagnosis of DVT. Furthermore, in two large series only a minority of patients (17–32%) with suspected DVT actually had the disease. Using history and physical alone, 40–60% of patients would receive unnecessary anticoagulation, which carries its own significant risk of morbidity. Diagnostic strategies must correctly diagnose DVT when present, and safely rule out DVT when absent. This has led to the development of clinical prediction rules utilising Well's criteria, D-dimer and pre-test probability of disease, in addition to diagnostic imaging modalities.

There have been different approaches for diagnostic imaging in VTE. As the use of emergency department-performed point-of-care ultrasound continues to expand, the diagnosis of DVT is becoming an essential component of daily practice. Comprehensive traditional venous ultrasound of the lower extremity involves interrogation and review of the entire lower-extremity vasculature. This requires significant resources and may not be readily available out of hours.

To overcome the time required for traditional comprehensive venous ultrasound, many studies (performed by both radiologists and vascular medicine) have validated simplified two-point compression ultrasound when used in combination with clinical pretest evaluations in ambulatory outpatients. In addition, emergency physician-performed two-point compression (versus comprehensive radiologist

Emergency Point-of-Care Ultrasound, Second Edition. Edited by James A. Connolly, Anthony J. Dean, Beatrice Hoffmann and Robert D. Jarman.

Companion website: www.wiley.com/go/connolly/ultrasound

ultrasonography) is both efficient and accurate in diagnosing DVT. A recent review evaluated six studies and reported a pooled sensitivity of 95% and specificity of 96% for emergency physician-performed ultrasound versus radiologist-performed scans for lower-extremity DVT. This technique, which focuses on areas of greatest turbulent flow and thus the highest probability areas of DVT, is performed rapidly.

Poppiti *et al*. showed that a limited venous ultrasound took 5.5 min to perform compared to 37 min for complete radiologist leg-ultrasonography. Safety, ease of use, speed, low cost and accessibility make two-point compression ultrasound especially useful for emergency physicians.

Clinical Indications

Venous ultrasonography of the lower extremity should be performed on any patient with a clinical suspicion of DVT. Using clinical prediction rules, only patients with a negative D-dimer and a low pre-test probability may safely be discharged without having undergone ultrasound.

Venous ultrasonography is also of value in atypical chest pain, cardiac arrest and undifferentiated shock when it may reveal the source of the patient's symptoms, though the absence of DVT does not exclude venous thromboembolus.

Scanning Technique and Normal Findings

Anatomy of the Lower Extremities and Views

The deep veins of the lower extremities include the popliteal, deep femoral, superficial femoral and common femoral veins (Figure 18.1). Despite its name, the superficial femoral vein (SFV) is part of the deep venous system and is sometimes referred to simply as the femoral vein to avoid confusion.

From proximal to distal, the external iliac vein becomes the common femoral vein (CFV) as it passes under the inguinal ligament. Immediately below the inguinal ligament the great saphenous vein (GSV), a superficial vein, merges with the CFV. Moving inferiorly, the latter vein then splits into the deep femoral vein (DFV) and superficial femoral vein (SFV). The deep vein travels deep into the thigh, while the SFV disappears distally into the obturator canal and emerges behind the knee as the popliteal vein (PV). The PV is joined by the veins from the lower leg (tibial and peroneal) and is usually superficial to the artery.

Variation in position of the PV can be a pitfall. Additionally, approximately one-third of the population will have a duplicated PV.

Necessary Views

Comprehensive traditional lower-extremity ultrasonography visualises the entire deep venous system in 1-cm increments, starting at the level of the CFV and proceeding down through the superficial femoral canal. The popliteal system is then evaluated moving distally to the level of the trifurcation in the upper calf and imaging the vasculature of the calf.

The two-point compression test, in contrast, assesses the vasculature in just two places: (i) at the CFV; and (ii) at the PV.

The first area of examination is the CFV. Controversy persists as to how much of the femoral vein and what branch points are assessed. It is recommended to start at the proximal femoral vein at the junction of the CFV and GSV. Starting at this point ensures a diagnosis of proximal thrombi in the GSV at the risk of extending into the CFV. The CFV should then be viewed distally, which generally involves three to four additional views and compressions at approximately 1 cm intervals.

The second segment involves a view of the popliteal fossa and vein. Generally, a single view of the popliteal artery and vein showing full compressibility is accepted in the literature, although it is suggested that the PV is followed to the trifurcation to improve accuracy.

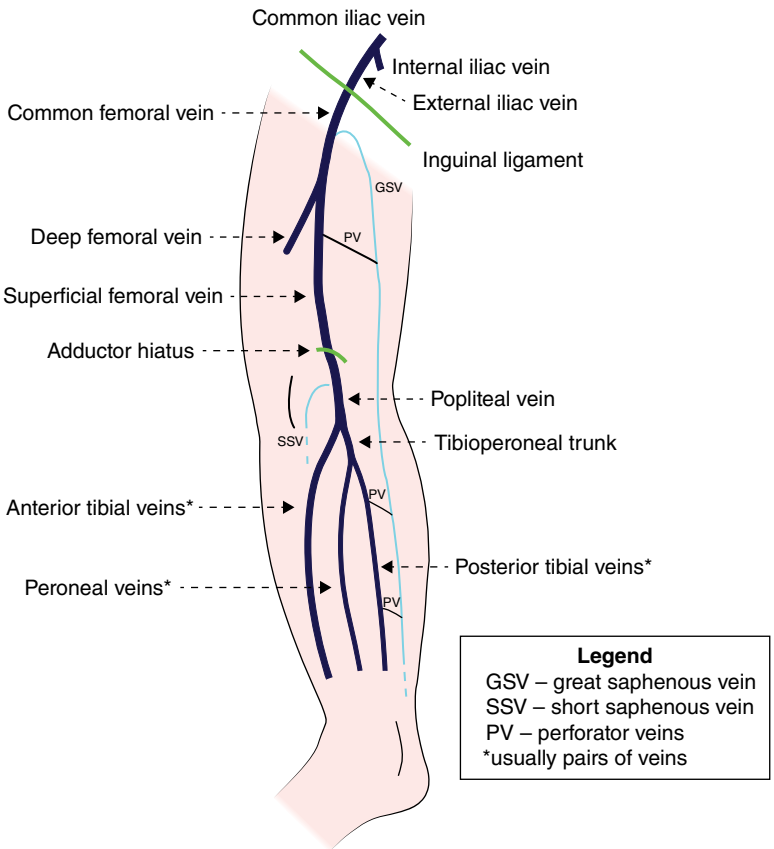

Figure 18.1 Normal anatomy of the lower extremity.

Focused Emergency Physician-Performed Venous Ultrasonography

Traditional comprehensive studies include many elements to assess for DVT, including Doppler evaluation for abnormalities in venous blood flow. The two-point compression test, however, only uses B-mode grey-scale compressibility of the veins. Compressibility alone can be relied on for confirming deep venous thrombosis, and Doppler does not add to the diagnostic accuracy.

Occasionally a clot is visualised, in which case (especially if the clot appears mobile) compression is not necessary due to concern that it may dislodge the clot. However, no cases of this happening have have been reported in the literature.

Scanning Technique

A high-frequency linear probe (5–10 MHz) should be used. The probe marker should be pointed toward the patient's right side throughout the examination. Occasionally, a lower-frequency probe will be necessary in larger patients.

With the patient in the supine position, the examination should started in the region of the CFV. If tolerated, the patient should be placed in 20–30 degrees reverse Trendelenburg position to increase venous distention. External rotation of the hip, and flexion at the knee, may also help to visualise the femoral region; correct positioning is shown in Figure 18.2.

View the CFV and GSV junction and demonstrate full compressibility of the vessel by

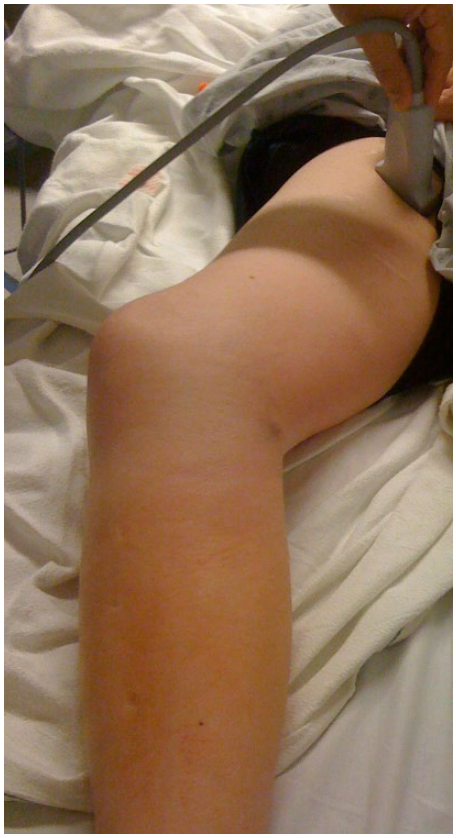

Figure 18.2 Patient positioning for scanning of the femoral vein.

applying direct pressure (Figure 18.3a–c). Move distally and compress the CFV until it bifurcates into the deep and superficial femoral veins (Figure 18.4). Enough pressure should be applied so that any superficial veins are seen to compress, as well as visualising some deformity of the artery with compression. Ensure that the probe is held perpendicular to the skin and that pressure is applied evenly over the vessels.

The probe is moved to the popliteal fossa to visualise the popliteal artery and vein. This can be done with the patient supine, with external rotation at the hip and flexion at the knee (Figure 18.5). Ideally it is done with the patient in the prone or laterl decubitus position. Again reverse Trendelenburg with the knee in 15–30 degrees of flexion improves access and distends the vessels. Visualise the more superficial PV and the deeper popliteal artery and apply pressure to compress the vein (Figure 18.6a and 6b). In general, less compression is needed for the PV than for the femoral vein.

A negative study is one where there is complete compressibility of all venous structures visualised. The two walls of the vein should touch one another.

Pathology

In the two-point compression examination, any vein that is not completely compressible is considered positive for DVT. Only complete compression of the vessel rules out DVT. It is important to note that this does not require actual visualisation of the thrombus.

In Figures 18.7 and 18.8, the femoral vein is not collapsible and thus is positive for DVT. Figure 18.9 shows a DVT in the PV.

Secondary Findings/ Advanced Techniques

Two-point compression ultrasound uses only compressibility. Other techniques used in ultrasound assessments performed by imaging specialists may be helpful in certain cases, although many studies show that its use does not improve accuracy. This is of particular concern with less experienced sonologists who are not trained in the use of Doppler.

Augmentation

Augmentation refers to the normal increase in flow seen when the lower extremity is squeezed distally. Using Doppler, the transducer is held over the vein and the lower extremity compressed distal to the probe. Under normal circumstances a rapid increase in blood flow should be visualised with compression distally (Figure 18.10). When there is a clot distal to the probe, this normal augmentation may be lost.

Respiratory Variation

The normal respiratory cycle leads to changes in blood flow under normal circumstances. On inspiration, the diaphragm descends and this

(a)

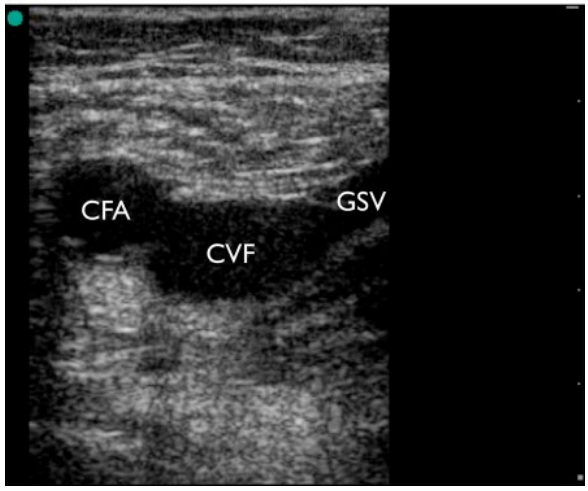

(b)

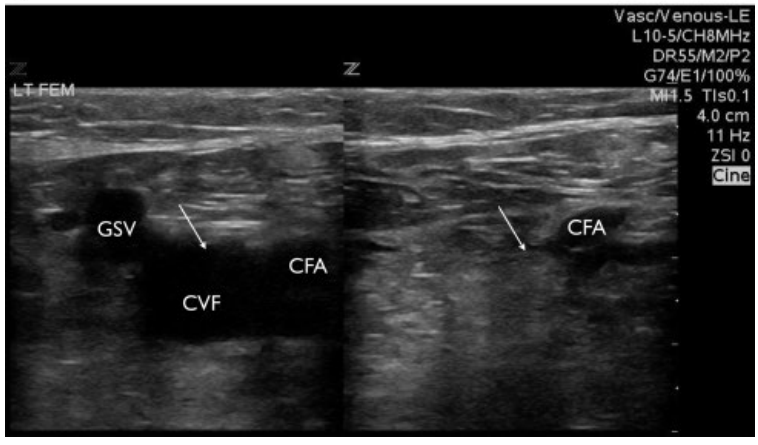

(c)

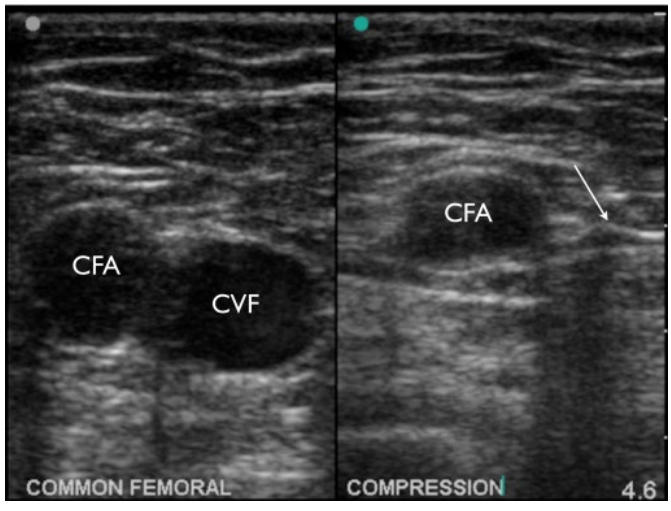

Figure 18.3 (a) View at the level of the common femoral vein (CFV) and greater saphenous vein (GSV). The common femoral artery is seen to the left (CFA). (b) Common femoral vein (CFV, white arrow) and common femoral artery (CFA) uncompressed (left) and with compression (right). (c) Common femoral vein (CFV, white arrow) and common femoral artery (CFA) uncompressed (left) and with compression (right).

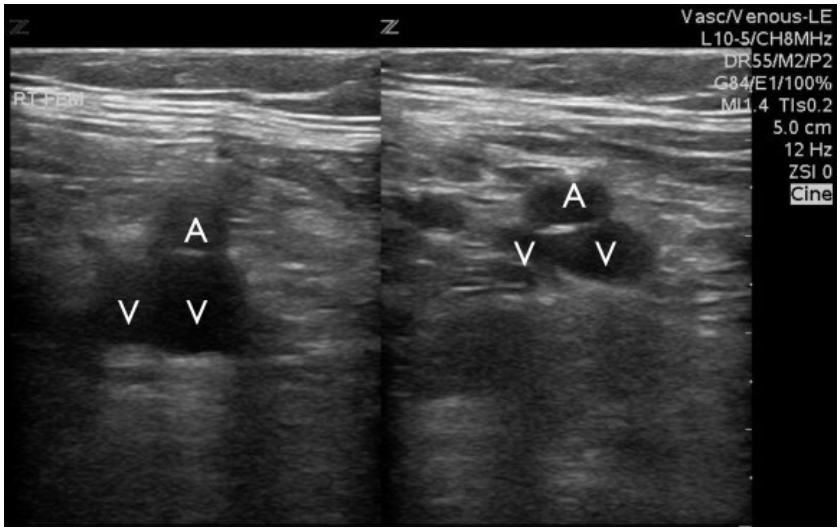

Figure 18.4 Compression at the level of the bifurcation of the common femoral vein into the deep (V) and superficial femoral vein (V). Note that the superficial vein, despite its name, is a component of the deep venous system. The compression in this image is incomplete for one of the veins (right image). A, femoral artery.

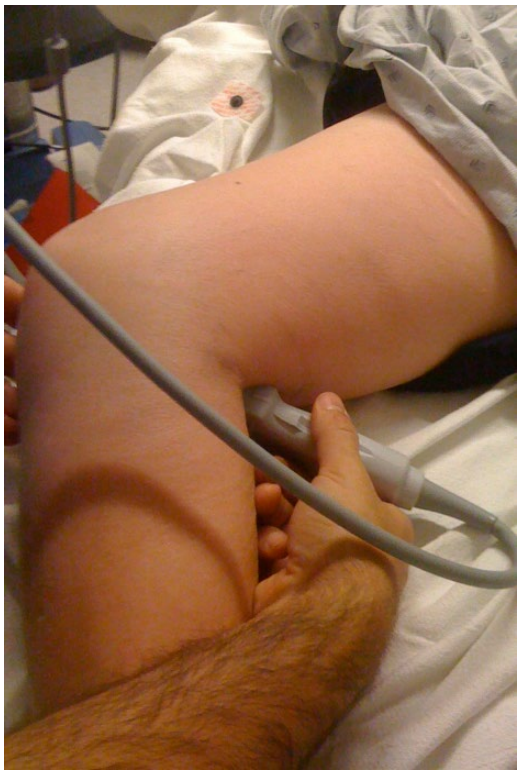

Figure 18.5 Position for evaluation of the popliteal vein.

leads to increases in intra-abdominal pressure; this compresses the inferior vena cava and leads to less venous outflow from the lower extremities. Doppler signals will show an increased flow during expiration and a decreased flow during inspiration. In the presence of a thrombus proximal to the probe, this normal respiratory variation may be lost.

Scanning Tips and Areas of Uncertainty

Probe

A high-frequency linear array probe is often used for DVT assessment. In a minority of patients a lower-frequency probe may be helpful for increased depth, although this comes at the cost of reduced resolution.

Compression

It is crucial to ensure that the vein completely collapses. Pressure should be applied evenly along the axis of the probe and the incident ultrasound beam, ideally perpendicularly to the skin surface sufficient to produce some distortion of the adjacent artery.

(a)

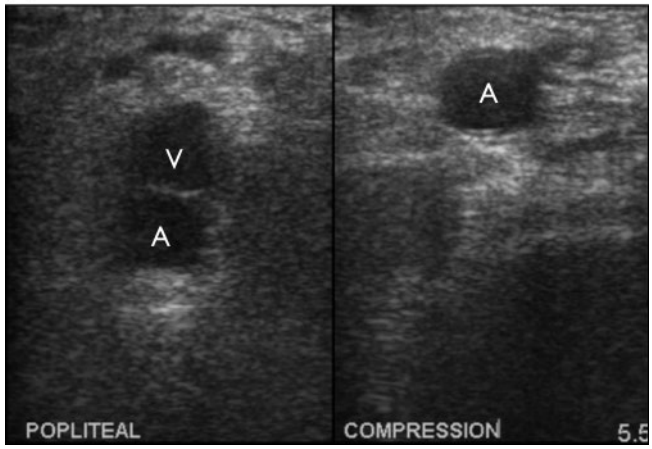

(b)

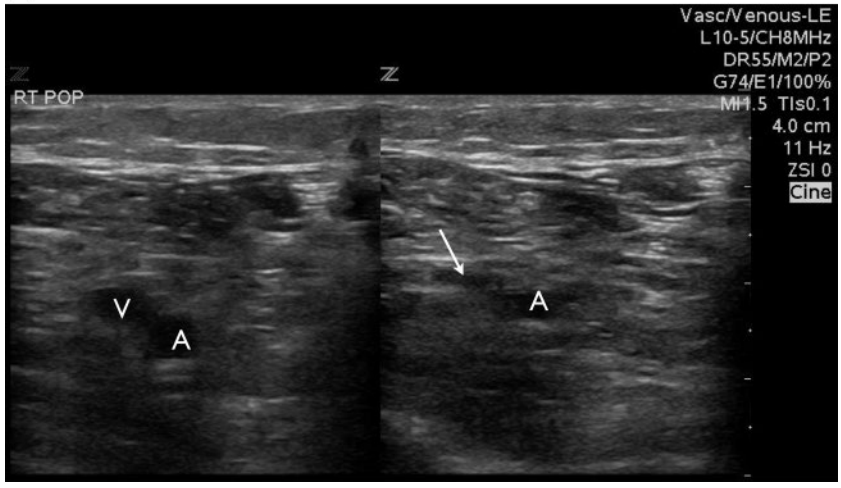

Figure 18.6 (a) Normal compression (right image) of the popliteal vein (V) and artery (A) showing a negative test for DVT.' (b) Normal compression of the popliteal vein (V) and artery (A) showing a negative test for DVT, right image with vein compression (arrow).

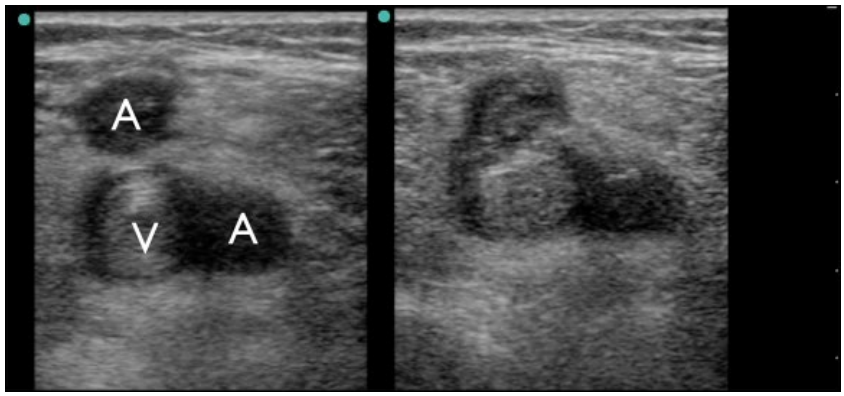

Figure 18.7 Left: Image showing a femoral vein (V) with hyperechoic thrombus, femoral artery (A). Right: Note the lack of compressibility.

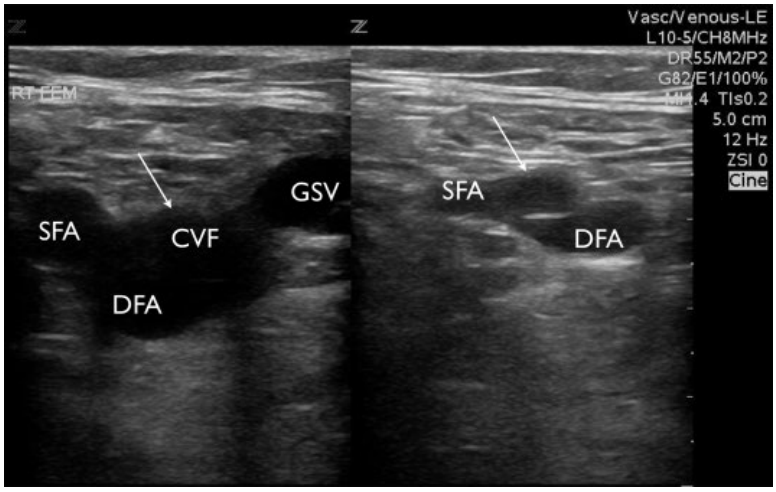

Figure 18.8 Additional example of femoral DVT. Left: Common femoral vein (CFV), greater saphenous vein (GSV) and superficial femoral artery (SFA) and deep femoral artery (DFA) uncompressed. Right: Note the lack of full compressibility of the vein (arrow).

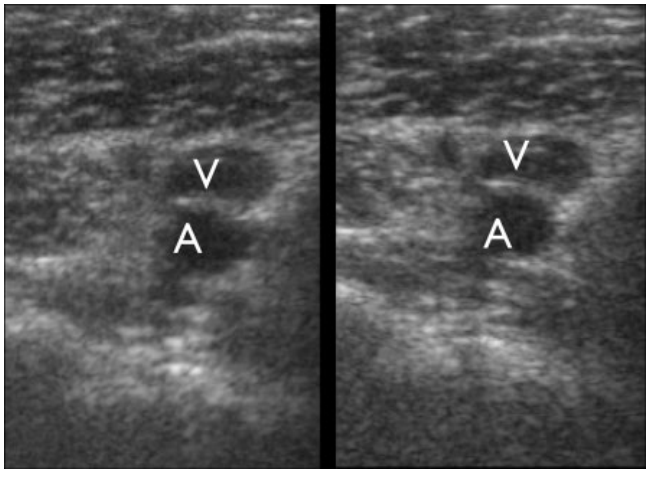

Figure 18.9 Positive finding for DVT in the popliteal vein (V). Left: No compression. Right: Compression is being applied with lack of compressibility. A, popliteal artery.

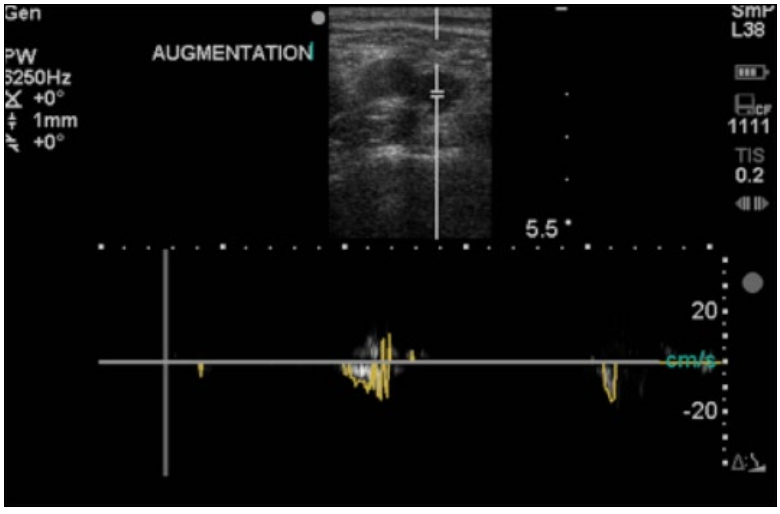

Figure 18.10 Normal augmentation using spectral Doppler mode.

Incidental Findings/Mimics

Occasionally, other structures may mimic a thrombus. A Baker's cyst may be visualised in the popliteal fossa (Figure 18.11), but this can be distinguished from a thrombus by visualising its confluence with the joint space. It will also lack flow on Doppler.

Lymph nodes are common in the femoral region and may be mistaken for a vessel with intraluminal thrombus. Lymph nodes, however, are more superficial and are highly vascular showing high Doppler signals compared to a venous clot. Furthermore, a lymph node is a finite structure, and moving the probe proximally or distally should identify the boundaries of a node, demonstrating that it is not a tubular structure (Figure 18.12). By moving the probe distally and proximally the node should disappear, while a vessel will not.

Pelvic Vein Thrombosis

In a small percentage of cases there may be an isolated pelvic vein thrombosis, which can be difficult to diagnose on ultrasound. A lack of respiratory variation is one way to assess for clots proximal to the transducer in the pelvis. However, this technique has been shown to only rarely provide any additional information in the hands of imaging specialists, and is beyond the skills of most clinician sonologists. In cases of high suspicion for pelvic clot, the use of computed tomographic venography (CTV) is necessary.

Slow Venous Blood Flow

Occasionally, blood flow within a vein may be slow and appear as a swirling of blood within the vessel lumen. This may appear echogenic and potentially be mistaken for a thrombus. However, the vein will remain fully compressible.

Distal Calf DVTs

Controversy regarding the clinical course and treatment of distal DVTs persists. For patients with a moderate or high pre-test probability of disease, a negative limited compressible ultrasound (as described above) is traditionally followed by a repeat ultrasound in one week or by follow-up full-leg ultrasound, due to the concern that a missed distal DVT may propagate. This algorithm has recently been questioned through indirect evidence questioning the significance of distal DVTs.

It had been thought that up to 25% of distal DVTs may propagate, increasing the risk of PE and post-thrombotic syndrome. However, many distal thrombi appear to resolve without anticoagulation, and it has been argued that

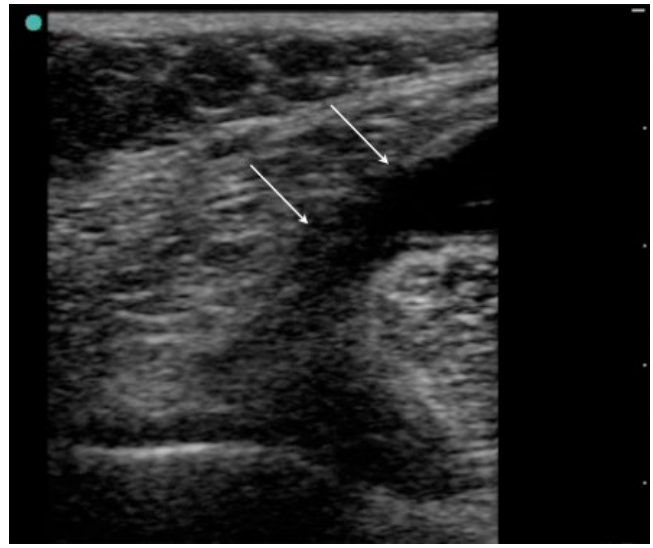

Figure 18.11 Baker's cyst (arrows).

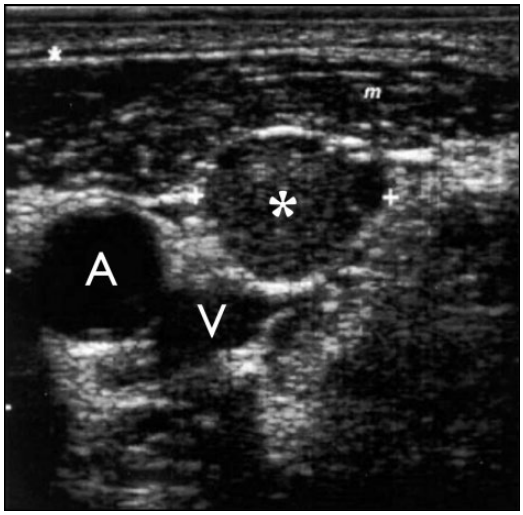

Figure 18.12 Lymph node (*), femoral artery (A) and femoral vein (V).

the detection and treatment of distal DVT is unnecessary and may place patients at increased risk due to bleeding risks of anticoagulation. In a meta-analysis conducted by Johnson *et al*. assessing the risk of thrombosis following negative whole-leg ultrasound, isolated distal DVT represented 52.1% of all DVTs diagnosed. The benefit of treating these DVTs with a three-month period of anticoagulation (which most practice guidelines still advocate) is controversial as anticoagulation carries an estimated annual risk for major bleeding of 1.1%.

In a recent randomised control trial in patients presenting with leg symptoms of DVT, Bernardi *et al*. compared the diagnostic strategies of whole-leg ultrasonography and repeat two-point compression sonography. The authors randomised 2098 outpatients to undergo: (i) two-point compression ultrasonography with D-dimer testing in patients with normal ultrasonography, and repeat ultrasonography at one week in patients with a positive D-dimer; or (ii) whole-leg colour Doppler ultrasonography in all patients on initial presentation. The two strategies led to similar rates for symptomatic venous thromboembolism over three months.

Another important finding in the latter study was that the initial whole-leg ultrasonography group had a higher prevalence of DVT than the group randomised to two-point ultrasonography plus D-dimer (26% and 22%, respectively). This difference was accounted for by 65 missed cases of isolated calf DVT in the two-point compression group. However, the two groups had similar long-term outcomes, and thus the diagnosis and treatment of isolated calf vein thrombosis may not be as critical as originally thought.

Overall, based on Bernardi's paper, patients with either an initial negative whole-leg investigation, or the combination of negative two-point compression study and negative D-dimer, may not require any additional follow-up or anticoagulation. Patients with an initial negative two-point compression study and a positive D-dimer still required a repeat two-point study one week later.

While indirect evidence has been provided that that isolated distal DVTs have a benign course, the widely accepted American College of Chest Physicians guidelines still recommend treating isolated calf DVTs with anticoagulation for at least six weeks. Currently, further research is indicated to define the optimal treatment strategy for distal DVTs.

Experience of Scanner

Most studies citing sensitivities of 89–100% and specificities of 76–99%, including a recent meta-analysis conducted by Burnside, were performed by a small number of highly trained practitioners, which suggests that caution is required when generalising to clinician sonologists. A recent study questioned the sensitivity and specificity among inexperienced clinicians. Kline *et al*. studied compression ultrasononography among a heterogeneous group of emergency department clinicians, and found sensitivities and specificities of 70% and 89%, respectively, versus radiologist-performed ultrasonography.

Need for Routine Bilateral Studies

Controversy exists regarding the need for routine bilateral lower-extremity ultrasound examinations *versus* examinations limited to the symptomatic leg. Some studies have suggested that thrombosis may occur in up to 14% of patients in the asymptomatic leg, and in either leg in up to 23% of patients with bilateral symptoms. Other studies suggest that it is unnecessary to examine an asymptomatic leg because these patients also typically have DVT in the symptomatic leg. Another rationale for limiting the examination to symptomatic legs is that management will likely not change if bilateral DVTs are found.

Role of Computed Tomography (CT) Scanning

As DVT and PE represent different manifestations of the same disease process, there has been increasing interest in evaluating for both processes simultaneously. Recent studies have compared the accuracy of CT venography (CTV) with lower-extremity venous ultrasonography and found a high concordance of 95.5% in the diagnosis of femoropopliteal DVT. When compared to CT venography, emergency physician- performed ultrasonography does not evaluate for more proximal clots, and may provide false-negative results in high-risk patients. CTV has the advantage of evaluating the iliac veins and inferior vena cava in patients where there is a high level of suspicion.

Summary

Faced with over one million visits annually for leg pain and swelling, investigations for DVT represent a common task for the emergency physician. Given this large patient population and the high potential for morbidity and mortality with both underdiagnosis and overdiagnosis, accurate evaluation is vital. While prediction rules exist and may aid the emergency physician, imaging is usually necessary to either exclude or make the diagnosis of DVT. In many settings, traditional comprehensive ultrasound may not be readily available 24/7 and may delay care in the emergency department or necessitate the practice of 'prophylactic' anticoagulation until the comprehensive examination can be made. This can lead to complications, in addition to the cost and inconvenience to the patient.

Emergency physician-performed point-of-care compression ultrasonography for DVT has been shown to have similar sensitivity and specificity to more comprehensive studies, and to increase emergency department efficiency. The American College of Emergency Physicians (ACEP) has listed DVT as one of the 11 core emergency ultrasonography applications making it an essential component of emergency medicine practice.

Pearls and Pitfalls

- Failure to identify the venous and arterial anatomy correctly is major source of error.
- Two-point compression ultrasound combined with evaluation of D-dimer is as accurate as extended duplex ultrasonography in the identification of proximal lower extremity DVT.
- Avoid mistaking lymph nodes for vessels.
- Two-point compression does not rule out deep pelvic vein clots.
- An absence of DVT on two-point compression does not exclude pulmonary embolism. However, the presence of lower extremity clots lends strong support to the diagnosis of PE.

Further Reading

Bernardi, E., Camporese, G., Büller, H.R., *et al.* Erasmus Study Group (2008) Serial 2-point ultrasonography plus D-dimer vs whole-leg color-coded Doppler ultrasonography for diagnosing suspected symptomatic deep vein thrombosis: a randomized controlled trial. *JAMA*, **300** (14), 1653–1659.

Birdwell, B.G., Raskob, G.E., Whitsett, T.L., *et al.* (1998) The clinical validity of normal compression ultrasonography in outpatients suspected of having deep venous thrombosis. *Ann. Intern. Med.*, **128**, 1–7.

Burnside, P.R., Brown, M.D., Kline, J.A. (2008) Systematic review of emergency imaging versus complete color-flow duplex venous scanning for detection of proximal deep venous thrombosis. *J. Vasc. Surg.*, **22** (5), 553–557.

Gallus, A.S., Baker, R.I., Chong, B.H., *et al.* (2000) Consensus guidelines for warfarin therapy. *Med. J. Aust.*, **172** (12), 600–605.

Goldhaber, S.Z. (1999) Pulmonary embolism. *N. Engl. J. Med.*, **339**, 93–104.

Goodacre, S., Sampson, F., Thomas, S., *et al.* (2005) Systematic review and meta-analysis of the diagnostic accuracy of ultrasonography for deep vein thrombosis. *BMC Med. Imaging*, **5**, 6.

Goodman, L.R., Stein, P.D., Matta, F., *et al.* (2007) CT venography and compression sonography are diagnostically equivalent: data from PIOPED II. *Am. J. Roentgenol.*, **189**, 1071–1076.

Johnson, S.A., Stevens, S.M., Woller, S.C., *et al.* (2010) Risk of deep vein thrombosis following a single negative whole-leg compression ultrasound. *J. Am. Med. Assoc.*, **303** (5), 438–445.

Kline, J.A., O'Malley, P.M., Tayal, U.S., *et al.* (2008) Emergency clinician-performed compression ultrasonography for deep venous thrombosis of the lower extremity. *Ann. Emerg. Med.*, **52** (4), 437–445.

Krakow, E., Ortel, T.L. (2005) Continuing anticoagulation following venous thromboembolism. *J. Am. Med. Assoc.*, **294** (24), 3088.

Lensing, A.W., Prandoni, P., Brandjes, D., *et al.* (1989) Detection of deep-vein thrombosis by real-time B-mode ultrasonography. *N. Engl. J. Med.*, **320**, 342–345.

Poppiti, R., Papanicolaou, G., Perese, S., Weaver, F.A. (1995) Limited B-mode venous physician-performed ultrasonography for lower-extremity deep vein thrombosis. *Acad. Emerg. Med.*, **15** (6), 493–498.

Righini, M., Paris, S., Le Gal, G., *et al.* (2006) Clinical relevance of distal deep vein thrombosis. *Thromb. Haemost.*, **95** (1), 56–64.

Shiver, S.A., Lyon, M., Blaivas, M., Adhikari, S. (2010) Prospective comparison of emergency physician-performed venous ultrasound and CT venography for deep venous thrombosis. *Am. J. Emerg. Med.*, **28**, 354–358.

19

Transcranial Doppler

John Gullett

Introduction

Transcranial Doppler ultrasound (TCD) is used to interrogate the intracranial vasculature by measuring the velocity and pulsatility of cerebral arterial blood flow. Flow in the anterior cerebral artery (ACA), middle cerebral artery (MCA), posterior cerebral artery (PCA) and the vertebrobasilar artery can all be assessed (see Figure 19.1). TCD has a role in the evaluation of a variety of pathological conditions, including vascular thrombosis, stenosis, vasospasm, intracranial pressure (ICP) elevation and intracranial haemorrhage.

Although the use of TCD in the emergency department or acute care setting is increasing, the use of this modality is still largely confined to vascular neurologists and specialised technicians. Its role in the emergency setting is still under investigation, but as the use of improved ultrasound systems becomes more prevalent and clinician-sonographer skills become more sophisticated, TCD may play an increasing role in the evaluation of many emergency neurological conditions, especially in settings without ready access to computed tomography (CT) imaging (Table 19.1).

Technique

TCD Technique

The patient should be resting in the supine position, and preferably without recent sedation. The sonographer should sit comfortably at the head of the bed, facing the patient's feet. A 2- to 3-MHz phased-array low-frequency transducer is used. Specific TCD software packages are available and may facilitate imaging.

A complete examination includes an evaluation of the internal carotid arteries, ACAs, MCAs, PCA in the circle of Willis and the vertebrobasilar vessels (Figure 19.2). Images should be obtained on both the right and left. For the identification of significant elevations in ICP, a limited examination focussing on decreased flow in either or both middle cerebral arteries may be sufficient to guide therapy. Limited focussed examinations may also be useful to monitor the changes in or evolution of a known abnormality.

Acoustic Windows

Transtemporal

The transtemporal window is used to insonate the MCA, the ACA, the PCA and the terminal

Emergency Point-of-Care Ultrasound, Second Edition. Edited by James A. Connolly, Anthony J. Dean, Beatrice Hoffmann and Robert D. Jarman.

Companion website: www.wiley.com/go/connolly/ultrasound

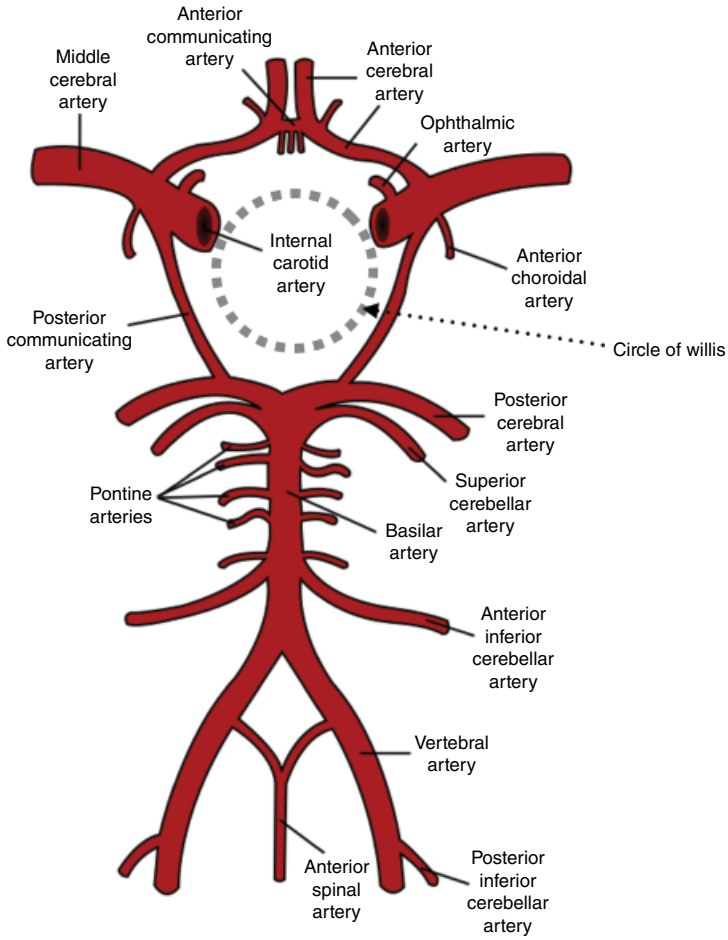

Figure 19.1 Circle of Willis and associated intracranial arterial circulation.

Table 19.1 Indications for TCD in the acute care setting.

Condition	TCD findings
Stroke	Arterial stenosis or occlusion
Subarachnoid haemorrhage	Vasospasm
Arteriovenous malformations (AVM)	Various findings. Used to monitor known AVM
Head trauma	Focal or diffuse decrease in arterial flow
Brain death	Absence or near-absence of cerebral blood flow

portion of the internal carotid artery (TICA), prior to its bifurcation.

After applying an appropriate amount of gel, the probe is placed at the pterion, just anterior to the ear and superior to the zygomatic arch. This declivity can be palpated, and usually is found just anterior to the point where the helix of the ear meets the skin of the temple. By convention, the transducer marker is directed anteriorly when scanning from either side of the head. The plane of the ultrasound is usually along an imaginary line to the lateral canthus of the eye, and is frequently thought of as the line that would be taken by the temples of a pair of

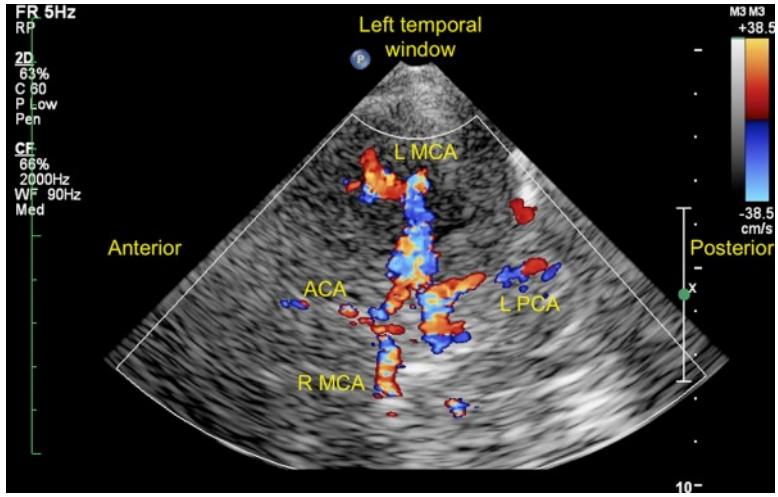

Figure 19.2 Normal circle of Willis, transtemporal view.

spectacles. The depth should be initially set at about 15 cm, allowing for a wide view that should reveal the signal from the contralateral wall of the skull. Approximately midway between the transducer and the contralateral calvarium, the hypoechoic brainstem should identified (the shape is often compared to a butterfly, a heart, or a 'Pacman' with 'mouth directed anteriorly'), and anterior to the brainstem the midline structures of the basal cistern and/or third ventricle can be identified. Subtle fanning of the transducer above and below this plane will reveal the circle of Willis, with the ipsilateral MCA curving toward the probe (Figure 19.3). The anatomical position of the MCA is anterior and lateral to the basal cistern. Flow in the MCA is directed towards the transducer, while flow in the ACA is away from the transducer. The PCA may be identified by its position immediately anterior to the cerebral peduncles and with the directionality of flow. Flow towards the transducer will indicate the P1 segment, while flow in the more distal P2 segment is directed away from the transducer.

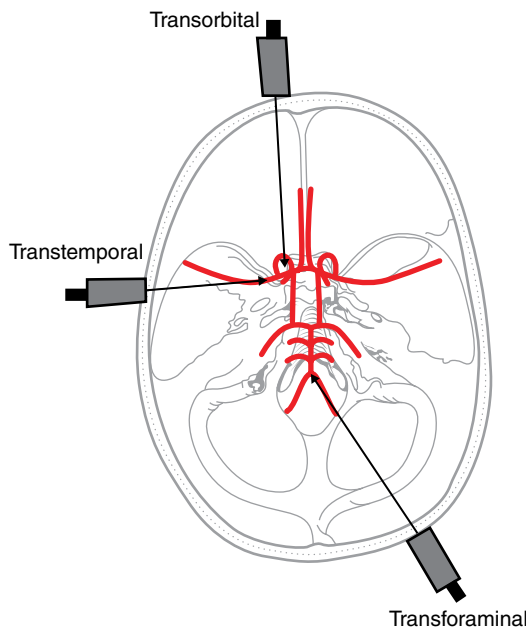

Figure 19.3 Location of probe placement for standard views.

Transforaminal

The transforaminal window provides visualisation of the distal vertebral arteries (VAs) and the basilar artery (BA). This window is optimally accessed with the patient seated and the head flexed slightly forward. In the intubated or incapacitated patient, the study may be performed by maintaining the patient's supine position and simply turning the patient's head to the side.

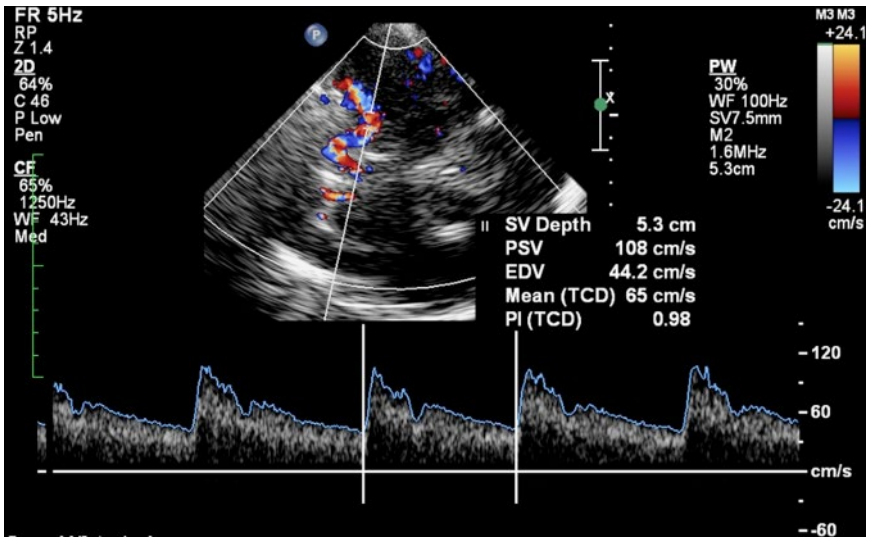

Figure 19.4 In this normal image of the left middle cerebral artery (MCA), the peak systolic velocity is normal (108 cm s^{-1}) with good forward flow during diastole (end-diastolic velocity: 44.2 cm s^{-1}). The pulsatility index (PI) is normal at 0.98.

The transducer is placed in the midline directly inferior to the occiput (Figure 19.3). The transducer orientation marker is directed to the patient's right. The probe should be angled cephalad roughly toward the patient's nose. The reference landmark is the hypoechoic medulla. The characteristic V-shaped appearance of the vertebral arteries can be seen extending superiorly from the basilar artery. Flow will be directed away from the transducer in both vessels.

Transorbital

The transorbital window allows visualisation of both the ophthalmic artery (OA) and the siphon of the ICA. The transducer orientation marker is directed to the patient's right. With this approach the transducer is placed so that it rests slightly on the closed eyelid. Flow will be directed towards the transducer.

Interpretation

TCD waveforms are analysed to assess the haemodynamics of cerebral blood flow. This analysis requires the interpretation of Doppler waveform morphology, flow velocity and direction, pulsatility index (PI) and resistance. The initial portion of the waveform is created by the systolic upstroke, with the remainder of the waveform being due to diminishing intra-arterial pressure during diastole. Under normal conditions systole causes a brisk acceleration of bloodflow to systolic peak velocity (see Figure 19.4). In the setting of proximal obstruction, a slower upstroke is seen as a slanted or rounded waveform. A globally slowed systolic upstroke, as opposed to a finding restricted to one vessel, is due to a central cause such as systolic cardiac dysfunction or aortic stenosis.

Cerebral blood flow velocity is a key concept in TCD. This finding is typically expressed as mean flow velocity (MFV), where:

$$\text{MFV} = \text{diastolic velocity} + (\text{systolic velocity} - \text{diastolic velocity})/3.$$

Each vessel has a characteristic MFV range (Table 19.2) Given a constant pressure, the velocity of flow is inversely related to the cross-sectional area of the vessel lumen, although abnormalities in flow velocity within a single vessel can be due to stenosis either proximally or distally, as well as ambient intracerebral pressure, requiring the evaluation of other vessels.

Table 19.2 Accepted guidelines for a normal TCD study.

Artery	Window	Depth (mm)	Direction	Mean flow velocity ($cm\,s^{-1}$)
MCA	Temporal	30–60	Towards probe	55 ± 12
ACA	Temporal	60–85	Away	50 ± 11
PCA	Temporal	60–70	Bidirectional	40 ± 10
TICA	Temporal	55–65	Toward	39 ± 09
ICA (siphon)	Orbital	60–80	Bidirectional	45 ± 15
OA	Orbital	40–60	Towards	20 ± 10
VA	Occipital	60–80	Away	38 ± 10
BA	Occipital	80–110	Away	41 ± 10

TCD, transcranial Doppler; MCA, middle cerebral artery; ACA, anterior cerebral artery; PCA, posterior cerebral artery; TICA, terminal internal carotid artery; ICA, internal carotid artery; OA, ophthalmic artery; VR, vertebral artery; BA, basilar artery.

The pulsatility index (PI) uses a comparison between systolic and diastolic flow, providing a measure of intracranial vascular resistance.

PI = (systolic velocity – diastolic velocity)/MFV.

Under normal healthy conditions, low-resistance beds (such as the brain) are characterised by a smooth systolic upstroke and continuous forward flow throughout diastole, reflected by a fairly low PI. High-resistance systems appear to have a sharper upstroke, a narrow peak, and little or no forward flow seen in diastole (Figure 19.5). A normal PI for most cerebral vessels is 0.5–1.19. A PI less than 0.5 suggests proximal arterial stenosis or occlusion or the presence of AVM. Conversely, a PI higher than 1.19 may represent distal stenosis, occlusion, arterial constriction or arteriosclerosis (stiff, non-compliant vessels). A distal obstruction will decrease diastolic forward flow, resulting in an elevated PI.

Flow directionality is noted for several reasons. Antegrade, or normal flow direction, may be reversed if the vessel is functioning as a collateral vessel, implying an obstruction elsewhere. There may be an alternating flow seen as retrograde in systole and antegrade in diastole, implying a progression toward collateral function.

Turbulence and bruits are found when the laminar flow in a vessel is disrupted, typically through areas of focal stenosis. This finding may be seen within the spectral waveform as a bright small (relatively low velocity) signal close to the baseline, known as a "visual bruit or spectral bruit".

Doppler findings in Common Pathological Conditions

1) Insonation at the site of focal narrowing: increased MFV.
2) Insonation distal to the narrowing: decreased MFV, delayed systolic upstroke.
3) Insonation proximal to an area of decreased vascular resistance (e.g., AVM): increased MFV, decreased PI.
4) Insonation proximal to area of increased vascular resistance (e.g., stenosis, spasm): decreased MFV, increased PI, sharper systolic upstroke.

Clinical Applications

Stroke

The use of TCD imaging in the evaluation of patients presenting with symptoms of acute stroke is a common practice among stroke

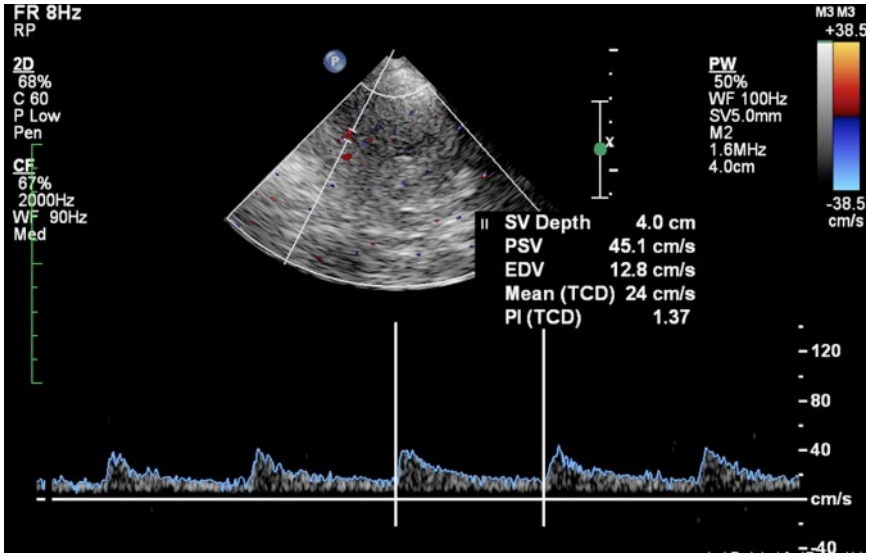

Figure 19.5 In this image of right middle cerebral artery Doppler flow (waveform at the bottom), the mean flow velocity (MFV) is low (24 cm s^{-1}) and there is an increased pulsatility index (PI) of 1.37. These findings are suggestive of a more distal intracranial arterial stenosis. This image would have been improved by adjusting the Doppler Velocity scale for improved resolution of the waveform (maximum velocity 50 cm/s).

neurologists. It has the advantages of being rapid and non-invasive, while providing real-time imaging of potentially compromised cerebral vasculature.

Emergency physicians have demonstrated that TCD – and, more recently, transcranial colour-coded duplex sonography; TCCS) – may be performed quickly and accurately at the bedside, providing a rapid evaluation of intracranial arterial thrombosis or stenosis. The bedside diagnosis of specific TCD patterns or decreased arterial flow velocities indicative of cerebral vascular obstruction can confirm the diagnosis of acute stroke, expediting the administration of appropriate therapies.

Head Injury

Traumatic brain injury (TBI) remains a significant cause of morbidity and mortality, and the evolving process of TBI is poorly understood. TCD is well-suited to evaluate cerebral blood flow as early as the emergency department or pre-hospital setting. TCD can be used to evaluate the haemodynamics of the cerebral vasculature in TBI patients, permitting real-time visualisation of cerebral vasospasm, as well as signs of increased ICP and altered cerebral perfusion pressure. Following severe head injury, alterations in cerebral blood flow (CBF) velocities may be detected using TCD. The presence of an increased ICP may be demonstrated via TCD waveforms that show an increased PI (due to decreased diastolic and mean velocities).

Subarachnoid Haemorrhage

Cerebral arterial vasospasm is a common and morbid complication of subarachnoid haemorrhage (SAH). Although vasospasm is uncommon in the immediate period following SAH, the presence of increased TCD velocities in the affected arteries may indicate its presence on subsequent evaluation. Although increased flow velocities may suggest the presence of vasospasm, other conditions such as hypertension, hyperaemia and hypervolaemia may also cause alterations in flow velocity. Markedly increased flow velocities of the middle cerebral artery compared to the ipsilateral extracranial internal carotid artery are suggestive of cerebral arterial vasospasm.

Brain Death

Brain death causes high resistance in the distal cerebral vascular bed, resulting in antegrade systolic flow and retrograde diastolic flow, such that an oscillating waveform pattern will be seen on TCD. This may evolve progress to a complete absence of CBF. Although these TCD findings may not be definitive, they may serve as an adjunct in the evaluation of the patient with suspected brain death.

Pearls and Pitfalls

- Take care to properly identify the intracranial vascular structure of interest. Directionality of flow and velocity measurements may vary significantly with the vessel being interrogated.
- Avoid relying on a single TCD examination in the evaluation of patients with suspected elevated ICP or vasospasm. Trends in cerebral arterial velocity measurements over time provide additional diagnostic information.
- TCD techniques require advanced training in the use of Doppler, and experience in recognition of cerebral anatomy. As in other ultrasound modalities, operator training and experience are important factors in obtaining adequate diagnostic information.
- It is important to recognize when a TCD exam is limited or inadequate. Limitations may be due to poor acoustic windows, as well as to an inability to visualize distal portions of intracranial arteries.

Further Reading

Aaslid, R., Huber, P., Nornes, H. (1984) Evaluation of cerebrovascular spasm with transcranial Doppler ultrasound. *J. Neurosurg.*, **60**, 37–41.

American College of Radiology (ACR); Society for Pediatric Radiology (SPR); Society of Radiologists in Ultrasound (SRU) (2012) AIUM practice guideline for the performance of a transcranial Doppler ultrasound examination for adults and children. *J. Ultrasound Med.*, **31** (9), 1489–1500.

Bellner, J., Romner, B., Reinstrup, P., Kristiansson, K.A., Ryding, E., Brandt, L. (2004) Transcranial Doppler sonography pulsatility index (PI) reflects intracranial pressure (ICP). *Surg. Neurol.*, **62** (1), 45–51; discussion 51.

Goertler, M., Kross, R., Baeumer, M., Jost, S., Grote, R., Weber, S., *et al.* (1998) Diagnostic impact and prognostic relevance of early contrast-enhanced transcranial color-coded duplex sonography in acute stroke. *Stroke*, **29** (5), 955–962.

Kassab, M.Y., Majid, A., Farooq, M.U., Azhary, H., Hershey, L.A., Bednarczyk, E.M., Graybeal, D.F., Johnson, M.D. (2007) Transcranial Doppler: an introduction for primary care physicians. *J. Am. Board Fam. Med.*, **20** (1), 65–71

Katz, M.L., Alexandrov, A.V. (2003) A Practical Guide to Transcranial Doppler Examinations, in *Littleton Guide to Transcranial Doppler Examinations*, Littleton-Summer Publishing, pp. 25–48.

Kirsch, J.D., Mathur, M., Johnson, M.H., Gowthaman, G., Scoutt, L.M. (2013) Advances in transcranial Doppler US: imaging ahead. *Radiographics*, **33** (1), E1–E14.

Marshall, S.A., Nyquist, P., Ziai, W.C. (2010) The role of transcranial Doppler ultrasonography in the diagnosis and management of vasospasm after aneurysmal subarachnoid hemorrhage. *Neurosurg. Clin. North Am.*, **21** (2), 291–303.

Nicoletto, H.A., Burkman, M.H. (2009) Transcranial Doppler series part III: interpretation. *Am. J. Electroneurodiagnost. Technol.*, **49** (3), 244–259.

Ojha, B.K., Jha, D.K., Kale, S.S., Mehta, V.S. (2005) Trans-cranial Doppler in severe head injury: evaluation of pattern of changes in cerebral blood flow velocity and its impact on outcome. *Surg. Neurol.*, **64** (2), 174–179; discussion 179.

Prunet, B., Asencio, Y., Lacroix, G., Montcriol, A., Dagain, A., Cotte, J., Esnault, P., Boret, H., Meaudre, E., Kaiser, E. (2012) Noninvasive detection of elevated intracranial pressure using a portable ultrasound system. *Am. J. Emerg. Med.*, **30** (6), 936–941.

Shafé, M., Blaivas, M., Hooker, E., Straus, L. (2004) Noninvasive intracranial cerebral flow velocity evaluation in the emergency department by emergency physicians. *Acad. Emerg. Med.*, **11** (7), 774–777.

Sloan, M.A., Alexandrov, A.V., Tegeler, C.H., Spencer, M.P., Caplan, L.R., Feldmann, E., *et al.* (2004) Therapeutics and Technology Assessment Subcommittee of the American Academy of Neurology. Assessment: transcranial Doppler ultrasonography: Report of the Therapeutics and Technology Assessment Subcommittee of the American Academy of Neurology. *Neurology*, **62** (9), 1468–1481.

Tazarourte, K., Atchabahian, A., Tourtier, J.P., David, J.S., Ract, C., Savary, D., Monchi, M., Vigué, B. (2011) Pre-hospital transcranial Doppler in severe traumatic brain injury: a pilot study. *Acta Anaesthesiol. Scand.*, **55** (4), 422–428.

White, H., Venkatesh, B. (2006) Applications of transcranial Doppler in the ICU: a review. *Intensive Care Med.*, **32** (7), 981–994.

20

Ocular Ultrasound

Anumeha Singh and Dietrich von Kuenssberg Jehle

Introduction

Many patients come to the emergency department with complaints of visual change or loss, ocular trauma, eye pain or other conditions that necessitate an accurate assessment of the eye and/or orbit. A number of techniques are available to aid the physician, including direct ophthalmoscopy, slit-lamp examination and tonometry. Bedside ultrasound offers a way to assess and record information about the eye not previously possible with these other modalities.

Ultrasound has been used by ophthalmologists for several decades. As multi-purpose, high-frequency probes are now available for many of the portable ultrasound machines found in emergency departments, emergency physicians take advantage of these diagnostic capabilities and perform bedside ultrasound ocular examinations as their scope of practice.

With the correct equipment and some practice, the emergency physician and ophthalmologist can learn to assess causes of acute non-traumatic visual loss, such as vitreous haemorrhage, vitreous detachment and retinal detachment. Traumatic problems can also be evaluated, including foreign body penetration and lens subluxation or dislocation. Structures posterior to the eye can also be imaged, especially if there is diagnostic uncertainty for retrobulbar air or haemorrhage. Knowing the normal appearance of these structures and the changes corresponding to various conditions can help the physician identify orbital cellulitis or increased intracranial pressure.

Scanning Techniques

Equipment

While specialised ocular probes are available and used commonly by ophthalmologists, they are rarely found in the emergency department. Today, however, many emergency department machines are fitted with linear, high-frequency probes that are typically capable of frequencies ranging from 5 to 15 MHz and are normally used for ultrasound-guided vascular access. This is the type of transducer that would be most commonly used for ocular scanning in the emergency department.

Technique

Patient Preparation

- *Closed eyelid* technique (Figure 20.1). The *open eye* technique is usually reserved for comprehensive ophthalmology ultrasound evaluations and requires local anaesthesia of the eye surface.

Emergency Point-of-Care Ultrasound, Second Edition. Edited by James A. Connolly, Anthony J. Dean, Beatrice Hoffmann and Robert D. Jarman.

Companion website: www.wiley.com/go/connolly/ultrasound

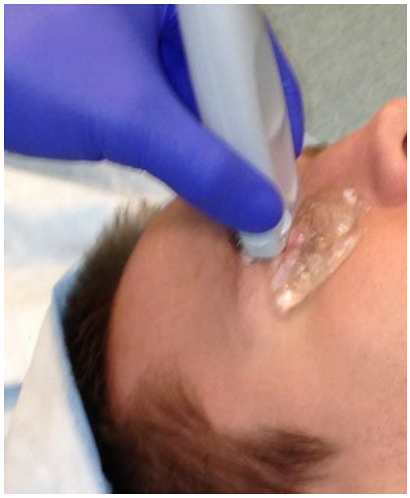

Figure 20.1 Closed-eye lid technique. A copious amount of gel is applied to the closed eye and the probe is placed over the area of interest, without making contact with the skin surface.

- The patient may be examined in an *upright, semi-erect or supine position*, depending on what the situation allows.
- A generous amount of gel should be applied to the upper eyelid to ensure proper contact and wave transmission. A stand-off pad can be used if feasible.

Transducer/Scanning

- Scanning across (*fanning motion*) the entire orbit in perpendicular planes accompanied by extraocular eye movements to both sides and up and down allows for thorough evaluation of the entire orbit.
- *Probe orientation*: There are three basic orientations in which the globe can be scanned:
  - *Transverse* scanning is accomplished by orienting the probe across the eye, and the patient's gaze usually directed up or down to allow insonation above or below the limbus of the cornea (thereby avoiding the crystalline lens).
  - In the *longitudinal* plane the probe pointer is directed cephalad and scanning can be directed to different parts of the globe with the patient's gaze directed laterally or medially.
  - The *axial* plane is obtained with the probe overlying the cornea and the gaze directed at the probe. Fanning can result in *paraaxial* scans where the lens is bypassed.
- *Evaluation for 'aftermovements'*: These are movements indicative of the mobility of a lesion, and are determined by observing motion following the cessation of rapid eye movement with B-mode scanning. Membranous structures such as vitreous or retinal detachments will display some aftermovement. More solid lesions such as choroidal detachments or tumours do not display aftermovement. The movement observed with vitreous detachments is more prominent and 'jiggly' than that seen with retinal detachments.

Normal Eye Anatomy on Ultrasound

The *anterior chamber* is filled with aqueous humor, and it is normally an anechoic space on ultrasound. Behind the iris lie the *ciliary body* peripherally and the *lens* centrally. The contour and position of the lens can be readily identified with emergency department ultrasound. Detailed visualisation of the anterior chamber is possible with very high-frequency ocular probes (20–60 MHz), but these are usually not available in the emergency department (Figure 20.2).

The *vitreous body* is behind the anterior elements and is seen as a large, normally anechoic structure completely filling the space behind the iris and lens. Its collagen fibres can sometimes be visualised when a high-enough gain is utilised (Figure 20.2).

The *posterior chamber* is comprised of the symmetrical, anechoic vitreous body, and the retina, choroid and sclera. At the posterior surface of the vitreous the retina, choroid and sclera are in contact with each other. However, the retina/choroid is slightly less echogenic than the denser sclera, and thus can occasionally be distinguished as a separate layer. The posterior eye should be a smooth surface without breaks, folds or elevations.

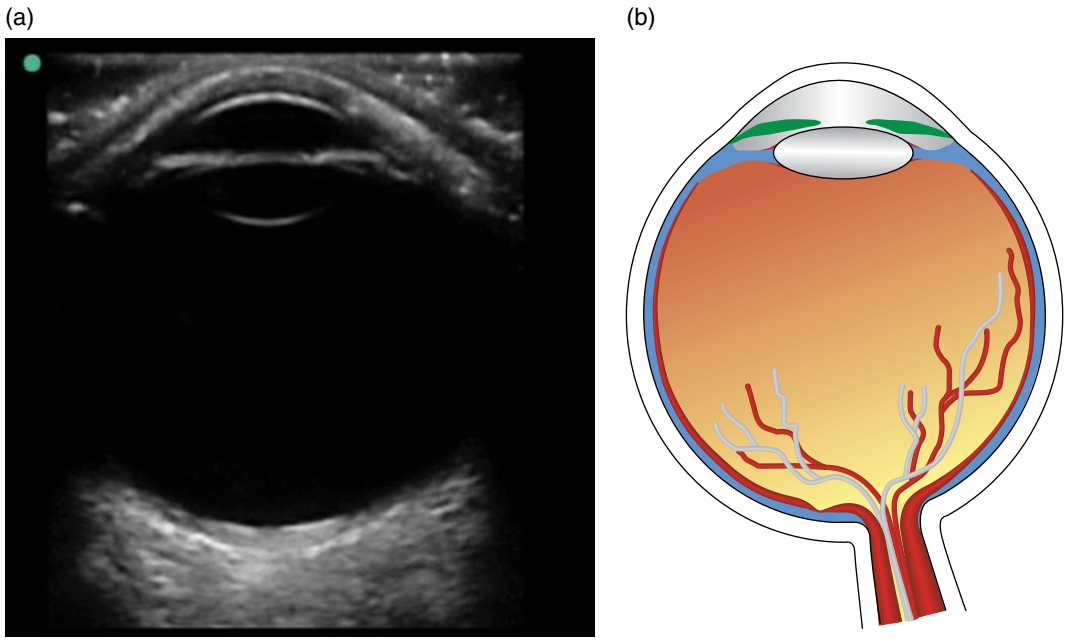

Figure 20.2 (a) Normal ocular ultrasound image. Courtesy of Beatrice Hoffmann, M.D.; (b) Illustration of ocular anatomy. Image courtesy of Matthew Nixon.

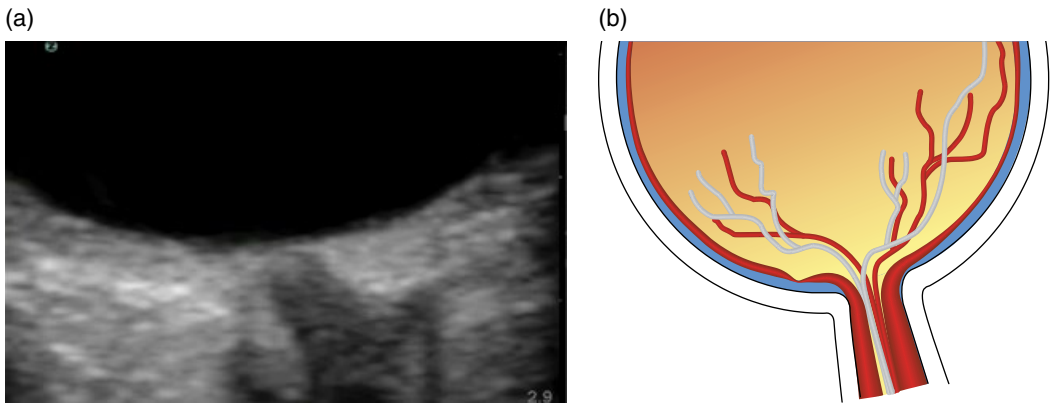

Figure 20.3 (a) Image with focus on the optic nerve. Image courtesy of Beatrice Hoffmann, M.D. (b): Illustration of the optic nerve. Courtesy of Matthew Nixon.

The *optic nerve* is hypoechoic in comparison to the remainder of the extraocular tissues and seen posterior to the vitreous (Figure 20.3).

Orbital vessels can be evaluated with colour Doppler imaging if the examiner has it available on his/her machine and is familiar with its use (Figure 20.4).

Common Ocular Pathologies Visualised on Bedside Ultrasound

Vitreous Haemorrhage

Vitreous haemorrhage can occur secondary to diabetic retinopathy, age-related macular

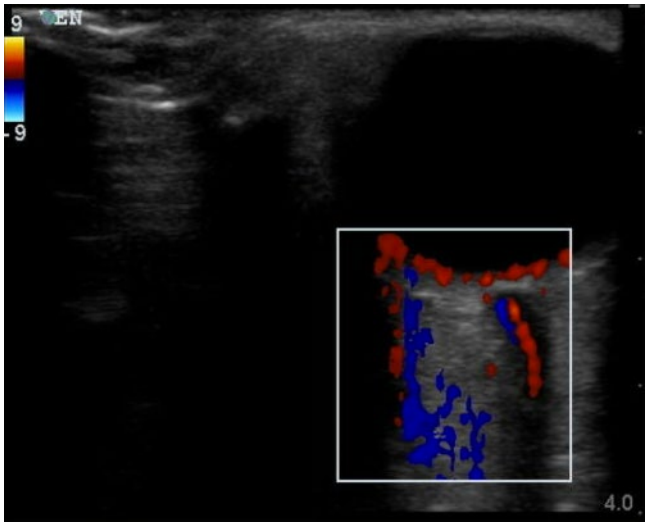

Figure 20.4 Colour Doppler imaging showing central retinal artery and vein within the optic nerve sheath and ciliary artery branches. Image courtesy of Beatrice Hoffmann, M.D.

degeneration, trauma, retinal vein occlusion or retinal tears.

Ultrasound Findings

The normal vitreous is not echogenic (except in the elderly). In the early stages of vitreous haemorrhage, as blood leaks in from the periphery, the vitreous will fill (or partially fill) with small dots and/or short lines of low reflectivity. With increased gain, vitreous fibres may become more apparent and be seen as echogenic structures.

- The appearance of the haemorrhage may differ depending on the time course of the presentation. In general, more severe acute haemorrhage with clot formation has higher echogenicity. Chronic haemorrhage may become less echogenic over time and may display layering or organisation. Eventually, the blood may clump into larger areas of distinct intra-vitreous echodensities.
- The older blood from more severe haemorrhage may also settle to the dependent portion of the globe, forming a thicker, more sonoreflective (echogenic) layer or pseudomembrane in the vitreous. This may give an appearance similar to retinal detachment; however, a pseudomembrane will taper as it extends superiorly. The edges of the pseudomembrane will disappear within the body of the vitreous, rather than having an insertion point into the optic nerve.
- Elderly patients may display diffuse, evenly scattered echoes in their vitreous humor as a normal finding. However, these echoes are very lowly reflective and are usually not noticed unless the gain is increased above normal. In this instance the examiner may confuse the echoes with the possibility of vitreous haemorrhage, but should remember to correlate findings to the clinical history and the opposite eye.

Posterior Vitreous Detachment

Posterior vitreous detachment (PVD) can occur as a result of normal aging (benign condition of the aging eye), trauma, vitreous haemorrhage or inflammation (Figure 20.5).

Ultrasound Findings

- As the edge of the vitreous separates from the retina it is seen by ultrasound as a thin, smooth and somewhat mobile membrane. Movement of the eye should result in a wave-like motion of the vitreous membrane. It may be slightly thicker in the presence of haemorrhage or if inflammatory debris is lying adjacent to the detached membrane.

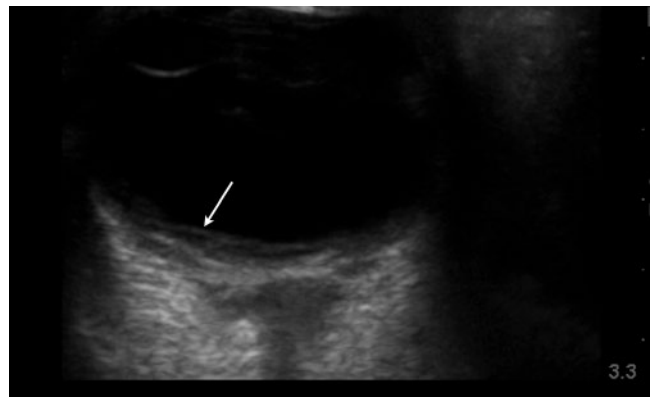

Figure 20.5 Posterior vitreous detachment (arrow) crossing the optic nerve. Image courtesy of Beatrice Hoffmann, M.D.

- The vitreous usually holds firm to the retina at the ora serrata, but may often not be attached. With complete detachment from the optic nerve head one may note a *Weiss ring* – a small ring of tissue (two small densities in cross-section) that usually anchors the membrane to the optic nerve head.
- Acute vitreous detachments tend to demonstrate very 'jiggly' motion, with aftermovement that is more prominent than what is seen with retinal detachments.
- In chronic PVD, the vitreous may become more stiff and dense and may resemble retinal detachment. Differentiation may be difficult and may depend on ophthalmology consultation.

Retinal Detachment

There are a number of potential aetiologies for retinal detachment. These include subretinal fluid accumulation (blood from trauma or tumour, or exudate from uveal effusion or inflammation), traction (from diabetic disease or trauma) or tears. Tears can represent an ocular emergency and occur more commonly in middle-aged or older patients with severe myopia (near-sightedness).

Ultrasound Findings

- When the retina separates from the choroid it is sonographically recognised as a brightly echogenic membrane, tethered at the optic disc and ora serrata, where the retina is most firmly attached. The motion is more restricted than that of PVD, as the retina is more strictly tethered. Mobility decreases with increasing time from detachment. Thus, acute changes in vision due to retinal detachment usually demonstrate a mobile membrane.
  - Always take note of the points of apparent insertion. These should not change as the patient moves the eye or as the examiner scans from multiple angles.
  - The retina may undergo complete detachment in cases of severe trauma, but this is rare.
- When detached, the retina may be perceived as a taut, smooth membrane, but more often it has a folded appearance within the vitreous, somewhat similar to a PVD. However, a detached retinal an almost always be seen tracking to the optic nerve head, and when scanned from multiple angles, with the patient moving the eye, the retinal structure demonstrates minor changes in form, unlike the more fluid and 'jiggly' appearing PVD.
- Extensive detachments may appear funnel- or T-shaped, tracking to the optic nerve (Figure 20.6). The three-dimensional form of the retina will not change much as the patient moves the eye due to the fact that the retina remains attached at the optic nerve.
- Small adhesions will lift the retina at a single point and result in a tent-like appearance, while larger adhesions lift a larger portion of the retina and result in a table-top appearance (Figure 20.7).

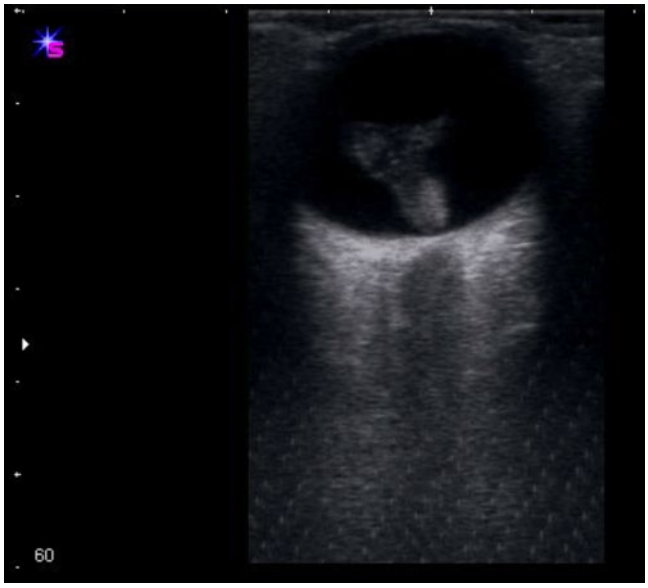

Figure 20.6 Large retinal detachment with retina tethering into optic nerve creating the classic V-shaped appearance.

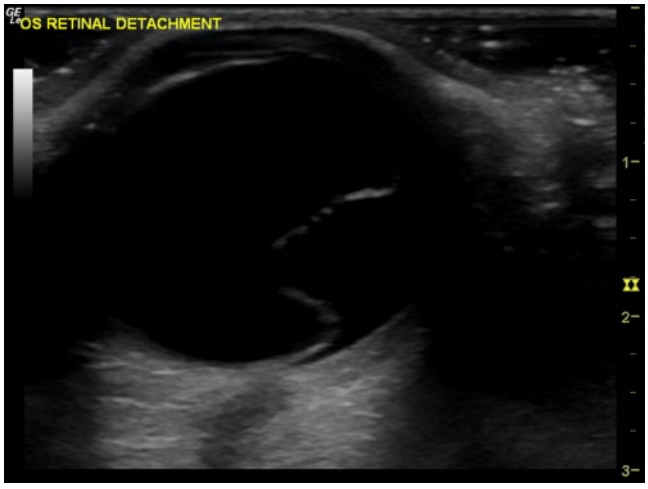

Figure 20.7 Larger retinal detachment with retina folding into the 'tabletop' appearance. Image courtesy of Beatrice Hoffmann, M.D.

Ruptured Globe

With either blunt or penetrating trauma the sclera can be perforated, resulting in a ruptured globe. It is important to note that in a patient with obvious or high suspicion for globe rupture, the application of any pressure to the orbit (as in ocular ultrasound) may lead to the leaking of vitreous fluid, and is contraindicated. If performed, it should be done with great caution using a thick layer of gel so that the transducer is not in contact with the eyelid. A ruptured globe will lead to loss of the usual spherical shape (Figure 20.8). However, in cases where globe rupture is not an initial concern, several echographic clues can assist in the diagnosis, including haemorrhage in the immediate episcleral space, a thickened or detached choroid, a detached retina in the area of concern, vitreous haemorrhage and a scleral buckling.

Ultrasound Findings

- Globe rupture leads to posterior scleral buckling, flattening of the anterior chamber, loss of architecture and flattening of the globe, or

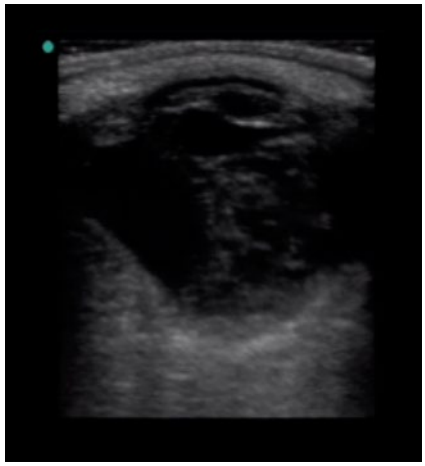

Figure 20.8 Patient with globe rupture. The spherical shape of the globe is disrupted, leading to a loss of architecture.

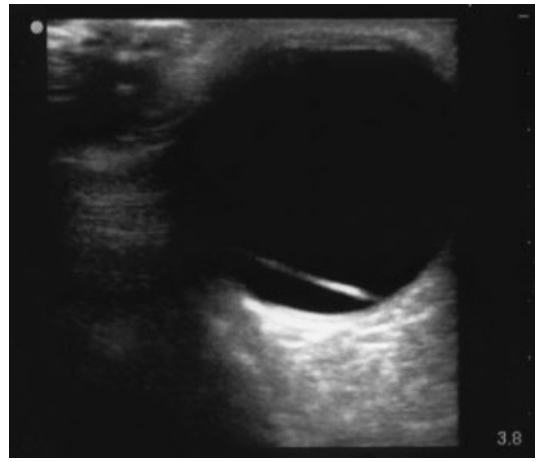

Figure 20.9 Foreign body (glass) found inside the globe.

vitreous haemorrhage (Figure 20.8). In addition, extrusion of the vitreous fluid or retina through the rupture site may be visualised. Blunt trauma may lead to posterior scleral rupture in some cases.

- In penetrating injury, vitreous haemorrhage in the tract of the penetration will either lead to the foreign body being retained within the globe, or will follow through to the exit wound through the posterior sclera.
- A scleral fold may result from penetrating or blunt trauma secondary to loss of vitreous and collapse of the scleral wall.
- Periorbital or intraocular air may be another finding noted with significant trauma.

Penetrating Foreign Body

Often, the penetration of foreign bodies is apparent from the history and external examination of the eye.

Ultrasound Findings

- Ultrasound detection of foreign bodies is highly variable according to the material of which the foreign body is composed, as well as its size and orientation.
- Small penetrating foreign bodies may create an isolated tract of haemorrhage within the vitreous.
- Metallic foreign bodies are highly echogenic and in most cases are easily detected, often with posterior shadowing. Spherical metals, such as BiBi pellets, can produce a great deal of comet-tail artefact.
- Glass shards can be more difficult to detect. The sound waves must strike perpendicular to a flat surface on the glass in order to be reflected back to the probe. Scanning should be done from multiple angles to detect the true placement and size of the piece(s) of glass (Figure 20.9).
- Organic matter, such as wood, will have varying degrees of echogenicity, although they are generally highly reflective in the immediate post-traumatic period.
- As an object penetrates the eye it may introduce eyelashes or small air bubbles into the tract of penetration. Eyelashes produce a bright signal without shadowing. Air bubbles may produce a signal suggestive of a solid foreign body, but the signal moves within the globe as the patient's head is placed in various positions, owing to the lower density of the air. These air bubbles usually resolve in just a few days after the insult.
- Some materials do not have the echogenicity required for ultrasound evaluation. Also, foreign bodies may be difficult to detect when they sit adjacent to the retina. Always correlate

ultrasound findings with the history, the examination by visual field, direct ophthalmoscopy, and other radiographic modalities.
- Although ultrasound can facilitate the diagnosis of intraocular foreign body, even the 'easily detectable' metallic foreign body may be missed on ultrasound.

Lens Subluxation or Dislocation

The lens is suspended behind the pupil by the zonular fibres. Their diameter is larger than that of a widely dilated pupil, so the outer rim of the lens is never visualised in normal eyes. Blunt trauma to the eye can stretch or rupture the zonular fibres, resulting in partial (subluxation) or complete dislocation of the lens.

Lens dislocation should be readily visualised on ultrasound examination, as the lens will move towards the dependent portion of the vitreous chamber.

Ultrasound Findings

- Owing to its superficial location, the lens should be imaged with the highest frequency probe available. A stand-off spacer will allow for a more extensive focal zone.
- The presence of cataracts may increase the echogenicity of the lens.
- Subluxation or dislocation is identified by the location of the lens anywhere other than its normal position directly behind the pupil. It may be subluxed anteriorly, laterally or posteriorly. If the lens has completely dislocated it is usually found floating deep in the vitreous substance or sliding along the surface of the retina.
- A grossly mis-shapen lens after severe blunt trauma suggests lens capsule rupture.

Extraocular Pathology

Optic Nerve Sheath Measurement in Elevated Intracranial Pressure (ICP)

A number of studies have described a correlation between optic nerve sheath diameter (ONSD) and ICP. The optic nerve attaches to the globe posteriorly and is surrounded by a cerebrospinal fluid-filled sheath that communicates with the intracranial cavity. Several studies explored the upper limits of ONSD from normal volunteers, and compared measurements with abnormal subjects. There is some overlap of OSND between the normal and increased ICP groups, however, Kimberly *et al*. reported a sensitivity of 88% and specificity of 93% for an ONSD > 5 mm to detect ICP > 20 cm H_2O in adults with traumatic brain injury. Other studies showed less reliable measurements.

Ultrasound Findings

- The optimal technique is using an axial scan with the eye directed forward.
- When measured at a point 3 mm posterior to the globe, a sagittal line through the optic nerve sheath can be measured. A transverse plane with the patients gaze directed to the feet can also be used (Figure 20.10). Typically each eye is measured two or three times to determine the optic nerve sheath diameter.
- ICP is equally distributed throughout the cranial vault, and transmission into the optic nerve sheath should affect both eyes equally.

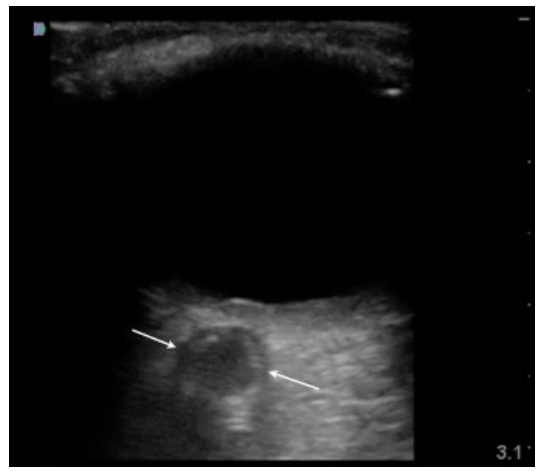

Figure 20.10 Increased optic nerve sheath (arrows) shown as a target-like appearance when viewed in short axis. Image courtesy of Beatrice Hoffmann, M.D.

The finding of increased nerve sheath diameter in only one eye should lead the physician to consider other causes for the finding (e.g., tumour obstructing fluid dynamics in that nerve sheath).

Papilloedema and Pseudotumour Cerebri

Optic nerve sheath measurements may also play a role in patients with suspected pseudotumour cerebri presenting to the emergency department. The ability to diagnose papilloedema using bedside ultrasound is of great utility as fundoscopic findings are late, and the ability to perform an accurate non-dilated fundoscopic examination can be difficult in the emergency department setting. There is evidence that the decrease in ICP after lumbar puncture correlates with sonographically measured decrease in ONSD.

Ultrasound Findings

- The optimal technique is as described above for optic nerve sheath measurement, with the additional finding of a prominent disc protruding into the posterior chamber.

Orbital Cellulitis

Orbital cellulitis is an infection of the post-septal orbital tissues.

Ultrasound Findings

- Attention is given to the tissues behind the globe, and the settings on the ultrasound machine must allow for the proper depth and gain to evaluate these areas.
- The extraocular muscles may appear thickened due to the inflammation of these tissues. Comparison with the contralateral eye may be helpful. Sub-Tenon's space may fill with fluid, resulting in a gap between the sclera and adjacent peri-orbital fat (both highly echogenic).
- The presence of multiple echolucent pockets in the orbital fat suggests an abscess with loculations. It is important to be able to recognise the difference in echogenicity between the muscle tissue and an abscess.

Retrobulbar Haemorrhage or Periorbital Haemorrhage

Peri-ocular trauma may result in the rupture of blood vessels posterior to the eye, but within the orbit. As this is a tightly enclosed space, haemorrhage in the retrobulbar area will initially push the globe forward. Trauma with facial fractures can introduce air into the retro-orbital or peri-orbital space. Air usually appears as hyperechoic lines or speckles with significant reverberation artefacts.

Ultrasound Findings

- Haemorrhage will be noted behind the globe. This will have the appearance of a fluid collection that may vary in echogenicity, depending on the age of the haemorrhage. This may be difficult to identify on ultrasound and can be easily missed if the haemorrhage is of similar echogenicity to that of surrounding structures.

Pearls and Pitfalls

- Stabilizing the examining hand is important to avoid motion artefact. Resting the hand on patient's nose, maxilla, or forehead can help.
- Special care must be taken while examining for global rupture cases as pressure on the globe will worsen the patient's condition.
- Ultrasound artefacts, including shadowing, edge artifact, contact artefact, reverberation artefact and gain artefact, can make interpretation difficult. Conversely, artifacts can also help to identify pathologic findings, for example, metallic foreign bodies produce both posterior acoustic shadowing and reverberation artefact that allows for ready identification within the otherwise echolucent vitreous humor.
- Always evaluate both eyes. If symptoms are unilateral, start with the normal eye to get a sense of the baseline anatomy.

Further Reading

Geeraerts, T., Launey, Y., Martin, L., *et al*. (2007) Ultrasonography of the optic nerve sheath may be useful for detecting raised intracranial pressure after severe brain injury. *Intensive Care Med.*, **33** (10), 1704–1711.

Kilker, B.A., Holst, J.M., Hoffmann, B. (2014) Bedside ocular ultrasound in the emergency department. *Eur. J. Emerg. Med.*, **21** (4), 246–253.

Kimberly, H.H., Shah, S., Marill, K., Noble, V. (2008) Correlation of optic nerve sheath diameter with direct measurement of intracranial pressure. *Acad. Emerg. Med.*, **15**, 201–204.

Newman, W.D., Hollman, A.S., Dutton, G.N., *et al.* (2002) Measurement of optic nerve sheath diameter by ultrasound: a means of detecting acute raised intracranial pressure in hydrocephalus. *Br. J. Ophthalmol.*, **86** (10), 1109–1113.

Singleton, J., Dagan, A., Edlow, J.A., Hoffmann, B. (2015) Real-time optic nerve sheath diameter reduction measured with bedside ultrasound after therapeutic lumbar puncture in a patient with idiopathic intracranial hypertension. *Am. J. Emerg. Med*., **33** (6), 860; e5–e7.

Tayal, V.S., Neulander, M., Norton, H.J., *et al.* (2007) Emergency department sonographic measurement of optic nerve sheath diameter to detect findings of increased intracranial pressure in adult head injury patients. *Ann. Emerg. Med.*, **49** (4), 508–514.

21

Airway/Ear, Nose and Throat (ENT) Sonography

Barton Brown and Srikar Adhikari

Introduction

Pain of the head and neck region, odynophagia, hoarseness, facial swelling and neck swelling are common problems and frequent causes of presentation to acute-care facilities. The aetiologies are numerous for these conditions, which vary in their need for urgent treatment. Patients with common conditions such as pharyngitis, tonsillitis, uncomplicated sialolithiasis and lymphadenitis can be treated as outpatients, employing symptomatic treatment or oral antibiotics. Other conditions such as peritonsillar abscesses, dental abscess, other deep-space facial abscesses and complicated facial fractures require urgent treatment. Clinical findings in patients presenting with face, neck or throat pain and swelling can be variable and difficult to distinguish.

Focused ear, nose and throat (ENT) sonography has emerged as an extremely valuable diagnostic tool for the rapid evaluation of facial and neck complaints that include odynophagia/dysphagia, facial swelling, neck masses and facial trauma. Ultrasound may reveal abscesses not identified with the physical examination. Ultrasound can also be used to reveal the pathology of a variety of other facial structures that may not be obvious on examination, including lymphadenitis, salivary gland pathology, thyroid pathology and other neck masses. In symptomatic patients with a subcutaneous mass, ultrasound can be used to successfully differentiate between adenitis, cellulitis and abscess.

Sonography is also a useful adjunct in the setting of facial trauma, where it can be used to evaluate for various facial fractures. Additionally, focused ultrasound can facilitate the ocular evaluation when fractures, swelling and bleeding make this difficult, or even impossible, from a clinical standpoint.

Scanning Technique

Probe Selection and Settings

Most of the structures of interest are superficially located, and do not require as much ultrasound penetration. This allows for the use of higher-frequency transducers, which enhance resolution and image quality. A 7.5–10 MHz linear transducer (or higher frequency if available) is commonly used. The small parts preset is most commonly used for the careful evaluation of superficial structures. If the area of interest is very superficial, an acoustic stand-off pad can be used to improve image resolution. For intraoral imaging, endocavitary transducers combine the benefits of a high-frequency transducer with a small footprint that can be placed in direct contact with the tonsils.

Emergency Point-of-Care Ultrasound, Second Edition. Edited by James A. Connolly, Anthony J. Dean, Beatrice Hoffmann and Robert D. Jarman.

Companion website: www.wiley.com/go/connolly/ultrasound

General Technique

The area of interest is usually visualised in at least two planes – typically the longitudinal plane and the transverse plane. Efforts should also be made to identify adjacent structures such as vessels, nerves and lymphatic tissue. The identification and mapping-out of adjacent structures can help to minimise complications if procedural intervention is required. Finally, the depth of the structures of interest should be noted, as this can facilitate drainage, if required.

Evaluation of Subcutaneous Masses

Ultrasound can be used to determine whether masses are cystic, solid or complex. Cystic or fluid-filled components are typically hypoechoic or anechoic, while solid masses can have a variety of sonographic appearances. Complex masses will have characteristics of both.

Odynophagia and Dysphagia

Peritonsillar Abscess

Peritonsillar abscess (PTA) is the most common deep infection of the head and neck (Figure 21.1a), most commonly affecting young adults. PTA typically forms in the superior pole of the tonsil, most often from the progression of an adjacent tonsillitis or the obstruction of Weber glands in the superior tonsil.

Diagnosis

Clinical differentiation of PTA from peritonsillar cellulitis can be difficult, leading to the need for imaging or for blind-needle aspiration. The latter technique has a reported false-negative rate of 10–24% and also risks complications such as puncturing of the carotid arteries, jugular veins or parotid gland. The main imaging modalities for PTA diagnosis are computed tomography (CT) and intraoral ultrasound. Intraoral ultrasonography is non-invasive and can be rapidly performed at the bedside in the emergency room. Other benefits include a lack of ionising radiation and cost-benefit advantages compared to CT. If a PTA is identified, real-time ultrasound can be used for procedural guidance. This allows the emergency physician to track the entire course of the needle and prevent complications such as puncturing the carotid artery.

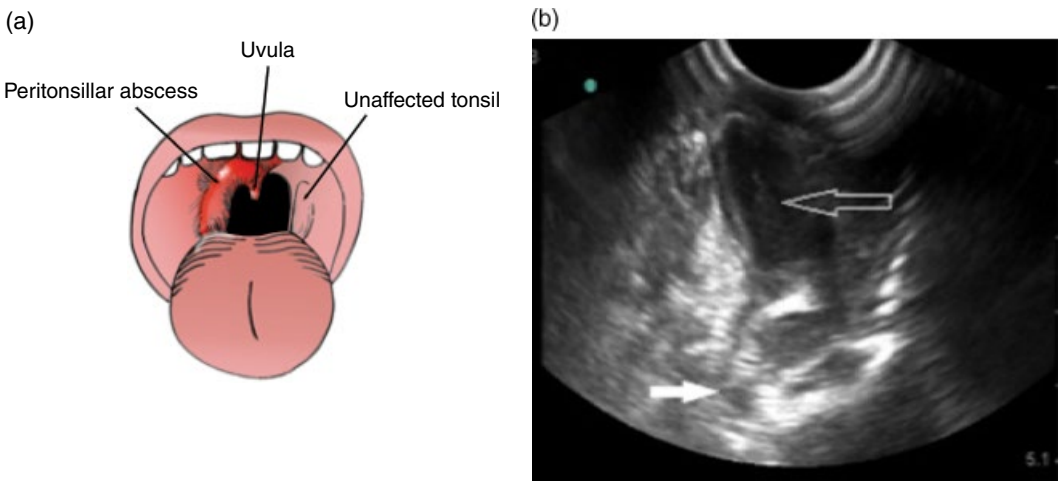

Figure 21.1 (a) Anatomical illustration of a peritonsillar abscess (PTA). (b) Appearance of a PTA obtained with an endocavitary probe. The hypoechoic area within the tonsil is the abscess cavity (open arrow). The internal carotid artery can be seen in the far field (solid arrow). Colour Doppler can be applied as needed to differentiate the artery from surrounding structures (not shown in this image). Figure reproduced with permission from Matthew Nixon.

Management

Pooled data from the best available prospective studies have not shown any significant differences in the initial success rates of blind-needle aspiration and incision and drainage. The initial success rates were 91.6% and 93.7%, respectively. Multiple studies have demonstrated the ability of the emergency physician to effectively use intraoral ultrasound for both the diagnosis of PTA and procedural guidance for needle drainage.

Technique

The endocavity probe can be covered with either a glove or condom and placed into the oral cavity over the area in question, after adequate topical and systemic analgesia has been administered. During the ultrasound evaluation of a PTA, the carotid artery and its relationship to the abscess cavity should be identified (Figure 21.1b). The carotid artery is generally located posterolateral to the tonsil and within 5–25 mm of a PTA. The use of Doppler can help to identify the carotid artery if it is not readily apparent. A PTA most commonly appears as a hypoechoic or complex cystic mass sonographically, typical of most abscesses. Once the abscess is identified, an 18-gauge, 2-inch (5 cm) needle can be inserted and aspirated under ultrasound guidance (Figure 21.2).

Epiglottitis

The epiglottis is structure that is readily evaluated by ultrasound by placing a high-frequency transducer on the anterior neck above the larynx. A prospective study evaluating 100 adult patients revealed the average epiglottic thickness to be 2.39 ± 0.15 mm. Case reports have described the evaluation of patients with suspected epiglottitis using ultrasound. This may prove to be a beneficial modality, particularly in cases where CT and laryngoscopy are not available, or the patient is too unstable for transport.

Swelling and Pain in the Face and Neck

Facial Abscesses

Facial abscesses are commonly encountered in the acute setting. Differentiating abscesses from cellulitis and other causes of facial swelling by clinical examination can be difficult, and imaging is often required to distinguish these entities. Bedside ultrasound is a valuable tool in these patients as it can not only be used to identify whether an abscess is present but also is reliable in detecting the stage of infection in patients with superficial facial swelling. Adjacent structures such as arteries, veins and

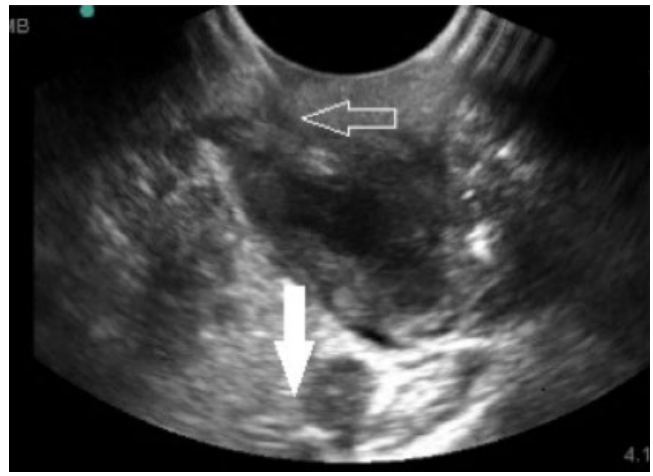

Figure 21.2 Ultrasound-guided PTA drainage. The hyperechoic needle (open arrow) can be seen entering the abscess cavity. The carotid artery can be seen in the far field (solid arrow). Vascular structures and the needle should both be visualised to help prevent inadvertent vascular puncture.

nerves can be mapped-out and avoided. If drainage is indicated, ultrasound then can be used for real-time procedural guidance. Following drainage, ultrasound can be used to re-assess the area to determine if adequate drainage has been accomplished.

Ultrasound Findings

Abscesses can take on a variety of ultrasound appearances, depending on the internal nature of the abscess cavity. Variable combinations of liquid and solid components may be seen. Abscesses that are mostly liquefied tend to have a more hypoechoic or anechoic appearance. The most common appearance of an abscess is a hypoechoic mass relative to adjacent structures (Figures 21.3). Necrotic debris or tissue appears as complex masses with variable echogenicity. Septae and gas may also be found within the abscess (Figure 21.4). Gentle pressure on an abscess may reveal movement of swirling of the liquid components (Video 21.1). Colour Doppler may show hyperaemia adjacent to the abscess cavity and an absence of flow within it. Once the abscess is identified, ultrasound can be used to drain the abscess in real time. The abscess area can also be re-assessed after or during drainage, to ensure that it is adequately drained.

Siailolithiasis/Sialoadenitis

Infection of the parotid gland can occur from viral (usually mumps virus) or bacterial (usually *Staphylococcus* sp.) pathogens. Sialoadenitis in adults is associated in approximately 50% of cases with sialolithiasis. More than 80% of salivary concretions are localised in the submandibular gland or in Wharton's duct, while approximately 15% of cases occur in the parotid gland or in Stensen's duct. Sublingual lithiasis is rare.

Sonographic Findings

Sialolithiasis can be identified by visualisation of the calculus, which typically demonstrates acoustic shadowing, along with dilation of the salivary ducts (Figures 21.5a and b). Differentiation of the salivary ducts from vessels can be aided with the use of colour Doppler (Figure 21.5c). Parotid gland inflammation is

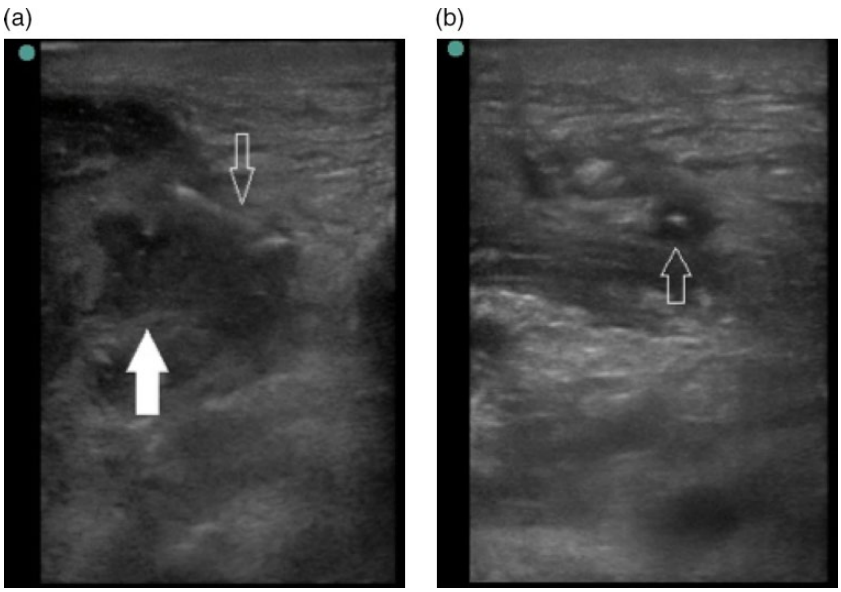

Figure 21.3 Complex fluid collection in the neck of a patient who reported the use of intravenous drugs. (a) Needle fragment detected in the superior portion of the abscess (open arrow), the needle is shown in longitudinal view. (b) Transverse image of the needle fragment (open arrow), surrounded by anechoic fluid (solid arrow).

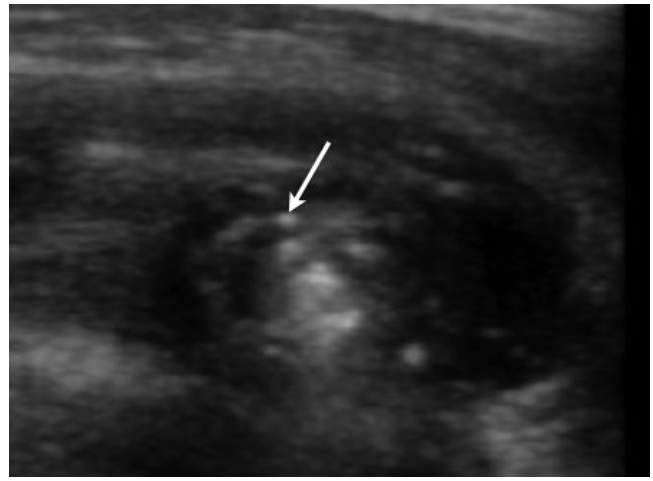

Figure 21.4 Complex fluid collection with internal gas. The acoustic mismatch from the gas within the abscess appears as brightly echogenic spots with irregular 'dirty' shadowing (arrow).

typically visualised as a diffusely enlarged gland with decreased echogenicity. Colour Doppler will typically show hyperaemia of the gland with infection. Intraglandular lymph nodes may be observed with a parotid gland infection. With bacterial parotitis, abscesses can develop within the parotid gland. Ultrasound can be particularly useful for guiding the needle drainage of these abscesses. With chronic glandular inflammation, ductal ectasia can develop.

Neck Masses

Ultrasound is a useful imaging modality in the assessment of neck masses, as it can be used to differentiate abscesses from cervical lymphadenitis, or abnormal enlarged lymph nodes or solid masses. It can also differentiate cystic from solid masses (Figure 21.6). Other neck masses that may be visualised by sonography include thyroid enlargement or masses, vascular abnormalities, salivary gland pathology and congenital abnormalities.

Sonographic Findings: Neck Masses

Grey scale and Doppler sonographic features are helpful in differentiating neck masses. Useful grey-scale features include size, shape, echogenicity and calcification. Solid masses can have a variety of appearances, depending on the aetiology. Cystic masses generally have an anechoic appearance, which is the sonographic appearance of most fluid-filled structures. Haemorrhage, infection and septations can all alter the sonographic appearance of cysts. Thyroglossal cysts and branchial cleft cysts are common causes of neck masses. Thyroglossal cysts are generally found medially, while branchial cleft cysts are found laterally.

Sonographic Findings: Lymphadenitis

Lymphadenitis appears as a hypoechoic mass with hilar vascularity demonstrated with Doppler ultrasound. Abscess cavities, on the other hand, do not demonstrate flow. Normal reactive lymph nodes are predominantly hypoechoic when compared with the surrounding structures. The use of colour Doppler has shown that metastatic lymph nodes have unique vascular patterns.

Facial Trauma

Facial Fractures

Ultrasound has been used to evaluate for fractures in the nasal bones and other facial fractures. Higher-frequency probes (15–30 MHz) are typically utilised for the evaluation of superficial facial bones; this enhances resolution as the areas of interest do not require much penetration.

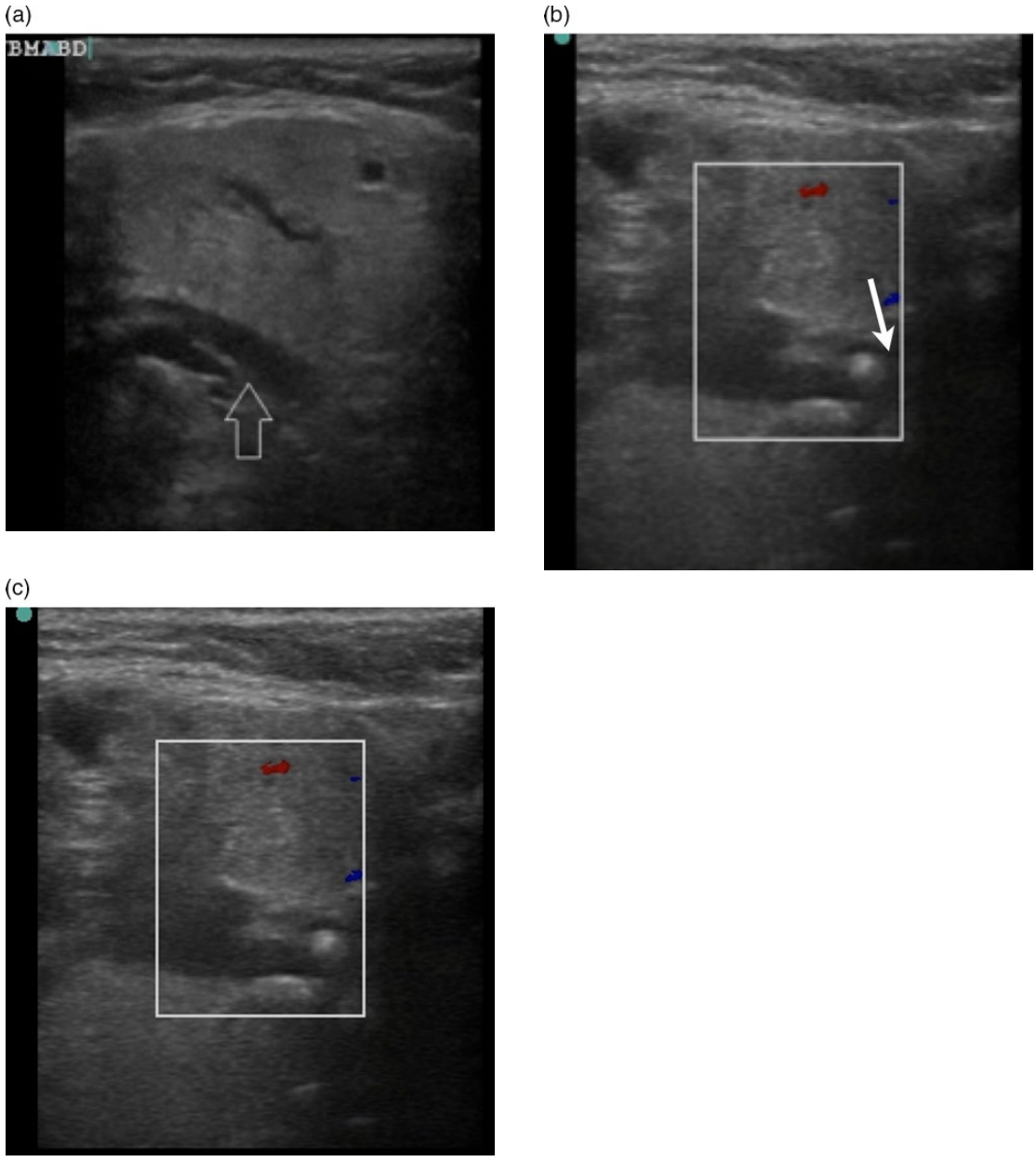

Figure 21.5 Images of the submandibular gland of a patient presenting with acute left lower face pain and swelling. (a) The proximal portion of Wharton's duct (open arrow), which was dilated. (b) Following the duct distally revealed the echoic obstructing calculus (arrow), with posterior acoustic shadowing. (c) Colour Doppler was applied but revealed no flow in the duct. Doppler can be used to help differentiate ductal structures from vessels.

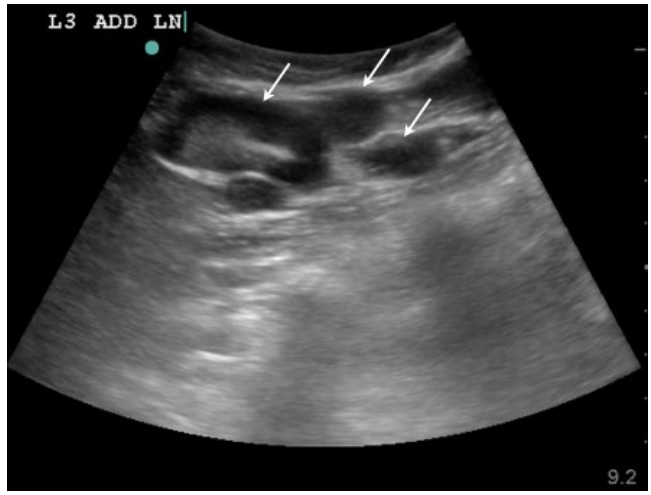

Figure 21.6 Several significantly enlarged lymph nodes in the lower anterior neck in a patient with lymphoma. Image courtesy of Beatrice Hoffmann MD.

Ocular Evaluation In Facial Trauma

Ultrasound can also be used to evaluate for pupillary reactivity and extraocular movements when significant facial trauma, facial fractures or swelling impede direct evaluation. Using a 7.5–10 MHz transducer, extraocular movements can be observed in real time. The evaluation of pupillary reactivity can be seen by shining a light in the unaffected eye and observing for a consensual response (Video 21.2).

Further Reading

Blaivas, M., Theodoro, D., Duggal, S. (2003) Ultrasound-guided drainage of peritonsillar abscess by the emergency physician. *Am. J. Emerg. Med.*, **21**, 155–158.

Dewitz, A. (2003) Soft tissue applications, in *Emergency Ultrasound* (eds O.J. Ma, J. Mateer), McGraw-Hill, New York, p. 385.

Galioto, N.J. (2008) Peritonsillar abscess. *Am. Family Phys.*, **77** (2), 199–202.

Hirai, T., Manders, E.K., Nagamoto, K., Saggers, G.C. (1996) Ultrasonic observation of facial bone fractures: report of cases. *J. Oral Maxillofac. Surg.*, **54** (6), 776–779; discussion 779–780.

Jenkins, C.N., Thuau, H. (1997) Ultrasound imaging in assessment of fractures of the orbital floor. *Clin. Radiol.*, **52** (9), 708–711.

Johnson, R.F., Stewart, M.G. (2005) The contemporary approach to diagnosis and management of peritonsillar abscess. *Curr. Opin. Otolaryngol. Head Neck Surg.*, **13** (3), 157–160.

Johnson, R.F., Stewart, M.G., Wright, C.C. (2003) An evidence-based review of the treatment of peritonsillar abscess. *Otolaryngol. Head Neck Surg.*, **128** (3), 332–343.

Katz, P. (2009) Clinical ultrasound of the salivary glands. *Otolaryngol. Clin. North Am.*, **42** (6), 973–1000.

Lyon, M., Blaivas, M. (2005) Intraoral ultrasound in the diagnosis and treatment of suspected peritonsillar abscess in the emergency department. *Acad. Emerg. Med.*, **12**, 85–88.

Peleg, M., Heyman, Z., Ardekian, L., Taicher, S. (1998) The use of ultrasonography as a diagnostic tool for superficial fascial space infections. *J. Oral Maxillofac. Surg.*, **56** (10), 1129–1131.

Promes, M. (1997) Miscellaneous applications, in *Ultrasound in Emergency and Ambulatory Medicine* (eds B. Simon, E. Snoey), Mosby, St Louis, p. 250.

Thiede, O., Krömer, J.H., Rudack, C., Stoll, W., Osada, N., Schmäl, F. (2005) Comparison of ultrasonography and conventional radiography in the diagnosis of nasal fractures. *Arch.*

Otolaryngol. Head Neck Surg., **131** (5), 434–439.

Werner, S.L., Jones, R.A., Emerman, C.L. (2004) Sonographic assessment of the epiglottis. *Acad. Emerg. Med.*, **11** (12), 1358–1360.

Ying, M., Ahuja, A., Brook, F., Metreweli, C. (2001) Vascularity and grey-scale sonographic features of normal cervical lymph nodes: variations with nodal size. *Clin. Radiol.*, **56**, 416–419.

Part 3

Paediatrics

22

Paediatric Musculoskeletal Point-of-Care Ultrasound

Paul Atkinson and Peter Ross

Introduction

Point-of-care ultrasound (PoCUS) has a number of indications in paediatric musculoskeletal (MSK) conditions, and provides many advantages over traditional imaging and diagnostic techniques. In general, PoCUS can be used to evaluate disease processes at the bedside, provide real-time information, is relatively low-cost and is more widely available than other modalities such as computed tomography (CT) scanning and magnetic resonance imaging (MRI). In paediatric populations, ultrasound can be particularly useful given that sedation is not required, there is no risk of ionising radiation, and ultrasound is uniquely suited for the visualisation and evaluation of the immature (i.e., cartilaginous) skeleton.

Ultrasound has a number of conventional uses in developmental MSK disease, including developmental dysplasia of the hip (DDH), foot anomalies and soft-tissue masses. However, in this chapter attention will be focussed on PoCUS and its application to more acute presentations, including infectious, inflammatory and traumatic conditions. For a discussion of PoCUS in the management of paediatric fractures, see Chapter 28.

Technique

The relatively superficial position of most MSK structures makes a high-frequency (9–17 MHz) linear-array probe ideal for the evaluation of most paediatric MSK conditions. The high-frequency probe maximises image detail in superficial areas, while lower-frequency probes that allow deeper penetration may be required to visualise deeper structures such as the hip or structures in older or obese children. Additionally, a probe with a relatively small footprint is preferred for paediatric applications because of the children's decreased size. As with any examination, optimal patient position and comfort are key, and PoCUS should be performed in a quiet room with the child's caregivers at the bedside. In terms of examiner technique, adequate ultrasound gel, appropriate probe manipulation (including positioning the probe perpendicular to the structure of interest), probe stabilisation using the hypothenar eminence and little finger of the examiner's hand, as well as multi-angle views to evaluate for anisotropy, are all important to obtaining high-quality clinically useful ultrasound images. The use of a water bath or small bag of saline between the probe and skin can be useful for

Emergency Point-of-Care Ultrasound, Second Edition. Edited by James A. Connolly, Anthony J. Dean, Beatrice Hoffmann and Robert D. Jarman.

Companion website: www.wiley.com/go/connolly/ultrasound

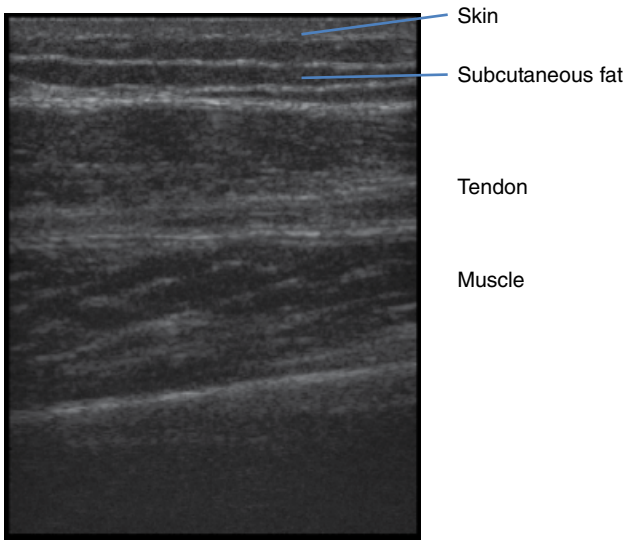

Figure 22.1 Normal muscle and tendon appearance.

visualising superficial structures, as the very near field may not include the skin. In order to maximise the information obtained it is important to take advantage of the dynamic nature of PoCUS and evaluate points of maximal tenderness, observe bones and tissues through a range of motion where appropriate, and compare contralateral structures, which can provide an invaluable normal comparison image.

Normal Anatomy

The anatomy specific to each condition will be discussed later, but a basic description of MSK anatomy from superficial to deep structures should prepare the reader for the more detailed discussions to follow. The skin (epidermis and dermis) appears as an echogenic outer layer with an underlying layer of hypoechoic subcutaneous fat. Additional connective tissue may appear as mildly echogenic streaking throughout the hypoechoic subcutaneous fat, and a thin layer of echogenic fascia overlies the striated muscle that has a 'marbled appearance', appearing as a slightly deeper grouping of multiple linear echogenic structures (fibrous septations) separated by hypoechoic muscle parenchyma (see Figure 22.1). Bones take on easily recognised shapes defined by hyperechoic cortex with posterior shadowing, while ligaments appear as echogenic fibrillar structures in tranverse planes (see Figure 22.2). Tendons also appear as fibrillar structures in traverse planes, but true to function take on an appearance of multiple linear structures, appearing similar to thinner muscle tissue often tapering to muscle insertion sites. Finally, normal cartilage appears hypoechoic with demarcations from the surrounding joint space and bone while immature cartilage is hypoechoic, sometimes with very thin hyperechoic margins.

Skin and Soft-Tissue Infection

PoCUS can be useful in the diagnosis, evaluation and also often the treatment of paediatric skin and soft-tissue infections. Common entities evaluated are cellulitis, abscess and acute haematogenous osteomyelitis.

Cellulitis is normally clinically apparent, but PoCUS can be helpful in following progress of the infection, and especially in identifying an abscess that may require drainage. In its early stages, cellulitis may appear normal on ultrasound, but with progression an increased echogenicity of the subcutaneous fat appears causing

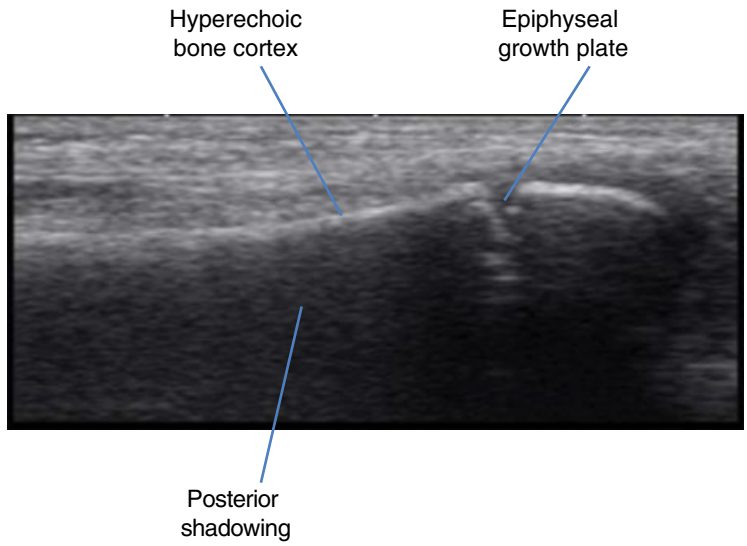

Figure 22.2 Normal long bone appearance.

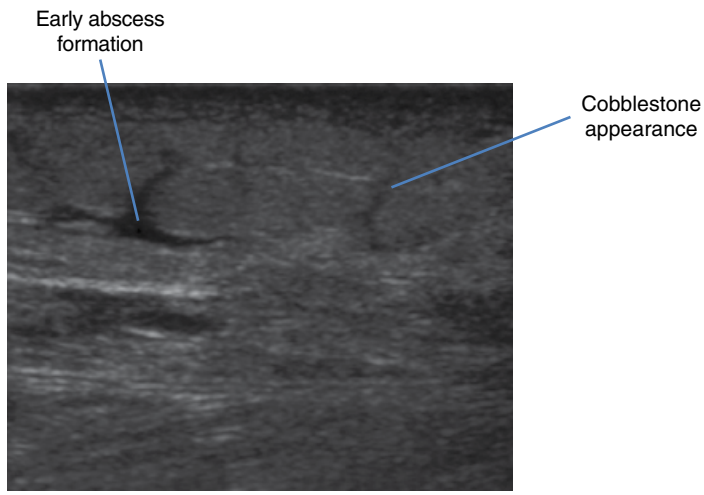

Figure 22.3 'Cobblestoning' of the subcutaneous tissue, as seen in cellulitis with small hypoechoic areas representing early abscess formation.

loss of the interface between fat and dermis. Abscesses appear as hypoechoic (dark) discrete collections (Figure 22.3).

Acute haematogenous osteomyelitis may present with fever, pain or sepsis. It may also present with non-specific symptoms, or associated with an overlying persistent soft-tissue infection. PoCUS in evaluation is limited but it can be useful when other modalities are not practical, and it is the best option for finding pus that may be drained. Changes seen in ultrasound include a periosteal reaction, the presence of subperiosteal abscesses, and increased vascularity. Periosteal reaction and subperiosteal abscesses are seen as hypoechoic collections of fluid, increased vascularity is assessed with colour flow Doppler (Figure 22.4).

Foreign Body

Retained foreign bodies (FBs) can be difficult to diagnose in children and are often initially missed, causing pain, overlying cellulitis, and

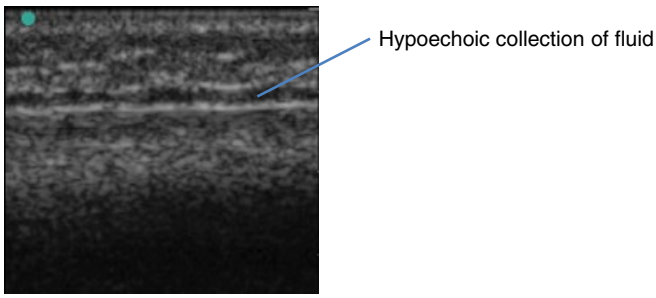

Figure 22.4 Periosteal reaction.

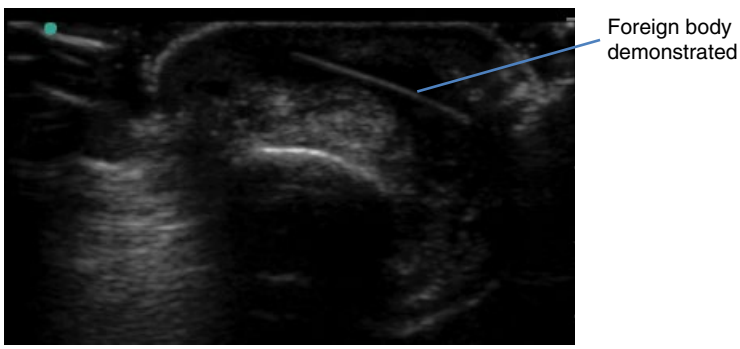

Figure 22.5 PoCUS demonstrating a subcutaneous foreign body.

sometimes abscess formation. Investigations using radiography will reveal radio-opaque materials such as metal and occasionally glass, but PoCUS can also demonstrate radiolucent glass, wood and plastic FBs. An ultrasound examination of FBs may also demonstrate a posterior or inferior shadow, making localisation easier than fluoroscopic examination. Ultrasound can also be used in real time to guide and confirm FB removal; this can be done either by guiding two locating needles to mark the FB, or by directly visualising forceps approaching the FB (Figure 22.5).

Dislocation/Subluxation

The most common dislocation/subluxation in children is subluxation of the radial head, often referred to as 'pulled elbow' or 'nursemaid's elbow'. This injury commonly occurs during maximal extension and traction of the arm (e.g., when a child is swung around with arms in extension). Although pulled elbows are often reduced without anaesthesia or imaging, the injury commonly involves a small avulsion of the olecranon and radiography, and ultrasound can be helpful in diagnosis and reduction. In radial head subluxation, the radial head slips out from underneath the overlying annular ligament and an increase in the distance between the radial head and capitellum can be observed (particularly during pronation) on ultrasound, as well as annular ligament tear and dynamic relocation. The second most common paediatric dislocation is anterior shoulder dislocation that predominantly occurs in adolescents. PoCUS may be helpful in confirming this injury and subsequent reduction, using the same technique as described for adults. The use of PoCUS has also been described in the diagnosis and management of congenital patella dislocation, which is usually observed in infants and is a good example of the use of ultrasound in the evaluation of cartilaginous (non-ossified) bones, as radiographs in congenital patella dislocation are often normal.

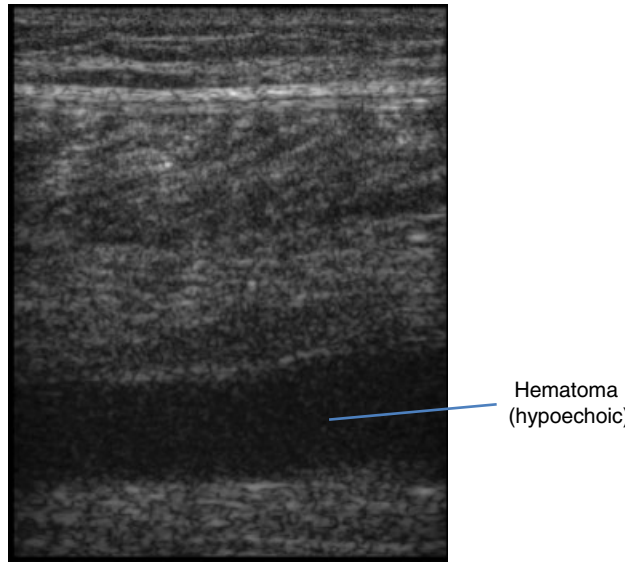

Figure 22.6 Muscle haematoma.

Ligament, Tendon and Muscle Injury

Ligament and tendon injuries are relatively less common in children than adults because the immature bones of children (particularly the epiphyseal plate) are weaker than the surrounding tendon and ligament complexes, and therefore are more susceptible to fracture. Given the relative weakness of immature bone, injuries to paediatric tendons typically occur at the tenoosseus junction, with the classic example being traction apophysitis of the anterior tibial tuberosity (also known as Osgood–Schlatter's disease). On ultrasound, the injury is characterised by irregular bony surfaces, thickened or fragmented tendons that have lost a crisp fibrillar appearance, and small hyperechoic pieces of avulsed bone. Osgood–Schlatter's disease is often evident on plain radiographs, but further information can be gained from ultrasound, as described above. Ultrasound can also be useful for the diagnosis of traction apophysitis at other sites, such as insertion of the hamstring muscles on the ischial tuberosity where plain radiographs are less helpful. Other ligament and tendon injuries, such as a medial gastrocnemius tear or rotator cuff injuries, are quite rare in children and if such injuries do occur they are typically in adolescents in whom the injuries can typically be managed similarly to adults. Muscle tears may be quantified by assessing for haematoma formation using ultrasound. Haematomas can be identified as deep hypoechoic areas within muscles (see Figure 22.6).

Procedures

The real-time format, safety profile and general ease of use of PoCUS make it a helpful tool in a variety of procedures that include aspirations, biopsies, vascular access, nerve blocks and others. In fact, the use of ultrasound is associated with increased procedural success, fewer complications (e.g., bleeding, infection), a decreased need for anaesthesia in children and shorter hospital stays. Although ultrasound is used for a variety of paediatric MSK procedures, including image-guided biopsy, the most common and well-developed application of PoCUS for the non-radiologist is fluid/joint aspiration. Indications for aspiration are both diagnostic and therapeutic, and include investigation of the potential septic joint and decompression of symptomatic effusion or haemarthrosis. Before

undertaking an aspiration, consent should be obtained from the guardians and child, and the risks of the procedure – including pain, bleeding and infection – should be explained. The position of the patient will vary with regard to the joint that is to be aspirated. Most capsules can be easily visualised, although it is particularly recommended that children be positioned supine with their legs straight when aspirating the hip. In terms of technique it is easiest to visualise the aspiration needle when it is in the plane of the ultrasound beam (the needle is introduced at the end of the probe; see Figure 22.7) at a shallow angle. In general, the key principles with regard to patient positioning and aspiration are to place the child in a comfortable position that provides the greatest visualisation of the effusion, and to directly observe the needle as it enters the area of greatest distension of the effusion. Given the usefulness of direct visualisation of aspiration, it is possible that ultrasound-guided joint aspiration may soon become the standard of care as it has for internal jugular central venous catheter placement.

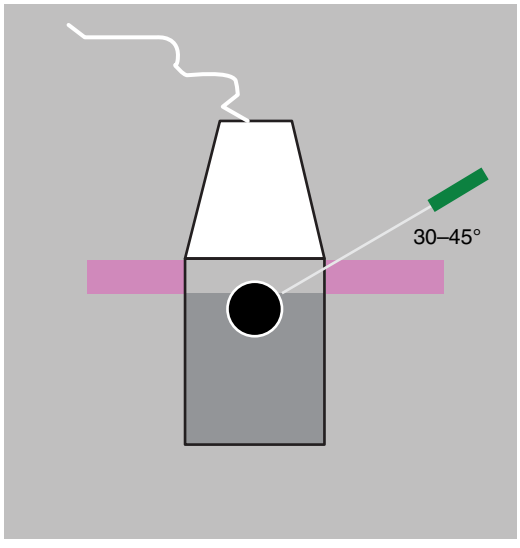

Figure 22.7 The 'in-plane' approach used for ultrasound-guided procedures.

Joint Effusions

Assessing for effusion is useful in a wide variety of disorders, including septic arthritis, collagen disease, reactive arthritis, coagulation disorders and in trauma. PoCUS allows rapid screening for the involvement of multiple joints, with a much greater sensitivity than that of the clinical examination and plain-film radiography.

The effusions appear as hypoechoic, compressible collections within the joint. Ensuring that they are negative for Doppler flow will differentiate them from surrounding vessels.

Although ultrasound can be used to accurately rule out, or detect, joint effusions, it cannot differentiate between an inflammatory, haemorrhagic or transudative cause, which requires clinical correlation and possibly aspiration.

Ultrasound can also be useful in detecting synovial thickening, increased blood flow to the synovium, and erosions of the bone or cartilage – all of which may be signs of early synovitis.

Ultrasound in Assessment of the Paediatric Hip

Technique

A high-frequency (7–12 MHz) probe with paediatric hip/MSK preset should be used if available. The depth should be adjusted so that the deepest point is just at the bone surface, and gain should be adjusted to best allow the visualisation of a hypo-echoic effusion.

When searching for an effusion the child should be placed supine with the hips neutral and the legs externally rotated to help force fluid into the anterior space of the joint capsule. The transducer is placed at an oblique angle parallel to the long axis of the femoral neck (Figure 22.8). Both hips should always be assessed for comparison. Note that this method is quite different from the technique used for assessing developmental hip dysplasia.

Anatomy

In this view there are several bony landmarks; the echogenic cortex of the femur should be seen, and it should be possible to identify the neck, head and growth plate. Caudal to the femur is the anterior margin of the acetabulum. The joint capsule can be seen just above the cortex, and superficial to the capsule is the illiopsoas muscle (Figure 22.9). The capsule normally has a concave margin, and a maximum depth of 2–5 mm. When comparing each side, the depth and shape of each capsule should be roughly symmetrical.

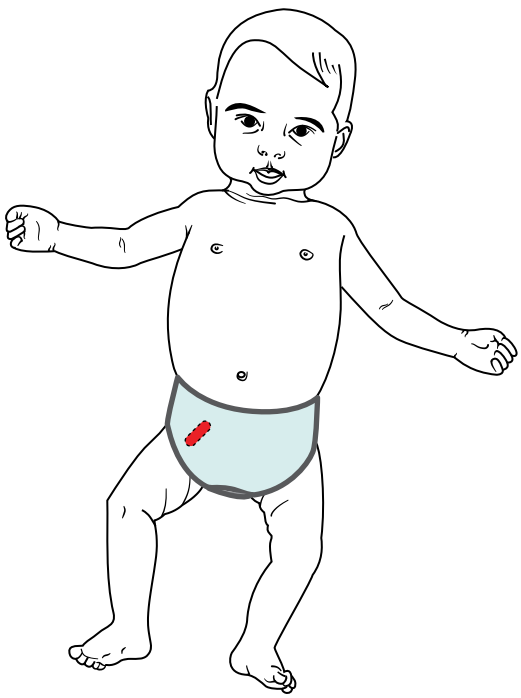

Figure 22.8 Probe position for examination of the paediatric hip.

The Painful (Irritable) Hip

Presentation with an atraumatic, painful hip is relatively common in children. Aetiologies include benign transient synovitis, Perthes' disease, slipped capital femoral epiphysis, early presentations of inflammatory arthropathies, septic arthritis and fracture. Typically, the child will limp or refuse to weight bear; however, it is difficult to differentiate between the aetiologies clinically as there is often a great deal of overlap in the symptoms and physical findings. Evaluation includes a detailed history and physical examination, imaging of the hip, and basic laboratory work including a complete blood count and inflammatory markers. One approach is outlined below. PoCUS alone cannot differentiate between transient synovitis and a septic arthritis; the main role of ultrasound is in assessing for the presence or absence of an effusion.

Effusion

Ultrasound can detect as little as 1 ml of synovial fluid, and overall is 90% sensitive in assessing for fluid within the joint. The absence of an

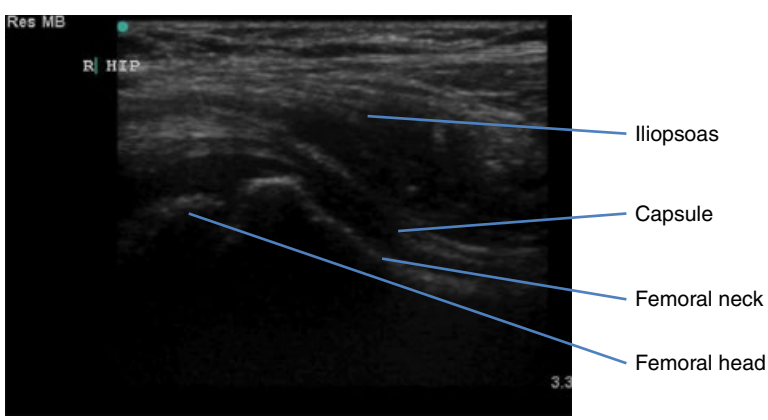

Figure 22.9 The normal appearance of the paediatric hip.

effusion effectively rules out septic arthritis; therefore, ultrasound can be quite effective in ruling out a septic hip. However, it is worth noting that osteomyelitis can be present in the absence of an effusion.

An effusion is said to be present when the capsule is convex at the anterior surface, is greater than 3 mm, or when one hip measures at least 2 mm greater than the contralateral side (Figure 22.10)

Ultrasound is sensitive in identifying effusions, but it cannot be used to reliably identify their cause. The presence of increased Doppler flow, or debris within the synovium, may suggest septic arthritis, but these findings are neither sensitive nor specific. When clinically suspicious, infection can be ruled out with aspiration of the joint and analysis of the synovial fluid.

Aspiration

PoCUS may be used to localise and guide an aspiration. However, the first question to ask is whether this invasive procedure is necessary. If fever, elevated inflammatory markers or overall clinical impression raise the suspicion of a septic process, aspiration is likely the safest course. In the absence of these consideration can be given to an approach of watchful waiting.

If aspiration is required, ultrasound localisation and guidance can increase the success rate. Ultrasound can be used to localise the effusion and to find where the capsular distension is greatest. Once this area is marked it can be tapped blindly, or ultrasound can be used to guide needle entry. In the short axis a ring-down effect can be seen, while in the long axis (in-plane) the needle itself may be visualised.

Developmental Dysplasia of the Hip

Ultrasound is commonly used in the evaluation of developmental dysplasia of the hip. However, interpretation of imaging and diagnosis is complex and requires a great deal of operator skill and experience, and is beyond the scope of this chapter.

Summary

Ultrasound has a number of advantages over other imaging techniques, including ease of use, real-time dynamic format, lack of ionising radiation, wide availability and low cost. These

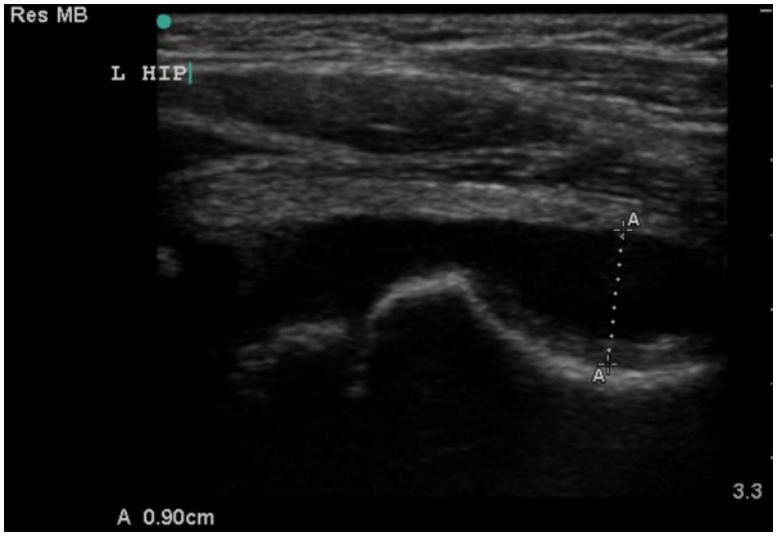

Figure 22.10 Hip effusion of 9 mm demonstrated by ultrasound.

advantages are clearly manifest in the diagnostic and therapeutic application of PoCUS to paediatric MSK conditions such as skin and soft-tissue infections, ligament and tendon injuries, dislocations, joint effusions and aspiration and foreign body removal.

Ultrasound can be used to detect quite small effusions within the hip joint, with 90% sensitivity. A lack of an effusion effectively rules out septic arthritis, or other causes of synovitis. Simply finding an effusion does not identify the aetiology. In cases where a septic arthritis is suspected, ultrasound can be used to localise the largest area of effusion and to guide needle entry for aspiration.

Finally, although PoCUS now has a number of established applications in paediatric MSK conditions, additional applications are very likely to emerge as research and clinician competency evolve.

Further Reading

Azam, Q., Ahmad, I., Abbas, M., Syed, A., Haque, F. (2005) Ultrasound and colour Doppler sonography in acute osteomyelitis in children. *Acta Orthop. Belg.*, **71** (5), 590–596.

Delaney, L.R., Karmazyn, B. (2011) Developmental dysplasia of the hip: background and the utility of ultrasound. *Semin. Ultrasound CT MRI*, **32**, 151–156.

Durston, W., Swartzentruber, R. (2000) Ultrasound guided reduction of pediatric forearm fractures in the ED. *Am. J. Emerg. Med.*, **18**, 72–77.

Fananpazir, G., Allison, S.J. (2011) Common application of musculoskeletal ultrasound in the emergency department. *Ultrasound Clin.*, **6**, 215–226.

Jacobson, J.A. (2007) Introduction to musculoskeletal ultrasound. *Ultrasound Clin.*, **2**, 569–576.

Karmazyn, B. (2011) Ultrasound in pediatric musculoskeletal disease: From head to toe. *Semin. Ultrasound CT MRI1*, **32**, 142–150.

Kim, K.C., Eckhardt, B.P., Craig, C., & Kuhns, L.R. (2004) Ultrasound of the annular ligament partial tear and recurrent pulled elbow. *Pediatr. Radiol.*, **34**, 999–1004.

Malcius, D., Jonkus, M., Kuprionis, G., Maleckas, A., Monastyreckiene, E., Uktveris, R., Rinkevicius, S., Barauskas, V. (2009) The accuracy of different imaging techniques in diagnosis of acute hematogenous osteomyelitis. *Medicina*, **45** (8), 624–631.

Nath, A.K., Sethu, A.U. (1992) Use of ultrasound in osteomyelitis. *Br. J. Radiol.*, **65** (776), 649–652.

Nath, A.K., Sethu, A.U. (2003) An update on use of ultrasound in osteomyelitis and importance of power Doppler. *Ultrasound Med. Biol.*, **29** (5S), S126.

Navarro, O.M., Parra, D.M. (2009) Pediatric musculoskeletal ultrasound. *Ultrasound Clin.*, **4**, 457–470.

Ramirez-Schrempp, D., Dorfman, D., William, B., Litelpo, A. (2009) Ultrasound soft tissue applications in the pediatric emergency department: To drain or not to drain? *Ped. Emerg. Care*, **25** (1), 44–48.

Riebel, T.W., Nasir, R., Nazarenko, O. (1996) The value of sonography in the detection of osteomyelitis. *Pediatr. Radiol.*, **26** (4), 291–297.

Squire, B.T., Fox, J.C., Anderson, C. (2005) ABSCESS: applied bedside sonography for convenient evaluation of superficial soft tissue infections. *Acad. Emerg. Med.*, **12**, 601–606.

Tayal, V.S., Hasan, N., Norton, H.J., *et al.* (2006) The effect of soft-tissue ultrasound on the management of cellulitis in the emergency department. *Acad. Emerg. Med.*, **13**, 384–388.

23

Point-of-Care Ultrasound in Paediatric and Neonatal Intensive Care

Mahmoud A. Elbarbary[†]

Introduction

The aim of this chapter is to explain the special utilisation of ultrasound in the context of the Neonatal Intensive Care Unit (NICU) and Pediatric Intensive Care Unit (PICU).

Intensive care unit (ICU) circumstances may have some peculiarities that differ from those of the emergency department with regards to:

- Patients stay longer in the ICU and may need repeated ultrasound scans.
- The scan can be more of a monitoring scope rather than a diagnostic scope.
- Scans are used for goal-directed therapy.
- Ultrasound-guided procedures in the ICU may differ from the types of procedure performed in the emergency department.
- Elective scans as well as emergency scans are considered.
- Peculiar indications may be encountered more frequently in the ICU.

Paediatric ICU Haemodynamic Management

Recent evidence has suggested that the incorporation of goal-directed ultrasound in the evaluation of non-traumatic, symptomatic, undifferentiated hypotension in NICU and PICU patients results in fewer viable diagnostic aetiologies, and can lead to a more accurate physician impression of the final diagnosis. The two basic components of the haemodynamic management are related to cardiac function and fluid status. Bedside ultrasound can facilitate assessment, diagnosis and the optimisation of interventions and follow-up of these two components.

Left Ventricular Global Systolic Function

This includes parameters such as fractional shortening (FS) and ejection fraction (EF), either by global visual assessment or by objective numerical measurement:

- Global eye-assessment: when the left ventricle empties more than half of its volume it is considered normal (i.e., an EF >55%). Mild impairment of the EF would equate to an EF of 45–55%, moderate to 30–44%, and severe impairment to <30%.
- Other objective parameters used to estimate ventricular function are described elsewhere in this book, and include M-mode, two-dimensional or Doppler assessment of trans-mitral flow that reflects the left ventricular end-diastolic pressure (LVEDP) and hence the left atrial pressure. These parameters can be useful for assessing the different aetiological causes of pulmonary oedema, assessment of fluid and inotrope

[†] Deceased.

Emergency Point-of-Care Ultrasound, Second Edition. Edited by James A. Connolly, Anthony J. Dean, Beatrice Hoffmann and Robert D. Jarman.

Companion website: www.wiley.com/go/connolly/ultrasound

titrations. These measurements are in addition to the measurement of cardiac output, which can be estimated based on the continuity equation.

Volume Status

This is assessed as previously described by the inferior vena cava (IVC) variability and global ventricular volume. The combination of the two assessments together is essential for the interpretation of different types of paediatric shock through four steps:

1) Gross *ruling out of pre-existing cardiac disease*. That is achieved by ruling out gross dilatation or hypertrophy of the left and right ventricles, or significant valvular abnormality.
2) *Assessment of the IVC for fluid status*. In hypovolaemia, inspiratory collapse is expected to be >50% in spontaneously breathing patients, or inspiratory distension of >20% in passive mechanical ventilation. The hypovolaemia can be either *absolute* (haemorrhage, dehydration, third space) or *relative* (sepsis, anaphylaxis, drugs). The responsiveness of the IVC following fluid therapy can guide fluid requirements. A dilated and fixed IVC may suggest pulmonary hypertension or cardiac tamponade if associated with right ventricular signs (see Step 3).
3) *Assessment of the right ventricle*. In the presence of a fixed, distended IVC, the right ventricle can be either small and hyperkinetic, suggesting cardiac tamponade, or dilated and hypokinetic, suggesting pulmonary hypertension or right ventricular infarct. Additional confirmatory signs for each of the two findings are useful: for cardiac tamponade, these include right atrial inversion/collapse in late systole (atrial diastole), which is an extremely sensitive sign, right ventricular inversion/collapse in early diastole (less sensitive, more specific), swinging heart, fluids or clots around the heart. For pulmonary hypertension, an assessment of Doppler flow across the tricuspid valve can give an accurate estimate of the pulmonary artery systolic pressure in the absence of pulmonary valve lesions. Septal shift towards the left ventricle also confirms a high right ventricular systolic pressure.
4) *Assessment of left ventricular function*. A hyperkinetic left ventricle will favour against the use of inotropes, while a hypokinetic left ventricle will support such use. Again, the combination of this step with step 2 (fluid status) will help in establishing the diagnosis, starting interventions and monitoring the effects of treatment on the patient.

This systematic four-step approach may be helpful with the decision to use volume versus inotropes. Effects can be monitored to achieve certain end points (goal-directed) regarding both ventricular filling and ventricular functions.

Mechanical Ventilation

Cardiac transmural pressure equals systemic pressure minus intrathoracic pressure. Therefore, positive pressure ventilation (PPV) in general helps the impaired left ventricle due to a reduction of the transmural pressure across the left ventricle free wall, thus reducing left ventricular afterload. In contrast, the PPV will constitute, in general, a burden on the impaired right ventricle because of a reduction of pre-load and increase in right ventricular afterload. Ultrasound can help in optimising the PPV to achieve the maximum benefit and avoid the unwanted side effects on the ventricles.

Combined lung and heart ultrasound will be able to achieve the optimum level of positive end expiratory pressure (PEEP) that can help in this condition, without deleteriously affecting the right ventricle. The trans-mitral flow estimation of LVEDP can be utilised during the weaning process from mechanical ventilation. The titration of optimum PEEP (Figure 23.1) can help the right ventricle by opening the collapsed alveoli and improving the functional residual capacity, and hence reducing the pulmonary vascular resistance. Repeated assessment using heart and lung ultrasound during

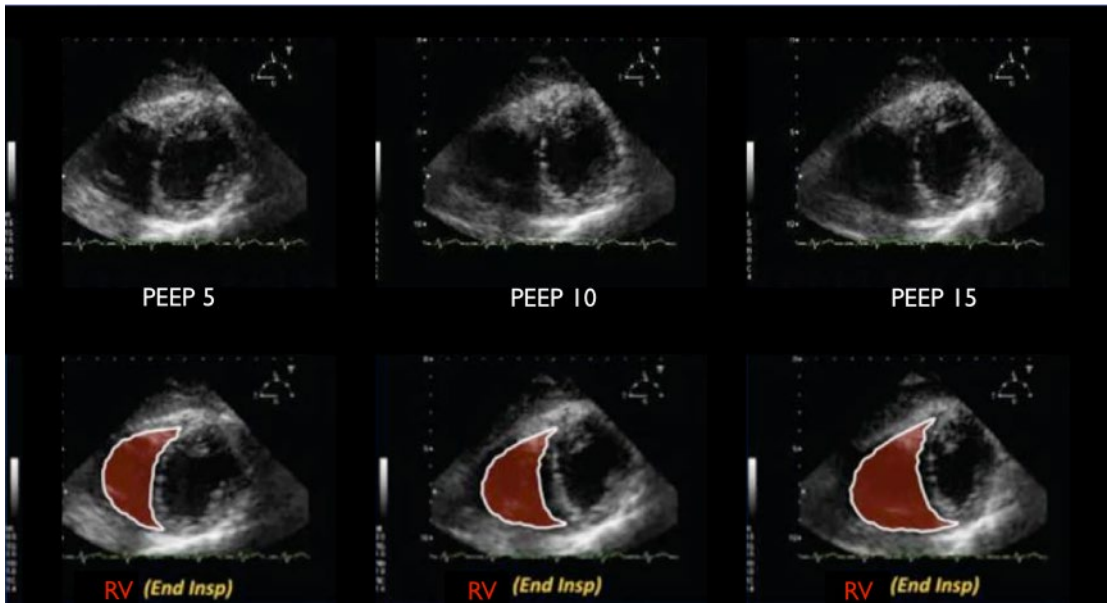

Figure 23.1 Effects of positive end-expiratory pressure (PEEP) of 5, 10 and 15 mmHg on the right ventricle.

PPV weaning will help in titrating both ventilator and circulatory support.

Diaphragmatic and vocal cord paralysis can lead to extubation failure. Bedside ultrasound can easily detect these two conditions. Diaphragmatic paralysis is shown in Figure 23.2. Ultrasound examinations of the vocal cords should be performed while the child is breathing spontaneously in a supine position with minimal neck extension, to allow a space for the probe to be placed and gently manipulated on the cricoid cartilage and trachea. A linear or curve-linear transducer with frequency of 8–12 MHz is recommended. The transducer should be placed in the axial (transverse) plane on the thyroid cartilage, which can be used as an acoustic landmark.

Video 23.1 shows an ultrasound of the diaphragm that can help in the identification of failure to wean from mechanical ventilation in case of paradoxical movement. Videos 23.3 a and b show ultrasounds of the vocal chords. These can be useful in evaluating cases of difficult-to-extubate, post-extubating stridor and croop.

Procedure-Related Peculiarities

Among procedures usually performed in the emergency department, but also carried out in the ICU and facilitated by ultrasound are lumbar puncture (Figure 23.3), paracentesis, pericardiocentesis (Figure 23.4 and Video 23.2), peripherally inserted central catheter (PICC) line insertion, abscess drainage, gallbladder drainage, supra-pubic drainage and transhepatic catheter placement. Video 23.4 shows the scanning for lumbar puncture procedures in paediatric patients.

Vascular Access in Paediatrics

A detailed account of the adult procedure is explained elsewhere and is also applicable to paediatric patients. However, the following points should be taken into consideration:

- Select a small-footprint transducer (8–15 Hz).
- Measurement of the probe–target distance should mimic the pressure that is sometimes

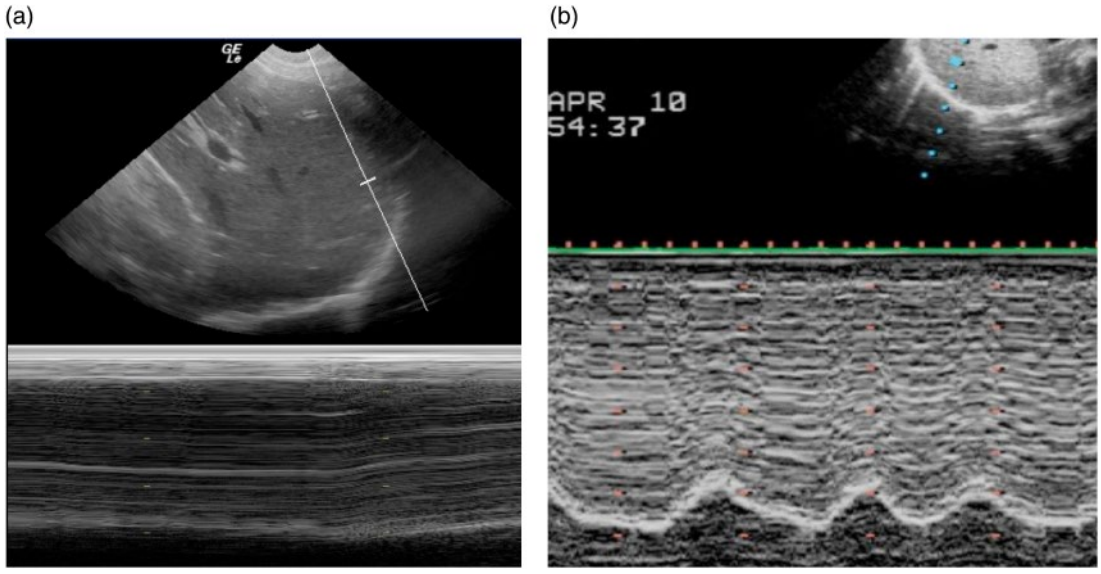

Figure 23.2 The use of M-mode ultrasound for diaphragmatic motion assessment. (a) M-mode placed through diaphragm showing no motion. (b) M-mode showing motion of the diaphragm.

made during the procedure, moving away from the use of 'zero pressure.'
- In case of difficult anatomy, a Doppler scan may be very helpful.
- Develop good posture and transducer-handling techniques.
- Be familiar with the anatomy.
- Once positioned, watch the screen, not the transducer.
- Let the screen guide your movements, not the transducer.
- In *neonates* use a separate 22–24 G cannula and baby wire instead of the central line introducer kit (Figure 23.5).

A short-axis technique (out-of plane) provides a view of the surrounding structures and allows the procedure in even a small field. A long-axis technique allows better needle tip and depth visualisation throughout the cannulation process. A *combined approach* is frequently used in paediatrics, starting with a short-axis technique first, after which the cannulation is completed in the long axis.

Videos 23.5 and 23.6 show vascular access techniques, including set-up, differentiation between venous and arterial flow, and how to rotate from short- to long-axis views.

Abdominal Surgical Emergencies in the Newborn

Necrotising Enterocolitis

Necrotising enterocolitis (NEC) is an acquired condition of diffuse necrotic injury to the mucosal and submucosal layers of the bowel. It is the most serious gastrointestinal disorder that occurs during the neonatal period. NEC mainly affects extremely low-birth weight (ELBW) infants but can also occur in full-term infants. The mortality rate for NEC is estimated to be 11.5–12.3 per 100 000 infant deaths, and greatly exceeds that of other gastrointestinal surgical disorders.

Radiographic findings are important in the staging of NEC and determining the need for surgical intervention. NEC can be suspected by using ultrasound, which can detect air bubbles localised within the wall of the intestine (pneumatosis intestinalis; Figure 23.6). Ultrasound finding of air in the portal system can

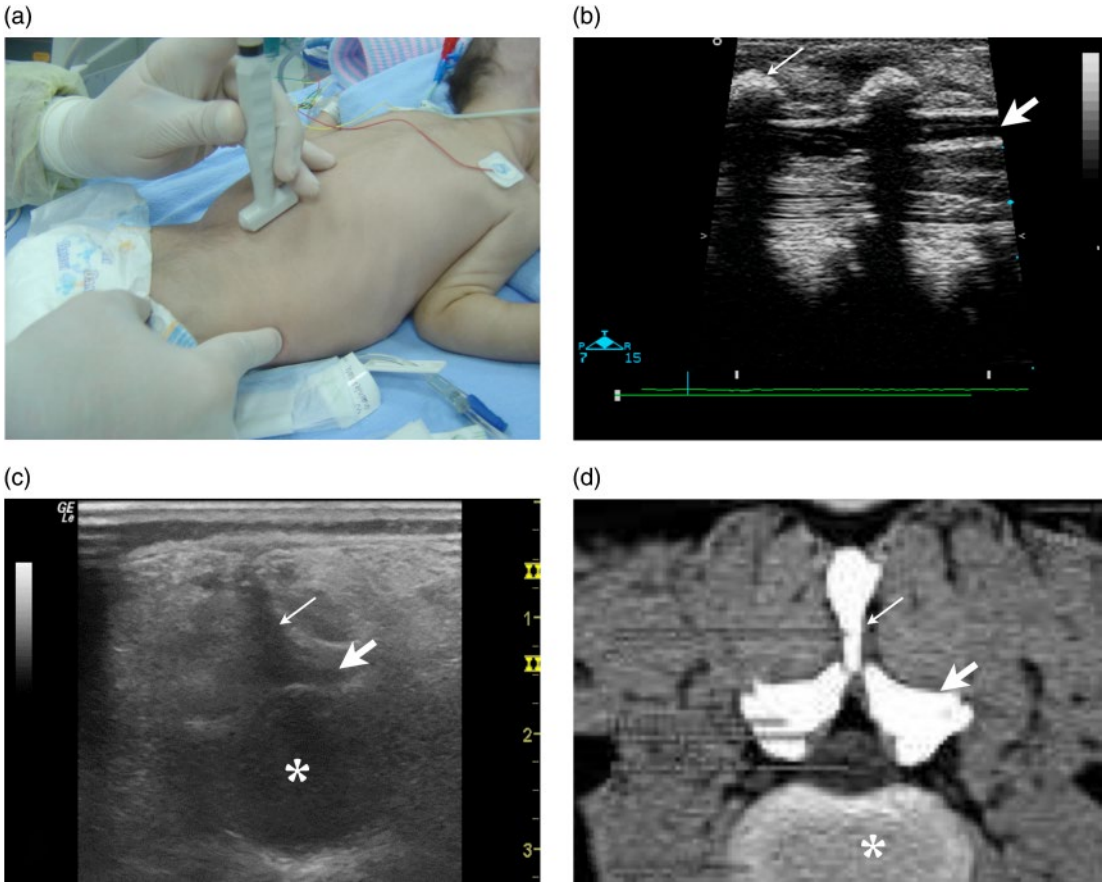

Figure 23.3 Ultrasound-guided lumbar puncture. (a) Patient and probe position. (b) Image of longitudinal view of lumbar spine and spinal canal with fluid (thick arrow). Spinous process (thin arrow). (c) Sonographic image and (d) CT image of vertebral body anatomy. Spinous process (thin arrows), transverse process (thick arrows). Vertebral body (stars).

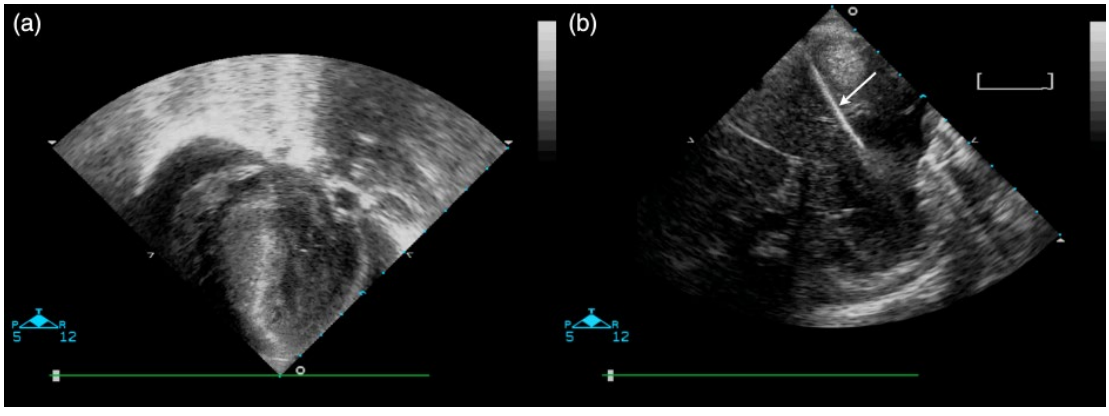

Figure 23.4 (a) TEE image of pericardial effusion. (b) Transthoracic image of pericardiocentesis needle (arrow) entering a pericardial effusion.

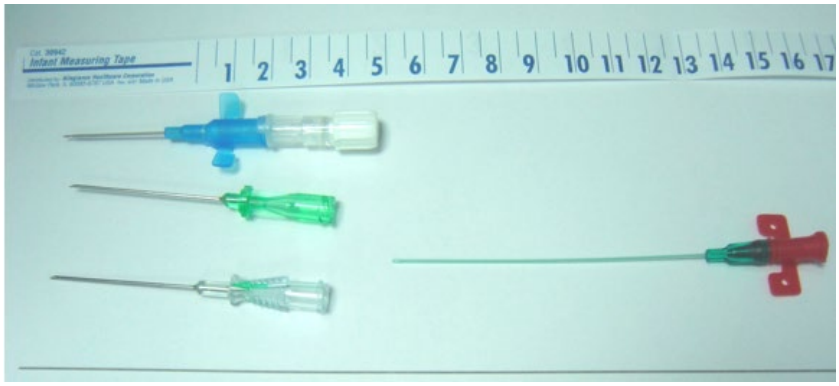

Figure 23.5 Cannulas used for paediatric vascular access.

also be indicative of NEC. Ultrasound Doppler may also be helpful in detecting hyperaemia or decreased blood flow in the wall of the intestine. These ultrasound findings, along with other clinical signs, can assist in making the diagnosis of NEC prior to bowel perforation and the development of peritonitis.

Ultrasound and Doppler flow should be measured using a small transducer suitable for neonates, with a frequency of 6–10 MHz. A higher frequency provides better resolution but a lower frequency provides deeper penetration.

Neonatal Bowel Obstruction

This is a serious condition that can be complicated by intestinal perforation. Early radiological studies in cases of neonatal bowel obstruction are needed to rule out intestinal malrotation with midgut volvulus. As many as 40% of patients with malrotation present within the first week of life. It is often difficult to differentiate malrotation from other causes of intestinal obstruction, such as intestinal atresia. Ultrasound can be helpful in diagnosing intestinal obstruction. If ultrasound findings demonstrate a dilated intestinal loop with a liquid content, and an adjacent very narrow loop of unused intestine, this can support the diagnosis of intestinal atresia. Finding the superior mesenteric vein (SMV) to the left of the superior mesenteric artery (SMA) is highly suggestive of malrotation.

Intraventricular Haemorrhage

Preterm infants, particularly those with ELBW, are at high risk of many of the complications of prematurity. Sudden deterioration can occur during the first few days of life due to various causes. Severe intraventricular haemorrhage (IVH) is an important complication due to impaired autoregulatory ability, which can result in rapid alterations in cerebral blood flow and blood pressure. These sudden changes can result in haemorrhage inside the lateral ventricles and haemorrhagic infarction in the brain parenchyma adjacent to the lateral ventricles (Grade IV IVH).

Grade IV IVH can manifest as sudden clinical deterioration with metabolic acidosis, hypotension, apnoea and bradycardia. Other problems of prematurity such as sepsis, pneumothorax and patent ductus arteriosus can also present with a similar clinical picture. A correct diagnosis would impact decisions for further management and support or avoid treatments.

The use of bedside ultrasound and a small transducer with a frequency of 5–10 MHz that fits at the infant's open anterior fontanel can easily yield the diagnosis (Figure 23.7).

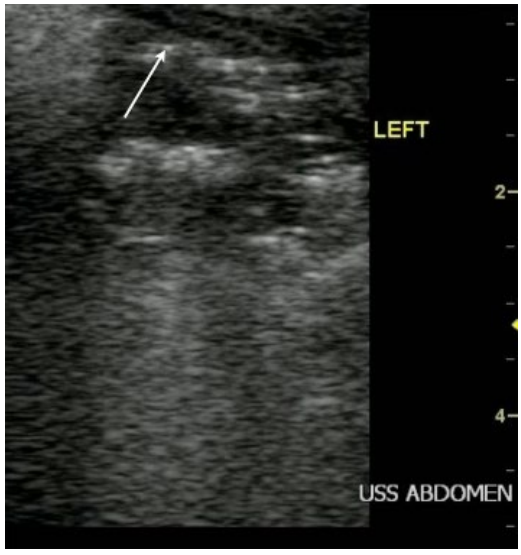

Figure 23.6 Pneumatosis intestinalis. White dots with shadows (arrow) indicative of air bubbles in the wall of the intestine.

Transient Tachypnoea of Newborn (TTN)

TTN, also called 'wet lungs' or type II respiratory distress syndrome, usually can be diagnosed during the hours after birth (see Chapter 40). It is not possible to detect before birth whether a child will have this condition.

TTN can occur in both premature babies (because their lungs are not yet fully developed) and full-term babies. Newborns at higher risk for TTN include those who are:

- Delivered by caesarean section (C-section).
- Born to mothers with diabetes.
- Born to mothers with asthma.
- Small for gestational age (small at birth).

Copetti and Cattarossi described a peculiar sign by ultrasound that was called the 'double lung point' (Figure 23.8). In infants with TTN, lung sonography showed a difference in lung echogenicity between the upper and lower lung areas. Very compact comet-tail artefacts were apparent in the inferior fields, but these were rare in the superior fields. This finding, which was termed the 'double lung point', was not observed in healthy infants, or in infants with respiratory distress syndrome, actelectasis, pneumothorax, pneumonia or pulmonary haemorrhage. Sensitivity and specificity of the double lung point was 100% for the diagnosis of TTN. It is worth knowing that in normal babies delivered by C-section, multiple B lines can be found bilaterally that disappear in a period of a few days.

Mechanical ventilation in neonates can result in several complications, among which can be included bronchopulmonary dysplasia. Ultrasound can be used to detect the development of such complications (see Figure 23.9).

Patent Ductus Arteriosus (PDA)

The presentation of neonatal shock can be due to closure of the ductus arteriosus in some ductal-dependent cardiac lesions, such as severe aortic coarctation, pulmonary atresia and transposition of the great arteries. An ultrasound examination of the PDA can help in establishing the diagnosis as well as in monitoring the effect of a prostaglandin infusion on opening the closing ductus. Detecting the direction of blood flow (by Doppler ultrasound) in the PDA can help in the diagnosis of pulmonary hypertension (right to left). In addition, a neonate can suffer from heart failure and become ventilator-dependent in the absence of an intracardiac lesion, due to the presence of a large PDA with a left-to-right shunt. In all of the previous conditions, an ultrasound examination of the PDA via the supra-sternal approach is of great value (Figure 23.10).

Videos 23.7 to 23.11 show cases of neonates and infants with patent ductus arteriosus (PDA). It is life-saving in duct-dependent lesions to start prostaglandin infusion to keep the PDA open and follow this routinely with POCUS.

Video 23.12 and 23.13 show cases of pulmonary hypertension. These cases are frequently encountered in PICU and NICU due to PPHN and RDS. Aside from the adult methods of estimation of pulmonary pressure, the direction of the flow across the patent ductus arteriosus (PDA) is crucial.

Video 23.14 shows a case of infective endocarditis in a child.

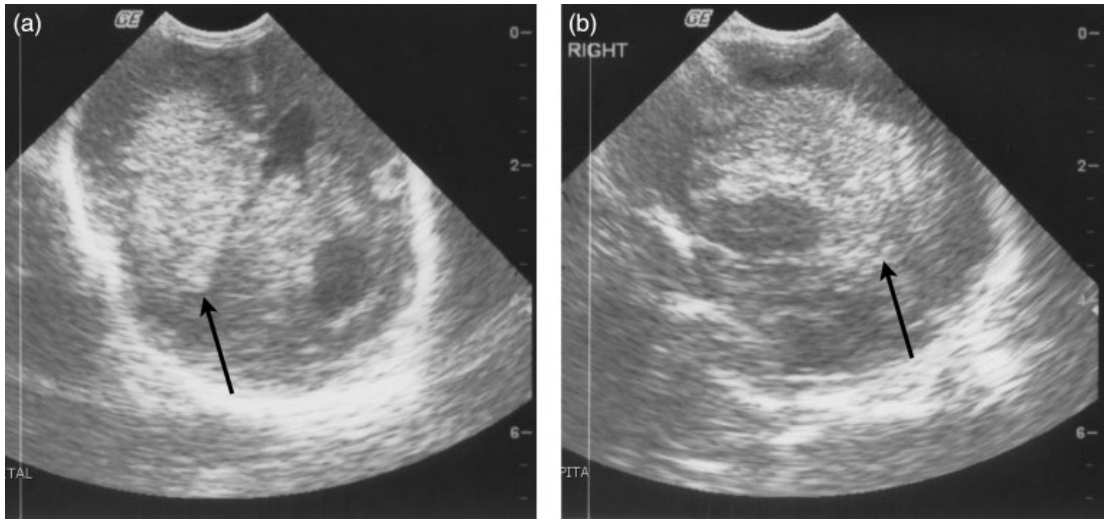

Figure 23.7 (a) Coronal section and (b) sagittal section of brain ultrasound scan, showing hyperechoic densities (arrows) in the area of the right lateral ventricle and the brain parenchyma adjacent to it, indicating right intraventricular and periventricular haemorrhage (grade IV IVH).

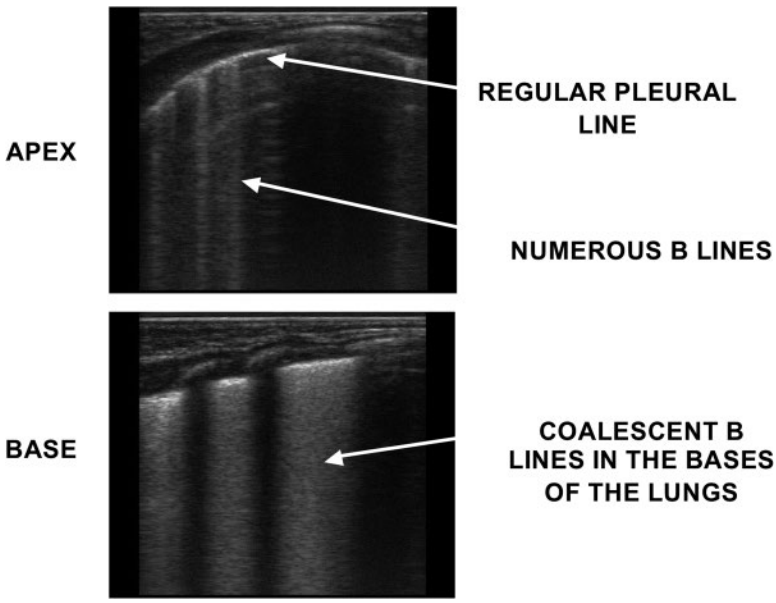

Figure 23.8 The double lung point for transient tachypnoea of the newborn.

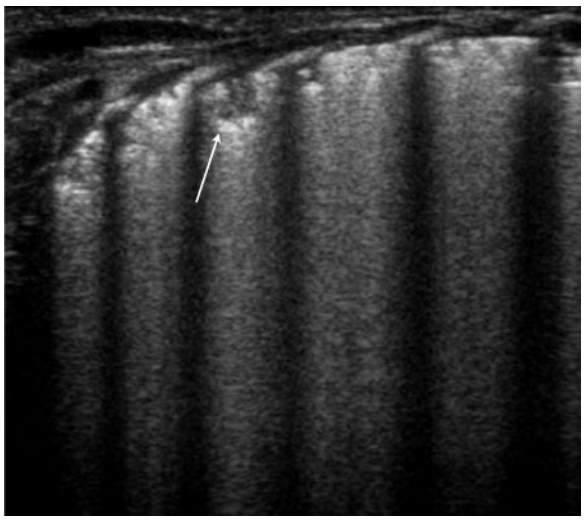

Figure 23.9 Bronchopulmonary dysplasia. The arrow indicates small sub-pleural consolidations. In addition, attenuation, irregularity, thickening and coarseness of the pleural line is present.

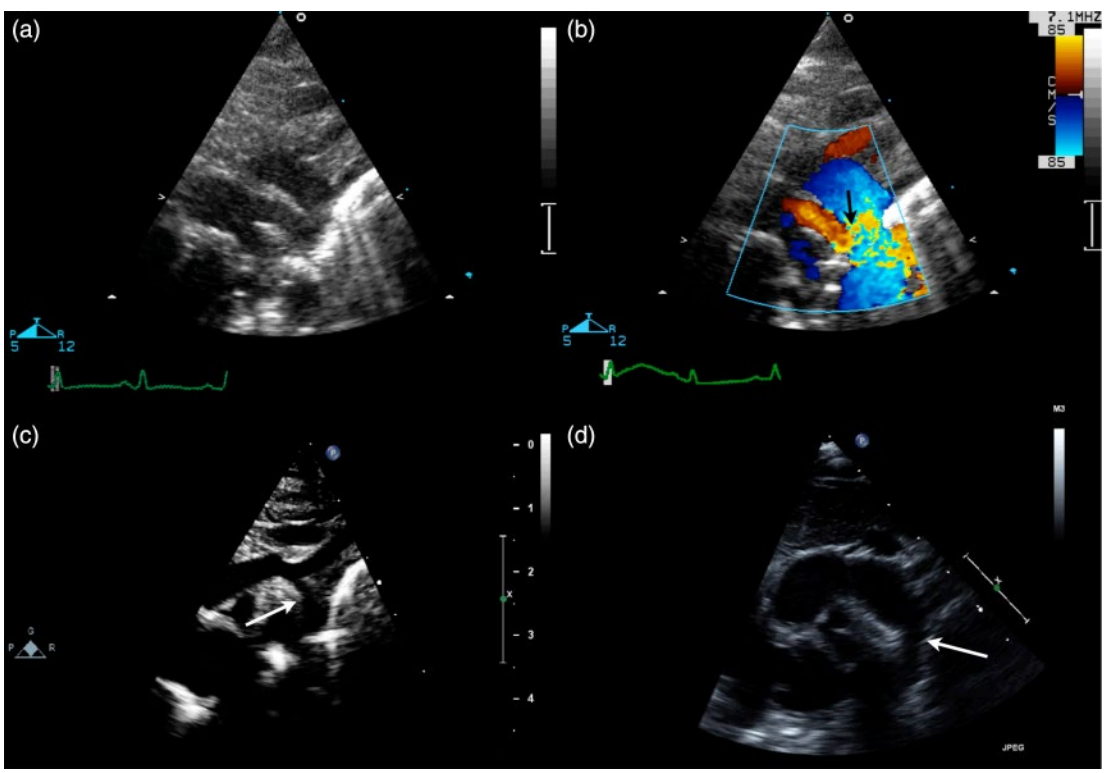

Figure 23.10 Supra-sternal window for viewing the aortic arch, possible coarctation and/or patent ductus arteriosus (PDA). PDA demonstrated by two-dimensional ultrasound (a) and Doppler ultrasound (b). PDA (arrow); (c, d) Aortic coarctation (arrows) with arch hypoplesia.

Further Reading

Chandler, J.C., Hebra, A. (2000) Necrotizing enterocolitis in infants with very low birth weight. *Semin. Pediatr. Surg.*, **9**, 63–72.

Copetti, R., Cattarossi, L. (2007) The 'double lung point': an ultrasound sign diagnostic of transient tachypnea of the newborn. *Neonatology*, **91** (3), 203–209.

Copetti, R., Cattarossi, L., Macagno, F., Violino, M., Furlan, R. (2008) Lung ultrasound in respiratory distress syndrome: a useful tool for early diagnosis. *Neonatology*, **94** (1), 52–59.

Froehlich, C.D., Rigby, M.R., Rosenberg, E.S., Li, R., Roerig, P.L., Easley, K.A., Stockwell, J.A. (2009) Ultrasound-guided central venous catheter placement decreases complications and decreases placement attempts compared with the landmark technique in patients in a pediatric intensive care unit. *Crit. Care Med.*, **37** (3), 1090–1096.

Shaath, G.A., Jijeh A., Alkurdi, A., Ismail, S., Elbarbary, M., Kabbani, M.S. (2012) Ultrasonography assessment of vocal cords mobility in children after cardiac surgery. *J. Saudi Heart Assoc.*, **24** (3), 187–190.

Spurney, C.F., Sable, C.A., Berger, J.T., Martin, G.R. (2005) Use of a hand-carried ultrasound device by critical care physicians for the diagnosis of pericardial effusions, decreased cardiac function, and left ventricular enlargement in pediatric patients. *J. Am. Soc. Echocardiogr.*, **18** (4), 313–319.

Vignon, P., Dugard, A., Abraham, J., Belcour, D., Gondran, G., Pepino, F., *et al.* (2007) Focused training for goal-oriented hand-held echocardiography performed by noncardiologist residents in the intensive care unit. *Intensive Care Med.*, **33**, 1795–1799.

24

Paediatric Abdominal Ultrasound

Jennifer R. Marin

Introduction

Ultrasound has been shown to be of considerable utility in the evaluation of children by imaging specialists. Reports on the topic of point-of-care ultrasound in paediatrics are few in number, but with appropriate training and experience point-of-care ultrasound is increasingly useful to clinicians at the bedside, particularly with the rising concern about the potentially deleterious effects of iatrogenic radiation exposure in childhood.

Pyloric Stenosis

Hypertrophic pyloric stenosis (HPS) is an acquired condition in which there is hypertrophy of the pyloric muscle and elongation of the pylorus. The condition typically develops between 2 and 12 weeks of life, and infants present with non-bilious, often projectile, vomiting.

The transducer should be placed over the 'olive'-sized mass in the right upper quadrant if it is palpable. Visualisation of the pyloris should initially be attempted with a high-frequency transducer. In most cases the distended stomach contains a large volume of fluid, creating an ideal sonographic window to identify the antrum and thereby the pylorus. If the stomach is filled with gas, the infant should be placed in the right lateral decubitus position to allow liquid contents to fill the gastric antrum, or even prone to improve visualisation. With severe distension, the pylorus may be positioned behind the stomach, and a lower-frequency transducer may be needed. If the stomach is empty, the infant may drink a small amount to assist with visualisation of the stomach.

The length of the pyloric channel should be measured. This view is often referred to as the 'string sign' (Figure 24.1). A measurement of >15 mm is considered abnormal. In the transverse plane the 'doughnut sign' should be sought (Figure 24.2); this is a central echogenic area of mucosa surrounded by hypoechoic thickened muscle. In this view, a pyloric diameter >11 mm or a muscularis thickness >3 mm is considered hypertrophic.

Other sonographic findings in the diagnosis of HPS include the 'nipple sign' (Figure 24.3), which is caused by the thickened, redundant pyloric mucosa protruding into the gastric antrum. Alternatively, the 'shoulder sign' (Figure 24.3), which is caused by the hypertrophied muscle bulging into the gastric antrum may be visualised. In addition, there may be delayed gastric emptying with a failure to image the descending duodenum, retrograde peristalsis, and exaggerated peristaltic waves. Pitfalls

Emergency Point-of-Care Ultrasound, Second Edition. Edited by James A. Connolly, Anthony J. Dean, Beatrice Hoffmann and Robert D. Jarman.

Companion website: www.wiley.com/go/connolly/ultrasound

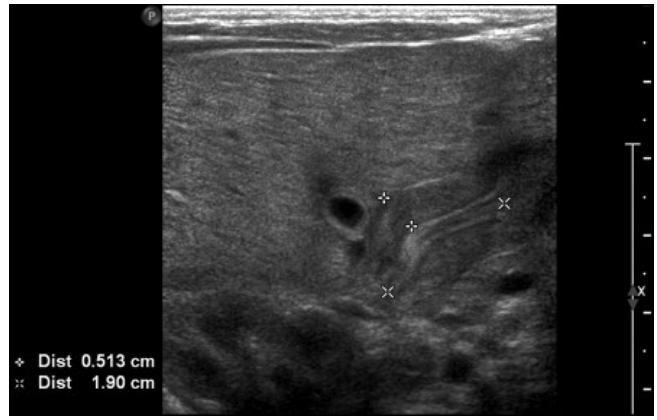

Figure 24.1 Pyloric stenosis. Longitudinal view through the pyloric channel, measuring 19 mm (normal ≤15 mm). The muscularis is also thickened at 5.13 mm (normal <3 mm).

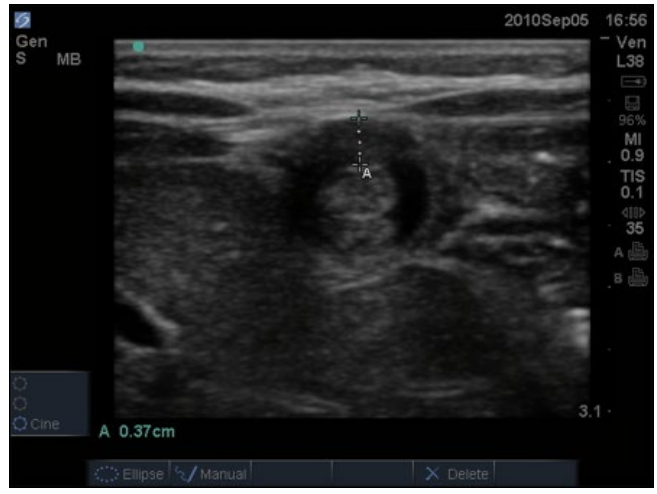

Figure 24.2 Pyloric stenosis. Transverse view demonstrating the 'doughnut' sign; the muscle thickness measured >3.7 mm (normal ≤3 mm). Image courtesy of Adam Sivitz, M.D.

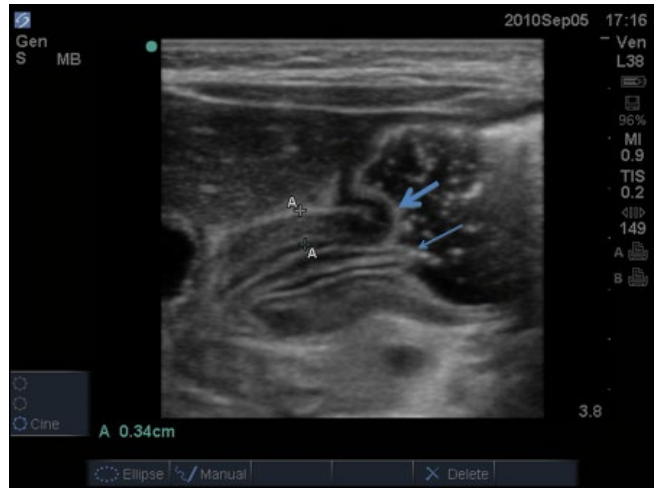

Figure 24.3 Pyloric stenosis. Longitudinal view demonstrating the 'nipple' sign (small arrow) and the 'shoulder' sign (large arrow). The hypertrophic muscularis is again seen. Image courtesy of Adam Sivitz, M.D.

include oblique sectioning of the pylorus which results in exaggerated measurements of thickness, a posterior displacement of the pylorus due to overdistension of the stomach, and pylorospasm (this is discussed in detail below).

Pylorospasm

The clinical presentation of pylorospasm can mimic that of pyloric stenosis and is distinguished by the transience of the sonographic abnormalities. During spasm, there may be some pyloric muscle thickening and/or elongation of the pyloric channel. However, pylorospasm should resolve within 5 min and therefore, if borderline measurements are obtained, the study should be repeated to distinguish the two diagnoses.

Intussusception

As the most common cause of intestinal obstruction in children aged between three months and six years, intussusception occurs when a segment of bowel telescopes on itself. Initially, this starts a vicious cycle of circulatory impairment with venous congestion leading to oedema that worsens congestion, ultimately leading to arterial obstruction and necrosis. The classic triad of intermittent abdominal pain, 'redcurrant jelly' stool and a palpable mass occurs in less than 40% of children, so clinicians should have a high index of suspicion for intussusception in a young child with paroxysmal abdominal pain and vomiting. In the past, a fluoroscopically guided enema with air and/or contrast was the preferred approach. More recently, however, ultrasound has emerged as an accurate diagnostic tool that avoids the risk of perforation.

A high-frequency transducer should be used and scanning should begin in the right lower quadrant and continue until the entire colon is scanned. The majority of intussusceptions are found in the right upper quadrant, or at the level of the mid-transverse colon. In the transverse view, the intussusception will appear as a 'swiss-roll' or 'doughnut' (Figure 24.4), or as a 'pseudokidney' in an oblique or longitudinal section (Figure 24.5). Colour Doppler may show hyperaemia initially, with decreased or absent flow with the onset of infarction.

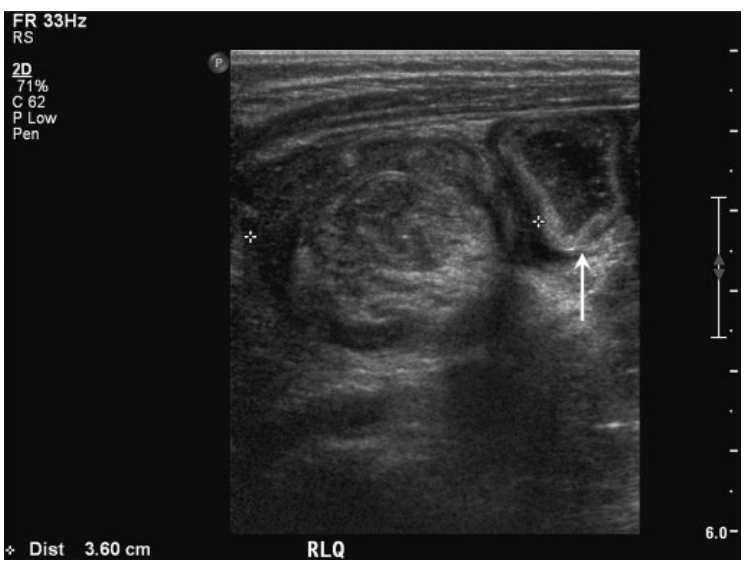

Figure 24.4 Transverse view of intussusception (between callipers). Note the adjacent fluid-filled loop of bowel (arrow). Non-peristaltic 'sentinel loops' are often see in real time adjacent to acute inflammatory conditions.

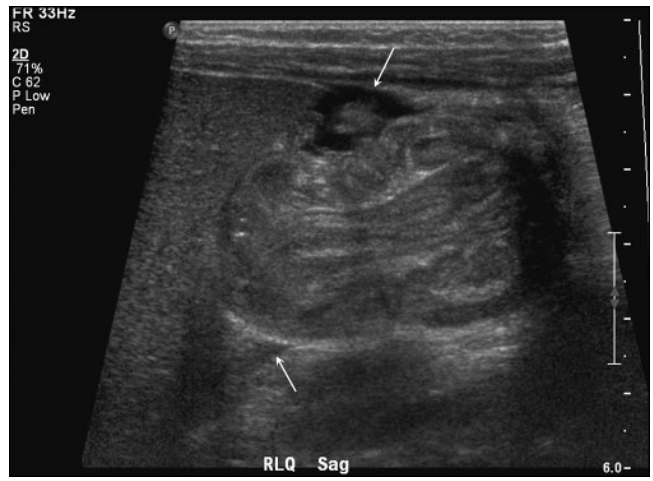

Figure 24.5 The 'pseudokidney' sign from an oblique or longitudinal view of intussusceptions. Note the adjacent peritoneal free fluid due to the inflammatory process (arrows).

Volvulus

Midgut volvulus occurs when the bowel twists around the superior mesenteric artery (SMA) as a result of embryological malrotation of the intestines. The diagnosis is usually made in early infancy, and patients present with bilious emesis. As with all ischaemic conditions, a timely diagnosis is essential.

Usually, a definitive diagnosis is made using upper gastrointestinal contrast radiography; however, there are ultrasound findings that may prompt a clinician to initially pursue this rather than alternative diagnoses. Sonologists should look for a reversal of the normal SMA/superior mesenteric vein (SMV) relationship, or the SMV may be seen directly anterior to the SMA. Midgut volvulus may be seen on colour Doppler and grey-scale ultrasound by the mesentery and SMV twisted around the SMA in the 'whirlpool sign' (Figure 24.6). This sign may be obscured by a dilated, gas-filled bowel. Other sonographic findings may include a dilated duodenum and malposition of the duodenojejunal flexure.

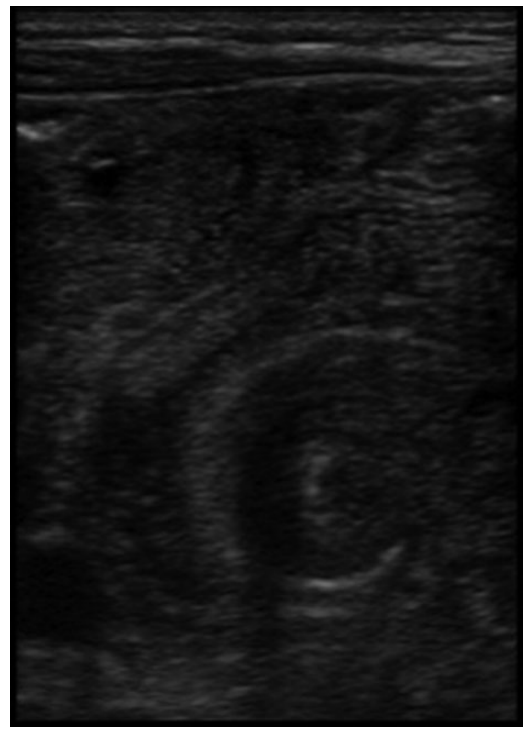

Figure 24.6 The 'whirlpool' appearance of midgut volvulus. Image courtesy of Adam Sivitz, M.D.

Appendicitis

Appendicitis is the most frequent surgical aetiology of abdominal pain in children presenting to emergency departments or outpatient clinics. There has been much debate regarding the use of ultrasound versus computed tomography in the diagnosis of appendicitis. The 'operator dependency' of ultrasound is reflected by the fact that the

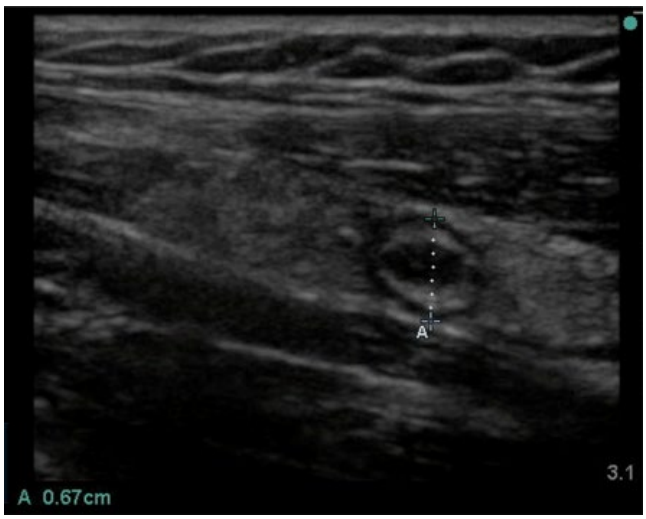

Figure 24.7 Transverse view of an inflamed appendix. As the callipers have not been placed outside the serosa the diameter is actually underestimated. Most enteric structures, including the appendix, have a three-layered sonographic appearance: a hyperechoic serosa; a hypoechoic muscularis; and a hyperechoic mucosa. This inflamed appendix contains hypoechoic fluid, which was non-compressible.

reported test characteristics of ultrasound are variable and institution-dependent.

Ultrasound for appendicitis requires a high-frequency linear transducer and a depth adjusted so that the psoas muscle is visualised in the far field. Using a graded compression technique, there is gentle, gradual pressure on the region examined by the transducer, which displaces and compresses the normal bowel loops. Compression is adequate if the iliac vessels and psoas muscle are visualised, since the appendix will be anterior to these structures. It is helpful to begin the examination at the point of maximal tenderness if the patient is able to verbalise this. If the appendix is not identified, scanning begins by identifying the ascending colon. The transducer is then moved inferiorly to identify the terminal ileum, which is easily compressible and usually demonstrates peristalsis. The appendix is about 1–2 cm below the terminal ileum. In most patients the appendix is draped over the psoas muscle, or is retrocaecal.

The sonographic findings are of an enlarged, non-compressible, blind-ending, hyperaemic tubular structure appearing as a 'target' in transverse section measuring >6 mm from outer wall to outer wall (Figure 24.7). In early appendicitis, ultrasound may demonstrate the submucosa as an inner echogenic lining in transverse view. Other findings include heterogeneity of the surrounding periappendiceal fat secondary to inflammation, an appendicolith (Figure 24.8), free fluid, and an abscess in the case of perforation. Prior to necrosis, colour flow Doppler will demonstrate hyperaemia within the appendiceal wall.

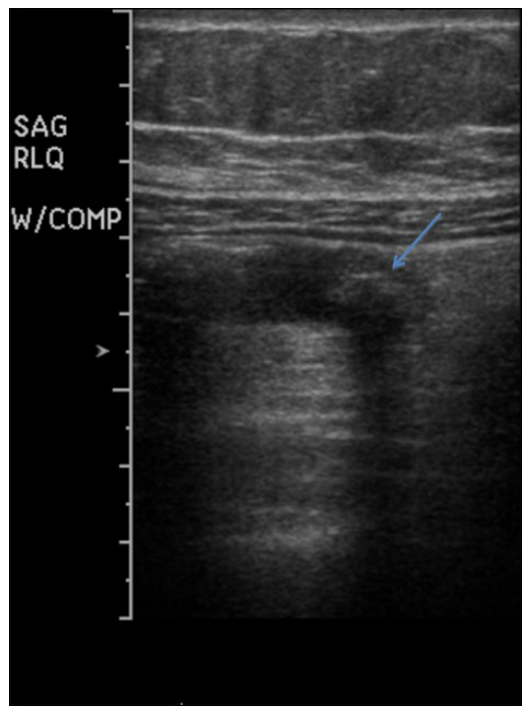

Figure 24.8 Appendicitis. Note the appendicolith (arrow) within the lumen of the appendix and the acoustic shadowing posterior to it.

Poor visualisation is responsible for most false-negative diagnoses. The appendix may not be found if graded compression is not tolerated, if it is located retrocaecal or following perforation. In these cases, its characteristic tubular structure may not be visualised, or is disrupted. In addition, the appendix may be difficult to identify in larger patients, or if it is normal and not inflamed, a retrocaecal appendix may be visualised by scanning in the coronal plane with the transducer parallel to the iliac wing. The sonologist should visualise the entire length of the appendix, as a limited examination may overlook inflammation limited to the appendiceal tip.

Further Reading

Alletag, M.J., Riera, A., Langhan, M., *et al.* (2011) Use of emergency ultrasound in the diagnostic evaluation of an infant with vomiting. *Pediatr. Emerg. Care*, **27** (10), 986–989.

Amodio, J., Fefferman, N. (2007) Ultrasound of pediatric abdominal and scrotal emergencies. *Appl. Radiol.* Available at: http://appliedradiology.com/articles/ultrasound-of-pediatric-abdominal-and-scrotal-emergencies [Accessed 27 December 2016].

Blumer, S.L., Zucconi, W.B., Cohen, H.L., *et al.* (2004) The vomiting neonate: a review of the ACR appropriateness criteria and ultrasound's role in the workup of such patients. *Ultrasound Q.*, **20** (3), 79–89.

Epelman, M. (2006) The whirlpool sign. *Radiology*, **240** (3), 910–911.

Maheshwari, P., Abograra, A., Shamam, O. (2009) Sonographic evaluation of gastrointestinal obstruction in infants: a pictorial essay. *J. Pediatr. Surg.*, **44** (10), 2037–2042.

Sivit, C.J. (2004) Imaging the child with right lower quadrant pain and suspected appendicitis: current concepts. *Pediatr. Radiol.*, **34** (6), 447–453.

Part 4

Adjunct to Practical Procedures

25

Ultrasound-Guided Vascular Access

Nova L. Panebianco

Introduction

Obtaining venous access is often a vital component of emergency department patient care. In patients with difficult venous access, or who urgently require central venous access for therapy and resuscitation, ultrasound guidance can reduce procedural time and complications, and is associated with greater patient satisfaction. The key points of this chapter include: (i) procedural set-up; (ii) transducer selection; (iii) vessel orientation; (iv) vessel selection; (v) catheter selection; (vi) issues of sterility; (vii) personnel requirements; and (viii) pitfalls associated with ultrasound-guided venous access.

With traditional technique, external landmarks and palpation were the sole guides for the placement of vascular access. Failure and complications could occur due to aberrant anatomy, intravascular volume depletion, thrombosed vessels, scarring of the vessel or operator error. Bedside ultrasound allows the direct visualisation of vessels, and with good technique may limit intravenous catheter placement failure and reduce complication rates. For this reason, the Agency for Healthcare Research and Quality in the United States, and the National Institute for Clinical Excellence in the United Kingdom, have recommended that central lines be placed under ultrasound guidance.

Ultrasound may also be used to guide peripheral intravenous catheter placement in patients with difficult intravenous access due to scarring of veins or a high body-mass index, thereby avoiding the need for the external jugular or central venous cannulation. Additionally, ultrasound can save time and is associated with increased patient satisfaction.

Despite the intuitive advantages of ultrasound guidance, poor technique can result in the same complications as traditional technique if improperly performed. For many beginners, ultrasound can actually increase the risk of failure because the ease of locating and seeing a target vessel on ultrasound gives the illusion that accessing it with a needle will be equally easy. Throughout this chapter it should be remembered that the key component of this procedure is continual awareness of *the one part of the needle that can cause injury to the patient*; namely the tip.

Technical Considerations

There are several technical considerations that must be addressed when attempting either central or peripheral ultrasound-guided venous access. As with most procedures, proper patient positioning, procedural set-up and operator comfort greatly increase the likelihood of success.

Procedural Set-Up

Before starting the procedure an inventory should be taken and the items needed for the procedure

Emergency Point-of-Care Ultrasound, Second Edition. Edited by James A. Connolly, Anthony J. Dean, Beatrice Hoffmann and Robert D. Jarman.

Companion website: www.wiley.com/go/connolly/ultrasound

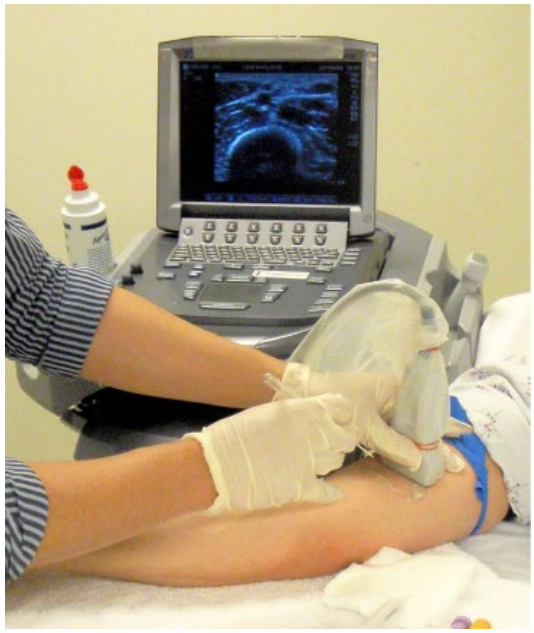

Figure 25.1 Correct set-up for ultrasound-guided peripheral venous access. The patient's arm is resting securely on a bedside table. The ultrasound screen is easily visualised by the sonographer, who uses the non-dominant hand to obtain the image on the ultrasound screen and keeps close contact with the patient's arm to prevent slipping. The transducer cord is kept out of the sterile field by being placed behind the sonologist's forearm. The dominant hand is used to insert the needle and catheter.

gathered. The patient and the operator should both be comfortable. For peripheral lines, this usually means that the operator is seated on a mobile, adjustable height stool. A mobile, adjustable-height table (more than one if available) is indispensible to set up the equipment and serve as a platform for the upper extremity when performing a peripheral intravenous line. The lights in the room should be dimmed, which will make visualising the needle on the ultrasound screen easier. The ultrasound machine should be positioned so that the sonographer can comfortably manipulate the needle, and see the ultrasound screen with minimal movement (Figure 25.1).

Transducer Selection and Orientation

In general, a high-frequency linear transducer is used for ultrasound-guided vascular access. A 'hockey stick' linear transducer is specifically designed for vascular access, and provides a nice platform for the fingers with its L-shaped design. All transducers have an indicator (notch, groove or mark) that corresponds to a screen indicator. The orientation of the transducer indicator and the orientation of the screen indicator should be concordant, regardless of the sonologist's orientation to the patient's body. This means that if an internal jugular vein is being accessed from above the patient's head, the left-hand side of the screen will now

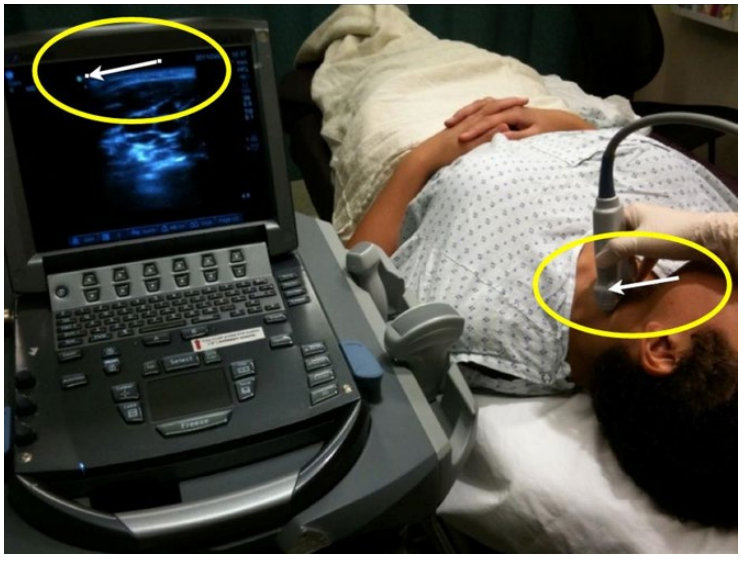

Figure 25.2 With the transverse approach, the scanning plane, the probe and the imaging screen are all oriented concordantly, as indicated by the white arrows. This relationship is maintained regardless of whether the arrow points to the right or left of the patient's body. With this arrangement, if the target vessel is seen to the *right* of the needle tip on the screen (from the operator's point of view), the operator knows to physically redirect the needle *in the same direction* as it is advanced into the patient, and vice-versa.

correlate with the left-hand side of the patient's body (see Figures 25.1 and 25.2). If the transducer and screen indicators are not concordantly oriented, movements of the needle in the patient will appear to move in the opposite direction than intended during the procedure. Prior to commencing, tap the surface of the probe to check that the left hand side corresponds with the left of the screen.

Personnel Requirements

Ultrasound-guided intravenous access, whether peripheral or central, can be performed using a one-person or two-person technique. The one-person technique can be either static or dynamic. In the dynamic one-person technique the person placing the line operates the ultrasound transducer with their non-dominant hand while manoeuvering the needle with their dominant hand. In the static technique, the operator uses the ultrasound to locate the target vessel, confirm its patency, and mark its location, depth and direction, and then attempts to place the intravenous line using this information, combined with traditional methods.

In the two-person technique, one person handles the transducer while a second person places the intravenous line. The two-person technique is more commonly used with central venous access. The advantages of the two-person technique are that it allows the person placing the line to concentrate on the procedure, retract redundant skin as necessary, and also provides an assistant to help with other aspects of the procedure. The disadvantage is that the operator loses control over what is shown on the viewing screen, making it more difficult to track the tip of the needle. Additionally, in a busy emergency department adequately trained personnel are rarely available to serve as assistants.

While the skills of the dynamic technique are more difficult to master, real-time guidance has several advantages. Notably, it takes less time, requires fewer percutaneous sticks, has a greater first-time success, decreases the number of back-wall vessel injuries, reduces the number of arterial sticks, and can be used to evaluate the line should resistance be met or a good flow not obtained from the vessel.

Vessel Selection

Before beginning the procedure the target vessel should be scanned through a length above and below the expected entry point to confirm its location, depth, diameter and course. The location of surrounding neurovascular structures should be noted (Figure 25.3.) Ideally, the vessel should be as straight as possible, and pressure should be applied to the vessel. If it

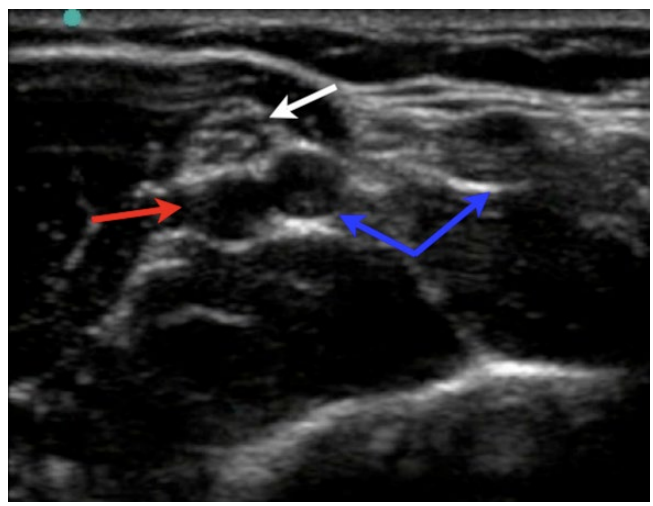

Figure 25.3 Transverse section of the upper arm. A nerve has a 'honeycomb' appearance (white arrow) and runs anterior to the artery (red arrow). Veins (blue arrows) tend to have thinner walls and larger diameters than their accompanying arteries.

does not collapse then it is either not a vein, or is not a patent vein. Colour flow Doppler may be applied to the target vessel, adjusting the settings for low-flow states. Spectral Doppler may also be applied, looking and listening for the bounding 'whoosh' of an artery versus the 'constant hum' of a vein.

Vessel diameter – not depth – is the most important factor in successful ultrasound-guided intravenous cannulation. However, deeper vessels are associated with early peripheral intravenous line failure. Thus, ideally, the vessel of choice would be relatively large and shallow. It takes very little effort to collapse a peripheral vein. However, if too much pressure is applied target vessels may collapse and not be identified; hence, a light touch is needed.

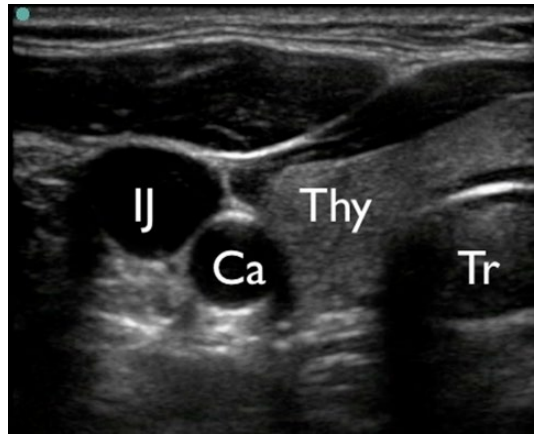

Figure 25.4 Normal anatomy of the left side of the neck, with the sonologist positioned above the patient's head in transverse plane. Note that in this view, the left side of the screen is pointing to the left side of the patient's body (see Figure 25.2). IJ, internal jugular; Ca, common carotid; Thy, thyroid; Tr, trachea.

Transducer Orientation

The transducer can be oriented transversely or longitudinally with respect to the vessel. There are advantages and disadvantages to each orientation. In the transverse plane (out of plane) the vessel is seen in cross-section. The benefit of this plane is that it provides perspective on surrounding structures, such as arteries and nerves (Figure 25.4). The transverse technique has been shown to be easier for novice sonographers. The drawback of this orientation is that once the needle tip has passed through the scanning plane of the transducer, its depth and location are unknown, leading to the risk of the needle being passed through back wall of the vessel or missing it completely, with damage to deeper structures (including arteries and pleura in the neck). This technique therefore requires that the operator move the transducer across the skin as she follows the tip of the needle into the vessel (described in detail below). This technique requires skill and practice to master.

At the start of the procedure using the transverse orientation the transducer should be placed over the target vessel in such a way that it appears in the middle of the screen. Depth should be adjusted so that as much of the screen as possible is devoted to the space between the skin and the posterior wall of the vessel. Focal adjustment, if available, should be about midway between the skin and the target vessel. If multiple focal zones are available, since with such shallow scanning, frame-rate is rarely an issue. The needle will puncture the skin adjacent to the middle of the transducer at a 30–45° angle to the skin. As soon as the needle has passed a few millimetres through the skin the needle tip, with its bright echo with shadowing and reverberation artefact, should be sought (Figure 25.5). As previously noted, *any part of the needle will cause the same shadow and reverberation artefact, as the tip*. The sonologist can only definitively identify the tip by seeing it disappear in real time as the transducer (and scanning plane) are moved beyond it, and seeing it re-appear on the screen as the transducer is moved back towards the needle. Once the needle tip is located, the operator should advance the transducer a few millimetres away from the needle until its echo/artefact disappears from the viewing screen. The needle is then advanced towards the scanning plane and the vessel until it is seen again on the screen. This process is repeated with 2–3 mm advances of the transducer, followed by advances of the needle with continual localisation of the needle tip, which can be redirected as it approaches the vein.

When the needle tip is seen within the vessel, the angle of the needle is reduced (usually to as close to parallel to the surface of the skin as possible) so that the tip does not pierce the back

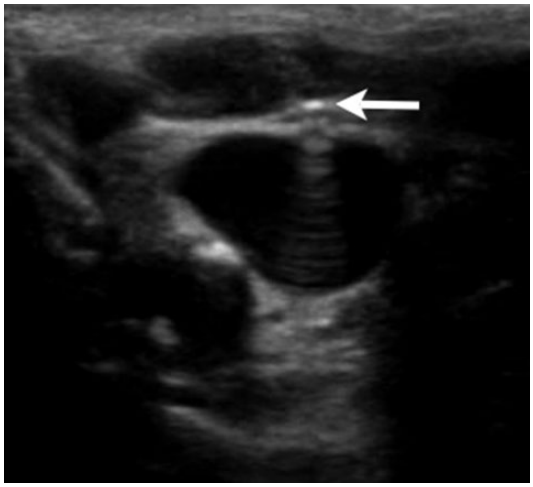

Figure 25.5 Bright echo of the needle (arrow) is seen touching the anterior wall of the internal jugular vein with characteristic reverberation ('comet tail') artefact seen behind it in the lumen of the vessel.

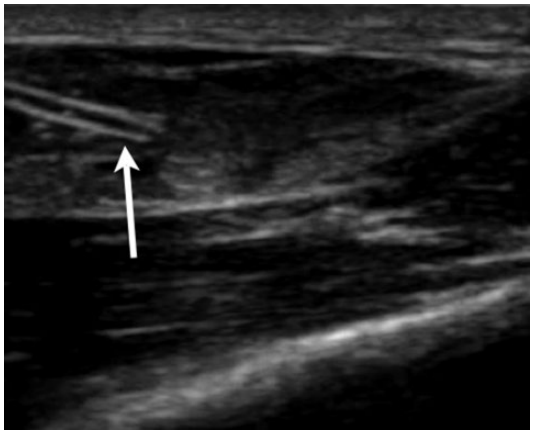

Figure 25.6 Longitudinal image of an angiocatheter blindly ending in soft-tissue (arrow).

wall and the catheter does not kink when advanced into the lumen. The needle should be advanced for at least1 cm within the lumen, *using the same direct ultrasound visualisation technique.* Failure to obtain complete entry of the catheter will result in dislodging the vein when the catheter is advanced (Figure 25.6).

In the longitudinal plane (in plane technique), the vessel will appear to course across the screen parallel to the skin. When placing an intravenous line in the longitudinal plane the (non-dominant) scanning hand remains fixed in one location, and the needle is advanced towards the vessel with the dominant hand in the exact scanning plane of the transducer. As with the transverse orientation, entry should start at a 30–45° angle to the skin. The needle should enter the skin as close as possible to the edge of the transducer, and the angle then lessened when the needle is seen within the lumen of the target vessel. If this is done properly, the needle tip can easily be seen entering the lumen of the vessel (Figure 25.7). Again, the needle should be advanced for at least 1 cm within the lumen, with direct ultrasound visualisation to ensure complete entry. Less-experienced sonologists find this technique more challenging because, if the needle leaves the plane of the ultrasound/vein, it is often difficult to re-orient the needle and/or transducer so that all three are once again in a single plane.

The disadvantage of the longitudinal orientation is that surrounding structures such as the arteries or nerves that course parallel to the vein are not seen, and these may be injured by the needle if it deviates from the plane of the ultrasound. Another problem with the longitudinal

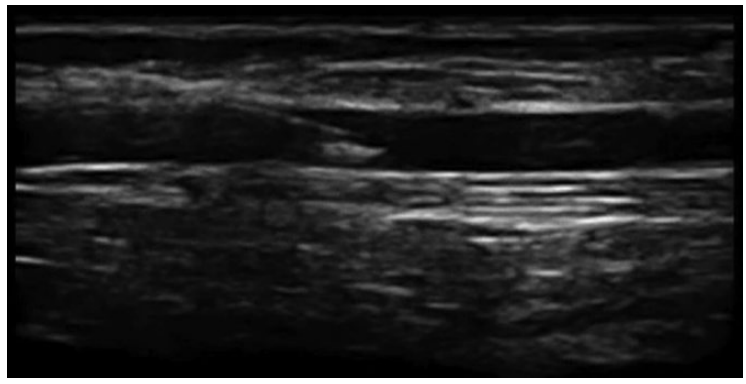

Figure 25.7 Needle within the lumen of a peripheral vein in longitudinal plane.

technique is that in access sites with limited space (e.g., paediatric patients or those with short necks) there may not be sufficient room for the longitudinally oriented transducer and needle. However, it does allow excellent depth control.

With the inherent advantages and limitations of both transverse and longitudinal planes, experienced operators frequently use both planes during the procedure. Rotating between transverse and longitudinal plane requires some practice and dexterity of the scanning hand, but it can give the operator the benefit of both orientations.

Catheter Selection

For central ultrasound-guided venous access, the equipment of stock central line kits is adequate. For ultrasound-guided peripheral access, extra-long catheters are ideal (48 mm or greater). Even if a shallow vessel is identified, a longer 48 mm catheter should be used to ensure that an adequate amount of the catheter sits in the vein. The deeper the vessel, the steeper the angle of approach that is needed to reach the vessel. However, with a steep angle of approach there is an increased risk of injuring the back wall of the vessel and causing kinking of the catheter at the point of entry. Conversely, a too-shallow angle of approach may lead to insufficient catheter reaching the vessel or remaining stably within it after placement.

Peripherally inserted central catheter ('PICC') lines, 'mid lines' (shortened PICC lines), paediatric central lines and a variety of other catheters have been used to obtain sufficiently long cannulas for access to deep peripheral veins and be left in place for up to 30 days.

Issues of Sterility

Ultrasound-guided central venous access is a sterile procedure. The patient should be prepped and draped using standard protocols. The ultrasound transducer should also be sterile for the procedure. Commercially available sterile kits include a transducer cover (ideally approximately 1 m long to cover the cord and avoid contamination of the field), sterile gel, and rubber bands to keep the sheath from slipping off. In an emergency, a sterile glove may suffice or a clear adherent surgical sterile dressing may be used.

When performing ultrasound-guided central venous access the operator should gown-up and the patient be prepped first. An assistant is necessary to place coupling gel inside the sterile sheath and direct the transducer into the sheath (which is held by the gowned operator). The transducer, covered in its sterile sheath, is then rested on the sterile field.

Peripheral ultrasound-guided intravenous lines need not be placed under full sterile technique. However, the transducer should be covered to protect the patient from any pathogens on the transducer, and to keep the transducer itself protected from the patient's blood. In most cases of ultrasound guided peripheral access the patient has some condition that makes traditional technique impossible. In such patients the peripheral IV that is obtained is highly "valuable" both to the patient and the healthcare team. Every effort should be made to ensure that such a line lasts as long as possible. This includes careful aseptic technique to minimize the likelihood of cellulitis of phlebitis. The skin should be fully and thoroughly washed and prepped with antiseptic solution using the technique recommended for obtaining blood cultures.

Pearls and Pitfalls

There are several pitfalls associated with ultrasound-guided venous access.

- As noted the commonest pitfall is failure to have continual sonographic localisation of the needle tip.
- It is possible to misidentify an artery for a vein, or a vein for an artery. Gentle compression, colour or spectral Doppler may help to distinguish arteries from veins.
- Evaluation of the vein will occasionally reveal thrombosis (Figure 25.8).
- Lymph nodes appear as non-tubular structures with a hypoechoic cortex and a relatively hyperechoic medulla. They may be differentiated from veins as they are not tubular, do not compress, and have colour flow in the medulla.
- Nerves often run parallel to veins and can appear dark if viewed at an oblique angle. However, when the scanning plane is oriented perpendicular to a nerve its characteristic

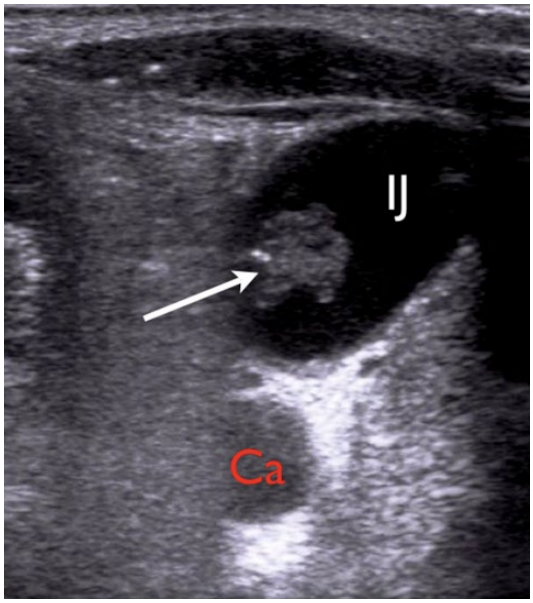

Figure 25.8 Partially occluding thrombus in the internal jugular vein. IJ, internal jugular vein; Ca, common carotid artery.

internal 'honeycomb' pattern can be seen (anisotropy) (Figure 25.3). As with other non-vascular structures, they will not compress with pressure and do not have colour flow.

Conclusions

Ultrasound-guided intravenous access in the critical care unit and emergency department settings can facilitate intravenous line placement in patients with difficult access or abnormal anatomy, and improve patient safety and satisfaction. It may also expedite care. However, technical proficiency is essential, and the necessary skills cannot be attained without effort and practice. Proper patient positioning, set-up, and awareness of the technical considerations and pitfalls of the procedure, are essential for success.

Further Reading

Blivas, M., Brannam, L., Fernandez, E. (2003) Short-axis versus long-axis approaches for teaching ultrasound-guided vascular access on a new inanimate model. *Acad. Emerg. Med.*, **10** (12), 1307–1311.

Constantino, T.G., Parikh, A.K., Satz, W.A., Fojtik, J. (2005) Ultrasonography-guided peripheral intravenous access versus traditional approaches in patients with difficulty intravenous access. *Ann. Emerg. Med.*, **46**, 456–461.

Fields, J.M., Toddman, R., Anderson, K., Dean, A.J., Panebianco, N.P. (2010) Early failure of ultrasound-guided peripheral intravenous catheters in the emergency department: it's not just about getting the IV – it's about keeping it. Abstract Presentation. American College of Emergency Physicians, September 2010, Las Vegas.

Karakisos, D., Labropoulos, N., De Groot, E., Patrianakos, A.P., Kouraklis, G., Poularas, J., Samonis, G., Tsoutsos, D.A. (2006) Real-time ultrasound-guided catheterisation of the internal jugular vein: a prospective comparison with the landmark technique in critical care patients. *Crit. Care*, **10** (6), R162.

Mills, C.M., Liebmann, O., Stone, M.B., Frazee, B.W. (2001) Ultrasonographically guided insertion of a 15-cm catheter into the deep brachial or basilic veins in patients with difficult intravenous access. *Ann. Emerg. Med.*, **50** (1), 68–72.

National Institute for Clinical Excellence (2002) *Guidance on the Use of Ultrasound Locating Devices for Placing Central Venous Catheters*. NICE, London [NICE Technology Appraisal No. 49]. Available at: https://www.nice.org.uk/guidance/ta49/resources/appendix-b-proposal-paper-presented-to-the-institutes-guidance-executive2. Accessed February 2017.

Resnick, J.R., Cydulka, R.K., Donato, J., Jones, R.A., Werner, S.L. (2008) Success of ultrasound-guided peripheral intravenous access with skin marking. *Acad. Emerg. Med.*, **5** (8), 723–730.

Rothschild, JM. (2001) Ultrasound guidance of central vein catheterization. In: *On Making Health Care Safer: A Critical Analysis of Patient Safety Practices*. Rockville, MD: AHRQ Publications; Chapter 21: 245–255. Available at: http://www.ahrq.gov/clinic/ptsafety/chap21.htm. Accessed February, 2017.

Shojania, K.G., Duncan, B.W., McDonald, K.M., Wachter, R.M., Markowitz, A.J. (2001) Making Health Care Safer: A Critical Analysis of Patient Safety Practices. *Evid. Rep. Technol. Assess. (Summ.)*, (**43**), i–x, 1–668.

26

Pericardiocentesis, Paracentesis and Thoracentesis

David B. Richards

Introduction

Pericardiocentesis, paracentesis and thoracentesis are invasive procedures that involve the introduction of a sharp object in the vicinity of a variety of vital organs. Ultrasound guidance has been shown to lower complication rates for all three procedures. Ultrasound allows direct visualisation of the target fluid, its location with respect to the surface, and adjacent or interposed structures. Guidance can be in real time or as a preliminary localisation and marking step prior to sterile access.

Pericardiocentesis

Emergency pericardiocentesis can prove to be life-saving in patients with haemodynamic instability, life-threatening respiratory compromise and pulseless electrical activity secondary to pericardial tamponade. Echocardiographic guidance significantly decreases the morbidity and mortality associated with pericardiocentesis, and should be within the armamentarium of most emergency physicians.

Pericardiocentesis involves the drainage of fluid from the pericardium for diagnostic or therapeutic purposes. Given the anatomical location and involved structures, pericardiocentesis is a procedure fraught with potential complications. It was first performed via a landmark-guided approach, with associated morbidity and mortality rates as high as 50% and 19%, respectively. A technique using electrocardiographic changes of injury to the myocardium to indicate needle location was first described in 1956. This was followed by the description of echocardiographic guidance in 1977 by Chandraratna. Since that time, echocardiographic guidance of the procedure has proven to be a safer approach and this now represents the standard of care at many centres. Training in echocardiography-guided pericardiocentesis is now part of the recommended ultrasound curriculum by the American College of Emergency Physicians. The safety and efficacy of sonographically guided pericardiocentesis has been established. In a series of 1127 consecutive echocardiography-guided pericardiocenteses over a 21-year period, Tsang reported a 97% overall procedural success rate with major complications encountered in 1.2%, including ventricular laceration, intercostal vessel injury requiring surgery, pneumothoraces requiring tube thoracostomy, ventricular tachycardia and bacteraemia. Minor complications such as transient chamber entry, small pneumothorax not requiring intervention and probable pleuropericardial fistulas were encountered in 3.5% of patients.

Performing the procedure with echocardiographic guidance allows direct visualisation of the pericardial fluid, the location of the fluid with respect to the surface, and real-time guidance of

Emergency Point-of-Care Ultrasound, Second Edition. Edited by James A. Connolly, Anthony J. Dean, Beatrice Hoffmann and Robert D. Jarman.

Companion website: www.wiley.com/go/connolly/ultrasound

the needle and catheter. Usually, a pericardial effusion needing drainage creates its own sonographic and access window, but if the access appears limited and the patient can tolerate it, a 30–45° elevation of the torso or semi-left lateral decubitus positioning may enlarge the target area, as determined by ultrasonography in real time.

A 2.5–5 MHz transducer with a small footprint is ideal for visualisation and performance of a pericardiocentesis. Following sterile preparation of the ultrasound transducer and the patient's chest wall, the probe can be placed in either a subxiphoid or parasternal long-axis location for visualisation of the pericardial fluid. The subxiphoid view typically provides the best overview of the heart and pericardium in a single view, and is particularly good for the identification of a circumferential pericardial effusion. The parasternal long-axis window is more important since it provides a view of the effusion and the preferred access pathway at one and the same time. An apical four-chamber view can be seen in Video 26.1.

The general approach to needle placement with echocardiographic guidance is to find *the largest fluid accumulation nearest the chest wall with no intervening vital structures.* Care should be taken to avoid the internal mammary artery, which runs in a cephalad–caudal direction 2–5 cm lateral to the sternum. Often, a parasternal approach, just lateral to the sternum and above the 5th rib, is the best needle insertion site for drainage of a circumferential pericardial effusion under live sonographic guidance. The subxiphoid needle approach used in the traditional 'landmark' technique was used because it obviated the risk of pulmonary puncture, pneumothorax, and laceration of the left anterior descending coronary artery if the presence of an effusion was not certain. All of these concerns can rapidly be addressed by ultrasound, so that the transhepatic approach is not the preferred approach when ultrasound is available unless it is the only access to a loculated effusion.

Prior to prepping the patient's skin a general exploration of the precordial anatomy and options should be made. Once the optimal site has been identified, a still image should be obtained when the target area of the effusion is at its thinnest (it usually varies with cardiac and respiratory motion) and a measurement should be made of the distance from the skin to the target, and the thickness of the effusion. A regular piece of ECG or monitor strip can be used to measure centimeters and millimetres along the shaft of the drainage needle to determine, before inserting the needle, the minimum and maximum depth that the needle can be inserted. In general emergency pericardiocentesis would be undertaken with trepidation for a collection that was less than 8mm thick along the anticipated track of the needle, since the needle has to be advanced until the catheter tip is completely within the effusion.

Identification of a pericardial effusion can be made with the transducer in several different locations. If space allows, the transducer can be placed directly next to the needle during actual performance of the procedure in order to optimise visualisation of the needle pathway and pericardial effusion. The angle of approach for the needle should be exactly the same as the angle of the transducer when the largest fluid collection closest to the surface is identified. If a two-step technique is used, during the ultrasound evaluation, the patient should be asked to take deep breaths in and out to ensure that the target fluid is present throughout the respiratory cycle. If possible, in-plane visualisation of the needle path during the procedure should be maintained. With this technique, the needle and the ultrasound beam should be almost parallel, so that the needle is easily seen; the tenting of the parietal pericardium, as the needle contacts and penetrates it, allows for needle tip localization. Care should be taken that the needle is advanced at least 4 mm after the first sign of fluid drainage, since it is essential that the catheter is not advanced over the needle until it also is fully within the effusion. As with central venous access, the most effective method of ultrasound guidance is real-time visualisation rather than the two-step method.

The administration of local anaesthesia along the needle tract is recommended if the clinical situation allows. Pericardiocentesis catheter placement typically involves accessing the

effusion with a 16- or 18-gauge catheter over an 8-cm needle, or the placement of a 5- to 8-Fr pigtail catheter, which has the advantage of side ports over a wire using a Seldinger technique.

Agitated saline can be injected as a sonographic contrast medium into the needle or catheter to confirm placement within the pericardial space (Videos 26.2 and 26.3). An aliquot (9 ml) of saline and 1 ml of air can be shuttled between two 10 ml syringes on a stopcock to create the solution. The agitated saline appears brightly echogenic and will highlight the pericardial space if the needle or catheter is properly positioned. Fluid can be removed, followed by removal of the catheter, or the catheter can be secured in place for ongoing drainage. A chest radiograph should be obtained after the procedure to ensure that a pneumothorax has not developed, even if echocardiographic guidance is used.

Paracentesis

Paracentesis is an important diagnostic procedure for patients with new-onset ascites, as well as those patients with pre-existing ascites who may have developed a new process, such as bacterial peritonitis. By identifying collections of ascitic fluid that are amenable to drainage, ultrasound has been shown to significantly increase the success rate of paracentesis in the emergency department. In a prospective randomised study comparing traditional versus ultrasound-guided technique, Nazeer reported that 95% of patients (40/42) were successfully aspirated in the ultrasound group compared to only 61% of those (27/44) in the non-ultrasound group. Furthermore, complications such as puncture of the bladder or bowel can be avoided by sonographic identification of these structures before the procedure is even begun. In patients with intra-abdominal adhesions from previous surgeries or infections, the ascitic fluid may be loculated.

A 3.5–5.0 MHz transducer is typically chosen for paracentesis to allow the identification of large collections of fluid that are amenable to drainage, often some distance from the surface. Ascitic fluid appears anechoic, while bowel containing fluid or air will have some degree of echogenicity (Figure 26.1).

After a collection of ascites has been selected by ultrasound it is important to avoid moving the patient, as this can change the location of the ascites. Areas of skin infection or dilated abdominal wall vessels should be avoided. Patients should be asked to take deep breaths in and out during the ultrasound evaluation to ensure that there are no intervening structures throughout the respiratory cycle. If access sites in the lower quadrants are selected, it is important to avoid the inferior epigastric arteries. The

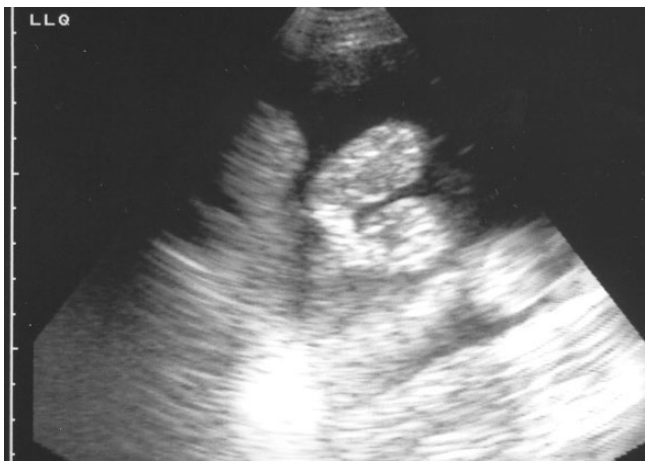

Figure 26.1 Hyperechoic loops of bowel floating in ascites. Image © A. J. Dean.

latter vessels arise from the external iliacs, immediately before they pass thorough the inguinal canal, so their origins can be identified by the femoral pulse in the groin. They course medially and superiorly, running up the interior abdominal wall, analogous to the internal mammaries in the chest, about 5 cm on either side of the midline. Their location can usually be mapped using colour-flow Doppler with appropriately adjusted (low-velocity) scale, depth and gain settings. The probe should be angled as far as possible from perpendicular to the abdominal wall to maximise the Doppler signal from these small vessels.

A candidate puncture site can be identified and marked prior to sterile preparation, or a real-time guidance approach can be used similar to that described for pericardiocentesis. After sterile preparation of the site and administration of local anaesthesia, a needle and catheter are used to enter the peritoneal cavity. Since ascitic fluid may be under pressure, and many of these patients have coagulopathy, it is recommended that a 'Z-tract' technique is used. (This involves applying lateral traction to the skin while advancing the needle through the abdominal wall; when the needle is removed this results in a needle track that does not make a direct line from the interior to the skin.) The fluid collection is entered under in-plane visualisation with the ultrasound and the fluid withdrawn.

Problems such as bowel or omentum obstructing the end of the catheter, or complete drainage of the pocket of fluid, can be identified easily using ultrasound. This problem can also be avoided by using a dedicated paracentesis kit with catheters that have several sideports in addition to that at the tip. Potential complications of paracentesis relate to circulatory dysfunction after the removal of a large volume of ascites, persistent leakage of fluid, and localised infection or haematoma formation. Ultrasound guidance increases the success rate and efficiency of paracentesis, and is a fast and easy-to-use tool for the treating clinicians.

Thoracentesis

Ultrasound has proven to be helpful both in diagnosing pleural effusions and in minimising the complications associated with thoracentesis. Ultrasound can localise very small effusions compared to plain radiography, with delays, logistical impediments associated with patient transfer and the risk of removal of the patient from the treatment area being avoided.

Pneumothorax is the most common serious complication of thoracentesis. In a meta-analysis of 24 studies examining the effect of ultrasound use on the incidence of pneumothorax, Gordon *et al.* reported a significant decrease in pneumothorax rate with ultrasound (odds ratio 0.3, 95% confidence interval 0.2–0.7). It is important to note that this effect has *not* been seen in patients who had sonographic localisation of fluid and skin marking in one department, followed by thoracentesis in another department by another provider. Only providers who performed localisation and thoracentesis without patient movement, or who performed the thoracentesis under live ultrasound guidance, had a lower incidence of pneumothorax.

A 3.5–5.0 MHz transducer with a small footprint allows for the best visualisation of pleural fluid. This allows the clinician to minimise rib shadows while having the depth to see the full extent of the effusion, identify, and avoid the lung and other underlying structures (Figure 26.2; see Video 26.4). Ultrasonographic characteristics of pleural effusions amenable to thoracentesis include: (i) dependent anechoic fluid; (ii) at least 15 mm of fluid between the parietal pleura and lung; and (iii) effusion seen one rib space above and below the anticipated thoracentesis site throughout the respiratory cycle (see Figure 26.2b).

As described for pericardiocentesis and paracentesis, either the real-time needle visualisation technique or the two-step skin marking method can be used. In the latter case, the patient should be marked in the exact position in which the procedure is performed. For most patients who can tolerate it, sitting on the edge of the stretcher with the upper trunk supported

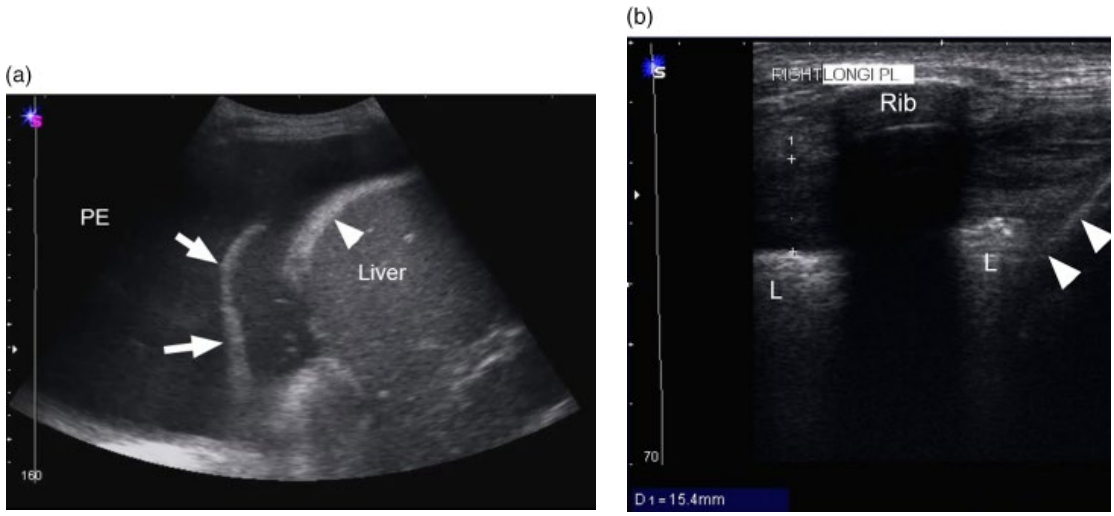

Figure 26.2 (a) A large right pleural effusion can be seen. The diaphragm (arrowhead) and completely atelectatic lung (arrows) can be seen. The lung is barely visible at the bottom of the image (see Video 26.1). (b) The pocket depth of a smaller pleural effusion is measured at 1.54 cm, barely sufficient for a safe thoracentesis. The rib-space on the left-hand side of the image would be used, if necessary, since it is a full rib-space clear of the diaphragm (arrowheads). Images © A. J. Dean.

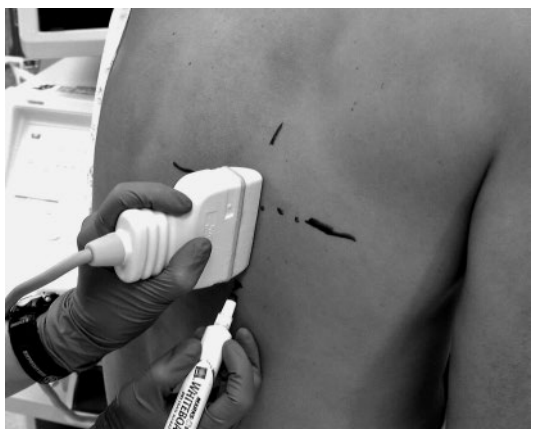

Figure 26.3 Patient positioning and technique for marking the thoracentesis site using the two-step method (see text for details). Image © A. J. Dean.

by bedside table is ideal (Figure 26.3). The first method may be challenging without assistance as it allows for only one hand to direct the needle passage through the chest wall. Given the growing amount of literature establishing the improved safety of thoracentesis with ultrasound it is now recommended as a 'best practice' at some centres.

Further Reading

American College of Emergency Physicians (2009) Emergency Ultrasound Guidelines. *Ann. Emerg. Med.*, **53**, 566.

Bishop, L.H., Jr, Estes, E.H., Jr, McIntosh, H.D. (1956) Electrocardiogram as a safeguard in pericardiocentesis. *J. Am. Med. Assoc.*, **162**, 264–265.

Chandraratna, P., First, J., Langevin, E., *et al.* (1977) Echocardiographic contrast studies during pericardiocentesis. *Ann. Intern. Med.*, **87**, 199–200.

Clarke, D., Cosgrove, D. (1987) Real-time ultrasound scanning in the planning and guidance of pericardiocentesis. *Clin. Radiol.*, **38**, 119.

Daniels, C., Ryu, J. (2011) Improving the safety of thoracentesis. *Curr. Opin. Pulm. Med.*, **17**, 232–236.

Gordon, C., Feller-Kopman, D., Balk, E., *et al.* (2010) Pneumothorax following thoracentesis. *Arch. Intern. Med.*, **170**, 332–339.

Heffner, J., Klein, J., Hampson, C. (2010) Diagnostic utility and clinical application of imaging for pleural space infections. *Chest*, **137**, 467–479.

Kohan, J., Poe, R., Israel, R., *et al.* (1986) Value of chest ultrasonography versus decubitus roentgenography for thoracentesis. *Am. Rev. Resp. Dis.*, **133**, 1124–1126.

Krikorian, J.G., Hancock, E.W. (1978) Pericardiocentesis. *Am. J. Med.*, **65**, 808–814.

Nazeer, S.R., Dewbre, H., Miller, A.H. (2005) Ultrasound-assisted paracentesis performed by emergency physicians vs. the traditional technique: a prospective, randomized study. *Am. J. Emerg. Med.*, **23**, 363.

Paracentesis: Multimedia. *eMedicine.* [Online] [Cited: December 28, 2010]. Available at: http://emedicine.medscape.com/article/80944-media.

Raptopoulos, V., Davis, L., Lee, G., *et al.* (1991) Factors affecting the development of pneumothorax associated with thoracentesis. *Am. J. Roentgenol.*, **156**, 917–920.

Schussler, J.M., Grayburn, P.A. (2010) Contrast guided two-dimensional echocardiography for needle localization during pericardiocentesis: a case report. *J. Am. Soc. Echocardiogr.*, **23**, 683.e1–683.e2.

Thomsen, T., Shaffer, R., White, B., *et al.* (2006) Paracentesis. *J. Am. Med. Assoc.*, **355**, e21.

Tsang, T., Barnes, M., Hayes, S., *et al.* (1999) Clinical and echocardiographic characteristics of significant pericardial effusions following cardiothoracic surgery and outcomes of echo-guided pericardiocentesis for management: the Mayo Clinic experience, 1979–1998. *Chest*, **116**, 322–331.

Tsang, T., El-Najdawi, E., Freeman, W., *et al.* (1998) Percutaneous echocardiographically guided pericardiocentesis in pediatric patients: evaluation of safety and efficacy. *J. Am. Soc. Echocardiogr.*, **11**, 1072–1077.

Tsang, T., Enriquez-Sarano, M., Freeman, W., *et al.* (2002) Consecutive 1127 therapeutic echocardiographically guided pericardiocenteses: clinical profile, practice patterns, and outcomes spanning 21 years. *Mayo Clin. Proc.*, **77**, 429–436.

Tsang, T., Seward, J. (2001) Pericardiocentesis under echocardiographic guidance. *Eur. J. Echocardiogr.*, **2**, 68–69.

Wong, B., Murphy, J., Chang, C.J., *et al.* (1979) The risk of pericardiocentesis. *Am. J. Cardiol.*, **44**, 1110–1114.

27

Suprapubic Aspiration and Catheterisation

Fernando Silva

Introduction

Suprapubic urinary bladder aspiration is a common urologic procedure, but is infrequently performed in the emergency and critical care setting. Nevertheless, it is a useful tool in the event of inability to pass a Foley catheter, and in infants it has been advocated by some as a more reliable source of a sterile urine specimen for culture than either a catheterised or mid-stream specimen, as there is no exposure of either the sample or catheter to the urethral and genital areas.

With ultrasound guidance, suprapubic aspiration is safe, with very low complication rates. Ultrasound guidance has a greater impact on the safety profile of suprapubic aspiration for non-urologists than for urologists, most likely due to the surgeons' operative familiarity with the urogenital anatomy, and the resultant ability to perform procedures in this region by landmarks alone. In contrast to the typical reaction of family members or spectators when confronted by this procedure, studies suggest that suprapubic access to the bladder may be less painful than the transurethral approach in many children. It may also be preferred by adult male patients with experience of traumatic catheterisations or urethral stricture. The suprapubic approach also has a lower risk of bacterial contamination of the bladder than urethral catheterisation.

Indications

There are two primary indications for suprapubic bladder aspiration: (i) relief of urinary retention; and (ii) collection of a sterile urine sample for culture. Suprapubic drainage of the bladder is indicated if the urine cannot be drained by the urethra for any physiological or anatomical reason (e.g., urethral stricture or trauma). If long-term drainage is anticipated, a suprapubic catheter can be placed; otherwise, the bladder is emptied with a simple needle puncture and aspiration. Suprapubic needle aspiration is the 'gold standard' method for obtaining a sterile urine sample. The technique is mostly used in infancy and early childhood, but is occasionally necessary in adults and the elderly.

Contraindications

The absolute contraindication is the inability to visualise the bladder or the presence of loops of bowel (usually due to adhesions) overlying the bladder on sonography. Relative contraindications include coagulopathy, overlying cellulitis or the presence of bladder cancer by history, or identified on sonography.

Emergency Point-of-Care Ultrasound, Second Edition. Edited by James A. Connolly, Anthony J. Dean, Beatrice Hoffmann and Robert D. Jarman.

Companion website: www.wiley.com/go/connolly/ultrasound

Technique

The following discussion focuses on the role of ultrasound in guiding the procedure. For technical details of the procedure itself, readers should consult a text on the topic. Sterile technique is used. The preparation consists of assembling the necessary equipment. For infants and children, a 22-gauge × 3.75 cm needle is adequate. The distance to the bladder lumen can be measured using ultrasound, but in most adults the distance to the bladder lumen is 5 cm or more, mandating the use of a 20-gauge spinal needle (with trochar). Even if it appears by ultrasound that the lumen can be reached with a shorter needle, the operator must beware that the bladder wall becomes thicker as the volume of urine decreases (i.e., during aspiration), so that there is the risk of the occluding the needle tip if it is only just inside the lumen of the bladder. If a cystostomy catheter is to be placed, the type and size of catheter and method of access will be determined by the kit that is available. Many kits use the Seldinger technique.

The choice of transducer depends on patient size and body habitus. A high-frequency linear-array probe is optimal in most patients. For children and adults with a high body-mass index a lower-frequency, curved-array probe may be necessary. Phased-array probes can be used to localise the bladder, but are suboptimal for real-time guidance due to their poor near-field resolution.

Both, static and dynamic techniques can be used. The primary goal of ultrasound guidance is to confirm that there is actually urine in the bladder and to determine a puncture site that gives direct access to the bladder, particularly avoiding the bowel. The first step is to identify a well-filled bladder above the pubic symphysis (see Figures 27.1 and 27.2). The point of peritoneal reflection from the anterior abdominal wall onto the dome of the bladder is identified. A transverse (coronal) scan is performed to identify the point at which the bladder is closest to the skin. Preference is given to the midline because the absence of any muscle layers in the linea alba makes it less vascular and therefore less prone to post-procedure bleeding. Longitudinal (sagittal) views will confirm a safe cephalocaudal distance between the anticipated access site and the dome of the bladder (Figure 27.2b–d). Trendelenberg positioning may displace the bowel superiorly, but does not change the location, shape or size of the bladder, and therefore is unlikely to materially increase the size of the window available for the tap.

If the static technique is being used, at this point the optimal location for needle puncture is marked on the skin. A measurement of the anticipated depth of entry of the bladder lumen is made. The operator makes a mental

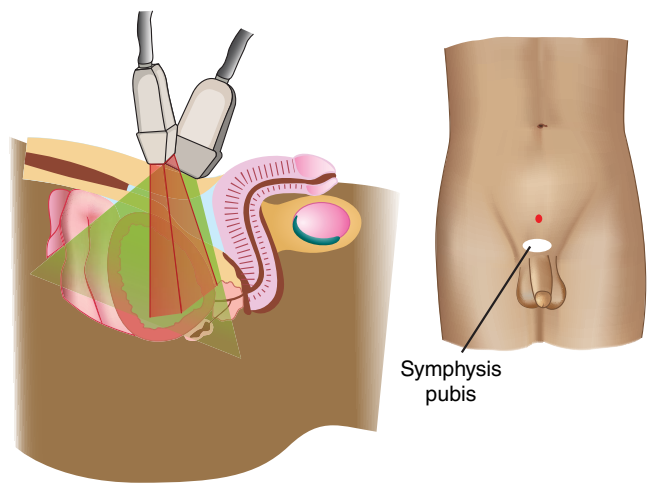

Figure 27.1 Left: the approximate location of a typical suprapubic tab in an infant is demonstrated. Right: the transverse and longitudinal scanning sections of a typical curved array transducer are demonstrated. The bladder and its surroundings are scanned in both the transverse and longitudinal planes for detection of the peritoneal limits and determination of the best puncture point, usually immediately above the symphysis pubis.

image of the direction of the needle path to enter the bladder most directly. The probe is removed, and the skin is prepped with cleansing solution and appropriately draped. Local anaesthetic is introduced at the site of anticipated puncture, followed by access to the bladder with the previously chosen type of needle. The needle is inserted while gently aspirating, such that a urine flash is obtained when the bladder is entered. After the urine flash it is important to continue to advance the needle for about 1 cm to ensure that the entire bevel of the needle is completely within the bladder.

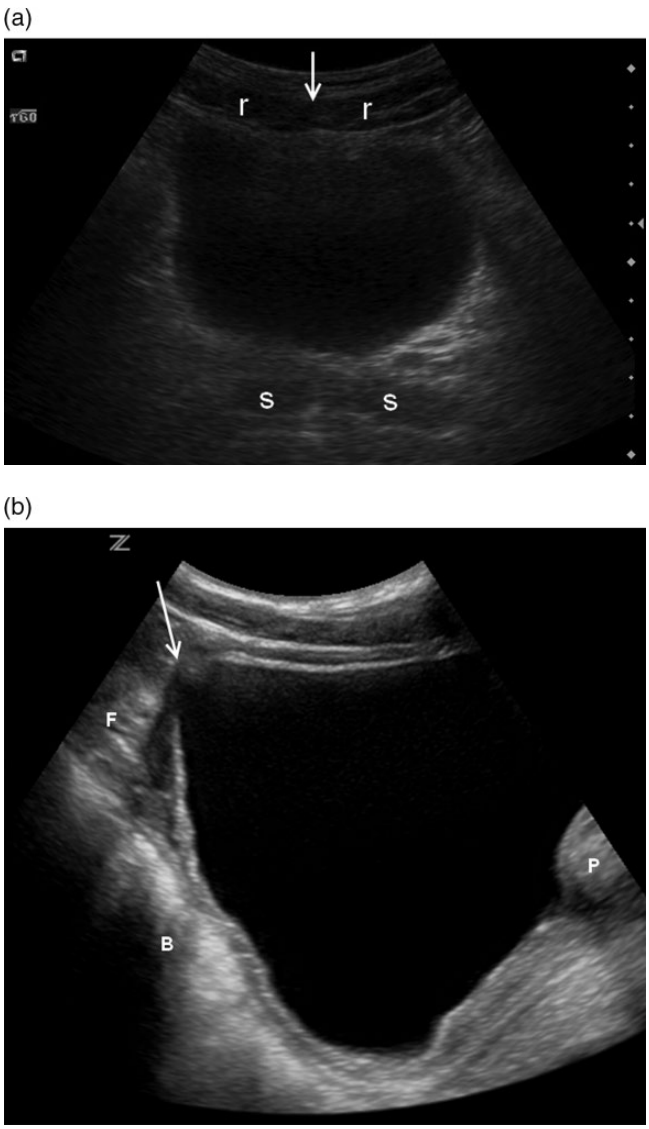

Figure 27.2 Sonographic views of the bladder. The transverse view (a) shows the two rectus abdominis muscles (r) and the intervening linea alba (arrow). The seminal vesicles (S) can also be seen. (b–d) show sagittal views of the bladder. The point at which the peritoneum reflects from the anterior abdominal wall onto the dome of the bladder is shown by the vertical arrow in panels (b) and (c). The reflection is cephalad to the scanning plane in panel (d). Properitoneal fat (F) sometimes extends to the dome of the bladder (B), as in (b) An enlarged prostate (P) can be seen in (c) and (d).

(c)

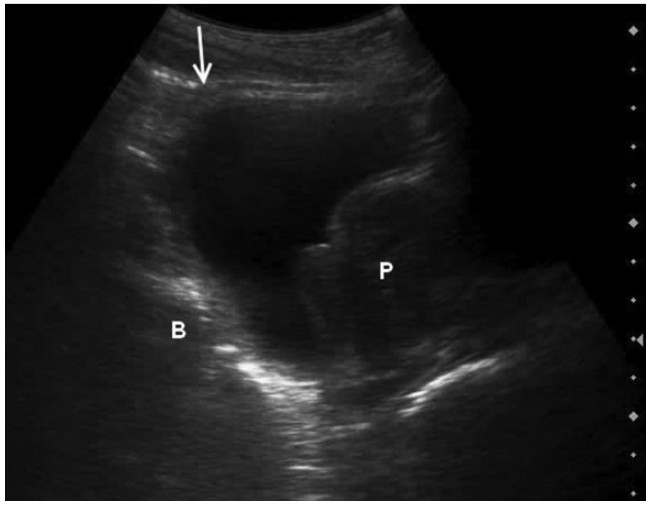

(d)

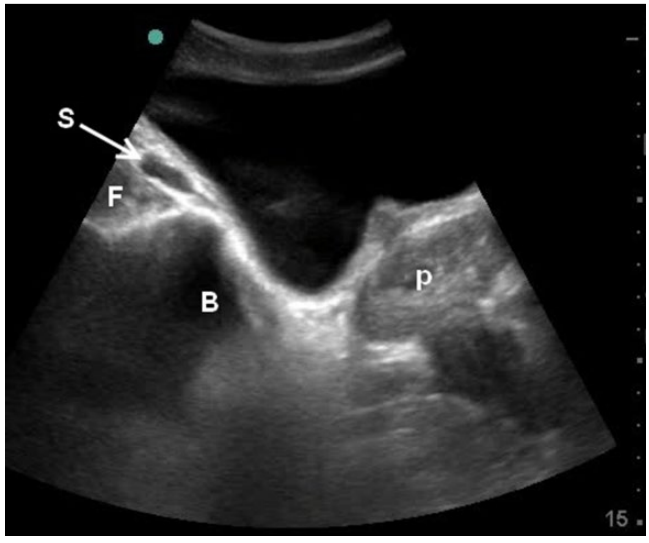

Figure 27.2 (Continued)

With the dynamic technique, after the initial overview, the transducer is placed in a sterile sheath, the skin prepped and draped, and the needle introduced under direct guidance. It should be remembered that because the needle and the incident ultrasound beam are almost parallel, neither the needle nor the needle tip will be directly visualised within the subcutaneous and fascial layers until the needle has entered the bladder lumen. The operator will be able to identify the needle tip indirectly as it tents the bladder mucosa immediately prior to puncture. As the needle passes into the bladder lumen, the tenting of the mucosa will be seen to suddenly resolve. Again, gentle aspiration will result in a urine flash as the bladder is entered. At this point the needle might be seen within the bladder lumen. Again, it is important to

continue to advance the needle for about 1 cm to ensure that the entire bevel of the needle is completely within the bladder.

Further Reading

Ahmed, S.J., Mehta, A., Rimington, P. (2004) Delayed bowel perforation following suprapubic catheter insertion. *BMC Urol.*, **4** (1), 16.

Barai, K.P., Islam, S. (2009) Suprapubic catheterization complicated by an iatrogenic enterocutaneous fistula: a case report. *Cases J.*, **2**, 9311.

Cundiff, G., Bent, A.E. (1995) Suprapubic catheterization complicated by bowel perforation. *Int. Urogynecol. J.*, **6**, 110–113.

Hardy, J.D., Furnell, P.M., Brumfitt, W. (1976) Comparison of sterile bag, clean catch and suprapubic aspiration in the diagnosis of urinary infection in early childhood. *Br. J. Urol.*, **48** (4), 279–283.

Mustonen, A., Uhari, M. (1978) Is there bacteremia after suprapubic aspiration in children with urinary tract infections? *J. Urol.*, **119** (6), 822–823.

NHS, National Patient Safety Agency – Rapid Response Report NPSA/2009/RRR005: Minimising risks of suprapubic catheter insertion; July 2009. Available at: www.npsa.nhs.uk/patientsafety/alerts-and-directives.

Pryles, C.V., Atkin, M.D., Morse, T.S., Welch, K.J. (1959) Comparative bacteriologic study of urine obtained from children by percutaneous suprapubic aspiration of the bladder and by catheter. *Pediatrics*, **24**, 983–991.

Tibbles, C.D., Porcaro, W. (2004) Procedural applications of ultrasound. *Emerg. Med. Clin. North Am.*, **22** (3), 797–815.

Titus, M., White, S. (2006) Suprapubic bladder tap aspiration in an elderly female. *J. Emerg. Med.*, **30** (4), 421–423.

Weathers, W.T., Wenzl, J.E. (1969) Suprapubic aspiration of the bladder. Perforation of a viscus other than the bladder. *Am. J. Dis. Child.*, **117** (5), 590–592.

28

Ultrasound in the Management of Fractures

Paul Atkinson and Peter Ross

Introduction

Point-of-care ultrasound (PoCUS) can provide an alternative to the traditional use of plain radiography and fluoroscopy in both the diagnosis and reduction of certain fractures. While the dose of radiation may be small, some fractures require repeated radiographs, need screening, or may be located close to potentially susceptible tissues such as the thyroid gland, as is the case in clavicle fractures. PoCUS may reduce the radiation exposure in these cases, which is especially important in children.

Fracture Diagnosis

Whilst there is ongoing debate as to whether PoCUS will replace radiography in general, it is well-suited for certain austere environments such as in the military field, disasters and in developing countries. PoCUS also has potential in pregnant patients, and in children where ultrasound may surpass the sensitivity of radiography in poorly ossified bones.

The sensitivity and specificity of PoCUS for diagnosing fractures is high for a wide variety of suspected fractures, including simple fractures of the sternum, ribs, femur, humerus and forearm bones. Accuracy is lower for compound fractures, small-bone fractures and Salter–Harris type I injuries. The diagnosis of clavicle fractures has excellent evidence and may be suitable as a primary imaging modality.

Extending the focussed assessment with sonography for trauma (FAST) examination to include screening for femoral fractures has been described as an extension of FAST.

Fracture Reduction

PoCUS guidance for forearm fracture reduction is a promising development, especially where there is a lack of real-time fluoroscopy or in reducing radiation dosages. The ability to check for fracture position prior to the application of a splint or cast can reduce the number of reduction attempts. Several studies have shown that ultrasound-guided forearm fracture reduction is very frequently successful on the first attempt, and that PoCUS determination of fracture position correlated well with radiography.

Obtaining POCUS Images of Bone

Generally, a high-frequency (typically 5–12 MHz) linear transducer (Figure 28.1) provides adequate depth and excellent resolution. For deeper structures, such as the femur, a lower frequency (typically 2–5 MHz) transducer may be required.

Emergency Point-of-Care Ultrasound, Second Edition. Edited by James A. Connolly, Anthony J. Dean, Beatrice Hoffmann and Robert D. Jarman.

Companion website: www.wiley.com/go/connolly/ultrasound

A basic knowledge of ultrasound physics will reveal the fact that ultrasound waves do not pass through high-resistance calcified tissues such as bone. Instead, all waves are reflected from the most superficial surface (cortex) of the bone, giving a clear picture of that surface which appears as an echogenic (white) line (Figure 28.2), but with any underlying structures remaining hidden from view (a dark acoustic shadow). Any breach or angulation of this surface will therefore be evident as a break or angle of the ultrasound image of the echogenic cortex. Care must be taken as often a strong reverberation artefact may be mistaken for the back of a bone, which is not generally visible.

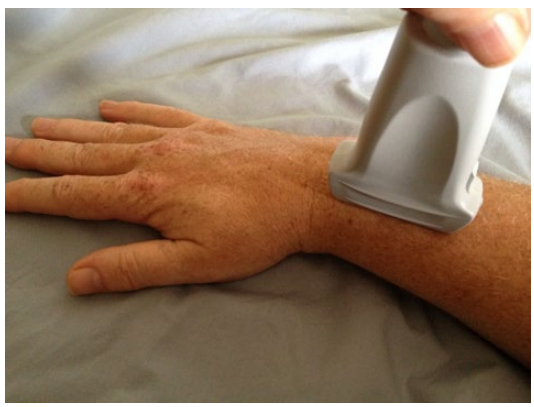

Figure 28.1 A high-frequency linear probe in longitudinal orientation on the dorsum of the wrist.

Technique

Before imaging, ensure maximal patient comfort by providing analgesia and placing the affected part in a comfortable supported position such as on a pillow. Minimise the pressure applied through the probe by using large amounts of gel and supporting the probe with two hands. If using PoCUS to guide reduction under sedation, pre-reduction images can be taken after the patient has been sedated.

Select a preset suitable for the evaluation of musculoskeletal structures and begin scanning close to – but not directly over – the site of the suspected fracture. Then proceed to gently move the probe along the bone, looking for signs of a fracture. In general, a longitudinal orientation is preferred. The bone can be viewed in two parallel planes, from different surfaces of the limb. For example, when scanning the distal radius, applying the probe longitudinal to the dorsum of the wrist (Figure 28.1) gives a view that resembles a lateral radiograph. By moving the probe to a longitudinal position on the radial aspect of the wrist, the image resembles the anteroposterior radiograph more closely.

Straight bones (e.g., humerus, radius, ulna) are easier to scan than bones that curve (e.g., clavicle, femur). Fractures appear as a breach or angulation of the smooth, hard, white, echogenic line of the bony cortex (Figure 28.3), a bony fragment, or an echo-poor (dark) area corresponding to a haematoma (Figure 28.4).

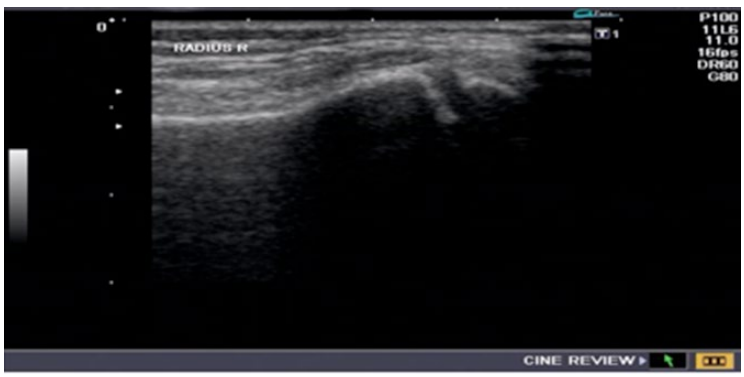

Figure 28.2 Typical image of bone on ultrasound. Note the bright echogenic cortical surface and the acoustic shadow.

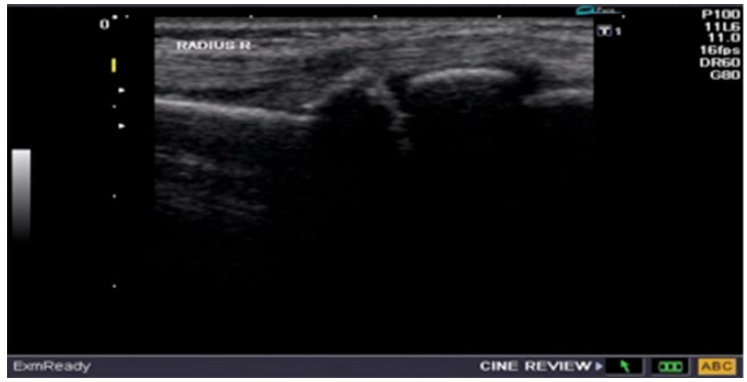

Figure 28.3 A fractured distal radius seen on ultrasound. Note the cortical breech and angulation.

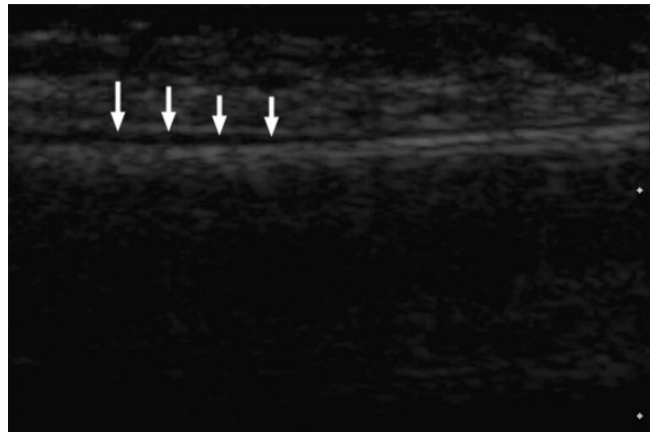

Figure 28.4 Diagnosis of a toddler's fracture by ultrasound. Note the dark echo-poor haematoma (arrows).

Pitfalls include incorrectly identifying an open growth plate, surface groove, or shadow from an overlying wound or foreign body as a fracture.

Toddler's Fracture

In younger children, fractures of certain lower-limb bones – commonly the tibia – may not be evident on plain radiography at initial presentation. In this setting, PoCUS may detect a localised cortical haematoma, diagnostic of an underlying fracture. This can be helpful when advising on prognosis and with decisions around casting or immobilisation.

Guidance for Fracture Reduction

The same technique is used as when diagnosing a fracture, with images obtained and stored before and after reduction of the fracture. Incomplete reduction detected by a combination of inspection, palpation and PoCUS should prompt further manipulation until a satisfactory position is obtained and a splint or cast can be applied. It is suggested that a post-reduction radiograph is recorded to ensure a good position in the cast or splint, as this cannot be obtained by PoCUS. The sequence of images is demonstrated in Figure 28.5.

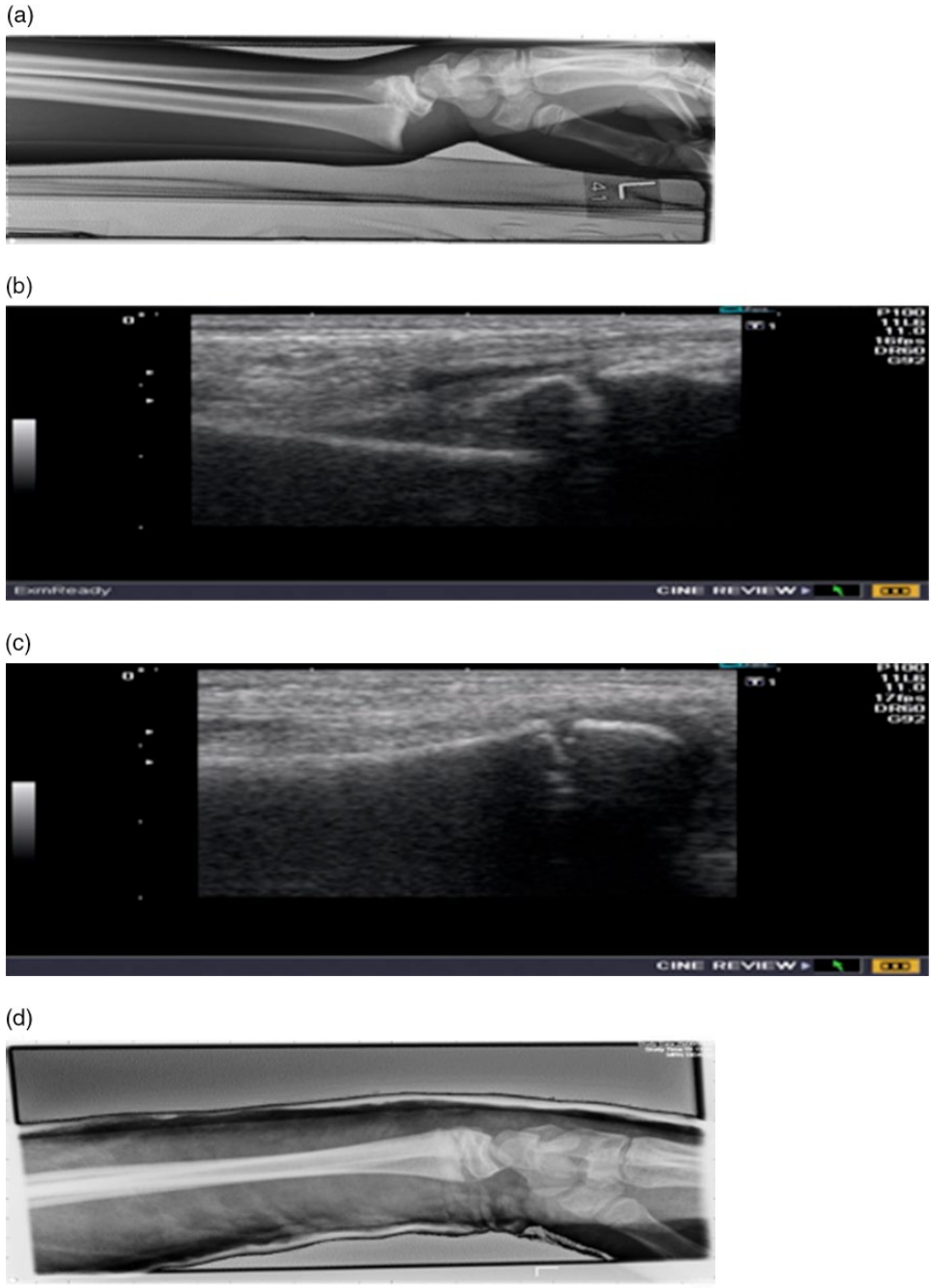

Figure 28.5 (a–d) The sequence of imaging during the reduction of a Salter–Harris type 2 distal radial fracture. (a) X-ray of fracture (b) US, same fracture (c) US, post reduction (d) X-ray, post reduction.

Table 28.1 Some available training resources for musculoskeletal PoCUS.

www.sonosite.com/education	The manufacturer Sonosite provides a variety of training workshops.
www.emergencyultrasound.net	A UK and Canadian group offering workshops in various elements of PoCUS.
www.sonoguide.com	One of ACEP's emergency ultrasound interactive learning resources.
www.hqmeded.com/node/20	Online video instruction on forearm fracture reduction.
www.mskus.com	Musculoskeletal Ultrasound is a private company that offers training workshops with both basic and advanced techniques.
http://www.noc.nhs.uk/ourservices/training/british_musculoskeletal_ultrasound.aspx	The British Musculoskeletal Ultrasound Course

Training

Clinicians not already proficient in PoCUS may consider learning this simple technique in isolation, although training in basic ultrasound image optimisation is recommended. Bedside training and supervision is the ideal way to learn this technique. Residency or fellowship training in PoCUS can be supplemented by specialised training courses or workshops for this and similar musculoskeletal ultrasound techniques (see Table 28.1). Self-directed learning by e-learning or text books can also be helpful, while simulation is becoming increasingly popular; the identification of fractures on chicken thigh bones and so forth can accurately resemble the 'real-life' experience.

Summary

Evidence supporting the use of PoCUS for both the diagnosis and guidance for reduction of fractures is growing. Currently, it seems reasonable to use PoCUS to supplement radiography for the diagnosis of many fractures, perhaps replace it for diagnosing clavicular fractures in young children, and to use it as an alternative to fluoroscopy for the reduction of certain forearm fractures.

Further Reading

Ackermann, O., Liedgens, P., Eckert, K., *et al.* (2009) Ultrasound diagnosis of forearm fractures in children: a prospective multicenter study. *Unfallchirurg.*, **112**, 706–711.

Atkinson, P., Iftikhar, K., Naveed, A., Kendall, R., van Rensburg, L., Madan, R. (2011) Ultrasound-guided paediatric forearm fracture reduction with sedation in the emergency department. *Clin. J. Emerg. Med.*, **13**, 173.

Atkinson, P., Lennon, R. (2003) Use of emergency department ultrasound in the diagnosis and early management of femoral fractures. *Emerg. Med. J.*, **20**, 395.

Beaudoin, F.L., Nagdev, A., Merchant, R.C., *et al.* (2010) Ultrasound-guided femoral nerve blocks in elderly patients with hip fractures. *Am. J. Emerg. Med.*, **28**, 76–81.

Chaar-Alvarez, F.M., Warkentine, F.W., Cross, K.P., *et al.* (2009) Bedside ultrasound diagnosis of non-angulated forearm fractures in the pediatric emergency department, in American

Academy of Pediatrics National Conference and Exhibition. Washington, DC, Section on Emergency Medicine.

Chen, L., Kim, Y., Moore, C.L. (2007) Diagnosis and guided reduction of forearm fractures in children using bedside ultrasound. *Pediatr. Emerg. Care*, **23**, 528–531.

Chien, M., Bulloch, B., Youssfi, M., *et al*. (2010) *Diagnosis of pediatric clavicle fractures [Abstract], in Pediatric Academic Societies*, Vancouver, BC.

Chinnock, B., Khaletskiy, A., Kuo, K., *et al*. (2009) Ultrasound-guided reduction of distal radius fractures. *J. Emerg. Med.*, E-published.

Cho, K.H., Lee, S.M., Lee, Y.H., *et al*. (2010) Ultrasound diagnosis of either an occult or missed fracture of an extremity in pediatric-aged children. *Korean J. Radiol.*, **15**, 84–94.

Cross, K.P., Padmanabhan, P., Stevenson, M.D. (2010) *Ultrasound-guided femoral nerve blocks in the pediatric emergency department [Abstract], in Pediatric Academic Societies*, Vancouver, BC.

Cross, K.P., Warkentine, F.W., Kim, I.K., *et al*. (2010) Bedside ultrasound diagnosis of clavicle fractures in the pediatric emergency department. *Acad. Emerg. Med.*, **17**, 687–693.

Durston, W., Swartzentruber, R. (2000) Ultrasound-guided reduction of pediatric forearm fractures in the ED. *Am. J. Emerg. Med.*, **18**, 72–77.

Eksioglu, F., Altinok, D., Uslu, M.M., *et al*. (2003) Ultrasonographic findings in pediatric fractures. *Turk. J. Pediatr.*, **45**, 136–140.

Fisher, N.A., Newman, B., Lloyd, J., *et al*. (1995) Ultrasonographic evaluation of birth injury to the shoulder. *J. Perinatol.*, **15**, 398–400.

Graif, M., Stahl-Kent, V., Ben-Ami, T., *et al*. (1988) Sonographic detection of occult bone fractures. *Pediatr. Radiol.*, **18**, 383–385.

Heiner, J.D., McArthur, T.J. (2009) A simulation model for the ultrasound diagnosis of long-bone fractures. *Simul. Healthcare*, **4**, 228–231.

Hubner, U., Schlicht, W., Outzen, S., *et al*. (2000) Ultrasound in the diagnosis of fractures in children. *J. Bone Joint Surg. Br.*, **82**, 1170–1173.

Hunter, J.D., Mann, C.J., Hughes, P.M. (1998) Fibular fracture: detection with high resolution diagnostic ultrasound. *J. Accident. Emerg. Med.*, **15**, 118.

Jones, G.P., Seguin, J., Shiels, W.E., *et al*. (2003) Fracture of the proximal humerus in a preterm infant. *Am. J. Perinatol.*, **20**, 249–253.

Katz, R., Landman, J., Dulitzky, F., *et al*. (1988) Fracture of the clavicle in the newborn. An ultrasound diagnosis. *J. Ultrasound Med.*, **7**, 21–23.

Lewis, D., Logan, P. (2006) Sonographic diagnosis of toddler's fracture in the emergency department. *J. Clin. Ultrasound*, **34**, 190–194.

Lyon, M., Blaivas, M. (2003) Evaluation of extremity trauma with sonography. *J. Ultrasound Med.*, **22**, 625–630.

Ma, O.J., Norvell, J.G., Subramanian, S. (2007) Ultrasound applications in mass casualties and extreme environments. *Crit. Care Med.*, **35** (5 Suppl.), S275–S279.

Marshburn, T.H., Legome, E., Sargsyan, A., *et al*. (2004) Goal-directed ultrasound in the detection of long-bone fractures. *J. Trauma*, **57**, 329–332.

McNeil, C.R., McManus, J., Mehta, S. (2009) The accuracy of portable ultrasonography to diagnose fractures in an austere environment. *Prehosp. Emerg. Care*, **13**, 50–52.

Melniker, L.A., Leibner, E., McKenney, M.G., *et al*. (2006) Randomized controlled clinical trial of point-of-care, limited ultrasonography for trauma in the emergency department: the first sonography outcomes assessment program trial. *Ann. Emerg. Med.*, **48**, 227–235.

Moritz, J.D., Berthold, L.D., Soenksen, S.F., *et al*. (2008) Ultrasound in diagnosis of fractures in children: unnecessary harassment or

useful addition to x-ray? *Ultraschall. Med.*, **29**, 267–274.

Noble, V.E., Legome, E., Marshburn, T. (2003) Long bone ultrasound: making the diagnosis in remote locations. *J. Trauma*, **54**, 800.

Patel, D.D., Blumberg, S.M., Crain, E.F. (2009) The utility of bedside ultrasonography in identifying fractures and guiding fracture reduction in children. *Pediatr. Emerg. Care*, **25**, 221–225.

Pistor, G., Graffstadt, H. (2003) Sonographic diagnosis of supracondylar fractures of the humerus. *Ultraschall. Med.*, **24**, 331–339.

Spencer, J.K., Adler, R.S. (2008) Utility of portable ultrasound in a community in Ghana. *J. Ultrasound Med.*, **27**, 1735–1743.

29

Ultrasound-Guided (USG) Peripheral Nerve Block (PNB)

Jens Børglum and Kenneth Jensen

Introduction

The first comprehensive textbook on nerve blocks using surface anatomy guidance (SAG) was published in 1922. The approaches to nerve blocks were expanded during a proliferative period during the 1980s and 1990s by the use of nerve stimulation guidance (NSG) as an adjunct to SAG. Hence, many studies were focused on which nerves to block, at which angles to apply the needle, and how many passes or injections were needed for success. Since then, technical advancements within the field of ultrasonography have improved. The first recorded ultrasound-guided (USG) application in 1994 of a real-time direct visualisation of the brachial plexus block at the supraclavicular level has led to an ever-increasing use of USG as a tool in the field of regional anaesthesia with the advent of more detailed, flexible and mobile ultrasound scanners. USG allows the physician to follow needle trajectory, navigate away from adjacent structures, observe the injected solution, and make real-time adjustments that are necessary for effective perineural spread of local anaesthetic.

Evidence Basis of USG Nerve Blocks

Although cohort studies on nerve localisation methods (USG versus NSG versus SAG) and novel approaches are still being published, randomised controlled trials (RCTs) investigating success rates, minimally effective doses and perineural catheter indications have become more widespread. Both types of study are needed for a proper view of the clinical promise that USG peripheral nerve blocks (PNBs) may deliver, since controlled evidence must always be applied to real-world factors. As a case in point, success rates have been investigated in many large-scale studies comprising thousands of patients; success rates may be defined as the ability to: (i) provide surgical anaesthesia with the use of the nerve block without the need to convert to general anaesthesia or use escape blocks; (ii) effectively block the sensory components of all targeted nerves; or (iii) provide effective postoperative analgesia without the need for opioids or escape blocks. The results of RCTs strongly suggest that USG may provide an extra benefit compared to NSG, since the number of studies showing this benefit outweigh those that do not. Cohort studies, however, are less clear on the subject and offer only a marginal benefit for USG over NSG or SAG. A brief overview of the disparities between RCTs and cohort studies in nerve blocks on the *upper extremity* is provided in Table 29.1. It has been found that RCTs consistently display smaller success rates than cohort studies, with equal variation, and with differences in success rates between methods of nerve localisation larger in RCTs

Emergency Point-of-Care Ultrasound, Second Edition. Edited by James A. Connolly, Anthony J. Dean, Beatrice Hoffmann and Robert D. Jarman.

Companion website: www.wiley.com/go/connolly/ultrasound

Table 29.1 Success rates in upper-extremity nerve blocks.

PNB and study type	USG	NSG	SAG	Unknown
Interscalene, Cohorts	96 ± 1 (4)	95 ± 2 (9)	–(0)	90 ± 5 (13)
Interscalene, RCTs	99 ± 0 (1)	91 ± 0 (1)	– (0)	– (0)
Supraclavicular, Cohorts	95 ± 3 (8)	94 ± 4 (5)	94 ± 1 (2)	87 ± 4 (6)
Supraclavicular, RCTs	81 ± 7 (3)	– (0)	– (0)	– (0)
Infraclavicular, Cohorts	92 ± 5 (5)	91 ± 2 (3)	– (0)	– (0)
Infraclavicular, RCTs	91 ± 3 (6)	74 ± 8 (4)	– (0)	– (0)
Axillary, Cohorts	94 ± 5 (10)	83 ± 12 (14)	77 ± 6 (8)	87 ± 1 (2)
Axillary, RCTs	91 ± 4 (3)	71 ± 4 (3)	– (0)	– (0)

Average success rates in percentage ± standard deviations between studies (defined as range divided by 4). Number of studies in (), according to method of nerve localisation. Studies were found by a Medline search using the search phrases 'interscalene', 'supraclavicular', 'infraclavicular', 'axillary' and 'success rate'", and by backtracking references in these studies. The list of studies is not intended to be fully exhaustive.

than in cohort studies. These differences between study types may be explained by better internal validity (more precise and more complete data acquisition) but *not* by better external validity of the RCTs (expertise and demographics equally uncontrolled). A recent meta-analysis of currently available RCTs for upper-extremity nerve blocks provides conclusive support for higher success rate and faster sensory onset of the blocks using USG, but remains unclear regarding benefits on block duration and procedure technicalities (such as the number of needle passes, procedure pain and vascular puncture). Current evidence does not support a reduced incidence of side effects following USG nerve blocks compared to NSG or SAG, since such studies require large numbers of participants and months of observation.

In conclusion, further quality studies on USG PNBs are required to accurately define their true clinical benefits over older methods (such as an improved learning curve, a consistently higher success rate, the effect of patient demographics, improved pharmacokinetics and better long-term patient safety). What is indisputable, however, is the fact that USG has definite advantages in certain clinical settings (Table 29.2). Most of these settings are difficult to properly investigate, but preliminary studies are underway. The best available evidence in USG PNB studies, according to analgesic purpose, is listed in Table 29.3.

Education in Regional Anaesthesia

In order to enhance the clinical implementation process, to support further education and to advance improvements in clinical practice, the American Society of Regional Anesthesia and Pain Medicine (ASRA) and the European Society of Regional Anaesthesia and Pain Therapy (ESRA) encouraged each institution that conducts USG PNB to support a quality improvement process. The joint committee of ASRA and ESRA advocated a focus on the following issues: (i) ten common tasks used when performing an USG nerve block; (ii) the core competencies and skills associated with UGS PNB; and (iii) a training practice pathway for postgraduate anaesthesiologists and a residency-based training pathway. The first proposal from the joint committee of ASRA and ESRA is provided in Table 29.4.

High block expertise requires both anatomical knowledge and extensive hands-on experience.

Table 29.2 Some theoretical advantages of USG PNBs over other methods of nerve localisation.

Beneficial USG nerve blocks	Examples: nerves and clinical settings
Nerves with no motor content	Saphenous nerve at the midfemoral level: knee surgery. Superficial cervical plexus (C3–C4): carotid artery and clavicle surgery.
Nerves with motor content of limited importance for mobility	Obturator nerves, anterior and posterior branch: hip and knee surgery. Transverse abdominis plane (TAP) block: gastrointestinal surgery.
Nerves not easily accessible	All nerves: patients with obesity or deformities. Sciatic nerve at gluteal or antero-medial level: patients with amputations or neuropathy (impaired motor ability).
Nerves with high risk of central or systemic spread	Lumbar plexus (psoas compartment): hip surgery. Sacral/parasacral plexus: hip surgery, amputations. Paravertebral nerves: pain in osteo-, myo- and dermatomes. Multiple blocks: high-volume toxicity issues.
Nerves adjacent to important structures	Brachial plexus and phrenic nerve at interscalene level, or brachial plexus at supraclavicular level: patients with chronic lung disease or risk of pneumothorax. Intercostal nerves: costal fractures (pneumothorax). Femoral nerve and artery in the inguinal crease, or brachial plexus at infraclavicular level: patients with coagulopathy.
Nerves sensitive to compression effects	All nerves: immobilised patients, or patients with HNPP (hereditary liability to nerve pressure palsies), or patients with local inflammation.
Nerves serving a fractured limb	All nerves: conditions in which muscle contractions are undesirable or painful.
Nerves in potential medico-legal disputes	All nerves: patients with existing nerve damage, or at high risk of surgical nerve damage. All nerves: patients in which precise documentation on the procedure is mandatory.

Overall, USG nerve blocks offer better visualisation of local anaesthetic spread, require lower volumes, and promise less (or better-documented) tissue trauma during the procedure.

Table 29.3 Best available evidence in USG PNB studies, according to analgesic purpose.

PNB	Acute/chronic pain	Surgical anaesthesia	Postoperative pain
Suprascapular	1b	–	2b
Interscalene	4	1b	2b
Supraclavicular	–	1b	2b
Infraclavicular	4	1b	1b
Axillary	–	1b	2b
TAP	2b	–	1b
Rectus sheath	–	–	1b
II/IH	–	–	1b
Femoral	1b	1b	1b
LCFN	4	4	–
Obturator	–	1b	1b
Saphenous	–	2b	2b
Sciatic, proximal	–	1b	2b
Sciatic, popliteal	4	1b	1b

Evidence levels: 1b = RCT; 2b = cohort study; 4 = case series. – = no studies available.

Table 29.4 Ten tasks helpful in performing USG peripheral nerve blocks.

1	Visualise key landmark structures including blood vessels, muscles, fascia, and bone.
2	Identify the nerves or plexus on short-axis imaging.
3	Confirm normal anatomy and recognise anatomic variation(s).
4	Plan for a needle approach that avoids unnecessary tissue trauma.
5	Maintain an aseptic technique with respect to the ultrasound equipment.
6	Follow the needle under real-time visualisation as it advances toward the target.
7	Consider a secondary confirmation technique, such as nerve stimulation.
8	When the needle tip is presumed to be in the correct position, inject a small volume of a test solution. If solution is not visualised during this test injection, presume that the needle tip is intravascular or out of the imaging plane.
9	Make necessary needle adjustments if an undesired pattern of local anaesthetic spread is visualised. The visualisation of local anaesthetic should occur through the entirety of the injection to avoid an intravascular injection.
10	Maintain traditional safety guidelines including the presence of resuscitation equipment, frequent aspiration, intravascular test dosing, standard monitoring, patient response, and assessment of injection characteristics.

As to the other proposals regarding core competencies and skills associated with USG PNB and the proposed training practice pathway at any institution, this chapter refers to the original publication. The aim of the chapter is to provide the reader with an easy pathway to perform USG PNB in daily clinical practice. The USG PNB can in reality be performed by any *trained* physician qualified in the field of emergency medicine, acute pain management and trauma, as well as physicians providing for surgical anaesthesia and postoperative pain management. In the following, recommendations will be provided as to how to perform the various USG PNB procedures and show relevant clinical photographs, together with ultrasound recordings to advise the reader accordingly.

Upper-Extremity Nerve Blocks

At this point, USG PNB of the brachial plexus and the peripheral nerves will be outlined (see Table 29.5). Recent findings have suggested that USG may provide significant advantages in brachial plexus blocks, including faster sensory onset and greater block success.

Table 29.5 Overview of relevant nerve blocks of the brachial plexus and its peripheral nerves. Recommended indications include surgical anaesthesia (SA) or postoperative pain management (PPM).

Brachial plexus and its peripheral nerves	Indications
Interscalene (ISC) block	Figure 29.1 Shoulder surgery (SA, PPM)
Supraclavicular (SCL) block	Figure 29.2 Surgery on the humerus, elbow, lower arm, wrist, hand (SA, PPM)
Lateral infraclavicular (LIC) block	Figure 29.3 Surgery on the humerus, elbow, lower arm, wrist, hand (SA, PPM)
Axillary (AX) block	Figure 29.4 Surgery on the elbow, lower arm, wrist, hand (SA, PPM)
Suprascapular nerve (SSN) block	Figure 29.5 Shoulder surgery (PPM)
Median nerve (MN) block at elbow level	Figure 29.6 Wrist and hand surgery (PPM)
Ulnar nerve (UN) block at elbow level	Figure 29.7 Wrist and hand surgery (PPM)
Radial nerve (RN) block at elbow level	Figure 29.8 Wrist and hand surgery (PPM)

USG Interscalene (ISC) Block

The patient is placed in a supine position with the head turned to the contralateral side (Figure 29.1). A linear transducer (6–15 MHz) is placed with its lateral end pointing lateral just above the clavicle to visualise the brachial plexus (BP) at the supraclavicular level, where the BP is seen with its multiple divisions (Figure 29.2). The BP is then tracked in a cranial direction until the superior, middle and inferior trunci is seen placed between the anterior and middle scalene muscles (Figure 29.1). The needle is inserted in-plane to the transducer in a lateral-to-medial direction and the tip of the needle is placed in the interscalene groove. The spread of the injectate should be observed to surround the three trunci (from cervical roots 5 to 7).

USG Supraclavicular (SCL) Block

The patient is placed in a supine position with the head turned to the contralateral side (Figure 29.2). A linear transducer (6–15 MHz) is placed with its lateral end pointing lateral just above the clavicle to visualise the BP at the supraclavicular level, where the BP is seen with its multiple divisions (Figure 29.2). The needle is inserted in-plane to the transducer in a lateral-to-medial direction. It is recommended that the tip of the needle is placed laterally to the subclavian artery above the first costa, keeping well away from the pleura. The spread of the injectate should be observed to lift the BP from the first costa. The local anaesthetic should surround the BP, and the physician must redirect the needle accordingly.

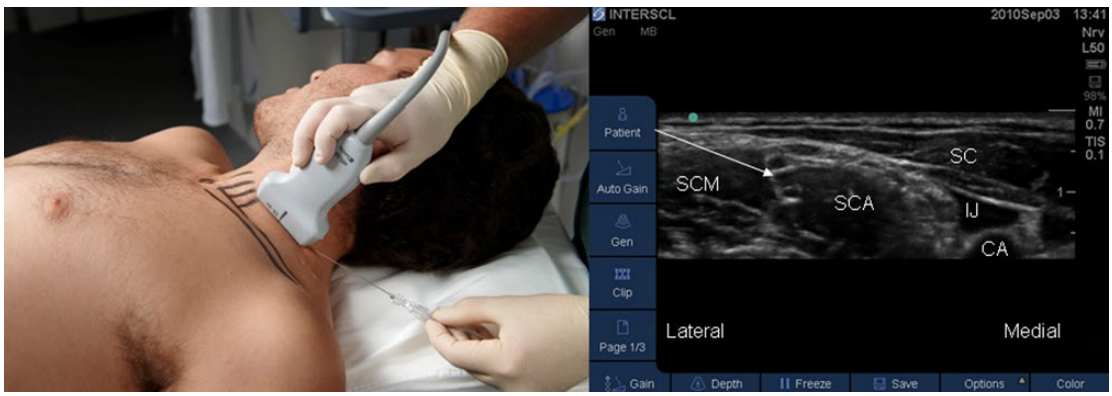

Figure 29.1 USG interscalene (ISC) block.

Figure 29.2 USG supraclavicular (SCL) block.

USG Lateral Infraclavicular (LIC) Block

The patient is placed in a supine position with the head turned to the contralateral side (Figure 29.3). A linear transducer (6–15 MHz) is placed in the parasagital plane with its cranial end below the clavicle and above the coracoid process (Figure 29.3). With the transducer placed in this fashion, the axillary artery (AA) (cranial) and vein (AV) (caudal) is visualised below the major and minor pectoral muscles (Figure 29.3). The lateral, posterior and medial cords of the BP are positioned in various ways around the AA (Klarstad and others). The needle is inserted in plane to the transducer in a cranial to caudal direction. It is recommended that the tip of the needle is placed at the 8 o'clock position in relation to the AA. The spread of the injectate should be observed to surround the AA, and the physician must redirect the needle accordingly.

USG Axillary (AX) Block

The patient is placed in a supine position (Figure 29.4). A linear transducer (6–15 MHz) is placed transversally to the humerus. With the transducer placed in this fashion, the AA and two or more veins are visualised (Figure 29.4). The median (MN), ulnar (UN) and radial (RN) nerves are seen laterally, medially and posteriorly to the AA, respectively. The musculocutaneous nerve (MC) is seen sandwiched between the biceps and coracoid muscles some distance from the AA. The needle is inserted in plane to

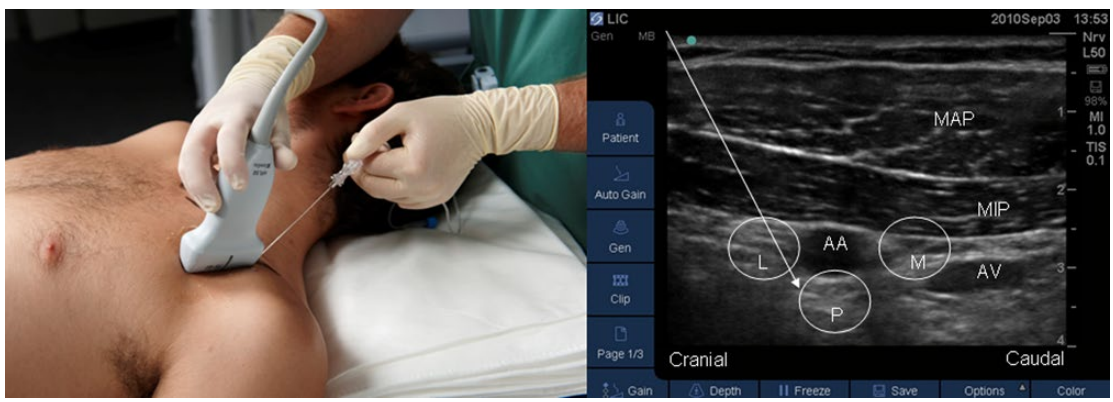

Figure 29.3 USG lateral infraclavicular (LIC) block.

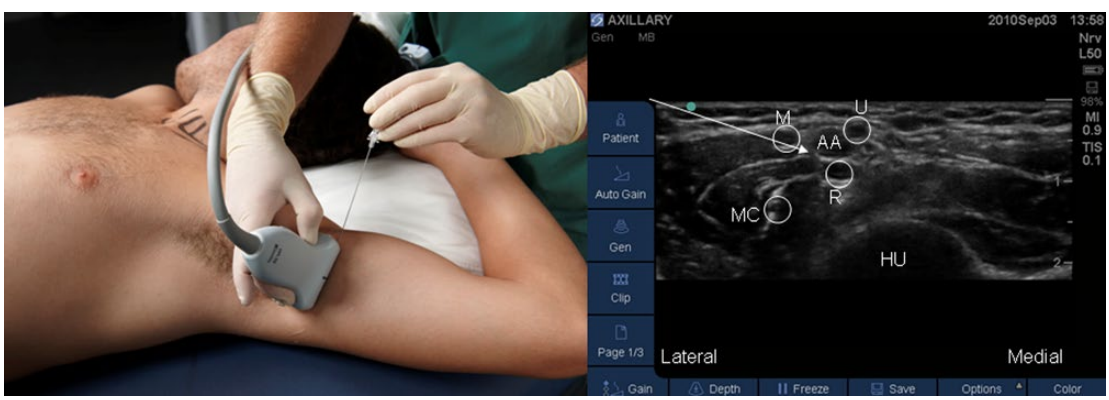

Figure 29.4 USG axillary (AX) block.

the transducer in a lateral-to-medial direction. The spread of the injectate should be observed to surround all four nerves, and the physician must redirect the needle accordingly.

USG Suprascapular Nerve (SSN) Block

This block is best performed with the patient sitting up with their back to the physician (Figure 29.5). A linear transducer (6–15 MHz) is placed parallel to the scapular spine. The ultrasound picture will show the scapular notch deep to the supraspinatus muscle (SPM). The scapular notch is roofed by the transverse scapular ligament (TSL), and the SSN is seen below the TSL in the scapular notch (Figure 29.5). The needle is inserted in-plane to the transducer in a lateral-to-medial direction. The spread of the injectate should be observed to expand below the TSL. It is indeed possible to provide for a continuous block of the SSN by inserting a catheter in the scapular notch.

USG Block of Peripheral Nerves at the Elbow Level

These nerve blocks are best used for supplementary blocks for wrist and hand surgery. A linear transducer (6–15 MHz) is placed in the cubid fossa transversally to the humerus (Figures 29.6–29.8). Medially to the brachial artery (BA) the median nerve (MN) is seen (Figure 29.6). Just above the medial epicondyle the ulnar nerve (UN) is seen before it disappears

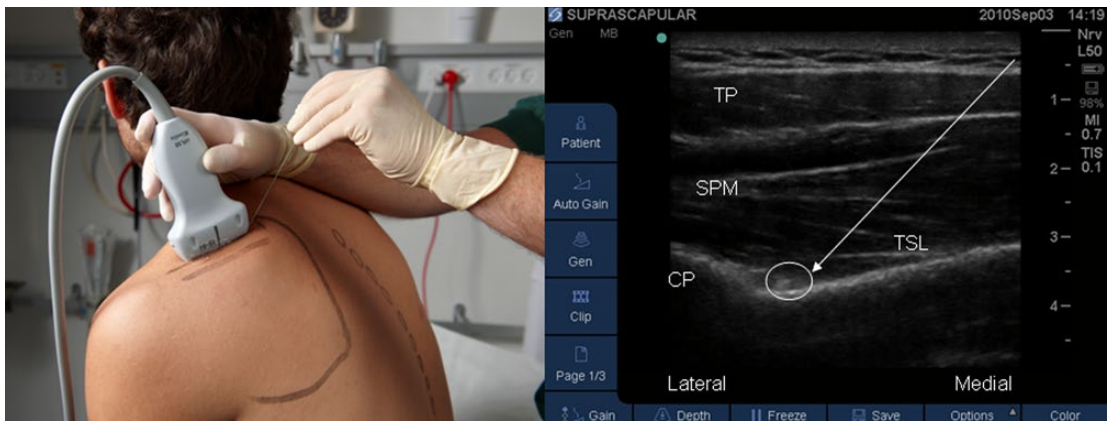

Figure 29.5 USG suprascapular nerve (SSN) block.

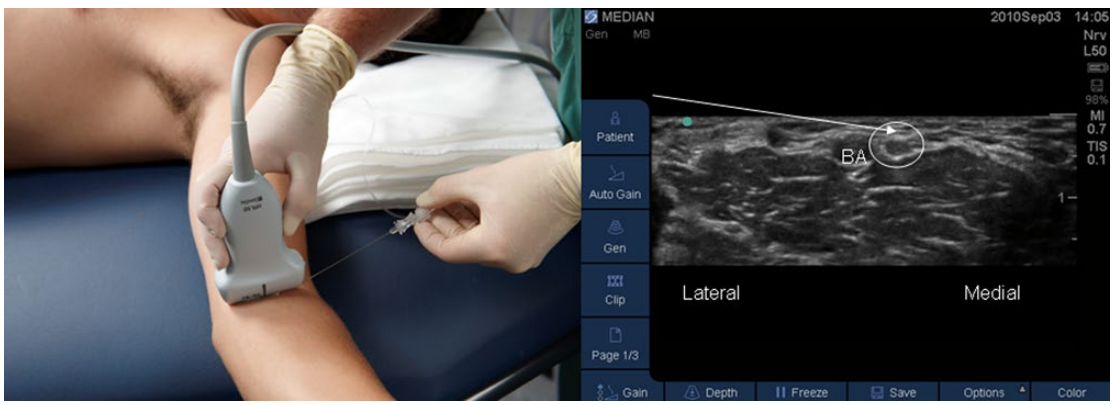

Figure 29.6 USG median nerve (MN) block.

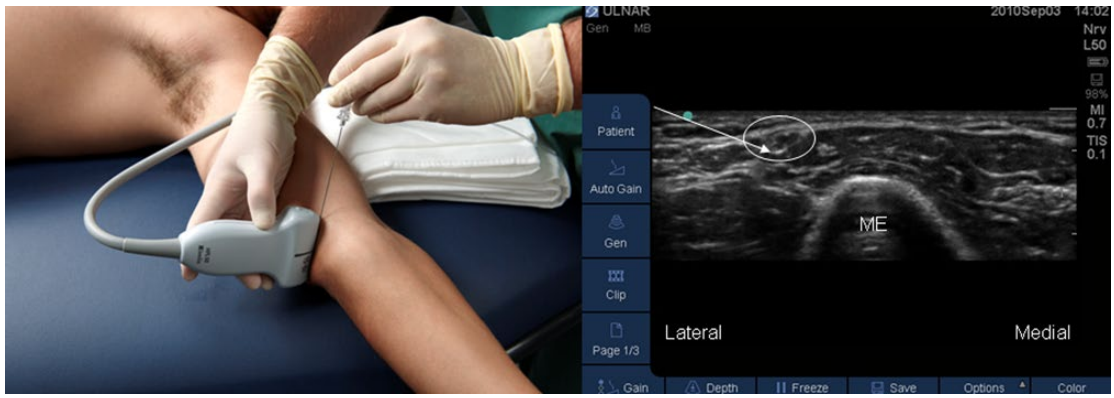

Figure 29.7 USG ulnar nerve (UN) block.

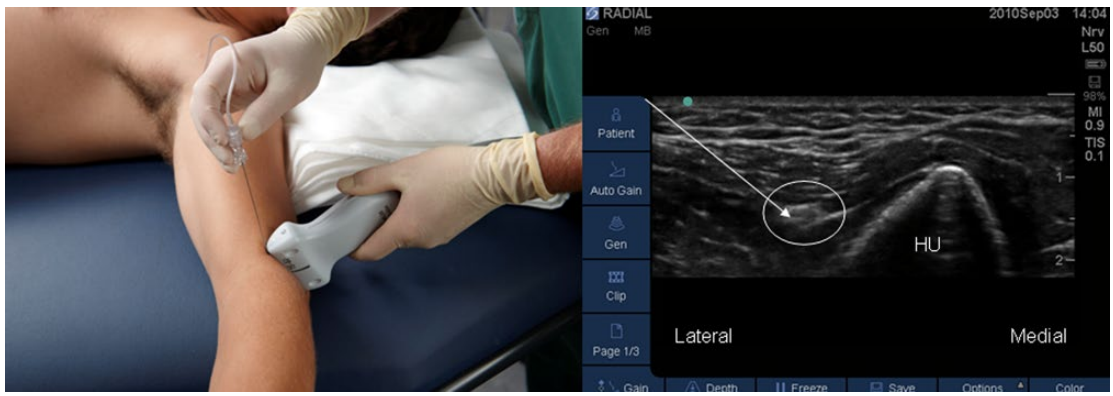

Figure 29.8 USG radial nerve (RN) block.

in the sulcus a few centimetres distally (Figure 29.7). The radial nerve (RN) is best seen laterally to the humerus and cranially to the elbow joint. It is recommended that the needle is inserted in-plane to the transducer in a lateral-to-medial direction. The spread of the injectate should be observed to surround the nerves at all three locations as necessary.

Lower-Extremity Nerve Blocks

There is level 1b evidence to recommend that ultrasound guidance improves the onset and success of sensory block, reduces local anaesthetic requirements, and reduces the time to perform lower-extremity peripheral nerve blocks. To date, no RCT has reported ultrasound as inferior to alternative techniques in any outcome. Nerve blocks for the lower extremities are listed in Table 29.6.

USG Femoral Nerve (FN) Block

The patient is placed in a supine position (Figure 29.9). A linear transducer (6–15 MHz) is placed parallel to the inguinal ligament transversally to the femoral artery (FA) and femoral vein (FV). The longitudinal or triangular shape of the FN is seen laterally to the FA below the fascia lata and fascia iliaca, but above the iliopsoas muscle (IPM) (Figure 29.9). The needle is inserted in-plane to the transducer in a lateral-to-medial direction. The spread of the injectate should be observed to surround the FN.

Table 29.6 Overview of relevant nerve blocks of the lumbosacral plexes and their peripheral nerves. Recommended indications include surgical anaesthesia (SA) or postoperative pain management (PPM).

Lumbar and sacral plexus, and their peripheral nerves	Indications
Femoral nerve (FN) block	Figure 29.9 Surgery on the hip, femur, knee (SA, PPM).
Lateral femoral cutaneous nerve (LFCN) block	Figure 29.10 Surgery on the hip (PPM). Thigh tourniquet pain (SA, PPM).
Obturator nerve (anterior branch) (ONA) and obturator nerve (posterior branch) (ONP) block	Figure 29.11 Surgery on the hip (ONA) and on the knee (ONP). Thigh tourniquet pain (ONA/ONP) (SA, PPM).
Saphenous nerve (SAN) block	Figure 29.12 Ankle and foot surgery (PPM).
Sacral plexus (SP) and sciatic nerve (SN) block – sacral/parasacral level (Mansour pivot technique)	Figure 29.13 Surgery on the hip, posterior thigh, knee, leg, ankle, foot (SA, PPM).
Sciatic nerve (SN) block: antero-medial thigh	Figure 29.14 Surgery on the posterior thigh, knee, leg, ankle, foot (SA, PPM).
Sciatic nerve (SN) block: popliteal level	Figure 29.15 Surgery on the knee, leg, ankle, foot (SA, PPM).

Figure 29.9 USG femoral nerve (FN) block.

USG Lateral Femoral Cutaneous Nerve (LFCN) Block

The patient is placed in a supine position (Figure 29.10). A linear transducer (6–15 MHz) is placed just below the anterior superior iliac spine (ASIS) and the sartorius muscle (SA) is located at this point lying just lateral to the IPM. The triangular shape of the SA is roofed by the fascia lata, and the LFCN runs below the fascia lata and above the SA (Figure 29.10). The needle is inserted in-plane to the transducer in a lateral-to-medial direction. The spread of the injectate should be observed to spread above the SA but below the fascia lata.

USG Obturator Nerve (ON) block (ONA, anterior branch; ONP, posterior branch)

The patient is placed in a supine position (Figure 29.11). A linear transducer (6–15 MHz) is placed parallel to the inguinal ligament, transversally to the femoral artery (FA). From this position the transducer is then moved gradually in a medial direction past the FV and the pectineus muscle (PM) until the three adductor muscles are localised medially to the PM. At this position, the ONA is seen between the adductor longus (AL) and adductor brevis (AB) muscles. The ONP is seen between the AB and the adductor magnus (AM) muscle (Figure 29.11).

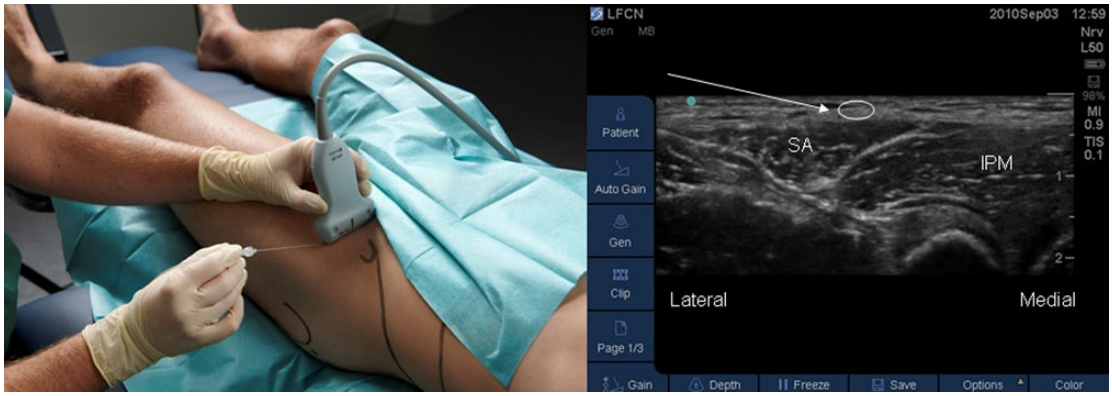

Figure 29.10 USG lateral femoral cutaneous nerve (LFCN) block.

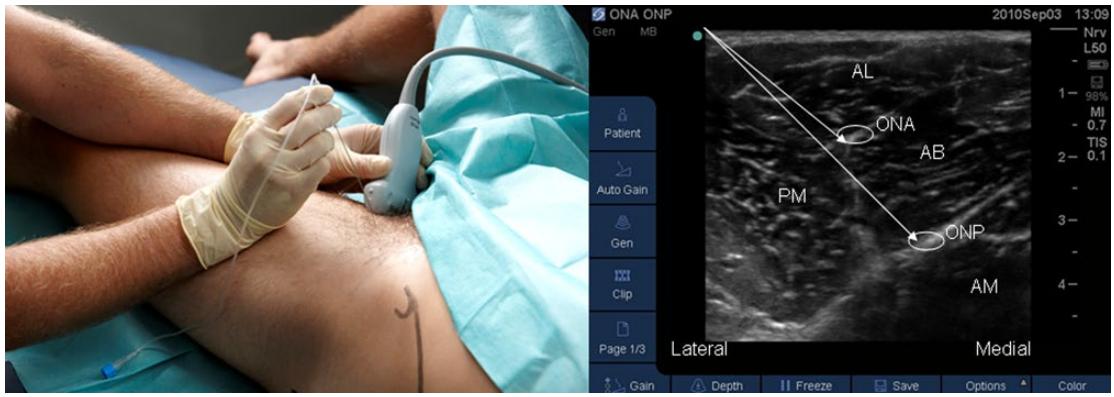

Figure 29.11 USG obturator nerve (ON) block. ONA (anterior branch), ONP (posterior branch).

The needle is inserted in-plane to the transducer in a lateral-to-medial direction. The spread of the injectate should be seen to advance in the fascial layers between the AL and AB and between the AB and AM, respectively.

USG Saphenous Nerve (SAN) Block

The patient is placed in a supine position (Figure 29.12). A linear transducer (6–15 MHz) is placed parallel to the inguinal ligament, transversally to the femoral artery (FA), and the FA is followed distally deep on the medial part of the thigh, where the FA is positioned below the SA in the adductor canal. At the medial part of the thigh the saphenous nerve (SAN) is always found laterally to the FA and below the SA that roofs the adductor canal (Figure 29.12). The needle is inserted in-plane to the transducer in a lateral-to-medial direction. The spread of the injectate should be seen to surround the SAN.

USG Sacral Plexus (SP) and Sciatic Nerve (SN) Block: Sacral/Parasacral Approach

The sciatic nerve is the largest nerve in the human body, and it runs in the posterior thigh, branching from the SP below the piriform muscle (PIM) ending in the popliteal fossa, where it divides into the tibial nerve (TN) and the common peroneal nerve (CP). The SN can be blocked all along this course. In this chapter it was decided to begin with an easy method of blocking the SP below the PIM. The patient is placed in a lateral decubitus position (Sim's

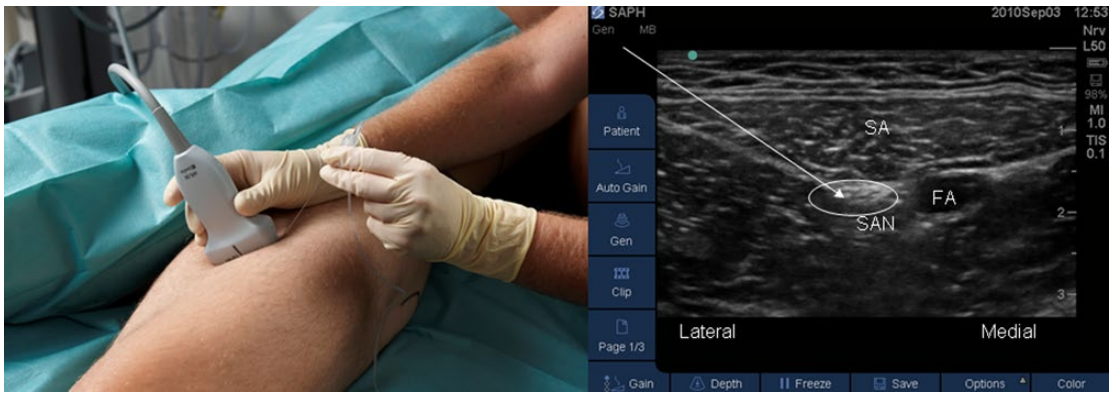

Figure 29.12 USG saphenous nerve (SAN) block.

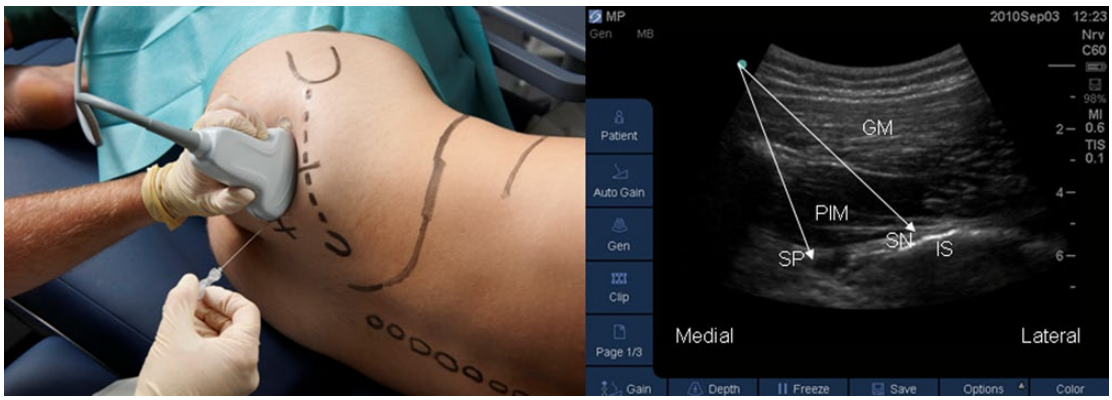

Figure 29.13 USG sacral plexus (SP) and sciatic nerve (SN) block – sacral/parasacral approach (Mansour pivot).

position), with the side to be anaesthetised facing upwards. The point of Mansour is localised 6 cm caudally to the inferior posterior iliac spine (IPIS). A curved-array transducer (2–5 MHz) is placed with its medial end at the point of Mansour. Using this point as a pivot, the transducer is rotated gradually until the lateral end of the transducer points towards the greater trochanter and the sacral plexus appears anterior to the triangular shape of the PIM at its medial base immediately next to the lateral border of the sacral bone (Figure 29.13). This pivoting manoeuvre is termed 'the Mansour pivot'. In order to block the SP or the SN at this level, it is advocated that the needle is inserted in-plane to the transducer from the medial to lateral end (Figure 29.13). To block the SP, the needle is inserted at a steep angle via the PIM towards the anterior side of the PIM, where the inferior gluteal artery is seen pulsating. To block the SN the needle is inserted at a more shallow angle, either via or below the PIM directing the tip towards the SN, which descends across the ischial spine (IS).

USG Sciatic Nerve (SN) Block: Antero-medial and Popliteal Approaches

The patient is placed in a supine position (Figures 29.14 and 29.15). For the antero-medial approach, a curved-array transducer (2–5 MHz) is placed 8 cm below the inguinal ligament transversally to the femur (FE) and SN (Figure 29.14). The SN is located just medially to the FE at the level of the lesser trochanter.

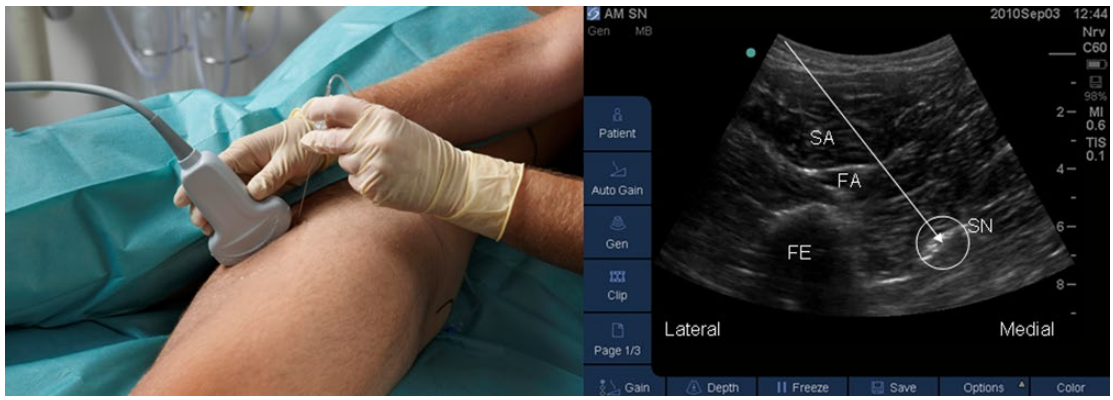

Figure 29.14 USG sciatic nerve (SN) block: antero-medial approach.

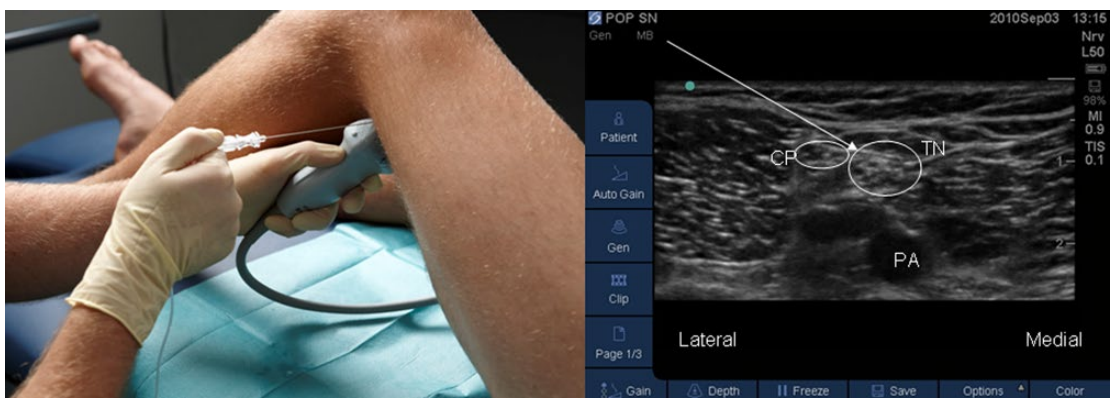

Figure 29.15 USG sciatic nerve (SN) block: popliteal approach.

The needle is inserted in-plane to the transducer in a lateral-to-medial direction, penetrating the sartorius muscle (SM) and bypassing the deep femoral artery (FA) before reaching the SN (Figure 29.14). The spread of the injectate should be observed to occur around the SN, with local anaesthetic deposited antero-laterally and infero-medially to the nerve. For the popliteal approach, a linear transducer (6–15 MHz) is placed in the popliteal fossa transversally to the popliteal artery (PA) and SN (Figure 29.15). The PA can easily be identified here. The tibial nerve (TN) is always observed posteriorly to the PA and anteriorly to the skin. The transducer is then shifted progressively in a cranial direction, keeping the TN in focus at all times. The common peroneal nerve (CP) is observed 4–10 cm cranially to the popliteal crease, where the PA was first identified. The needle is inserted in-plane to the transducer in a lateral-to-medial direction (Figure 29.15). The spread of the injectate should be observed to cover the CP and TN just at the bifurcation of the SN.

Truncal Nerve Blocks

It has recently been stated that although relatively few studies have compared ultrasound guidance with other established techniques, the available evidence suggests that it is a safe and effective means to facilitate correct needle placement and adequate spread of local anaesthetic for truncal blocks. At this point, the

Table 29.7 Overview of recommended truncal nerve blocks. Indications only include postoperative pain management (PPM).

Truncal nerve blockade	Indications
Ilioinguinal/iliohypogastric (II/IH) block	Figure 29.16 Open and laparoscopic inguinal hernia repair (PPM).
Rectus sheath (RS) block	Figure 29.17 Midline incisions and trochar holes (PPM).
Intercostal nerve (ICN) block	Figure 29.18 Parasaggital plane. Thoracic and breast surgery and trauma (PPM).
Bilateral Dual – Transversus Abdominal Plane (BD-TAP) block	Figure 29.19 Medial intercostal TAP block (MIC-TAP) block (PPM). Figure 29.20 Lateral intercostal TAP block (LIC-TAP) (PPM). Figure 29.21 Classic TAP block (CL-TAP) (PPM).

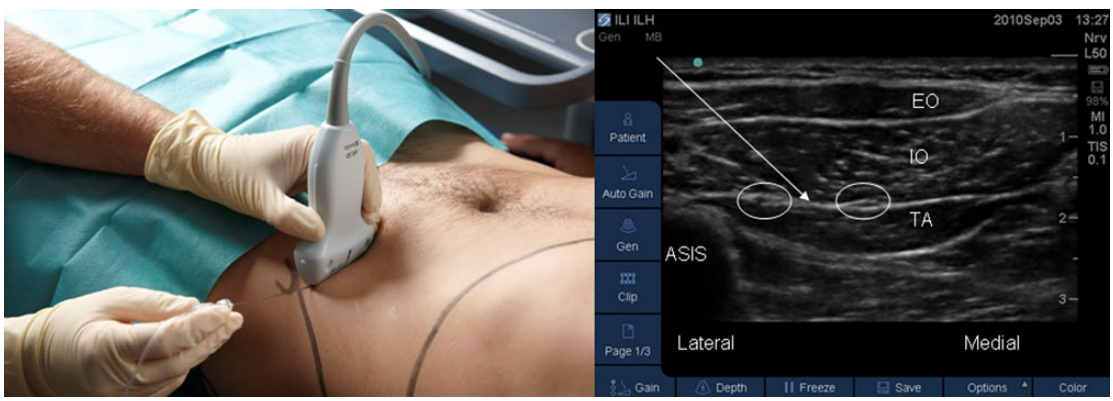

Figure 29.16 USG ilioinguinal/iliohypogastric (II/IH) nerve block.

thoracic paravertebral block will not be described as it should only be considered by specially trained physicians. The recommended truncal nerve blocks and their indications are listed in Table 29.7.

USG Ilioinguinal/Iliohypogastric (II/IH) Nerve Block

This is actually a block of the ventral ramus of the L1. The patient is placed in a supine position, and the anterior superior iliac spine (ASIS) is localised by palpation (Figure 29.16). A linear transducer (6–15 MHz) is placed with its lateral end at or just superior to the ASIS. The needle is inserted in-plane to the transducer in a lateral-to-medial direction, and the neurovascular plane between the OI and the TA is located. The II and IH nerves can often be seen together with the deep circumflex iliac artery in the neurovascular plane. The tip of the needle is placed in this plane, and the spread of the injectate should be observed to expand in the fascial neurovascular plane.

USG Rectus Sheath (RS) Block

The RS block may have been overshadowed by the TAP block, but the evidence base for its use is very good. The patient is placed in a supine position, and a linear transducer (6–15 MHz) is placed with its medial end just above the linea alba (Figure 29.17). The needle is inserted in-plane to the transducer in a medial-to-lateral

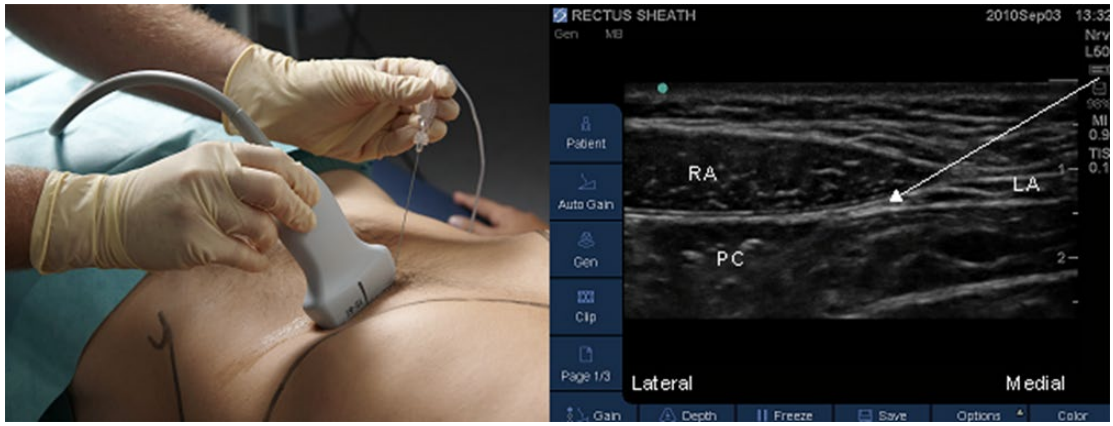

Figure 29.17 USG rectus sheath (RS) block.

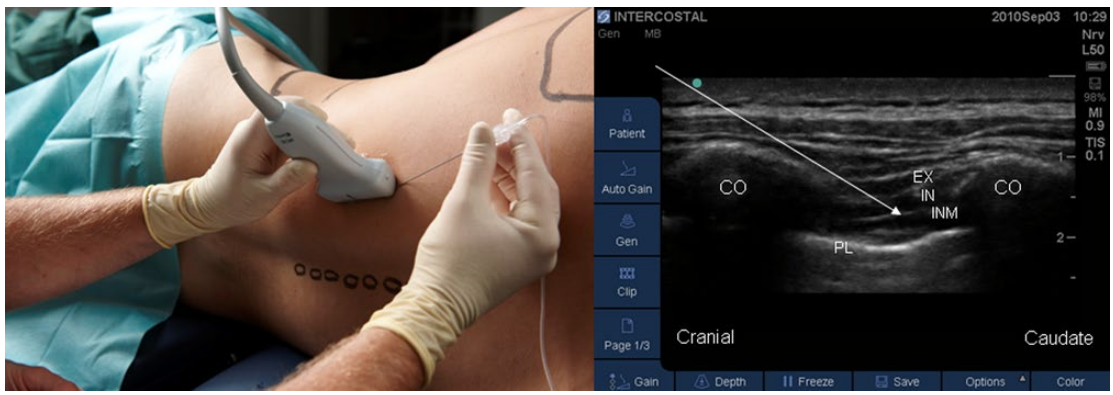

Figure 29.18 USG intercostal nerve (ICN) block: parasaggital plane.

direction, and the division between the belly of the rectus abdominis muscle and the posterior rectus sheath is visualised. The tip of the needle is placed in this space. The spread of the injectate should be observed to advance in a lateral direction.

USG Intercostal Nerve (ICN) Block: Parasaggital Plane

The patient is placed in the lateral decubitus position, and a linear transducer (6–15 MHz) is placed in a saggital paravertebral plane (Figure 29.18). The needle is inserted in-plane to the transducer in a cranial-to-caudal direction, and the three intercostal muscles (external, internal and innermost) are visualised between two costae. The tip of the needle is placed in the fascial plane between the internal and innermost intercostal muscles. The spread of the injectate should be observed to occur in this fascial plane. It is very important to visualise the tip of the needle at all times and its close proximity to the parietal pleura.

USG Bilateral Dual TAP (BD-TAP) Block

With the aim to render the entire abdominal wall pain-free after surgery, it is essential to anaesthetise all the antero-lateral rami of the thoracoabdominal nerves (Th6–12). In doing so, it is important to target both the uppermost intercostal TAP plexus (Th6–9) just below the xiphoid process medially to the costal curvature

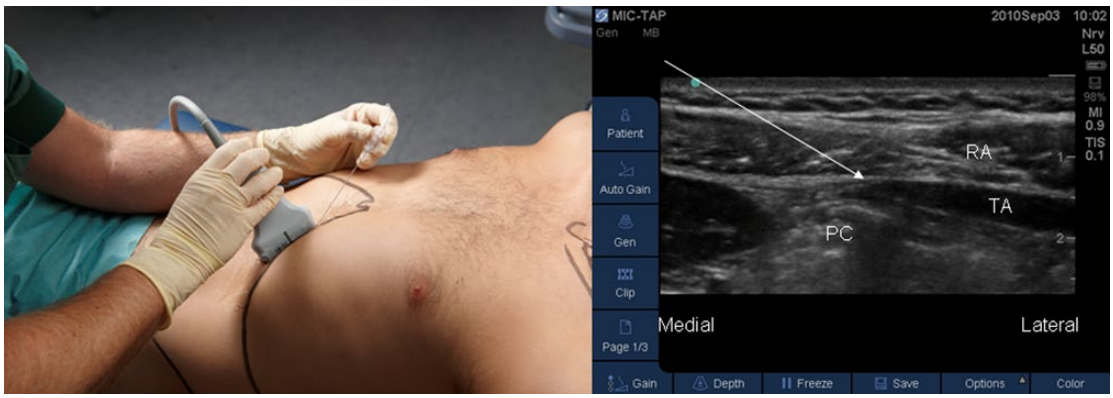

Figure 29.19 USG medial intercostal TAP (MIC-TAP) block.

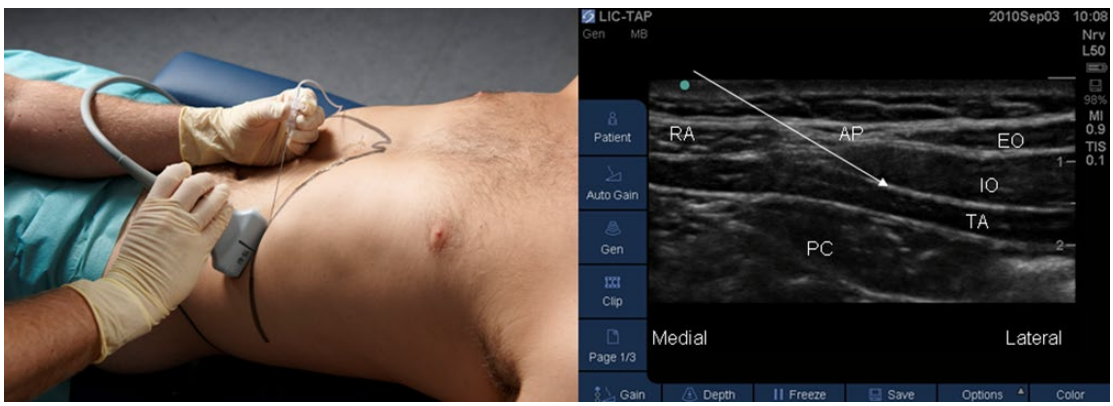

Figure 29.20 USG lateral intercostal TAP (LIC-TAP) block.

(Figures 29.19 and 29.20) and the more caudal TAP plexus in the anterior axillary line above the iliac crest and below the costal curvature (Th10–12) (Figure 29.21). There are two ways to achieve this goal. The physician must employ either the oblique subcostal TAP block technique, or utilise the BD-TAP block approach. It is recommended that the more simple BD-TAP block technique, which is a four-point USG single-shot TAP block approach, is used. In some patients the transverse abdominis muscle (TA) reaches below the rectus abdominis muscle (RA). To target the uppermost branches of the intercostal TAP plexus the physician must then use the USG medial intercostal TAP (MIC-TAP) block, where the TAP lies in the fascial plane between the RA and the TA (Figure 29.19). If the TA is first seen laterally to the RA at the formation of the aponeurosis, the USG lateral intercostal TAP (LIC-TAP) block must be employed to target the intercostal TAP plexus between the internal oblique (IO) and the TA muscles (Figure 29.20). Having anaesthetised the intercostal TAP plexus either by the MIC- or LIC-TAP block, the physician must now target the lower TAP plexus (Th10–12) with the classic TAP (CL-TAP) block (Figure 29.21). Thus, the BD-TAP block consists of either a MIC- and a CL-TAP or a LIC- and a CL-TAP bilaterally. For all TAP blocks the patient is placed in a supine position, and a linear transducer (6–15 MHz) is placed with its medial end pointing medially (Figures 29.19–29.21). The needle is inserted in-plane to the transducer in a medial-to-lateral

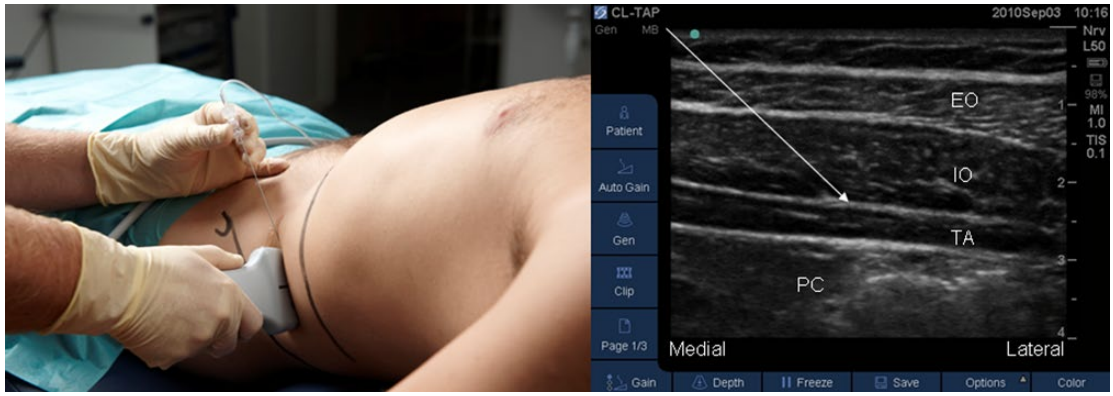

Figure 29.21 USG classic TAP (CL-TAP) block.

direction in the fascial neurovascular plane between the RA and TA (MIC-TAP), or between the OI and TA (MIC- and CL-TAP). The spread of the injectate should be observed to spread in a lateral direction.

Further Reading

Abrahams, M.S., Horn, J.-L., Noles, L.M., Aziz, M.F. (2010) Evidence-based medicine. Ultrasound guidance for truncal blocks. *Region. Anesth. Pain Med.*, **35**, S36–S42.

Bærentzen, F., Jensen, K., Maschmann, C., Belhage, B., Børglum, J. (2012) Ultrasound-guided block of the ilioinguinal and iliohypogastric nerves for inguinal herniotomy. A randomized study. *Anesth. Analg.*, **37** (5), 502–507.

Børglum, J., Bartholdy, A., Hautopp, H., Krogsgaard, M., Jensen, K. (2011) Ultrasound-guided continuous suprascapular nerve block after surgery for adhesive capsulitis: one case and a short topical review. *Acta Anaesth. Scand.*, **55** (2), 242–247.

Børglum, J., Maschmann, C., Belhage, B., Jensen, K. (2011) Ultrasound-guided (USG) bilateral dual transversus abdominis plane (BD-TAP) block: description of a four-point ultrasound-guided TAP block approach. *Acta Anaesthesiol. Scand.*, **55** (6), 658–663.

Hebbard, P.D., Barrington, M.J., Vasey, C. (2010) Ultrasound-guided continuous oblique subcostal transversus abdominis plane blockade: description of anatomy and clinical technique. *Region. Anesth. Pain Med.*, **35**, 436–441.

Jensen, K., Børglum, J. (2011) Predictors of failure of interscalene nerve blocks for shoulder surgery. A 4-year cohort study. Spring 2011 ASRA 36th Annual Regional Anesthesia Meeting and Workshops May 5-8, 2011 Las Vegas, Nevada.

Kapral, S., Krafft, P., Eibenberger, K., Fritzgerald, R., Gosch, M., Weinstabl, C. (1994) Ultrasound-guided supraclavicular approach for regional anesthesia of the brachial plexus. *Anesth. Analg.*, **78**, 507–513.

Koscielniak-Nielsen, Z.J. (2008) Ultrasound-guided peripheral nerve blocks: what are the benefits? *Acta Anaesth. Scand.*, **52**, 727–737.

Labat, G. (1922) *Regional anaesthesia. Its technique and clinical application*. W.B. Saunders, New York.

Liu SS, MD, Justin Ngeow, BA, and Raymond S. John, BA. Evidence basis for ultrasound-guided block characteristics. Onset, quality, and duration. *Region. Anesth. Pain Med.*, **35**, S26–S35.

Liu, S.S., *et al*. (2009) Ultrasound-guided regional anesthesia and analgesia. *A qualitative systematic review. Region. Anesth. Pain Med.*, **34**, 47–59.

Mansour, N.Y. (1993) Reevaluating the sciatic nerve block: another landmark for consideration. *Region. Anesth.*, **18**, 322–323.

McCartney, C.J.L., Lin, L., Shastri, U. (2010) Evidence basis for the use of ultrasound for upper-extremity blocks. *Region. Anesth. Pain Med.*, **35**, S10–S15.

Neal, J.M., Brull, R., Chan, V.W.S., Grant, S.A., Horn, J.-L., *et al*. (2010) The ASRA evidence-based medicine assessment of ultrasound-guided regional anesthesia and pain medicine. Executive summary. *Region. Anesth. Pain Med.*, **35**, 1–9.

Neal, J.M., *et al*. (2009) Upper extremity regional anesthesia: essentials of our current understanding, 2008. *Region. Anesth. Pain Med.*, **34**, 134–170.

Orebaugh, S.L., *et al*. (2009) Interscalene block using ultrasound guidance: impact of experience on resident performance. *Acta Anaesth. Scand.*, **53**, 1268–1274.

Prasad, A., Perlas, A., Ramlogan, R., Brull, R., Chan, V. (2010) Ultrasound-guided popliteal block distal to sciatic nerve bifurcation shortens onset time. *Region. Anesth. Pain Med.*, **35**, 267–271.

Rozen, W.M., Tran, T.M., Ashton, M.W., Barrington, M.J., Ivanusic, J.J., Taylor, G.I. (2008) Refining the course of the thoracolumbar nerves: a new understanding of the innervation of the anterior abdominal wall. *Clin. Anat.*, **21**, 325–333.

Salinas, F.V. (2010) Ultrasound and review of evidence for lower extremity peripheral nerve blocks. *Region. Anesth. Pain Med.*, **35**, S16–S25.

Sites, B.D., Chan, V.W., Neal, J.M., Weller, R., Grau, T., Koscielniak-Nielsen, Z.J., Ivani, G. (2010) The American Society of Regional Anesthesia and Pain Medicine and the European Society of Regional Anaesthesia and Pain Therapy joint committee recommendations for education and training in ultrasound-guided regional anesthesia. *Region. Anesth. Pain Med.*, **35** (2), 74–80.

Willschke, H., Marhofer, P., Bösenbeerg, A., *et al*. (2005) Ultrasonography for ilioinguinal/iliohypogastric nerve blocks in children. *Br. J. Anaesth.*, **95**, 226–230.

www.cebm.net.

30

Foreign Body and Abscess

Erskine J. Holmes

Introduction

Foreign bodies are often difficult to visualise using plain film radiography. Diagnostic uncertainty can be compounded by late presentation and the lack of a clear history. Abscess identification on clinical grounds alone can also be difficult, especially where there is coexisting cellulitis or difficulty in demonstrating fluctuance due to depth. Ultrasound – either alone or in conjunction with other imaging techniques – can be extremely useful in the localisation and treatment of these conditions.

The identification of soft-tissue foreign bodies and abscesses requires an understanding of normal soft-tissue anatomy. As with most ultrasound techniques, the practitioner will better recognise pathology by first having a good understanding of normal anatomy. In general, this comes with practice, but comparison with normality can be useful and may be best achieved by scanning normal soft tissue prior to scanning the area of suspected abnormality. This has the additional benefit in children of reducing anxiety before scanning a potentially painful area of soft tissue. Foreign bodies frequently occur in the hands and feet, and a good understanding of the relevant anatomy is key to diagnosis and avoiding iatrogenic complications associated with intervention.

Technique

Probe selection is important. A high-frequency linear-array transducer with a suitably sized footprint is key to good image acquisition. In practical terms, many machines are fitted with a linear probe capable of scanning with a range of between 7 and 14 MHz. These linear probes, despite having a large footprint, are usually adequate for most soft-tissue work. Smaller footprint probes, specifically designed for superficial soft-tissue imaging, are available but in pragmatic terms they are not usually part of the emergency department armamentarium. The probe should be held perpendicular to the skin, scanning in at least two planes with adequate amounts of acoustic-couplant gel.

Pearls and Pitfalls

- *Misinterpretation of normal anatomy*: Interfaces between different tissues can be brightly echogenic. Misinterpretation of normal echogenic tissue interfaces can be avoided by careful meticulous scanning in various directions and familiarity with the normal appearances of tendons, nerves and bones (including sesamoid and accessory ossicles). Note should be made of important adjacent structures to avoid iatrogenic procedural injury.

Emergency Point-of-Care Ultrasound, Second Edition. Edited by James A. Connolly, Anthony J. Dean, Beatrice Hoffmann and Robert D. Jarman.

Companion website: www.wiley.com/go/connolly/ultrasound

- *Image optimisation*: Visualisation of superficial structures may be improved using an acoustic stand-off pad. As well as being commercially available, an improvised stand-off can be made using a sterile glove containing water. With extremity soft-tissue sonography, immersion of the limb within a water bath can also improve visualisation, and may be preferable. Care must be taken to ensure that the probe is suitable for use with a water bath and ensures operator and patient safety. The idea behind both of these techniques is to move the superficial soft-tissue structures further away from the probe and into the transducer focal zone. Machine technology permitting, dynamic adjustment of depth, focal zone and image gain will aid in the identification of pathology. Images of a finger foreign body demonstrated using a water bath are shown in Figure 30.1.
- *Artefact avoidance*: Imaging may be technically limited by air within the soft tissues, pain at the site, and the small size of the foreign body. Care should be taken, with local anaesthetic infiltration of the area so as not to introduce air artefact or significantly distort the tissues. Using a nerve or regional block is often preferential to local anaesthesia for these reasons.
- *Foreign body localisation*: A sterile needle can be guided through soft tissues using ultrasound to localise the foreign body and facilitate procedural removal. Ultrasound-guided removal in real time is possible but is technically difficult and often not practical. Following the removal of a foreign body the best practice is to re-scan where possible to ensure there are no additional retained foreign bodies.
- *Abscess identification*: Abscesses are typically round or elliptical in shape, and hypoechoic with post-acoustic enhancement. Depending on the abscess contents they may sometimes appear isoechoic or hyperechoic. Also, depending on the tenderness of the area the probe can be used to gently compress the skin, and swirling of abscess contents can occur. Colour Doppler is useful to distinguish an abscess from an inflamed enlarged lymph node. Lymph node vessels typically enter through the node hilum and have a very typical appearance in comparison to the surrounding reactive hyperaemia seen with abscesses. Typical appearances of abscess/collections are shown in Figure 30.2.

Foreign Body Echogenicity, Shadowing and Reverberation Artefact

In the acute phase, foreign bodies often appear echogenic with clean shadowing. Reverberation artefacts may occur and are seen more often with smooth or flat surfaces, such as with metal or glass. They are characterised by regularly spaced echogenic parallel lines deep to the structure being imaged. Reverberation will vary with probe position and beam angle, and will be most apparent when imaging a flat smooth foreign body perpendicular to the ultrasound beam. Comet tail artefacts are also seen, more commonly with small rounded objects.

With time, a hypoechoic rim develops around the foreign body due to tissue reaction. This can aid in the identification of a suspected foreign body. The use of colour flow Doppler may reveal increased vascularity in keeping with a local tissue reaction and hyperaemia.

With more time, appearances can change further, with walling-off or loss of the hypoechoic rim as it is replaced with chronic granulomatous tissue.

The typical appearances of some foreign bodies are shown in Figure 30.3.

Summary

Soft-tissue ultrasound has been shown to be highly sensitive and specific in both foreign body and abscess identification. It is a valuable tool and should be thought of as an extension to clinical examination, especially when the clinical picture is not clear. The visualisation of adjacent normal structures helps avoid potentially catastrophic iatrogenic procedural injury.

(a)

(b)

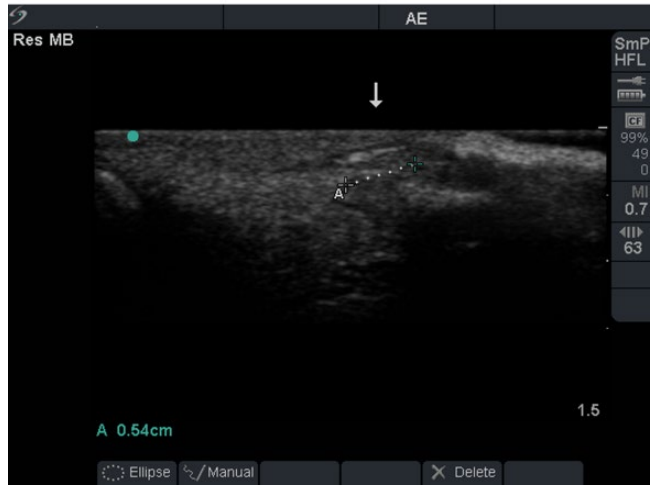

(c)

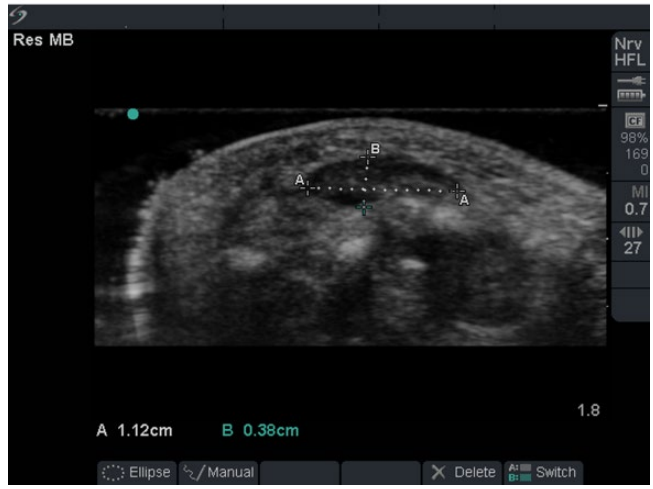

Figure 30.1 (a) Foreign body (A-A) within a finger, using the water-bath technique, transverse view. (b) Foreign body (A) within a finger, using the water-bath technique, longitudinal view. The measurement marker is deep to the foreign body. (c) Fourteen-day-old baby with acute swelling on the dorsum hand (water-bath technique). Abnormal soft tissue can be seen superficial to the echogenic metacarpals.

(a)

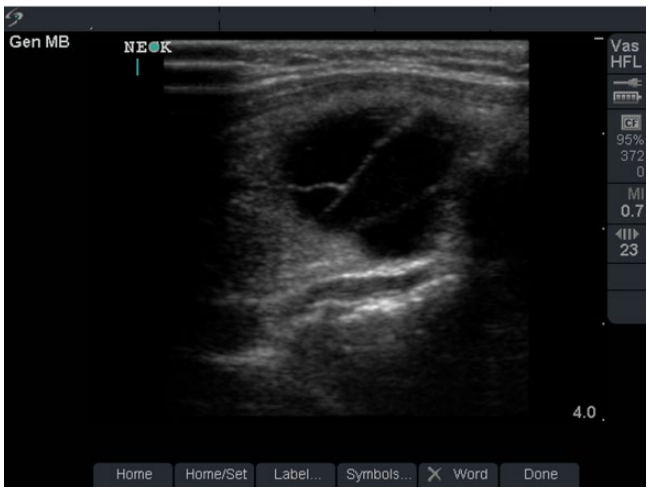

(b)

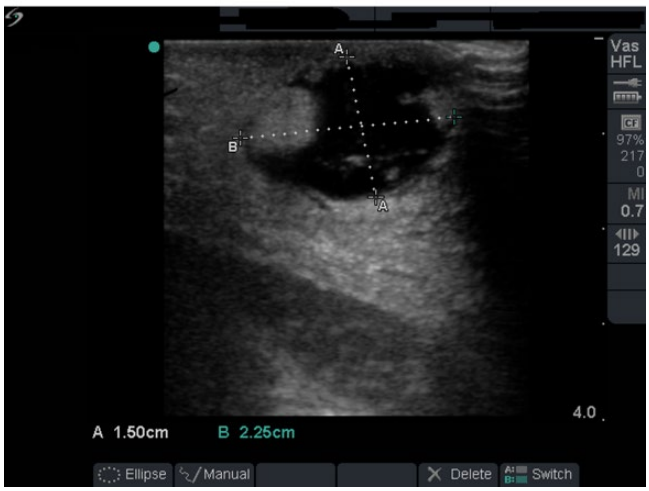

(c)

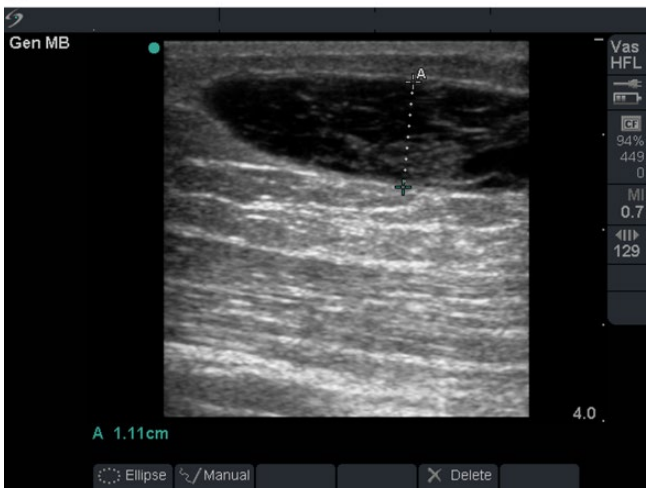

Figure 30.2 (a) Abscess with internal septations demonstrating posterior acoustic enhancement. (b) Abscess demonstrating posterior acoustic enhancement. (c) Soft-tissue fluid collection demonstrating mixed echogenicity.

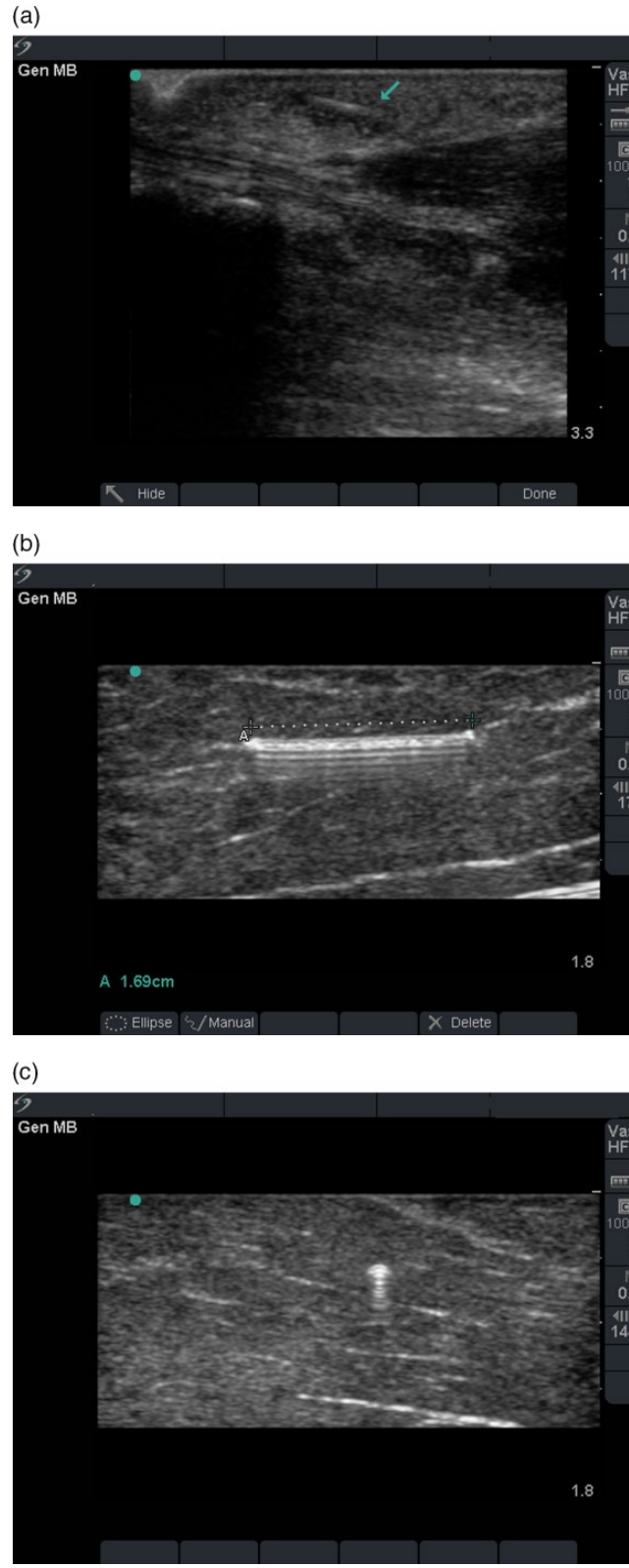

Figure 30.3 (a) Foreign body (arrow). (b) Thick metallic foreign body with reverberation artefact. (c) Thin metallic foreign body with reverberation artefact. (d) Thin metallic foreign body with reverberation artefact. (e) Wooden foreign body with posterior shadowing, longitudinal view. (f) Wooden foreign body with posterior shadowing, transverse view.

(d)

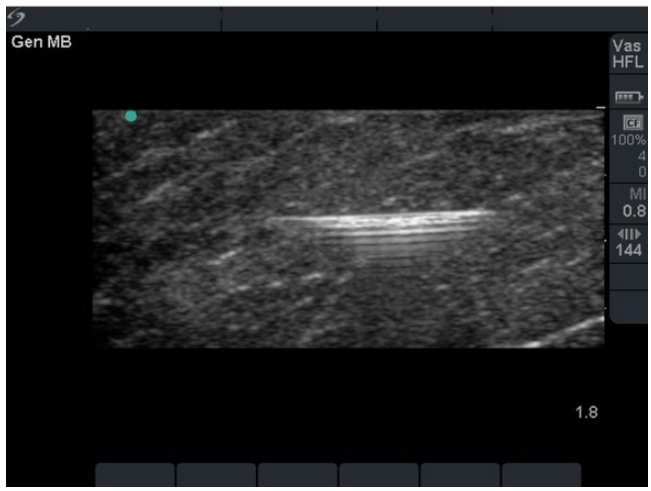

(e)

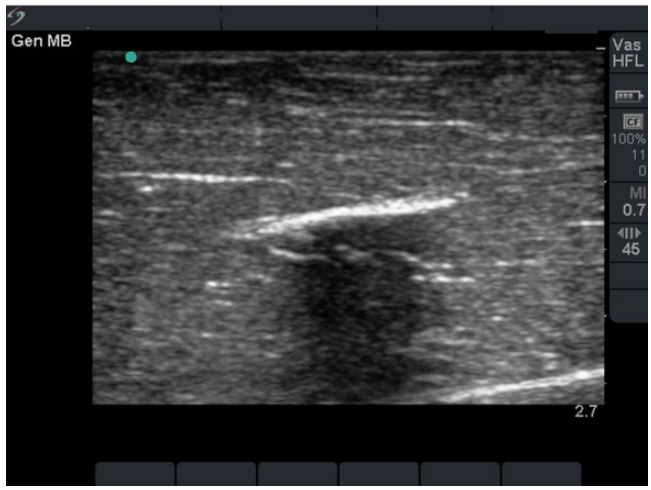

(f)

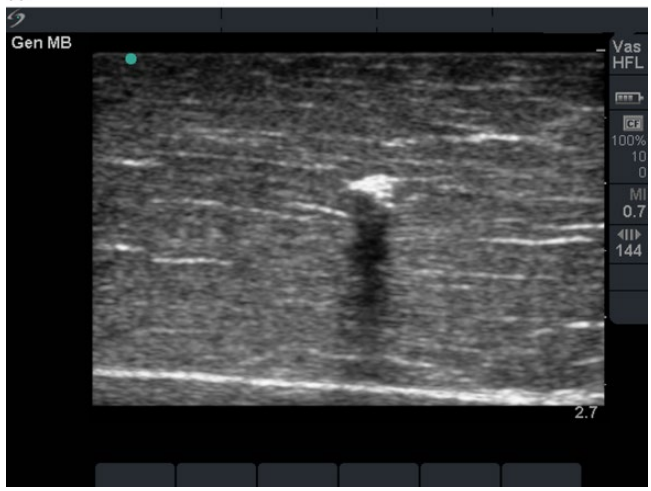

Figure 30.3 (*Continued*)

31

Ultrasound of the Airway

Christopher T. Wall, Seth R. Strote, Liberty V. Caroon and Robert F. Reardon

Introduction

Ventilation is paramount in the care of critically ill patients, and airway management is one of the tenets of emergency and critical care medicine. Traditionally, direct visualisation of the endotracheal tube (ETT) passing through the vocal cords has been the only way in real time to see the distal tube enter the trachea. However, such direct visualisation is not always achievable due to difficult anatomy, excessive secretions or blood obscuring the view, or other pathological conditions. Post-intubation confirmation for ETT placement include end-tidal carbon dioxide monitoring, chest auscultation, ETT expiratory vapour and oxygen saturation monitoring. However, none of these parameters is 100% reliable, nor do they provide anatomical evidence of ETT position.

Ultrasound provides a portable, non-invasive and inexpensive method for both static and real-time assessment of the airway before, during and after intubation. Ultrasonography can provide direct and indirect indicators for difficulties of endotracheal intubation, by providing valuable information about airway and surrounding structures prior to intubation (Figure 31.1). Ultrasonography can be used for real-time or dynamic guidance, following each step of ETT placement. Lastly, several techniques and assessments have been described to confirm tracheal versus oesophageal endotracheal tube placement.

To begin, sonography of the upper airway requires a high-frequency transducer due to the superficial nature of structures. Generally, this can be accomplished with a 10-5 MHz linear transducer externally, or 8-2 MHz micro-convex transducer sublingually. Due to the high acoustic impedance of air, the inside of the trachea, nasal and oral cavities cannot be visualised with ultrasound; however, the anterior and lateral walls of structures can easily be appreciated. This information can help determine the difficulty of direct laryngoscopic intubation in these patients.

Pre-Intubation Evaluation

Prior to intubation, the 10-5 MHz linear transducer can be used in the transverse plan at the level of the anterior neck crease, just superficial to the hyoid bone. Initially, the sonographer can direct the transducer more cephalad in order to measure the anterior soft-tissue thickness from the skin to the bright, hyperechoic reflection of the hyoid bone (Figure 31.2). The examiner can then move the transducer caudally to measure the anterior soft-tissue thickness at the level of the thyrohyoid membrane. This measurement can often be recorded using two distances: (i) from

Emergency Point-of-Care Ultrasound, Second Edition. Edited by James A. Connolly, Anthony J. Dean, Beatrice Hoffmann and Robert D. Jarman.

Companion website: www.wiley.com/go/connolly/ultrasound

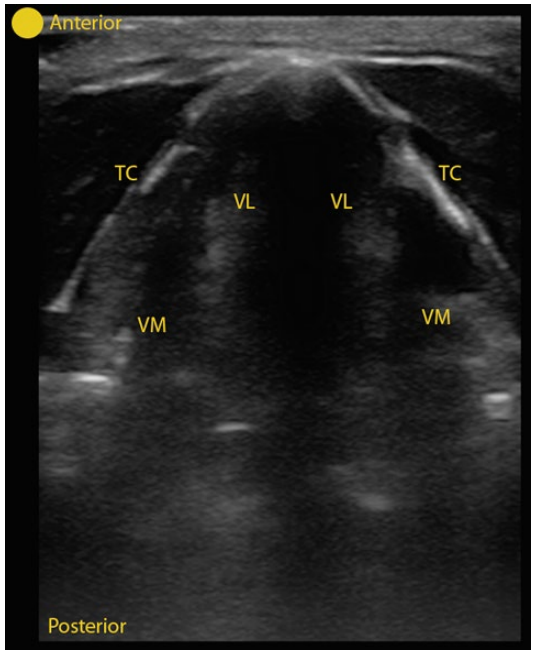

Figure 31.1 Normal transverse view of the larynx showing part of the thyroid cartilage (TC) and the vocal ligaments (VL) and vocalis muscles (VM) bilaterally.

the skin to the anterior edge of the epiglottis; and (ii) from the skin to the inner wall of the anterior vocal cords (Figures 31.3 and 31.4). Increased soft-tissue thicknesses measured at these three locations have been shown to correlate with difficult endotracheal intubation. In urgent settings, this pre-screening evaluation was obtained in less than 2 minutes.

Endotracheal Tube Confirmation

Several methods have been described to confirm tracheal placement of an ETT using sonography, the majority using indirect sonographic signs. There are, however, a few methods, which directly visualise tracheal intubation.

Visualisation of Tracheal Intubation in Real Time

Visualisation of the ETT passing through the vocal cords has been described in children. This technique requires two operators. The sonographer

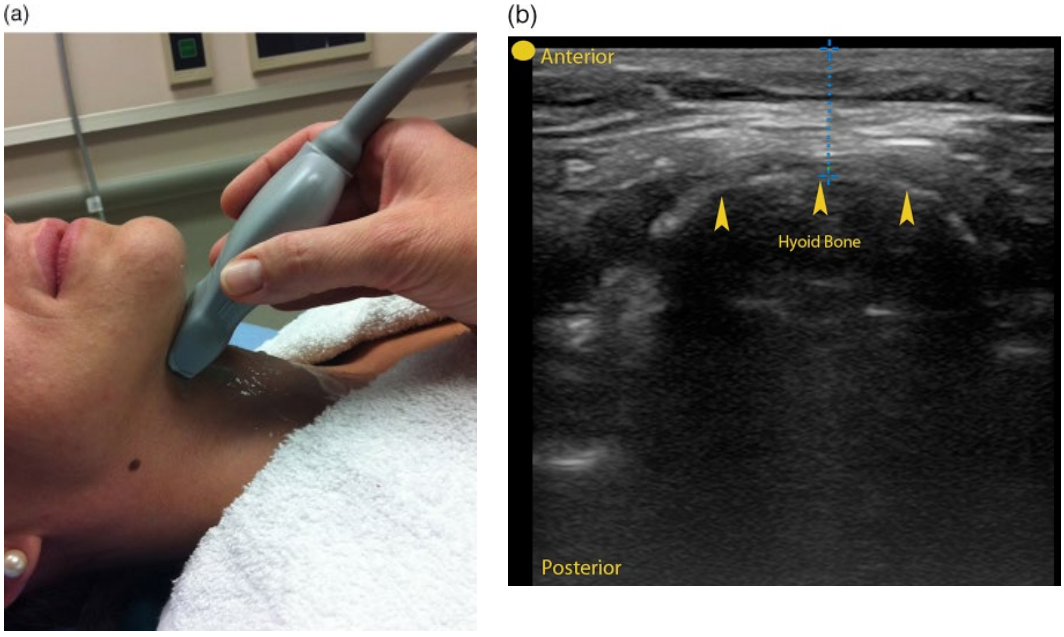

Figure 31.2 (a) Transducer placement for transverse imaging of the hyoid bone and anterior neck soft-tissue measurement. (b) Transverse image of the airway at the hyoid bone with measurement of the anterior soft tissue, which can be used as screening for difficult airways.

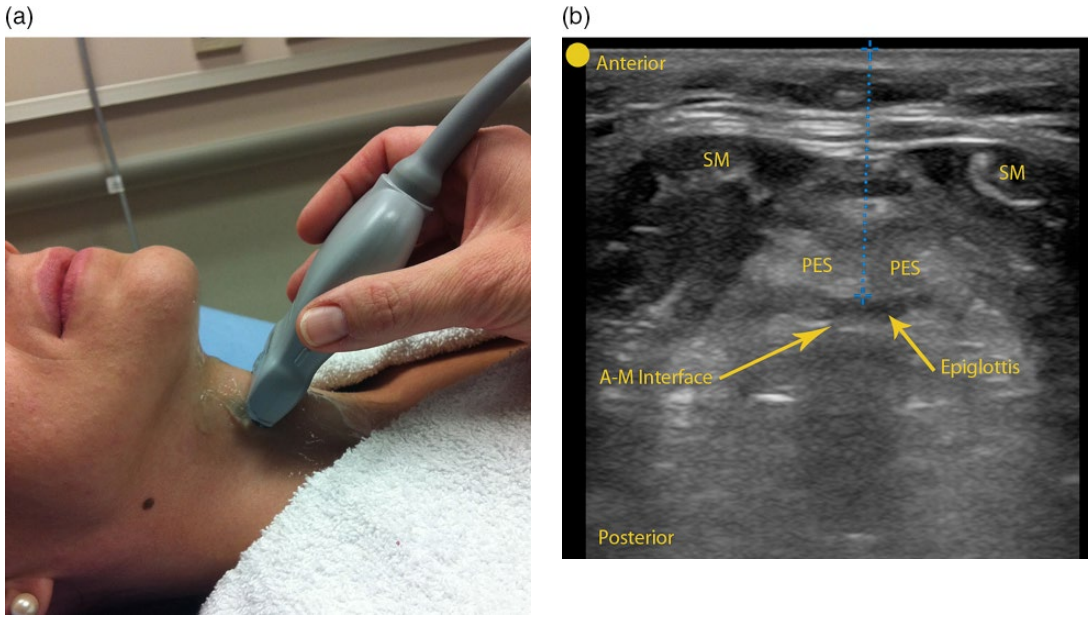

Figure 31.3 (a) Placing the transducer in the transverse plane aiming slightly cephalad allows imaging of the epiglottis. (b) The distance measured from skin to epiglottis can aid in predicting a difficult airway and identifying the pre-epiglottic space (PES) and strap muscles (SM), as well as the hyperechoic air–mucosal interface (A-M Interface).

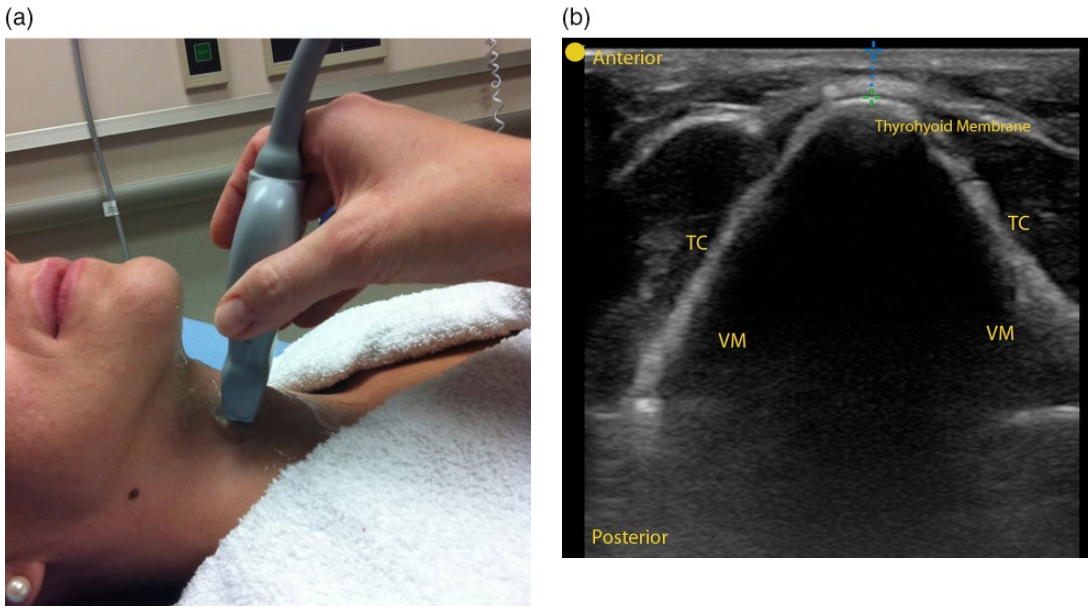

Figure 31.4 (a) Fanning the transducer slightly caudal brings the thyrohyoid membrane into view. (b) In this transverse view the skin-to-membrane distance can again help predict a difficult intubation. TC, thyroid cartilage; VM, vocalis muscles.

places a linear high-frequency (10-5 MHz) transducer transversely in the midline on the patient's neck just above the suprasternal notch and scans cephalad until the vocal cords come into view. True vocal cords can be visualised as paired hyperechoic linear structures in an inverted 'V'. They should have mobility with respirations and swallowing (Figure 31.5). As the second physician passes the ETT into the trachea and through the glottis, the cords will be observed to widen. The ETT itself is not visualised due the acoustic impedance of the air in and around the tube. The distortion of the glottis as the ETT passes confirms placement. This method will also allow the sonographer to appreciate oesophageal intubation.

An alternative method for confirming ETT placement in real time is to observe a change in the air artefact within the trachea. The empty trachea tends to produce a periodic resonance artefact, whereas a comet tail artefact is produced in the intubated trachea (Figure 31.6). However, these artefacts are not always present and the clinical utility of this is situation unproven.

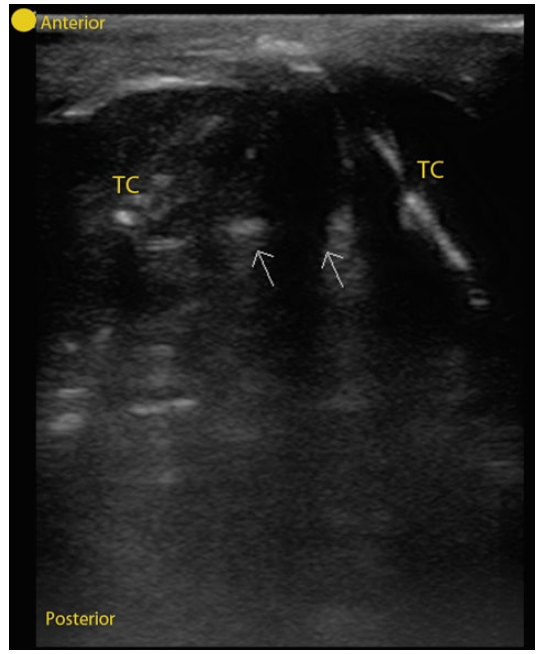

Figure 31.5 Transverse view of the normal vocal cords (arrows) at the level of the thyroid membrane, which will be actively displaced as the ETT and cuff pass through. TC, thyroid cartilage.

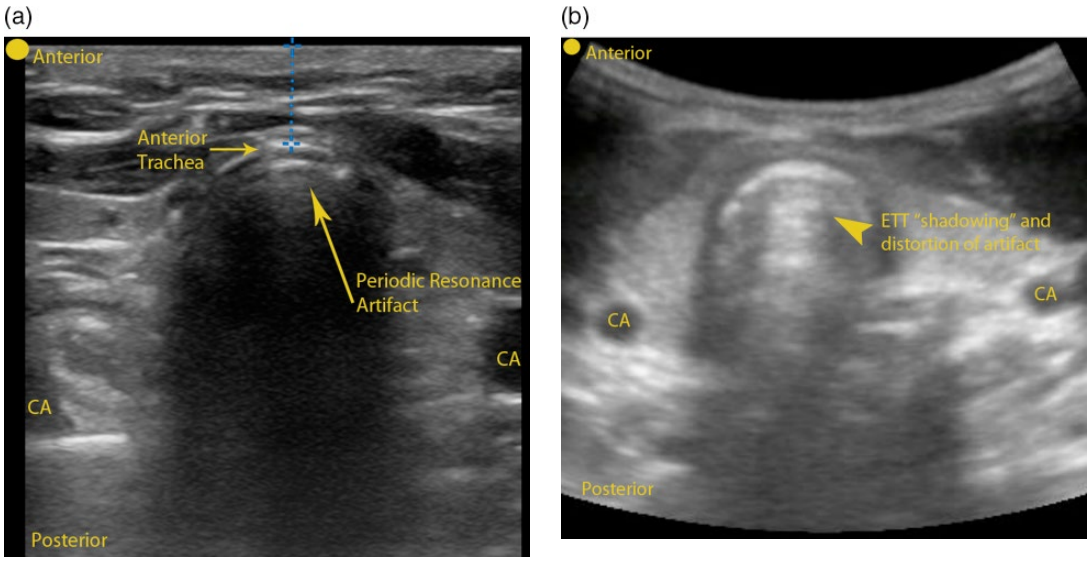

Figure 31.6 At the suprasternal notch, two comparative transverse views without (a) and with (b) ETT placement showing the periodic resonance artefact or comet tailing without the ETT. CA, carotid artery.

Lastly, inflating the ETT cuff with saline or foam can be utilised to confirm tracheal placement of the ETT. Air within the trachea normally interferes with good sonographic visualisation of the ETT, but saline or foam allows sound waves to pass, so that the ETT can be visualised directly. This technique utilises a longitudinal view and is enhanced by gentle movement of the ETT (Figure 31.7). At the level of the suprasternal notch, visualisation of the cuff directly posterior can yield a sensitivity and specificity of 100% for correct ETT depth.

Real-Time Assessment of Oesophageal Intubation

Identifying the absence of an oesophageal intubation can serve as an excellent indirect means of confirming tracheal placement of the ETT. Again, this technique requires two operators for real-time assessment. The sonographer should use a high frequency (10-5 MHz) linear transducer placed midline and transversely across the trachea, approximately 1 cm inferior to the cricoid ring. The trachea should be easily visualised in the midline with surrounding thyroid tissue. A periodic resonance artefact may be visualised due to air in the trachea. The oesophagus may or may not be seen lateral to the trachea. If the ETT is advanced into the oesophagus instead of the trachea, the sonographer is able to detect in real time the distension of the oesophagus by the ETT. To further aid the sonographer, small oscillations of the ETT can be made to allow its better visualisation. If oesophageal intubation is confirmed by this method the tube should be withdrawn and another attempt at intubation made.

Assessment of Sliding Lung Sign

Sliding lung sign (SLS) can be used as another indirect indicator for the correct placement of the ETT. SLS occurs as the visceral and parietal pleura slide over one other, producing the characteristic sliding lung sign and comet tail artefact. SLS is obtained by placing a linear or curved-array transducer aimed cephalad in the 3rd or 4th intercostal space on the anterior chest. The pleural interface is visualised as an hyperechoic line between superior and inferior rib shadows (see Chapter 2). Movement at the pleural interface should always be assessed on both sides of the chest for comparison. If present, the SLS confirms ETT placement in the trachea due to proper ventilation of the lung parenchyma. Right main stem intubation can also be detected by this method, as only the right SLS sign is present. Sonographers should be aware that an absence of SLS does not confirm incorrect tube placement as other pathological conditions can also lead to an absence of SLS.

Assessment of Diaphragmatic Movement

Ideal ETT placement should result in an equal bilateral movement of the diaphragm with ventilation, as described by Hsieh *et al.* in children. The sonographer assesses for equal bilateral movement of the diaphragm by using a phased-array (5-2 MHz) transducer in the mid-upper abdomen, directly beneath the xiphoid process, for bilateral scanning of the diaphragm. Using the left lobe of the liver as an acoustic window, both hemi-diaphragms should be visualised. M-mode can aid in assessing the diaphragm for the sinusoidal rhythm of respirations. Assessing bilateral diaphragm movement caudally with contractions on respirations or due to positive-pressure ventilation confirms correct ETT placement. This method, like SLS, can be used to assess for right main stem intubation if only the right hemi-diaphragm exhibits movement. Caution must be applied, however, as oesophageal intubation may result in a paradoxical movement of the diaphragm with ventilation due to increased intra-abdominal pressure.

Pre-Extubation Evaluation

Finally, prior to extubation ultrasound can be helpful in predicting post-extubation stridor, based on the air-column width when the cuff is

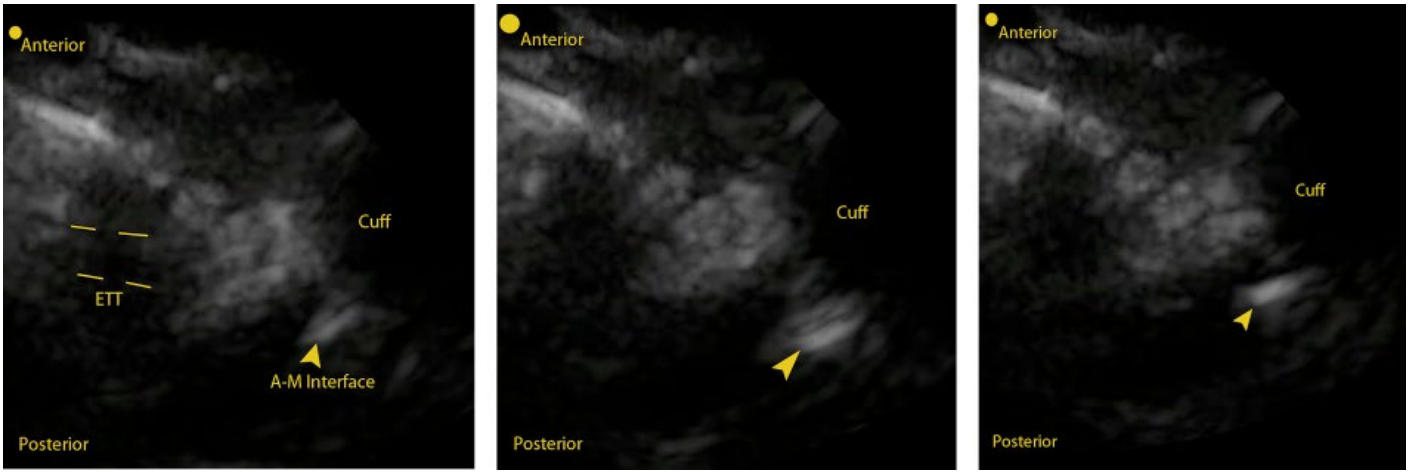

Figure 31.7 In a longitudinal view at the suprasternal notch, oscillation of saline into the cuff displaces the posterior wall of the trachea in sync. This is evidenced here by displacement of the anterior air–mucosal interface (A-M Interface) of the oesophagus in series (left to right).

deflated. For this, the linear transducer is used at the level of the cricothyroid membrane and the vocal cords are visualised in the transverse plane. Using the callipers transversely from vocal cord to vocal cord laterally, a width measurement of the intra-luminal air-column within the ETT is taken with the cuff inflated and then deflated (Figure 31.8). An initial study showed a significant difference in widths of 6.4 mm and 4.5 mm between non-stridorous post-extubation and stridorous post-extubation patients, respectively. Thus, ultrasound can be used as an adjunct to cuff leak in patients where post-extubation stridor is a concern.

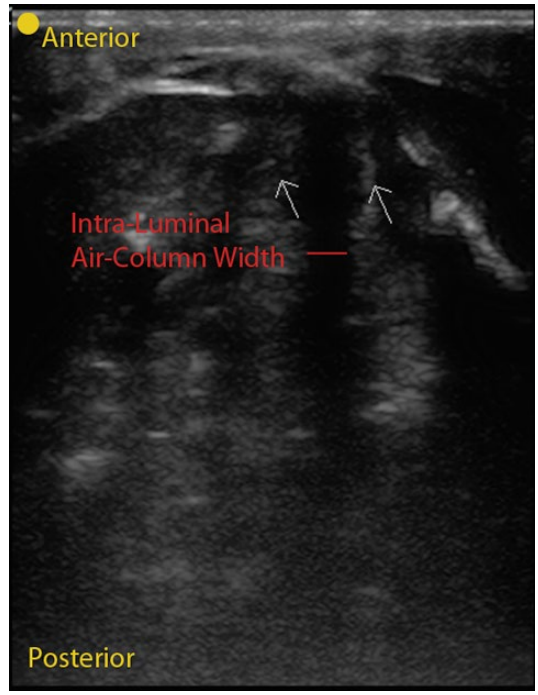

Figure 31.8 Transverse view of the vocal cords in a non-intubated patient, measuring intra-luminal air-column width which can predict post-extubation stridor in an intubated patient.

Alternative Evaluations

As the field of bedside ultrasound continues to expand, further validated studies will confirm other measurements capable of helping to guide clinical assessment. An example is the sublingual view using the micro-convex (8-2 MHz) transducer, which allows the assessment of oropharyngeal and glottis structures (Figure 31.9).

Other areas of visualisation that have expanded from initial airway ultrasound procedures include evaluation of the epiglottis in a patient with a sore throat and muffled voice or stridor.

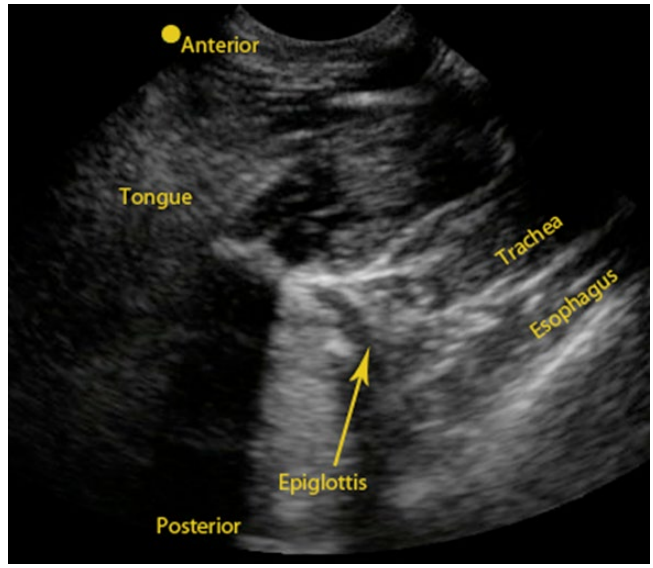

Figure 31.9 The structures of the posterior oropharynx can be visualised using the (8-2 MHz) micro-convex transducer in the longitudinal plane sublingually.

The epiglottis can be measured using bedside ultrasound with the linear transducer in the transverse plane centred on the thyrohyoid membrane (Figure 31.10). Other studies have demonstrated the correlation of epiglottic diameter enlargement in adult patients with acute epiglottitis, as confirmed by indirect laryngoscopy. As the epiglottis is one of the most easily identifiable structures in the upper airway, further research may prove sonography to be a reliable bedside method for evaluating patients with potential acute epiglottitis.

Ultrasound has enhanced the safety of a wide variety of needle-guided procedures by allowing the visualisation of underlying structures. The cricothyroid membrane can be quickly and easily identified with ultrasound in the longitudinal plane using the (10-5 MHz) linear transducer. This is especially helpful in morbidly obese patients when landmarks are difficult to palpate (Figure 31.11).

The limitations of airway ultrasound must be well recognised; extensive subcutaneous emphysema can obscure ultrasound images, or paratracheal masses can distort normal anatomy.

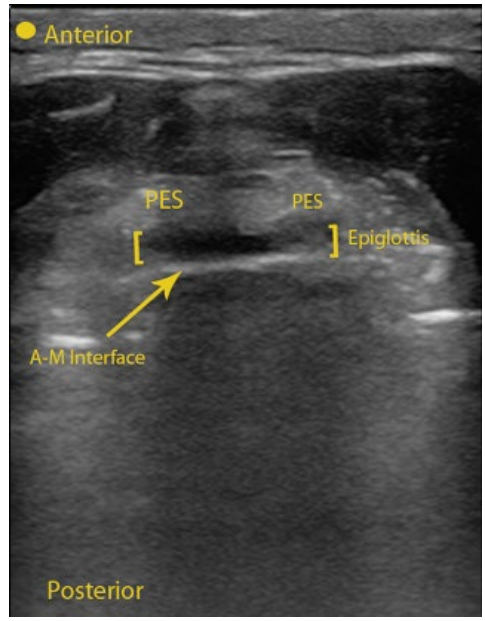

Figure 31.10 In the transverse plane at the thyrohyoid membrane the epiglottis can be viewed non-invasively to rule out epiglottitis by measuring the width of the structure at midline and each end laterally. PES, pre-epiglottic space.

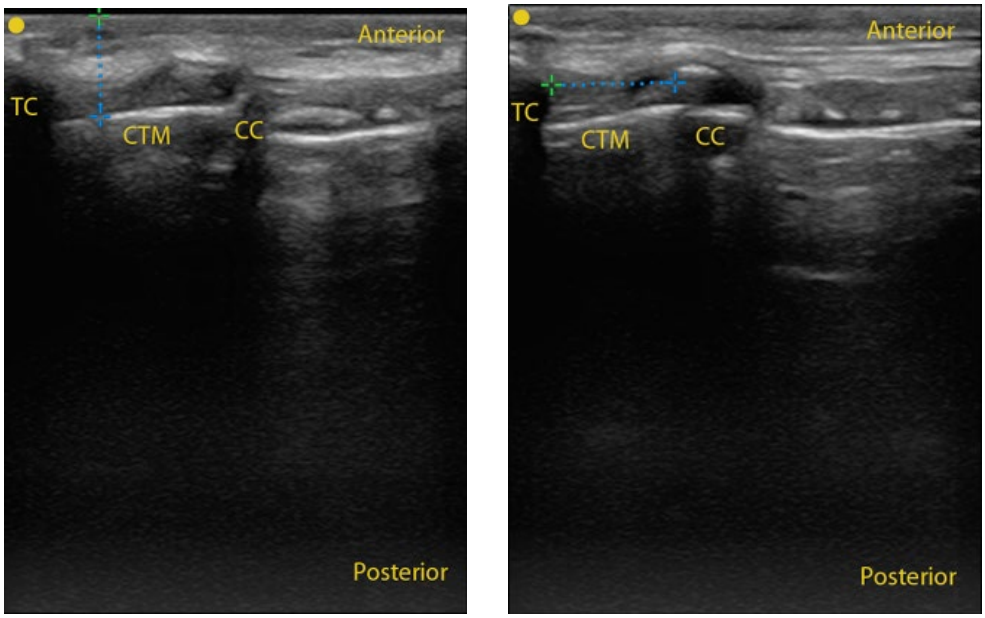

Figure 31.11 A patient's cricothyroid membrane (CTM) can be quickly identified in the longitudinal plane for an emergency surgical airway. The anterior soft-tissue depth can be quickly measured or estimated for cricothyrotomy prior to or in real time using this procedure. TC, thyroid cartilage; CC, cricoid cartilage.

It may also be difficult or even impossible to scan the upper airway of patients who cannot extend their necks.

Further research is required to clarify the role of airway ultrasound in emergency medicine and critical care. However, it seems clear that bedside ultrasound has a role in the assessment of upper airway anatomy, as well as being an adjunct for the confirmation of correct ETT location and depth.

Further Reading

Adhikari, S., Zeger, W., Schmier, C., *et al*. (2011) Pilot study to determine the utility of point-of-care ultrasound in the assessment of difficult laryngoscopy. *Acad. Emerg. Med.*, **18** (7), 754–758.

Bektas, F., Soyuncu, S., Yigit, O., Turhan, M. (2010) Sonographic diagnosis of epiglottal enlargement. *Emerg. Med. J.*, **27** (3), 224–225.

Blaivas, M., Tsung, J.W. (2008) Point-of-care sonographic detection of left endobronchial main stem intubation and obstruction versus endotracheal intubation. *J. Ultrasound Med.*, **27** (5), 785–789.

Chun, R., Kirkpatrick, A.W., Sirois, M., *et al*. (2004) Where's the tube? Evaluation of hand-held ultrasound in confirming endotracheal tube placement. *Prehosp. Disast. Med.*, **19** (4), 366–369.

Ding, L.W., Wang, H.C., Wu, H.D., Chang, C.J., Yang, P.C. (2006) Laryngeal ultrasound: a useful method in predicting post-extubation stridor. A pilot study. *Eur. Respir. Physiol.*, **27** (2), 384–389.

Drescher, M.J., Conard, F.U., Schamban, N.E. (2000) Identification and description of esophageal intubation using ultrasound. *Acad. Emerg. Med.*, **7** (6), 722–725.

Ezri, T., Gewurtz, G., Sessler, D.I., *et al*. (2003) Prediction of difficult laryngoscopy in obese patients by ultrasound quantification of anterior neck soft tissue. *Anaesthesia*, **58** (11), 1111–1114.

Galicinao, J., Bush, A.J., Godambe, S.A. (2007) Use of bedside ultrasonography for endotracheal tube placement in pediatric patients: a feasibility study. *Pediatrics*, **120** (6), 1297–1303.

Hsieh, K.S., Lee, C.L., Lin, C.C., Huang, T.C., Weng, K.P., Lu, W.H. (2004) Secondary confirmation of endotracheal tube position by ultrasound image. *Crit. Care Med.*, **32** (9 Suppl.), S374–S377.

Hung, T.Y., Li, S., Chen, P.S., *et al*. (2011) Bedside ultrasonography as a safe and effective tool to diagnose acute epiglottitis. *Am. J. Emerg. Med.*, **29** (3), 359, e351–e353.

Jain, P. (2008) High-resolution sonography of sublingual space. *J. Med. Imag. Radiat. Oncol.*, **52** (2), 101–108.

Knapp, S., Kofler, J., Stoiser, B., *et al*. (1999) The assessment of four different methods to verify tracheal tube placement in the critical care setting. *Anesth. Analg.*, **88** (4), 766–770.

Komatsu, R., Sengupta, P., Wadhwa, A., *et al*. (2007) Ultrasound quantification of anterior soft tissue thickness fails to predict difficult laryngoscopy in obese patients. *Anaesth. Intensive Care*, **35** (1), 32–37.

Lichtenstein, D.A., Menu, Y. (1995) A bedside ultrasound sign ruling out pneumothorax in the critically ill. Lung sliding. *Chest*, **108** (5), 1345–1348.

Marciniak, B., Fayoux, P., Hebrard, A., Krivosic-Horber, R., Engelhardt, T., Bissonnette, B. (2009) Airway management in children: ultrasonography assessment of tracheal intubation in real time? *Anesth. Analg.*, **108** (2), 461–465.

Raphael, D.T., Conard, F.U., III (1987) Ultrasound confirmation of endotracheal tube placement. *J. Clin. Ultrasound*, **15** (7), 459–462.

Shiga, T., Wajima, Z., Inoue, T., Sakamoto, A. (2005) Predicting difficult intubation in apparently normal patients: a meta-analysis of bedside screening test performance. *Anesthesiology*, **103** (2), 429–437.

Singh, M., Chin, K.J., Chan, V.W., Wong, D.T., Prasad, G.A., Yu, E. (2010) Use of sonography for airway assessment: an observational study. *J. Ultrasound Med.*, **29** (1), 79–85.

Sustic, A. (2007) Role of ultrasound in the airway management of critically ill patients. *Crit. Care Med.*, **35** (5 Suppl.), S173–S177.

Tsui, B.C., Hui, C.M. (2008) Sublingual airway ultrasound imaging. *Can. J. Anaesth.*, **55** (11), 790–791.

Tsui, B.C., Hui, C.M. (2009) Challenges in sublingual airway ultrasound interpretation. *Can. J. Anaesth.*, **56** (5), 393–394.

Vaghadia, H., Jenkins, L.C., Ford, R.W. (1989) Comparison of end-tidal carbon dioxide, oxygen saturation and clinical signs for the detection of oesophageal intubation. *Can. J. Anaesth.*, **36** (5), 560–564.

Weaver, B., Lyon, M., Blaivas, M. (2006) Confirmation of endotracheal tube placement after intubation using the ultrasound sliding lung sign. *Acad. Emerg. Med.*, **13** (3), 239–244.

Part 5

Syndromic Approach

32

Chest Pain and Dyspnea

Lawrence A. Melniker

Introduction

Uncertainty in medical decision-making results from the fact that the clinical phenotype of an illness involves multidimensional interactions of various physiological mechanisms. Difficulty communicating the history of the illness may be exacerbated by patient and clinician differences in expressiveness and understanding. Uncertainty is common throughout the practice of medicine, and causes variability in the clinical process of care and resource utilisation, which is associated with worse outcomes and greater expense.

Patient-centred variability in signs and symptoms is, for the most part, uncontrollable. Conversely, variability in clinician evaluation and assessment of the patient can be controlled and must be limited, when possible. It is in the mitigation of clinical uncertainty and the consequent unnecessary variability in practice that point-of-care sonography may play its most vital role.

Chest pain and *dyspnoea* are among the most common complaints seen in the emergency department, accounting for nearly 20% of all visits. It must be constantly considered whether a chest pain is due to ischaemic heart disease, and/or is a shortness of breath caused by congestive heart failure?

Clinical sonographic protocols for the evaluation of the heart and chest are presented in Chapters 2 to 6 of this textbook. A multi-modal algorithmic approach, inclusive of clinical sonography, in patients with chest pain and/or dyspnoea may reduce diagnostic uncertainty and improve patient outcomes. This is evidenced in the medical literature.

Jones *et al.* studied the diagnostic thinking effectiveness of emergency physicians in the initial evaluation of patients with non-traumatic hypotension. The patient encounters were randomised to either initial physician evaluation inclusive of ultrasound or without ultrasound. The physician's differential diagnosis in rank order of presumed likelihood was then recorded. All patients without ultrasound were then scanned and the physician's differential with rank was recorded again. The aim of this study was to assess whether a goal-directed ultrasound protocol could help clinicians correctly identify the aetiology of non-traumatic hypotension. The addition of an ultrasound-containing evaluation to standard care allowed the clinicians to compile a significantly shorter and more accurate list of possible aetiologies of non-traumatic hypotension. The sonographic information was associated with less clinical uncertainty, as shown by the reduction in size of the differential list and higher rank of the final diagnosis.

Emergency Point-of-Care Ultrasound, Second Edition. Edited by James A. Connolly, Anthony J. Dean, Beatrice Hoffmann and Robert D. Jarman.

Companion website: www.wiley.com/go/connolly/ultrasound

Chest Pain and Acute Coronary Syndrome

In the United States, approximately six million patients present to the emergency department each year for the evaluation of suspected acute coronary syndrome (ACS). Some 70% of chest pain presentations are non-cardiac in origin. Uncertainty in defining the very low-risk subset is high, as are the consequences of incorrect stratification. Past medical and history of present illness has sensitivity under 50% and initial electrocardiogram (ECG) is less than 25% sensitive, though nearly 100% specific. The TIMI (Thrombolysis In Myocardial Infarction) score (a 0–7 Likert scale) includes historical, presentation and ECG characteristics, which are specific but not sufficiently sensitive. Patients with TIMI <3 have composite outcomes (Acute Myocardial Infarction (AMI) and death) of 5–7%.

Consensus guidelines recommend the use of cardiac biomarkers in assessing suspected ACS but, due to their time-dependent nature, baseline measurements have sensitivities under 50% and 2-hour delta measurements are about 70% sensitive. New emerging markers, such as ischaemia-modified albumin (IMA), have a higher sensitivity at the expense of a lower specificity. Recent guidelines recommend a troponin cut-off point that corresponds to the 99th percentile of a healthy population; however, most conventional troponin methods lack sufficient precision at this low level. Commercially available highly sensitive troponin assays have sensitivity for baseline measurements in the range of 70%, with 90% specificity, 50% positive predictive value, and 95% negative predictive value for ACS. Thus, at the initial presentation, the 'Standard Model' of clinical acumen, ECG and biomarkers still yields a clinical uncertainty of 10–20%.

A time-independent assessment of vascular health might enhance the accuracy of the evaluation of patients with suspected ACS. Using ultrasonography, measuring the carotid artery intima-media thickness (IMT) has been performed since the mid-1980s and has become established as a predictor of cardiovascular disease in large longitudinal studies. Recent studies have shown that examining the carotid artery IMT is as good a predictor of the condition of the coronary arteries as examining one coronary artery and predicting the condition of another. Therefore, IMT assessment is an accurate point-of-care test of cardiovascular health. Assessing the patient's vascular health can provide essential information to the evaluating physician attempting to make time-critical diagnostic and treatment decisions.

Therefore, using an algorithmic approach, inclusive of history, ECG, biomarkers and clinical sonography, a patient with a reassuring history – normal ECG, negative highly sensitive troponin I and healthy vasculature – may truly be at very low risk, while a similar patient with a substantially increased IMT may not.

Non-Ischaemia-Related Chest Pain

In addition to ischemic heart disease, causes of chest pain may include pulmonary embolus, disorders of the pericardium, pleura and the chest wall, as well as oesophageal and spinal. A combination of focused cardiac and lung ultrasound can elucidate multiple causes of chest pain.

Pulmonary Embolism

The diagnosis of pulmonary embolism (PE) remains challenging with a high degree of clinical uncertainty and a high probability of death when the diagnosis is missed. PE is the most unexpected mortal event at autopsy, being correctly diagnosed antemortem in 18–39% of cases. Signs and symptoms have been employed in several prediction rules. For example, Well's criteria have yielded sensitivities as high as 94% but are non-specific (45–50%), with interobserver reliabilities of 60–70%. Blood levels of the N-terminal prohormone of brain natriuretic peptide (NT-proBNP) have been studied in patients with suspected PE and had good

predictive accuracy for 30-day all-cause mortality; AUC = 0.85 (95% CI 0.73–0.93). NT-proBNP and troponin T levels correlate with cor pulmonale findings on echocardiography.

The role of focused cardiac and lung ultrasound techniques in diagnosing acute PE has been investigated in severe cases with haemodynamic compromise. Its role in the complete clinical spectrum of patients with suspected PE is less well-defined, however. Studies have assessed the utility of evaluating for PE based on one parameter or a combination of a clinical score, focused cardiac and lung ultrasound, and lower-extremity compression. A multi-modal approach has shown 89% sensitivity and 74% specificity, with a total accuracy of 82%. In patients with massive PE with cor pulmonale, the sensitivity and negative predictive values were 97% and 98%, respectively. Right ventricular dysfunction is an important predictor of outcomes (positive predictive value 55%; negative predictive value 95%), though focused cardiac ultrasound alone was poorly sensitive (approximately 50%), but highly specific (nearly 90%). Thus, the integration of clinical likelihood and ultrasound provides a practical approach to patients with suspected PE, decreases clinical uncertainty, and promotes a rapid implementation of appropriate management.

Focused cardiac ultrasound (FoCUS) is useful in evaluating a variety of pathological conditions affecting the pericardium, especially pericardial effusion. Patient history and physical examination findings of pericardial effusion are insensitive (35–50%) but specific (75–85%), while Beck's triad is a late and specific finding of cardiac tamponade. A physiology of tamponade is detectable by FoCUS revealing right atrial collapse and right ventricular diastolic collapse, and these findings are highly sensitive and specific. The accuracy of FoCUS in diagnosing pericardial effusion is about 90–100%, and of tamponade about 80–90%. False-negative echocardiographic studies may be seen in patients with pulmonary hypertension, and false-positive studies for cardiac tamponade may occur in severe hypovolaemia. Both, M-mode and two-dimensional imaging may be useful in diagnosing pericardial thickening related to restrictive disease.

Clinical signs and symptoms of pleural disease are not reliably present, but are specific. Pneumothorax can be a life-threatening injury and its care requires expeditious and accurate diagnosis and possible intervention. Numerous studies have compared thoracic ultrasound with chest X-radiography (CXR) using computed tomography (CT) scanning as the criterion standard. The sensitivity of thoracic ultrasound is 85–95% and the specificity 90–100%. The sensitivity of CXR is 30–40% and, again, the specificity is 90–100%. The negative predictive value of thoracic ultrasound for pneumothorax is 95–100%, while that of CXR is 75–80%. The 'lung point' sign is pathognomonic for pneumothorax.

Systematic reviews and meta-analyses of thoracic ultrasound for pleural effusion detection have been conducted, and have demonstrated high sensitivity and specificity [means of 93% (95% CI 89–96%) and 96% (95% CI 95–98%), respectively]. Pleural changes (specifically thickening and nodularity) when detected sonographically may also differentiate benign versus malignant effusions.

Various definition and clinical severity schema have been developed for pneumonias of various types (community-acquired, healthcare-associated and ventilator-associated) which range in sensitivities from 45% to 90% and specificities from 15% to 60%. No specific biomarkers are presently in use for pneumonias.

The usefulness of sonography in the diagnosis of pneumonia and bronchopneumonia has been well evidenced, especially in children. Ultrasound has been compared with conventional radiology and, in some studies, with CT. These studies have shown that the infective lung diseases that cause alveolar consolidation present similar, characteristic ultrasound patterns. The diagnostic sensitivity of ultrasound (93–97%) is at least that of conventional CXR (56–77%). In children and young adults, the test characteristics have been shown to be an overall sensitivity of 86% (95% CI 71–94%), specificity

of 89% (95% CI 83–93%), positive likelihood ratio (LR) of 7.8 (95% CI 5.0–12.4) and negative LR of 0.2 (95% CI 0.1–0.4) for diagnosing pneumonia by visualising lung consolidation with sonographic air bronchograms.

Dyspnoea: Congestive Heart Failure (CHF) versus Non-CHF-Related

In the United States, CHF affects over five million people, and over 600 000 new cases are diagnosed each year. Care of heart-failure patients costs over US$ 30 billion annually, including one million hospital admissions and with hospitalisation accounting for over half of the expense. More than 75% of patients admitted to hospital with heart failure arrive through the emergency department. There is currently wide variability in practice regarding hospital admission for patients with decompensated heart failure. Hospital admission rates vary widely across geographical regions, with evidence suggesting that emergency physicians overestimate the probability of short-term death or severe complications for patients with heart failure. Among dyspnoeic patients in the acute-care setting, clinical uncertainty is associated with increased morbidity and mortality, especially in those with heart failure. In addition to heart failure, a number of disorders can cause dyspnoea, including chronic obstructive pulmonary disease (COPD), asthma, pneumonia, sepsis, pulmonary embolism, deconditioning, metabolic acidosis, anxiety and many others. Patients with final diagnoses of asthma, COPD, pneumonia or, in particular, sepsis have a higher than expected mortality if erroneously treated for heart failure. Moreover, delaying the treatment of CHF may increase mortality, delay hospital discharge, and increase treatment costs.

The initial presumptive diagnosis of acute decompensated heart failure often is made based on the patient's history and a physical examination. Unfortunately, history and physical findings are neither sensitive nor specific for the diagnosis of heart failure. Physical examination findings historically attributed to heart failure are often absent in patients with the subsequent diagnosis of CHF. Furthermore, findings often attributed to asthma or COPD exacerbations, such as wheezing, can be found in patients with CHF. No single history or physical finding has been shown to be more accurate than the clinician's overall assessment at differentiating patients with CHF from other causes of dyspnoea. Still, initial clinical judgement is not reliable either, having a good specificity (86%) but lacking adequate sensitivity (61%).

CXR is quick, inexpensive and readily available in most emergency departments. However, one in every five patients admitted from the emergency department with CHF have no signs of congestion on CXR. These patients are more likely to have a diagnosis other than CHF on admission. CXR also has a poor diagnostic performance in identifying other causes of dyspnoea, such as emphysema and pneumonia.

A CT scan of the chest is able to image the pulmonary vasculature and parenchyma as well as other thoracic structures. Numerous studies have demonstrated the clinical utility of CT in correctly identifying PE, pneumonia, COPD, pneumothorax and heart failure, as well as many other clinically significant abnormalities in patients with dyspnoea. Despite its diagnostic accuracy, CT of the chest is of limited utility in the unstable, acutely dyspnoeic patient as it cannot be performed at the bedside and requires an interruption of treatment and monitoring.

Pulmonary function tests (PFTs) have been used for many years for distinguishing dyspnoea of pulmonary origin from that of cardiac origin. However, PFTs often require the patient to be transported out of the emergency department and require he/she to be both cooperative and stable in order for the tests to be completed.

Because no isolated symptom, sign or radiographic finding has a sufficient predictive value in identifying CHF, several scores have been developed for use as screening instruments. The Framingham, Boston, Göteberg, NHANES, Duke, Walma and Georghiade came into use as research screening instruments for the selection of heart-failure patients for therapeutic and

epidemiological studies. Data from history, physical and, in some cases CXR, PFTs and response to therapy, have been incorporated into these scoring systems in an effort to create more useful and reliable instruments in the diagnosis of heart failure. While widely accepted, these diagnostic instruments have failed to show any significant improvement in diagnostic accuracy. Several studies comparing the aforementioned scores with echocardiographic findings and with cardiologists' assessments as 'gold standards' have shown that, although any one of these instruments can have good negative predictive value (over 90% in one study), their positive predictive value is poor (as low as 10% for Göteberg criteria, and at best 88% for Boston criteria), thus limiting their usefulness as clinical diagnostic instruments.

The American Heart Association (AHA) recommends a comprehensive two-dimensional echocardiogram as the single most useful diagnostic test in the evaluation of patients with heart failure. The AHA further recommends that when the aetiology of dyspnoea is in doubt, echocardiography can elucidate the origin of dyspnoea by documenting or ruling out the common causes of pulmonary congestion, whether left-sided valvular disease, depressed systolic function or diastolic dysfunction, as well as various cardiomyopathies. Emergency physicians with training in FoCUS can accurately determine left ventricular systolic function by differentiating poor, moderate and normal ejection fractions with high levels of agreement. While FoCUS can be a useful adjunct in the evaluation of patients with dyspnoea, it has its limitations. Patients with dyspnoea due to heart failure may be misidentified, as the combination of heart failure and normal systolic function is more common than was once generally appreciated. Isolated diastolic dysfunction is not easily identified by non-invasive assessment. In one study of outpatients with symptoms of breathlessness suspected of cardiac origin, 18% had a profile consistent with isolated diastolic dysfunction. Furthermore, dyspnoeic patients with a history of chronic heart failure may have an abnormal systolic function at baseline, and without a prior study available for comparison may be misdiagnosed with CHF where another aetiology is the cause of their symptoms.

BNP and NT-proBNP measurements specifically have been shown to be useful in differentiating dyspnoea due to heart failure from dyspnoea due to lung disease, with a negative predictive value for CHF of 99% using the cut-off NT-proBNP level of $80\,pg\,ml^{-1}$. BNP and NT-proBNP also appear to be useful in uncovering new-onset heart failure in patients with a history of pulmonary disease (asthma or COPD). BNP and NT-proBNP levels detect more patients with new-onset heart failure than clinical suspicion alone. High clinical suspicion detected only 37% of patients with heart failure compared to 93% by BNP, while high clinical suspicion detected only 23% of patients with new-onset heart failure. Among these patients 82% had elevated NT-proBNP levels.

Relying on BNP or NT-proBNP alone also has its limitations. BNP levels in patients with a history of heart failure, but with non-cardiac aetiologies of dyspnoea, overlap with those seen in patients with acute decompensated heart failure with a positive predictive value of the BNP assay alone being only 79% and its accuracy rate 83%. In the case of NT-proBNP, using the age-specific cut-offs of $450\,pg\,ml^{-1}$ in patients aged <50 years and $900\,pg\,ml^{-1}$ in patients aged >50 years, the positive predictive value is at best 77% and accuracy only 85% for patients aged >50 years. An elevated body mass index can negatively affect the negative predictive value of both assays. Overweight and obese patients with CHF have lower circulating NT-proBNP and BNP levels, thus limiting the sensitivity of these assays in this population.

Lung ultrasonography is useful in the detection of pulmonary interstitial fluid. Indeed, studies comparing ultrasound to pulmonary capillary wedge pressure (PCWP) found that lung ultrasound has good sensitivity and specificity (90% and 86%, respectively) in detecting extravascular lung volume at levels where CXR often shows no findings suggestive of pulmonary oedema.

Ultrasound detection of interstitial fluid does not necessarily imply a cardiogenic origin, as pneumonia, adult respiratory distress syndrome and chronic interstitial lung disease can produce comet-tail images. However, preliminary research in cardiology patients has shown some clinically significant correlations between abnormalities on lung ultrasonography and heart failure, with the number of comet-tail artefacts correlated to PCWP and extravascular lung water.

Clinical judgement alone often misidentifies the aetiology of dyspnoea, and emergency physicians often rely on additional diagnostic tools to increase the accuracy of diagnosis. CXR and BNP measurements have added diagnostic value to the initial clinical assessment. However, the measurement of BNP and NT-proBNP cannot be useful if it is not available before therapeutic interventions are instituted, and these assays are still unavailable as point-of-care tests in most emergency departments. While CXR is readily available at most institutions, the diagnostic value of portable films is limited. It is not always possible – nor feasible – to promptly evaluate the dyspnoeic patient with more sophisticated testing such as PFTs and CT scanning.

A clinical assessment, which includes ultrasonography of the heart to determine left ventricular function, and of the lungs to seek evidence of interstitial fluid, may serve as a useful diagnostic strategy in differentiating patients with CHF from those with dyspnoea of another cause.

Further Reading

Jones, A.E., Tayal, V.S., Sullivan, D.M., Kline, J.A. (2004) Randomized, controlled trial of immediate versus delayed goal-directed ultrasound to identify the cause of non-traumatic hypotension in emergency department patients. *Crit. Care Med.*, **32** (8), 1703–1708.

33

Bedside Ultrasound as an Adjunct in the Evaluation and Management of Critically Ill Patients

Anthony J. Dean and Sarah A. Stahmer

Introduction

Critically ill patients are often unable to provide a clear history, the utility of the physical examination is limited by the patient's ability to cooperate, and the temporal and logistic impediments of diagnostic testing necessitate a limited, time-sensitive approach. In cardiopulmonary arrest (CPA) – the final, pre-mortal phase of respiratory and circulatory instability – evaluation is further telescoped and proceeds concomitantly with treatment according to the time-honoured priorities of 'Airway, Breathing, Circulation'. With such critically ill patients, ultrasonography – which can identify many common causes of undifferentiated respiratory or circulatory compromise – can be applied to evaluate response to therapy and can deployed at the bedside within seconds is obviously of great value. Continual technological improvements in ultrasound have given rise to higher-resolution images on more affordable, mobile and user-friendly equipment. A growing body of literature supports the use of bedside ultrasound in the management of the critically ill by intensivists, emergency physicians and paramedics, as well as care-providers in military, austere environment and natural-disaster settings. In this chapter, a brief integrated review will be provided of the sonographic approach to the critically ill. To avoid redundancy, the reader is referred to the relevant chapters elsewhere in this text to review specific techniques.

The regions to be assessed in the sonographic evaluation of the critically ill are listed in Table 33.1, while common findings by organ system, and their significance, are listed in Table 33.2. As with any diagnostic test, ultrasound findings will be interpreted in the context of the overall clinical picture. With limited clinical clues, a methodical sequential approach is advisable, and a variety of protocols have been proposed (see References and Chapter 34). More commonly, there are some clinical data to direct the sonographic evaluation. For example, a patient who had complained of abdominal pain prior to a syncopal event might have the aorta and peritoneal spaces examined first. Conversely, a patient with a history of cancer and distended neck veins should probably be first evaluated for cardiac tamponade and pulmonary embolus. The present discussion will focus on the way that evaluation of individual organs or regions are combined with the management of syndromes of critical illness, namely airway, shock, dyspnoea and cardiopulmonary arrest.

'ABC: Airway …'

A detailed discussion of the role of ultrasound in airway management is found in Chapter 31. Occasionally, ultrasound can be rapidly deployed to confirm the location of an endotracheal tube

Emergency Point-of-Care Ultrasound, Second Edition. Edited by James A. Connolly, Anthony J. Dean, Beatrice Hoffmann and Robert D. Jarman.

Companion website: www.wiley.com/go/connolly/ultrasound

Table 33.1 Body regions to be investigated and sonographic findings to be sought by ultrasonography in the evaluation of the critically ill.

Ultrasonography of the thorax
Evaluation of the pericardium (Current chapter)
Effusion ± tamponade
Evaluation of the heart (Current chapter and Chapters 5, 6, 35, 36)
Empty hyperdynamic heart
Global wall motion abnormalities
Focal wall motion abnormalities [#]
Sonographic findings of pulmonary embolus [#]
Sonographic findings of right-sided myocardial infarction[#]
Gross dynamic or structural abnormalities of the heart valves[#]
Evaluation of the proximal and descending aorta (Chapter 3)
Intimal flap[#]
Thoracic aneurysm[#]
Evaluation of the lungs and pleural spaces (Chapter 2)
Sonographic findings of pneumothorax
Sonographic findings of tension pneumothorax
Massive pleural effusion
Massive pulmonary consolidation
Pulmonary oedema
Ultrasonography of the abdomen
Inferior vena cava[*] (Chapter 10)
Evaluation of size, collapse index
Identification of intraluminal clot or other obstruction
Evaluation of the abdominal aorta (Chapter 7)
Abdominal aortic aneurysm
Intimal flap, pseudolumen
Evaluation of the peritoneal cavity (Chapter 8)
Free fluid
Sonographic findings of pneumoperitoneum[#]
Lower-extremity limited compression ultrasonography (see Chapter 18)

[#] Conditions which can be identified, but cannot be reliably excluded with EMBU.
[*] The IVC is usually examined in the subxiphoid window concurrently with the evaluation of the thorax.
EMBU, Emergency Medicine Bedside Ultrasonography.

that is suspected of having been dislodged or misplaced in the oesophagus (Figure 33.1). An evaluation of the symmetry of lung sliding in a patient on positive-pressure ventilation can also be used to exclude right main stem bronchus intubation.

Intravascular Volume Assessment

The first goal in addressing the circulatory needs of the patient in shock is directed to optimising intravascular volume. This is most rapidly and non-invasively performed at the bedside with inferior vena cava (IVC) assessment (see Chapter 10). A collapsed IVC is almost always associated with a small hyperdynamic, tachycardic heart. The cause of severe hypovolaemia is usually clear on clinical grounds, although occasionally a case of unheralded intraperitoneal haemorrhage is revealed by ultrasound, often with a pelvic source in women of childbearing age. When searching for free fluid in the pleural and peritoneal spaces, a systematic approach should be used analogous to that of the Focussed Assessment by Sonography in Trauma examination (see Table 33.3 and Chapter 8).

A plethoric, non-collapsing IVC can have many causes, the most common being one or more of volume overload, renal failure or heart failure.

The diagnosis of heart failure can be correlated with cardiac findings (see discussion below). In patients with unheralded renal failure, an ultrasound examination of the kidneys (see Chapter 15) is indicated to exclude bilateral obstruction. The unexpected discovery of bilateral hydronephrosis is made not uncommonly, especially in patients with a history of malignancy.

While a patient in shock who is found to have a flat or underfilled IVC is almost always hypovolaemic, the converse is often not the case. Hypotensive patients with an apparently well-filled IVC may still benefit from additional volume resuscitation. A variety of tests have been investigated to identify 'fluid-responsive shock', several of which use ultrasound. The most reliable and widely accepted is the assessment of cardiac output (CO) before and after a fluid bolus or a passive straight-leg raise test. The basic technique involves obtaining a Doppler waveform of blood flow at the aortic or the pulmonic valve (accessed via the apical four-chamber or high parasternal short-axis windows, respectively). The tracing of the Doppler waveform

Table 33.2 Clinical significance of various sonographic findings in the assessment of severe dyspnoea, hypotension, and during cardiopulmonary resuscitation.

Organ of interest and sonographic finding	Clinical significance
Heart and mediastinum	
Pericardial effusion ± right atrial or ventricular collapse during diastole	Pericardial effusion ± tamponade. Consider acute ventricular rupture, aortic dissection
Small hyperdynamic heart, end-systolic ventricular collapse, LVEF >75%	Intravascular hypovolaemia.
Well-filled hyperdynamic heart	Peripheral vasodilation: consider sepsis, anaphylaxis, vasodilators, severe anaemia
Small heart with normal LVEF and thick ventricles	Consider diastolic dysfunction
Large heart with thinned walls, very low EF	End-stage dilated cardiomyopathy
Dilated RV, ± paradoxical septal motion, ± RV hypokinesis, ± intracardiac thrombus, IVC dilation, McConnell's sign, TR, acute PA hypertension (TR jet velocity >2 m s^{-1} with dilated IVC or >2.5 m s^{-1} with normal/underfilled IVC)	Haemodynamically significant pulmonary embolus. [RV infarct very similar but no TR, no ultrasound signs of acute pulmonary hypertension].
Focal wall motion abnormalities	Acute coronary syndrome
Difficulty identifying the heart on all views	Consider tension pneumothorax
Marked displacement of heart in subxiphoid view to left or right	Right or left tension pneumothorax (respectively)
Intimal flap in aortic arch (high PSLA or suprasternal views) or descending aorta (PSLA view)	Aortic dissection
Gross dynamic or structural abnormalities of the heart valves	Papillary muscle rupture, endocarditis
Decrease or absence of myocardial wall motion; absence of valve closure or of valve motion; presence of intracardiac gel-like densities.	Each represents progressive cardiac dysfunction in PEA. Consider ischaemic, toxic, metabolic causes.
Abdomen	
Intraperitoneal free fluid	Haemoperitoneum versus ascites
Aorta for AAA and intimal flap	Acute AAA, aortic dissection
Slit-like IVC or respiratory IVC collapse of >75%	Intravascular hypovolaemia
IVC distended; absence of normal respiratory variation	Consider volume overload, CHF (right and/or left), pulmonary embolus, acute RV infarct
Absence of normal sliding of parietal-visceral peritoneum interface, linear reverberation artefacts	Pneumoperitoneum
Pleural spaces and lung	
Pleural free fluid ± internal echodensities	Pleural effusion; if internal echodensities: consider empyema versus clotted blood
Absence of 'pleural sliding' sign	Pneumothorax
Multiple B-lines	Increased extravascular lung water. Common causes include CHF, ARDS, interstitial pneumonitis, etc.

(Continued)

Table 33.2 (Continued)

Organ of interest and sonographic finding	Clinical significance
'Hepatisation' of lung	Pulmonary consolidation (pneumonia, atelectasis, contusion, tumour, etc)
Lower extremities	
Non-compressible common femoral and or popliteal veins	DVT

Abbreviations: AAA, abdominal aortic aneurysm; ARDS, adult respiratory distress syndrome; CHF, congestive heart failure; DVT, deep venous thrombosis; LVEF, left ventricular ejection fraction; IVC, inferior vena cava; PEA, pulseless electrical activity; PSLA, parasternal long axis; RV, right ventricle; TR, tricuspid regurgitation.

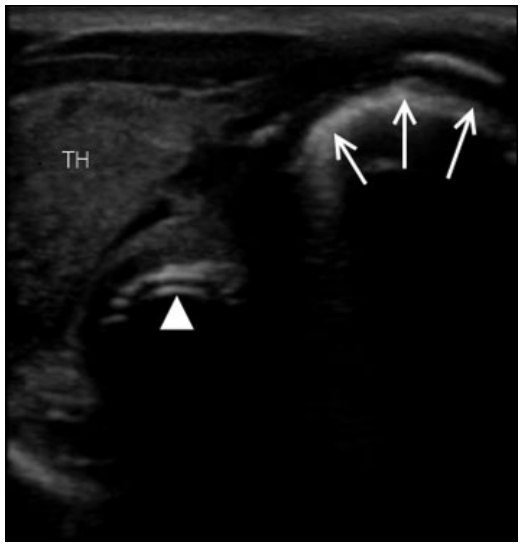

Figure 33.1 Transverse view of the neck at the level of the right thyroid (TH) shows the shadowing mass of the trachea (arrows). On the patient's right, there is a second shadowing mass due to a misplaced endotracheal tube (ETT). The apex of the arrowhead indicates the inner wall of the ETT. The anterior wall may also generate reverberation artefact identifiable in both the oesophagus and in the trachea (with correct placement). Image reproduced with permission; © Beatrice Hoffmann.

Table 33.3 Regions and potential spaces to be evaluated in the search for pathological fluid collections.

Right costal and subcostal region, midclavicular to posterior axillary line (from superior to inferior)
- Pleural space
- Subphrenic space
- Morison's pouch
- Right colic gutter/inferior pole of right kidney

Subxiphoid
- Pericardial space

Left costal and subcostal region, midclavicular to posterior axillary line (from superior to inferior)
- Left pleural space
- Subphrenic space
- Splenorenal space
- Left colic gutter/inferior pole of left kidney

Suprapubic
- Pouch of Douglas/rectouterine space

allows for a calculation of the velocity-time integral (VTI) of the systolic flow across the valve in a single cardiac cycle. The unit of the VTI value is centimetres. The resulting 'aortic distance' (or 'pulmonic distance') represents the 'length' of a conceptual cylinder of blood that is ejected through the orifice of the valve during a single cardiac contraction. The stroke volume (SV) can then be calculated by multiplying this 'distance' by the cross-sectional area of the valve. Rather than expending the time to attempt to measure the diameter or area of the valve (which has been shown to be inherently inaccurate with significant inter- and intra-observer variability), these values can be more reliably obtained from the Nidorf nomograms (see references), which show the valvular area to be tightly correlated with height (typically an easily obtainable piece of patient information). For ease of calculation,

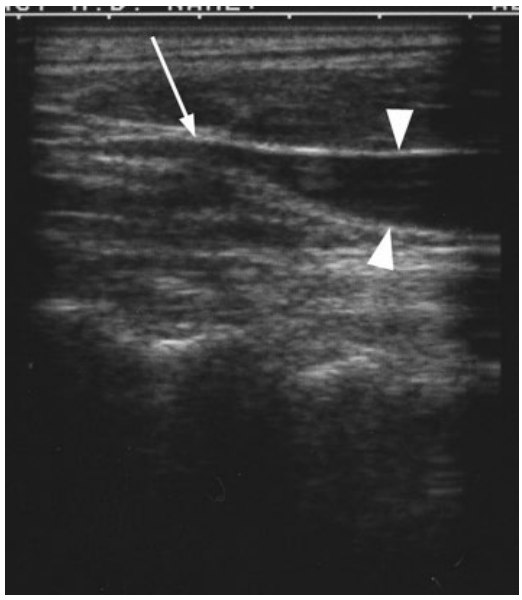

Figure 33.2 In a longitudinal view, the fluid column of blood within the internal jugular vein (between arrowheads) tapers to a point. The highest apex of the fluid column (arrow, end expiration) should be marked. Measurements may be more accurate scanning in a transverse plane. See text for method of computation of right atrial pressure.

an approximate median valve area is 3 cm^2 (range: 2 to 4.5 cm^2). Multiplying the SV by the heart rate gives the CO. Of note, the VTI can be substituted for the CO in this assessment if the heart rate does not change, because all other variables are constant. A more detailed discussion of the measurement of cardiac output and its clinical utility is available in Chapter 36.

Because the use of Doppler is beyond the skills and training of many point-of-care sonologists, a range of parameters have been sought as surrogates for aortic/pulmonic VTI. These include carotid blood flow, systolic velocity variation and systolic flow time. Measurements have been made in the aorta, carotid or radial arteries. Detailed discussion of these parameters is beyond the scope of this chapter because they continue to be actively investigated with debate about their applicability in various settings, and their validity.

Sonographic assessment of the internal jugular vein (IJ) can also be used to estimate right atrial pressure. This may be easier than a physical examination in patients with thick necks and/or a high body-mass index. Using a linear array probe in a longitudinal plane, the IJ is identified and the patient is elevated to the point at which the vein can be seen tapering to a point of collapse in the neck (see Figure 33.2). At this point, the vein tapers in a cephalad direction. The superior extent of the jugular venous column will be seen to undulate with respirations and cardiac contraction. The examiner should maintain light contact with the skin or the vein will collapse artefactually. The vertical height from the point of complete collapse to the sternal angle of Louis is added to 5 cm for a measure of central venous pressure (CVP). If the vein is not distended with the patient supine, the CVP is extremely low.

Sonographic Evaluation of the Heart

Pericardial Effusion and Tamponade

Common causes of non-traumatic pericardial effusions include neoplastic, uraemic, infectious and inflammatory processes. They can also develop ideopathically. Echocardiographers have proposed various classifications of pericardial effusions. For the most part these are of little value to a care provider presented with a patient in shock, since rapidly forming pericardial effusions can cause tamponade with circumferential effusions of 5 mm (documented with as little as 80 ml of fluid), especially in patients dependent on high filling pressures (Video 33.1). False-positive diagnoses of pericardial effusions have been caused by misidentification of epicardial fat, pleural effusions and vessels posterior to the heart (e.g., descending aorta, pulmonary vessels or coronary sinus). Epicardial fat is usually non-circumferential, moves with the underlying myocardium, has an irregular 'lumpy' outline, tends to lie in the interventricular and interatrial groves, and with well-adjusted gain demonstrates internal echoes (see Videos 33.2 and 33.5). In contrast to effusions, epicardial fat usually becomes thinner

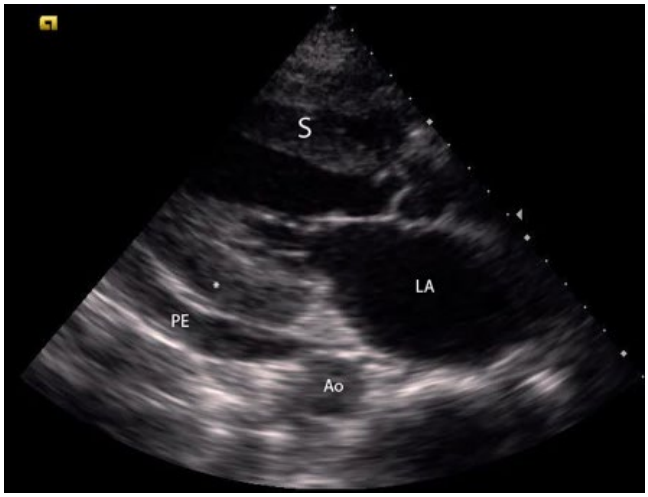

Figure 33.3 Parasternal long axis view showing a pericardial effusion (PE) characteristically tapering anterior to the descending aorta (Ao). Image from Video 33.3. S, septum; LA, left atrium; *, left ventricular free wall.

towards the apex. In distinction to pleural effusions, pericardial fluid conforms to the shape of the pericardial sac and, in the parasternal axis view, can be seen tracking anterior to the descending aorta (see Figure 33.3 and Video 33.3). It should be noted that Beck's triad is a late finding., With ultrasound it should be possible to diagnose tamponade prior to the onset of hypotension. Right ventricular diastolic collapse is the most sensitive and specific sign, although false positives (most commonly resulting from severe hypovolaemia) and false negatives (most commonly due to pulmonary hypertension, but also atrial septal defect and aortic insufficiency) examinations can occur (Figure 33.4 and Video 33.4). Right atrial collapse is more sensitive, but less specific because it can also be caused by hypovolaemia and acute obstructive airway disease (exaggerated fluctuations of inspiratory and expiratory intrathoracic pressures). The larger the proportion of the cardiac cycle in which atrial collapse occurs, the more likely it is due to increased intrapericardial pressure. Conversely, it is most likely to be due to other factors when seen transiently, especially at the beginning of diastole. It should be noted that the normal atrium *contracts* (diminishing size with *convex* walls). This should be distinguished from *collapse*, which involves a period of actual *concavity* of the atrial wall (see Videos 33.5 and 33.6). Except in cases of severe hypovolaemia, the absence of a plethoric IVC effectively makes tamponade extremely unlikely.

If tamponade occurs in the setting of chest pain, consideration should be given to aortic dissection or ventricular free wall rupture. The distinction between these may be difficult on clinical, electrocardiographic or sonographic grounds. If proximal dissection is suspected, the aortic arch should be evaluated via high parasternal or sternal notch views (Figure 33.5), which can identify a flap in up to 80% of cases in the hands of experts. Since a great deal rides on the identification of proximal dissection, the descending aorta should also be checked, as this would effectively rule in the disease in the setting of appropriate thoracic symptoms (see Figure 33.6 and Video 33.7). Positional pleuritic chest pain, repetitive unprovoked vomiting and restlessness or agitation are suggestive of ventricular free wall rupture, which may occasionally be seen sonographically. In either case, a cardiothoracic surgeon will be urgently needed.

Shock States due to Cardiac Dysfunction

In the absence of findings of intravascular volume depletion or tamponade, the echocardiographic evaluation continues with a qualitative assessment of the cardiac chambers and cardiac wall motion. The amount and quality of information available from this evaluation will depend on the skills and experience of the

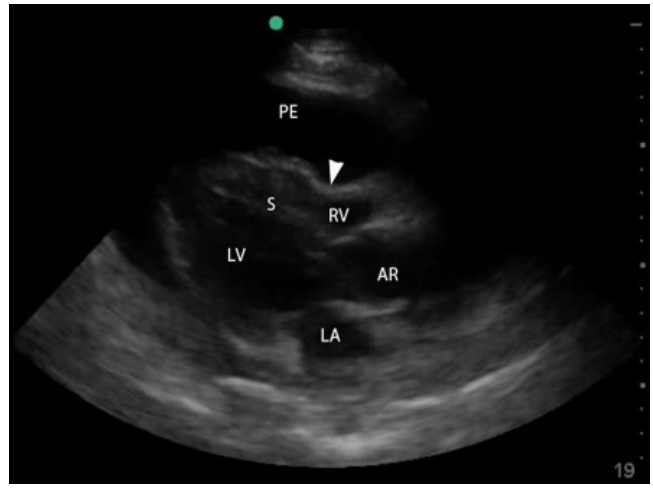

Figure 33.4 Parasternal long axis view demonstrating tamponade with right ventricular (RV) collapse (arrowhead). Image from Video 33.4. AR, aortic root; LA, left atrium; LV, left ventricle; PE, pericardial effusion; S, septum.

sonologist. The following discussion focuses on key elements of the examination that are more commonly encountered and most likely to be rapidly identifiable. A systematic approach involving a more extensive examination is the Focussed Assessment by Transthoracic Echocardiography (FATE) protocol (as discussed in Chapter 35). The utility of this protocol is recognised by the British Intensive Care Society, which makes it the basis of its certificate programme for competency in basic cardiac ultrasound.

A well-filled heart and IVC that are hyperdynamic suggest distributive shock due to sepsis, anaphylaxis or vasodilator toxicity. A large heart with global hypokinesis can be the result of end-stage dilated cardiomyopathy, or have a more immediate cause from acute ischaemic, metabolic, septic or toxicological insults [see the discussion of pulseless electrical activity (PEA) below] (Figure 33.7; Video 33.8a and b). The assessment of focal wall motion abnormalities is beyond the purview of all but experienced echocardiologists. However, derangements of myocardial function sufficient to cause haemodynamic compromise are readily identifiable, and numerous studies have shown that visual estimates are as accurate as more arcane and time-consuming measurements in assessing left ventricular ejection fraction (LVEF).

An examination showing severely depressed myocardial contractility will mandate caution in the administration of fluids, and may prompt a consideration of diuresis if the heart is severely dilated, as well as the initiation of inotropic therapy, early percutaneous transluminal angioplasty and/or intra-aortic balloon pump. Conversely, the demonstration of mildly depressed, normal or hyperdynamic cardiac function excludes acute myocardial dysfunction as a primary cause of hypotension, and usually indicates an acute and unrelated process such as sepsis or dehydration (see Video 33.9a and b). Absence of clinically significant heart failure can also be confirmed by a B-line evaluation of the lungs (see Chapter 2). Few or absent B-lines make significant left ventricular failure and/or impaired gas exchange very unlikely causes of a patient's circulatory and/or respiratory embarrassment.

Diastolic dysfunction (defined as, and often referred to as 'heart failure with preserved systolic function') is very common. In many series, diastolic dysfunction is responsible for more than 50% of cases of heart failure, and it also contributes to the symptoms of many patients with systolic failure. It behoves the bedside sonologist to be able to recognise some basic sonographic findings of this disease because its pharmacological management is fundamentally different from that of heart failure due to dilated

(a)

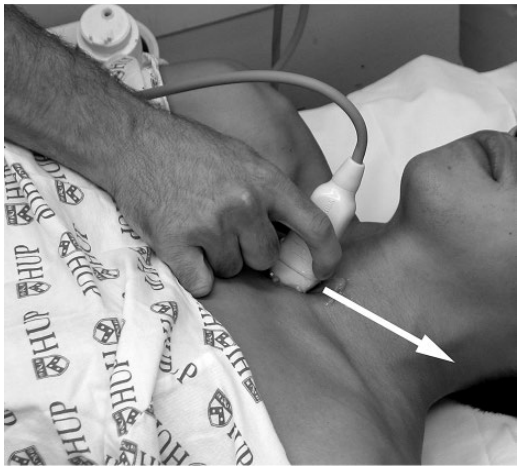

(b)

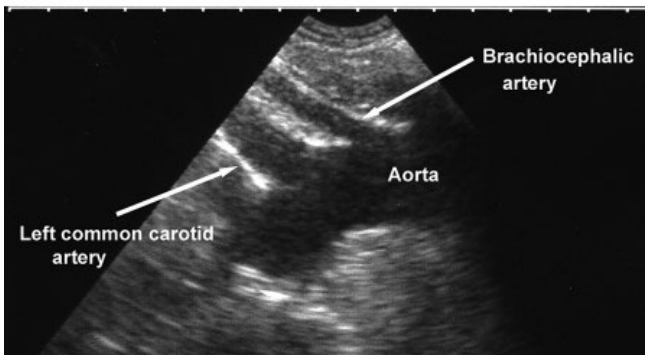

Figure 33.5 (a) Probe positioning for suprasternal views of the aortic arch. The arrow indicates the direction of the probe 'pointer' approximately 30° clockwise from the sagittal plane. The patient should be positioned with as much neck extension as possible (a bolster under the shoulders may help). Ideally, a small-footprint probe is used. (b) The suprasternal image. The aortic root is on the right of the image, the arch (obscured) would be on the left.

cardiomyopathy and/or systolic failure. The typical scenario is a patient with acute heart failure whose ultrasound reveals a relatively normal-sized heart with a normal or high LVEF. The left ventricular wall thickness (LVWT; normal range 7–13 mm measured in diastole) is increased, and the left ventricular end-diastolic ventricular diameter (LVEDD; normal range 40–60 mm) is decreased (see Figure 33.8 and Video 33.10). Both of these measures are correlated with habitus and gender (small habitus and women have lower ranges). While it is impracticable to memorise nomograms of these relationships, it is useful to bear them in mind when interpreting these measurements. Thus, a 45-kg patient with a LVWT of 11 mm and a 100-kg patient with a LVEDD of 45 mm would both be justifiably suspected of diastolic dysfunction. Clinically, patients with systolic heart failure may describe days or weeks of slow progressive decompensation, whereas those with acute diastolic failure tend to present with an unheralded and precipitous onset of symptoms from a stable baseline. Any stress can lead to relative myocardial ischaemia, which is the final common pathway of acute luseotropic dysfunction. Chronic hypertension and metabolic syndrome/diabetes are significant risk

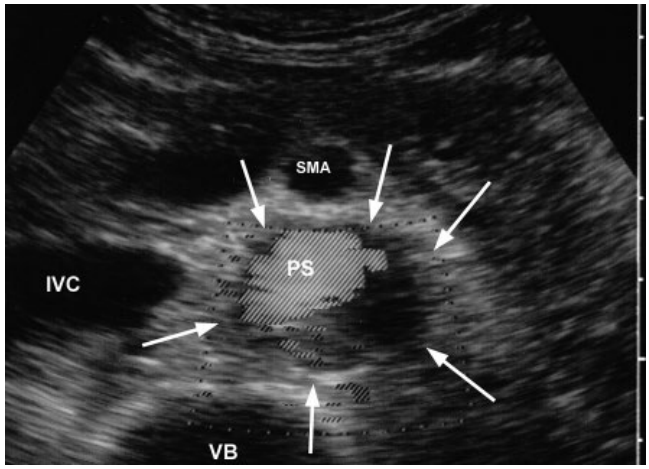

Figure 33.6 Colour-flow Doppler image of a transverse view of the aorta (arrows) at the level of the superior mesenteric artery (SMA) reveals the aorta with flow limited to only a half of the vessel, most likely the pseudolumen (PS). In many cases, flow continues on both sides of the flap, which with optimal gain settings appears as a fluttering membrane (as demonstrated in Video 33.7). In the setting of characteristic chest pain, dissection of the abdominal aorta (see Video 33.7) is presumptive evidence of a type A dissection. As is typical in dissection, this aorta is *not* aneurysmal (see 1-cm hatch-marks on right of image). IVC, inferior vena cava; VB, vertebral body.

Figure 33.7 A case of dilated cardiomyopathy with a very enlarged left ventricular end-diastolic diameter (84 mm), and effacement of the ventricular walls. This image is from Video 33.8b.

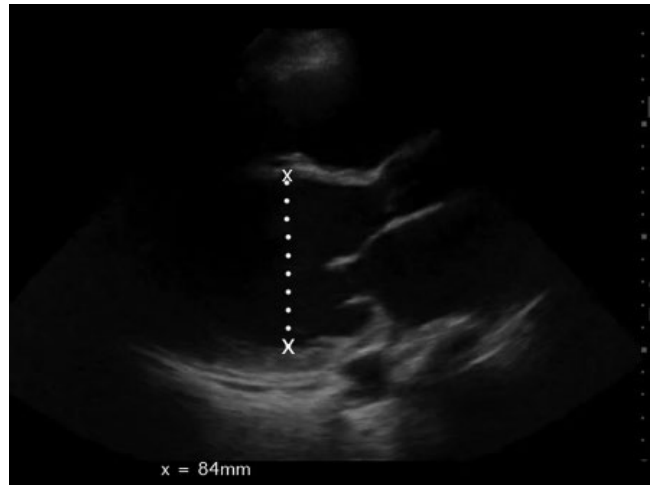

factors. The sonographic findings of diastolic heart failure can be confirmed with Doppler assessment of mitral valve inflow velocity and tissue Doppler assessment of septal motion and/or annular plane systolic excursion measurements, all of which are beyond the scope of this chapter.

Right Ventricular Abnormalities and Pulmonary Embolus (PE)

In contrast to small or moderate-sized pulmonary emboli, those sufficient to cause haemodynamic instability result in gross, readily identifiable echocardiographic abnormalities (see Table 33.4). The first parameter to be

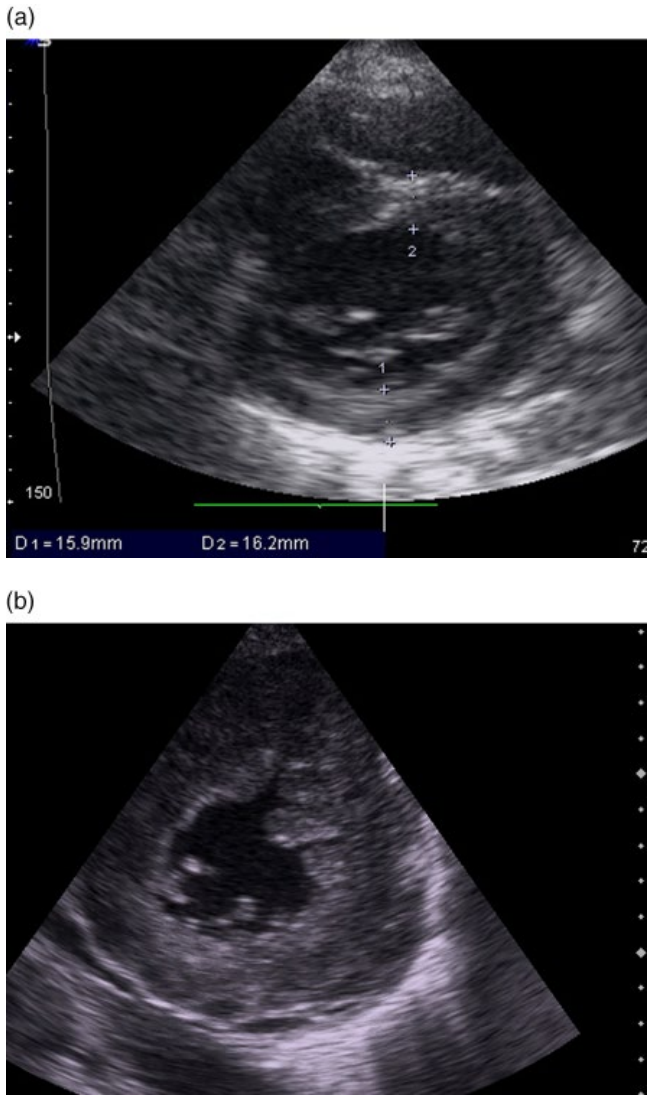

Figure 33.8 (a,b) Parasternal short-axis views of severely hypertrophied ventricles in diastole. While calliper measurements have not been made in panel (b), the 1 cm hash-marks on the right of the image demonstrate an increased wall thickness of about 30 mm and a severely diminished end-diastolic diameter of about the same. A small pericardial effusion is present in panel (b).

assessed is the right-to-left ventricular ratio, usually estimated at end-diastole at the level of the tips of the tricuspid and mitral leaflet tips. This is normally <60%, but in patients with acute PE the ratio is almost always >100%. Chronic pulmonary hypertension also causes right ventricular dilation, but will be accompanied by a thickened (≥7 mm) ventricular wall, whereas in PE the right ventricular wall is effaced (<5 mm) (Figures 33.9–33.11; see Videos 33.11–33.13). Paradoxical septal motion is abnormal septal wall motion *towards* the right

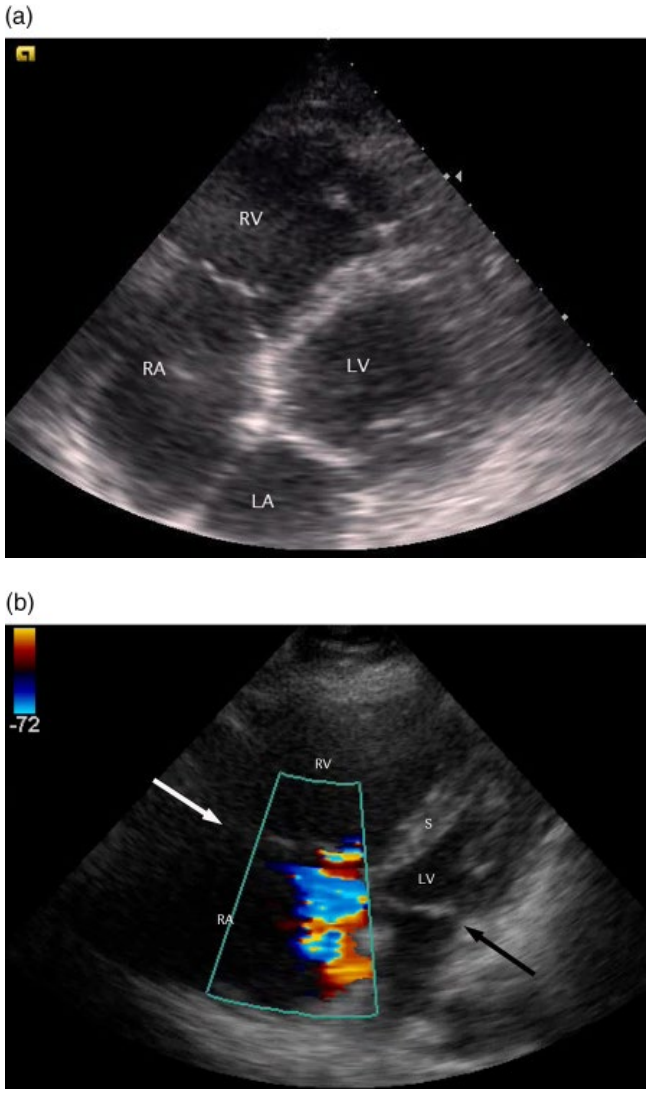

Figure 33.9 (a) Four-chamber view with the abnormally dilated right ventricle (RV) larger than the left (LV). There is also significant right atrial (RA) dilation suggestive of tricuspid regurgitation and/or elevated right central venous pressure. (b) Regurgitation is confirmed, with the white arrow indicating the location of the poorly visualised tricuspid valve and the black arrow indicating the mitral valve. Image taken from Video 33.11. S, septum.

ventricle in systole, and *away from* the right ventricle in diastole. It too can be seen with both acute and chronic pulmonary hypertension (Figure 33.11; Videos 33.12 and 33.13). It occurs when the diastolic pressure of the right ventricle exceeds that of the left ventricle. It can occur as a result of right-sided congestion or left-sided underfilling, or a combination of the two. Other findings associated with acute haemodynamically significant PE include septal flattening (also described as a 'D'-shaped left ventricle) and McConnell's sign (Videos 33.11 and 33.12).

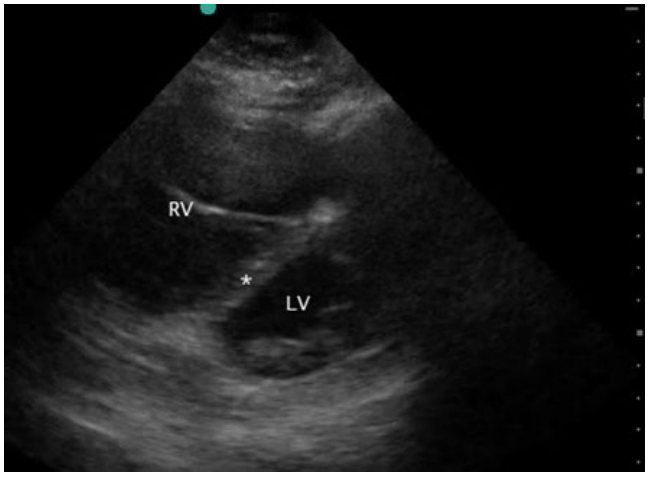

Figure 33.10 Short-axis view with a compressed 'D'-shaped left ventricle (LV), with a flattened septum (*) and significantly dilated right ventricle (RV). The transverse linear structure under the letters 'RV' is a leaflet of the open tricuspid valve, also seen intermittently in diastole in Video 33.12.

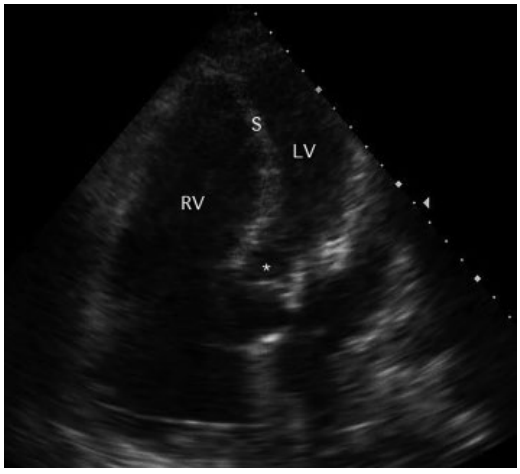

Figure 33.11 Dilated right ventricle (RV), underfilled left ventricle (LV), and significantly bowing of the septum suggesting elevated right ventricular pressure. While possible with acute pulmonary embolus, this degree of RV dominance is usually seen with chronic pulmonary hypertension and longstanding progressive RV hypertrophy. See Video 33.13. *, aortic outflow tract.

The latter is the finding of right ventricular free wall hypokinesis combined with apical sparing. Right ventricular infarct and PE may cause similar clinical, haemodynamic and sonographic findings. If the distinction cannot be made electrocardiographically, Doppler assessment of the tricuspid valve will almost invariably reveal tricuspid regurgitation with PE, which is rarely seen in right ventricular infarct (see Figure 33.9b).

Evaluation of the Lungs and Pleural Spaces

Evaluation of the pleura and lungs for pneumothorax, large pleural effusion, empyema, pulmonary consolidation and pulmonary oedema are described in detail elsewhere in this book. Each of these conditions can be the cause of critical illness and should be sought when clinical circumstances prompt suspicion of their presence. In the case of massive pleural effusion, drainage should proceed using ultrasound guidance. Lung ultrasound may be particularly useful in distinguishing between an acute exacerbation of chronic obstructive pulmonary disease and interstitial or alveolar oedema causing impaired gas exchange. The latter is identified by the presence of diffuse and widespread B-lines. Any cause of increased extravascular lung water can give rise to this ultrasound finding, including congestive heart failure, volume overload, acute respiratory distress syndrome, interstitial pneumonitis and toxic lung injury.

Table 33.4 Sonographic findings to be assessed in patients suspected of acute haemodynamically significant pulmonary embolus.

Sonographic finding	Sonographic technique and notes
Basic ultrasound techniques	
LV to RV diameter ratio	Ap4Ch or SX-4Ch. Measure below MV and TV leaflet tips. Normal usually <0.6. Definitely abnormal if >1.0
Septal wall flattening	PSSA, PSLA, SX-4Ch, SX-SA
'D'-shaped LV	PSSA, SX-SA
Paradoxical septal motion	Ap4Ch, PSLA, PSSA
McConnell sign	Ap4Ch or SX4Ch. RV hypokinesis with apical sparing
IVC distended, non-collapsible	
Intracardiac thrombus in transit	
More advanced ultrasound techniques	
Tricuspid regurgitant jet velocity	Ap4Ch (or PSSA, or any view demonstrating jet)

Abbreviations: Ap4Ch, apical four-chamber view; IVC, inferior vena cava; LV, left ventricle; MV, mitral valve; PSLA, parasternal long axis; PSSA, parasternal short axis; RV, right ventricle; SA, short axis plane; SX, subxiphoid or subcostal view; TV, tricuspid valve; 4Ch: four-chamber plane.

Usually, the specific aetiology of the increased lung water can be distinguished by a combination of the clinical circumstances and ultrasound evaluation of the IVC and heart.

Bedside Ultrasound in the Setting of Cardiac Arrest

For the purposes of bedside ultrasonography, the traditional dichotomisation of cardiac arrest patients into those with shockable and non-shockable cardiac rhythms is useful (see Figure 33.12). For the former group, the primary treatment is electrical. Except for asystole, other rhythms constitute pulseless electrical activity (PEA) or electromechanical dissociation (EMD). For patients in this group, the goal is rapid diagnosis and treatment of those in whom the PEA is reversible. A variety of algorithms have been developed to use ultrasound as the first step, as it can identify several of the more common causes including pericardial tamponade, intravascular volume depletion, acute right-sided heart strain (pulmonary embolus), pneumothorax, severe aberration of cardiac function (cardiogenic shock) and an absence of cardiac motion (true electromechanical dissociation). One such algorithm for patients found to be in PEA is shown in Figure 33.13. Specific ultrasound examinations of the heart, pleura, lungs and IVC to make these diagnoses are described elsewhere in this chapter and this book. In addition to these applications, there are reports of sonography to identify ventricular fibrillation during apparent asystole by electrocardiogram monitoring and pacemaker placement and capture.

Several studies have demonstrated that ultrasound can be used in arrest in compliance with ALS guidelines. Based on the results of these studies, the following recommendations can be made. Where feasible, ultrasound evaluation of the heart should be performed using the subxiphoid window. This allows views of the IVC, and sometimes of the heart, concurrent with cardiac compressions. The four-chamber plane is most useful. While cardiac massage is ongoing,

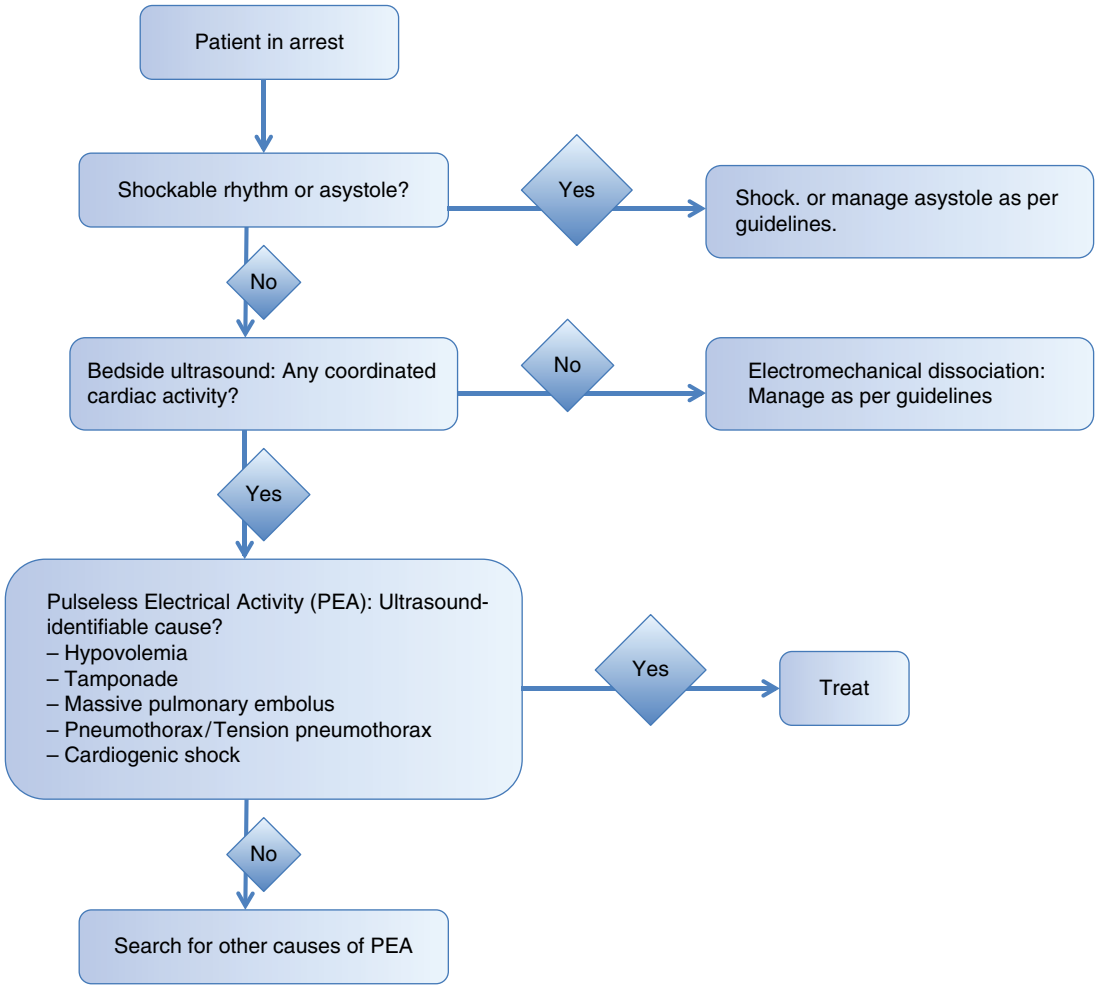

Figure 33.12 Integration of bedside ultrasound in the management of cardiopulmonary arrest.

the pleura (via views in the mid-clavicular and mid-axillary lines) can be assessed for massive pleural effusions, although evaluation for pneumothorax is almost never feasible due to the continual thoracic motion of cardiac compressions. If adequate images of the heart cannot be obtained during cardiac compressions, views should be obtained during pulse checks.

Many studies have been conducted to assess the prognostic significance of the sonographic absence of wall motion during cardiac arrest. The results are not completely consistent, reflecting the subjective nature of 'absence of wall motion' (see Video 33.14); however, the vast majority of data suggest that the absence of cardiac activity makes survival to hospital admission rare, and survival to hospital discharge exceedingly unlikely. While hard-and-fast rules cannot be made, these findings suggest that an ultrasound determination of cardiac activity, with due consideration of other clinical factors, including age, comorbid conditions, time prior and subsequent to the initiation of cardiopulmonary resuscitation, is a useful adjunct in decision-making regarding the termination of resuscitative efforts.

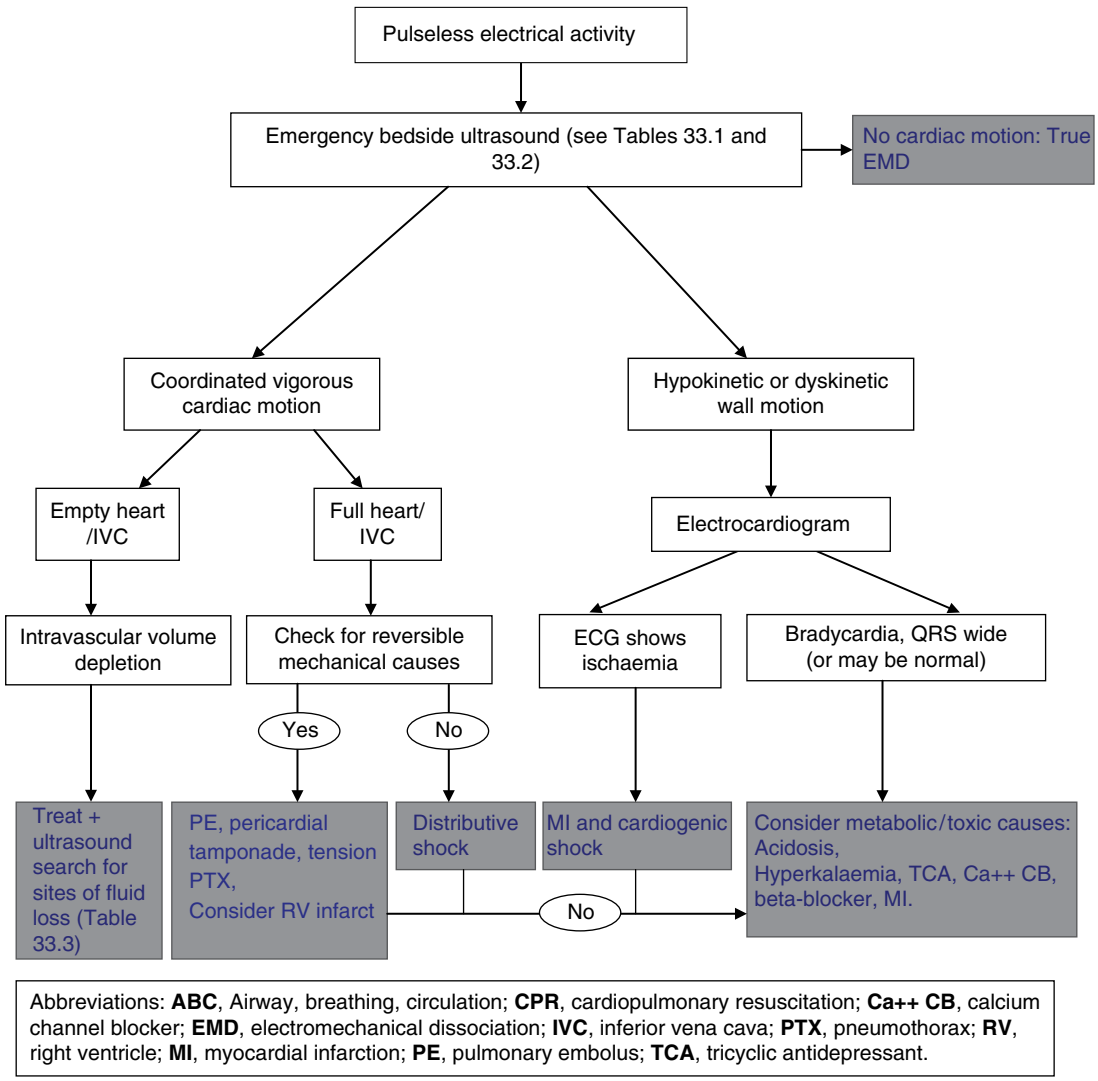

Figure 33.13 An algorithm for use of emergency bedside ultrasonography (EMBU) in the management of pulseless electrical activity. Boxes in blue are end-points with specific management or therapy. Adapted with permission from Hendrickson, R.G., Dean, A.J.. Costantino, T.G. (2001) A novel use of ultrasound in pulseless electrical activity: the diagnosis of an acute abdominal aortic aneurysm rupture. *J. Emerg. Med.*, **21** (2), 141–144.

Further Reading

Blaivas, M., Graham, S., Lambert, M.J. (2000) Impending cardiac tamponade, an unseen danger? *Am. J. Emerg. Med.*, **18** (3), 339–340.

Cheriex, E.C., Sreeram, N., Eussen, Y.F.J.M., Pieters, F.A.A., Wellens, H.J.J, (1994) Cross sectional Doppler echocardiography as the initial technique for the diagnosis of acute pulmonary embolism. *Br. Heart J.*, **72**, 52–57.

Goldberger, J.J.. Himelman, R.B., Wolfe, C.L., Schiller, N.B. (1991) Right ventricular infarction: recognition and assessment of its hemodynamic significance by two-dimensional echocardiography. *J. Am. Soc. Echocardiogr.*, **4** (2), 140–146.

Henry, W.L.. Gardin, J.M., Ware, J.H. (1980) Echocardiographic measurements in normal subjects from infancy to old age. *Circulation*, **62** (5), 1054–1061.

Levine, M.J.. Lorell, B.H., Diver, D.J., Come, P.C. (1991) Implications of echocardiographically assisted diagnosis of pericardial tamponade in contemporary medical patients: detection before hemodynamic embarrassment. *J. Am. Coll. Cardiol.*, **17** (1), 59–65.

Lipton, B. (2000) Estimation of central venous pressure by ultrasound of the internal jugular vein. *Am. J. Emerg. Med.*, **18**, 432–434.

Mark, D.G., Ku, B.S., Carr, B.G., Everett, W.W., Okusanya, O., Horan, A., Gracias, V.H., Dean, A.J. (2007) Directed bedside transthoracic echocardiography: preferred cardiac window for left ventricular ejection fraction estimation in critically ill patients. *Am. J. Emerg. Med.*, **25** (8), 894–900.

McGowan, J.H., Cleland, J.G. (2003) Reliability of reporting left ventricular systolic function by echocardiography: a systematic review of 3 methods. *Am. Heart J.*, **146** (3), 388–397.

Moore, C.L., Rose, G.A., Tayal, V.S., Sullivan, M., Arrowood, J.A., Kline, J.A. (2002) Determination of left ventricular function by emergency physician echocardiography of hypotensive patients. *Acad. Emerg. Med.*, **9**, 189–193.

Nidorf, S.M., Picard, M.H., Triulzi, M.O., Thomas, J.D., Newell, J., King, M.E., Weyman, A.E. (1992) New perspectives in the assessment of cardiac chamber dimensions during development and adulthood. *J. Am. Coll. Cardiol.*, **19**, 983–988.

Algorithms for use of ultrasound in the critically ill.

Beaulieu, Y. (2007) Bedside echocardiography in the assessment of the critically ill. *Crit. Care Med.*, **35** (5 Suppl.), S235–S249.

Hendrickson, R.G., Dean, A.J., Costantino, T.G. (2001) A novel use of ultrasound in pulseless electrical activity: the diagnosis of an acute abdominal aortic aneurysm rupture. *J. Emerg. Med.*, **21** (2), 141–144.

Jensen, M.B., Sloth, E., Larsen, K.M., Schmidt, M.B. (2004) Transthoracic echocardiography for cardiopulmonary monitoring in intensive care. *Eur. J. Anaesthesiol.*, **21**, 700–707.

Neri, L.. Storti, E., Lichtenstein, D. (2007) Toward an ultrasound curriculum for critical care medicine. *Crit. Care Med.*, **35** (5 Suppl.), S290–S304.

Niendorff, D.F., Rassias, A.J., Palac, R., Beach, M.L., Costa, S., Greenberg, M. (2005) Rapid cardiac ultrasound of inpatients suffering PEA arrest performed by nonexpert sonographers. *Resuscitation*, **67** (1), 81–87.

Rose, J.S., Bair, A.E., Mandavia, D., Kinser, D.J. (2001) The UHP ultrasound protocol: a novel ultrasound approach to the empiric evaluation of the undifferentiated hypotensive patient. *Am. J. Emerg. Med.*, **19** (4), 299–302.

34

Point-of-Care Ultrasound in Resuscitation and Cardiac Arrest: The FEEL Protocol

Elena Costantini, Peter M. Zechner, Frank Heringer, Colleen Cuca, Felix Walcher and Raoul Breitkreutz

Echocardiography in the Context of Advanced Cardiac Life Support (ACLS)

Focussed resuscitation and peri-resuscitation echocardiography is a relatively new and evolving application of point-of-care sonology that may significantly benefit those patients who have reversible causes of cardiac arrest. The potential role of ultrasound imaging as an adjunct to ACLS was recognised in 2010 the ACLS guidelines of the American Heart Association (AHA), the European Resuscitation Council (ERC) and the International Liaison Committee on Resuscitation (ILCOR). At the same time, an increased emphasis was placed on the importance of minimally interrupted, high-quality chest compressions accompanying any ACLS intervention. Notably, chest compressions may be paused only briefly (for less than 10 s), and solely to enable specific tasks such as a pulse check. While many focussed echocardiography protocols such as FATE, BLEEP, CLUE and FOCUS have been described for the use in critically ill patients, none of these was specifically designed to operate within the constraints of current ACLS recommendations. In this chapter, attention is focussed on the ACLS-compliant use of sonography in cardiac arrest or pulseless states.

Pulseless electrical activity (PEA) is defined as a state of cardiovascular collapse (absent pulses) in the presence of electrical cardiac activity. Echocardiography in the peri-resuscitation setting may distinguish between two forms of PEA with very different prognoses:

- Pseudo PEA, which includes patients presenting with coordinated electrical and myocardial kinetic activity on echocardiography ('PEA with cardiac activity'). These patients have a very high likelihood of return of spontaneous circulation (ROSC).
- True PEA, which includes patients without any sonographically detectable wall motion ('PEA without cardiac kinetic activity', also referred to as 'electromechanical dissociation'; EMD). This is associated with a much worse outcome.

If PEA with cardiac activity is identified, ultrasound can be extremely effective in identifying many of the more common reversible causes. The FEEL (the Focussed Echocardiography Examination in Life) support examination offers an ACLS-compliant approach to the use of ultrasonography in cardiac arrest. Details of the examination are shown in Figure 34.1.

Emergency Point-of-Care Ultrasound, Second Edition. Edited by James A. Connolly, Anthony J. Dean, Beatrice Hoffmann and Robert D. Jarman.

Companion website: www.wiley.com/go/connolly/ultrasound

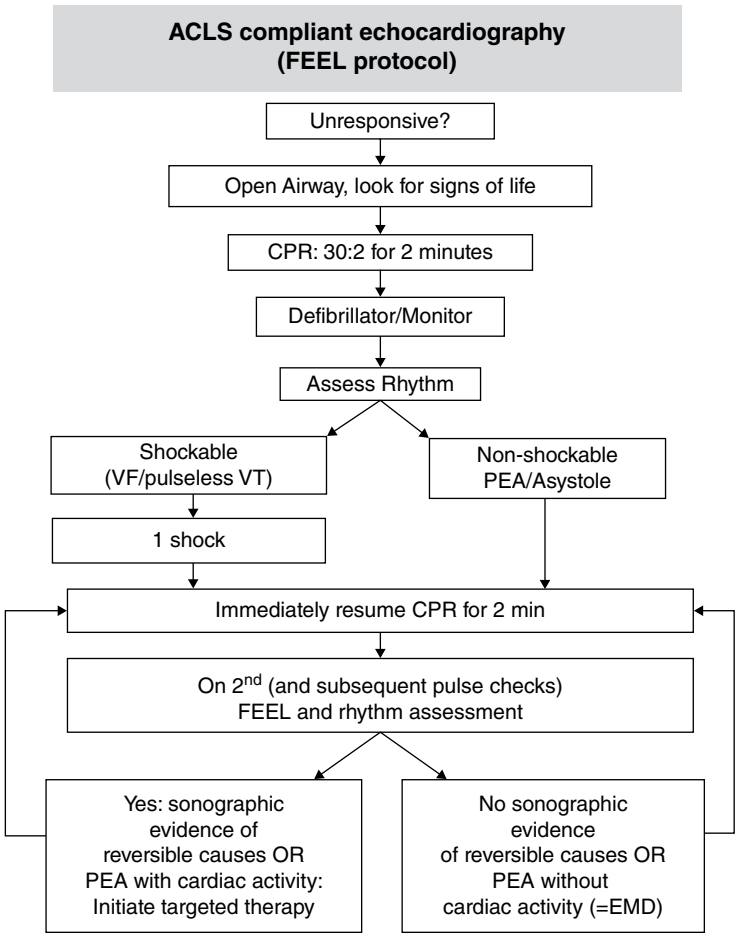

Figure 34.1 The focussed echocardiography evaluation in life support (FEEL) examination. ACLS-conformed integration of point-of-care cardiac ultrasound into the CPR algorithm. Note that the ACLS is the dominant driving force. For abbreviations, see the text.

Details of the FEEL Examination

Set-Up and Workflow

In the workflow of the FEEL examination, sonographic images are obtained exclusively during the brief breaks from cardiac compressions for rhythm analysis and pulse check after the initial minimum of 2 minutes of uninterrupted cardiopulmonary resuscitation (CPR). The ultrasound machine should be turned on and adjusted, and a sonologist with experience in cardiac echocardiography should be comfortably situated before the compression break. It should not be necessary to modify the placement of the defibrillator pads. The sonologist should be in direct verbal communication with the team leader and the ACLS team, who should know and understand the nature and goals of the FEEL examination. The transducer should be positioned with coupling gel on the chest immediately before the start of the compression break in order to obtain adequate images within the 10-s pause. It is vital that the compression breaks are not extended due to the sonologist searching for 'a good window'. If an adequate window cannot be obtained the sonologist should remove the probe within 10 s, and make preparations to scan an alternative window during the next pause.

A useful technique that may further decrease the hands-off time is first to use the record

feature to film a small loop, and then to review the loop away from the patient to allow a prompt resumption of cardiac compressions.

In almost all cases it is best to start with the sub-xiphoid window. This view is relatively easy to master, provides good imaging in supine patients, is often effective in mechanically ventilated patients. It can also be set up during chest compressions. It provides information about all four chambers and allows evaluation of the inferior vena cava (IVC).

The IVC can also be visualised via the right intercostal approach, which may provide better images during chest compressions. If other views are needed, parasternal and apical windows may be interrogated during subsequent pulse checks. The features of the various cardiac planes and windows are discussed in detail in Chapters 4 and 5, but briefly, the parasternal long-axis view shows left ventricular function, the left ventricular inflow and outflow tracts, the mitral valve, and the right ventricle. The apical four-chamber view permits an assessment of right and left ventricular functions, right ventricle:left ventricle (RV:LV) ratios, and the pericardial space. These views may be more challenging in supine, mechanically ventilated patients.

Anatomical Structures and Associated Diagnostic Entities to be Identified

The FEEL examination permits a rapid assessment of ventricular function by the absence, presence and quality of endocardial inward motion, and of myocardial wall thickening. If coherent myocardial activity is seen, ventricular function should be assessed (normal, severely impaired or absent). Hypovolemia is suggested by small ventricles with near or complete end-systolic collapse and 'kissing trabecular muscles. The ventricle is likely to be hyperkinetic unless there has been myocardial damage arising from prolonged hypovolemic shock, sepsis or antecedent heart disease.

In general, the IVC will be plethoric in arrest, and anything less than a fully distended and circular vessel is suggestive of relative intravascular hypovolemia that might benefit from further fluid resuscitation.

The RV:LV ratios should be estimated. A ratio greater than 1 is highly suggestive of right ventricular dilatation (especially in the absence of a thickened hypertrophic RV wall) and should prompt consideration of massive pulmonary embolus as the cause of the patient's arrest.

The identification of a circumferential pericardial effusion should be followed by a search for diastolic collapse of any chamber, especially the right or left ventricles. However, the identification of a large effusion and any concern for tamponade in the setting of arrest should probably prompt pericardiocentesis unless there are compelling reasons not to do it.

In the event that a cause for the patient's arrest is identified by ultrasound, the ACLS team leader should immediately be advised. Ultrasound findings should be reviewed with the team and integrated with other components of the clinical picture in order to optimise peri-resuscitation care. Anomalous findings can sometimes prompt consideration of previously overlooked conditions (e.g., acute valvulopathy, displacement of the mediastinum suggestive of occult tension pneumothorax, or large volumes of unheralded intra-abdominal fluid suggestive of vascular catastrophe).

Pearls and Pitfalls

- The primary role of the FEEL examination is to provide information that can be used to improve or guide resuscitative efforts. This would seem to represent a fundamental improvement over 'blind' CPR. Because many treatable causes of PEA (e.g., toxicological, hypoxaemia, hypothermia, endotracheal tube malfunction) are sonographically occult, decisions to terminate resuscitative efforts should be based on all available clinical evidence, and not ultrasound alone.
- Similar to all applications of ultrasonography, the FEEL examination is operator-dependent. As such, the sonologist should be rigorously trained, and cognisant of his or her limitations. As previously noted, the FEEL examination should never become a reason for failing to comply with ACLS algorithms.

Future Directions for Ultrasound in Resuscitation

A recent prospective observational study demonstrated that the application of ALS-compliant echocardiography in pre-hospital care is feasible, and alters the diagnosis and management in a significant number of patients. In this study, a total of 230 patients was included, with 204 undergoing an echocardiographic examination during ongoing cardiac arrest (n = 100) or in a state of shock (n = 104). Images of diagnostic quality were obtained in 96% of observed cases. In a high percentage of cases with initial ECG-diagnosed asystole or with PEA, coordinated cardiac motion was detected, associating those cases with increased survival.

Other potential applications of focussed echocardiographic or ultrasound or transoesophageal examinations during resuscitation may include the detection of aortic dissection or abdominal aortic aneurysm, pneumothorax, or bleeding in the chest or abdomen. Case reports have shown that fine ventricular fibrillation missed by surface ECGs or be wrongly interpreted as asystole.

The results of limited studies have suggested that the skills required for the focussed point-of-care sonography in the FEEL examination can be achieved with relatively brief training, in combination with generic ACLS training programmes. Training should be multi-modal, and include fundamental theory, visual pattern recognition, psychomotor skill testing and simulator-based team training within time-critical ACLS scenarios. The use of simulated arrest scenarios will allow for the further study of various training approaches, as well as the identification of potential disruptions of ACLS protocols that may arise as a result of using ultrasound.

Conclusions

The FEEL examination is an ACLS-compliant use of ultrasonography to enhance resuscitation and to detect and treat reversible conditions in cardiac arrest scenarios. It can be used by cardiologists and non-cardiologists alike. The impact of echocardiography on patient outcomes for both in-hospital and pre-hospital arrest represents a potentially exciting avenue for future resuscitation research.

Further Reading

Blaivas, M., Fox, J.C. (2001) Outcome in cardiac arrest patients found to have cardiac standstill on the bedside emergency department echocardiogram. *Acad. Emerg. Med.*, **8** (6), 616–621.

Breitkreutz, R., Price, S., Steiger, H.V., Seeger, F.H., Ilper, H., Ackermann, H., Rudolph, M., Uddin, Sh., Weigand, M.A., Müller, E., Walcher, F. (2010) Focused echocardiographic evaluation in life support and peri-resuscitation of emergency patients: a prospective trial. *Resuscitation*, **81**, 1527–1533.

Breitkreutz, R., Walcher, F., Seeger, F.H. (2007) Focused echocardiographic evaluation in resuscitation management: Concept of an advanced life support-conformed algorithm. *Crit. Care Med.*, **35** (5), S150–S161.

Nolan, J.P., *et al*. (2010) European Resuscitation Council Guidelines for Resuscitation 2010. *Resuscitation*, **81**, 1219–1276.

Price, S., Ilper, H., Uddin, Sh., Steiger, H.V., Seeger, F.H., Schellhaas, S., Heringer, F., Rüsseler, M., Ackermann, H., Via, G., Walcher, F., Breitkreutz, R. (2010) Peri-resuscitation echocardiography: training the novice practitioner. *Resuscitation*, **81**, 1534–1539.

Salen, P., O'Connor, R., Sierzenski, P., Passarello, B., Pancu, D., Melanson, S., Arcona, S., Reed, J., Heller, M. (2001) Can cardiac sonography and capnography be used independently and in combination to predict resuscitation outcomes? *Acad. Emerg. Med.*, **8** (6), 610–615.

Via, G., Breitkreutz, R., Price, S., *et al*. (2009) WINFOCUS ECHO-ICU Group (World Interactive Network Focused on Critical UltraSound ECHO ICU Group). Detailed echocardiography (echo) protocols for the critical patient. *J. Trauma*, **66** (2), 589–590.

35

Non-Invasive Haemodynamics

Erik Sloth, Christian Alcaraz Frederiksen and Peter Juhl-Olsen

Basic Haemodynamics

From basic physiological considerations it is apparent that imaging of the heart will enhance the foundation for assessment of the haemodynamic determinants (Table 35.1):

- *Preload* can be assessed by ultrasound using relatively simple volumetric methods for one-, two- or three-dimensional quantification of cardiac chamber dimensions, areas or volumes. In combination with respiratory changes of the inferior vena cava (IVC), volume responders can be predicted with high probability.
- *Afterload* requires both knowledge about ventricular dimensions and myocardial thickness, both of which parameters can be easily assessed using ultrasound. It should be emphasised that, according to Laplace's law, the assessment of afterload is a question of disclosing a small cavity together with a hypertrophic myocardium versus a dilated or thin-walled ventricle.
- *Myocardial function* and ejection fraction are often considered equivalent. An ejection fraction >55% is normal, while <25% is severely reduced. Several quantitative or semi-quantitative methods can be used. It is important to take into account that the ejection fraction implies that a reduction in left ventricular size will increase the percentage of emptying, and dilatation of the cavity will have the opposite effect. Thus, the left ventricle ejection fraction (LVEF) should always be correlated to the diastolic dimension.
- *Eyeballing* is the predominant method for the assessment of LVEF, but there are many other methods. There are great expectations for more objective measures of myocardial deformation, such as speckle tracking ultrasound, which is less user-dependent than Doppler-based methods.
- *Diastolic function* can be evaluated from a combination of different Doppler-based methods. However, none of these methods is suitable for point-of-care use. Instead, the presence of left ventricle hypertrophy in combination with left atrial enlargement can be used as a predictor for diastolic dysfunction. Systolic and diastolic heart failure accounts for approximately 50% each, and since they are fundamentally different the distinction between them is essential. Varieties of pathological conditions exist, and this often presents a major challenge for the medical team. By means of non-invasive ultrasound techniques the most crucial diagnoses are often quite easy to rule out (see Table 35.1).

From the above points it is evident that systolic and diastolic function, together with significant pathology, are difficult to assess without imaging capabilities. In conjunction with Doppler measurements the ultimate utility of ultrasound is reached.

Emergency Point-of-Care Ultrasound, Second Edition. Edited by James A. Connolly, Anthony J. Dean, Beatrice Hoffmann and Robert D. Jarman.

Companion website: www.wiley.com/go/connolly/ultrasound

Table 35.1 Important physiological and pathophysiological haemodynamic determinants.

Right and left ventricle physiological determinants	
Systolic	**Diastolic**
Preload	Compliance
Afterload	Relaxation
Contractility	Heart rate
Heart rate	
Pathophysiological determinants	
Hypovolaemia, e.g., bleeding and sepsis	Pneumothorax
Pericardial effusion	Valve disease
Pulmonary embolus	Aorta dissection
Pleural effusion	Myocardial infarction
	Post myocardial septal defect

By means of continuous-wave Doppler-mediated pressure estimations based on Bernoulli's principle, it is possible to assess right ventricle peak systolic pressure or a pressure gradient across the aortic valve. Both measurements can be performed from the apical view across the tricuspid valve and aortic valve, respectively. To achieve the correct right ventricular pressure, the right atrial pressure should be added to the Doppler pressure measurement. The right ventricle pressure equals pulmonary artery pressure if the pulmonary artery is unobstructed. Using colour Doppler, valve incompetence and septum defects can be visualised. Finally, a variety of Doppler methods can be used for the assessment of cardiac output.

Practical Approach

Appreciating the potential of ultrasound for dynamic imaging of the heart, pleura, great vessels and right/left ventricle interplay, a wide range of focussed echocardiography protocols have been described (FATE, FEEL, H.A.R.T., CLUE and FUSE), with FATE (Focus Assessed Transthoracic Echocardiography) as the most comprehensive. All essential information is printed on a laminated FATE card (Figure 35.1).

FATE is a rapid and systematic protocol for circulatory problem-solving (see Figure 35.1). Time needed for the initial evaluation is typically around 70 s, depending on patient condition, and the procedure can be performed even with the patient in the sitting position. FATE includes the following five steps:

1) *Look for obvious pathology*: It is important to identify all significant pathology, since an unrecognised pathology may prevent correct treatment (see Table 35.1) and inappropriate administration of inotropic support, thereby disguising major problems. In severe circulatory failure, several haemodynamic determinants often need to be optimised (see Table 35.1). All echocardiographic views can contribute to the evaluation of pathology.
2) *Assess wall thickness and chamber dimensions*: Chamber dimensions are essential for the assessment of right and left ventricular loading conditions. It is noteworthy that concentric left ventricular hypertrophy entails a reduced left ventricular dimension that is not necessarily equivalent to hypovolaemia. Most echocardiographic views can be used with the parasternal long-axis view in favour (position 3 in the FATE protocol).
3) *Assess myocardial function*: Start with eyeballing. This will give information on both global and regional myocardial function. A combination of multiple two-dimensional imaging planes is recommended.
4) *Imaging pleura on both sides*: This is very important because pleural effusion in itself can cause severe haemodynamic instability, especially with other concomitant disorders.
5) *Relate the information to the clinical context*: This is the most important step – synthesis of the findings. Often, a comprehensive evaluation implies the use of many different Doppler echocardiographic measurements.

Future Perspectives

Pocket ultrasound machines have already been manufactured and will set a new standard for non-invasive haemodynamic optimisation.

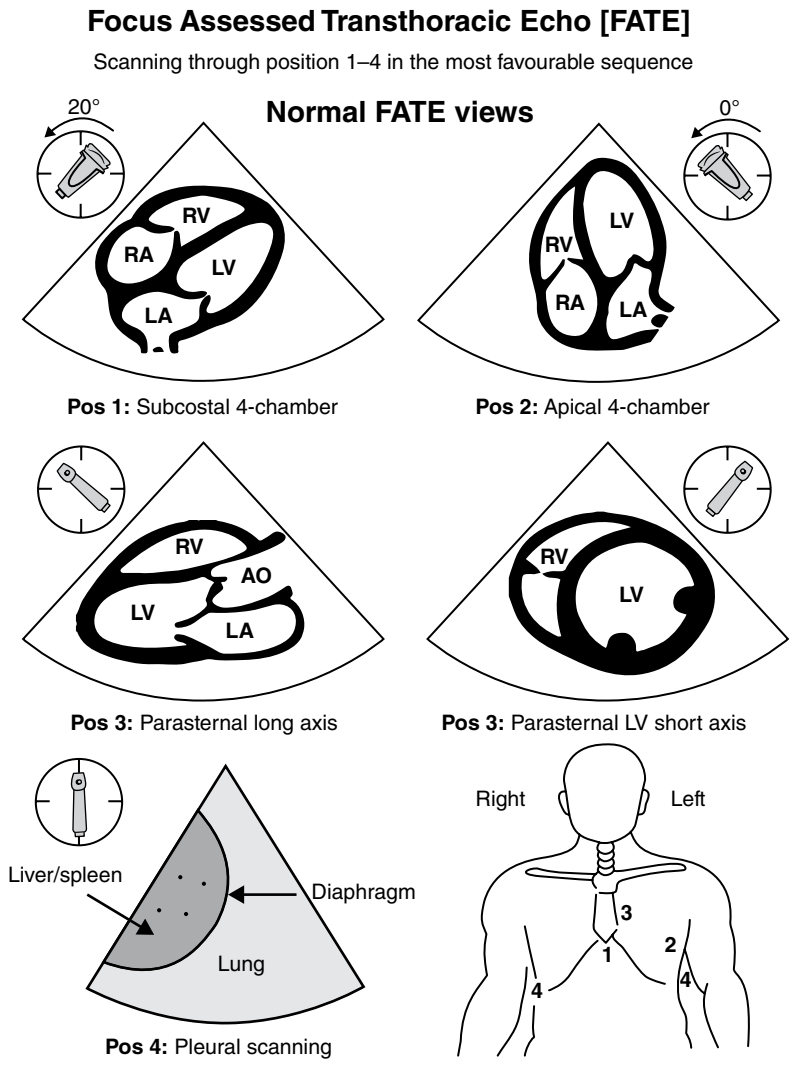

Figure 35.1 Laminated FATE card (page 1 of 4). All standard imaging planes are found together with guidance to interpret the echocardiographic findings and apply the findings in the haemodynamic clinical context. FATE card reproduced from (and can be ordered free of charge at): www.fate-protocol.com.

Further Reading

Barbier, C., Loubieres, Y., Schmit, C., Hayon, J., Ricome, J.L., Jardin, F., *et al.* (2004) Respiratory changes in inferior vena cava diameter are helpful in predicting fluid responsiveness in ventilated septic patients. *Intensive Care Med.*, **30** (9), 1740–1746.

Cahalan, M.K., Lurz, F.C., Schiller, N.B. (1988) Transoesophageal two-dimensional echocardiographic evaluation of anaesthetic effects on left ventricular function. *Br. J. Anaesth.*, **60** (8 Suppl.1), 99S–106S.

Frederiksen, C.A., Juhl-Olsen, P., Larsen, U.T., Nielsen, D.G., Eika, B., Sloth, E. (2010) New pocket echocardiography device is interchangeable with high-end portable system when performed by experienced examiners. *Acta Anaesthesiol. Scand.*, **54** (10), 1217–1223.

Gabriel, R.S., Klein, A.L. (2009) Modern evaluation of left ventricular diastolic function using Doppler echocardiography. *Curr. Cardiol. Rep*.,**11** (3), 231–238.

Jensen, M.B., Sloth, E., Larsen, K.M., Schmidt, M.B. (2004) Transthoracic echocardiography for cardiopulmonary monitoring in intensive care. *Eur. J. Anaesthesiol.*, **21** (9), 700–707.

Paulus, W.J., Tschope, C., Sanderson, J.E., Rusconi, C., Flachskampf, F.A., Rademakers, F.E., *et al*. (2007) How to diagnose diastolic heart failure: a consensus statement on the diagnosis of heart failure with normal left ventricular ejection fraction by the Heart Failure and Echocardiography Associations of the European Society of Cardiology. *Eur. Heart J.*, **28** (20), 2539–2550.

36

Doppler Assessment of Haemodynamics

Brendan E. Smith and Veronica M. Madigan

Introduction

If the term 'ultrasound' is mentioned to most clinicians it usually conjures up pictures of a beating heart or a squirming foetus, or even a beating heart within a squirming foetus! Whilst the tendency is to think of point-of-care ultrasound (PoCUS) in terms of images only, there is another modality of PoCUS which concerns itself with flow and with the measurement of velocities and pressures; this is the Doppler mode.

Principles of Doppler Measurements

The realisation that a train whistle has a higher pitch when coming first towards us, but then lowers when moving away from us, is a familiar experience. The change in frequency is directly proportional to the relative velocity of the source and observer, and also depends on the cosine of the angle between them, and the velocity of sound in the medium. This change in pitch is known as the Doppler shift. If the frequency shift can be measured, then the relative velocity can be calculated. For an emitted frequency denoted by *fe*, the observed frequency *fo* is found from:

$$fo = \left(\frac{Vm + Vr}{Vm + Vs}\right) fe \quad \text{or} \quad fo = \left(1 - \frac{Vs - Vr}{Vm}\right) fe$$

where *Vm* is the velocity of sound in the medium, *Vr* is the velocity of the receiver relative to the medium, and *Vs* is the velocity of the source relative to the medium. By rearranging these equations, it is possible to estimate the relative velocities if the source is known and the frequencies observed. This is the method used by traffic police to check the speed of a vehicle: they use an emitter with a known frequency and compare it to the reflected frequency reflected from an on-coming vehicle. A similar technique is used in assessing blood flow because red blood cells (RBCs) are very good reflectors of ultrasound. In this case, there are *two* Doppler shifts – one when the incident beam hits the red blood cells, and another as that beam is reflected from them. In this case the change in frequency is dependent on the velocity of the RBCs and the angle between the direction of motion of the RBCs and the probe. In Figure 36.1, blood is flowing through an artery at an actual velocity *Va*. The observer (the ultrasound probe) is looking at an angle to the line of flow, Θ. The observed velocity *Vo* is less than the real value by a factor of cosine Θ.

Taking all these effects together, the velocity of flow can be calculated from the formula:

$$Va = \left(\frac{fDs \times Vm}{2\, fe.\cos\theta}\right)$$

Emergency Point-of-Care Ultrasound, Second Edition. Edited by James A. Connolly, Anthony J. Dean, Beatrice Hoffmann and Robert D. Jarman.

Companion website: www.wiley.com/go/connolly/ultrasound

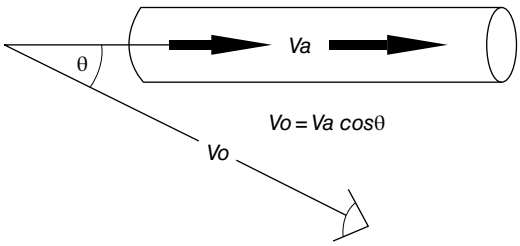

Figure 36.1

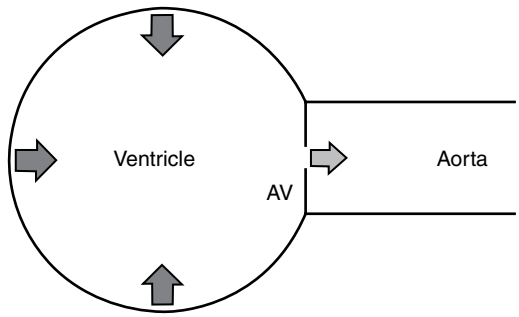

Figure 36.2

where *Va* is the actual flow velocity, *fDs* is the Doppler shift frequency, *fe* is the emitted frequency, *Vm* is velocity of sound in the tissues, and Θ is the angle of probe alignment. There are two ways that the Doppler effect can be use, namely qualitative and quantitative.

Qualitative (Colour) Doppler

The ultrasound machine can be arranged so that flows towards the probe (positive Doppler shift) can be shown in one colour, while flows away from the probe (negative Doppler shift) are shown in a different colour. It is customary to shows flow toward the probe in red, and flow away from the probe in blue. But more is possible: the shade of red can be made lighter or darker according to the Doppler shift, so higher velocities are shown in brighter reds and lower velocities shown in darker reds. The same can be done for blue.

At lower velocities, fluids maintain a smooth laminar pattern of flow, but as velocity increases turbulence occurs. In turbulent flow there will be some red cells travelling towards the probe and some travelling away from it. Are both reds and blues of various shades seen? Sometimes yes, but more usually the colours from adjacent areas merge and in a millisecond the flow at any one point may change direction, and therefore colour. What is usually seen is a blend of red and blue which appears green or white. If white is seen then high-velocity turbulence is present, whereas dark green or swirling greens, blues and reds indicate low-velocity turbulence. This can be of considerable value in cases of valvular heart disease or septal defects, but it can also be used in the examination of peripheral arteries and veins.

Quantitative Doppler

While colour Doppler can give an immediate impression of flow direction and velocity, Doppler can also be used to measure the actual velocity of flow and even the pressures involved. The velocity measurement has been described above, but how does Doppler measure pressures?

In medicine, there is a tendency to think of blood pressure generating blood flow. In haemodynamics, it is better to think of the heart as a volume pump which forces an incompressible liquid (blood) through the resistance of the peripheral circulation. This resistance to flow will then generate a pressure gradient from a high upstream pressure to a low downstream pressure. This means that a high-velocity flow must be due to a higher pressure gradient across the resistance element. Since velocities can be measured very accurately with Doppler, they can be used to measure pressure gradients. Figure 36.2 shows the relationship of the left ventricle, the aorta and the aortic valve.

It emerges that the pressure gradient across the aortic valve, $\Delta P_{(mmHg)}$, is approximately $4V^2$ This is known as the *modified Bernoulli equation*, and the formula has good clinical accuracy. If the systolic velocity of blood passing through the aortic valve is $4\,m\,s^{-1}$, the pressure gradient

across the valve must be $4 \times 4^2 = 64$ mmHg, a value which indicates aortic stenosis.

The same idea can be used to gauge pulmonary artery pressure. If there is a regurgitant jet at the tricuspid valve, which is increasingly more likely as pulmonary artery pressure rises, then the pressure gradient can be measured between the right ventricle and the right atrium. If the velocity of the jet is measured as $3\,m\,s^{-1}$, then the atrioventricular gradient is 36 mmHg. If the right atrial pressure is 10 mmHg, then the right ventricular pressure is around 46 mmHg. If the velocity across the pulmonary valve was measured as $1.25\,m\,s^{-1}$, then the gradient here must be 6.25 mmHg, so the pulmonary artery pressure is [46 – 6.25], or just below 40 mmHg. This applies in the peripheral circulation just as well, and can be used to estimate the severity of an arterial stenosis for example.

Doppler Measurement of Flow Volumes

If a pipe of radius **r** is considered with fluid flowing through it at a velocity of V, then at steady state the quantity of fluid flowing per unit time (Qt) is V multiplied by the cross-sectional area (XSA) or $Qt = V \times \pi r^2$. For a peripheral artery or vein where flow is more or less at constant velocity, all that is needed to know for measuring the flow rate is the internal diameter or radius of the vessel and the Doppler velocity.

Pulsatile Flow Measurements

Pulsatile flow is a little more tricky, since what is needed is the mean flow velocity. If the Doppler flow velocities for the aortic valve are measured, for example (see Figure 36.3), the ejection waveform is found to be roughly triangular in shape, with a velocity range of zero at the base to around $1.4\,m\,s^{-1}$ at the peak. The length of this pulse is around 350 ms, and it is then followed by diastole where there is zero flow through the valve. The total cycle time is around 800 ms, denoted by *t* in Figure 36.3.

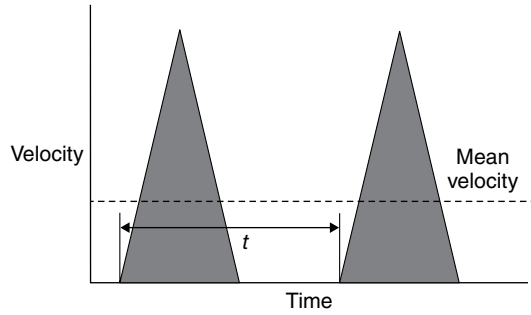

Figure 36.3

The mean velocity can be calculated by finding the area under the ejection curve by integrating the velocity with respect to time *t*. This is simply known as the velocity-time integral (VTI). If the VTI is multiplied by the XSA, the results is the stroke volume (SV): $SV = VTI \times XSA$. (Most ultrasound machines will trace the ejection waveform and calculate the VTI. This is also done automatically in devices specifically designed to measure cardiac output, such as the ultrasonic cardiac output monitor or 'USCOM' or the Cardio-Q transoesophageal monitor). The cardiac output is then simply expressed as: $VTI \times XSA \times HR$, where HR is the heart rate. Unfortunately, the measurement of aortic valve area and/or diameter is time-consuming and not very reliable. The pulmonary valve is even more difficult to measure. So, is there an easier way?

Nidorf found that the valve annulus diameter for heart valves, and for the aortic and pulmonary valves in particular, are very closely correlated with the patient's height and body weight. Predictions based on nomograms have been shown to give more accurate results than those of experienced sonologists making M-mode measurements. Thus, to obtain a cardiac output measurement the only task to perform manually is to obtain the best flow signal velocity when the probe is in approximate alignment with the axis of flow for that valve. This brings in a crucial factor with Doppler. Doppler can *underestimate* velocity if the ultrasound beam is angled to the axis of flow, but it can *never overestimate*

velocity. The highest velocity will be achieved with the best alignment of the flow axis and the probe.

Continuous-Wave Doppler and Pulsed-Wave Doppler

In continuous-wave Doppler (CWD), a transmitting crystal sends out a continuous beam of ultrasound while a receiving crystal 'listens' to the echoes coming back. Any echoes from the field of view, whatever the depth, are included in the sample. The width of the beam may be 20–30° or more. Thus, a wide range of tissue is scanned for information. With pulsed-wave Doppler (PWD), a discrete pulse is emitted and then the receiving crystal 'listens' for the echoes to this one pulse. By setting an exact time period or window from the emission of the pulse to sampling of its echoes, the system analyzes the Doppler shift at a given depth. If the sampling angle is made fairly narrow, say 10°, then sampling is effectively being made from a relatively small and discrete block of tissue, termed the 'sampling volume'.

At first sight, it may seem that PWD is the more precise tool to use, but for reasons that are beyond the space available in this introductory chapter PWD is limited as flow rates toward or away from the probe increase, and by deeper targets. CWD does not have this limitation. In haemodynamic practice, CWD is the preferred option for high-velocity flows like the aorta and pulmonary artery, and for valve regurgitant jets. Lower-velocity targets such as flow through a patent ductus arteriosus (PDA) or s septal defect are better for PWD.

Quantifying Haemodynamics

Although Doppler can be used to measure stroke volume, cardiac output, ejection velocity, flow time, flow rates and even waveform morphology, it can do even more. These values can be taken and combined to derive other indices of haemodynamics. Systemic vascular resistance (SVR) (or more accurately, systemic vascular *impedance*, as the input to the major vessels is pulsatile not constant) is simply mean blood pressure divided by cardiac output, and is equivalent to the ventricular afterload. It is also possible to calculate inotropy or myocardial contractility, ventricular end-diastolic volume (which is the ultimate indicator of preload), myocardial stroke work and cardiac power output, and even impedance matching of the ventricle and the arterial tree to optimise energy transfer.

Inotropy Measurement

In Figure 36.4, every time the child moves the pump handle through a full sweep she will generate one stroke volume of the pump. She will produce this stroke volume at a hydrostatic pressure and at a flow velocity which is determined by the force on the pump handle. But what if her father were to operate the pump instead? He would still produce the same stroke volume, but he would produce it in a much shorter time and with a higher pressure and flow velocity than his daughter could manage. Clearly, the difference is due to the power that he possesses relative to his daughter.

If these variables can be measured for the heart, then its instantaneous output power – which is

Figure 36.4

a function of its inotropy – can also be calculated. The stroke volume, flow time and flow velocity can be measured with Doppler, and the mean blood pressure by the usual means. From these values it is possible to calculate both the potential energy generated by the heart pumping blood from the low-pressure space of the left ventricle in diastole into the high-pressure zone of the aorta, and also the kinetic energy of the blood entering the aortic root.

Potential energy (PE) is the product of change of pressure and the volume of blood pumped into the high-pressure zone, or $PE = \Delta P \times \Delta V$. The change in pressure, ΔP, is: [mean arterial pressure – central venous pressure (CVP)], or [output pressure – input pressure]. The kinetic energy for any moving mass is given by the formula $KE = \frac{1}{2}mV^2$, where m is the mass of the object and V its velocity. Applying this to the heart, where the mass of blood is SV × density, and adding in the PE, the Smith–Madigan formula for inotropy is obtained:

$$\text{Inotropy} = \text{PE} / \text{Flow Time} + \text{KE}/\text{Flow Time}$$
$$= \frac{\text{BPm} \times \text{SV} \times 10^{-3}}{7.5 \times \text{FT}} + \frac{\text{D} \times \text{SV} \times 10^{-6} \times \text{Vm}^2}{2 \times \text{FT}}$$

where BPm = (mean arterial pressure – CVP) in mmHg, SV = stroke volume in ml, D = density in kg m^{-3}, Vm = mean velocity, and FT = systolic flow time in ms. The factors 7.5, 10^{-3} and 10^{-6} are required to convert mmHg, milliseconds and ml to kPa, seconds and m^3, respectively, to conform to SI values.

Power is the energy output per unit time, in this case the flow time. The left-hand term shows the power required for blood pressure, while the term on the right is the power required for blood flow. Both of these must be the product of ventricular power, or inotropy. Working through the equation, the result will be in Watts, the SI unit of power. If inotropy is divided by the body surface area (BSA), then just as with cardiac output and cardiac index, it is possible to derive the Smith–Madigan Inotropy Index (SMII), which is inotropy/BSA. Normal subjects have an SMII of 1.6–2.2 $W\,m^{-2}$, with much lower values being seen in heart failure.

Potential Energy to Kinetic Energy Ratio (PKR)

In the Smith–Madigan formula above, PE and KE were calculated The energy of blood pressure and the energy of blood flow must have an optimum ratio. Pressure without flow is pointless, but no matter how high the flow rate there must be adequate perfusion pressure for the tissues. Where is the optimum point?

In practice it is found that in healthy individuals the PE:KE ratio (PKR) is around 30:1. In excessively vasoconstricted states this can be 100:1 or more, while in the hyperdynamic phase of septic shock it is typically less than 5:1. Studies have shown that just increasing the inotropy level to a given value may not result in commensurate systemic benefits. Inotropic and vasoconstrictive effects need to be balanced. The PKR is a simple indicator of when the matching of pressure and flow is near optimal.

Left Ventricular End-Diastolic Volume (LVEDV)

The strict definition of preload is the presystolic length of the cardiac myocyte sarcomere. The *in vivo* correlate is ventricular end-diastolic volume. Pressure-based estimates of preload such as IVC diameter, CVP or pulmonary occlusion pressure (wedge pressure) are unreliable because they are affected by ventricular compliance. The direct measurement of ventricular volume is possible, but it is time-consuming, requires considerable expertise and has high interobserver variability. Alternatively, it can be done by using existing information regarding the heart's inotropy level.

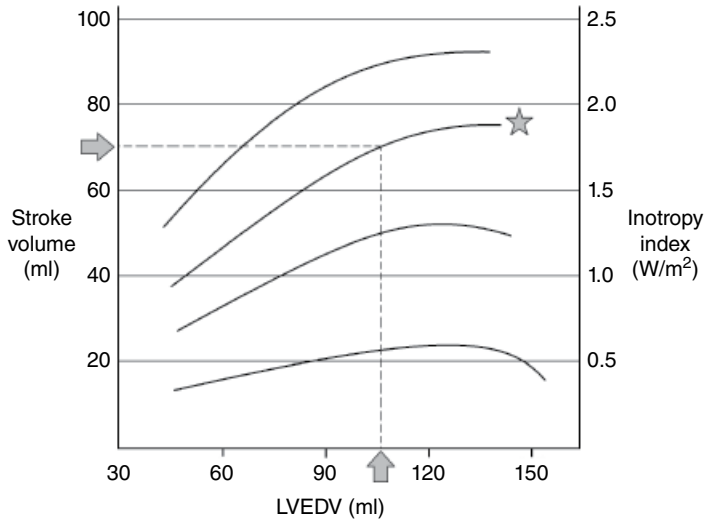

Figure 36.5

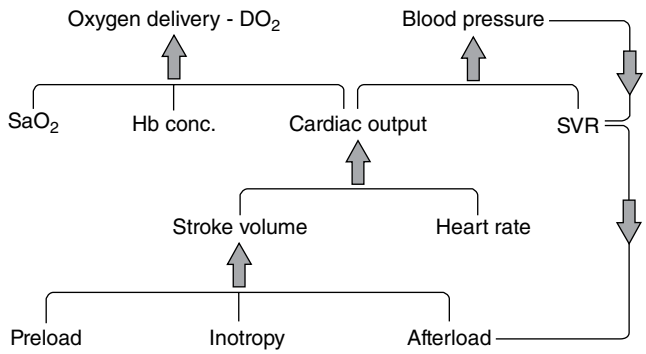

Figure 36.6

Starling's curves (see Figure 36.5) are familiar to medical practitioners. For any given LVEDV there will be a corresponding stroke volume, the magnitude of which depends on the myocardial contractility or inotropy, with high contractility curves at the top and low contractility curves at the bottom. However, this process also works in reverse.

If the stroke volume is known to be 70 ml (arrow on the y-axis in Figure 36.5), and the SMII is 1.8 W m^{-2} (starred curve), then the LVEDV must be around 105 ml (arrow on x-axis). This would equate to an ejection fraction of 70/105 = 66%, a normal value which fits the normal inotropy index of 1.6–2.2 W m^{-2}. Although this methodology is still undergoing validation, the initial results suggest that it correlates very well with sophisticated echocardiographic measurements.

Putting the Jigsaw Together

From Figure 36.6 it can be seen that if the preload, inotropy and afterload are known, then the three determinants of stroke volume are known:

- Stroke volume × heart rate = cardiac output.
- Cardiac output × SVR = blood pressure.
- CO × haemoglobin concentration × 1.34 × oxygen saturation = oxygen delivery, DO_2.

If the arterial and mixed venous oxygen contents are known, then the [cardiac output × arteriovenous oxygen content] difference yields oxygen consumption, VO_2. Thus, the haemodynamic jigsaw can be solved at the point-of-care.

Summary

So now we can measure fundamental and vital physiological parameters, and we can do it non-invasively. Many ultrasound machines now incorporate several of these calculations, along with nomograms to predict valve orifice diameters, automated flow tracing, pulse oximetry and so on and one, the USCOM, can perform all these measurements and calculations in real time on a beat to beat basis. Even data formerly considered to be the exclusive domain of highly sophisticated echocardiography is now readily available at the point of care. That makes Doppler ultrasound a very potent clinical tool. Hopefully this chapter will help you to incorporate it into your clinical practice.

Further Reading

Allan, P.L., Dubbins, P.A., Pozniak, M.A., McDicken, W.N. (2006) *Clinical Doppler Ultrasound*, 2nd edition. Churchill Livingstone-Elsevier: Oxford.

Hattle, L., Angelsen, B. (1985) *Doppler Ultrasound in Cardiology - Physical Principles and Clinical Applications*. Lea & Febiger, Philadelphia.

Klabunde, R.E. (2005) *Cardiovascular Physiology Concepts*. Lippincott Williams & Wilkins, Philadelphia.

Smith, B.E. Available at: www.learnhemodynamics.com.

37

Algorithmic Bedside Approach to the Major Trauma Patient in Extremis

Robert Arntfield and Andrew W. Kirkpatrick

Bedside Approach to Blunt Abdominal Trauma

When approaching the haemodynamically unstable trauma victim, the clinician must be aware that the odds of death are high, and that life-threatening pathology, usually – but not always severe hypovolaemia – must be urgently corrected. Survival typically requires localisation and correction of the problem, not just ongoing resuscitation (Figure 37.1). In an adult, haemorrhage sufficient to induce cardiovascular collapse or shock is typically from a limited number of discrete anatomical sites, notably intra-thoracic, intra-peritoneal, retroperitoneal, from multiple long bone fractures, or from external bleeding. Generally, while severe trauma is conceptualised as either being blunt, penetrating or thermal in nature, blast injuries – especially with improvised weapons – may confuse these neat boundaries, emphasising the need for reassessing the anatomy and physiology rather than the pattern.

The Advanced Trauma Life Support (ATLS) course remains the standard and tried approach to resuscitating the trauma patient in a hierarchal manner, serving to both prioritise and address the greatest threats to life rapidly. The initial approach to all serious trauma utilises the ABCDE concept. Thus, the airway is first addressed and either determined to be patent or secured with any number of airway maintenance devices, although a cuffed endotracheal tube remains standard. There is a limited role for ultrasound at this stage of care, unless a surgical/percutaneous airway is required, or there is doubt after placement as to the correct positioning of the tube.

Once the airway has been secured, breathing is next assessed. This has traditionally consisted of assessing the anterior chest for the hyper-resonance associated with a tension pneumothorax (PTX), and the lateral chest for the dullness of a massive haemothorax (HTX). As either of these diagnoses is associated with diminished air entry and respiratory embarrassment, a tube thoracostomy (TT) is warranted for either. If an experienced ultrasonographer is available however, both HTX/PTXs can be identified within seconds, and the size of each potentially evaluated. It is critical that an inexperienced user not make these diagnoses however, and that TTs be placed liberally as the risk-benefit ratio in those patients in extremis warrants liberal placement.

Once respiration is assured, the circulation is quickly assessed. It is essential that external bleeding is controlled as blood loss is seen to be the leading cause of potentially preventable trauma death. Resuscitation, localisation and correction must be as contiguous as possible.

The pericardial space is quickly identified to detect cardiac injury, the most treatable of

Emergency Point-of-Care Ultrasound, Second Edition. Edited by James A. Connolly, Anthony J. Dean, Beatrice Hoffmann and Robert D. Jarman.

Companion website: www.wiley.com/go/connolly/ultrasound

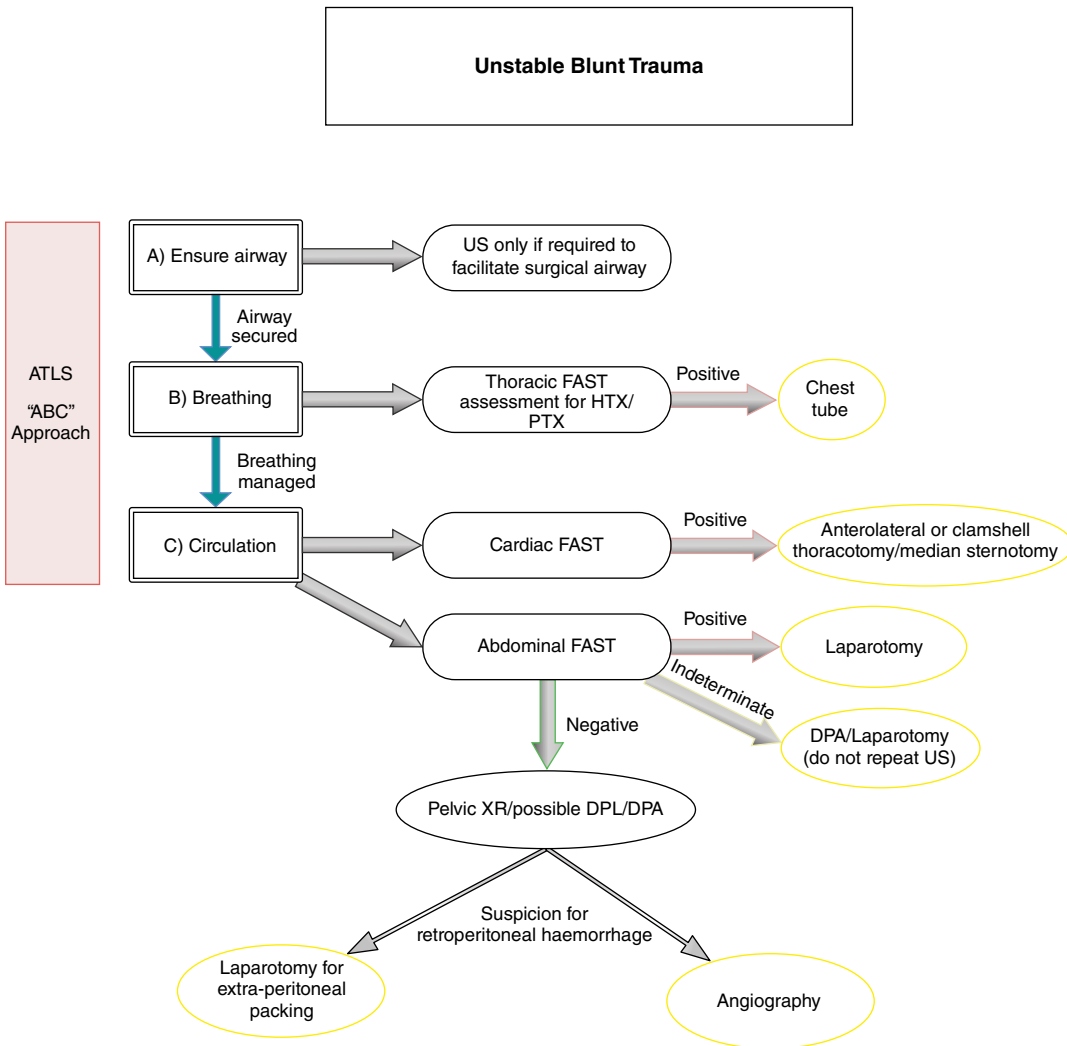

Figure 37.1 Algorithm for unstable blunt thoracoabdominal trauma.

which is pericardial tamponade. Visualising the heart first also allows the gain to be adjusted for the optimal depiction of blood. An unstable patient where the pericardial window of the FAST scan is positive should be immediately transferred to an operating theatre, if their physiology will allow it, as resuscitative thoracotomy performed in such an environment is associated with much better outcomes than those undertaken in the emergency room.

If the pericardium is normal, most physicians will move on to the abdominal examination. While a wealth of information can be inferred from the cardiac function (e.g., relative volume status and even potential valvular injury), these details should be sought after a primary survey has been completed, as the source of hypovolaemia requires blood loss into a large body cavity or externally.

When a FAST examination is true positive, the right upper quadrant is the anatomical location that will be most often positive (80%), compared to the left upper quadrant (55%) or pelvis (40%). A positive examination in any one of

these sites constitutes a positive examination for the purposes of proceeding to laparotomy in a physiologically compromised patient.

It is important to emphasise that decisions can only be made when the images generated are clearly positive or negative, and that clear anatomical structures are recognised allowing fluid to be recognised as being present or absent. If the images are unclear, and these details are uncertain, then the FAST is not negative, it is indeterminate (IND). Most common causes of an IND FAST are patient rather than operator-dependent, such as obesity or subcutaneous emphysema. Thus, some other modality should be used rather than persisting with the ultrasound examination.

If the FAST is clearly negative, and the haemorrhage has not been localised to an external or thoracic site, it may be retroperitoneal – a possibility made much more likely by a significant pelvic fracture. Both, physical examination and an emergency pelvic X-ray are required, and a diagnostic peritoneal aspiration (rather than lavage) will increase the confidence that a major haemoperitoneum is not being missed. Thereafter, while some centres will address presumed pelvic fracture-related bleeding with a surgical approach consisting of extraperitoneal pelvic packing and/or emergency pelvic bony stabilisation, many others will commit to transporting the patient to an angiographic suite for emergency angioembolisation of presumed vascular injury. There is a risk however in committing to a resuscitative intervention offering solely interventional angiography, or solely operative therapies, in physically separate locations.

Be wary, as a fracture of the anterior pelvis which tracks up the abdominal wall can look like a bladder and so cause confusion.

If the clinician has made the correct deduction of the site of bleeding then this is often life-saving, but it may be disastrous if the opposite intervention is what was required. Whilst in the future, hybrid-trauma operating theatres with combined operative and angiographic capabilities will simplify decision-making, as such patients in extremis will be taken to a single omni-capable suite, this is currently a critical task for which immediate and accurate bedside ultrasound is critical.

Penetrating Torso Injury

Penetrating mechanisms remains a common cause of traumatic injury, for which operative intervention is frequently required. In patients who are unstable after penetrating torso trauma, determining and controlling haemorrhagic and obstructive causes of shock remain the physician's most pressing challenges. Even if adequate supportive care is instituted, including a definitive airway, intravenous volume support and a warm environment, conditions such as haemopericardium, pneumothorax, haemothorax or haemoperitoneum may all progress to death if left undetected and uncorrected.

When using ultrasound to assess the unstable patient after penetrating torso injury (Figure 37.2), the sequence of scanning is important. The pericardial space is most sensitive to ongoing incremental bleeding given its small overall size and direct influence on cardiac output. Thus, the cardiac FAST view should be carried out first. While the sensitivity and specificity of the cardiac FAST view has been shown to be exceptional, being mindful of the potential for cardiac lesions to present as massive haemothorax (via decompression in to the pleural space) leading to a falsely negative cardiac FAST is important in high-risk precordial lesions.

The abdomen may then be assessed in the usual fashion with the three views of the abdominal FAST examination (as reviewed in Chapter 8). Using the FAST examination for penetrating abdominal trauma has been shown to be specific, but not sensitive. In the unstable patient who has demonstrable haemoperitoneum on ultrasound, assurance must be made that there is no co-morbid intrathoracic (particularly cardiac) injuries that may be co-contributing to instability. If thoracic assessment is negative, immediate laparotomy is appropriate, in the previously healthy (non-cirrhotic) patient.

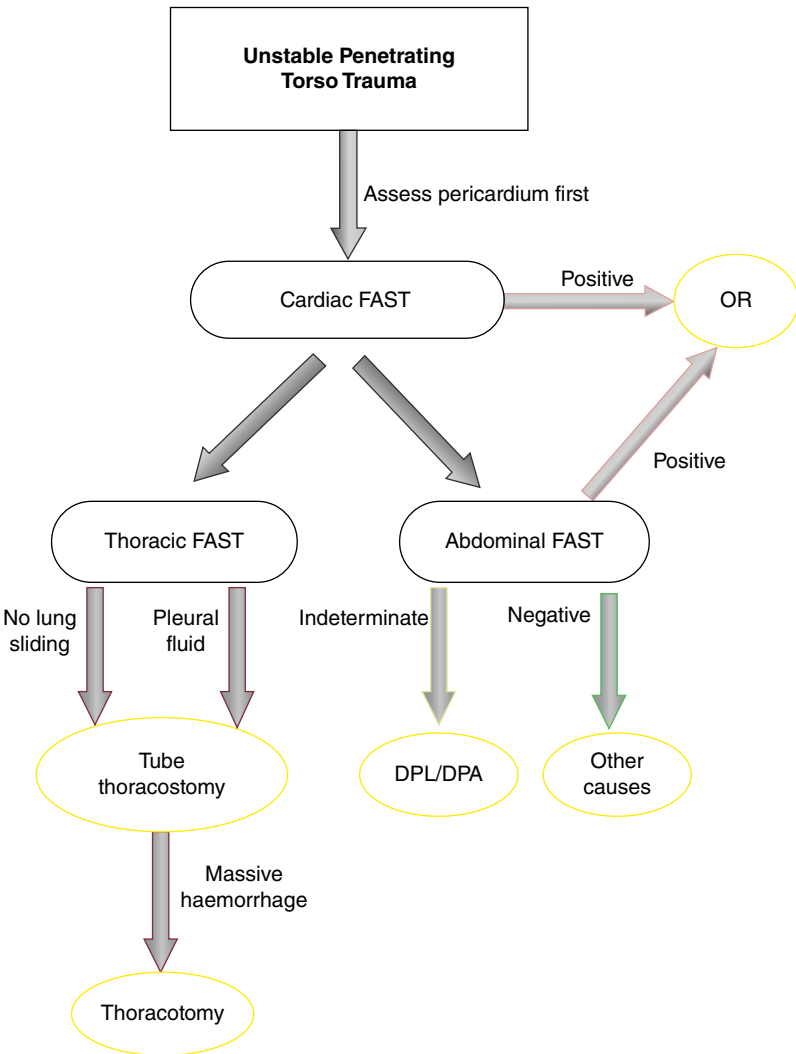

Figure 37.2 Algorithm for unstable penetrating thoracoabdominal trauma.

Assessment of the thorax for both HTX and PTX may then take place. Any loss of lung sliding or fluid cranial to the diaphragm in an unstable patient should prompt immediate tube thoracostomy. While there are other reasons besides PTX as to why lung sliding may not be present at the pleural junction (apnoea, atelectasis, pleural adhesions, and possibly bullous emphysema), the high-risk unstable patients represent a situation that warrants the assumption of PTX with absent sliding. Even urgent tube thoracostomies must always be placed with care however, abandoning the procedure if no actual pleural cavity is present upon dissection, as may occasionally occur with prior thoracic surgery or pleural disease. If more than 1500 ml of blood is drained acutely and the patient remains unstable, then thoracotomy should be performed.

In the event of an unstable patient who has a negative FAST, including the assessment of pericardium, thorax and abdomen, a consideration of more rare penetrating injuries such as retroperitoneal vascular (e.g., aortic) injury or high

spinal cord injury (with resultant neurogenic shock) may be suspected as the cause of instability.

Severe Head Injury

As treatment of the primary brain injury is still so limited, it is critical that any secondary brain injury be minimised. Thus, for a severely head-injured patient the initial treatment must prioritise aggressive supportive care and the early identification and treatment of neurosurgical lesions. This means practically that it is crucial to transport such patients to the computed tomography (CT) scanner as quickly as other life-threatening injuries can be excluded. For simplicity, the use of bedside ultrasound for severe head injury translates into quickly satisfying either the blunt or penetrating algorithms (Figure 37.1 and 37.2) to ensure that the patient can most safely be physically transported to the CT scanner. It may also guide an aggressive use of osmotic agents where there is a time-critical expanding brain lesion.

It is through such a rapid assessment for other injuries, such as haemoperitoneum, haemopericardium, PTX or HTX that trauma ultrasound may be most useful in this set of severely head-injured patients. If left undetected, such injuries may herald unanticipated swings in blood pressure or gas exchange that may cause secondary neuronal insult through hypotension or hypoxaemia. As neuroimaging is required in nearly all circumstances, detecting such injuries prior to CT scanning is of critical importance to avoid resuscitation attempts in less than ideal locations, such as while in transit or in the radiology suite.

In the future, ultrasound may assume a more primary role, such as in the approximation of intracranial pressure through the measurement of optic nerve sheath diameter or transcranial Doppler velocities, which have generated much enthusiasm and research. Though these techniques are of great appeal, they are subject to a great deal of technical nuance and, in resource-replete hospitals with CT capabilities, delaying definitive neuroimaging to apply these techniques cannot yet be endorsed. However, it is hoped that future research will permit a revision of these conclusions in the future.

Further Reading

Ball, C.G., Kirkpatrick, A.W., D'Amours, S.K. (2011) The RAPTOR: Resuscitation with angiography, percutaneous techniques and operative repair. Transforming the discipline of trauma surgery. *Can. J. Surg.*, **54** (5), E3–E4.

Ball, C.G., Williams, B.H., Wyrzykowski, A.D., Nicholas, J.M., Rozycki, G.S., Feliciano, D.V. (2009) A caveat to the performance of pericardial ultrasound in patients with penetrating cardiac wounds. *J. Trauma: Injury Infect. Crit. Care*, **67** (5), 1123–1124.

Blaivas, M., Lyon, M., Duggal, S. (2005) A prospective comparison of supine chest radiography and bedside ultrasound for the diagnosis of traumatic pneumothorax. *Acad. Emerg. Med.*, **12** (9), 844–849.

Boulanger, B.R., Brenneman, F.D., Kirkpatrick, A.W., McLellan, B.A., Nathens, A.B. (1998) The indeterminate abdominal sonogram in multisystem blunt trauma. *J. Trauma*, **48**, 52–56.

Boulanger, B.R., Kearney, P.A., Tsuei, B., Ochoa, J.B. (2001) The routine use of sonography in penetrating torso injury is beneficial. *J. Trauma*, **51**, 320–325.

Burlew, C.C., Moore, E.E., Smith, W.R., Johnson, J.L., Biffl, W.L., Barnett, C.C., *et al*. (2011) Preperitoneal pelvic packing/external fixation with secondary angioembolization: optimal care for life-threatening hemorrhage from unstable pelvic fractures. *J. Am. Coll. Surg.*, **212** (4), 628–635; discussion 635–637.

Chun, R., Kirkpatrick, A.W., Sirois, M., Sargsyan, A.E., Melton, S., Hamilton, D.R,, *et al*. (2004) Where's the tube? Evaluation of hand-held ultrasound in confirming endotracheal tube placement. *Prehospital Disast. Med.*, **19**, 366–369.

Cullinane, D.C., Schiller, H.J., Zielinski, M.D., Bilaniuk, J.W., Collier, B.R., Como, J., *et al*.

(2011) Eastern Association for the Surgery of Trauma Practice Management Guidelines for Hemorrhage in Pelvic Fracture – Update and systematic review. *J. Trauma*, **71** (6), 1850–1868.

Demetriades, D., Murray, J., Sinz, B., Myles, D., Chan, L., Sathyaragiswaran, L., Noguchi, T., Bongard, F.S., Cryer, G.H., Gaspard, D.J. (1998) Epidemiology of major trauma and trauma deaths in Los Angeles County. *J. Am. Coll. Surg.*, **187** (4), 373–383.

Heetveld, M.J., Harris, I., Schlaphoff, G., Balogh, Z., D'Amours, S.K., Sugrue, M. (2004) Hemodynamically unstable pelvic fractures: Recent care and new guidelines. *World J. Surg.*, **28**, 904–909.

Hsieh, K.S., Lee, C.L., Lin, C.C., Huang, T.C., Weng, K.P., Lu, W.H. (2004) Secondary confirmation of endotracheal tube position by ultrasound image. *Crit. Care Med.*, **32**, S374–S377.

Hyacinthe, A.C., Broux, C., Francony, G., Genty, C., Bouzat, P., Jacquot, C., *et al*. (2011) Diagnostic accuracy of ultrasonography in the acute assessment of common thoracic lesions after trauma. *Chest*, **141** (5), 1177–1183.

Kirkpatrick, A.W. (2007) Clinician-performed focused sonography for the resuscitation of trauma. *Crit. Care Med.*, **35**, S162–S172.

Kirkpatrick, A.W., Ball, C.G., D'Amours, S.K., Zygun, D. (2008) Acute resuscitation of the unstable adult trauma patient: Bedside diagnosis and therapy. *Can. J. Surg.*, **51**, 57–69.

Kirkpatrick, A.W., Ball, C.G., Rodriguez-Galvez, M., Chun, R. (2009) Sonographic depiction of the needle decompression of a tension hemo/pneumothorax. *J. Trauma*, **66** (3), 961.

Kirkpatrick, A.W., Sirois, M., Ball, C.G., Laupland, K.B., Goldstein, L., Hameed, M., *et al*. (2004) The hand-held FAST exam for penetrating abdominal trauma. *Am. J. Surg.*, **187**, 660–665.

Kortbeek, J.B., Al Turki, S.A., Ali, J., Antoine, J.A., Bouillon, B., Brasel, K., *et al*. (2008) Advanced trauma life support, 8th edition, the evidence for change. *J. Trauma*, **64** (6), 1638–1650.

Kristensen, M.S. (2011) Ultrasonography in the management of the airway. *Acta Anaesthesiol. Scand.*, **55** (10), 1155–1173.

Ma, O.J., Mateer, J.R., Ogata, M., Kefer, M.P., Wittman, D., Aprahamian, C. (1995) Prospective analysis of a rapid trauma ultrasound examination performed by emergency physicians. *J. Trauma*, **38**, 879–885.

Mohanty, K., Musso, D., Powell, J.N., Kortbeek, J.B., Kirkpatrick, A.W. (2005) Emergent management of pelvic ring fractures: an update. *Can. J. Surg.*, **48**, 49–56.

Plummer, D., Brunette, D., Asinger, R., Ruiz, E. (1992) Emergency department echocardiography improves outcome in penetrating cardiac injury. *Ann. Emerg. Med.*, **21** (6), 709–712.

Ract, C., Moigno, S., Bruder, N., Vigué, B. (2007) Transcranial Doppler ultrasound goal-directed therapy for the early management of severe traumatic brain injury. *Intensive Care Med.*, **33** (4), 645–651.

Rozycki, G.S., Feliciano, D.V., Ochsner, M.V., Knudson, M.M., Hoyt, D.B., Davis, F., Hammerman, D., Figueredo, V., Harviel, J.D., Han, D.C. (1999) The role of ultrasound in patients with possible penetrating cardiac wounds: a prospective multicenter study. *J. Trauma*, **46** (4), 543–551.

Rozycki, G.S., Feliciano, D.V., Oschner, G., Knudson, M.M., Hoyt, D.B., Davis, F., *et al*. (1999) The role of ultrasound in patients with possible penetrating cardiac wounds: a prospective multicenter study. *J. Trauma*, **46**, 543–552.

Rozycki, G.S., Ochsner, M.G., Feliciano, D.V., Thomas, B., Boulanger, B.R., Davis, F.E., *et al*. (1998) Early detection of hemoperitoneum by ultrasound examination of the right upper quadrant: A multicenter study. *J. Trauma*, **45**, 878–883.

Weaver, B., Lyon, M., Blaivas, M. (2006) Confirmation of endotracheal tube placement after intubation using the ultrasound sliding lung sign. *Acad. Emerg. Med.*, **13**, 239–244.

38

A Syndromic Approach with Sonography to the Patient with Abdominal Pain

Jonathan Fischer and Pablo Aguillera

Introduction

Abdominal pain accounts for 5–10% of all emergency department visits in the United States. Some causes of abdominal pain (e.g., acute abdominal aortic aneurysm) are rapidly and irreversibly progressive so that a swift diagnosis is essential for successful therapeutic intervention. Other disease processes are somewhat less time-sensitive (e.g., biliary colic), but immediate diagnosis by ultrasound increases the efficiency of the diagnostic work-up and decreases time to surgical intervention when indicated. The addition of sonography to the evaluation of patients with undifferentiated abdominal pain has been shown to significantly improve the clinician's diagnostic accuracy. Patient satisfaction is increased and the short-term use of healthcare resources reduced by bedside ultrasound. In this chapter, the aim is to discuss issues and approaches when using ultrasound as an adjunct in the evaluation of patients presenting with acute abdominal pain.

Background

Goal-Oriented Scanning

Point-of-care sonography is focused in scope. It is often directed to answering only a specific 'yes or no' question arising from the clinical setting; for example, "…does this patient have an abdominal aortic aneurysm (AAA)?" When evaluating undifferentiated abdominal pain the sonologist rarely has just one clinical question in mind; however, maintaining a dichotomous mindset for each of several possible diagnostic entities (e.g., "…does the patient have an AAA or impacted gallstone or spontaneous bacterial peritonitis?") will maintain the clinician's focus, and ensure a clear sense of both the goals and limitations of the sonographic examination.

Skill Development

Effective use of point-of-care ultrasound requires proficiency in image acquisition, image interpretation, and integration of the sonographic data into clinical decision-making. These skills require study, practice time and expert supervision. Studies on this subject are limited, but various data suggest that 15–40 hours of didactic training and two to four weeks of proctored practice provides adequate *basic* competency. It is *to be anticipated* that novice clinical sonographers will initially have difficulty in acquiring or interpreting images. However, after a relatively short period of learning most clinicians can use ultrasound to rapidly obtain important information at the bedside of many of their patients. Conversely, experienced sonologists

Emergency Point-of-Care Ultrasound, Second Edition. Edited by James A. Connolly, Anthony J. Dean, Beatrice Hoffmann and Robert D. Jarman.

Companion website: www.wiley.com/go/connolly/ultrasound

are always mindful of the limits of both their skills and the diagnostic test itself, being sure to correlate their sonographic findings with the patient's entire clinical picture.

General Technique

The fundamental elements of a high-quality ultrasound scan are:

- Scanning with a slow and steady motion.
- Identification of key anatomical features.
- Imaging structures in their entirety in two orthogonal planes.

A slow and steady scanning technique will help to identify both *subtle abnormalitie*s, such as the presence of a complex collection of free fluid in the right lower quadrant, and *small abnormalities*, such as a small stone in the neck of the gallbladder (GB) (see Figure 38.1). Anatomical landmark identification is critical. First, because it helps the sonographer to be certain that he/she is indeed interrogating the correct structure, for example, to avoid erroneous measurement of the superior mesenteric artery instead of the aorta (see Figure 38.2). Second, landmarks are needed to ensure a complete examination. For example, the fundus, body and the neck of the GB all need to be evaluated to reliably exclude cholelithiasis (see Video 38.1). Structures should be scanned in two orthogonal (i.e.. perpendicular) planes in order to thoroughly evaluate organs, to clarify the size and shape of pathological findings, and to define spatial relationships with neighbouring structures. Orthogonal scanning also frequently helps to differentiate between artifactual and real findings (see Figure 38.3).

Clinical Applications

Many factors contribute to the challenge of the sonographic evaluation of patents with suspected acute intra-abdominal pathology. These include: (i) the vague and referred nature of visceral pain sensation; (ii) the increasing prevalence of abdominal obesity; and (iii) the extremes of ages, such as aging populations (with a diminished perception of abdominal symptoms) and the young patient with a still-limited ability to communicate symptoms and region of pain. Point-of-care sonography is an efficient way to focus the evaluation, including the choice of alternative imaging tests.

Some diagnoses should be rapidly excluded by ultrasound, while others can be potentially confirmed. Although ultrasound is highly sensitive and specific for certain diseases (e.g., abdominal

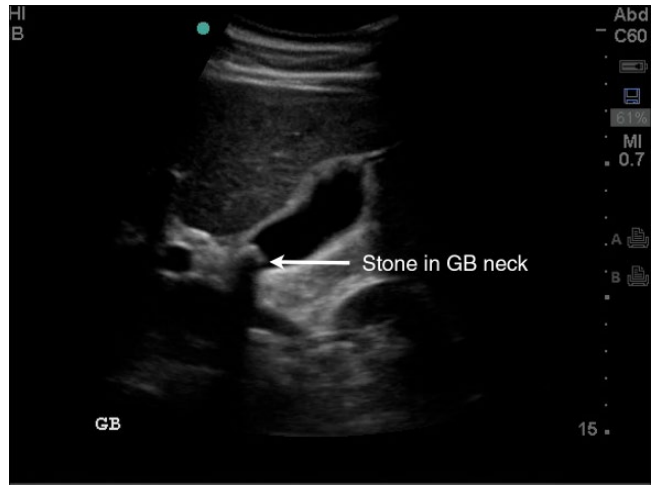

Figure 38.1 Slow scanning and close inspection of the entire structure enabled identification of this small stone in the gallbladder (GB) neck.

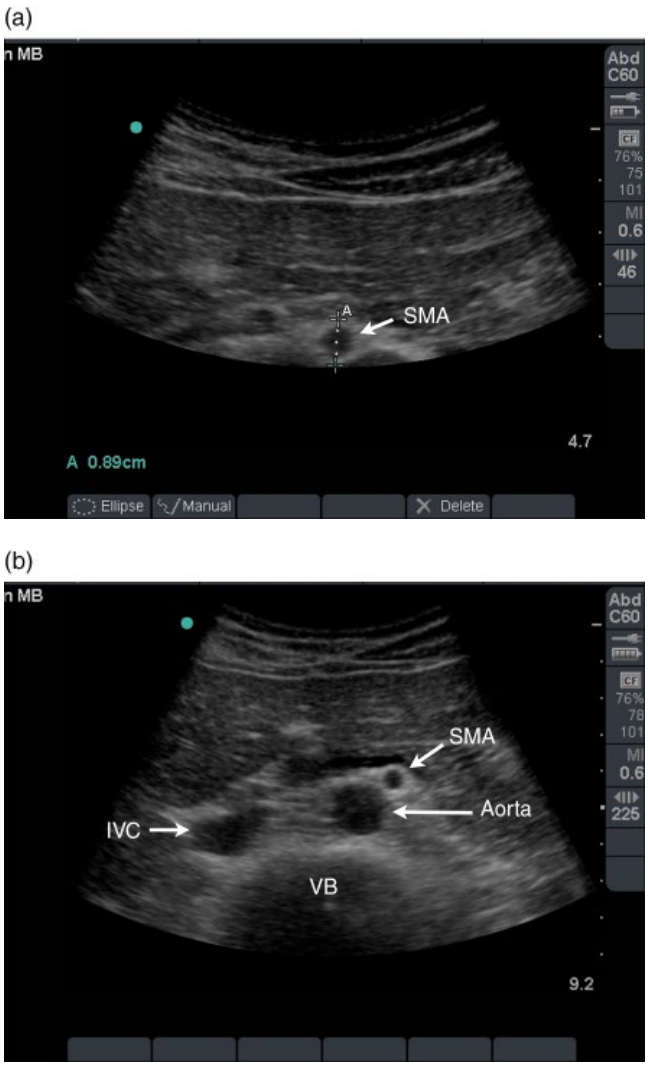

Figure 38.2 (a) The clinician sonographer has erroneously measured the superior mesenteric artery (SMA) rather than the aorta diameter. (b) The screen depth has been increased and the vertebral body (VB) can clearly be visualised, which enables accurate identification of the aorta, inferior vena cava (IVC) and SMA.

aortic aneurysm), clinician-performed sonography lacks the required high sensitivity to exclude some others. Consequently, if the clinician-performed ultrasound appears negative when there is significant clinical suspicion of pathology, further diagnostic exploration is warranted.

Potential Approach

The clinician should begin the ultrasound evaluation to evaluate for the most serious and emergent differential diagnosis. If AAA is likely, a leading differential diagnosis, the abdominal aorta and Morrison's pouch should be imaged first. If there is acute abdominal pain after colonoscopy and biopsy, the sonographer should check for free intra-abdominal air, and so forth.

A summary of bedside ultrasound findings, accuracy, and degrees of difficulty for various acute intra-abdominal conditions is listed in Table 38.1.

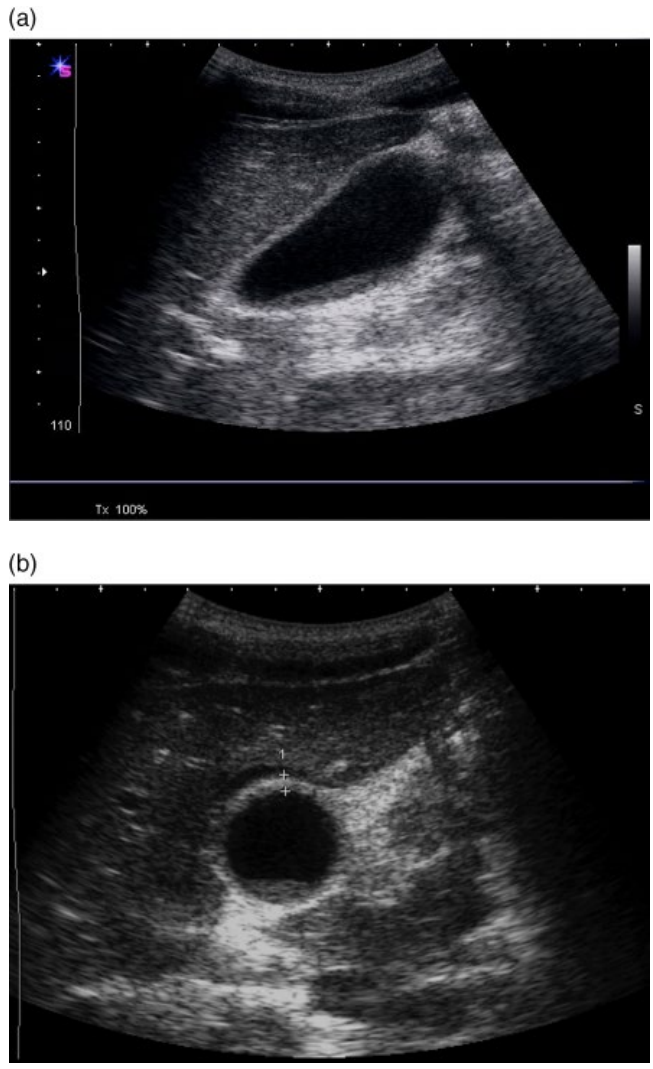

Figure 38.3 (a) This long-axis view of the gallbladder (GB) reveals a dependent echogenic layer. (b) It is only upon visualisation of the GB in the orthogonal plane that the layer can be confidently identified as sludge rather than a side lobe artifact.

Pearls and Pitfalls

Pearls

- *Ensure that you are physically comfortable while scanning.* Raise the gurney to a height that allows you to easily reach all scanning areas. Place the ultrasound machine so that you can view the screen without straining your back and neck (see Figure 38.4). Creating an ergonomic work-space will more than repay the time spent in set-up, and will avoid the tendency to perform a hurried or slip-shod examination due to muscle fatigue.
- *Know the basic ultrasound artifacts.* Keen recognition of artifacts is not only helpful for identifying artifactual findings, but it can often be the key to finding pathology. Artifacts related to pathological findings are sometimes easier to identify than the pathology itself, and it is only by knowing the artifact that a pathology can be diagnosed (see Figure 38.5).
- *Adjust for bowel gas.* Shadowing from bowel gas can frequently obstruct views during

Table 38.1 A summary of point-of-care ultrasound for intra-abdominal pathologies listed in approximate order of difficulty and required expertise.

Differential diagnosis	Sensitive enough to rule-out*	Specific enough to rule-in*	Scan difficulty	Key findings
Urinary retention	Yes	Yes	Beginner	High post-void residual bladder volume
Suspected ectopic	Yes	Unknown**	Beginner	
Abdominal aortic aneurysm	Yes	Yes	Beginner	Maximal aorta outer wall to outer wall measurement >3 cm
Intraperitoneal free fluid	No	Yes	Beginner	Anechoic fluid tracking adjacent to intra-abdominal organs and within potential spaces
Biliary colic with cholelithiasis	Yes	Yes	Beginner	Echogenic foci with shadowing. Sonographically, no signs of acute cholecystitis
Ileus	Yes	Unknown**	Advanced	Dilated loops of fluid-filled bowel with visible valvulae conniventes, increased peristalsis with rapid progression of contents and collapsed distal bowel
Cholecystitis	Yes	No	Intermediate	Sonographic Murphy's sign, ± gallbladder wall thickening, ± pericholecystic fluid
Appendicitis	No	Yes	Advanced	Blind-ended, non-compressible tubular structure that is >6 mm, non-peristalsing and tender to probe palpation
Intraperitoneal free air	No	Unknown**	Advanced	Hyperechoic areas with posterior reverberation artifact and free fluid with internal echoes that exhibit posterior reverberation
Intussusception	Unknown**	Unknown**	Advanced	'Target sign' or 'Pseudokidney sign'
Large bowel obstruction	Unknown**	No	Advanced	Colonic distention abruptly transitioning to collapsed bowel
Strangulated abdominal wall hernia	Yes	Unknown**	Advanced	
Diverticulitis	No	Unknown**	Advanced	Colonic mural thickening >5 mm, pericolic fat echogenicity changes, loss of compressibility, non-inflamed diverticula away from involved region, +/− visualisation of inflamed diverticula

* Assuming a technically adequate scan.

** There is insufficient data regarding this scan in the hands of clinician sonographers to determine this value. For scans where either sensitivity or specificity is known, but the other is listed as 'Unknown', the known value was determined based on studies with radiologists performing or interpreting the ultrasounds.

Figure 38.4 (a) The clinician sonographer is forced to strain his body to see the ultrasound screen because the machine is not positioned in front of him and the bed has not been raised. (b) After raising the gurney and removing a chair to allow proper placement of the ultrasound machine, the clinician sonographer can now scan comfortably.

sonography of intra-abdominal organs. The following manoeuvers may be helpful:
  - Apply steady pressure to the probe and simultaneously jiggle it to displace the bowel.
  - Use a lateral decubitus position to shift the intra-abdominal contents.
  - Use harmonic frequency scanning, if available.
- *Visualise the target from different angles.* For example, image the gallbladder neck both subcostally in the mid-clavicular line and intercostally from the anterior axillary line.
- *Make use of respiratory diaphragmatic excursion.* Respiratory movement of the upper abdominal organs caused by respiration can be a friend (not an enemy). Cooperative patients can be asked to 'take a deep breath and hold it'. For patients who cannot cooperate it is possible to systematically scan partly or completely through some organs (e.g., gallbladder or kidneys) by holding the probe still in the transverse plane while diaphragmatic excursion moves the target organ through the scaning plane.

Pitfalls

- ***Contradictory sonographic and clinical findings.*** When these occur, re-evaluate both the patient and the ultrasound findings. Use further imaging and/or laboratory testing as needed.
- ***Failure to recognise a study as limited and/or non-diagnostic.*** It is critical to acknowledge when it is not possible to perform a complete scan, or when poor image quality limits the ability to interpret the images. Some very important diagnoses (e.g., saccular abdominal aortic aneurysm) can easily be overlooked if any part of the complete organ is not visualised (see Figure 38.6). If a study is non-diagnostic, proceed as you would have if the ultrasound had not been performed at all.

(a)

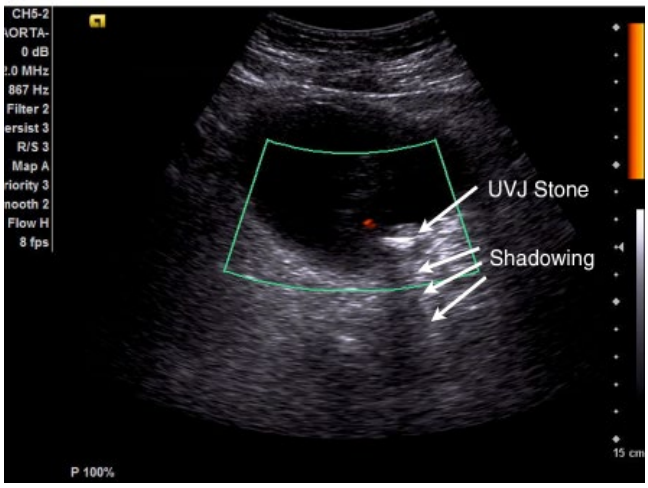

(b)

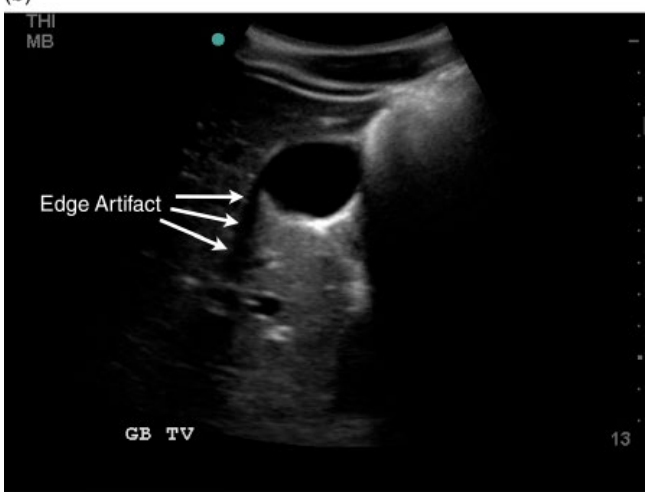

Figure 38.5 (a) Recognition of shadowing in the region of the left ureterovesicular junction (UVJ) led to identification of this UVJ stone. (b) Edge artifact (lateral cystic shadowing) is an artifactual finding which might easily be mistaken for a stone impacted in the gallbladder (GB) wall or neck. Sonographic interrogation in multiple planes can help confirm that the finding arises from the edge and not from within the GB.

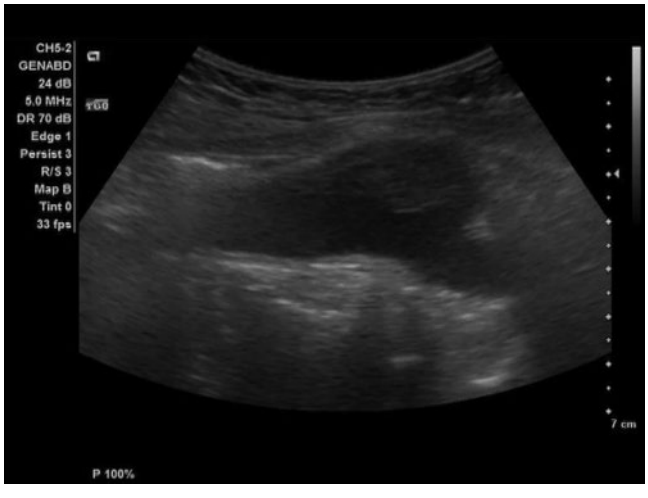

Figure 38.6 This saccular abdominal aortic aneurysm could have easily been missed if the entirety of the abdominal aorta was not visualised. Recognition of an inadequate study is critical to avoid false reassurance.

Further Reading

Kuhn, M., Bonnin, R., Davey, M.J., Rowland, J.L., Langlois, S.L.P. (2000) Emergency department ultrasound scanning for abdominal aortic aneurysm: accessible, accurate, and advantageous. *Ann. Emerg. Med.*, **36**, 219–223.

Laméris, W., van Randen, A., van Es, H.T., *et al.* (2009) Imaging strategies for detection of urgent conditions in patients with acute abdominal pain: diagnostic accuracy study. *Br. Med. J.*, **339**, b2431.

Lindelius, A., Törngren, S., Nilsson, L., Pettersson, H., Adami, J. (2009) Randomized clinical trial of bedside ultrasound among patients with abdominal pain in the emergency department: impact on patient satisfaction and health care consumption. *Scand. J. Trauma Resusc. Emerg. Med.*, **17**, 60.

Lindelius, A., Törngren, S., Pettersson, H., Adami, J. (2009) Role of surgeon-performed ultrasound on further management of patients with acute abdominal pain: a randomized controlled clinical trial. *Emerg. Med. J.*, **26**, 561–566.

Lindelius, A., Törngren, S., Sondén, A., Pettersson, H., Adami, J. (2008) Impact of surgeon-performed ultrasound on diagnosis of abdominal pain. *Emerg. Med. J.*, **25**, 486–491.

McCaig, L.F., Nghi, L. (2002) *National Hospital Ambulatory Medical Care Survey: 2000. Emergency Department Summary. Advance data from vital and health statistics, no. 326.* National Center for Health Statistics, Hyattsville, MD, p. 14.

Plummer, D., Clinton, J., Matthew, B. (1998) Emergency department ultrasound improves time to diagnosis and survival in ruptured abdominal aortic aneurysm [abstract]. *Acad. Emerg. Med.*, **5**, 417.

39

A Syndromic Approach to the Pregnant Patient

Joseph Wood

Introduction

The coexistence of pregnancy confers not just an increased risk of certain conditions but also an increased utility for point-of-care ultrasound, as it does not involve radiation and is repeatable over time. Previous syndrome-based approaches have been outlined for specific symptoms and should be referred to. In pregnancy, these may be augmented by the following considerations.

Abdominal Pain

Abdominal pain is a common complaint in pregnancy, and point-of-care ultrasound (PoCUS) may have great utility in aiding the diagnosis of these conditions.

Right Upper Quadrant (RUQ) and Epigastric Pain

In pregnancy there is an increased incidence of gallstone and sludge formation during pregnancy. In patients with upper abdominal pain or mid-back pain, a PoCUS examination of the RUQ can be very helpful.

Demonstrating the presence of gallstones with a positive sonographic Murphy's sign is highly suggestive of cholecystitis as the cause of the patient's pain.

The presence of pericholecystic fluid, and thickening of the anterior wall of the gallbladder in addition to a gallstone and sonographic Murphy's sign locks in the diagnosis of acute cholecystitis.

While gallstones are common in pregnancy, HELLP (triad of haemolysis, elevated liver enzymes and low platelets) must always be high in the initial diagnosis of any pregnant patient complaining of upper abdominal pain.

Flank and/or Back Pain

Symptomatic nephrolithiasis increases in the second and third trimesters of pregnancy. A transabdominal ultrasound examination is extremely helpful in detecting hydronephrosis and obstruction of the ureter (hydroureter).

The initial PoCUS view of the kidney should be a coronal view of both the RUQ and left upper quadrant (LUQ) (these views are identical to those utilised in a FAST examination). It is important to appreciate however that right-sided hydronephrosis may be physiological in pregnancy.

Pyelonephritis may manifest as fever and flank pain with urinary symptom. A PoCUS examination may be useful if it reveals coexisting pathology such as perirenal abscesses, calculi or obstruction.

The presence of these complications on PoCUS is likely to lead to more formal imaging studies.

Emergency Point-of-Care Ultrasound, Second Edition. Edited by James A. Connolly, Anthony J. Dean, Beatrice Hoffmann and Robert D. Jarman.

Companion website: www.wiley.com/go/connolly/ultrasound

Right Lower Quadrant (RLQ) Pain

Appendicitis should be a consideration in any patient with RLQ and/or right iliac fossa pain. Localised tenderness and rebound should not be attributed solely to pregnancy. Pregnant patients with these signs will usually require imaging studies of some form. Compression graded ultrasound may be a helpful diagnostic tool, but its accuracy is highly operator-dependent.

Clinicians who lack substantial experience with this sonographic imaging technique should defer to clinicians with demonstrated competence.

Positive sonographic findings include non-compressible, blind-ended and tubular multi-layered structures of maximal diameter >6 mm. It has been suggested that, in the right hands, the diagnostic accuracy of ultrasound in pregnant patients is similar to that in non-pregnant patients during the first and second trimesters. However a non- visualised appendix does not exclude appendicitis. The third trimester gravid uterus frequently obscures the ultrasound examination, such that other imaging studies or diagnostic laparoscopy are required.

Lower Abdominal Pain

Lower abdominal pain is a frequent complaint in pregnancy. PoCUS examinations may be used to demonstrate many pathologies, including ovarian cysts or urinary retention secondary to an incarcerated uterus.

Nausea/Vomiting

Nausea and vomiting are common problems during pregnancy, peaking at the five-week period and lasting for up to 20 weeks of gestation.

Hyperemesis is a condition that includes persistent nausea, vomiting and weight loss with the presence of ketonuria. The utility of ultrasound in this situation is in detecting the potential causes of hyperemesis (including gestational trophoblastic disease and multiple gestation, both of which are known to be risk factors for hyperemesis). Gestational trophoblastic disease shows a heterogeneous mass with multiple anechoic structures or a so-called 'snowstorm pattern' within the uterus.

RUQ ultrasound can also be used to evaluate the hepatobiliary system for hepatobiliary disease processes, as hyperemesis may cause mild elevations in liver enzymes.

Dyspnoea

Physiological changes during pregnancy include elevation of the diaphragm and an increased baseline respiratory rate. Therefore, subjective shortness of breath is a relatively common feature.

PoCUS is of immense value as it may help to detect other conditions, without the need for ionising radiation. Examples include:

- *Pulmonary oedema*: this can be induced by tocolytics, fluid overload and underlying cardiac disease. Comet-tail artefacts arising from lung-wall interfaces correlate not only with the presence of pulmonary oedema but also with its severity.
- *Pneumonia*: this is a clinical diagnosis and often requires chest X-radiography, although consolidation may be suggested on sonographic evaluation of the chest (see Chapter 2), so that the use of X-rays may potentially be avoided.
- *Pulmonary embolus (PE)*: Pregnancy is accompanied by an increased risk of thromboembolism. In patients with otherwise unexplained shortness of breath, a PoCUS examination demonstrating deep-vein thrombosis (DVT) will greatly favour pulmonary emboli as the cause of the patient's dyspnoea (though a negative DVT scan does not exclude PE). Similarly, right ventricular dilatation in this scenario is highly predictive, but again not always present.

Trauma

All female trauma patients of reproductive age receiving a Focused Assessment with Sonography in Trauma (FAST) in trauma should

ideally also be screened as part of that scan for pregnancy, since this is highly likely to lead to modifications of the subsequent trauma evaluation and management.

An enlarged uterus reduces the risk of visceral injury, small bowel injury, and damage to retroperitoneal structures.

The FAST exam is used as per normal to detect haemoperitoneum, tamponade and haemothorax. It can also be used to evaluate the foetal heart rate. This is especially useful as a rapid reassurance following trauma; however, this simple PoCUS should generally be followed by more formal foetal monitoring.

If a subchorionic haematoma is observed, placental abruption is likely, although an absence of this finding does not rule out abruption. Unfortunately, the sensitivity of ultrasound for placental abruption is only about 50%.

Vaginal Bleeding

- *First trimester bleeding*: For details of first-trimester bleeding see Chapter 11.
- *Late pregnancy bleeding*: After the first trimester the rate of ectopic pregnancy will diminish. In late pregnancy, as placental maturity increases, bleeding is more likely due to *placenta praevia*. In painless vaginal bleeding of late pregnancy the priority is thus to check the placental location by using transabdominal ultrasound in order to rule out praevia prior to a pelvic examination. If pain is present with a vaginal bleed, the important differential is placental abruption. Unfortunately, ultrasound is not sensitive enough to detect retroplacental haematoma.
- *Post partum bleeding*: Primary post-partum haemorrhage occurs within 24 hours of birth. Secondary haemorrhage occurs between 24 hours and 12 weeks post-partum.

During the evaluation of Vaginal bleeding an examination should be made for any intra-uterine abnormality, such as clots or retained products. Transabdominal/transvaginal ultrasound is thus a useful adjunct to speculum examination.

Difficult Labour in a Resource-Poor/Austere Environment

In resource-poor environments or rural settings the identification of certain specific conditions is an area where future developments may be aimed to reduce foeto-maternal mortality. The recognition of *multiparous pregnancy*, *abnormal lie* and *placenta praevia* should prompt early transfer to a centre that can better manage these conditions.

Pearls and Pitfalls

- Point-of-care ultrasound has great potential in pregnancy to reduce the exposure of patients to ionising radiation.
- Point-of-care ultrasound has a sensitivity of only 50% for abruption.
- All FAST scans in females of child-bearing age should seek pregnancy.
- Screening dyspnoeic pregnant patients is likely to lead to more rapid, appropriate investigations.
- In lower abdominal pain of pregnancy a non-visualised appendix does not exclude appendicitis.

Further Reading

Available at: http://www.guideline.gov/summary/summary.aspx?doc_id=13683&nbr=007017&string=pyelonephritis

Awwad, J.T., Azar, G.B., Seoud, M.A., Mroueh, A.M., Karam, K.S. (1994) High-velocity penetrating wounds of the gravid uterus: review of 16 years of civil war. *Obstet. Gynecol.*, **83** (2), 259.

Barloon, T.J., Brown, B.P., Abu-Yousef, M.M., Warnock, N., Berbaum, K.S. (1995) Sonography of acute appendicitis in pregnancy. *Abdom. Imaging*, **20** (2), 149.

Cusick, S.S., Tibbles, C.D. (2007) Trauma in pregnancy. *Emerg. Med. Clin. North Am.*, **25**, 861–872.

Larrey, D., Rueff, B., Feldmann, G., Degott, C., Danan, G., Benhamou, J.P. (1984) Recurrent jaundice caused by recurrent hyperemesis gravidarum. *Gut*, **25** (12), 1414.

Lichtenstein, D., Mézière, G., Biderman, P., Gepner, A., Barré, O. (1997) The comet-tail artifact. An ultrasound sign of alveolar-interstitial syndrome. *Am. J. Respir. Crit. Care Med.*, **156** (5), 1640–1646.

Rasmussen, P.E., Nielsen, F.R. (1988) Hydronephrosis during pregnancy: a literature survey. *Eur. J. Obstet. Gynecol. Reprod. Biol.*, **27** (3), 249.

Stothers, L., Lee, L.M. (1992) Renal colic in pregnancy. *J. Urol.*, **148** (5), 1383.

40

The Use of Ultrasound in Evaluating Dyspnoea/Respiratory Distress in Infants and Children

Roberto Copetti and Luigi Cattarossi

Lung Diseases of the Newborn

Transient Tachypnoea of the Newborn

Transient tachypnoea of the newborn (TTN) is a common cause of neonatal respiratory distress, which has a similar frequency worldwide. TTN has low morbidity, but it can be severe and should be differentiated from other pulmonary or cardiac diseases (such as pneumothorax, pneumonia, sepsis, respiratory distress syndrome and congenital heart disease).

All infants with TTN show, on the first ultrasound examination, bilateral coalescent B-lines of the lung base (echographic 'white lung') and a normal or near-normal appearance of the lung in the superior fields. This finding is evident in both lungs, though not always symmetrically. The bound between the inferior pulmonary fields, where the artifacts are coalescent, and the superior fields is so sharp that the lung picture is specific. It is important to note that the pleural line is normal also in the areas of 'white lung'. This ultrasound finding was named 'double lung point' because it seems to observe two contiguous different lungs in the same patient (Figure 40.1; Video 40.1).

Respiratory Distress Syndrome

Neonatal respiratory distress syndrome (RDS), also known as hyaline membrane disease, is due – at least in part – to an insufficiency of pulmonary surfactant, and is mainly confined to preterm infants.

All infants show B-lines, which are coalescent, diffuse and symmetrically distributed in both lungs (Video 40.3). This pattern determines a picture of echographic 'white lung'. The pleural line is always extensively thickened, irregular, not well-defined and coarse. Multiple subpleural hypoechoic areas that are generally small are observed mainly in the posterior and lateral scans, indicating lung consolidations. Larger consolidations with a tissular pattern and with evidence of air or fluid bronchograms may be observed more frequently in the posterior fields. These findings are immediately present at birth before clinical deterioration. Scans of the anterior thoracic wall are sufficient for the diagnosis.

The three most important signs for the ultrasound diagnosis are: (i) bilateral coalescent B-lines involving all the lung ('white lung'); (ii) and absence of spared areas (areas of lung with a normal appearance); and (iii) pleural line abnormalities (Figure 40.2; Video 40.2).

Bronchopulmonary Dysplasia

Bronchopulmonary dysplasia (BPD) is a form of chronic lung disease that develops in preterm neonates treated with oxygen and positive-pressure ventilation. The diagnosis is made on the basis of oxygen requirements at 36 weeks' gestation.

Emergency Point-of-Care Ultrasound, Second Edition. Edited by James A. Connolly, Anthony J. Dean, Beatrice Hoffmann and Robert D. Jarman.

Companion website: www.wiley.com/go/connolly/ultrasound

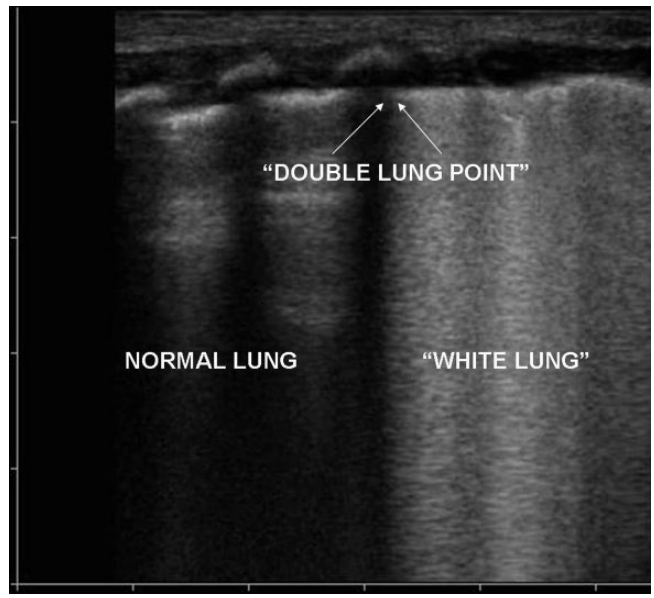

Figure 40.1 Longitudinal scan showing a clear sharp difference between the upper and lower lung fields ('double lung point').

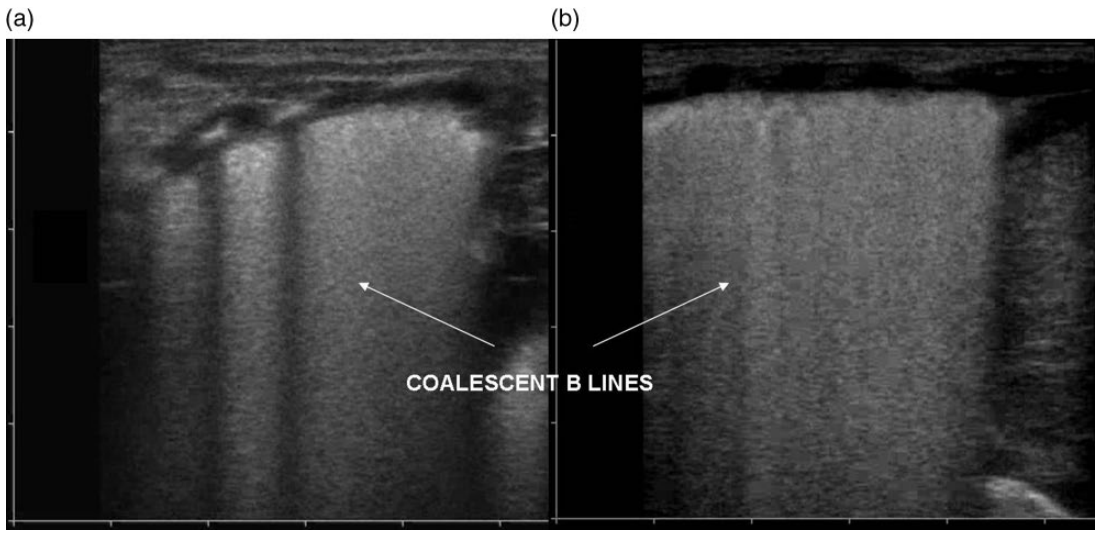

Figure 40.2 Superior field of the lung (a) and inferior field (b) in a newborn with respiratory distress syndrome. In both areas there is evidence of coalescent B-lines ('white lung'). The pleural line is not well defined and coarse.

In infants with BPD there is evidence of multiple B-lines that have a non-homogeneous distribution, with diffuse changes in the pleural line that is thickened with multiple small subpleural consolidations. Generally, there is evidence of spared areas and the entity of alveolar-interstitial syndrome and pleural line changes correlate to the severity of the clinical stage (Figure 40.3).

Pulmonary Atelectasis

Pulmonary atelectasis is a frequent occurrence in ventilated newborns. Often, chest X-radiography diagnosis is difficult due to the underlying

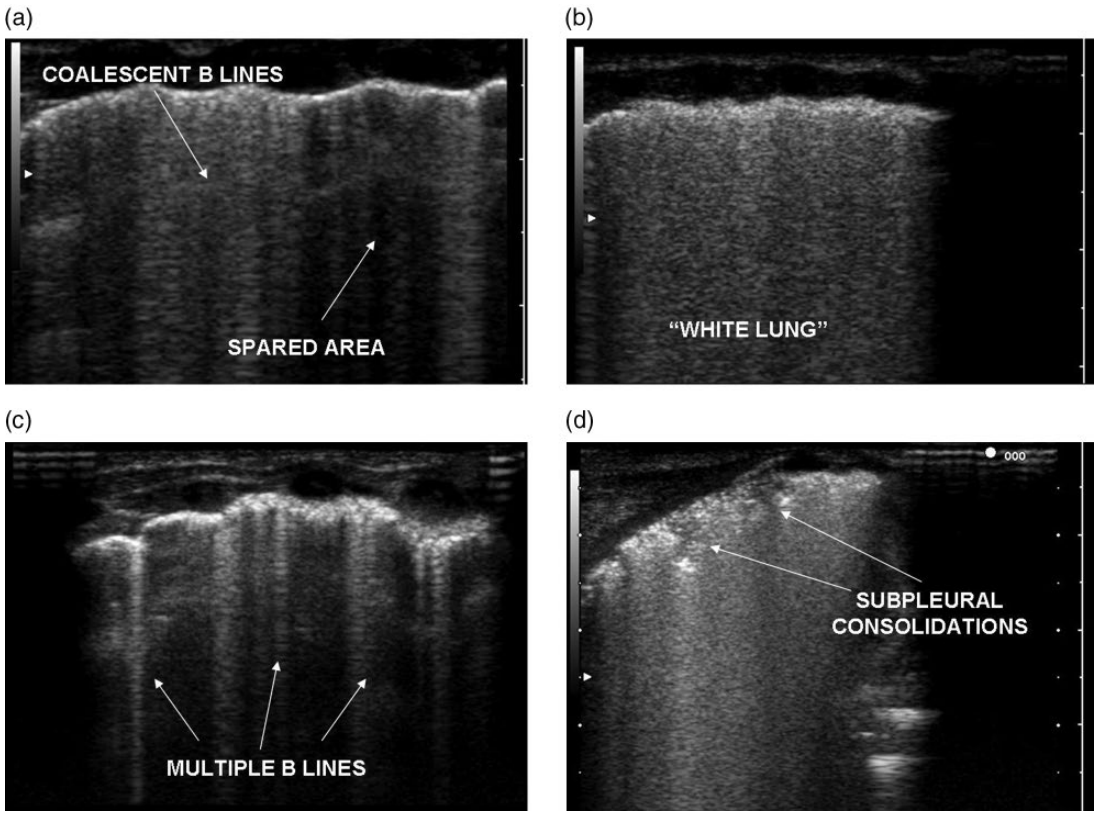

Figure 40.3 (a–d) Different images of lung areas of infants with bronchopulmonary dysplasia.

respiratory disease. The dynamic ultrasound signs are very useful for the diagnosis. and may be monitored at the bedside.

The ultrasound appearance of atelectasis is characterised by a liver-like appearance of the lung with 'lung pulse', an absence of lung sliding and a parallel course of air bronchograms, as described in adult patients (Figure 40.4). The evidence of dynamic air bronchograms rules out obstructive atelectasis. These data are very important because lung consolidation may often be caused by alveolar collapse (i.e., pulmonary haemorrhage, RDS) and in ventilated newborns by hypoventilation due to insufficient ventilatory pressure.

Pneumothorax

Pneumothorax is frequent in newborns. Chest X-radiography has the same diagnostic limitation that is well-known in adults. Transillumination is the bedside procedure used by neonatologists. The ultrasound signs are the same as described in adults, namely: (i) an absence of 'lung sliding'; (ii) an absence of B-lines; and (iii) the presence of 'lung point' in a non-massive pneumothorax (Video 40.4).

Lung Diseases of the Infant and Child

Bronchiolitis

Bronchiolitis is an acute, infectious, inflammatory disease of the upper and lower respiratory tract that may result in obstruction of the small airways. Diagnosis is made based on age and seasonal occurrence, tachypnoea and the presence of profuse coryza and fine rales, wheezes (or both) upon auscultation of the lungs.

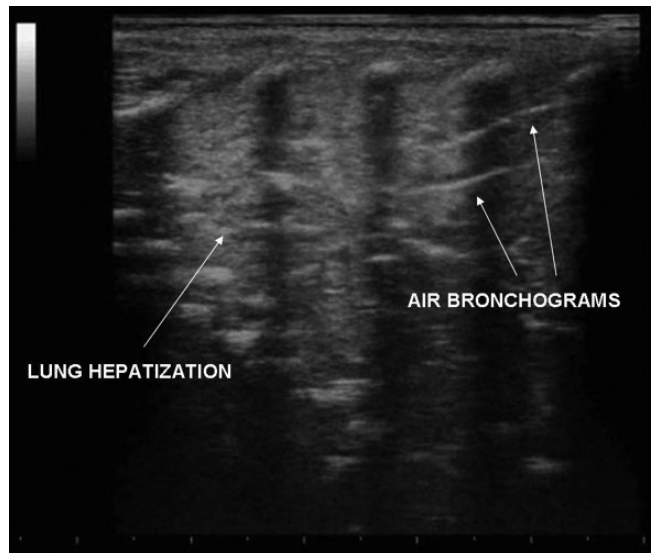

Figure 40.4 Liver-like appearance of the lung and parallel course of air bronchograms in pulmonary atelectasis.

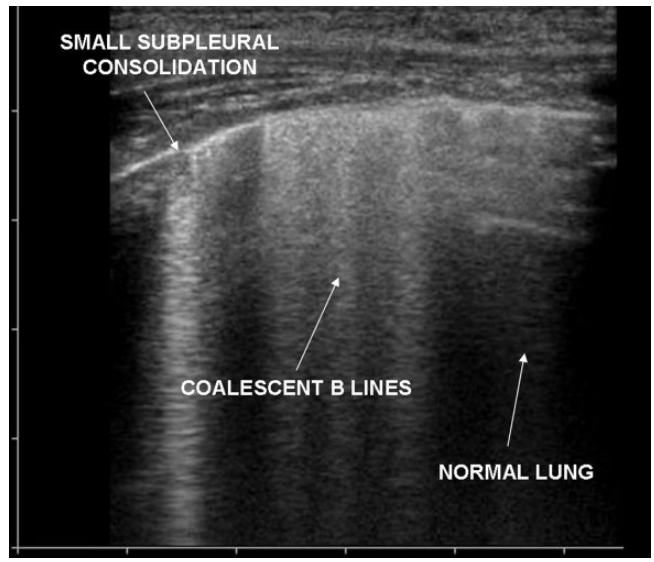

Figure 40.5 Typical picture of bronchiolitis with evidence of a small subpleural consolidations, and an area of coalescent B-lines near an area of normal lung.

Often the ultrasound findings are peculiar, and this is important because in some patients with more severe symptoms chest X-radiography may be avoided.

In patients with bronchiolitis, bilateral involvement of the lungs was constantly observed. Typically, areas of normal lung are observed adjacent to areas with subpleural consolidations (1–3 cm) due to small areas of atelectasis. These consolidations are surrounded by B-lines that can appear coalescent (Figure 40.5). Larger consolidations are less frequent and generally observed in more severe disease. Small pleural effusions can also be seen.

Pneumonia

Children and infants with pneumonia may present with a number of clinical symptoms and signs, such as fever, cough and tachypnoea.

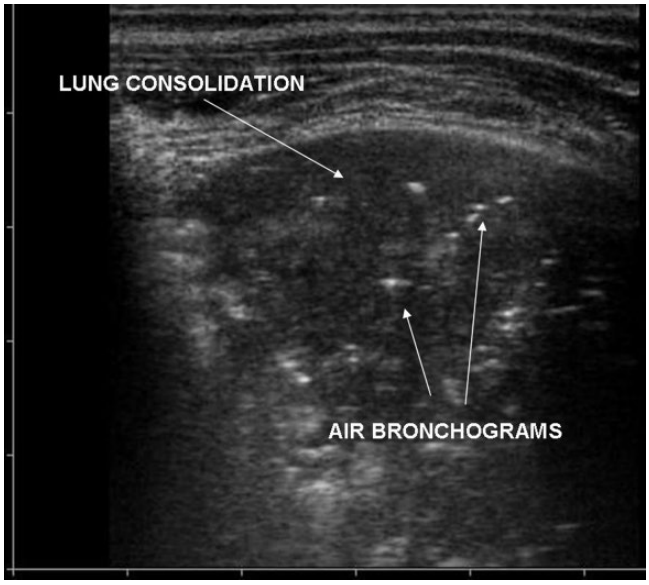

Figure 40.6 Typical ultrasound image of pneumonia in a paediatric patient with hyperechoic air bronchograms. In real time these would be seen to move together and apart with respiration, indicating that they are arborizing tubular structures. The transition from consolidated to normal lung is typically "shredded" in appearance.

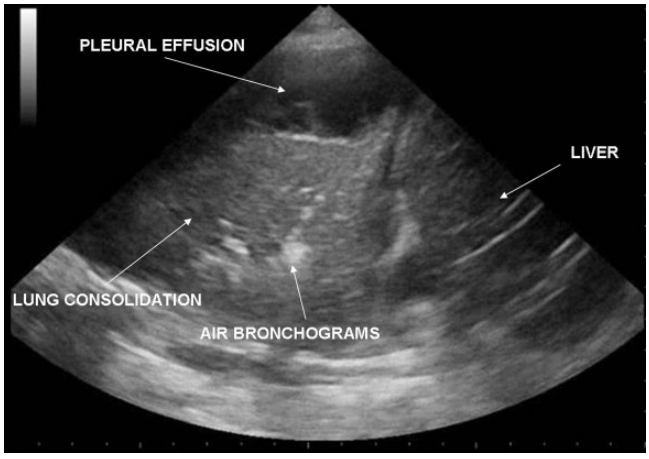

Figure 40.7 Another typical image of pneumonia, but in this case, in contrast to that Figure 40.6, there is an overlying effusion. The appearance of the diaphragm with an overlying consolidation in this image should be contrasted with its usual echogenic appearance (caused by impedance mismatch) when abutted by normal (air-filled) lung.

A minority of children present with fever of unknown origin and may have no respiratory symptoms or signs. Chest X-radiography is still considered to be the first imaging step for diagnosing pneumonia in children.

In children, pneumonia appears as a hypoechogenic area with poorly defined borders and compact underlying comet tail artifacts. Vertical artifacts in varying numbers are often seen in areas adjacent to the consolidation. The pleural line is less echogenic in the area affected by lung consolidation. Lung sliding is reduced or absent. In the case of large consolidations, branching echogenic structures – representing air bronchograms – are seen in the infected area. Dynamic air bronchograms can be observed, and this finding rules out atelectasis. Multiple lenticular echoes, representing air-trapping in the smaller airways, are also frequently present. Fluid bronchograms, described in post-obstructive pneumonia, are identified as anechoic tubular structures, with hyperechoic walls and without a colour-Doppler signal. Pleural effusion is easily detected on ultrasound and appears as an anechoic area in the pleural space (Figures 40.6–40.8).

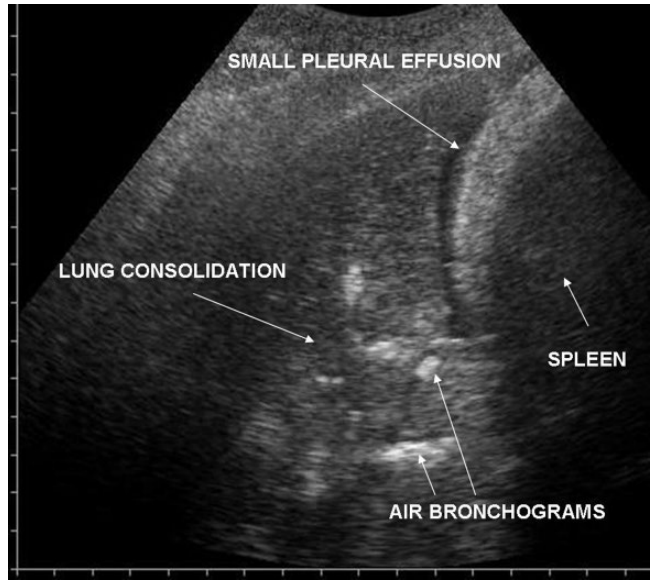

Figure 40.8 In this case, the upper part of the image shows almost complete atelectasis, indicated by the absence of air bronchograms. The lower part of the image shows a few air-filled bronchi. There is a subpulmonic effusion adjacent to the diaphragm.

In pediatric patients, as in adults, lung ultrasound demonstrates a diagnostic accuracy that is higher than, or at least not inferior to, that of chest X-radiography.

Further Reading

Copetti, R., Cattarossi, L. (2007) The 'double lung point': an ultrasound sign diagnostic of transient tachypnea of the newborn. *Neonatology*, **91**, 203–209.

Copetti, R., Cattarossi, L. (2008) Ultrasound diagnosis of pneumonia in children. *Radiol. Med.*, **113** (2), 190–198.

Copetti, R., Cattarossi, L., Macagno, F., *et al*. (2008) Lung ultrasound in respiratory distress syndrome: a useful tool for early diagnosis. *Neonatology*, **94** (1), 52–59.

Lichtenstein, D., Mezière, G., Seitz, J. (2009) The dynamic air bronchogram. A lung ultrasound sign of alveolar consolidation ruling out atelectasis. *Chest*, **135** (6), 1421–1425.

Lichtenstein, D.A., Lascols, N., Prin, S., *et al*. (2003) The 'lung pulse': an early ultrasound sign of complete atelectasis. *Intensive Care Med.*, **29** (12), 2187–2192.

41

Point-of-Care Ultrasound for Human Immune-Deficiency Virus (HIV) and Tuberculosis (TB) Co-Infection: The FASH Scan

Hein Lamprecht

Introduction

New tuberculosis (TB) infections are surging in patients infected with the human immune-deficiency virus (HIV). This is a concerning trend that largely affects communities in under-developed nations, where patients at high risk live in densely and extremely poor living conditions with limited access to healthcare.

Healthcare facilities in low-resource settings are usually severely overcrowded. The 2007 World Health Organization (WHO) guidelines for diagnosing TB in HIV-positive patients make point-of-care ultrasound ideally suitable for diagnosing the TB co-infection in smear-negative patients (Figure 41.1). Clinicians trained in bedside ultrasound may gain immediate access to imaging results, and are able to expedite the diagnosis and treatment of both infections with significant morbidity and mortality benefit. The impact of point-of-care imaging is amplified where comprehensive formal imaging access may be delayed due to nearly non-existent healthcare infrastructure and depleted resources.

Relationship Between HIV and TB

HIV has changed the pathology, histology, clinical presentation and epidemiology of TB. Between 20% and 25% of all newly diagnosed TB patients, who are co-infected with HIV, present with extrapulmonary tuberculosis (EPTB). Furthermore, 76% of all HIV patients who present with EPTB have CD4 counts of less than 100 per microlitre.

PTB and disseminated TB (spread via blood or lymphatic system) are both regarded as AIDS-defining conditions. The most common sites for EPTB, in order of prevalence, are: lymph glands, pleura, genitourinary tract, skeletal, joints, meninges, small and large bowel, peritoneum, pericardium and skin.

Role of Point-of-Care Ultrasound in High-Prevalence HIV and TB Co-Infection Settings

HIV patients who are suspected to have TB co-infection should be worked-up diagnostically as per the latest 2007 WHO guidelines (see Figure 41.1).

TB sputum testing is the first step in diagnosing TB co-infection. The WHO 2007 guidelines recommend two sputum tests to improve the low single-smear yield. All TB-positive sputum test patients should be started immediately on a TB treatment regime followed by an antiretroviral regime.

HIV patients who test negatively on their TB sputum should continue with their diagnostic work-up aided by supplementary investigations.

Emergency Point-of-Care Ultrasound, Second Edition. Edited by James A. Connolly, Anthony J. Dean, Beatrice Hoffmann and Robert D. Jarman.

Companion website: www.wiley.com/go/connolly/ultrasound

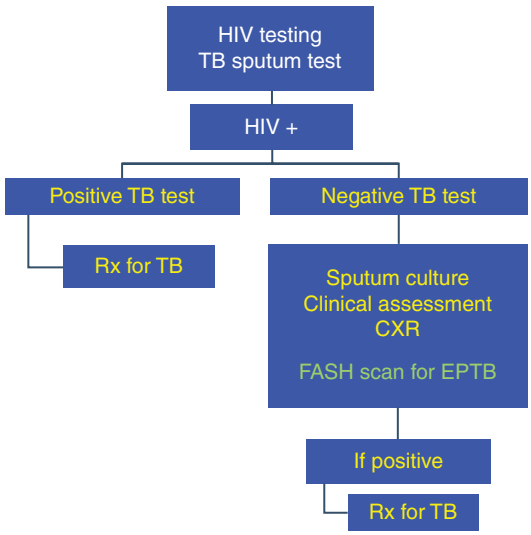

Figure 41.1 Simplified flow chart of HIV testing and TB screening and treatment.

The respective yields for confirming TB diagnosis are:

- Chest X-radiography examination (CXR) – 17.6%.
- Comprehensive clinical assessment – 41.2%.
- Ultrasound imaging (FASH point-of-care or comprehensive consultative ultrasound) – 41.2%.
- Sputum culture – 70% for single sputum sample and 91% for two sputum samples. However, sputum cultures can take up to eight weeks to provide results.

Patients who confirm positive for TB with any of these diagnostic aids should also be immediately started on TB treatment followed by an HIV treatment regime.

Focussed Assessment with Sonography in HIV/TB (FASH Scan)

The term FASH ultrasound scan examination was first coined by Dr Tom Heller, a physician with special interest in infectious diseases, while working in rural Southern Africa. The FASH scan examination includes a key list of ultrasound findings according to the ease of skill required to perform the examination and their diagnostic and therapeutic significance. The aim of the FASH scan ultrasound examination is to identify EPTB sites in HIV-positive patients who have tested negative on both their TB sputum smears (see Figure 41.1 and Table 41.1).

FASH Scan and Diagnosis of AIDS

Research has shown that 76% of HIV patients with EPTB have CD4 counts less than 100 μl^{-1}. Imaging investigations (including the FASH scan) increase the likelihood of detecting the presence of EPTB in patients who may be otherwise difficult to diagnose due to the low sputum TB testing yield. All HIV patients who are diagnosed with EPTB are categorised as stage 4 disease. Their outcomes will be improved by immediate TB antimicrobial treatment and co-trimoxazole antibiotic prophylaxis, followed by antiretroviral treatment after the shortest possible time interval. The risk of immune reconstitution inflammatory syndrome (IRIS) should deter the length of the time interval prior to commencing HIV treatment.

The FASH scan components have varying value in predicting the presence of EPTB. In HIV patients pericardial effusions are 90.5% likely to be caused by TB. The detection of abdominal lymph nodes is 97.1% specific for EPTB, with a positive likelihood ratio of 11.4. The presence of multiple TB splenic abscesses is an indicator of a severely immune-compromised patient. The FASH scan has the dual benefit of detecting EPTB and grossly predicting the severity of the patient's immune status suppression.

Role of the FASH Scan in Low-Prevalence HIV and TB Co-infection Settings

The FASH scan test's sensitivity and specificity for detecting EPTB in HIV co-infected patients are 95.5% and 98.5%, respectively.

Table 41.1 The FASH scan components.

Views	Objectives	Technique and probe selection
1. Perihepatic view (Figures 41.2 and 41.3)	To identify intraperitoneal fluid (ascites) in Morrison's pouch and perihepatic space. To identify right pleural effusion	Similar to the FAST scan. Refer to Chapter 8.
2. Perisplenic view (Figure 41.4)	To indentify intraperitoneal fluid (ascites) in the perisplenic space. To identify left pleural effusion	Similar to the FAST scan. Refer to Chapter 8.
3. Sub-xiphoid view (Figure 41.5)	To identify fluid (effusion) in the pericardial space	Similar to the FAST scan. Refer to Chapter 8.
4. Pelvic view (Figure 41.6)	To identify intraperitoneal fluid (ascites) in the retro- and perivesicle spaces	Similar to the FAST scan Refer to Chapter 8.
5. Liver sweep (Figure 41.7)	To identify focal fibrotic/ hyperechoic (granulomatous) and hypoechoic (micro-abscess) hepatic lesions. To identify hepatomegaly	Repeat the sweep with both low- and high-frequency probes to increase the sensitivity in identifying the lesions. Sweep from the left lobe's external border to the right lobe's external border in both the horizontal and vertical planes, using both probes.
6. Spleen sweep (Figure 41.8)	To identify multiple focal lytic spleen lesions and micro-abscesses	Repeat the sweep with both low- and high-frequency probes to increase the sensitivity in identifying lesions. Sweep all areas in both the spleen's long and short axes.
7. Aorta, iliac and portal vessels sweep (Figures 41.9 and 41.10)	To identify perivascular intra-abdominal lymph nodes, >1.0 cm in diameter (especially paraortic, coeliac and iliac artery regions).	Sweep all vessels in both the transverse and sagittal planes, starting at point where the aorta enters the abdomen, behind the liver, moving the probe distal to the aorta bifurcation, continuing down both iliac vessels until they disappear from view. Identify and follow the hepatic artery as it leaves the aorta in the transverse position, joined by the portal vein and common bile duct until all three structures disappear into the liver parenchyma.

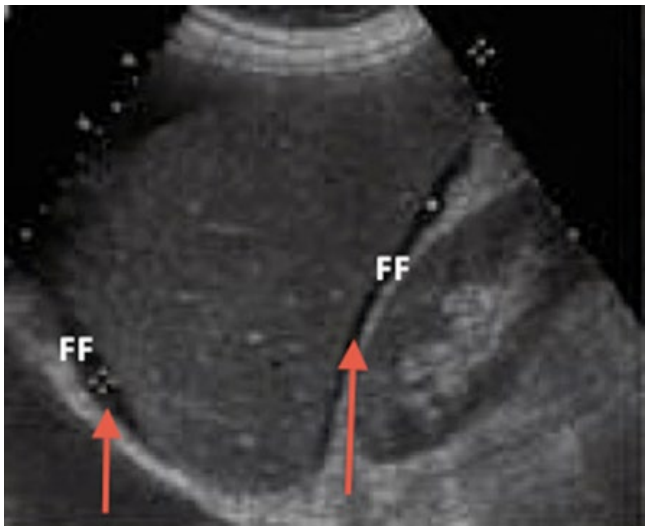

Figure 41.2 Perihepatic view ascites.

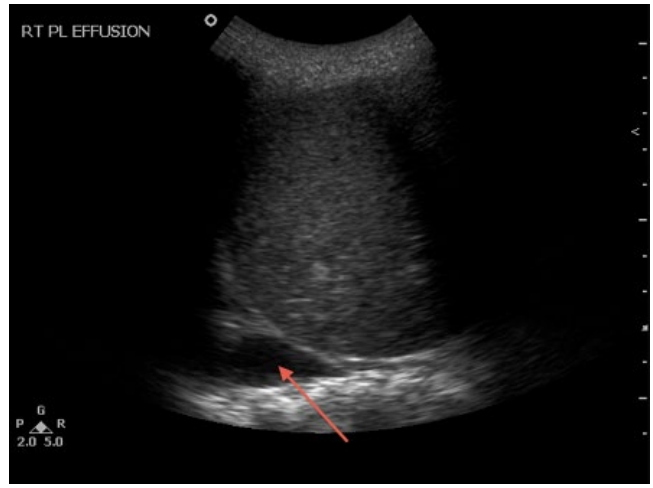

Figure 41.3 Perihepatic view, right pleural effusion.

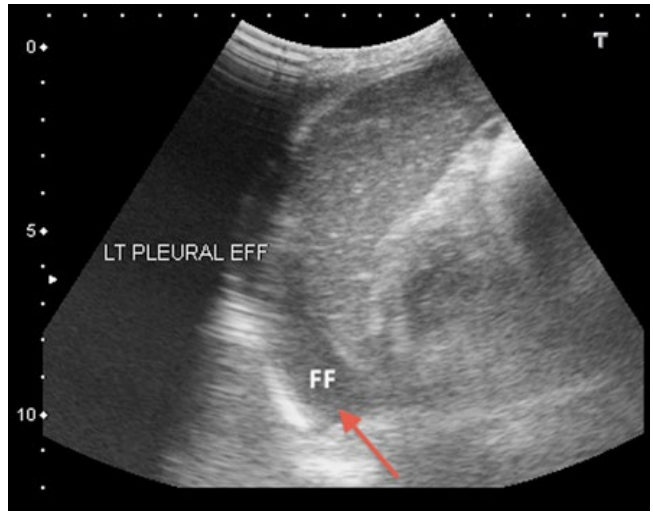

Figure 41.4 Perisplenic view, left pleural effusion.

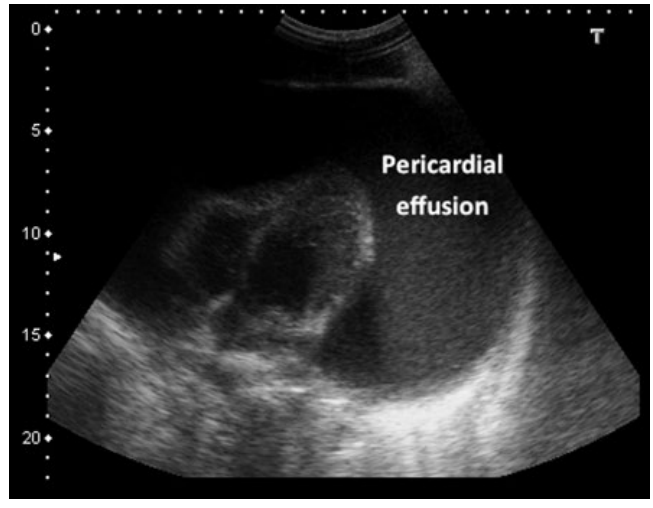

Figure 41.5 Sub-xiphoid view, pericardial effusion.

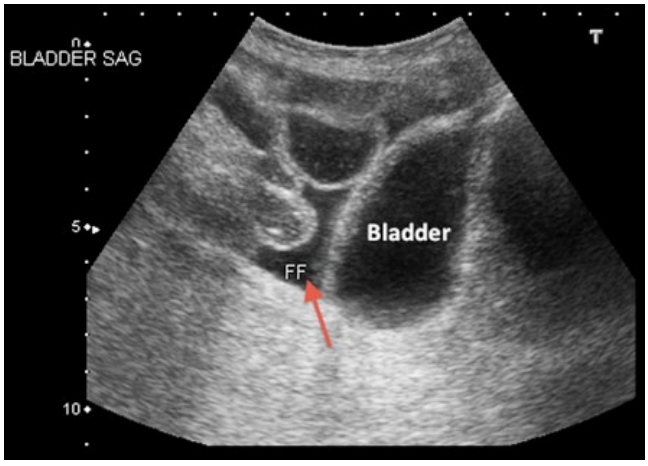

Figure 41.6 Pelvic view, ascites.

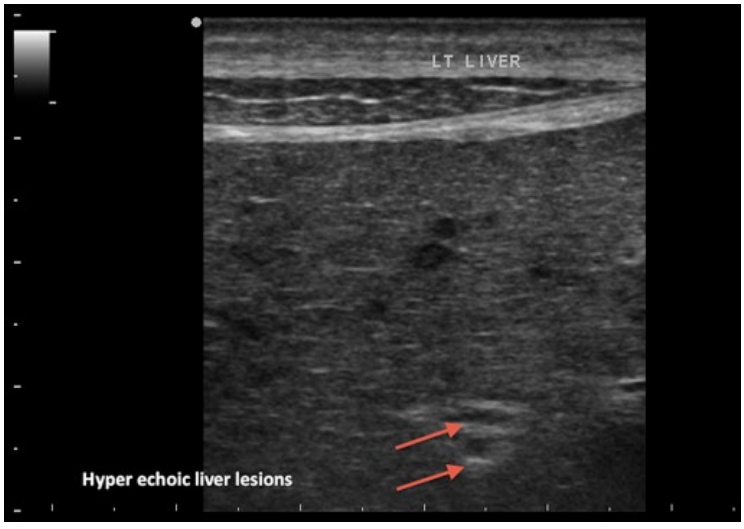

Figure 41.7 Hepatic view, micro-abscesses and hyperechoic lesions.

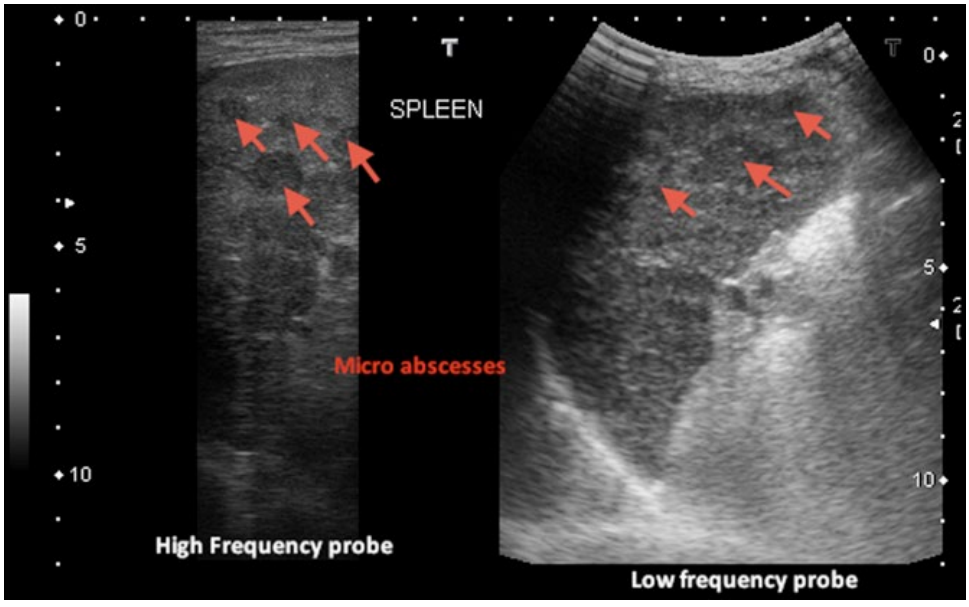

Figure 41.8 Splenic view, micro-abscesses show more clearly when using a high-frequency probe.

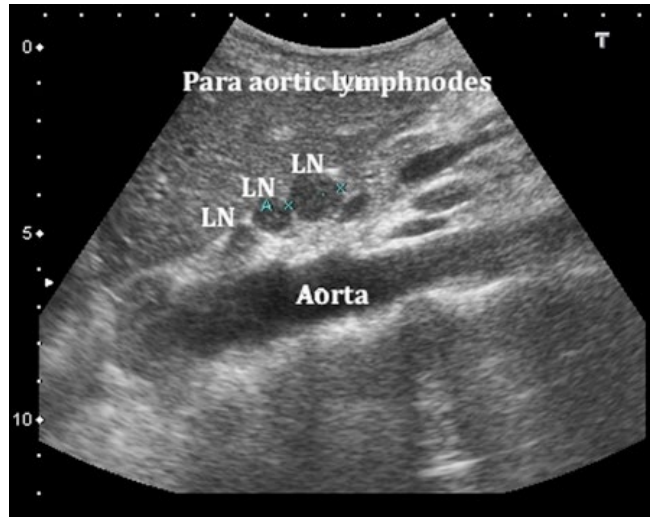

Figure 41.9 Longitudinal aorta/superior mesenteric artery view revealing multiple perivascular lymph nodes.

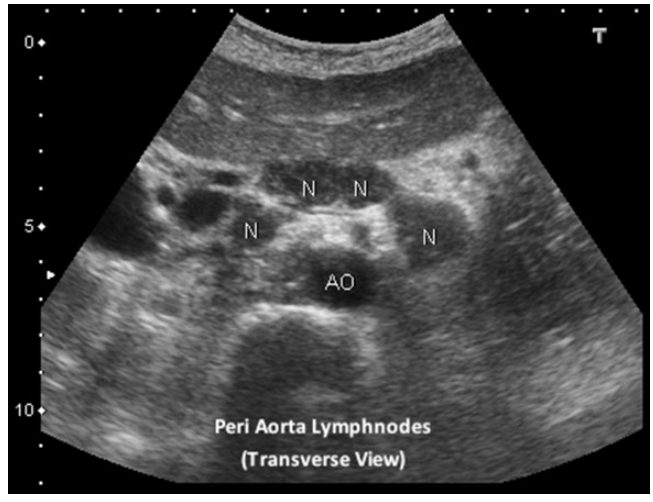

Figure 41.10 Transverse aorta/superior mesenteric artery view revealing the same multiple perivascular lymph nodes.

In high-prevalence settings the positive predictive value (PPV) will be high and the negative predictive value (NPV) low, which renders the test valuable as a supplementary diagnostic aid. Where the prevalence of HIV and TB co-infections is low, the PPV will be low and NPV high, which undermines the FASH scan's validity as a front-line diagnostic test. Fortunately, in many of these low-HIV/TB prevalence settings patients have access to well-developed healthcare systems with effective alternative HIV/TB diagnostic tests.

For instance, in 2007 there were 948 new cases of TB per 100 000 of the population diagnosed in South Africa, of which 73% were co-infected with HIV. If these figures are compared indirectly to the United Kingdom's incidence of 15 new cases of TB per 100 000 population in 2010, of which none was co-infected with HIV, the FASH scan's external validity as a diagnostic test is questionable due to basic clinical epidemiological principles.

However, the common advantage for using the FASH scan is the speed at which ultrasound images can be created, especially in high-risk patients. If the clinician detects any of the positive FASH scan findings, high-risk TB/HIV patients should be isolated until the final diagnosis is known.

Pearls and Pitfalls

Notable advantages and disadvantages of the FASH scan include:

- It assists in diagnosing EPTB in sputum-negative patients with confirmed HIV.
- It has a high positive predictive value in high-HIV/TB prevalence settings.
- It serves as a valuable supplemental diagnostic tool in low-resource healthcare systems.
- It expedites the diagnosis of EPTB in HIV-positive patients.
- It expedites TB treatment in HIV patients, which leads to lower morbidity and mortality.
- The findings of EPTB may be a predictor of an HIV patient's immunity status (CD4 count), which assists with the timing of starting antiretroviral treatment.
- In low-HIV/TB prevalence settings useful additional tool to enable earlier isolation and so improve Staff Safety.

Further Reading

Adler, D., Mgalula, K., Price, D., Taylor, O. (2008) Introduction of a portable ultrasound unit into the health services of the Lugufu refugee camp, Kigoma District, Tanzania. *Int. J. Emerg. Med.*, **1** (4), 261–266.

Al Zahrani, K., Al Jahdali, H., Poirier, L., Rene, P., Menzies, D. (2001) Yield of smear, culture and amplification tests from repeated sputum induction for the diagnosis of pulmonary tuberculosis. *Int. J. Tuberc. Lung Dis.*, **5** (9), 855–860.

Aubry, P., Reynaud, J.P., Nbonyingingo, C., Ndabaneze, E., Mucikere, E. (1994) [Ultrasonographic data of the solid organs of the abdomen in stage IV human immunodeficiency virus infection. A prospective study of 101 cases in central Africa]. *Ann. Gastroenterol. Hepatol. (Paris)*, **30** (2), 43–52.

de Geus, A. 1993) Scarcity of radiodiagnostic services in developing countries. *Trop. Geogr. Med.*, **45** (3), 97.

Dixit, R., Arya, M.K., Panjabi, M., Gupta, A., Paramez, A.R. (2010) Clinical profile of patients having splenic involvement in tuberculosis. *Indian J. Tuberc.*, **57** (1), 25–30.

Health Protection Agency (2011). Available from: www.hpa.org.uk/Topics/InfectiousDiseases/InfectionsAZ/Tuberculosis. [Accessed 13 October 2013].

Heller, T., Wallrauch, C., Lessells, R.J., Goblirsch, S., Brunetti, E. (2010) Short course for focused assessment with sonography for human immunodeficiency virus/tuberculosis: preliminary results in a rural setting in South Africa with high prevalence of human immunodeficiency virus and tuberculosis. *Am. J. Trop. Med. Hyg.*, **82** (3), 512–515.

Hudson, C.P., Wood, R. (2003) Ultrasound for the diagnosis of HIV-associated tuberculosis. *S. Afr. Med. J.*, **93** (6), 440–441

Koole, O., Thai, S., Khun, K.E., Pe, R., van Griensven, J., Apers, L., *et al*. (2011) Evaluation of the 2007 WHO guideline to improve the diagnosis of tuberculosis in ambulatory HIV-positive adults. *PLoS ONE*, **6** (4), e18502.

Longo-Mbenza, B., Tonduangu, K., Seghers, K.V., Mubagwa, D. 91997) [HIV infection and pericardial disease invasion in Africa]. *Arch. Mal. Coeur Vaiss.*, **90** (10), 1377–1384.

Monill-Serra, J.M., Martinez-Noguera, A., Montserrat, E., Maideu, J., Sabate, J.M. (1997) Abdominal ultrasound findings of disseminated tuberculosis in AIDS. *J. Clin. Ultrasound*, **25** (1), 1–6.

Ocama, P., Katwere, M., Piloya, T., Feld, J., Opio, K.C., Kambugu, A., *et al*. (2008) The spectrum of liver diseases in HIV infected individuals at an HIV treatment clinic in Kampala, Uganda. *Afr. Health Sci.*, **8** (1), 8–12.

Patel, M.N., Beningfield, S., Burch, V. (2011) Abdominal and pericardial ultrasound in suspected extrapulmonary or disseminated tuberculosis. *S. Afr. Med. J.*, **101** (1), 39–42.

Reichel, C., Theisen, A., Rockstroh, J.K., Muller-Miny, H., Spengler, U., Sauerbruch, T. (1996) Splenic abscesses and abdominal tuberculosis in patients with AIDS. *Z. Gastroenterol.*, **34** (8), 494–496.

Sculier, D., Vannarith, C., Pe, R., Thai, S., Kanara, N., Borann, S., *et al*. (2010) Performance of abdominal ultrasound for diagnosis of tuberculosis in HIV-infected persons living in Cambodia. *J. Acquir. Immune Defic. Syndr.*, **55** (4), 500–502.

Sinkala, E., Gray, S., Zulu, I., Mudenda, V., Zimba, L., Vermund, S.H., *et al*. (2009) Clinical and ultrasonographic features of abdominal tuberculosis in HIV positive adults in Zambia. *BMC Infect. Dis.*, **9**, 44.

Training in diagnostic ultrasound: Essentials, principles and standards (1998) Report of a WHO Study Group. *World Health Organ. Tech. Rep. Ser.*, **875**, i-46; back cover.

World Health Organization (2007) Treatment of Tuberculosis Guidelines (2007), pp. 1–144.

World Health Organization (2009) WHO global TB control report. Contract No.: WHO/HTM/TB/2009.411.

42

Fever and Ultrasound

Gabriel Simon and Beatrice Hoffmann

Introduction

The use of bedside ultrasound in patients presenting for evaluation of a febrile illness depends on the practice setting in which it is being employed. In highly resourced environments, ultrasound can be used in a focussed, complementary fashion to supplement the results of laboratory and other advanced imaging studies. In austere or resource-poor environments, given its portability and ease of deployment, it could be argued that a bedside ultrasound machine is the single most versatile stand-alone piece of diagnostic equipment. The combination of patient history, physical examination, bedside ultrasound and an inexpensive urinary dipstick will diagnose a causative infectious process in the majority of cases. In a German study of routine whole-body ultrasound in 200 patients admitted to the hospital with fever, a specific cause was confirmed by ultrasound in 57% of cases. New causes of fever not initially suspected by patient history or routine screening laboratory and imaging tests were found in 12%.

A complete ultrasound examination of patients presenting with fever might include a wide range of body regions and scanning techniques. Region-specific examples of typical causes of febrile illness amenable to ultrasound diagnosis are listed in Table 42.1.

A symptom-based approach will help focus the ultrasound examination in most cases. The majority of patients with a febrile illness in the developed world will present with a background of normal cognition and an intact immune system. Infection will result in local inflammation. This leads to irritative symptoms specific to the affected organ system, and pain. The sonographer can then direct their efforts to the region of discomfort. A useful oversimplification would be – if it hurts or if it is the leading symptom on history, scan it.

In patients presenting with minimal localising or generalised symptoms or an impaired level of consciousness, a step-wise approach focussing on high-yield examinations is best. The discussion below describes the rationale for a selection of key screening ultrasound exams in febrile patients. Each of these are described in detail in other areas of this text.

Pneumonia

Patient history and physical examination can be unreliable in making the diagnosis of pneumonia. Classic features such as cough or abnormal lung sounds are frequently absent. Although chest x-radiography (CXR) will readily diagnose most cases of pneumonia, as many as 30% will

Emergency Point-of-Care Ultrasound, Second Edition. Edited by James A. Connolly, Anthony J. Dean, Beatrice Hoffmann and Robert D. Jarman.

Companion website: www.wiley.com/go/connolly/ultrasound

Table 42.1 Common diseases causing fever amenable to diagnosis using bedside ultrasound.

Region	Disease
ENT	Peritonsillar abscess, lymphadenitis
Thorax	Pneumonia, endocarditis, empyema, pulmonary embolism
Abdomen	Cholecystitis, liver abscess, splenic infarct or abscess, appendicitis, diverticulitis, enteritis, colitis, intra-abdominal abscess, pyelonephritis, perforated viscus
Pelvic	Pelvic inflammatory disease, tubo-ovarian abscess, endometritis
Genito-urinary system	Pyelonephritis, renal obstruction with suspected infection, epidydimitis, orchitis, prostatitis
Soft tissue and Musculoskeletal (MSK)	Cutaneous abscess, cellulitis, thombophlebitis, septic arthritis, lymphoma
Systemic infections and diseases	HIV and tuberculosis (TB) co-infection with extra-pulmonary or disseminated TB. Lymphoma

be falsely negative initially. Ultrasound appears to have a substantially higher sensitivity for pneumonia than CXR when employed by an experienced sonographer. In a recent emergency department study of 49 patients performed by one experienced sonologist, bedside ultrasound correctly diagnosed all 32 cases of pneumonia found on CXR, and an additional eight cases of pneumonia missed on CXR later confirmed by computed tomography (CT).

Standard lung windows should be scanned sequentially looking for areas of hypoechoic irregular subpleural infiltrate, air bronchograms (Figure 42.1), ultrasonic B-lines, lung abscess and areas of pleural irregularity with an absence of lung sliding. The lung bases should then be scanned for fluid collections and possible empyema.

Using ultrasound to confirm the presence of a parapneumonic effusion is clinically important. Many of these patients will require diagnostic thoracentesis and surgical drainage if infection is confirmed.

Endocarditis

Endocarditis produces fever and non-specific constitutional symptoms in its early phases. A brief bedside ultrasound examination of the mitral, aortic and tricuspid valves is a reasonable screen for sometimes very large hyperechoic valvular vegetations. Transthoracic echocardiography (TTE) in the hands of a non-cardiologist has a high potential for diagnostic error in this setting. Persistent clinical suspicion for endocarditis should lead to referral for formal TTE or transoesophageal echocardiography (TEE) as indicated (Figure 42.2). Comprehensive echocardiography should also be used when available to confirm a preliminary diagnosis of endocarditis.

Biliary

Elderly patients with biliary sources of fever may present with advanced stages of infection, while experiencing only minimal pain and discomfort. The results of laboratory testing are often misleading. The gallbladder, positioned adjacent to the liver, is easily screened with bedside ultrasound. Performing a right upper quadrant ultrasound in older patients with fever and no obvious source of infection is particularly useful.

Splenic Infarct and Abscess

Splenic infarct resulting from endocarditis and splenic abscess (Figure 42.3) represent uncommon but important causes of occult fever. This finding can be missed by other diagnostic modalities. The spleen is easy to locate in the left upper quadrant, and has favourable ultrasonic tissue characteristics similar to liver parenchyma.

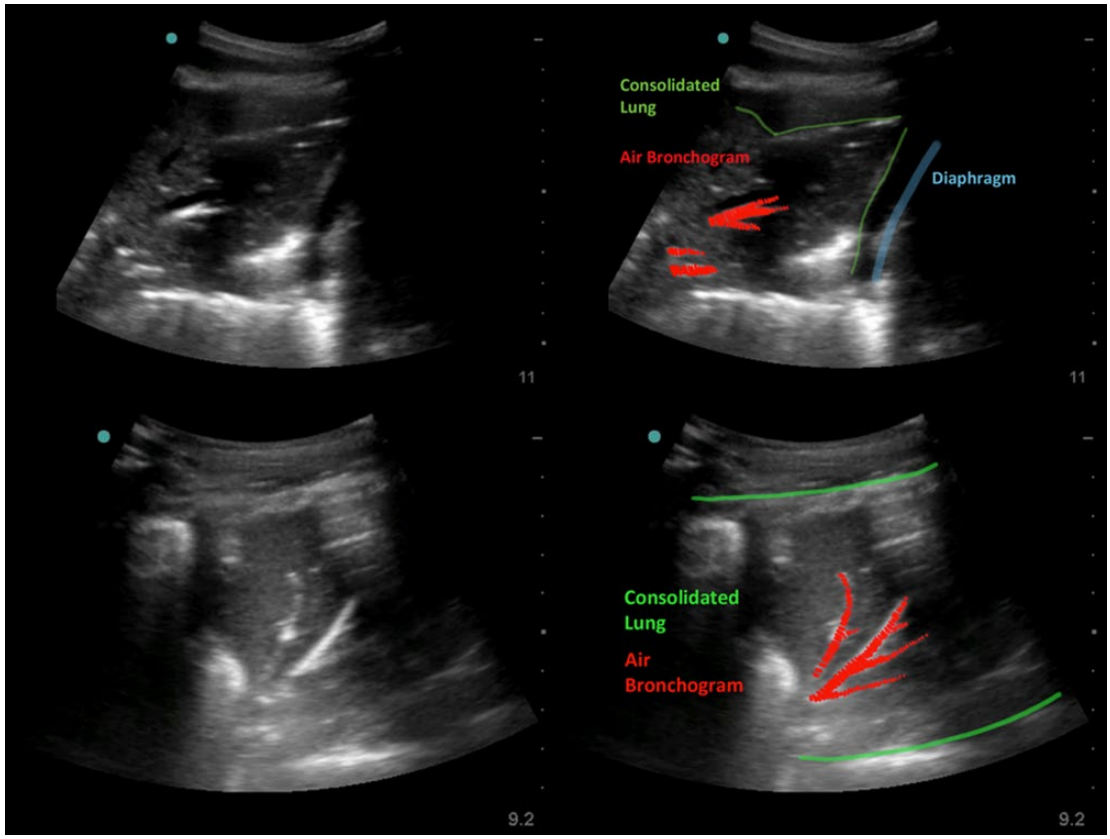

Figure 42.1 Lobar pneumonia with air bronchograms (arrows).

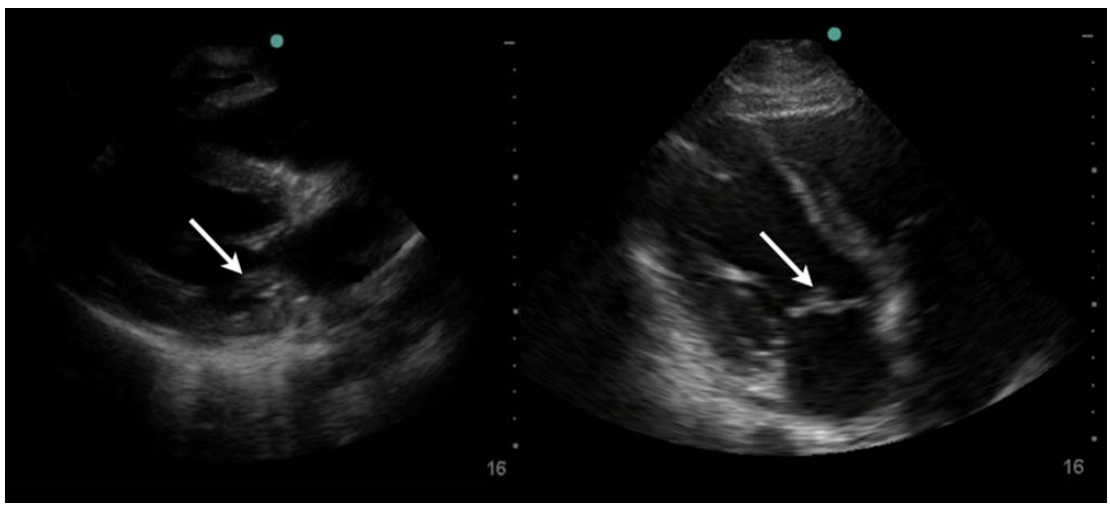

Figure 42.2 Two young patients with fever and chest pain and subtle new murmur on physical examination. Left: small vegetation on mitral valve (arrow). Right: large vegetation on mitral valve (arrow). Both cases of endocarditis were later confirmed with TEE.

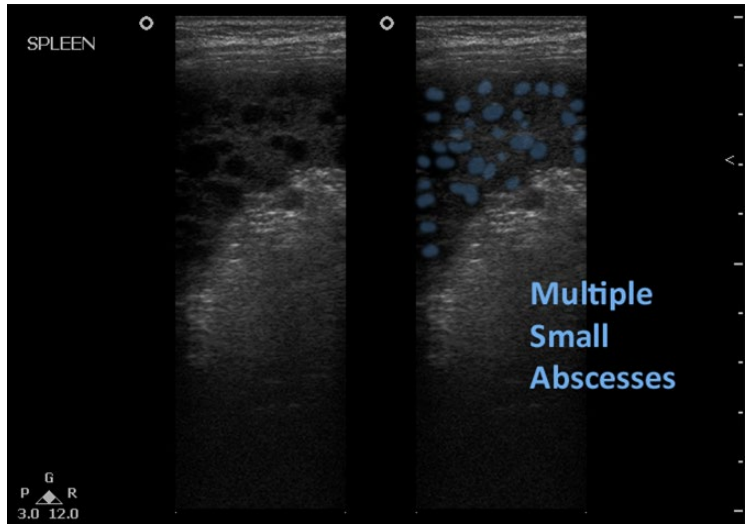

Figure 42.3 Multiple small splenic abscesses in a patient with previously undiagnosed HIV and suspected disseminated extra-pulmonary tuberculosis. Image courtesy of Hein Lamprecht MD.

Intra-Abdominal Abscess

Occult intra-abdominal abscess is another relatively frequent cause of fever in patients without an obvious source. Systematic scanning of the entire abdomen is performed to screen for these anechoic fluid collections.

Thrombophlebitis

Infections and other inflammatory processes occurring adjacent to vessels may produce either bland or septic thrombophlebitis. These are often unsuspected based on initial physical examination. Using compression and colour Doppler sonography to evaluate venous structures in the area of clinical concern may help diagnose important concomitant vessel thrombosis.

Cutaneous Abscess

Recent research has indicated that subcutaneous fluid collections are present in nearly half of emergency department patients with what appears to be uncomplicated cellulitis. The routine application of ultrasound in patients with cellulitis will often reveal an abscess requiring incision and drainage.

Pearls and Pitfalls

- Sonography may be a feasible screening test for patients with undifferentiated fever.
- Sonography could reduce the time to diagnosis and also the number of diagnostic tests needed to determine the source.
- If the source is identified, sonography may be valuable in assessing the extent of the infection or disease.

Further Reading

Colice, G.L., Curtis, A., Deslauriers, J., Heffner, J., Light, R., Littenberg, B., Sahn, S., Weinstein, R.A., Yusen, R.D. (2000) Medical and surgical treatment of parapneumonic effusions: an evidence-based guideline. *Chest*, **118** (4), 1158–1171.

Cunha, B.A. (2007) Fever of unknown origin: clinical overview of classic and current concepts. *Infect. Dis. Clin. North Am.*, **21** (4), 867–915, vii.

Görg, C., Ozbatur, H. (2009) The value of a standardized ultrasound in patients with fever. *Ultraschall. Med.*, **30** (4), 396–400.

Metlay, J.P., Kapoor, W.N., Fine, M.J. (1997) Does this patient have community-acquired pneumonia? Diagnosing pneumonia by history and physical examination. *J. Am. Med. Assoc.*, **278** (17), 1440–1445.

Parker, L.J., Vukov, L.F., Wollan, P.C. (1997) Emergency department evaluation of geriatric patients with acute cholecystitis. *Acad. Emerg. Med.*, **4** (1), 51–55.

Parlamento, S., Copetti, R., Di Bartolomeo, S. (2009) Evaluation of lung ultrasound for the diagnosis of pneumonia in the ED. *Am. J. Emerg. Med.*, **27** (4), 379–384.

Syrjälä, H., Broas, M., Suramo, I., Ojala, A., Lähde, S. (1998) High-resolution computed tomography for the diagnosis of community-acquired pneumonia. *Clin. Infect. Dis.*, **27** (2), 358–363.

Tayal, V.S., Hasan, N., Norton, H.J., Tomaszewski, C.A. (2006) The effect of soft-tissue ultrasound on the management of cellulitis in the emergency department. *Acad. Emerg. Med.*, **13** (4), 384–388.

Part 6

Different Environments

43

The Role of Ultrasound in Pre-Hospital Care

Tim Harris, Adam Bystrzycki and Stefan M. Mazur

Introduction

Pre-hospital care (PHC) is organised differently across the globe and consists of: (i) primary work, where the patient is attended in a non-medical environment; or (ii) retrieval work, where the patient is being moved from one medical facility to another to provide care for injuries and illness outside the expertise of the referring unit. In the United States, primary work is mostly paramedic-based but it may involve doctors in some countries. Doctors bring with them a set of advanced skills which may be used to benefit a small cohort of the sickest patients. One such skill is ultrasound. In this chapter, attention is focused primarily on the primary retrieval role.

Why is There an Interest in Ultrasound in Pre-Hospital Care?

During recent years, ultrasound (US) has developed and is of value to answer specific questions and to improve the accuracy with which procedures are performed. The instruments used have become smaller, tougher, weather-proof and more portable. Among other improvements, the battery life has increased, and screens have been developed that can not only be viewed in direct sunlight but also produce far better images at lower cost than even 10 years ago. Indeed, some of the machines now available are targeted at the pre-hospital arena and are robust enough even for military use.

The role of US in pre-hospital care (PHC) is two-fold:

- To promote earlier, more accurate diagnoses, so enhancing patient care.
- To minimise the risks of procedures.

The management of many medical emergencies and traumatic injuries is influenced by early care delivery. In this time-critical arena portable US helps in making diagnoses earlier facilitating timely definitive care. The PHC environment presents a risk to both patients and clinicians, and time spent there should be minimised. For this reason, US should only be used to answer questions when management will be changed or improved. Thus, while commonly performed US scans may be largely transferable to PHC, the practitioner will often truncate their scans, concentrating on one question at a time.

For this reason, the best approach is not by using protocolised image acquisition but rather by a single organ and single question.

Emergency Point-of-Care Ultrasound, Second Edition. Edited by James A. Connolly, Anthony J. Dean, Beatrice Hoffmann and Robert D. Jarman.

Companion website: www.wiley.com/go/connolly/ultrasound

Protocolised scans (e.g., eFAST, FATE, RUSH, etc.) are well described elsewhere in this book, and while these promote a safe structured approach to using US, which may be transferred to PHC, looking at their components offers a better approach to US in PHC. The uses described are examples of what can be achieved.

The noise of the PHC environment makes the use of auditory cues less reliable but does not affect US images. US has been described as a 'visual stethoscope', and for this reason it may offer clinicians more therapeutic gain pre-hospital than in it!

The major potential for harm from PHC US is that of increased on-scene time delaying transport to definitive care. Thus, most scans should be performed during transport, unless required in an emergency – such as to identify potential pneumothoraces in intubated patients. However, US studies are quick to perform, with most authors reporting times of 2–6 minutes.

The Evidence Base for Pre-Hospital Ultrasound?

To date, no randomised PHC US studies have been conducted, and even the two more widely used US studies – thoracic and abdominal US – do not show improved outcomes. Hence, much of what will be discussed here is either extrapolated from in-hospital US use or based on the experience of the authors.

Focussed US is an evolving field, and common sense suggests that an earlier, more accurate diagnosis with more precise triage should improve patient care. US represents a safe imaging modality, and provided that the practitioner is acting well within their competency in an established governance system, does not unnecessarily delay patient care and presents their findings accurately, harm to the patient is unlikely. Indeed, the potential for benefit is significant.

Established Roles for US and their Applications in PHC

Focused Assessment by Sonography in Trauma

The two main causes of death in trauma are traumatic brain injury and blood loss. FAST has been successfully used in the pre-hospital environment, both at scene and during transport. By identifying free fluid in the abdomen or pericardium the clinician can ensure that the patient is transported to the correct facility, and that the receiving hospital is correctly prepared. For example, there will be a need to activate massive transfusion protocols, free the computed tomography (CT) scanner and/or ensure that resources such as operating theatre and a trauma/cardiothoracic surgeon are available.

Since there is evidence that reducing the time to trauma laparotomy improves outcome, one of the most important factors may be in reducing the time from injury occurrence to definitive operative procedure. In some systems this may come about with the realisation that permissive hypotension may be more relevant, that additional on scene therapy be limited and more rapid time to scene departure be instituted.

Clinical examination and physiological parameters alone are unreliable in making this decision, and so improvement may be made by conducting a pre-hospital FAST study. As trauma systems mature it may also be possible to identify a subgroup of patients who could benefit from being transferred directly to the operating theatre rather than to the resuscitation room.

PHC US has been shown to alter the disposition or management of trauma patients, and performs better than clinical assessment alone. At present, there is no evidence that patient care was delayed as a consequence of US scanning.

The *best time to perform US studies pre-hospital is during transport*, as this will minimise any potential delay to a definitive operative procedure.

US studies performed in the pre-hospital arena may be truncated once diagnostic information has been obtained. If blood is found on one abdominal view, then the pre-hospital clinician's time may be better spent on resuscitation or looking to exclude other causes of shock, such as pneumothoraces, rather than the completion of a scanning protocol.

Although previous studies have described mixed results for FAST in the PHC setting, more recent studies have shown similar accuracy to studies performed in hospital. Overall, performing a FAST at scene or in transport is associated with a sensitivity of 99% and a specificity of 93%, as compared to in-hospital studies. FAST has also been reported as a possible procedure in hostile military environments, with similar sensitivities/specificities.

Cardiac Ultrasound for Trauma

In patients with significant chest trauma – particularly penetrating trauma – on-scene ultrasound has the potential to be life-saving. The pericardial view can be performed either as part of the traditional FAST scan or in isolation, and may identify haemopericardium and any resultant pericardial collection.

In traumatic cardiac arrest the priority is to identify reversible causes of these conditions. Tension pneumothorax, pericardial effusion and hypovolaemia can be identified, at least in part, by using US.

In peri-arrest or recently arrested patients with evidence of penetrating trauma, the detection of pericardial effusion pre-hospital should lead to an immediate pre-hospital thoracotomy, if the team has skills to perform this. Survival figures of 7.5% have been reported for pre-hospital thoracotomy performed on patients with no signs of life when performed within 10 minutes of cardiac arrest. In trauma patients with a cardiac output, identifying the presence of a pericardial effusion pre-hospital allows the receiving hospital to ensure that the team are ready to take the patient for immediate surgery.

Focussed echocardiography can also provide important information on the volume status of critically unwell patients. The ventricle may appear empty with the walls in close apposition at end-systole and the inferior vena cava (IVC) may be small, usually taken as less than 12–15 mm in vertical height. This is best measured 3–5 cm distal to the junction of the hepatic veins with the IVC.

In medical patients with undifferentiated hypotension, or who have arrested, cardiac US can be used to help assess the aetiology. Patients with a larger right than left ventricle may have pulmonary embolism and thus benefit from thrombolysis; indeed, there are many case reports to support this intervention in selected cases; this diagnosis is supported by a dilated inferior vena cava, measured as described above but with a vertical dimension of over 25 mm, paradoxical septal movement, and a normal right ventricular free wall diameter.

A focussed cardiac US scan may also assist in differentiating electromechanical dissociation (or pseudo- pulseless electrical activity; PEA) from true PEA. The causes include hypovolaemia, massive pulmonary embolism, coronary thrombosis and poisoning. The former three diagnoses are all suggested by echocardiographic appearances.

Finally, the absence of left ventricular activity may suggest a dismal prognosis and help in the decision to cease resuscitation.

Aortic Abdominal Aneurysm

The diagnosis of aortic abdominal aneurysm (AAA) is challenging if reliance is placed on clinical assessment alone. Confirmation of this disease process is likely to alter the PHC management significantly, in much the same way as identifying bleeding in trauma patients. It may prompt the clinician to transport the patient to an appropriate facility and to apply hypotensive resuscitation principles. The clinician could also contact the receiving hospital, so enabling a massive transfusion protocol, vascular surgeon, specialist anaesthetist and operating theatre to be prepared.

Alternative diagnoses such as renal calculi may also be identified by US. However, it is not suggested that a comprehensive scan be performed pre-hospital as this delays transport times and is less likely to alter the initial treatment.

Lung Ultrasound

The traditional approach to the dyspnoeic patient using focussed history, physical examination and chest X-radiography all perform poorly in the critically ill. The situation is even worse in the challenging pre-hospital environment, when extraneous noise can make auscultation impossible and where radiology is unavailable, hence the interest in lung ultrasound.

Early diagnosis allows the early institution of targeted medical (e.g., bronchodilation or after-load reduction) or surgical (thoracostomy) therapy, and has the potential to improve outcome. An ideal investigative strategy would be one that is:

- Low-cost.
- Readily available.
- Not influenced by the environment.
- Can be learned with relative ease.
- Is reproducible.
- Can be completed in a short time.
- Has good diagnostic performance (specific and sensitive).

Ultrasound approaches this ideal.

It is not possible to image the lungs using ultrasound with the same mindset as solid or fluid filled organs, as much of what is identified is artefact. It is, however, the different patterns of artefacts that are generated by normal and diseased lungs and pleura, which gives lung US its diagnostic performance.

The role of pulmonary US in PHC is to identify the likely cause of acute dyspnoea and to institute treatment. However, not all findings should promote treatment. A pleural effusion is best drained under sterile conditions in hospital, unless consequent upon trauma in a patient requiring intubation when the likelihood of a co-existing pneumothorax – and hence a possibility of tension physiology with positive-pressure ventilation – must be balanced against the risks of drainage.

Pre-Hospital Lung Ultrasound

While most studies have described chest US in the critical care environment, there have been a few small studies that have demonstrated the feasibility of US in the pre-hospital setting after a natural disaster.

Busch described the use of portable ultrasound on the Norwegian Air Rescue Service, and in experienced hands the standardised examination, which included FAST, lung sonography and apical two-chamber cardiac imaging, was completed within 2.5 minutes. This particular report represents actual clinical use, as the inclusion criteria were abdominal/thoracic and obstetric trauma, circulatory/respiratory compromise, PEA in cardiac arrest, acute abdomen and monitoring during transport. Although at least 'moderate' imaging was obtained in 90% of patients, there was only one experienced point-of-care physician-sonographer performing the examinations.

Mazur *et al.* have described the use of ultrasound in an Australian Aeromedical Retrieval Service for a whole range of procedures, including thoracic US, but make no comment on the time required to undertake these scans.

Lung Ultrasound in Trauma

Clinical examination alone is poor at making these diagnoses in the multi-trauma patient, particularly pre-hospital. The role of US in trauma was originally the detection of free fluid in the abdomen or pericardium. Extending this study to the chest is now common practice.

Kirkpatrick *et al.* described scanning anteriorly for pneumothorax using a high-frequency linear transducer, while others have proposed use of a lower-frequency phased-array or curvilinear probe employed for the remainder of the FAST examination. These techniques have been described in the pre-hospital environment by many authors.

The diagnosis of pneumothorax pre-hospital may allow critical chest drainage interventions to be undertaken in a more timely manner. This is particularly important in the following situations:

- The spontaneously breathing patient with a pneumothorax who is undergoing pre-hospital intubation, where a few cycles of positive-pressure ventilation has the potential to convert a simple pneumothorax into a tension pneumothorax.
- In patients with prolonged transport times, especially in confined transport frames such as helicopters and aeroplanes, where there is limited access to sides of the body against bulkheads.

The ability to diagnose and treat (haemo) pneumothorax with chest drainage prior to transport may ensure an earlier appropriate application of critical interventions for the benefit of the patient. However, in spontaneously ventilating patients with no physiological embarrassment, identifying a pneumothorax should *not* immediately lead to drainage as this is best performed in a sterile hospital environment and may increasingly be managed conservatively, even in ventilated patients.

Ultrasound may lead to a reduction in the number of pre-hospital drainage procedures performed.

Lung Ultrasound for Dyspnoea

The medically unwell patient with dyspnoea presents a diagnostic and management challenge pre-hospital, with similar physical signs produced by very differing disease processes. Auscultation has a 61% diagnostic accuracy for pleural effusion, dropping to 35% for alveolar consolidation, and can be expected to be even less accurate pre-hospital due to environmental noise and distractions.

Ultrasound offers a relatively cheap and portable imaging modality which is well-suited to pre-hospital use and performs well for lung pathology. The diagnostic accuracy is 93% for pleural effusion, 97% for alveolar consolidation, and 95% for alveolar-interstitial syndrome. This is markedly better than chest X-radiography (even if it were available), and has a similar inter-rater variability (kappa 0.73–0.79).

The Blue Protocol is a step-wise diagnostic approach to the dyspnoeic patient, but has only been validated in the intensive care unit setting. It is cumbersome in PHC, and the important diagnoses are to identify the correct aetiology of wheeze (pulmonary oedema or obstructed lung disease) and (haemo)pneumothoraces causing critical ventilatory embarrassment. Lung US will be of most use when long transport times are required, and with aeromedical rather than road transport. Whether such a systematic scanning protocol can be used reliably and expeditiously in the pre-hospital setting remains to be seen.

Pre-hospital lung US can nevertheless be used to distinguish between pulmonary oedema and exacerbation of chronic obstructive pulmonary disease, and also to diagnose pneumothorax as well as haemothorax and pleural effusions.

Emerging Roles for Ultrasound in Trauma Care

US and Airway Care

Intubation is a common PHC procedure and should be performed to the same standard in PHC as in hospital. Difficult intubation is likely more common both in trauma patients and in PHC. Unrecognised oesophageal intubation results in potentially fatal hypoxia, and the confirmation of endotracheal tube (ETT) placement has been recommended (see Guidelines 2000 for Cardiopulmonary Resuscitation and Emergency Cardiovascular Care). Correct ETT placement is most commonly confirmed by direct visualisation of the tube passing between the cords and end-tidal capnography. The former approach is not always possible, while the latter requires the presence of some ventilation, cardiac output and cellular metabolism. A recent meta-analysis demonstrated that capnography has a sensitivity of 93%.

Ultrasound can be used in real time to observe the ETT being placed. This is an advantage over other methods as it allows the confirmation of tube placement prior to any ventilation, thus potentially preventing gastric insufflation. Unfortunately, the paucity of literature, which mostly relates to cadavers, means that these benefits remain theoretical.

One small study performed in an operating theatre suggested that laryngeal US can be used to identify tracheal placement of the ETT with 100% sensitivity and 100% specificity. A large Turkish cadaver study involving 560 intubations (50% oesophageal) demonstrated a sensitivity of 95.7% and specificity of 98.2%.

To identify correct placement of the ETT a 5–10 MHz linear transducer is placed horizontally over the anterior larynx just above the suprasternal notch, as this more caudal placement is likely associated with better accuracy than placing it over the cricoid ring. In cases of oesophageal intubation, the oesophagus is displaced laterally (usually to the left) in relation to the tracheal, and two anechoic circular structures – the trachea and oesophagus – are displayed. If correctly placed in the trachea the ETT reflects sound waves, producing strong echos with reverberation artefact, and the oesophagus is not visualised.

Ultrasound can also be used to demonstrate pleural sliding (see section on pneumothorax), the implication being that if there is pleural slide then there is ventilation and the ETT has been correctly placed. Similarly, US can be used to demonstrate movement of the diaphragm with ventilation. However, with these methods the ETT may be sited above the cords and the signs also lose reliability with pneumothorax or contusion.

Comparing pleural and diaphragmatic movement between the left and right sides may also help to identify right main stem intubation, with the left side of the chest demonstrating reduced movement.

Ultrasound may also improve on clinical assessment for the prediction of a difficult airway; though this is of little benefit for PHC where most airways interventions are time critical, and identifying a potentially difficult airway is unlikely to change management choices. The accuracy of this is not well-validated and its role in PHC not explored.

Finally, US may have a role in identifying the cricoid membrane to facilitate surgical cricothyroidotomy. Rescue airways are rare, and few practitioners are experienced with them as they are performed under stressful conditions. Hence, complications are common at between 9% and 40%.Ultrasound techniques have been described which identify the cricoid membrane in a mean of 24 s, using a linear 7.5 MHz transducer. To date, no hospital or PHC studies have been reported to determine if US reduces complications or improves success rates. However, it is easy to suggest a role in patients where landmarks are challenging and a surgical airway is being considered as the primary airway option.

Ultrasound and Vascular Access

Ultrasound is widely used to identify patent peripheral and central veins. Complications of central cannulation are common at between 0.3% and 18.8%, under even ideal conditions. Pre-hospital and emergency placement is associated with a high incidence of malplacement, with reported rates of between 1% and 38%.

Ultrasound has been shown to reduce the number of attempts required for successful central cannulation, failure rates, time to successful placement and complications. The use of US is also recommended by the National Institute for Health and Care Excellence (NICE).

There is now good evidence that US improves the accuracy of central cannulation for internal jugular, femoral and subclavian veins in adults and children. Central cannulation is rarely required in PHC as the sites are best preserved for sterile catheter placement in hospital. However, in patients with difficult access central cannulation (usually femoral) may be required.

The use of US to assist with difficult peripheral cannulation is of significant potential use in PHC. In an emergency department study focussed on

patients with difficult venous access, the use of US was found to be associated with a decreased time to gain access (13 versus 30 minutes (95% CI 0.8–45.6) and a higher success rate (97% versus 33%, 95% CI 39–71%). The present authors are not aware of any study examining this point in PHC. Either a single-operator or a two-operator technique can be used, the most widely used area being the upper arm.

For femoral access the transducer is placed just below and parallel to the inguinal ligament, with the probe midline over the femoral pulse. The femoral vein is medial to the artery. The vein is cannulated using either a Seldinger or direct method. The transducer tip is then directed into the vein. In hospital, the transducer is placed in a sterile sheath but this is rarely practical pre-hospital. The techniques of vascular access with US are well described elsewhere.

Intraosseous Access and Ultrasound

Intraossoeus access is increasingly used in PHC for both paediatric and adult patients when peripheral cannulation is difficult. The procedure is rapid and good flow rates are obtained. Confirmation of placement is by either by marrow aspiration or noting the easy flow of infused fluids.

Of promise in a small cadaver study, colour power Doppler was used to assess whether the needle was inserted intraosseously (IO), as opposed to subcutaneously (SC). The method used to confirm placement was to observe the flow of crystalloid within the bone cortex. US correctly identified all placements as IO or SC (sensitivity 100%, specificity 100%), whereas clinical assessment demonstrated a sensitivity of 88% and specificity of 25%. No studies of this technique have yet been conducted in a PHC environment.

Cranial Ultrasound

Clinical assessment for raised intracranial pressure (ICP) is neither sensitive nor specific, and many factors may be causal of impaired consciousness. Knowledge of which patients have increased ICP has a potential role in PHC in identifying patients in whom a CT brain is of paramount importance before even clinical indicators, such as asymmetrical pupils become apparent.

The study is performed using a linear transducer held over the closed upper eyelid. The optic nerve is identified and lined up opposite the probe. The optic sheath is examined 3 mm behind the point where the optic nerve enters the globe. Measurements greater than 5 mm are considered abnormal.

As the ICP increases, the optic nerve and sheath become oedematous and swell. US can be used to measure the diameter of the optic nerve, and is a sensitive test in this setting. Whilst an optic nerve sheath under 5 mm in transverse section suggests normal ICP, a high abnormal reading may have several causes, including raised ICP. However, further studies with greater patient numbers are required to confirm these findings. Although the technique has also been explored in children, the available evidence suggests it may lack the clinical sensitivity and specificity required for clinical use.

It is possible that haemodynamically stable patients can be transferred directly to the CT scanner rather than to the resuscitation room. Knowledge concerning ICP is important to help the clinician determine to what systolic blood pressure the patient should be resuscitated. Patients with blood loss – particularly from penetrating disease – are resuscitated to a sub-physiological blood pressure to minimise further blood loss (so-called hypotensive or hypovolaemic resuscitation). However, hypotension (and hypoxia) may worsen traumatic brain injury, and systolic pressures of 100–110 mmHg are recommended. Identifying any isolated head injuries is also of benefit.

Finally, many small adjustments can be made by the PHC clinician to minimise intracranial hypotension, including the use of pre-induction fentanyl and loosening the cervical collar and ETT ties.

Stroke

Stroke is the third commonest cause of death in the United Kingdom, accounting for 11% of all deaths. The majority of strokes (70–80%) are due to vessel occlusion by thrombus or emboli. In selected patients, thrombolysis within 4.5 hours (and perhaps longer) of stroke onset has been shown to improve outcome, and consequently a rapid identification and transfer has assumed significant importance.

Transcranial Doppler studies may be performed using the phased-array probes found on many 'point-of-care' machines. These may demonstrate total (no flow) or subtotal occlusion (the peak flow velocity will increase at the stenosis and then fall distal to it) of the middle cerebral artery or one of its branches. The site of the arterial occlusion is linked to clinical outcome, and repeat sonographic studies may identify patients with a limited response to thrombolysis who require treatment escalation, such as invasive radiological techniques. This highlights a potential role in monitoring patients transferred from smaller remote locations, where the presence of CT has allowed thrombolysis to be delivered, to tertiary centres.

Evidence also exists that higher-energy US may in itself exert a thrombolytic effect, and at lower energy levels improve recanilisation with thrombolysis, offering a therapeutic advantage. This approach has been used at remote locations, for example on Mount Everest when an experienced clinician felt that ischaemic stroke was probable in a patient who was several days' trek from any tertiary care. Similar use in isolated locations, such as Antarctic stations, may have a role.

There is also evidence of increasing haemorrhagic transformation using higher US energies, and hence there may be a potential risk but limited clinical knowledge is currently available.

In one study where the role of PHC transcranial US in the early diagnosis of stroke was explored, the procedure was found to be feasible and facilitated further in-hospital assessment.

The same technology may be used in traumatic brain injury and subarachnoid haemorrhage to identify a reduced blood flow consequent to a raised ICP or vasospasm, respectively. Unfortunately, the role in PHC is untested and likely to be relevant only for a small group of retrieved patients to assist in physiological optimisation pre-transport. However, the skill base required to perform transcranial studies is most likely beyond most doctors working in PHC.

Ultrasound in the Diagnosis of Fractures

Ultrasound has been reasonably well studied in fracture assessment for both adults and children. It has the advantage of being able to assist in the assessment of associated soft-tissue injuries, and performs well against plain radiography in the hands of emergency physicians in austere environments. Indeed, a recent military report suggested a sensitivity of 100% and specificity of 94% in 44 subjects with suspected fractures.

Ultrasound may also be used to help identify dislocations and guide the reduction of these as well as fractures with an accuracy similar to that for plain films. In remote environments, US may help determine who requires Medivac and who remains on location: soft-tissue injuries may recover sufficiently rapidly to continue placement. US may also see a battlefield role in helping to decide who is to be evacuated by air from a battlefield.

Finally, it may be possible to define treatable injuries and offer immediate care. The obvious example here is a dislocated shoulder, where diagnostic confirmation enables relocation at scene, saving the patient from prolonged pain and an increasingly difficult re-location as muscle spasm progresses.

Bone is an excellent reflector of US energy, and thus the cortex appears as a dense white line. Fractures are readily identifiable and appear as a step or irregularity in the cortical line. A linear high-frequency probe is used and,

as with plain films, the images are obtained in two perpendicular planes.

The Role of Ultrasound in Mass-Casualty Situations

A mass-casualty incident is one in which the number of patients with injuries exceeds the available medical resources to provide care in a timely manner. The potential role of ultrasound in pre-hospital mass-casualty scenarios is poorly defined. Since ultrasound enables the rapid identification of life-threatening injuries, a potential role would be to complement triage systems. The potential use of US includes employing the EFAST examination to identify pneumothoraces, intra-abdominal or pericardial free fluid (presumed blood), to assess crush injuries, to determine foetal viability and to define the aetiology of undifferentiated hypotension.

Monitoring pneumothoracies may allow a cause for later physiological deterioration to be identified and corrected, whilst knowledge about the extent of intra-abdominal injuries may assist in planning evacuation. Indeed, Mazur and Rippey have demonstrated the use of ultrasound in a mass-casualty situation where secondary triage for prolonged air transport was required with limited transport resources. These authors used US to help exclude significant intra-abdominal pathology and to diagnose chest injuries in patients who were the victims of a cyclone. As portable US becomes more prevalent amongst pre-hospital care providers its role – if any – in mass-casualty and disaster scenarios should become clearer.

Ultrasound may help within the hospital or in field units when other imaging facilities are overwhelmed, and demonstrated its versatility during the recent earthquakes in China. In a case report, 1207 patients underwent US examinations, including 115 US-guided interventions. This represented about 37% of the total patient case load. US was used (initially outdoors due to safety concerns for the hospital infrastructure) to assess patients, primarily with the EFAST examination. However, as the disaster progressed US was used for ongoing assessment and interventions as the workforce and patients were able to return to the hospital.

Ultrasound was used to assist in-hospital triage in the 1991 Armenian earthquake, with pathology being identified in 96 of 400 screened patients, most of whom had crush injuries Four false-negative scans that occurred in patients with either technically difficult imaging or injuries (i.e., where US is not a choice investigation), retroperitoneal disease, bowel injury and contained splenic haematoma.

More technologically advanced scans were used in the 1999 Turkish earthquake, where Doppler studies of the renal arteries were used to identify patients with severe crush injury by assessing the resistive index. These studies were performed during the first three days of the patients' admission to hospital.

There is considerable scope for the role of US at the scene of major incidents. One retrospective chart study modelled the potential role of US as a triage tool at scene, whereby 359 patients were identified via their attendance at a major trauma centre. Of these patients, 286 were retrospectively triaged as P2s/yellow. The authors noted that 20 patients had a positive FAST, and six of them underwent surgery within 24 hours of arrival at hospital. As well as rapidly defining injuries, US has the potential to assist with triage by further dividing P2s based on the presence or absence of free intraperitoneal fluid, thus defining a group requiring priority transport.

Other case reports detail the pre-hospital use of portable US by disaster medical assistance teams as part of the ongoing care of victims of mass-casualty or disaster events, and may have the most benefit in being able to rule out significant pathology and allow scarce resources to be focussed on those most likely to benefit. These reports demonstrate that US can be carried and used by pre-hospital providers in mass-casualty situations. Any evidence of patient benefit remains anecdotal, however.

Images from echocardiography and FAST studies have been transmitted to hospital for interpretation from remote locations. This includes the international space station and a simulated space trip to Mars, as well as remotely guided diagnosis and treatment in the Arctic Circle. All of these studies demonstrated excellent accuracy and easily obtained diagnostic information.

Further Reading

Abboud, P.A., Kendall, J.L. (2004) Ultrasound guidance for vascular access. *Emerg. Med. Clin. North Am.*, **22**, 749–773.

Báez, A.A., Lane, P.L., Sorondo, B., Giráldez, E.M. (2006) Predictive effect of out-of-hospital time in outcomes of severely injured young adult and elderly patients. *Prehosp. Disaster Med.*, **21** (6), 427–430.

Bair, A., Panacek, E., Wisner, D., *et al*. (2003) Cricothyroidotomy: a 5-year experience at one institution. *J. Emerg. Med.*, **24**, 151–156.

Beck-Razi N, Fischer D, Michaelson M, Engel A, Gaitini D. (2007) The utility of focused assessment with sonography for trauma as a triage tool in multiple-casualty incidents during the second Lebanon war. *J. Ultrasound Med.*, **26**, 1149–1156.

Bickell, W.H., Wall, M.J., Jr, Pepe, P.E., *et al*. (1994) Immediate versus delayed fluid resuscitation for hypotensive patients with penetrating torso injuries. *N. Engl. J. Med.*, **331**, 1105–1109.

Blaivas, M., Kuhn, W., Reynolds, B., Brannam, L. (2005) Change in differential diagnosis and patient management with the use of portable ultrasound in a remote setting. *Wilderness Environ. Med.*, **16**, 38–41.

Blaivas, M., Sierzenski, P., Theodoro, D. (2002) Significant hemoperitoneum in blunt trauma victims with normal signs and clinical examination. *Am. J. Emerg. Med.*, **20**, 218–221.

Blaivas, M., Theodoro, D., Sierzenski, P. (2003) Elevated intracranial pressure detected by bedside emergency ultrasound of the optic nerve sheath. *Acad. Emerg. Med.*, **10**, 376–381.

Boulanger, B.R., McLellan, B.A., Brennemann, F.D., Juan, O., Kirkpatrick, A.W. (1999) Prospective evidence of the superiority of a sonography-based algorithm in the assessment of blunt abdominal injury. *J. Trauma*, **47**, 632–637.

Brain Injury Foundation, American Association of Neurological Surgeons, Joint section on Neurotrauma and Critical Care (2000) Initial Management. *J. Neurotrauma*, **17**, 463–469.

Busch, M. (2006) Portable ultrasound in prehospital emergencies: a feasibility study. *Acta Anaesthesiol. Scand.*, **50** (6), 754–758.

Byhahn, C., Binbold, T., Zwissler, B., Maier, M., Walcher, F. (2008) Prehospital ultrasound detects pericardial tamponade in a pregnant victim of stabbing assault. *Resuscitation*, **76**, 146–148.

Cai Leung Tsui, Hin Tat Fung, Kin Lai Chung, V. Chak Wah Kam (2008) Focussed abdominal sonography for trauma in the emergency department for blunt abdominal trauma. *Int. J. Emerg. Med.*, **1**, 183–187.

Chang, R., Amilton, R., Carter, W. (1998) Declining rate of cricothyroidotomy in trauma patients with an emergency medicine residency: implications for skills training. *Acad. Emerg. Med.*, **5**, 247–251.

Chun, R., Kirkpatrick, A., Sirois, M., *et al*. (2004) Where's the tube? Evaluation of hand-held ultrasound in confirming endotracheal tube placement. *Prehosp. Emerg. Care*, **19**, 366–369.

Clarke, J.R., Trooskin, S.Z., Doshi, P.J., Greenwald, L., Mode, C.J. (2002) Time to laparotomy for intra-abdominal bleeding from trauma does affect survival for delays up to 90 minutes. *J. Trauma*, **52**, 420–425.

Corral, E., Silva, J., Suarez, R.M., Nunez, J., Cuesta, C. (2007) A successful emergency thoracotomy performed in the field. *Resuscitation*, **75** (3) 530–533.

Costantino, T.G., Parikh, A.K., Satz, W.A., Fojtik, J.P. (2005) Ultrasonography-guided peripheral intravenous access versus traditional approaches in patients with difficult intravenous access. *Ann. Emerg. Med.*, **46**, 456–461.

Dan, D., Mingsong, L., Jie, T., Xiaobo, W., Zhong, C., Yan, L., Xiaojin, L., Ming, C. (2010) Ultrasonographic applications after mass casualty incident caused by Wenchuan earthquake. *J. Trauma*, **68** (6), 1417–1420.

Deakin, C.D. (2007) From agonal to output: An ECG history of a successful pre-hospital thoracotomy. *Resuscitation*, **75** (3), 525–529.

Dean, A.J., Ku, B.S., Zeserson, E.M. (2007) The utility of handheld ultrasound in an austere medical setting in Guatemala after a natural disaster. *Am. J. Disaster Med.*, **2** (5), 249–256.

Do, J.R., McManus, J., Harrison, B. (2006) Use of ultrasonography to avoid an unnecessary procedure in the prehospital combat environment: a case report. *Prehosp. Emerg. Care*, **10** (4), 502–506.

Dronen, S., Thompson, B., Nowak, R., Tomlanovich, M. (1982) Subclavian vein catheterization during cardiopulmonary resuscitation: a prospective comparison of the supraclavicular and infraclavicular percutaneous approaches. *JAMA*, **247**, 3227–3230.

Durston, W., Swartzentruber, R. (2000) Ultrasound guided reduction of the forearm fractures. *Am. J. Emerg. Med.*, **18**, 72–77.

McManus, J.G., Morton, M.L., Crystal, C.S., *et al*. (2008) Use of ultrasound to assess acute fracture reduction in emergency care settings. *Am. J. Disaster Med.*, **3**, 241–247.

Emerman, C.L., Bellon, E.M., Lukens, T.W., May, T.E., Effron, D. (1990) A prospective study of femoral versus subclavian vein catheterization during cardiac arrest. *Ann. Emerg. Med.*, **19**, 26–30.

Ezri, T., Gewurtz, G., Sessler, D., *et al*. (2003) Prediction of difficult laryngoscopy in obese patients by ultrasound quantification of anterior neck soft tissue. *Anaesthesia*, **58**, 1111–1114.

Farrow, G.B. (2001) Portable ultrasound on deployment: A pilot study. *ADF Health*, **2**, 55–58.

Forster, R., Pillasch, J., Zielke, A., Malewski, U., Rothmund, M. (1992) Ultrasonography in blunt abdominal trauma: influence of the investigator's experience. *J. Trauma*, **34**, 264–269.

Friese, R.S., *et al*. (2007) Abdominal ultrasound is an unreliable modality for the detection of hemoperitoneum in patients with pelvic fracture. *J. Trauma*, **63**, 97–102.

Galetta, S., Byrne, S., Smith, J. (1989) Echographic correlation of optic nerve sheath size and cerebrospinal fluid pressure. *J. Clin. Neuropathalmol.*, **9**, 79–82.

Gerscovich, E., Cronan, M., McGahan, J., *et al*. (2001) Ultrasonographic evaluation of diaphragmatic motion. *J. Ultrasound Med.*, **20**, 597–604.

Goksu, E., Sayrac, V., Oktay, C., Kartal, M. (2010) How stylet use can effect confirmation of endotracheal tube position using ultrasound. *Am. J. Emerg. Med.*, **28**, 32–36.

Goldfarb, G., Lebrec, D. (1982) Percutaneous cannulation of the internal jugular vein in patients with coagulopathies: an experience based on 1000 attempts. *Anesthesiology*, **56**, 321–323.

Goletti, O., Ghiselli, G., Lippons, F.V., *et al*. (1994) The role of ultrasonography in blunt abdominal trauma: results in 250 consecutive cases. *J. Trauma*, **36**, 178–181.

Graif, M., Stahl-Kent, V., Ben-Ami, T., Strauss, S., Amit, Y., Itzchak, Y. (1988) Sonographic detection of occult bone fractures. *Pediatr. Radiol.*, **18**, 383.

Grechenig, W., Clement, H.G., Fellinger, M., Seggl, W. (1998) Scope and limitations of ultrasonography in the documentation of fractures – an experimental study. *Arch. Orthop. Trauma Surg.*, **117**, 368–371.

Gruessner, R., Mentges, B., Duber, C., Ruckert, K., Rothmund, M. (1989) Sonography versus peritoneal lavage in blunt abdominal trauma. *J. Trauma*, **29**, 242–244.

Guidance on the use of ultrasound locating devices for placing central venous catheters, September 2002, Technology appraisal 49, http://www.nice.org.uk/nicemedia/live/11474/32461/32461.pdf.

Guidelines 2000 for Cardiopulmonary Resuscitation and Emergency Cardiovascular care: Part 6: Advanced cardiovascular life support: section 3. Adjuvant for oxygenation, ventilation and airway control. The American

Heart Association in collaboration with the International Liaison Committee on Resuscitation. *Circulation*, **102** (Suppl. 8), 195.

Gunst, M., Ghaemmaghami, V., Sperry, J., Robinson, M., O'Keeffe, T., Friese, R., *et al.* (2008) Accuracy of cardiac function and volume status estimates using the bedside echocardiographic assessment in trauma/critical care. *J. Trauma*, **65** (3), 509–516.

Halberg, M.J., Wweeney, T.W., Owens, W.B. (2009) Bedside ultrasound for verification of shoulder reduction. *Am. J. Emerg. Med.*, **27** (1), 134.e5–e6.

Hansen, H., Helmke, K. (1997) Validation of the optic nerve sheath response to changing cerebrospinal fluid pressure: ultrasound findings during intrathecal infusion tests. *J. Neurosurg.*, **87**, 34–40.

Härtl, R., Gerber, L.M., Iacono, L., Ni, Q., Lyons, K., Ghajar, J. (2006) Direct transport within an organized state trauma system reduces mortality in patients with severe traumatic brain injury. *J. Trauma*, **60** (6), 1250–1256; discussion 1256.

Heegaard, W., Hildebrandt, D., Spear, D., Chason, K., Nelson, B., Ho, J. (2010) Prehospital Ultrasound by Paramedics: Results of Field Trial. *Acad. Emerg. Med.*, **17** (6), 624–630.

Helmke, K., Hanson, H. (1996) Fundamentals of transorbital sonographic evaluation of the optic nerve sheath expansion under intracranial hypertension, I: experimental study. *Pediatr. Radiol.*, **26**, 701–705.

Helmke, K., Hanson, H. (1996) Fundamentals of transorbital sonographic evaluation of the optic nerve sheath expansion under intracranial hypertension, II: experimental study. *Pediatr. Radiol.*, **26**, 706–710.

Hilty, W.M., Hudson, P.A., Levitt, M.A., Hall, J.B. (1997) Real-time US-guided femoral vein catheterization during cardiopulmonary resuscitation. *Ann. Emerg. Med.*, **29**, 331–337.

Hind, D., Calvert, N., McWilliams, R., Davidson, A., Paisley, S., Beverley, C., *et al.* (2003) Ultrasonic locating devices for central venous cannulation: meta-analysis. *Br. Med. J.*, **327**, 361–367.

Hoffmann, R., Nerlich, M., Muggia-Sullam, M., *et al.* (1992) Blunt abdominal trauma in cases of multiple trauma evaluated by ultrasonography: a prospective analysis of 291 patients. *J. Trauma*, **32**, 452–458.

Holmes, A.E.M., Holmes, J.F., Harris, D., Battistella, F.D. (2004) Performance of abdominal ultrasonography in blunt trauma patients with out-of-hospital or emergency department hypotension. *Ann. Emerg. Med.*, **43** (3), 354–361.

Hrics, P., Wilber, S., Blanda, M.P., Gallo, U. (1998) US-assisted internal jugular catheterization in the ED. *Am. J. Emerg. Med.*, **16**, 401–403.

Hsieh, K., Lee, C., Lin, C., *et al.* (2004) Secondary confirmation of endotracheal tube placement by bedside ultrasound. *Crit. Care Med.*, **32** (Suppl.), S374–S377.

Huffer, L.L., Bauch, T.D., Furgerson, J.L., *et al.* (2004) Feasibility of remote echocardiography with to support medical activities in the austere medical environment. *J. Am. Soc. Echocardiogr.*, **17**, 670–674.

Jang, T., Audin, C. (2005) The use of serial ocular ultrasound in the care of patients with head injury (letter). *Ann. Emerg. Med.*, **45**, 335–336.

Jastremski, M.S., Matthias, H.D., Randell, P.A. (1984) Femoral venous catheterization during cardiopulmonary resuscitation: a critical reappraisal. *J. Emerg. Med.*, **1**, 387–389.

Jorgensen, H., Jensen, C., Dirks, J. (2010) Does pre-hospital ultrasound improve the treatment of the trauma patient? *Eur. J. Emerg. Med.*, **17**, 249–253.

Keven, K., Ates, K., Yagmurlu, B., *et al.* (2001) Renal Doppler ultrasonographic findings in earthquake victims with crush injury. *J. Ultrasound Med.*, **20**, 675–679.

Keyes, L.E., Frazee, B.W., Snoey, E.R., Simon, B.C., Christy, D. (1999) US-guided brachial and basilic vein cannulation in emergency department patients with difficult intravenous access. *Ann. Emerg. Med.*, **34**, 711–714.

Kimura, A., Otsuka, T. (1991) Emergency center ultrasonography in the evaluation of hemoperitoneum: a prospective study. *J. Trauma*, **31**, 20–23.

Knapp, S., Kofler, J., Stoiser, B., *et al.* (1999) The assessment of four methods to verify tracheal tube placement in the critical care setting. *Anesth. Analg.*, **88**, 766–770.

Lapostolle, F., Petrovic, T., Catineau, J., Lenoir, G., Adnet, F. (2005) Training emergency physicians to perform out-of-hospital ultrasonography (letter). *Am. J. Emerg. Med.*, p. 572.

Le, A., Hoehn, M., Smith, M., Spentzas, T., Schlappy, D., Pershad, J. (2009) Bedside sonographic measurement of optic nerve sheath diameter as a predictor of increased intracranial pressure in children. *Ann. Emerg. Med.*, **53**, 785–791.

Leigh-Smith, S., Harris, T. (2005) Tension pneumothorax – time for a re-think? *Emerg. Med. J.*, **22**, 8–16.

Leung, J., Duffy, M., Finck, H. (2006) Real-time ultrasonographically-guided internal jugular vein catheterization in the Emergency Department increases success rates and reduces complications: A randomized, prospective study. *Ann. Emerg. Med.*, **48**, 540–547.

Li, J. (2001) Capnography alone is imperfect for endotracheal tube placement confirmation. *J. Emerg. Med.*, **20**, 223–229.

Lichtenstein, D.A. (2007) Ultrasound in the management of thoracic disease. *Crit. Care Med.*, **35** (5 Suppl.), S250–S261.

Liu, M., Lee, C., P'eng, F.K. (1993) Prospective comparison of diagnostic peritoneal lavage computed tomographic scanning and ultrasonography for the diagnosis of blunt trauma. *J. Trauma*, **35**, 267–270.

Lockey, D.J., Davies, G. (2007) Pre-hospital thoracotomy: A radical resuscitation intervention come of age? *Resuscitation*, **75**, 394–395.

Ma, G., Hayden, S., Chan, T., *et al.* (1999) Using ultrasound to visualise and confirm endotracheal intubation (abstract). *Acad. Emerg. Med.*, **6**, 515.

Ma, O.J., Norvell, J.G., Subramanian, S. (2007) Ultrasound applications in mass casualties and extreme environments. *Crit. Care Med.*, **35** (5 Suppl.), S275–S279.

Mace, S., Hedges, J. (2004) Cricothyroidotomy and translaryngeal jet ventilation, in *Clinical Procedures in Emergency Medicine*, 4th edition (eds Roberts and Hedges), WB Saunders, Philadelphia, Chapter 6.

Mansfield, P.F., Hohn, D.C., Fornage, B.D., Gregurich, M.A., Ota, D.M. (1994) Complications and failures of subclavian-vein catheterization. *N. Engl. J. Med.*, **331**, 1735–1738.

Mazur, S., Pearce, A., Alfred, S., Sharley, P. (2007) Use of point-of-care ultrasound by a critical care retrieval team. *Emerg. Med. Austr.*, **19**, 547–552.

Mazur, S.M., *et al.* the F.A.S.T.E.R. trial. (2008) Focused assessment by sonography in trauma during emergency retrieval: A feasibility study. *Injury Int. J. Care Injured*, **39**, 512–518.

Mazur, S.M., Rippey, J. (2009) Transport and use of point-of-care ultrasound by a Disaster Medical Assistance Team. *Prehosp. Disast. Med.*, **24** (2), 140–144.

McGahan, J.P., Rose, J., Coates, T.L., Wisner, D.H., Newberry, P. (1997) Use of ultrasonography in the patient with acute abdominal trauma. *J. Ultrasound Med.*, **16**, 653–662.

McKenney, M.G., Martin, L., Lentz, K., *et al.* (1996) 1,000 consecutive ultrasounds for blunt abdominal trauma. *J. Trauma*, **40**, 607–610.

McNeil, C.R., McManus, J., Mehta, S. (2009) The accuracy of portable ultrasonography to diagnose fractures in an austere environment. *Prehosp. Emerg. Care*, **13**, 50–52.

Melanson, S.W., McCarthy, J., Stromski, C.J., Kostenbader, J., Heller, M. (2006) Aeromedical trauma sonography by flight crews with a miniature ultrasound unit. *Prehosp. Emerg. Care*, **5**, 399–402.

Merrer, J., De Jonghe, B., Golliot, F., Lefrant, J., Raffy, B., Barre, E., *et al.* (2001) Complications of femoral and subclavian venous catheterization in critically ill patients. *JAMA*, **286**, 700–707.

Miletic, D., Fuckar, Z., Mraovic, B., *et al.* (1999) Ultrasonography in the evaluation of hemoperitoneum in war casualties. *Mil. Med.*, **164**, 600–602.

Miller, A.H., Roth, B.A., Mills, T.J., *et al.* (2002) US guidance versus the landmark technique for the placement of central venous catheters in

the emergency department. *Acad. Emerg. Med.*, **9**, 800–805.

Farahmand, N., Sirlin, C.B., Brown, M.A., Shragg, G.P., Fortlage, D., Hoyt, D.B., Casola, G. (2005) Hypotensive patients with blunt abdominal trauma: performance of screening US. *Radiology*, **235**, 436–443.

Nicholls, S., Sweeney, T., Ferre, R., Strout, T. (2008) Bedside sonography by emergency physicians for the rapid identification of the landmarks relevant to cricothyroidotomy. *Am. J. Emerg. Med.*, **26**, 852–856.

Noble, V.E., Lamhaut, L., Capp, R., *et al.* (2009) Evaluation of a thoracic ultrasound training module for the detection of pneumothorax and pulmonary edema by prehospital physician care providers. *BMC Med. Educ.*, **9**, 3.

Pearce, A., Mark, P., Gray, N., Curry, C. (2006) Responding to the Boxing Day tsunami disaster in Aceh, Indonesia: Western and South Australian contributions. *Emerg. Med. Austral.*, **18**, 86–92.

Polk, J.D., Fallon, W.F. (2000) The use of focussed assessment with sonography for trauma (FAST) by a prehospital air medical team in the trauma arrest patient. *Prehosp. Emerg. Care*, **4**, 82–84.

Polk, J.D., Fallon, W.F., Kovach, B., Mancuso, C., Stephens, M., Malangoni, M.A. (2001) The 'airmedical FAST' for trauma patients – The initial report for a novel application for sonography. *Aviat. Space Environ. Med.*, **72**, 432–436.

Price, D.D., Wilson, M.D., Murphy, T.G. (2000) Trauma ultrasound feasibility during helicopter transport. *Air Med. J.*, **19** (4), 144–146.

Roberts, J., McManus, J., Harrison, B. (2006) Use of ultrasonography to avoid an unnecessary procedure in the prehospital combat environment: a case report. *Prehosp. Emerg. Care*, **10**, 502–506.

Rothlin, M.A., Naf, R., Amgwerd, M., Candinas, D., Frick, T., Trentz, O. (1993) Ultrasound in blunt abdominal and thoracic trauma. *J. Trauma*, **34**, 488–495.

Rozycki, G.S., Ochsner, M.G., Schmidt, J.A., *et al.* (1995) A prospective study of surgeon-performed ultrasound as the primary adjuvant modality for injured patient assessment. *J. Trauma*, **39** (3), 492–498.

Rozycki, G.S., Ochsner, M.G., Jaffin, J.H., Champion, H.R. (1993) Prospective evaluation of surgeons' use of ultrasound in the evaluation of trauma patients. *J. Trauma*, **34**, 516–526.

Sarkisian, A.E., Khondkarian, R.A., Amirbekian, N.M., *et al.* (1991) Sonographic screening of mass casualties for abdominal and renal injuries following the 1988 Armenian earthquake. *J Trauma*, **31**, 247–250.

Scalea, T.M., Sinert, R., Duncan, A.O., Rice, P., Austin, R., Kohl, L., *et al.* (1994) Percutaneous central venous access for resuscitation in trauma. *Acad. Emerg. Med.*, **1**, 525–531.

Schmitt, J., Ma, G., Hayden, S., *et al.* (2000) Suprasternal versus cricothyroid ultrasound probe position in the confirmation of the endotracheal tube placement by bedside ultrasound (abstract). *Acad. Emerg. Med.*, **7**, 526.

Sheridan, R.L., Petras, L., Lydon, M. (1997) Ultrasonic imaging as an adjunct to femoral vein catheterization in children. *J. Burn Care Rehabil.*, **18**, 156–158.

Stone, M.B., Teismann, N.A., Wang, R. (2007) Ultrasound confirmation of intraosseous needle placement in an adult unembalmed cadaver model. *Ann. Emerg. Med.*, **49**, 515–519.

Strode, C.A., Rubal, B.J., Gerhardt, R.T., *et al.* (2003) Satellite and mobile wireless transmission of focused assessment with sonography in trauma. *Acad. Emerg. Med.*, **10**, 1411–1414.

Sutic, A. (2007) Role of ultrasound in the airway management of critically ill patients. *Crit. Care Med.*, **35** (5), S173–S177.

Swanson, R.S., Uhlig, P.N., Gross, P.L., McCabe, C.J. (1984) Emergency intravenous access through the femoral vein. *Ann. Emerg. Med.*, **13**, 244–247.

Sznajder, J.I., Zveibil, F.R., Bitterman, H., Weiner, P., Bursztein, S. (1986) Central vein catheterization: failure and complication rates by three percutaneous approaches. *Arch. Intern. Med.*, **146**, 259–261.

Sztajnkrycer, M.D., Baez, A.A., Luke, A. (2006) FAST ultrasound as an adjunct to triage using the START mass casualty triage system: a preliminary descriptive system. *Prehosp. Emerg. Care*, **10**, 96–102.

Tayal, V., Neulander, M., Norton, H., Foster, T., Saunders, T., Blaivas, M. (2007) Emergency department sonographic measurements of the optic nerve sheath diameter to detect findings of increased intracranial pressure in adult head injury patients. *Ann. Emerg. Med.*, **49** (4), 508–514.

Volpicelli, G. (2007) Significance of comet tail artifacts at lung ultrasound. *Am. J. Emerg. Med.*, **25** (8), 981–982.

Walcher, F., Kirschning, T., Müller, M.P., *et al*. (2010) Accuracy of prehospital focused abdominal sonography for trauma after a 1-day hands-on training course. *Emerg. Med. J.*, **27**, 345–349.

Walcher, F., Kortüm, S., Kirschning, T., Weihgold, N., Marzi, I. (2002) Optimierung des traumamanagements durch präklinische sonographie. *Unfallchirurg*, **105**, 986–994.

Walcher, F., Weinlich, M., Conrad, G., Schweigkofler, U., Breitkreutz, R., Kirsching, T., *et al*. (2006) Prehospital ultrasound imaging improves management of abdominal trauma. *Br. J. Surg.*, **93**, 238–242.

Weaver, B., Lyon, M., Blaivas, M. (2005) Confirmation of endotracheal tube placement after intubation using the ultrasound lung sliding sign. *Acad. Emerg. Med.*, **8**, 239–244.

Weinberg, B., Diakoumakis, E.E., Kass, E.G., Seife, B., Zvi, Z.B. (1986) The air bronchogram: sonographic demonstration. *Am. J. Roentgenol.*, **147** (3), 593–595.

Weiss, D.B., Jacobson, J.A., Karunakar, M.A. (2005) The use of ultrasound in evaluating orthopaedic trauma patients. *J. Am. Acad. Orthop. Surg.*, **13**, 525–533.

Werner, S., Smith, C., Goldstein, J., Jones, R., Cydulka, R. (2007) Pilot study to evaluate the accuracy of ultrasound in confirming endotracheal tube placement. *Ann. Emerg. Med.*, **49**, 75–80.

Westfall, M.D., Price, K.R., Lambert, M., Himmelman, R., Kacey, D., Dorevitch, S., *et al*. (1994) Intravenous access in the critically ill trauma patient: a multicentered, prospective, randomized trial of saphenous cutdown and percutaneous femoral access. *Ann. Emerg. Med.*, **23**, 541–545.

Yuen, C.K., Mok, K.L., Kan, P.G., Wong, Y.T. (2009) Bedside ultrasound for the verification of shoulder reduction with lateral and anterior approaches. *Am. J. Emerg. Med.*, **27**, 503–504.

Yuen, C.K., Mok, K.L., Kan, P.G., Wong, Y.T. (2009) Ultrasound diagnosis of anterior shoulder dislocation. *Hong Kong J. Emerg. Med.*, **16** (1), 29–34.

Appendix A1

Selected Protocols for Cardiac and Critical Care Ultrasound

Among critically ill patients there are several commonly encountered and vitally important mechanical, anatomic and physical derangements that are readily identifiable by ultrasound. A number of tools have been developed to assist the clinician in the use of ultrasound in this pressurized context. Protocols have been developed with a variety of focuses, including shortness of breath, hypotension, undifferentiated shock, pulseless electrical activity, cardiac arrest, as well as for different contexts ranging from the initial evaluation of the undifferentiated patient to the longer-term management of the critically ill, which includes assessment of response to therapeutic interventions. Some representative examples are included in this Appendix, in addition to others that appear in the text.

With a range of skills among sonologists, differences of clinical focus, improvements in ultrasound technology, and evolving practice domains among clinicians using ultrasound, there is no 'one size fits all' protocol. The clinician should consider all of these factors in selecting an approach in any given clinical situation.

A1.1 DEFG for Basic Echocardiography

This protocol is a mnemonic for a systematic echocardiographic evaluation of the heart by the sonologist with basic ultrasound skills. It does not include assessment of the inferior vena cava, which many would include in such an evaluation.

Emergency Point-of-Care Ultrasound, Second Edition. Edited by James A. Connolly, Anthony J. Dean, Beatrice Hoffmann and Robert D. Jarman.

Companion website: www.wiley.com/go/connolly/ultrasound

*DEFG for basic echo

D	Dimensions	**Any obvious dimension abnormalities?** RV:LV ratio should be less than 60% On PLAX, remember 4,5,6: - Root of aorta less than 4 cm - Left atrium diameter less than 5 cm - Left ventricle diameter (end diastole) less than 6 cm Left ventricle wall thickness: - 1 cm end diastole - Thickens by 30% in systole
E	Effort	**How is the heart contracting?** Less than normal – normal – more than normal
F	Fluid	**Is there fluid around the heart?** - Small < 1 cm - Moderate 1–2 cm - Large > 2 cm *(PLAX/PSAX views good for this)* **Is there fluid adjacent to the heart (e.g. pleural fluid)?**
G	Gradients	**Pressure gradients cause blood flow across valves:** - What valves can you see? - Do they look normal? - Are they opening and closing normally? - Is there any gross stenosis or regurgitation on colour Doppler?

A1.2 The FATE (Focus-Assessed Transthoracic Echocardiography) Tool

The FATE (Focus-Assessed Transthoracic Echocardiography) tool was developed by Dr Eric Sloth and his team (see Chapter 35) and is publicly accessible for download http://www.fate-protocol.com/130067GE_Fate_Card.pdf (accessed 14 March 2017). It provides visual reminders of the key windows, views, and findings of cardiac echocardiography. It includes some more advanced skills including M-mode applications and the qualitative assessment of right/left heart interactions.

regionmidtjylland midt

Focus Assessed Transthoracic Echo (FATE)

Scanning through position 1–4 in the most favourable sequence

Basic FATE views

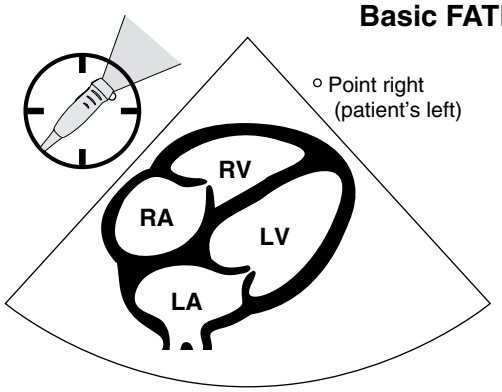

Pos 1: Subcostal 4-chamber

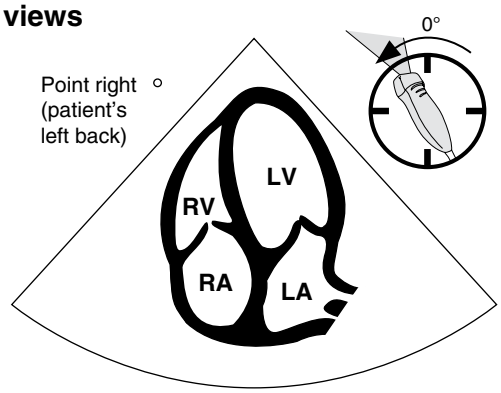

Pos 2: Apical 4-chamber

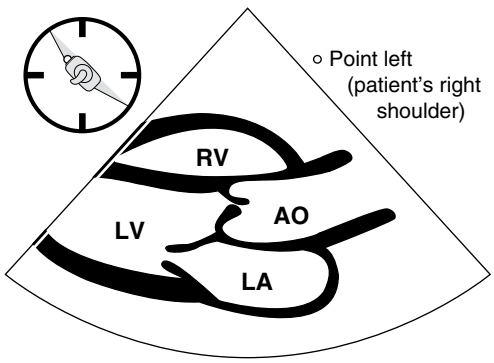

Pos 3: Parasternal long axis

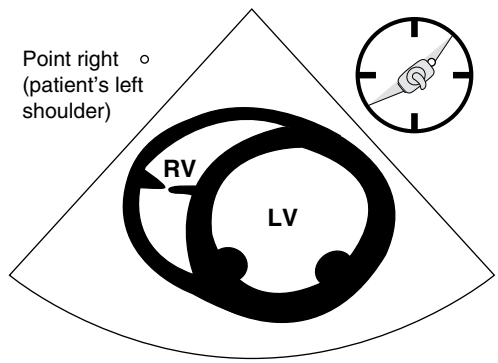

Pos 3: Parasternal LV short axis

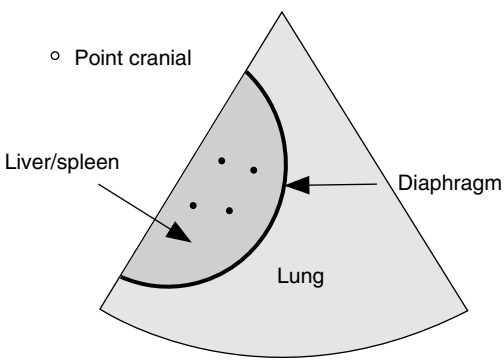

Pos 4: Pleural scanning

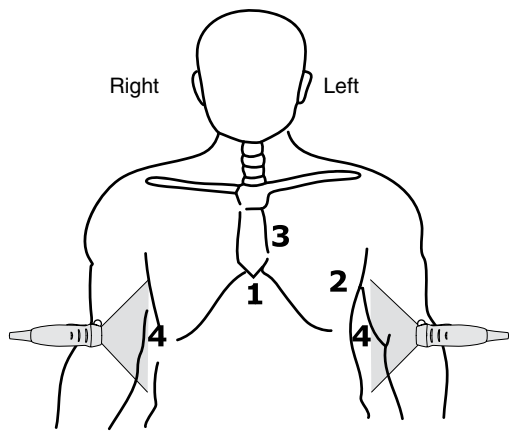

Focus Assessed Transthoracic Echo (FATE)

(European Journal of Anaesthesiology 2004; **21**: 700–707)

1. Look for obvious pathology
2. Assess wall thickness + chamber dimensions
3. Assess bi - ventricular function
4. Image pleura on both sides
5. Relate the information to the clinical context
6. Apply additional ultrasound

Dimensions and contractility:

$$\textbf{FS} = \frac{\textbf{(LVDd – LVSd)}}{\textbf{LVDd}}$$

EF ~ 2 x FS

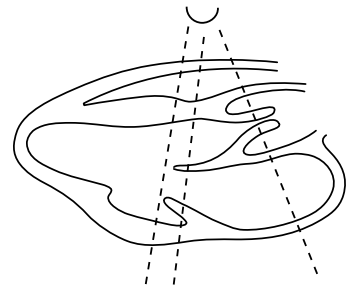

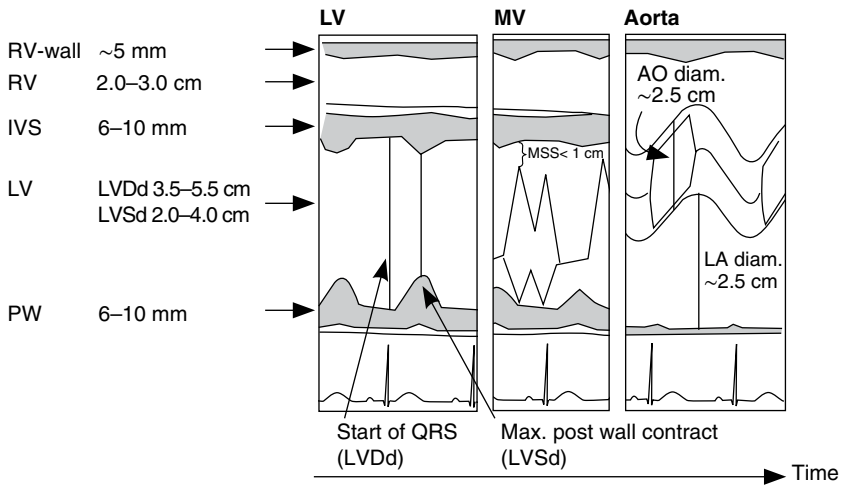

The global function of the heart is determined by the interaction between:

Right ventricle		Left Ventricle	
Systole:	Diastole:	Systole:	Diastole:
Preload	Compliance	Preload	Compliance
Afterload	Relaxation	Afterload	Relaxation
Contractility	Heart rate	Contractility	Heart rate
Heart rate		Heart rate	

Hemodynamic instability, perform a systematic evaluation of these determinants plus concomitant pathology:
(e.g. pericardial effusion, pulmonary embolus, pleural effusion, pneumothorax, valvulopathy, dissection, defects)

Important pathology

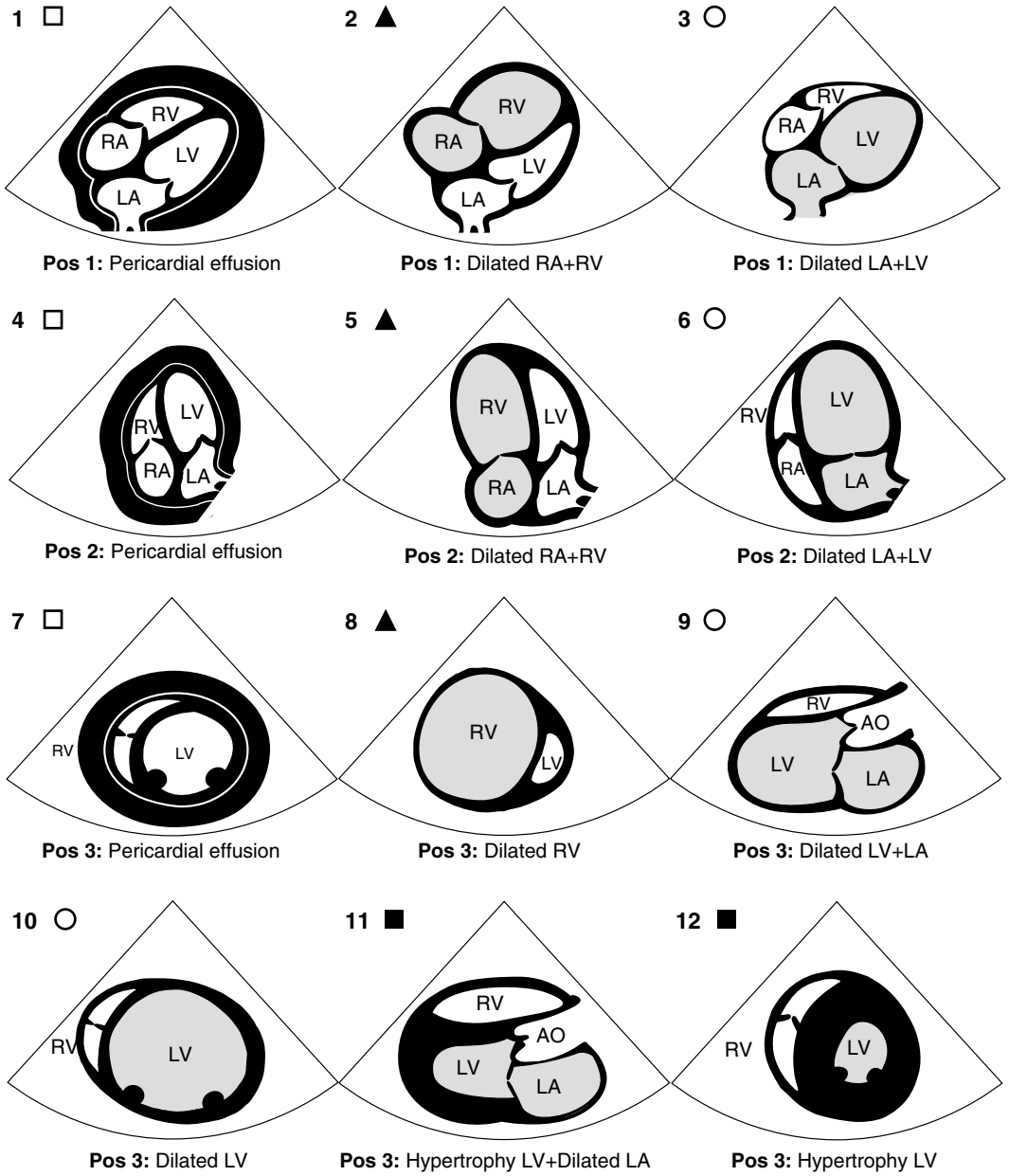

PATHOLOGY TO BE CONSIDERED IN PARTICULAR:

□ Post OP cardiac surgery, following cardiac catheterisation, trauma, renal failure, infection.

▲ Pulmonary embolus, RV infarction, pulmonary hypertension, volume overload.

○ Ischemic heart disease, dilated cardiomyopathy, sepsis, volume overload, aorta insufficiency.

■ Aorta stenosis, arterial hypertension, LV outflow tract obstruction, hypertrophic cardiomyopaty, myocardial deposit diseases.

Extended FATE views

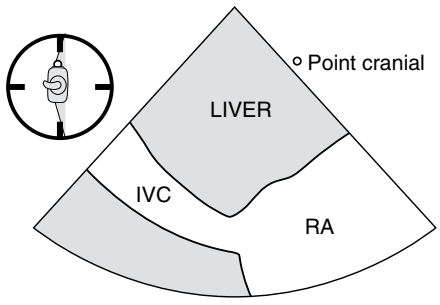

Pos 1: Subcostal vena cava

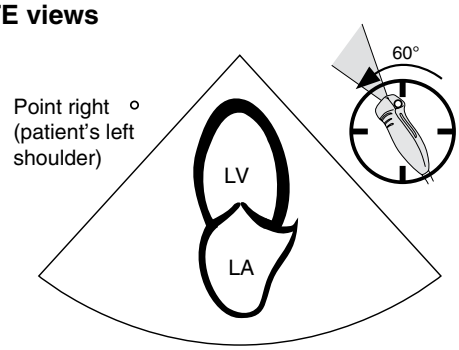

Pos 2: Apical 2 - chamber

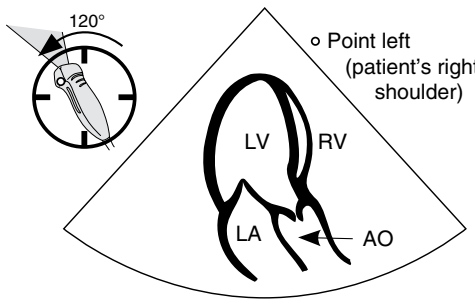

Pos 2: Apical long - axis

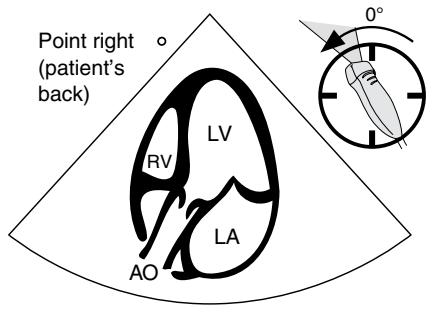

Pos 2: Apical 5 - chamber

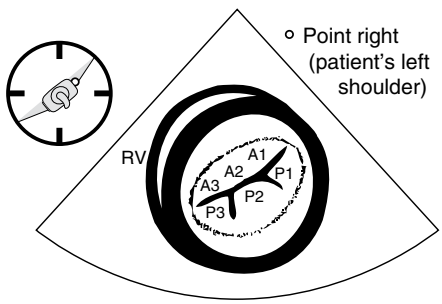

Pos 3: Parasternal short axis mitral plane

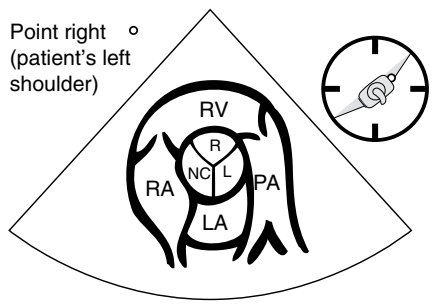

Pos 3: Parasternal aorta short axis

CW: Peak pressure: V^2 x 4; AO < 2 m/s; PA < 1 m/s; TI < 2.5 m/s

PW: Mitral inflow desc. time 140–240 ms; MAX E < 1.2 m/s; E/A >1 (age dependent)

TVI: E/e'< 8–10; IVC < 20 mm; 50% collaps during inspiration is normal

Systolic ventricular function

Ventricle		M-Mode	Normal	Mild ↓	Moderately ↓	Severely ↓
LV	Pos 3, PS long	EF (%)	≥ 55	45–54	30–44	< 30
LV	Pos 3, PS long	FS (%)	≥ 25	20–24	15–19	< 15
LV	Pos 3, PS long	MSS (mm)	< 10	7–12	13–24	> 24
LV	Pos 2, AP 4ch	Mapse (mm)	≥ 11	9–10	6–8	< 6
RV	Pos 2, AP 4ch	Tapse (mm)	16–20	11–15	6–10	< 6
Right and left ventricle eye balling use all views						

For additional information: www.usabcd.org

A1.3 ACES (Abdominal and Cardiac Evaluation with Sonography in Shock)

The ACES (Abdominal and Cardiac Evaluation with Sonography in Shock) algorithm was developed to assist in the evaluation of undifferentiated hypotension. As with many protocols for use in this context, the ultrasound examination starts with the immediate assessment of gross cardiac function and the inferior vena cava. (see Atkinkinson, P.R., McAuley, D.J., Kendall, R.J., Abeyakoon, O., Reid, C.G., Connolly, J., Lewis, D. (2009) Abdominal and Cardiac Evaluation with Sonography in Shock (ACES): an approach by emergency physicians for the use of ultrasound in patients with undifferentiated hypotension. *Emerg. Med. J.*, **26** (2), 87–91.

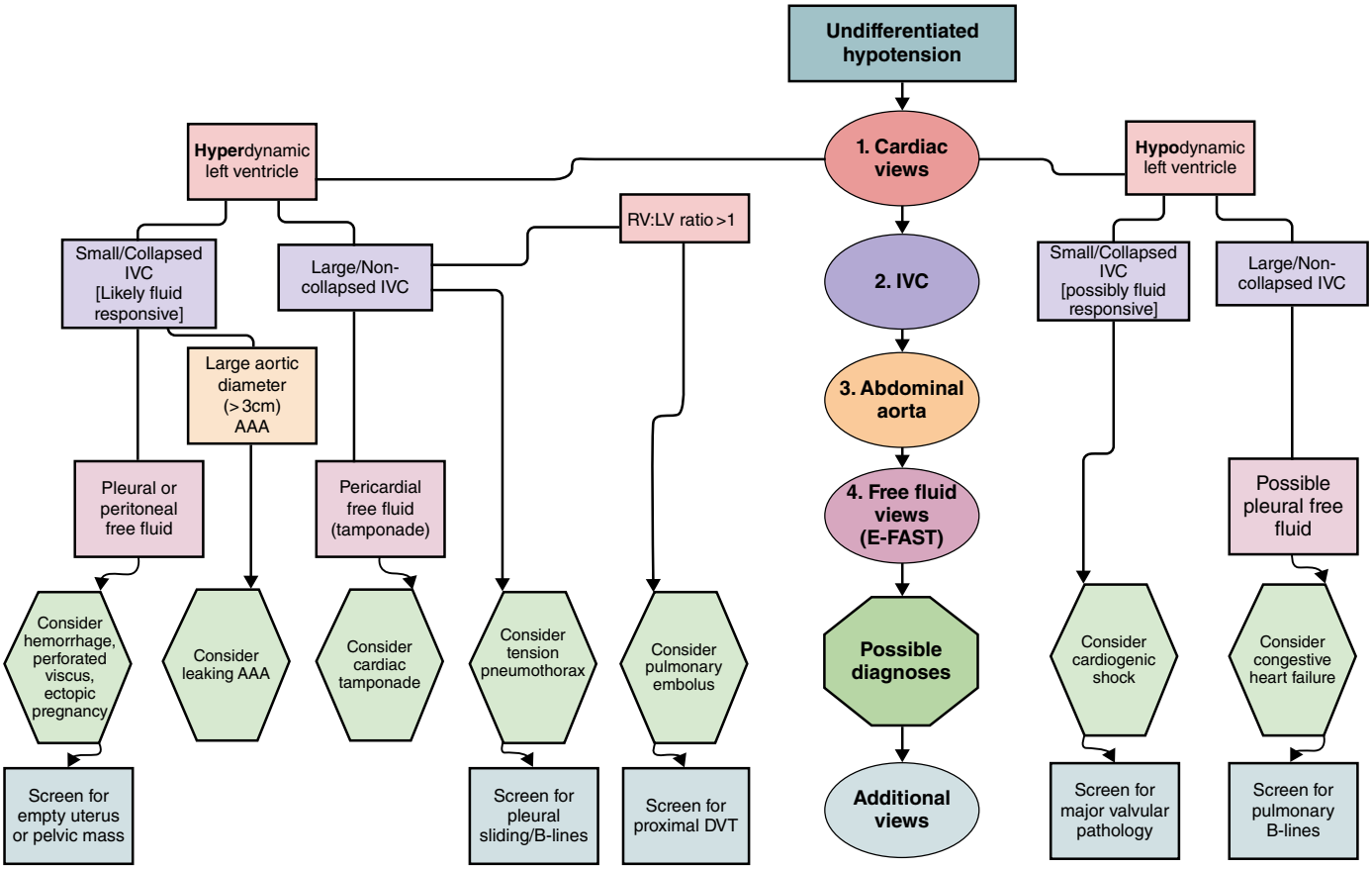
Undifferentiated hypotension
1. Cardiac views
2. IVC
3. Abdominal aorta
4. Free fluid views (E-FAST)
Possible diagnoses
Additional views
Hyperdynamic left ventricle
Small/Collapsed IVC [Likely fluid responsive]
Large/Non-collapsed IVC
RV:LV ratio >1
Large aortic diameter (>3cm) AAA
Pleural or peritoneal free fluid
Pericardial free fluid (tamponade)
Consider hemorrhage, perforated viscus, ectopic pregnancy
Consider leaking AAA
Consider cardiac tamponade
Consider tension pneumothorax
Consider pulmonary embolus
Screen for empty uterus or pelvic mass
Screen for pleural sliding/B-lines
Screen for proximal DVT
Hypodynamic left ventricle
Small/Collapsed IVC [possibly fluid responsive]
Large/Non-collapsed IVC
Possible pleural free fluid
Consider cardiogenic shock
Consider congestive heart failure
Screen for major valvular pathology
Screen for pulmonary B-lines

A1.4 RUSH (Rapid Ultrasound for Shock and Hypotension) Examination

The RUSH (Rapid Ultrasound for Shock and Hypotension) examination was developed by a group on the EMCrit website in 2006. Since then it has been widely used by clinicians in Emergency Medicine and Critical Care. It is publicly accessible (https://emcrit.org/rush-exam/original-rush-article/; accessed 14 March 2017). The protocol shown here is adapted for cardiac arrest.

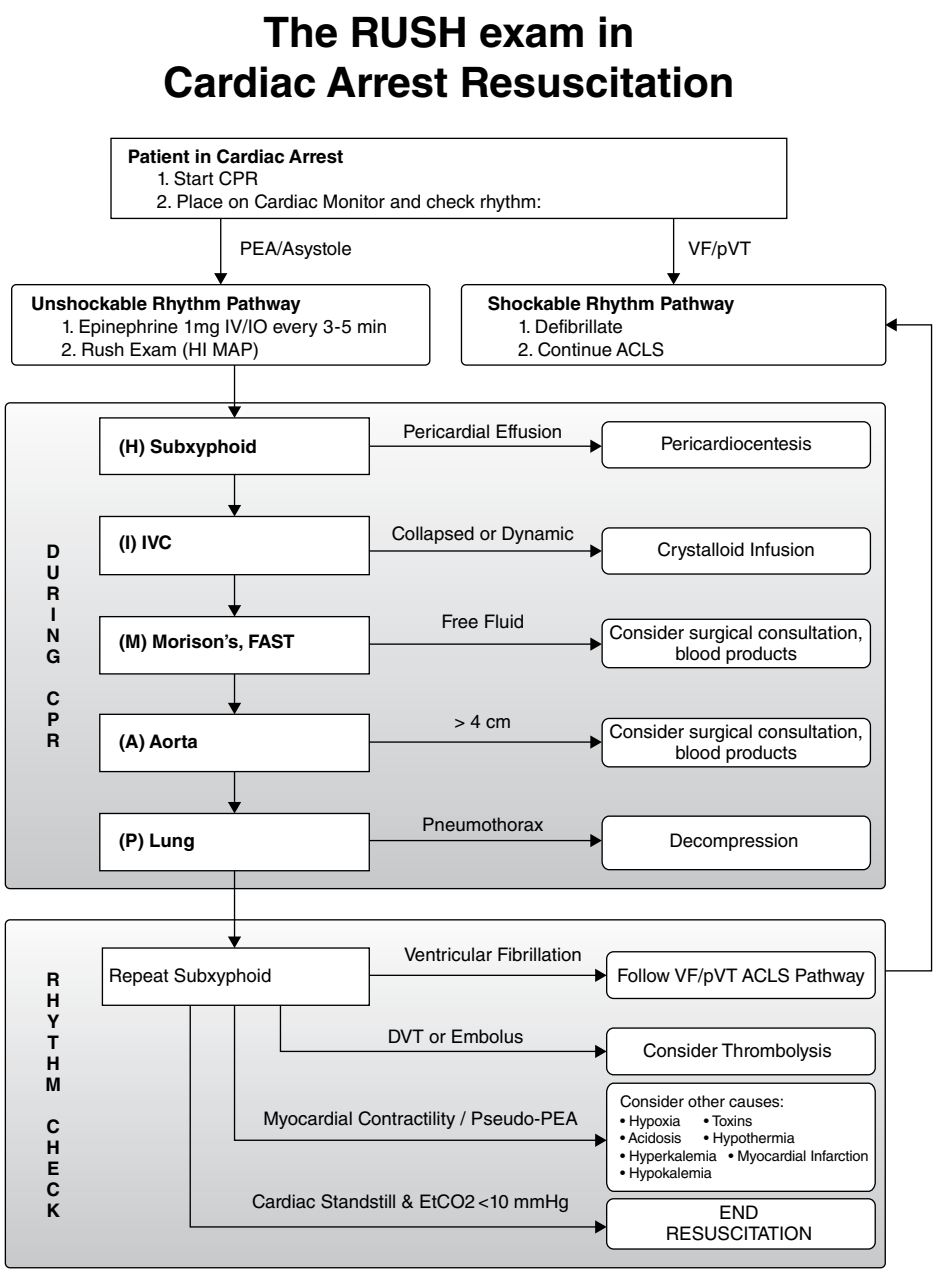

A1.5 Patients in Cardiopulmonary Arrest

This algorithm was developed for use in patients presenting in cardiopulmonary arrest. Similar to Figure A1.4, it is directed at differentiating patients with mechanical causes from those with ischemic, metabolic, or 'electrical' causes. The shaded boxes are end-points with specific management or therapy as per current recommendations. [Adapted with permission from Hendrickson, R.G., Dean, A.J., Costantino, T.G. (2001) A Novel Use of Ultrasound in Pulseless Electrical Activity: The Diagnosis of an Acute Abdominal Aortic Aneurysm Rupture. *J. Emerg. Med.*, **21** (2), 141–144.

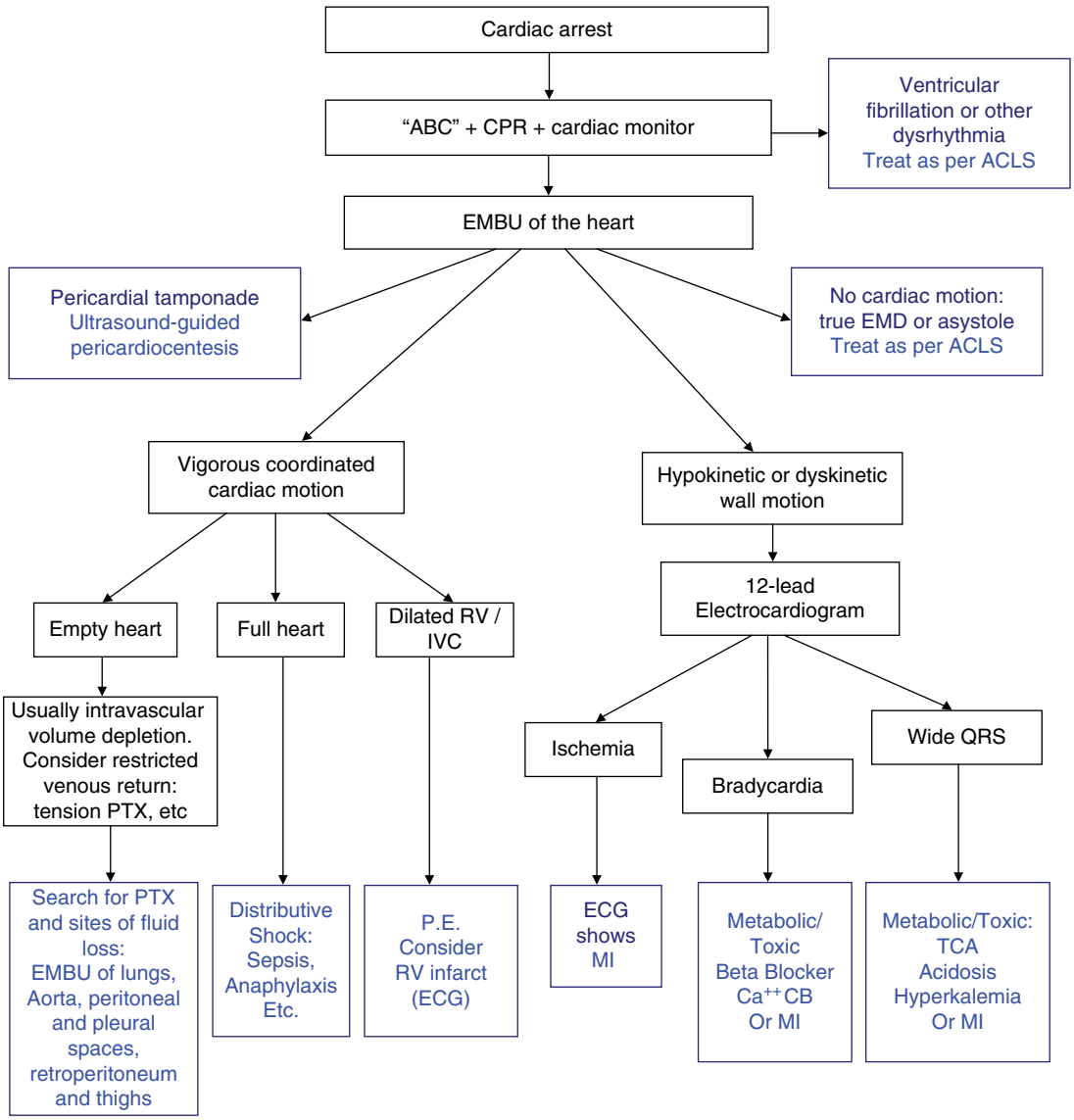

Abbreviations: ABC: Airway, breathing, circulation; CPR: cardiopulmonary resuscitaton; Ca^{++} CB: Calcium channel blocker; EMBU: emergency bedside ultrasonography; EMD: electromechanical dissociation; IVC: inferior vena cava; RV: right ventricle; MI: myocardial infarction; P.E.: pulmonary embolus; PTX: pneumothorax; TCA: cyclic antidepressant.

A1.6 The SHoC Protocols

Protocols for the evaluation of hypotension (Figures A1.6a and A1.6b), and for the evaluation of patients in cardiac arrest (Figures A1.6c and A1.6d) have been developed by a consensus panel of experts from the International Federation of Emergency Medicine (IFEM). Figures A1.6b and A1.6d provide the background scanning technique for the protocols that appear in Figures A1.6a and A1.6c, respectively. Figure A1.6e is a graphical representation of the priorities of scanning from 'core' elements (labelled red) through 'supplementary' elements, to those that can be considered 'additional' (marked yellow). Downloaded from http://www.ifem.cc/resources/ifem-policies-guidelines/(accessed 14 March 2017), with permission of the Canadian Association of Emergency Physicians and the authors).

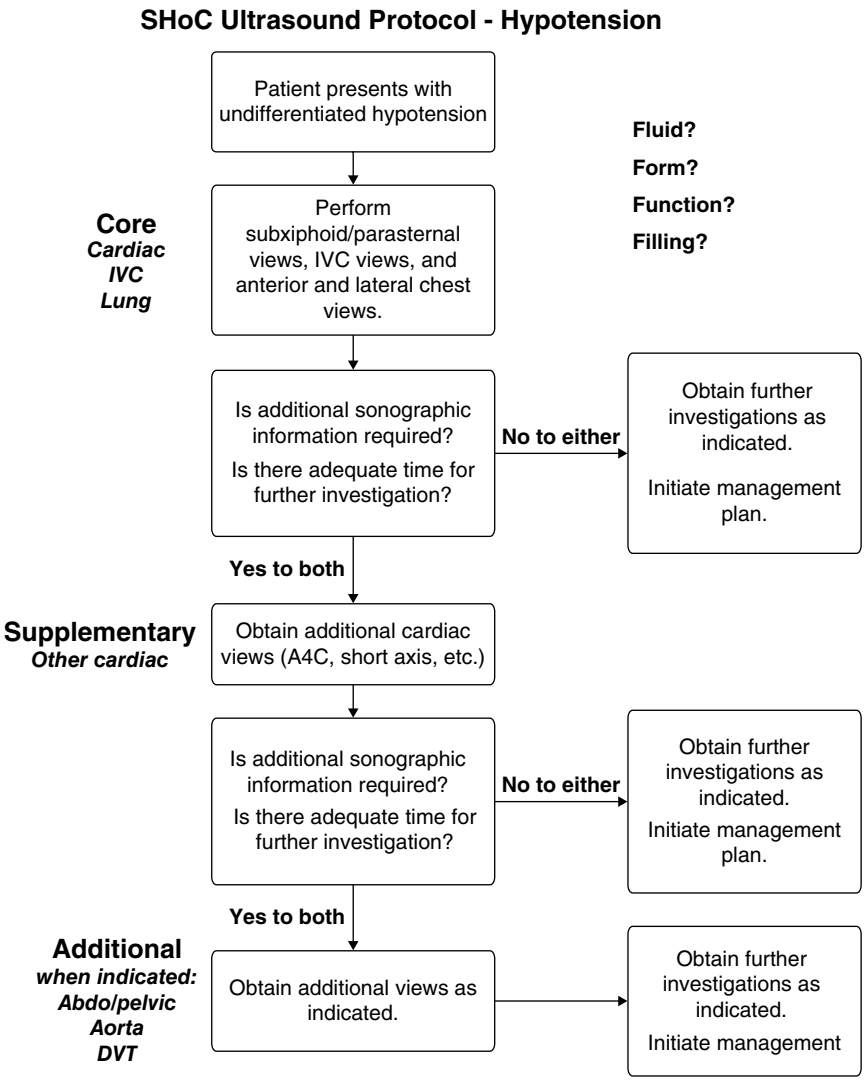

Figure A1.6a The SHoC protocol for patients presenting with undifferentiated hypotension.

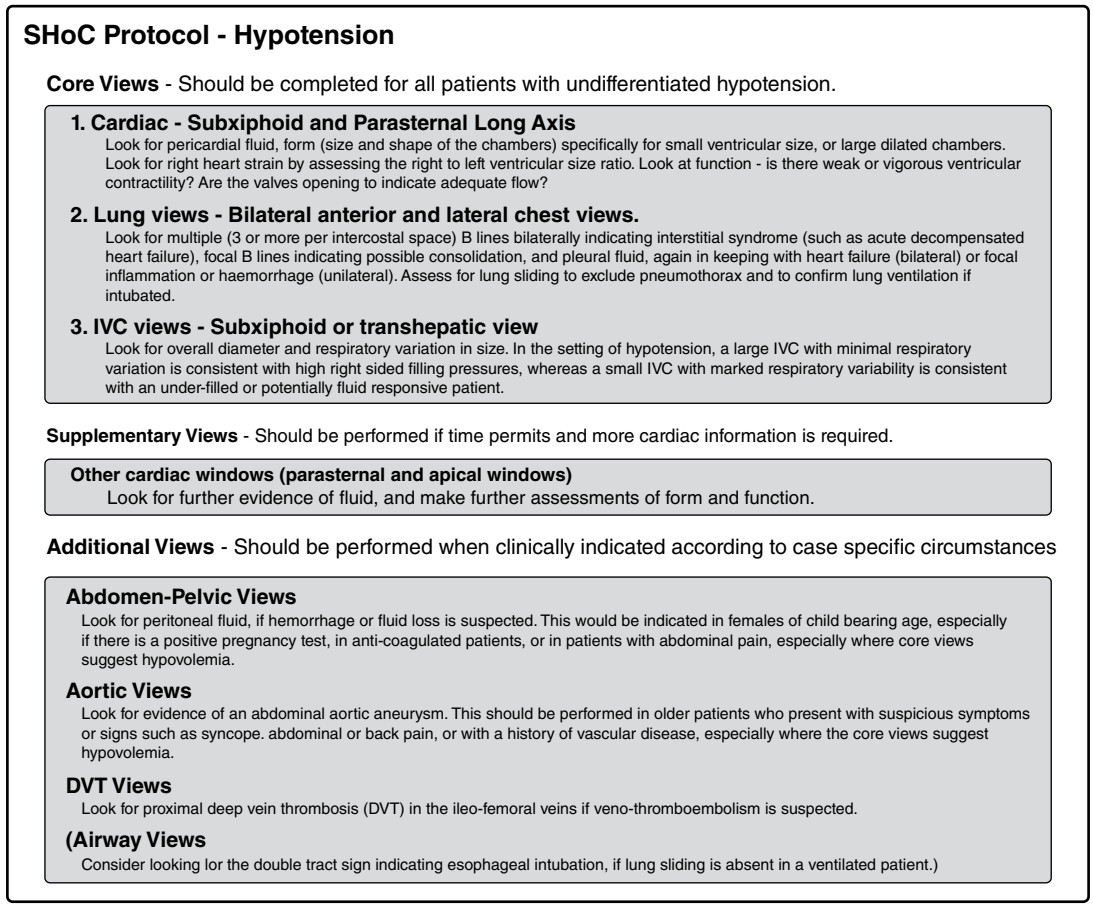

Figure A1.6b The core, supplementary, and additional ultrasound views likely to be needed to assess patients with undifferentiated hypotension in the protocol shown in Figure A1.6a.

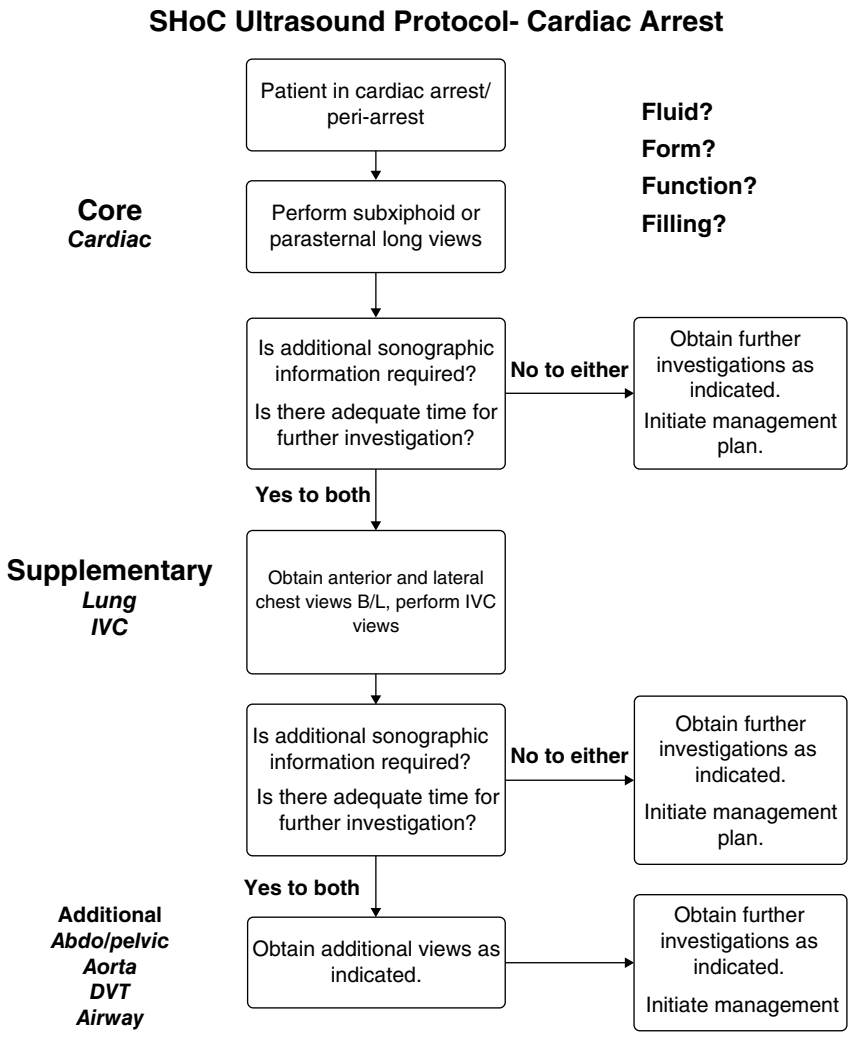

Figure A1.6c The SHoC protocol for patients presenting in cardiac arrest.

SHoC Protocol - Cardiac Arrest

Ensure that chest compressions are not interrupted to perform PoCUS. Use the rhythm/pulse check break to perform scans (less than 10 seconds interruption to CPR)

Core views - should be completed for all patients during cardiac arrest.

1. Cardiac - Subxiphoid or Parasternal Long Axis
Look for pericardial fluid, form (size and shape of the chambers) specifically for small ventricular size, or large dilated chambers. Look for right heart strain by assessing the right to left ventricular size ratio. Look at function - is there weak or vigorous ventricular contractility? Are the valves opening to indicate adequate flow.

Supplementary views - should be performed if time permits and more information is required.

2. Lung views - Bilateral anterior and lateral chest views.
Assess for lung sliding to exclude pneumothorax, and to confirm adequate bilateral ventilation if intubated. Look for multiple (3 or more per intercostal space) B lines bilaterally indicating interstitial syndrome (such as acute decompensated heart failure), focal B lines indicating possible consolidation, and pleural fluid, again in keeping with heart failure (bilateral) or focal inflammation or hemorrhage (unilateral).

3. IVC views - Subxiphoid or transhepatic view
Look for overall diameter and respiratory variation in size. In the setting of cardiac arrest, a large IVC with minimal respiratory variation is commonly seen due to the low flow state, whereas a small IVC with marked respiratory (ventilatory) variability is consistent with an under-filled or potentially fluid responsive patient.

Additional views - should be performed when clinically indicated according to case specific circumstances

Abdomen-Pelvic Views
Look for peritoneal fluid, if hemorrhage or fluid loss is suspected. This would be indicated in females of child bearing age, especially if there is a positive pregnancy test, in anti-coagulated patients, or in patients with abdominal pain, especially where core views suggest hypovolemia.

Aortic Views
Look for evidence of an abdominal aortic aneurysm. This should be performed in older patients who present with suspicious symptoms or signs such as syncope, abdominal or back pain, or with a history of vascular disease. especially where the core views suggest hypovolemia.

DVT Views
Look for proximal deep vein thrombosis (DVT) in the ileo-femoral veins if veno-thromboembolism is suspected.

Airway Views
Scan the anterior neck and look for the double tract sign indicating esophageal intubation, if lung sliding is absent in a ventilated patient.

Figure A1.6d The core, supplementary, and additional ultrasound views likely to be needed to assess patients in cardiac arrest in the protocol shown in Figure A1.6c.

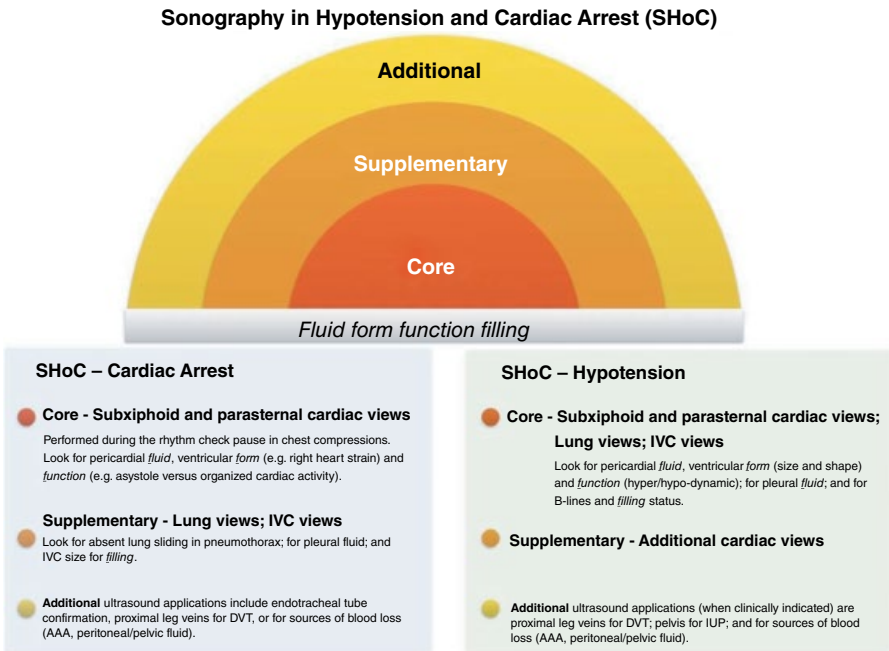

Figure A1.6e The conceptual arrangement of core, supplementary, and additional ultrasound views used in the SHoC protocols.

Index

Emergency Point-of-Care Ultrasound, Second Edition. Edited by James A. Connolly, Anthony J. Dean, Beatrice Hoffmann and Robert D. Jarman.

Companion website: www.wiley.com/go/connolly/ultrasound

q

r